

Department of Chemistry

**Biogeochemical cycles (C, N, S, P and Fe) of modern and
ancient microbialites (Western Australia)**

Anais Pagès

**This thesis is presented for the Degree of
Doctor of Philosophy
of
Curtin University**

January 2014

Declaration

To the best of my knowledge and belief this thesis contains no material previously published by any other person except where due acknowledgment has been made.

This thesis contains no material which has been accepted for the award of any other degree or diploma in any university.

Anais Pagès

Perth, January 30th, 2014

Abstract

Stromatolites are “accretionary sedimentary structures, commonly thinly layered, megascopic and calcareous, produced by the activities of mat-building communities of mucilage-secreting microorganisms, mainly photoautotrophic prokaryotes”. They represent the earliest traces of life, with macro-fossil specimens reported in the rock record back to 3430 Ma. Stromatolites were dominant structures in the rock record until 600 Ma reflecting a crucial role in Earth’s evolution, particularly in oceans and the oxidation of the atmosphere. Yet, the general lack of microfossils or molecular fossils during this period of life’s early evolution makes the study of microbial assemblages highly challenging and prone to scrutiny. In addition, little is known about the sources – i.e., at a microbial species level - biogeochemical processes and preservation pathways of these ancient microbial macrostructures. Modern microbial mats, including laminated lithifying smooth mats reported in the World Heritage listed Shark Bay, Western Australia are considered modern analogues of early-formed stromatolites. Consequently, the study of these specimens provides an opportunity to gain a better understanding of the evolution of early life and conduct a molecular comparison with ancient microbial structures with the hope of correlating molecular microfossils (i.e., biomarkers). Studies of modern microbial mats and diagenetic pathways supporting their biomarker preservation are critically important for discerning early microbial assemblages, complex and dynamic elemental cycles and the true nature of macroscopic biosignatures (e.g. organic petrography).

The analysis of biomarkers and their stable isotopic composition bears a great potential for the investigation of recent and ancient stromatolites. These data can be used to characterise microbial assemblages, identify organic sources and to reconstruct environmental settings. This PhD study explored this potential and identified the advantages biomarker and stable isotope analyses bring to the microbial characterisation of mat communities. Complimentary methods including 16s *r*RNA analysis, diffusive equilibration in thin films (DET) and diffusive gradients in thin films (DGT) samplers were also applied to contribute to a more holistic characterisation of microbial communities.

Abstract

The main focus of this project was the characterisation of modern microbial mats from Shark Bay in terms of microbial communities and biogeochemical processes, as presented in [Chapters 2-5](#). The preservation pathways of biosignatures in modern and ancient stromatolites were investigated in [Chapters 6 and 7](#). A more detailed synopsis of the research these chapters describe follows.

In [Chapter 2](#), DET and DGT samplers were deployed in a modern smooth stromatolite from Nilemah, Shark Bay, in order to observe, for the first time, two-dimensional distributions of porewater solutes during both day and night time periods. Two-dimensional sulfide and alkalinity distributions revealed a strong spatial heterogeneity and a minor contribution of sulfide to alkalinity. Regions of high sulfide concentrations below the microbial mat suggested significant anaerobic activity in the underlying sediments. Phosphate distributions were also very heterogeneous, while iron(II) distributions were quite similar during day and night with a few hotspots of mobilisation. In some areas of the mat, phosphate and iron(II) distributions suggested that phosphate was most likely being trapped by iron(III) oxyhydroxides to form iron-phosphate complexes. Lipid biomarkers from the three successive layers of the mat were also analysed in order to characterise the microbial communities regulating the analyte distributions. The major hydrocarbon products detected in all layers included *n*-alkanes and isoprenoids, whilst other important biomarkers included hopanoids. The hydrocarbon distribution of the three layers reflected several changes in microbial community structure with mat depth; the most significant increase in bacterial input and a concomitant decrease in eukaryotes including land plant contributions. The relatively high abundance of *n*-C_{17:0} *n*-alkane (*n*-C_{17:1} *n*-alkene was also present) and steroids (C₂₇-C₂₉ sterenes, dominated by C₂₇/cholestene) in the aliphatic fraction of all mat layers confirmed significant cyanobacterial and other eukaryotic inputs, respectively. Diploptene, probably deriving from cyanobacteria, but possibly also methylotrophs or sulfate reducing bacteria, was the most abundant hopanoid in all layers, and its relative abundance decreased with depth. Phospho-lipid fatty-acid (PLFA) profiles similarly revealed a decrease in cyanobacterial markers (i.e 16:0, 16:1 ω 7 and 18:1 ω 9) with depth, whereas sulfate-reducing bacteria (SRB) markers (i.e *iso*-17:1 ω 9 and 10-Me16:0) increased in abundance in accordance with rising sulfide concentrations with depth. Our

Abstract

results contribute to a growing body of evidence that laminated microbial mats are highly complex ecosystems. In addition to vertical stratifications of physicochemical conditions, there is considerable lateral variations in environmental conditions controlling solute concentrations, and therefore in the distributions of the microbial communities which regulate and generate these physicochemical variables.

In [Chapter 3](#), microelectrode measurements of oxygen and sulfide as well as silver foil analyses were performed in a modern layered microbial mat (with three distinct layers) from Nilemah, Shark Bay, in order to determine the redox conditions and sulfate-reducing activity during day and night. High resolution, two-dimensional distributions of porewater analytes were additionally monitored using colourimetric DET and DGT techniques. The colourimetric DET and DGT techniques were used to investigate the co-distributions of sulfide, iron(II), phosphate and alkalinity - the latter related to carbonate precipitation/dissolution dynamics over the diurnal cycle. Oxygen was detected in the two upper layers of the mat during the day, but only the first layer at night. Two-dimensional distributions of sulfide, iron(II) and phosphate showed a high degree of spatial heterogeneity under both light and dark conditions. However, there was a clear shift in overall redox conditions between light and dark conditions as shown by the general concentration profile trends. During light deployments, iron(II) and sulfide concentrations were generally low throughout the entire microbial mat. In contrast, during the dark of night, anoxic conditions prevailed resulting in higher concentrations of iron(II) and sulfide and the migration of the sulfide boundary towards the upper layer of the mat. Similar to iron(II), phosphate profiles showed an increase in concentration at night probably due to release through the dissolution of iron-phosphate complexes under anaerobic conditions. However, two-dimensional distributions revealed that hot spots of phosphate and iron(II) did not coincide, implying that porewater phosphate was mainly regulated by diurnal metabolic changes in the mat. Alkalinity profiles demonstrated an increase in concentration at night, probably related to high rates of sulfate-reduction under dark conditions. Overall, these results demonstrated that microbial activity played a significant role in regulating porewater solute concentrations, especially through photosynthetic processes. Two-dimensional

Abstract

porewater analyte distributions showed significant small-scale heterogeneity, highlighting the advantage of two-dimensional methods.

In Chapter 4, the influence of important abiotic conditions on microbial communities of different types of mats was investigated. The distributions and stable isotopic values of lipid biomarkers (aliphatic hydrocarbons, and PLFAs), and bulk carbon and nitrogen isotope values were analysed in four microbial mats (pustular, smooth, colloform mats and microbial pavement) along a tidal flat gradient to systematically investigate the differences between the lipid and isotopic composition of the microbial mats at different water depths. The PLFA and hydrocarbon analyses revealed that cyanobacteria represented a dominant community in all four microbial mats. However, more depleted $\delta^{13}\text{C}$ values and lower C:N ratios were evident with depth and these data may relate to a possible higher abundance of cyanobacteria in the shallower structures and higher macrophyte input in the deeper microbial mats. In all mats, a predominance of odd-over-even long-chain *n*-alkanes ($\text{C}_{21}\text{-C}_{33}$) was observed and is indicative of a terrestrial plants or macrophyte source. The molecular proxy P_{aq} , based on relative abundances of long-chain *n*-alkanes (C_{23} , C_{25} , C_{29} and C_{31}), was calculated to distinguish the relative biomass inputs of 1) submerged/floating aquatic macrophytes; and 2) emergent and terrestrial plants P_{aq} values indicated the pustular, smooth and colloform mats were dominated by a mixed contribution from terrestrial plants and submerged macrophytes. The lower P_{aq} value of the microbial pavement, however, suggested a higher contribution from seagrass beds to this deepest structure. SRB were also present in all mats, based on the detection of diagnostic PLFA (e.g., 10-Me-16:0). The $\text{C}_{25:1}$ highly branched isoprenoid (HBI) alkene was identified in the pustular and smooth mats and its enriched carbon isotopic composition in comparison with other hydrocarbons suggested the presence of diatoms in these shallower mats. The lipid, isotope and nutrient analyses were extended to two additional microbial laminated smooth mats from other Shark Bay sites (i.e., Garden Point and Rocky Point) presenting lower salinity levels and compared with the hypersaline Nilemah smooth mat data to investigate for any potential relationship between salinity and the structure or function of these microbial ecosystems. The data reflected a predominance of cyanobacteria and also a common presence of sulfate-reducing bacteria in the mats at all three salinities.

Abstract

However, *iso-17:1 ω 9* PLFA was particularly abundant in the Garden Point mat suggesting a high abundance of sulfur-cycling organisms in this mat which of the three was at an intermediate salinity. Furthermore, the C_{25:1} HBI alkene diatom marker was identified in the Nilemah mat only, whilst PLFAs indicative of diatoms were measured in distinctly lower abundance in the less saline mats suggesting that diatoms may respond better to higher salinities.

The influence of the abiotic conditions of water depth and salinity on microbial metabolites was further investigated in [Chapter 5](#). The distributions of intact polar lipids (IPLs) and lipophilic pigments were analysed in the same four microbial mats studied in [Chapter 4](#) (pustular, smooth, colloform mats and microbial pavement). The lipophilic pigment distributions of these mats was also compared to those of the mats studied over two decades earlier by Palmisano et al. (1989) to observe community changes in the mats over this time. The IPL and lipophilic pigment composition of the Nilemah mats highlighted the presence of sulfur-cycling organisms, and possibly phosphate-limited conditions, along the littoral gradient. Alphaproteobacteria and cyanobacteria were detected in all mats, although the smooth mat presented a much lower diversity of cyanobacterial IPLs, probably reflecting a lower diversity in cyanobacterial species in this mat. Other subtle differences between the mat communities were detected, suggesting that water depth does influence microbial mats communities to some degree. The concentration in bacteriochlorophyll *a*, for instance, decreased with depth, highlighting a decrease in purple phototrophic bacteria (*Chromatiaceae*) with depth. In addition, chlorophyll *c*, indicative of diatoms, was only detected in the shallow pustular and smooth mats. These results were concordant with the higher abundance of lipid biomarkers ([Chapter 4](#)) of diatoms in the shallower mats. The IPL and lipophilic pigment composition of the Garden Point and Rocky Point were also analysed to continue the investigation of salinity control. The highest diversity of IPLs was found in the least saline Rocky Point mat, which might imply only a smaller subset of organisms survive the harsh conditions of higher salinity. Cyanobacterial IPLs were present in the mats at all three salinities, although at lower diversity in the most saline Nilemah mat. The chlorophyll *c* of diatoms was only detected in the Nilemah smooth mat, supporting the lipid data ([Chapter 4](#)) which also showed diatoms were more abundant in the most

Abstract

saline site. The much higher abundances of purple phototrophic bacteria in the Garden Point mat did not seem to be related to salinity, but might associate with the relatively calm waters of this location, favouring the development of thick microbial layers. The present lipophilic pigment distribution of the Shark bay mats reflected a number of differences to those of Hamelin Pool mats analysed by Palmisano et al. (1989), which again highlighted the structural dynamics of these microbial communities. Presently, diatoms are exclusively present in the shallower mats, whilst the deepest colloform mats present a high abundance of cyanobacteria. This contrast the 1989 report (Palmisano et al., 1989) of an absence of diatoms in shallow mats and their high abundance in the colloform mats. A comparison of the two data sets also indicated the abundance of purple phototrophic bacteria has increased over the last 25 years, as yet another example of the sensitivity of microbial communities to even small changes in environmental conditions.

In [Chapter 6](#), the preservation pathways of biosignatures in modern stromatolites were investigated. The preservation of highly functionalised biolipids in the geological record is crucial for the reconstruction of paleoenvironments and verifying microbial assemblages related to early-life. Sulfurisation is one important diagenetic pathway for the preservation of biolipids. Desulfurisation, using Raney-nickel, is a useful method for identifying S-bound carbon skeletons and was applied here to four layers of a living, well-laminated, smooth microbial mat from Garden Point, Shark Bay. The innovative measurement of the two-dimensional distribution of dissolved sulfide and iron (II) within these mats was also undertaken in order to assess the environmental conditions. Anoxic conditions, high sulfide and low iron (II) concentrations are prerequisites for the formation of organic sulfur compounds (OSC) and our results demonstrated that such biogeochemical conditions were present and favoured the sulfurisation process in the mat. PLFAs were also analysed for evidence of the viable biomass in all layers, including the deepest layer containing FeS. Various PLFA markers of sulfate-reducing bacteria (i.e. *iso-17:1 ω 9* and 10-Me16:0) were detected as well as unusual long-chain fatty acids presenting a similar distribution to fatty acids analyzed in ooids from the Bahamas and Shark Bay and associated with the presence of sulfate-reducing bacteria. Significantly, the present research represents the first discovery of sulfur-bound

Abstract

aliphatic and aromatic compounds within a modern stromatolite. The aliphatic hydrocarbon products included *n*-alkanes, isoprenoids, steroids and triterpanes with a strong predominance of 17 β (H),21 β (H)-hopanes. Sulfur-bound carotenoids from sulfur cycling organisms (green and purple sulfur bacteria) were also identified in the upper three layers. The presence of isorenieratane in the third layer indicated anoxic and sulfidic conditions. The presence of reduced carotenoids suggested the abiotic reduction *via* hydrogen sulfide from bacterial sulfate-reduction within this contemporary ecosystem. These results provided compelling evidence for the sulfurised preservation of “living fossils” of early-life and highlighted the role of sulfate-reducing bacteria in the preservation of biosignatures through time.

In [Chapter 7](#), biomarker signatures in a 2.3 billion years old microbial mat from the Turee Creek group were investigated. Hydropyrolysis (HyPy) has been recently established as a reliable method to release kerogen-bound biomarkers which can then be unequivocally associated with the stratigraphic interval of the sample. No steranes or hopanes were detected in the freely extractable saturated fraction. However, after HyPy treatment of the kerogen, C₂₇, C₂₈ and C₂₉ steranes and diasteranes in both 20*S* and 20*R* isomeric configuration, with a slight predominance of 20*S*, were observed. The kerogen was also separately treated by HCl to investigate carbonate-bound biomarkers. HCl dissolved the carbonate and released from it steranes and sterols. No further steranes were released following subsequent HyPy treatment of the carbonate-free kerogen, confirming that those detected following initial HCl treatment were carbonate-bound. As the steroid biomarkers were exclusively entrapped in the carbonate matrix, the morphology and other spectral features of the carbonate were examined for diagenetic features. Thin-section analysis of the carbonate revealed that no later re-precipitation occurred suggesting the carbonates were contemporary to the formation of the microbial mat (1.8 Ga at the earliest but most likely 2.3 Ga). Raman spectroscopy revealed a spectrum similar to other low-metamorphic grade, old carbonate rocks and matched the lowest temperature spectrum for the kerogen formation (140°C or lower). Analysis of two additional samples from the Turee Creek group (a stromatolite and a clotted mat) confirmed that steroids were only present in the laminated smooth mat. Additional work will be required to confirm the indigenous signature of steroids in this sample.

Abstract

However, the entrapment of biosignatures within the carbonate matrix appears to represent a pathway of exceptional biomarker preservation through geological time.

Acknowledgements

This PhD project has been a great and challenging journey. It is the work of many wonderful people who contributed to its achievement and I am delighted to have received so much support from them.

First, I would like to thank my supervisor Prof Kliti Grice for providing me excellent scientific support and guidance whilst still allowing me to approach my study in the way that I wanted. I am very grateful that she allowed me to participate in a high number of national and international conferences and three memorable field trips to Shark Bay. My PhD project has been a wonderful experience and I am delighted that Kliti offered me this opportunity and always trusted my scientific ideas and opinion. Thanks to her, I feel that I became a lot more knowledgeable and it was great pleasure to work in the amazing facilities that she is offering.

I would also like to express my gratitude to my co-supervisor Associate Prof. Paul Greenwood for always supporting me in time of doubts, for his advice and continuous help and his valuable input to the writing of this thesis.

In addition, I would like to thank Prof Lorenz Schwark for very interesting discussions regarding my results and his highly valuable scientific advice. I am also glad that he strongly encouraged me to further pursue the work on ancient microbial mats and stromatolites.

Additionally, I am very grateful to Dr David Welsh and Associate Prof. Peter Teasdale for allowing me to use their facilities and for a wonderful long-term collaboration. I am delighted that I was able to work with them again and I deeply trust and value their advice.

Acknowledgements

Many thanks to Prof. Martin Van Kranendonk! It was a real pleasure to work with him and I am very grateful for his highly valuable contribution to my work and providing very detailed description of the geological settings of my samples. I am also glad he provided me exceptional samples, even though it was only a few months before I completed my PhD!

I also wish to acknowledge my colleagues at WA-OIGC for their continuous support with labwork and writing. I would like to give a special thanks to my dear friend Ines Melendez, Svenja Tulipani, Caroline Jaraula, Chloe Plet, Hendrik Grotheer and Aileen Robert with whom I shared wonderful moments out of University and for cheering me up in moments of doubts. I strongly hope that we will stay in contact in the future and visit each other in different parts of the world. I am also grateful to Geoff Chidlow for taking the time to discuss with me and for his excellent technical support, Robert Lockhart for his enormous help with hydrolysis experiments, and Stephen Clayton for his support with compound specific isotope analyses. Many thanks to Dr's Tobias Ertefai, Cédric Hubas and Tarik Meziane for their valuable help with sample analysis. Thanks also to Tanya Chambers, Alicia Harrison, Marija Predojevic and other administrative staff for their significant help regarding travel and field trip organisations.

I also had the wonderful opportunity to participate in various field trips to Shark Bay and would like to thank everyone involved in these field trips, particularly Dr Ricardo Jahnert, Prof.'s Pieter Visscher and Lindsay Collins for helping me with the sampling, data collection and teaching me some much about Shark Bay!

Furthermore, I am grateful to Prof. Roger Summons for MRM-GC-MS analysis of my samples and his scientific input. Also many thanks to Dr Greg Skrzypek and Douglas Ford for their support with $\delta^{13}\text{C}$ analysis of OM and carbonates.

I also would like to thank Dr Pia Atahan for inviting me to ANSTO and allowing me to present my work during the Biomarker Workshop.

Acknowledgements

I would like to acknowledge Curtin University for a CIPRS scholarship and CSIRO for a top-up scholarship. I also thank the ARC for funding (QEII Discovery, Discovery projects and an ARC Linkage grant) awarded to my supervisor to help pursue the research on early-life apparition on Earth.

I also wish to acknowledge the two reviewers of my thesis who spent significant time and effort providing constructive comments on my work.

Finally, I would like to deeply acknowledge my loving family, especially my parents who always supported me in every way they could and believed in me. Un grand merci a vous! Last, I would like to thank Michael Vacher who has been sharing my life for many years and was always there for me, supported me and encouraged me and simply, makes me happy.

Primary publications

This thesis is assembled by publications, either accepted with minor revisions, submitted or in preparation, which form the individual chapters and are listed below.

Chapter 2

A. Pagès, K. Grice, M. Vacher, P.R. Teasdale, D.T. Welsh, W.W. Bennett, P. Greenwood. Characterising microbial communities and processes in a modern stromatolite (Shark Bay) using lipid biomarkers and two-dimensional distributions of porewater solutes. *Environmental Microbiology*, in press (2014) impact factor 5.76.

Chapter 3

A. Pagès, D.T. Welsh, P.R. Teasdale, K. Grice, M. Vacher, W.W. Bennett, P.T. Visscher.

Diel fluctuations in solute distributions and biogeochemical cycles in hypersaline microbial mats from Shark Bay, Western Australia. *Marine chemistry*, in press (2014) impact factor 3.00.

Chapter 4

A. Pagès, K. Grice, R. Jahnert, T. Ertefai, G. Skrzypek, P. Greenwood.

Organic geochemical studies of modern microbial mats from Shark Bay – Part I. Influence of depth and salinity on lipid biomarkers and their isotopic signatures. *Geobiology*, under review (2014) impact factor 3.04.

Chapter 5

A. Pagès, C. Hubas, K. Grice, N. Thiney, R. Jahnert, T. Ertefai, T. Meziane. Organic geochemical studies of modern microbial mats from Shark Bay – Part II. Influence of depth and salinity on intact polar lipid and lipophilic pigment distributions. *Geobiology*, in preparation (2014) impact factor 3.04.

Primary publications

Chapter 6

A. Pagès, K. Grice, R. Jahnert, M. Vacher, P.R. Teasdale, D.T. Welsh, L. Collins, M.J. Van Kranendonk, J. Cleverley, P. Greenwood.

Keeping the smell down: Microbial environment and community diversity in a modern stromatolite from Shark Bay, Western Australia. *Geobiology*, under review (2014) impact factor 3.04.

Chapter 7

A.Pagès, K.Grice, L. Schwark, R. Lockhart, D. Flannery, M.J. Van Kranendonk
Investigation of biomarker distributions in a Paleoproterozoic microbial mat from the Turee Creek group, Pilbara, Western Australia. In preparation.

Statement of Contribution of Others

Chapter 2

Experiments were designed by Anais Pagès and Kliti Grice and executed by Anais Pagès. The DET and DGT probes were made at the Environmental Future Centre, Griffith University, Australia under the supervision of Peter Teasdale and David Welsh and with the assistance of William Bennett. The DGT and DET samplers were deployed in the field (Shark Bay, Western Australia) with the assistance of Michael Vacher. Paul Greenwood helped with the analysis of phospho-lipid fatty acids at the School of Plant Biology, University of Western Australia, Australia. Anais Pagès wrote the manuscript with contributions from all co-authors. All of whom also provided intellectual input in discussions. Kliti Grice provided analytical facilities except where mentioned otherwise. This research was funded by an ARC Discovery Grant (Grice, Greenwood, Snape, and Summons).

Chapter 3

Experiments were designed by Anais Pagès and Kliti Grice and executed by Anais Pagès. The DET and DGT probes were made at the Environmental Future Centre, Griffith University, Australia under the supervision of Peter Teasdale and David Welsh and with the assistance of William Bennett. The DGT and DET samplers were deployed in the field (Shark Bay, Western Australia) with the assistance of Michael Vacher. Peter Visscher provided the microelectrode (sulfide and oxygen) and silver foil measurements in the mat. Anais Pagès wrote the manuscript with contributions from all co-authors. All of whom also provided intellectual input in discussions. Kliti Grice provided analytical facilities except where mentioned otherwise. This research was funded by an ARC Discovery Grant (Grice, Greenwood, Snape and Summons).

Statement of Contribution of Others

Chapter 4

Experiments were designed by Anais Pagès and Kliti Grice and executed by Anais Pagès and Tobias Ertefai. The samples were taken with the assistance of Tobias Ertefai and Ricardo Jahnert. Paul Greenwood assisted with the analysis of phospho-lipid fatty acids at the School of Plant Biology, University of Western Australia, Australia. $\delta^{13}\text{C}$ analysis and of $\delta^{15}\text{N}$ of organic matter and carbonates were performed by Greg Skrzypek at the School of Plant Biology, University of Western Australia, Australia. Anais Pagès wrote the manuscript with contributions from all co-authors. All of whom also provided intellectual input in discussions. Kliti Grice provided analytical facilities except where mentioned otherwise. This research was funded by an ARC Discovery Grant (Grice, Greenwood, Snape and Summons).

Chapter 5

Experiments were designed by Anais Pagès, Tobias Ertefai and Kliti Grice and executed by Anais Pagès and Tobias Ertefai. The samples were taken with the assistance of Tobias Ertefai and Ricardo Jahnert. Intact polar lipids were analysed at Bremen University with the assistance of Tobias Ertefai. Pigment distributions were analysed at the Natural History Museum, Paris, France with the assistance of Cédric Hubas, Najet Thiney and Tarik Meziane. Anais Pagès wrote the manuscript with contributions from all co-authors. All of whom also provided intellectual input in discussions. Kliti Grice provided analytical facilities except where mentioned otherwise. This research was funded by an ARC Discovery Grant (Grice, Greenwood, Snape, and Summons).

Statement of Contribution of Others

Chapter 6

Experiments were designed by Anais Pagès and Kliti Grice and executed by Anais Pagès. The DET and DGT probes were made at the Environmental Future Centre, Griffith University, Australia under the supervision of Peter Teasdale and David Welsh. The DGT and DET samplers were deployed in the field (Shark Bay, Western Australia) with the assistance of Michael Vacher. The sample of microbial mat for organic analysis was sampled with the assistance of Ricardo Jahnert and Lindsay Collins. Paul Greenwood helped with the analysis of phospho-lipid fatty acids at the School of Plant Biology, University of Western Australia, Australia. Anais Pagès wrote the manuscript with contributions from all other co-authors including James Cleverley and Martin Van Kranendonk. All of whom also provided intellectual input in discussions. Kliti Grice provided analytical facilities except where mentioned otherwise. This research was funded by an ARC Discovery Grant (Grice, Greenwood, Snape and Summons).

Chapter 7

Experiments were designed by Anais Pagès, Lorenz Schwark and Kliti Grice and executed by Anais Pagès with some technical support from Geoff Chidlow, Greg Skrzypek and Stephen Clayton. Robert Lockhart provided assistance with the hydrolysis analysis. Martin Van Kranendonk provided the set of samples and performed the microscopic analysis. David Flannery performed the Raman Spectroscopy. Anais Pagès wrote the manuscript with contributions from all co-authors. All of whom also provided intellectual input in discussions. Kliti Grice provided analytical facilities except where mentioned otherwise. This research was funded by an ARC Discovery Grant (Grice, Greenwood, Snape and Summons).

Secondary publications

Manuscript and abstracts based on research that was conducted during the preparation of this thesis.

Peer reviewed journal articles not part of thesis research

M.J. Van Kranendonk, J.W. Schopf, K. Williford, K. Grice, **A. Pagès**, A. B. Kudryavtsev, V.A. Gallardo, C. Espinoza, T. Ushikubo, K. Kitajima, A. Lepland, M.R. Walter, K.E. Yamaguchi, E. Hegner, M. Ikehara, I. Melendez, D. Flannery, J. Valley.

A chemoautotrophic, sulfur-cycling microbial community dating from the rise of atmospheric oxygen. Under review, *Geobiology* (2013), impact factor 3.04.

Conference abstracts

A. Pagès, K. Grice, R. Jahnert, L. Collins, M. Vacher, R. Summons, P.R. Teasdale, D.T. Welsh, J. Cleverley, M.J. Van Kranendonk, P. Greenwood. Abiotic sulfurisation of a modern ecosystem and the preservation of early-life. The International Biogeoscience Conference, Nagoya, Nov. 2013, oral presentation.

A. Pagès, K. Grice, R. Jahnert, L. Collins, M. Vacher, R. Summons, P.R. Teasdale, D.T. Welsh, J. Cleverley, M.J. Van Kranendonk, P. Greenwood. Abiotic sulfurisation of a modern ecosystem and the preservation of early-life. 26th International Meeting of Organic Geochemistry (IMOG), Tenerife, Sep. 2013, poster presentation.

J.J. Brocks, B.J. Bruisten, **A. Pagès**, K. Grice. Phototrophs and ore formation. Goldschmidt Conference, Florence, Aug. 2013, oral presentation.

P.R. Teasdale, D.T. Welsh, D. Robertson, **A. Pagès**, W.W. Bennett. A new view of sediment biogeochemistry and heterogeneity: use of two-dimensional, high resolution DET and DGT techniques. Conference on DGT and the Environment, Lancaster, Jul. 2013, oral presentation.

Secondary publications

P.R. Teasdale, D.T. Welsh, D. Robertson, **A. Pagès**, W.W. Bennett. Passive sampler techniques for investigating biogeochemical processes within heterogeneous estuarine sediments. 12th International Biogeochemistry Symposium, Plymouth, Jul. 2013, oral presentation.

A. Pagès, K. Grice, R. Jahnert, L.Collins, M. Vacher, R. Summons, P. R. Teasdale, D.T.Welsh, J. Cleverley, M.J. Van Kranendonk, P.Greenwood. Abiotic sulfurisation of a modern ecosystem and the preservation of early-life. 12th Australasian Environmental Isotope Conference, Perth, Jul. 2013, oral presentation.

A. Pagès, K. Grice, R. Jahnert, L.Collins, M. Vacher, R. Summons, P. R. Teasdale, D.T.Welsh, J. Cleverley, M.J. Van Kranendonk, P.Greenwood. Abiotic sulfurisation of a modern ecosystem and the preservation of early-life. Australian Astrobiology meeting, Sydney, Jul. 2013, oral presentation.

A. Pagès, K. Grice, R. Jahnert, L.Collins, M. Vacher, R. Summons, P. R. Teasdale, D.T.Welsh, J. Cleverley, M. Van Kranendonk, P.Greenwood. Abiotic sulfurisation of a modern ecosystem and the preservation of early-life. 17th Australian Organic Geochemistry Conference, Sydney, Dec.2012, oral presentation.

M.J. Van Kranendonk, J.W. Schopf, K. Williford, K. Grice, **A. Pagès**, A.B. Kudryavtsev, V.A. Gallardo, C. Espinoza, T. Ushikubo, K. Kitajima, A. Lepland, M.R. Walter, K.E. Yamaguchi, E. Hegner, M. Ikehara, I. Melendez, D. Flannery, J. Valley. A 2.3 Ga sulfuretum at the GOE: microfossil and organic geochemistry evidence from the 2.3 Ga Turee Creek Group, Western Australia. International Geological Congress, Brisbane, Aug. 2012, oral presentation.

M.J. Van Kranendonk, J.W. Schopf, K. Williford, K. Grice, **A. Pagès**, A.B. Kudryavtsev, V.A. Gallardo, C. Espinoza, T. Ushikubo, K. Kitajima, A. Lepland, M.R. Walter, K.E. Yamaguchi, E. Hegner, M. Ikehara, I. Melendez, D. Flannery, J. Valley. A 2.3 Ga sulfuretum at the GOE: microfossil and organic geochemistry evidence from the 2.3 Ga Turee Creek Group, Western Australia. Astrobiology Science conference, Atlanta, Apr. 2012, oral presentation.

Secondary publications

A. Pagès, K. Grice, R. Lockhart, A. Holman, I. Melendez, M. Van Kranendonk, P. Greenwood, C. Jaraula. Biomarkers of sulfate reducing bacteria from a variety of different aged samples including a modern microbial mat. American Geophysical Union (AGU) Fall Meeting, San Francisco, Dec. 2011, oral presentation.

A. Pagès, K. Grice, R. Lockhart, A. Holman, I. Melendez, M. Van Kranendonk, P. Greenwood, C. Jaraula. Biomarkers of sulfate reducing bacteria from a variety of different aged samples including a modern microbial mat. Royal Society of WA 13th annual postgraduate symposium, Perth, Sep. 2011, oral presentation.

A. Pagès, K. Grice, R. Lockhart, R. Capon. Hydroxyrolysis and stable isotope analyses of extant biomass to yield biomarkers preserved in the rock record. 11th Australasian Environmental Isotope Conference, Cairns, Jul. 2011, oral presentation.

Invited talks

A. Pagès, K. Grice, R. Jahnert, L. Collins, M. Vacher, R. Summons, P. R. Teasdale, D.T. Welsh, J. Cleverley, M. Van Kranendonk, P. Greenwood. Abiotic sulfurisation of a modern ecosystem and the preservation of early-life. Australian national nuclear research and development organisation (ANSTO), Sydney, Jan. 2013, invited speaker.

A. Pagès, K. Grice, R. Lockhart, A. Holman, I. Melendez, M. Van Kranendonk, P. Greenwood, C. Jaraula. Biomarkers of sulfate reducing bacteria from a variety of different aged samples including a modern microbial mat. Stanford University, San Francisco, Dec. 2011, invited speaker.

Abbreviations

A-B-C

Bchl: Bacteriochlorophyll
BSIA: Bulk stable isotope analysis
BL: Betaine lipid
BLAST: Basic local alignment search tool
BSR: Bacterial sulfate reduction
CA: Carbonate alkalinity
CARD-FISH: Catalyzed reporter deposition-FISH
CF: Continuous flow
Chl: Chlorophyll
CPI: Carbon preference index
CSIA: Compound specific stable isotope analysis

D

DAG: Diacylglycerol
DCM: Dichloromethane
DET: Diffusional equilibration in thin-film
DGDG: Diglycosyldiacylglycerol
DGT: Diffusional gradient in thin-film
DIC: Dissolved inorganic carbon
DNA: Deoxyribonucleic acid
DOC : Dissolved organic carbon

E-F

EA: Elemental analyser
EDTA: Ethylenediaminetetraacetic acid
e.g: *exempli gratia* (for example)
EtOH: Ethanol
EPC: Electronically pressure controlled
EPS: Exopolymeric substances
FA: Fatty acid
FAME: Fatty acid methyl ester
FISH: Fluorescence *in situ* hybridisation

Abbreviations

G-H-I

GC: Gas chromatography
GC-MS: GC tandem mass spectrometry
GC-MRM: GC- multiple reaction monitoring
Gly: Glycolipids
GlyA-DAG: Monoglycosyldiacylglycerol
GSB: Green sulfur bacteria
HBI: Highly branched isoprenoid
HP: Hewlett Packard
(3)-HP: Hydroxypropionic acid
HPLC: High Pressure Liquid Chromatography
HPLC-ESI-MS: High-performance liquid chromatography-electrospray ionization-MS
HyPy: Hydropyrolysis
IAEA: International atomic energy agency
i.e.: *id est* (that is)
irMS: Isotope-ratio-MS
IPL: Intact polar lipid

J-K-L-M-N-O

MeOH: Methanol
MgDVP: Mg -2,4-divinyl phaeoporphyrin a₅ monomethyl ester
MSD: Mass selective detector
m/z: Mass-to-charge ratio
N.b.: *Nota bene* (note well)
NCBI: National center for biotechnology information
OH-FA: Hydroxy fatty acid
OL: Ornithine lipid
OM: Organic matter
OSC: Organic sulfur compound

P-Q

PAGE-TBE: polyacrylamide gel electrophoresis-Tris-borate-EDTA
PC-DAG: Phosphatidylcholine with DAG
PCR: Polymerase chain reaction
PE-DAG: Phosphatidylethanolamine with DAG
PG-DAG: Phosphatidylglycerol with DAG
PLFA: Phospho-lipid fatty-acid
Ph: Phytane
Pr: Pristane
PSB: Purple sulfur bacteria
PST: Phosphate specific transport
PSU: Practical salinity unit
PUFA: Polyunsaturated fatty acid
PZE: Photic zone euxinia

Abbreviations

R-S-T

REDOX : Reduction /oxidation

RIP: Raman index of preservation

RNA: Ribonucleic acid

SI: Saturation index

SQ-DAG: Sulfoquinovosyldiacylglycerol

SRB: Sulfate-reducing bacteria

T°: Temperature

TCA: Tricarboxylic acid

TLE: Total lipid extract

TOC: Total organic carbon

TFS-WP : Thermo Fisher Scientific – Water Parameter

U-V-W-X-Y-Z

UV: Ultra-violet

VSMOW: Vienna standard mean ocean water

VPDB: Vienna Pee Dee Belemnite

WA: Western Australia

WHWL: Winter high water level

WP: Water parameters

Table of Contents

Declaration.....	ii
Abstract.....	iii
Acknowledgements	xi
Primary Publications	xiv
Statement of Contribution of Others	xvi
Secondary Publications	xix
Abbreviations.....	xxii
Table of contents	xxv
Table of figures	xxxiv
Table of tables	xli

Table of Contents

Introduction and Overview.....	3
Early-life and stromatolites	3
Modern microbial mats	7
• Microbial communities: Characterisation and organisation	7
➤ <i>Light gradient</i>	7
➤ <i>Chemical gradients</i>	8
➤ <i>Organisation of microbial communities and mat formation</i>	8
• Study site: Shark Bay	11
• Types of microbial mats in Shark Bay	12
Characterisation of microbial communities	15
• Significance of biomarkers	15
➤ <i>Diagenesis and preservation of biosignatures</i>	18
➤ <i>Aliphatic hydrocarbons in microbial mat settings</i>	19
✓ Common organic geochemical analytical methods	21
➤ <i>Phospho-lipid fatty acids (PLFAs) in microbial mat settings</i>	22
➤ <i>Intact Polar Lipids (IPLs)</i>	24
➤ <i>Lipophilic pigments</i>	26
• Significance of stable isotopes in organic geochemistry	27
➤ <i>Isotopic fractionation</i>	27
➤ <i>Notation, standards and instrumentation</i>	28
➤ <i>Bulk stable isotope analysis (BSIA)</i>	29
✓ Methods and instrumentation	30
➤ <i>Compound specific stable isotope analysis (CSIA)</i>	31
✓ Methods and instrumentation	31
➤ <i>Significance of $\delta^{13}\text{C}$ analysis</i>	32
Study of biogeochemical cycling.....	34
• Complex biogeochemical cycling in microbial mats.....	34
➤ <i>Carbon and oxygen cycles in microbial mats</i>	35
➤ <i>Iron and sulfur cycles in microbial mats</i>	36
➤ <i>Nitrogen cycle in microbial mats</i>	38
• Diffusional Equilibration in Thin-films (DET) and Diffusional Gradient in Thin-films (DGT) samplers	41
➤ <i>Heterogeneity in microbial mats</i>	41
➤ <i>Description of DET technique</i>	42
➤ <i>Description of DGT technique</i>	43
➤ <i>DET and DGT deployments in sediment</i>	44
Aims of the thesis	46
References	48

Table of Contents

Chapter 2: Characterising microbial communities and processes in a modern stromatolite (Shark Bay) using lipid biomarkers and two-dimensional distributions of porewater solutes.

Chapter 2	69
Abstract	69
Introduction	70
Materials and Methods	73
• Sampling site.....	73
• Sample description	74
• DET/DGT probes	74
➤ <i>Preparation of DGT and DET gels and assembly of combined DET-DGT probes</i>	74
➤ <i>Deployment of combined DET-DGT probes</i>	75
➤ <i>Analysis of sulfide and alkalinity co-distributions</i>	76
➤ <i>Analysis of iron(II)-phosphate and co-distributions</i>	76
• Lipid biomarkers	77
➤ <i>Sampling</i>	77
➤ <i>Extraction</i>	77
➤ <i>Column chromatography</i>	77
➤ <i>Phospho-Lipid Fatty Acids (PFLAs)</i>	78
➤ <i>Gas-Chromatography Mass-Spectrometry (GC-MS)</i>	78
Results and Discussion	79
• Two-dimensional distributions of solutes indicative of microbial activity	79
➤ <i>Co-distribution of alkalinity and sulfide</i>	79
➤ <i>Co-distribution of phosphate and iron(II)</i>	85
• Lipid biomarkers	87
➤ <i>Hydrocarbons</i>	87
➤ <i>Phospho-lipid fatty acids (PLFAs)</i>	92
• Microbial communities and biogeochemical cycles.....	95
Conclusions	96
References	98

Table of Contents

Chapter 3: Diel fluctuations in solute distributions and biogeochemical cycles in hypersaline microbial mats from Shark Bay, Western Australia.

Chapter 3	109
Abstract	111
Introduction	111
Materials and Methods	111
• Site and sample descriptions	113
• Microelectrode profiles of oxygen, sulfide and pH.....	113
• 2D mapping of sulfate-reducing activity using $^{35}\text{SO}_4^{2-}$ -labelled silver foils	116
• Preparation of DGT and DET gels, and assembly of combined DET-DGT probes	116
• Deployment of combined DET-DGT probes.....	117
• Analysis of Fe(II), phosphate and sulfide co-distributions	118
• Analysis of alkalinity distributions.....	119
Results and discussion	119
• Microelectrode profiles of oxygen and sulfide	119
• Small scale two-dimensional heterogeneity in sulfide, iron(II) and phosphate distributions.....	120
• Biogeochemical changes over a diel cycle	127
• Alkalinity measurements and the carbonate cycle	136
Conclusions	138
References	140
Appendix	147

Table of Contents

Chapter 4: Organic geochemical studies of modern microbial mats from Shark Bay – Part I. Influence of depth and salinity on lipid biomarkers and isotopic signatures.

Chapter 4.....	152
Abstract.....	153
Introduction	153
Materials and methods	154
• Sampling sites along salinity gradient	156
• Description of microbial mats along depth gradient.....	158
• Lipid laboratory preparation	159
➤ <i>Sampling</i>	159
➤ <i>Extraction</i>	159
➤ <i>Column chromatography</i>	160
• Identification and isotopic characterisation of lipid biomarkers	161
➤ <i>Gas-Chromatography Mass-Spectrometry (GC-MS)</i>	161
➤ <i>GC- Isotope Ratio Mass Spectrometry (GC-iRMS)</i>	162
• Bulk parameters	163
➤ <i>Sample preparation</i>	163
➤ <i>Measurements</i>	163
• Water parameters.....	164
Results	165
• Depth gradient.....	165
➤ <i>Bulk parameters</i>	165
➤ <i>Aliphatic hydrocarbons and their carbon isotopic compositions</i>	166
➤ <i>Phospho-lipid fatty acids (PLFAs) and their carbon isotopic compositions</i>	168
• Salinity gradient	170
➤ <i>Bulk parameters</i>	170
➤ <i>Aliphatic hydrocarbons</i>	171
➤ <i>Phospho-lipid fatty acids</i>	173
Discussion.....	175
• Nilemah mats of different depth.....	175
➤ <i>Common features of all microbial mats</i>	175
➤ <i>Changes along the Nilemah littoral gradient</i>	178
• Salinity gradient	182
• Implications for paleoenvironmental applications	182
Conclusions	186
References	187

Table of Contents

Chapter 5: Organic geochemical studies of modern microbial mats from Shark Bay – Part II. Influence of depth and salinity on intact polar lipids and lipophilic pigment distributions.

Chapter 5.....	198
Abstract.....	199
Introduction	200
Materials and Methods	201
• Sampling sites	201
• Description of microbial mats.....	201
• Lipid biomarkers	202
➤ <i>Sampling.....</i>	202
➤ <i>Intact polar lipid (IPL) extraction.....</i>	202
➤ <i>Analysis of intact polar lipids by high performance liquid chromatography–mass spectrometry (HPLC-MS).....</i>	202
➤ <i>Pigment extraction.....</i>	202
➤ <i>Analysis of pigments by HPLC</i>	203
Results	204
• Depth gradient.....	204
➤ <i>Intact polar lipids (IPLs).....</i>	204
➤ <i>Lipophilic pigments.....</i>	207
• Salinity gradient	209
➤ <i>Intact polar lipids (IPLs).....</i>	209
➤ <i>Lipophilic pigments.....</i>	211
Discussion.....	212
• Depth gradient.....	212
➤ <i>Common features for all mats.....</i>	212
➤ <i>Changes along the littoral gradient.....</i>	213
➤ <i>Changes in Hamelin Pool microbial mat communities through time.....</i>	215
• Salinity gradient	220
Conclusions	222
References	224

Table of Contents

Chapter 6: Keeping the smell down: Microbial environment and community diversity in a modern stromatolite from Shark Bay, Western Australia.

Chapter 6	231
Abstract	231
Introduction	232
Methods	233
• Sampling site.....	233
• Sample description	234
• Biogeochemical methods: DGT and DET samplers.....	234
• Molecular phylogenetic methods	235
• Organic Geochemical Methods	237
➤ <i>Sampling</i>	237
➤ <i>Extraction</i>	237
➤ <i>Column chromatography</i>	237
➤ <i>Phospho-lipid fatty acids (PFLAs)</i>	238
➤ <i>Cleavage of C-S bonds by Raney nickel</i>	238
➤ <i>Gas-Chromatography Mass-Spectrometry (GC-MS)</i>	238
➤ <i>GC-multiple reaction monitoring-MS (GC-MRM-MS)</i>	239
➤ <i>GC- Isotope-Ratio Mass-Spectrometry (GC-iRMS)</i>	239
➤ <i>Measurement of $\delta^{13}C$ of bulk carbonate</i>	240
Results and discussion	240
• Porewater chemistry: co-distributions of iron(II) and sulfide.....	240
• Microbial diversity of the smooth mat.....	243
• Lipid biomarkers	246
➤ <i>Aliphatic hydrocarbons</i>	246
➤ <i>Compound-specific carbon isotopic signatures of hydrocarbons</i>	249
➤ <i>Phospho-lipid fatty acids (PLFAs)</i>	250
• Significance of sulfur in the modern stromatolite	252
Conclusions	256
References	258

Table of Contents

Chapter 7: Investigation of biomarker distributions in a Paleoproterozoic microbial mat from the Turee Creek group, Pilbara, Western Australia.

Chapter 7	269
Abstract	270
Introduction	270
Geology and methods	271
• Geological context.....	271
• Sample description	271
Organic geochemical analysis	272
➤ <i>Sampling</i>	272
➤ <i>Extraction</i>	273
➤ <i>Column chromatography</i>	273
➤ <i>HydroPyrolysis (HyPy)</i>	273
➤ <i>Carbonate dissolution</i>	274
➤ <i>Analysis of samples by Gas Chromatography – Mass Spectrometry</i>	275
➤ <i>Procedure followed for the analysis of the samples</i>	275
Results	277
• Free saturated and alcohol hydrocarbons.....	277
• Saturated hydrocarbons after HyPy on kerogen.....	278
• Carbonate-bound saturated and alcohol hydrocarbons	281
• Saturated hydrocarbons after HyPy on carbonate-free kerogen.....	282
Discussion	283
• Diagenetic features of carbonate	284
• Raman spectroscopy analysis of the microbial mat.....	285
• Comparison with two additional samples from the Turee Creek group	287
• HyPy technique evaluation	288
Conclusions	289
References	290

Table of Contents

Conclusions and outlook	293
Biogeochemical cycles in modern microbial mats.....	294
Influence of abiotic conditions on microbial mats communities.....	296
Rapid turnover in microbial communities	298
Preservation pathway of biosignatures in microbialites	299
Future perspectives	300
Bibliography	301
Appendix.....	338

Table of Figures

Chapter 1

Figure 1.1: Large domical to coniform stromatolites from the Tumbiana Formation, Fortescue Group (Bolhar and Van Kranendonk, 2007).	4
Figure 1.2: Geological timescale with important biological events, and observations of well-preserved Precambrian biomarkers and crude oil (modified from Brocks and Summons, 2003).	6
Figure 1.3: Schematic of a laminated microbial mat organisation and biogeochemical gradients (modified from (Navarrete, 1999).	10
Figure 1.4: Model of microbial mat formation (Dupraz et al., 2011) (a) Typical diffusion of O ₂ through the water-sediment interface in the absence of microbial activity. (b) Cyanobacteria colonize the sediment, fixing (reduce) CO ₂ to form biomass using solar energy (photosynthesis) and using water as an electron donor. O ₂ is a product (visible in the upper millimeter of the depth profile). (c) The autotrophically-produced organic matter is degraded by aerobic heterotrophs (aerobic respiration) using O ₂ as final electron acceptor. The consumption of oxygen results in, or is reflected by, a sharper O ₂ gradient in the sediment (arrows) and the formation of an anoxic zone below the active cyanobacterial layer. (d). Anaerobic heterotrophs then develop in the anoxic zone (mostly SRB in this example). (e) SRB produce sulfide compounds, which can then feed anoxygenic photosynthesis and aerobic sulfide oxidation. (f) Examples of a hypersaline mat from the Bahamas showing classical zonation of bacterial guilds.	10
Figure 1.5: Map of Shark Bay with the locations of Nilemah, Garden Point and Rocky Point highlighted (modified from Jahnert and Collins, 2013).	12
Figure 1.6: Sky view of Nilemah embayment showing the location of the different types of mats studied along the tidal flat. (Google Earth image).	13
Figure 1.7: Distribution along the littoral gradient and internal/external fabrics of the different types of microbial mats in Nilemah (modified from Jahnert and Collins, 2013).	13
Figure 1.8: Dominant microbial species present in the different types of mats from Nilemah (Jahnert and Collins, 2013).	15
Figure 1.9: The Universal Phylogenetic Tree annotated with examples of diagnostic biomarkers for some taxonomic groups (modified from Brocks and Summons, 2003).	17
Figure 1.10: Flowchart of analytical steps applied to the modern microbial mats. DCM = Dichloromethane, MeOH: Methanol, GC-irMS = gas chromatography-isotope ratio mass spectrometry; GC-MS = gas chromatography-mass spectrometry; Ra-Ni: Raney-Nickel; BSIA = bulk stable isotope analysis, EA = elemental analysis.	22
Figure 1.11: Carbon and oxygen cycling in microbial mats during daytime and night time (modified from Canfield and Des Marais, 1993).	36
Figure 1.12: Sulfide and iron(II) interactions in microbial mats during daytime and night time (modified from Wieland et al., 2003).	38
Figure 1.13: Key processes involved in the nitrogen cycle (Herbert, 1999).	39

Table of Figures

Figure 1.14: Nitrogen cycling in marine sediments (modified from Herbert, 1999).	40
Figure 1.15: Schematic of a DGT/DET sampler.	43
Figure 1.16: Cross-section through a DGT sampler in sediment. Concentration gradients are shown for three cases: a) sustained, b) unsustained and c) partially sustained (Zhang et al., 2002). ...	44

Appendix 1

Figure A 1.1: Structure referred to in the text.	67
--	----

Chapter 2

Figure 2.1: Two-dimensional distributions of sulfide and alkalinity from DGT and DET samplers in the mat during day and night. The white lines represent the entire mat. The black dotted lines represent the limits between the first, second and third layers. The region above the top white line represents the water and the area underneath the deeper white line represents the sediment.	80
Figure 2.2: Two-dimensional distributions of phosphate and iron(II) from DET samplers in the mat during day and night. The white lines represent the entire mat. The black dotted lines represent the limits between the first, second and third layers. The region above the top white line represents the water and the area underneath the line represents the sediment.	85
Figure 2.3: Total ion chromatograms from gas chromatography-mass spectrometry (GC-MS) analysis of the aliphatic hydrocarbon fractions from layers 1-3 of the smooth mat.	89
Figure 2.4: M/z 85 fragmentogram from GC-MS analysis of the aliphatic hydrocarbon fractions from layers 1-3 of the smooth mat.	90
Figure 2.5: Lipid biomarker distribution over depth: (A) aliphatic hydrocarbons (short-chain/ C_{16} - C_{22} n -alkanes, long-chain/ C_{27} - C_{33} n -alkanes, hopanoids, steroids); (B) short C_{16} - C_{22} and long C_{27} - C_{33} chain n -alkanes and highly branched isoprenoids (phytane, phytene and phytadiene isomers); (C) hopanoids (C_{27} $\beta\beta$ hopane, C_{29} $\beta\beta$ hopane, C_{30} $\beta\beta$ hopane, C_{31} $\beta\beta$ hopane, diploptene, C_{31} hopene); (D) steroids (C_{27} sterene, C_{28} sterene, C_{29} sterene).	92

Chapter 3

Figure 3.1: Photographs of A, View of Nilemah, Shark Bay. The smooth mats are located close to the waterline. B, a smooth microbial mat. C, a sample of the smooth mat showing the characteristic vertical layering in cross-section. D, a close-up view of the smooth microbial mat.	114
Figure 3.2: Representative oxygen and sulfide profiles measured with microelectrodes in the layered microbial mat during light ($I = 1982 \mu\text{E}\cdot\text{m}^{-2}\cdot\text{s}^{-1}$) and dark deployments ($I = 0 \mu\text{E}\cdot\text{m}^{-2}\cdot\text{s}^{-1}$). The yellow layer represents the first layer of the mat, the green layer represents the second layer characteristic of cyanobacteria and the grey layer represents the deepest part of the mat.	120

Table of Figures

- Figure 3.3:** Two-dimensional distributions of sulfide measured by five DGT probes in the microbial mat during light and dark deployments. The width of all gels is 14 mm. The white dotted line represents the mat surface. 124
- Figure 3.4:** Two-dimensional co-distributions of sulfide, iron(II) and phosphate measured in the layered microbial mat by combined DGT/DET probes during light (probe B) and dark (probe I) deployments. The width of all gels is 14 mm. The white dotted line represents the mat surface..... 127
- Figure 3.5:** Mean depth profiles of sulfide, iron(II) and phosphate concentrations during light and dark deployments. Error bars indicate the standard error of the mean (n=5). The yellow layer represents the first layer of the mat, the green layer represents the second layer characteristic of cyanobacteria and the grey layer represents the deepest part of the mat. 128
- Figure 3.6:** Visualisation of sulfide heterogeneity at the mat-water interface in probe G using a smaller concentration scale (0 to 100 μM). The white dotted line represents the mat-water interface. 130
- Figure 3.7:** 2D distribution of sulfate reducing activity in a smooth mat from Nilemah measured in April 2012; density and size of black and grey pixels indicate locations and relative degree of sulphate reducing activity. Darker pixels represent higher levels of sulfate-reducing activity. The size of the pixel indicates the approximate true size of the sulfate-reducing activity (see text and Visscher et al. 2000). The numbers on the right side (1-4) indicate the layer's number (1 = tan surface layer; 2 = green cyanobacterial layer; 3 = thin layer of purple sulfur bacteria (not always present in smooth mats); 4 = black layer of FeS. 132
- Figure 3.8:** Mean depth profiles of alkalinity concentrations during light and dark deployments. Error bars indicate the standard error of the mean (n=5). The yellow layer represents the first layer of the mat, the green layer represents the second layer characteristic of cyanobacteria and the grey layer represents the deepest part of the mat. 138

Appendix 3

- Figure A 3.1:** Two-dimensional distributions of iron(II) measured by five DET probes in the layered microbial mat during light and dark deployments. The white dotted line represents the mat surface. The region above the top white line represents the water. The width of all gels was 14 mm..... 138
- Figure A 3.2:** Two-dimensional distributions of phosphate measured by five DET probes in the layered microbial mat during light and dark deployments. The white dotted line represents the mat surface. The region above the top white line represents the water. The width of all gels was 14 mm. No data was available for the small white areas on probes C and F due to physical damage..... 138

Table of Figures

Figure A 3.3: Two-dimensional distributions of alkalinity measured by five DET probes in the layered microbial mat during light and dark deployments. The white dotted line represents the mat surface. The region above the top white line represents the water. The width of all gels was 14 mm. 138

Chapter 4

Figure 4.1: Google Earth image of Shark Bay showing the location of investigated tidal flats (Nilemah, Garden Point and Rocky Point) and photographs of the microbial mats investigated along the Nilemah S3 tidal flat gradient. The pustular mat was the shallowest mat (0.20-0.80m, D1), followed by the smooth mat (0.80-1.20m, D2), the colloform mat (1-1.50m, D3) and the microbial pavement that was the deepest structure (2-6m, D4). Rocky Point presented the lowest salinity (40psu, S1), Garden Point an intermediate salinity (54psu, S2) and Nilemah the highest salinity (64psu, S3)..... 157

Figure 4.2: A) % carbon and C:N ratios and B) $\delta^{13}\text{C}$ and $\delta^{15}\text{N}$ of the total biomass in the different microbial mats from Nilemah..... 165

Figure 4.3: Total ion chromatograms from GC-MS analysis of the aliphatic hydrocarbon fractions of the Nilemah mats. The squares indicate cyanobacterial markers and the dashes indicate diatom markers..... 167

Figure 4.4: The $\delta^{13}\text{C}$ values of hydrocarbons of Nilemah mats at different water depths (D1-D4). The maximum standard deviation of the $\delta^{13}\text{C}$ values is $\pm 0.3\%$. The squares indicate cyanobacterial markers and the dashes indicate potential diatom markers..... 168

Figure 4.5: Histograms showing relative abundances of PLFA (%) for the different types of the Nilemah mats. Data from GC-MS analysis of PLFA fractions. The pie charts indicate the relative proportion of cyanobacterial PLFAs, sulfate-reducing bacteria PLFAs, diatom PLFAs and PLFAs from other sources for each mat. 169

Figure 4.6: $\delta^{13}\text{C}$ of PLFA, biomass and CO_2 (calculated from the DIC according to Mooke *et al.*, 1974) of the Nilemah mats. The maximum standard deviation of the $\delta^{13}\text{C}$ values is $\pm 0.4\%$. The squares indicate cyanobacterial markers and the triangles indicate potential sulfate-reducing bacteria markers. 170

Figure 4.7: A) % carbon and C: N ratios and B) $\delta^{13}\text{C}$ and $\delta^{15}\text{N}$ of the total biomass in S1, S2 and S3. 171

Figure 4.8: Total ion chromatograms from GC-MS analysis of the aliphatic hydrocarbon fractions of S1, S2 and S3. The squares indicate cyanobacterial markers and the dashes indicate diatom markers. 172

Figure 4.9: Histograms showing relative abundances of PLFA (%) for S1, S2 and S3. Data from GC-MS analysis of PLFA fractions. The pie charts indicate the relative proportion of cyanobacterial PLFAs, sulfate-reducing bacteria PLFAs, diatom PLFAs and PLFAs from other sources for each mat..... 174

Table of Figures

Figure 4.10: $\delta^{13}\text{C}$ of values of PLFA, biomass, CO_2 (calculated from the DIC according to Mook *et al.*, 1974) of S1, S2 and S3. The maximum standard deviation of the $\delta^{13}\text{C}$ values is $\pm 0.3\%$. The squares indicates cyanobacterial markers and the triangles indicate potential sulfate-reducing bacteria markers.175

Chapter 5

Figure 5.1: Bar chart representing the concentrations in IPL ($\mu\text{g.kg}^{-1}$ of TOC) in the different types of mats from Nilemah, Hamelin Pool.205

Figure 5.2: Bar chart representing the relative abundance of IPLs groups (%) in the different types of mats from Nilemah, Hamelin Pool. The arrow indicates the increase in depth.205

Figure 5.3: Bar chart representing the relative abundance of lipophilic pigments (%) in the different types of mats from Nilemah, Hamelin Pool.208

Figure 5.4: Bar chart representing the concentrations in IPL ($\mu\text{g.kg}^{-1}$ of TOC) in the smooth mats from the different Shark Bay sites.210

Figure 5.5: Bar chart representing the relative abundance of IPLs groups (%) in the smooth mats from the different Shark Bay sites. The arrow indicates the increase in salinity.210

Figure 5.6: Bar chart representing the relative abundance of lipophilic pigments (%) in the smooth mats from the different Shark Bay sites. The arrow indicates the increase in salinity.211

Figure 5.7: Bar chart representing the concentration in echineone, chl *a*, β -carotene and bac *a* in the different types of mats from Hamelin Pool from this study (blue bars) and the previous study by Palmisano *et al.* (1989) (pink bars).218

Figure 5.8: Bar chart representing the concentration in bac *a* in the smooth mats from the different Shark Bay sites.221

Chapter 6

Figure 6.1: Sampled microbial smooth mat presenting 4 distinct layers: the first a pale yellow-green layer, a second purple layer, a third dark green-brown layer and a fourth black layer.234

Figure 6.2: Two-dimensional distributions of sulfide (DGT) and iron(II) (DET) samplers in the microbial mat under daylight conditions. The white lines represent the entire mat. The region above the top white line represents the water and the area underneath the line represents the sediment. The black dotted lines represent the four different layers of the mat.241

Figure 6.3: A. Phylogenetic affiliations and proportion of groups of bacteria and archaea present in the smooth mat. B. Relative proportion of the 10 most abundant bacterial groups.244

Figure 6.4: Phylogenetic tree of the Garden Point microbial mat 16s ribosomal RNA gene sequences. The size of the nodes is directly proportional to the number of sequences observed for the given taxonomic units it represents.245

Figure 6.5: Total ion chromatograms from gas chromatography-mass spectrometry (GC-MS) analysis of the aliphatic hydrocarbon fraction of the fourth layer of the microbial mat.247

Table of Figures

Figure 6.6: Mass fragmentogram ($m/z = 85$) of the aliphatic hydrocarbon fraction of the fourth layer of the microbial mat.....	248
Figure 6.7: $\delta^{13}\text{C}$ of values of hydrocarbons from the saturate fraction of the fourth layer of the microbial mat analysed by gas chromatography – isotope ratio – mass spectrometry (GC-irMS) analysis. The maximum standard deviation of the $\delta^{13}\text{C}$ values is $\pm 0.3\%$	250
Figure 6.8: Total Ion Chromatogram and $\delta^{13}\text{C}$ values obtained from GC-MS and GC-irMS analysis of the phospho-lipid fatty acid fraction of the fourth layer of the mat. The maximum standard deviation of the $\delta^{13}\text{C}$ values was $\pm 0.3\%$	252
Figure 6.9: Total Ion Chromatogram of the sulfur-bound aliphatic hydrocarbons from the fourth layer of the smooth mat measured by GC-MS. The black dots indicate even carbon-numbered n -alkanes.....	253
Figure 6.10: Mass fragmentogram ($m/z = 191$) of the sulfur-bound aliphatic hydrocarbons from layer 3.....	254
Figure 6.11: Partial GC-MRM chromatograms ($m/z\ 217 \rightarrow 372$; $217 \rightarrow 400$). A: Steroid standard. B: sulfur-bound aliphatic fraction of layer 4.....	256
Figure 6.12: The role of sulfate-reducing bacteria in biosignature preservation. Sulfate-reducing bacteria produce H_2S that favour early diagenetic sulfurisation and preservation of organic matter under specific environmental conditions (anoxic, high sulfide and low Fe^{2+} concentrations). They also produce EPS (exo-polymeric substances) that tend to accumulate organic sulfur compounds favouring organic matter preservation and binds Ca^{2+} promoting lithification of the microbialite. Finally, bacterial sulfate-reduction raises the alkalinity favouring carbonate precipitation. Microbial mat lithification occurs if the precipitation of carbonates exceeds their dissolution by aerobic heterotrophs, sulfide oxidisers and fermenters.....	257
Chapter 7	
Figure 7.1: (A) Photography of the outcrop microbial mat and (B) photography of a fresh surface of the mat.....	272
Figure 7.2: Flow chart of the experimental procedure.....	276
Figure 7.3: Total Ion Chromatogram (TIC) of the freely extractable saturated hydrocarbons measured by Gas Chromatography-Mass Spectrometry (GC-MS).....	277
Figure 7.4: TIC of the freely extractable alcohol hydrocarbons measured by GC-MS.....	278
Figure 7.5: Mass fragmentogram ($m/z = 217$) of the saturated hydrocarbons, measured by GC-MS, after applying HyPy on the kerogen.....	279
Figure 7.6: Total Ion Chromatogram of the carbonate-bound saturated hydrocarbons measured by GC-MS.....	281
Figure 7.7: Total Ion Chromatogram of the carbonate-bound alcohol hydrocarbons measured by GC-MS.....	282
Figure 7.8: Total Ion Chromatogram of the saturated hydrocarbons, measured by GC-MS, after HyPy on carbonate-free kerogen.....	283

Table of Figures

Figure 7.9: Thin-sections showing the first phase (A) Cross-polarised light thin section view of finely laminated microbial mat with weakly radiating palisade structure in fine-grained bedded dolomite (B) Plane light thin section view of finely bedded fine-grained carbonate (black arrow) with neomorphic recrystallization of carbonate into rhombs (white arrow) (C) Plane polarised light thin section view of laminated microbial mat comprising two distinct phases: a fine-grained dark phase that defines bedding and a second, discordant phase of coarser, sparry dolomite (D) Closeup of second phase, coarse sparry carbonate cored by clear silica (macroquartz).....	285
Figure 7.10: Raman spectrographic analysis of kerogen from the sampled Turee Creek microbial mat compared with another low-grade sample from the Neoproterozoic Maddina Formation (Fortescue Group) and the spectra libraries from Schopf et al. (2010) and Wiederkehr et al. (2002) that indicate very low temperature of metamorphism ($\leq 140^{\circ}\text{C}$) and high degree of preservation, similar to that of the Paleoproterozoic Gunflint Formation.	286
Figure 7.11: Photographs of the additional studied samples from the Turee Creek group: A) a microbialite presented a “clotted” texture and B) a stromatolite.	287
Figure 7.12: Total Ion Chromatogram of the carbonate-bound saturated hydrocarbons of the stromatolite, measured by GC-MS.....	288

Table of Tables

Chapter 1

Table 1.1: Comparison of lipids from the three domains of life (modified from Itoh et al., 2001)...	18
Table 1.2: Specific PLFA for various organisms (modified from Allen, 2006).....	24
Table 1.3: Stable isotope abundances (atom %, Faure and Mensing, 2005 and references therein)..	27
Table 1.4: Day and night metabolic processes of main functional groups present in microbial mats (modified from Visscher and Stolz, 2005).	34

Chapter 2

Table 2.1: Distribution of PLFAs in the smooth mat (layers 1-3): PLFA are represented in % abundances of total PLFA.	94
Table 2.2: Two-dimensional distributions of phosphate and iron(II) from DET samplers in the mat during day and night. The white lines represent the entire mat. The black dotted lines represent the limits between the first, second and third layers. The region above the top white line represents the water and the area underneath the line represents the sediment.....	95

Appendix 3

Table A 3.1: Correlation between phosphate and iron(II) concentrations (r values) for 2D images and 1D profiles for each probe.	152
---	-----

Chapter 4

Table 4.1: Main characteristics of the three study sites.	158
Table 4.2: Main characteristics of the microbial mats sampled along the Nilemah tidal flat.....	158
Table 4.3: Carbon and nitrogen contents, molar ratios, $\delta^{13}\text{C}$ and $\delta^{15}\text{N}$ and other environmental parameters of the Nilemah mats. $\delta^{13}\text{C}_{\text{CO}_2}$ (dissolved) was calculated from $\delta^{13}\text{C}_{\text{DIC}}$ according to Mook et al., 1974. $\delta^{13}\text{C}_{\text{HCO}_3}$ ($\sim\delta^{13}\text{C}_{\text{DIC}}$) using the equations of $\delta^{13}\text{C}_{\text{CO}_2} = \varepsilon (\text{CO}_2\text{-HCO}_3) \times (1000 + \delta^{13}\text{C}_{\text{HCO}_3})/1000$ and $\varepsilon (\text{CO}_2\text{-HCO}_3) = 24.12 - 9866/T$, where T is absolute temperature and $\varepsilon (\text{CO}_2\text{-HCO}_3)$ is the fractionation between dissolved CO_2 and HCO_3	166
Table 4.4: Carbon and nitrogen contents, molar ratios, natural abundances of $^{13}\text{C}/^{12}\text{C}$ and $^{15}\text{N}/^{14}\text{N}$ and other environmental parameters for S1, S2 and S3. $\delta^{13}\text{C}_{\text{CO}_2}$ was calculated from $\delta^{13}\text{C}_{\text{DIC}}$ according to Mook <i>et al.</i> , 1974. n.m.: not measured. n.d.: not determined.	171
Table 4.5: Value of molecular proxy P_{aq} , based on relative abundance of long-chain <i>n</i> -alkanes and suggested sources for these <i>n</i> -alkanes in the Nilemah mats.	180

Table of Tables

Chapter 5

Table 5.1: Overview of IPL detected in the mats.	206
Table 5.2: Summary of pigments that could be identified with the HPLC method used in this study and their taxonomic affinities (compiled from Jeffrey et al., 1997; Leavitt and Hodgson, 2001) and relative abundances of the pigments (%) identified in the different Nilemah mats. N. B. the % of chl <i>a</i> , chl <i>a</i> epimer and chl <i>a</i> allomer were combined.....	208
Table 5.3: Comparison of lipophilic pigments identified in the different types of mats from Hamelin Pool from this study and the previous study by Palmisano et al. (1989). X indicates that the pigment was present.	217

Chapter 7

Table 7.1: Identification of steranes and sterols in the sample.....	280
---	-----

Chapter 1

Introduction and Overview



Chapter 1

Early-life stromatolites

Modern microbial mats

- Microbial communities: characterisation and organisation
 - Light gradient
 - Chemical gradients
 - Organisation of microbial communities and mat formation
- Study site: Shark Bay
- Types of microbial mats in Shark bay

Characterisation of microbial communities

- Significance of biomarkers
 - Diagenesis and preservation of biosignatures
 - Aliphatic hydrocarbons in microbial mat settings
 - ✓ Common organic geochemical analytical methods
 - Phospho-lipid fatty acids (PLFAs) in microbial mat settings
 - Intact Polar Lipids (IPLs)
 - Lipophilic pigments
- Significance of stable isotopes in organic geochemistry
 - Isotopic fractionation
 - Notation, standards and instrumentation
 - Bulk stable isotope analysis (BSIA)
 - ✓ Methods and instrumentation
 - Compound specific stable isotope analysis (CSIA)
 - ✓ Methods and instrumentation
 - Significance of $\delta^{13}\text{C}$ analysis

Study of biogeochemical cycling

- Complex biogeochemical cycling in microbial mats
 - Carbon and oxygen cycles in microbial mats
 - Iron and sulfur cycles in microbial mats
 - Nitrogen cycle in microbial mats
- Diffusional Equilibration in Thin-films (DET) and Diffusional Gradient in Thin-films (DGT) samplers
 - Heterogeneity in microbial mats
 - Description of DET technique
 - Description of DGT technique
 - DET and DGT deployments in microbial mats

Aims of the thesis

Early-life and stromatolites

Stromatolites are defined as “accretionary sedimentary structures, often thinly layered, megascopic and calcareous, produced by the activities of mat-building communities of mucilage-secreting microorganisms, mainly photoautotrophic prokaryotes” (Schopf et al., 2007). Other definitions relate to the biogenic, organosedimentary nature of stromatolites (Walter, 1976; Semikhatov et al., 1979). Stromatolites constitute some of the most widespread and easily identifiable structures of Precambrian carbonate platforms, ranging from simple domes and cones to more complex columnar structures that extend for hundreds of metres vertically and hundreds of kilometres laterally (Grotzinger and Knoll, 1999). However, the presence of microfossils and palimpsest microstructures in stromatolites is extremely rare as these originally calcareous structures undertook diagenetic changes that affected mat-building communities (Grotzinger and Knoll, 1999). Grotzinger and Knoll (1999) stated that “it is probably conservative to estimate that even less than 1 % of all stromatolites ever described have a fossilised microbiota associated with them”.

However, studies on Proterozoic cherty stromatolites that unequivocally presented microfossils revealed that the structures of Archean stromatolites were striking similar to biogenic Proterozoic stromatolites (Mendelson and Schopf, 1992; Schopf, 1999; Knoll, 2003; Schopf et al., 2005). Ancient stromatolitic structures have been observed, for instance, in the Transvaal Supergroup, South Africa (~2560 Myr), the Fortescue group, Western Australia (~2723 Myr) (Figure 1.1), the Steeprock group, Canada (~2800 Myr) and the Insuzi group, South Africa (~2985 Myr). The oldest known stromatolites were reported in the 3430 Myr Strelley Pool Chert (SPC) (Pilbara Craton, Australia) (Allwood et al., 2006). An abiogenic origin was affirmed for the formation of these stromatolites. In addition, patterns in their structural diversity, complexity and environmental associations implied the existence of organisms at this time (Allwood et al., 2006).

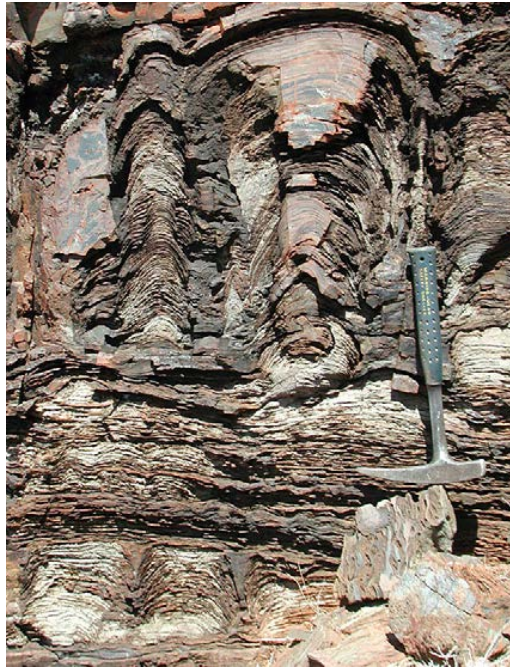


Figure 1.1: Large domical to coniform stromatolites from the Tumbiana Formation, Fortescue Group (Bolhar and Van Kranendonk, 2007).

Stromatolites are dominant structures in the rock record up to 600 Myr (Awramik, 1984) implying that benthic microbial communities were flourishing and played a crucial role in Earth's evolution. Hoehler et al. (2001) reported that photosynthetic organisms in modern microbial mats produce H_2 and CO-gases as well as CH_4 . The authors suggested that fluxes of such gases would have been dominant during times when stromatolites strongly contributed to biological productivity (Walter, 1976). In addition, fluxes of H_2 from these microbial systems most likely played a crucial role in oceans and oxidation of the atmosphere (Hoehler et al., 2001).

These major changes in environmental conditions contributed to the evolution of the biosphere and the apparition of eukaryotes during the Proterozoic (Knoll et al., 2006) (Figure 1.2). Molecular fossils were used to investigate the rise of eukaryotes and steroids, lipid biomarkers of eukaryotic organisms (Volkman, 1986), were found in the 2700 Ma shales from the Pilbara Craton, Western Australia (Brocks et al., 1999). However, Rasmussen et al. (2008) disputed the origin of the biomarkers and reassessed the oldest eukaryotic origin to 1780-1680

Myr (Knoll et al., 2006). Nonetheless, steroids were also identified in Huronian oil-bearing fluid inclusions (2450-2200 Myr) suggesting the existence of eukaryotes at this period (Dutkiewicz et al., 2006).

Of all biogenic carbonates, microbial carbonates are the most common facies and have the longest geological history (Riding, 2000). They represent the most conspicuous trace of life during the Precambrian (Riding, 2000). Yet, the lack of microfossils or biomarkers during this period of life emergence makes the study of early microbial assemblages highly challenging and prone to scrutiny. In addition, little is known about the biogeochemical processes and preservation pathways of these ancient microbial macrostructures and their associated biosignatures (Semikhatov et al., 1979; Grotzinger and Knoll, 1999). Archean stromatolites only rarely show close structural similarities with modern lithifying microbial mats (Grotzinger and Knoll, 1999; Riding, 2000; Flannery and Walter, 2011). Modern microbial mats, including laminated lithifying smooth mats have been reported in the World Heritage listed Shark Bay, Western Australia (Jahnert and Collins, 2012; 2013) and have been described as modern analogues of their ancient ancestors (Logan, 1961). Consequently, these modern microbial mats might provide a better understanding of the evolution and community organisation of these microbial structures. Studies of modern microbial mats and their preservation pathway are critically important for discerning early microbial assemblages, complex and dynamic biogeochemical cycles and the true nature of macroscopic biosignatures.

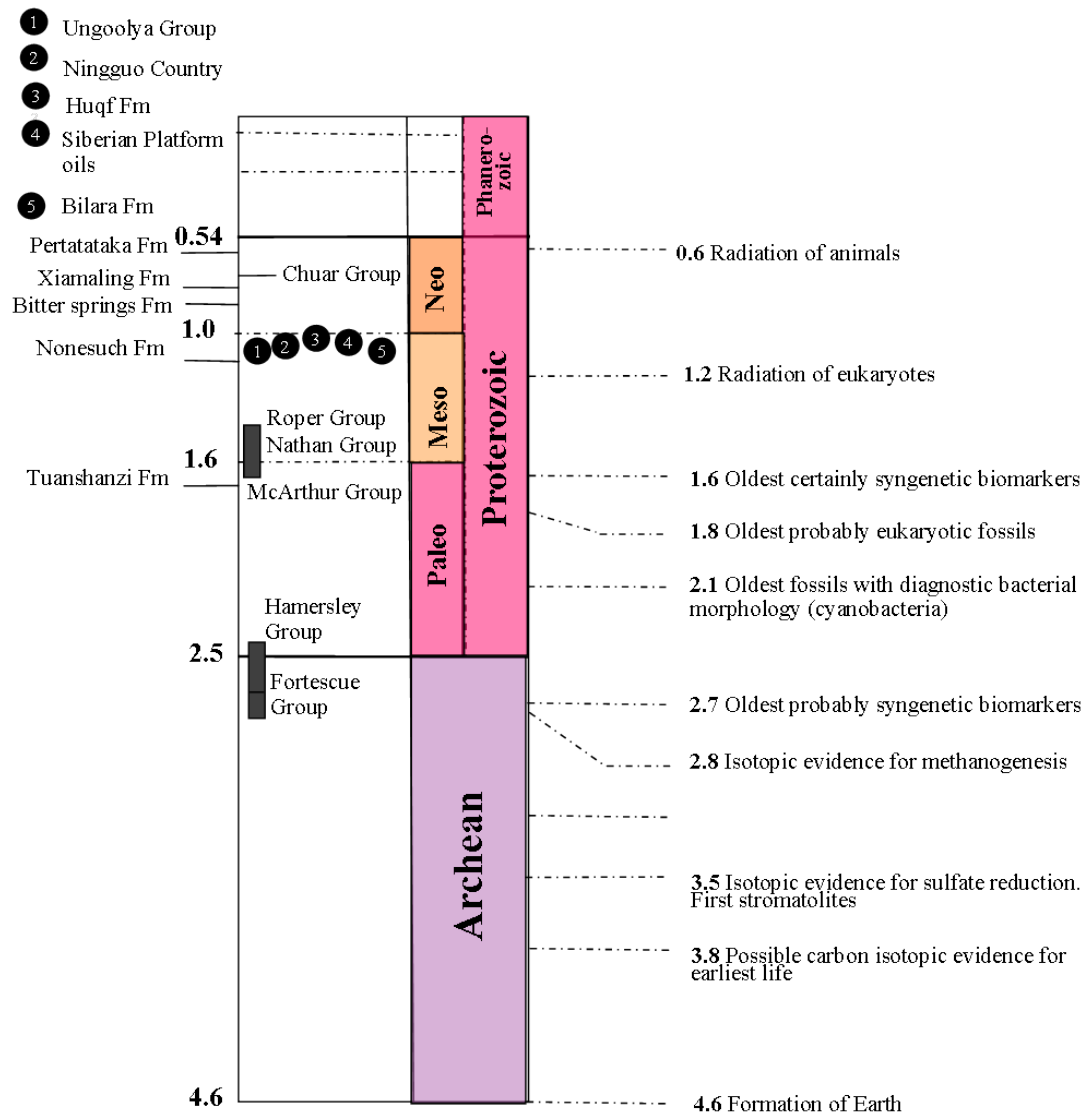


Figure 1.2: Geological timescale with important biological events, and observations of well-preserved Precambrian biomarkers and crude oil (modified from Brocks and Summons, 2003).

Modern microbial mats

- **Microbial communities: Characterisation and organisation**

Modern microbial mats are the macroscopic assemblage of complex microbial communities in which the primary production is usually dominated by photoautotrophic microorganisms (Atlas and Bartha, 1998). In laminated microbial mats, microbial communities orient themselves vertically along microscale chemical, physical gradients and potential electron donors and acceptors in order to optimise biogeochemical processes (van Gemerden, 1993). This results in a vertical distribution of main functional groups visible to the naked eye as distinct coloured layers within the mats. Microbes interact to change the oxidation states of C, N, O, S (Canfield and Des Marais, 1991) and diurnal changes in the light environment drive shifts in the dominant biogeochemical processes (Jørgensen and Des Marais, 1988).

➤ *Light gradient*

The light flux reaching the surface of the mat can be measured both as downward irradiance (the total down-welling light that passes through a horizontal plane) and as scalar irradiance (the sum of all light that converges upon a given point within the mat) (Des Marais, 2003). Because of high abundance of photosynthetic organisms, bacterial mucilage and minerals in mats, light absorption occurs mainly through the activity of light-harvesting pigments of the photoautotrophic bacteria. As absorption and scattering of light are required within the mat, scalar irradiance can significantly vary from downward irradiance (Jørgensen and Des Marais, 1988). Previous studies reported that mat matrix can substantially influence the penetration of light at depth and the microbial community distribution (Jørgensen et al., 1987). For instance, cyanobacteria-dominated mats that utilise light that has been filtered by overlying diatoms exhibit the highest photosynthetic rates at wavelengths between 550 and 650 nm (Jørgensen et al., 1987), a region that lies between the absorption maxima of chlorophyll *a*. However, planktonic cyanobacteria exposed to a larger spectrum of light show important activity at wavelengths that match with the absorption maxima of chlorophyll *a* (Jørgensen and Des Marais, 1988). Light is required for

photosynthetic activity and the light gradient clearly affects the distribution of microbial mats (Des Marais, 2003). Nonetheless, UV radiations can have a negative impact on microbial communities potentially causing inhibition of primary productivity.

➤ *Chemical gradients*

The significant photosynthetic activity that takes place in the daytime photic zone of the mat generates steep and variable gradients in pH, oxygen and sulfide concentrations (Revsbech et al., 1983). Cyanobacteria and anoxygenic photoautotrophs perform photosynthesis that generates organic matter beneficial to other microbial communities. However, the associated production of oxygen can inhibit anaerobic processes and favours chemoautotrophic and chemical oxidations of reduced species (van Gemerden, 1993). Thus, the oxic area of the mat demonstrates a dynamic balance between O₂ production (photosynthesis) and O₂ consumption (respiration) by heterotrophic bacteria and sulfide oxidisers. Conversely, under dark conditions, as oxygen concentrations are rapidly depleted in the absence of photosynthesis, the oxic-anoxic boundary rapidly moves towards the upper mat layer and heterotrophic anaerobic processes dominate. These process shifts result in steep and fluctuating chemical gradients (De Wit and Van Gemerden, 1988; De Wit et al., 1989) that are expected to influence iron(II) and nutrient distributions as well as the precipitation/dissolution of carbonates.

➤ *Organisation of microbial communities and mat formation*

Four groups of microorganisms are dominant in microbial mats: oxygenic cyanobacteria, colorless sulfur oxidisers, purple sulfur bacteria and SRB (Figure 1.3). The cyanobacteria represent the first microbial community colonizing the sediment and which start to build the microbial mats (Figure 1.4). Aerobic heterotrophs are also of high importance since they degrade the organic carbon produced by cyanobacteria using O₂ as an electron acceptor (Figure 1.3) and favour the presence of SRB in the mat as their activity generates oxygen depletion deeper in the mat. Fermentative microorganisms produce growth substrates for SRB. Strict anaerobic SRB are found in the anoxic layers of the mat but some oxygen-tolerant

SRB can live closer to the mat surface. Sulfate-reduction is a key respiratory pathway (anaerobic respiration) (Canfield and Des Marais, 1993) using sulfate as the terminal electron acceptor and leading to the production of sulfide (Table 1.4). The production of sulfide by SRB feeds aerobic sulfide oxidation and anoxygenic photosynthesis. Less abundant groups include nitrifying and denitrifying bacteria, and methanogenic bacteria (van Gemerden, 1993).

In more complex microbial mats, a green layer characteristic of green sulfur bacteria (GSB) can be observed under the layer of purple sulfur bacteria (Nicholson et al., 1987) (Figure 1.3; Figure 1.4). GSB include green and brown pigmented sulfur-bacteria (*Chlorobiaceae*) which are obligate anaerobic phototrophs fixing CO₂ via anoxygenic photosynthesis and utilising H₂S produced by SRB as an electron donor (Table 1.4). As a consequence of their high oxygen sensitivity, these microorganisms are exclusively found in the photic and anoxic zone of the mat. These organisms also make specific bacteriochlorophylls and secondary pigment carotenoids for photosynthesis.

The presence of a green layer underneath the purple sulfur bacteria does not necessarily demonstrate the presence of GSB as ‘inverted mats’ have been observed where the purple sulfur bacteria form the top layer and the cyanobacteria occur beneath them (van Gemerden et al., 1989). In some microbial mats, a black layer containing insoluble iron sulfide (FeS) has also been observed as sulfide can subsequently react with ferrous iron (Fe²⁺) to produce FeS in the anoxic regions of the mat (Stal, 2001).

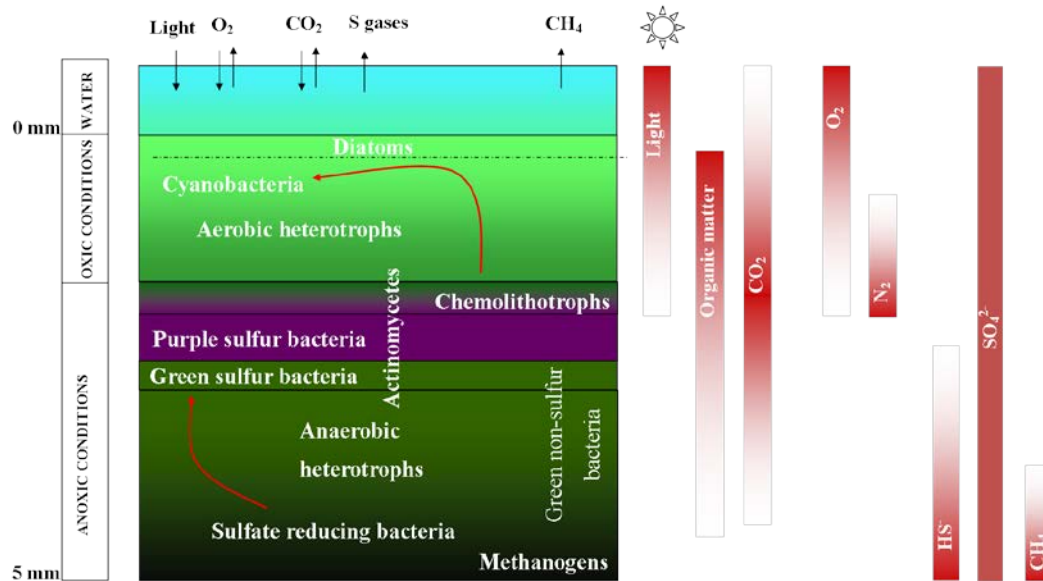


Figure 1.3: Schematic of a laminated microbial mat organisation and biogeochemical gradients (modified from (Navarrete, 1999)).

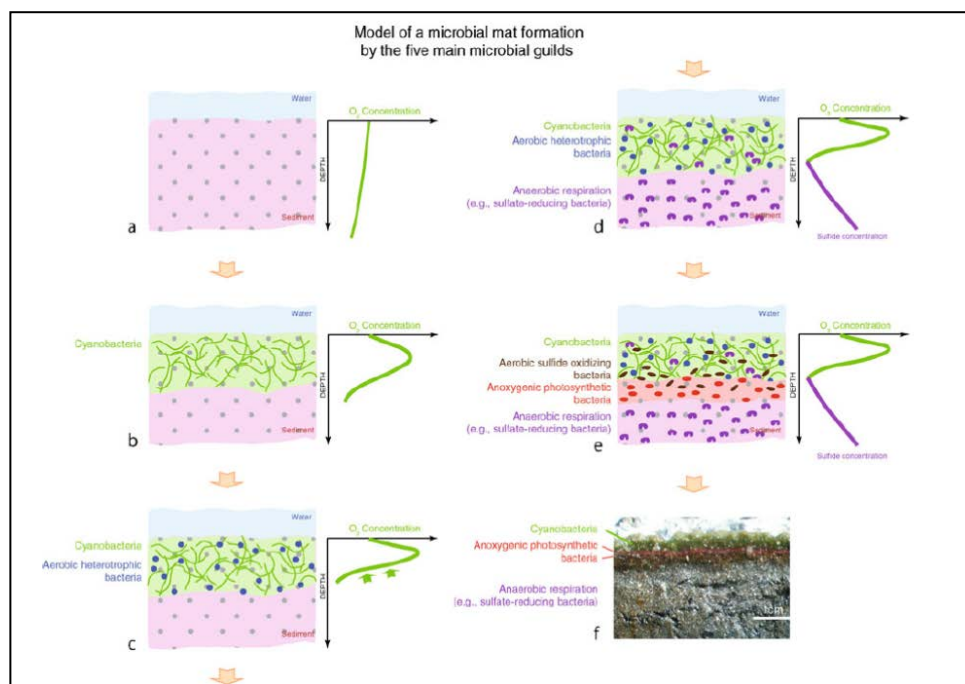


Figure 1.4: Model of microbial mat formation (Dupraz et al., 2011) (a) Typical diffusion of O_2 through the water-sediment interface in the absence of microbial activity. (b) Cyanobacteria colonize the sediment, fixing (reduce) CO_2 to form biomass using solar energy (photosynthesis) and using water as an electron donor. O_2 is a product (visible in the upper millimeter of the depth profile). (c) The autotrophically-produced organic matter is degraded by aerobic heterotrophs (aerobic respiration) using O_2 as final electron acceptor. The consumption of oxygen results in, or is reflected by, a sharper O_2 gradient in the sediment (arrows) and the formation of an anoxic zone below the active cyanobacterial layer. (d) Anaerobic heterotrophs then develop in the anoxic zone (mostly SRB in this example). (e) SRB produce sulfide compounds, which can then feed anoxygenic photosynthesis and aerobic sulfide oxidation. (f) Examples of a hypersaline mat from the Bahamas showing classical zonation of bacterial guilds.

- **Study site: Shark Bay**

Shark Bay is located in Western Australia, about 800 km north of Perth. Three sites were investigated in Shark Bay during this study: Nilemah, Garden Point and Rocky Point (Figure 1.5). In Nilemah, the water is hypersaline because of limited rainfall and intense evaporation (Logan and Cebulski, 1970) and the pH ranges between 7.5 and 8.4 (Jahnert and Collins, 2013). Microbial mats were sampled along the tidal flat of Nilemah which is located on the southern area of Hamelin Pool (S 26°25.5' E 114°3.5'). Hamelin Pool is the easterly embayment of this semi-enclosed shallow (<10 m) area and extends up to 1400 km². Hence, the pools' volume is relatively small ~7 km³, favouring high rates of evaporation. The Hamelin Pool water is evaporated on average ~23% in relation to the open ocean. This evaporative loss is compensated by an inflow through the shallow Faure Sill. Consequently, 70–200% of the pools' volume is replaced every year because of combined tidal fluctuation and evaporation losses (Price et al., 2012). The water is oligotrophic and phosphorus is the limiting nutrient while requirements in nitrogen are met by cyanobacterial nitrogen fixation (Smith and Atkinson, 1983). As the beach ridges of Hamelin Pool are dominated by the Hamelin Coquina barrier which formed through the accretion of a high abundance of bivalve shell, the seawater is supersaturated in calcium carbonate (Jahnert and Collins, 2012). Microbial mats cover 300 km² of the area (Jahnert and Collins, 2012). Microbial community organisation in these mats strongly depends on physical and chemical parameters such as salinity, alkalinity, light intensity, depth, waves and wind intensity (Logan, 1974).

Garden Point is a re-entrant located on the eastern area of Henry Freycinet embayment, located on the western part of Shark Bay (see Jahnert and Collins, 2013 for detailed maps). In this area, metahaline calm waters favour the formation of coarse stratified microbial mats. The pH ranges between 7.8 and 8.7 in this area (Jahnert and Collins, 2013). Rocky Point, located on the western side of L'Haridon Bight, is a tidal flat covering 8 km². The water inflow in this area is highly restricted, favouring microbial growth. The formation of microbial deposits in this area occurred before the formation of microbial mats in Garden Point. Rocky Point presents metahaline waters and a pH varying between 7.4 and 8 (Jahnert and

Collins, 2013). The three sites presented different salinities: Nilemah presented a salinity of 64 practical salinity units (psu) (hypersaline – 60 to 70psu), Garden Point 54 psu (metahaline – 40 to 60psu) and Rocky Point 40 psu (metahaline).



Figure 1.5: Map of Shark Bay with the locations of Nilemah, Garden Point and Rocky Point highlighted (modified from Jahnert and Collins, 2013).

- **Types of microbial mats in Shark Bay**

Nine different types of microbial mat were identified in Hamelin Pool based on their specific surface morphology: colloform, gelatinous, smooth, pincushion, tufted, pustular, film, reticulate and blister mats (Logan, 1974; Playford, 1990). More recent studies of different sites in Shark Bay revealed that Nilemah presented five mat types along the littoral gradient: the shallowest tufted mat, the intertidal pustular mat, the subtidal smooth mat, the subtidal colloform mat and also the microbial pavement (Figure 1.6) (Jahnert and Collins, 2012; 2013).

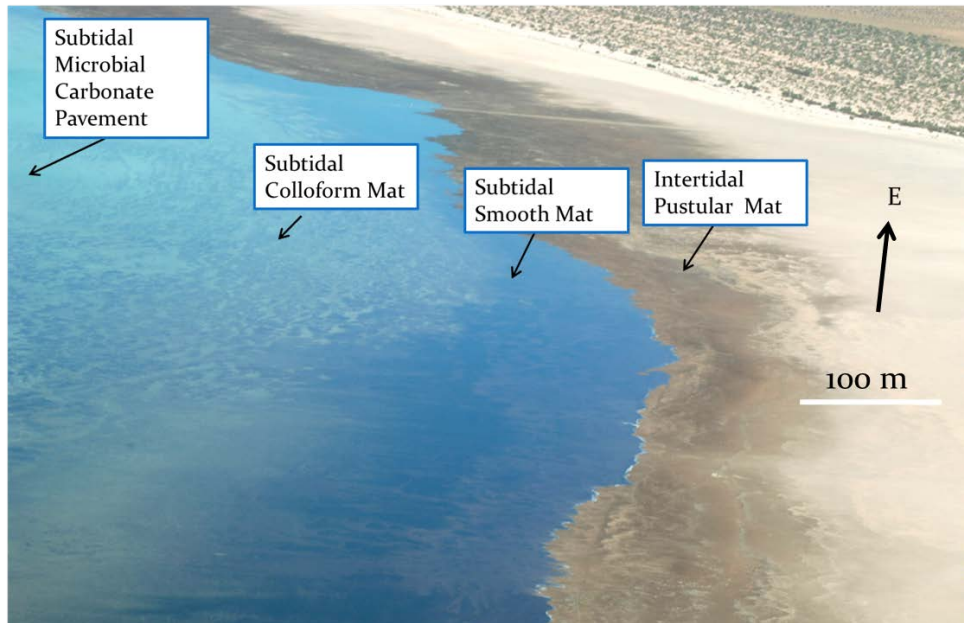


Figure 1.6: Sky view of Nilemah embayment showing the location of the different types of mats studied along the tidal flat. (Google Earth image).

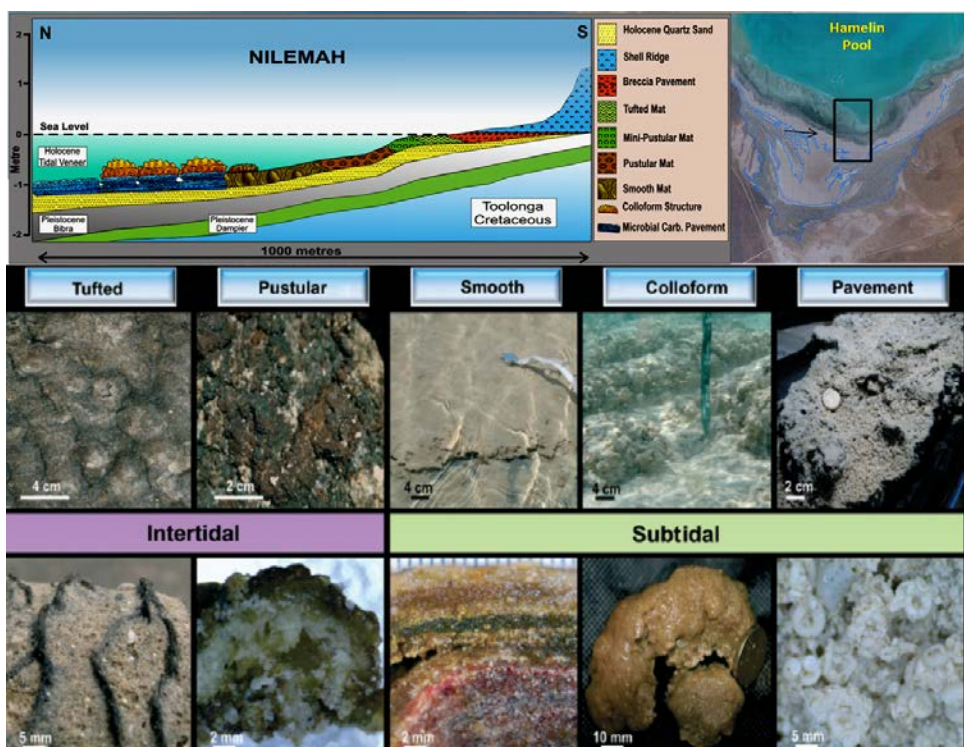


Figure 1.7: Distribution along the littoral gradient and internal/external fabrics of the different types of microbial mats in Nilemah (modified from Jahnert and Collins, 2013).

All mats presented different macroscopic and microscopic structures and different microbial assemblages (Jahnert and Collins, 2012; 2013) (Figure 1.7).

Tufted mats occur in the upper intertidal zone, between 0 and 0.20 m depth, and are growing in scallops because of long filaments made by *Lingbya* sp. (Hoffman, 1976; Figure 1.8). This type of mat normally thrives over shallow muddy substrates where sediments permanently retain moisture. Strong winds, tides and storms favour the accumulation of quartz sand and bivalve shell fragments at the surface of the mats. The Nilemah intertidal pustular mats, present between 0.20 and 0.80 m depth, contain coccoid cyanobacteria and exhibit an irregular clotted fabric characteristic of thrombolitic deposits covered by brown mucilage produced from the organomineralisation of gelatinous mucilage (Golubic and Hoffman, 1976). The laminated smooth mats observed between 0.80 and 1.20 m water depth present flat surfaces and are composed of “sub-horizontal millimetric laminae made of fine-grained carbonate sediments interbedded with laminae of microbial organic matter that had become lithified as micrite laminae” (Jahnert and Collins, 2012). At the surface of this mat, filamentous cyanobacteria produce exo-polymeric substances (EPS) that bind the sediment and favour a relatively flat surface. In Shark Bay, microbial smooth mats are considered to be pioneering microbial assemblages colonizing newly deposited sediments (Burne and Johnson, 2012). The colloform mats present a globular shape with coarse laminated wavy structure made of peloids and lithified micrite. Coccoid cyanobacteria and diatoms are responsible for the production of mucilage binding bioclasts that are further converted to lithified laminae (Jahnert and Collins, 2013). The microbial pavement, carbonate cryptomicrobial deposits containing fragments of bivalves, algae and micro-gastropods, is the deepest microbial deposit in Nilemah (Jahnert and Collins, 2013).

A more detailed description of the microbial mats has been reported elsewhere (Jahnert and Collins, 2012; 2013).

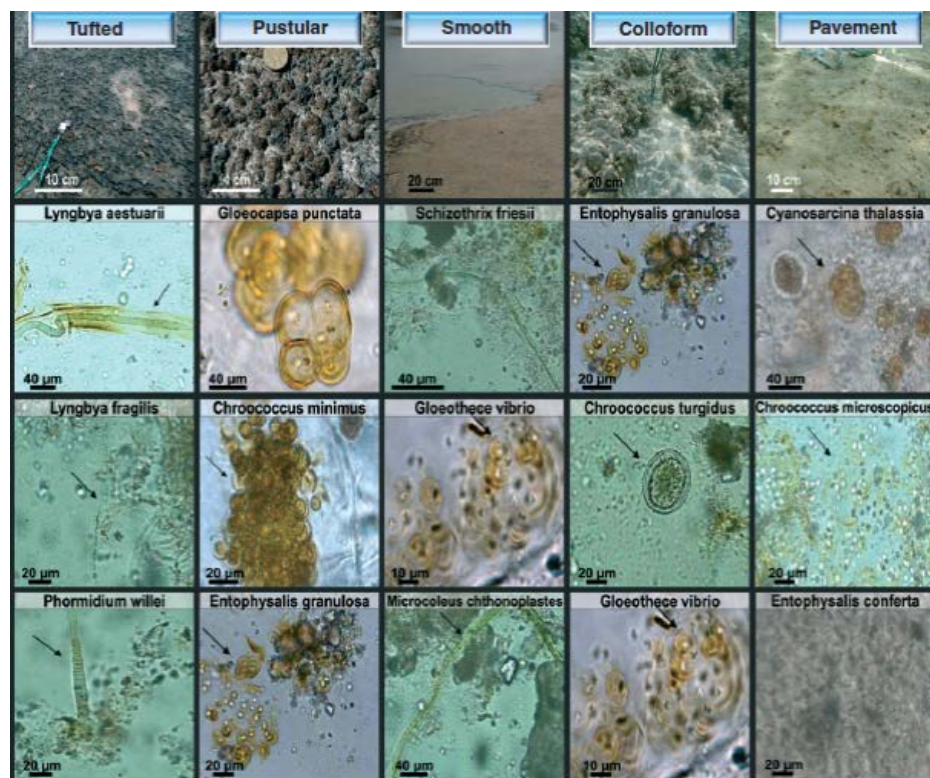


Figure 1.8: Dominant microbial species present in the different types of mats from Nilemah (Jahnert and Collins, 2013).

Because of strict restrictions related to permits and sample collections in Shark Bay, three different main field missions were needed to collect the entire set of microbial mats studied in this PhD (May 2010 – Chapters 3 and 4, April 2011 – Chapter 6 and April 2012 – Chapter 2 and 3).

Characterisation of microbial communities

- **Significance of biomarkers**

Biomarkers are molecular compounds detected in sedimentary OM or oils which can be ascribed to a particular biosynthetic origin. Some organic compounds have exceptional preservation potential and even if more reactive functional groups are often lost after burial during diagenesis (with the exclusion of exceptional preservation conditions (e.g. Melendez et al., 2013)), the main carbon skeletons often get preserved and can be potentially related to specific taxonomic groups (Peters et al., 2005; Brocks and Grice, 2011 for a review). Consequently, biomarker distributions can help characterise the source of OM and the environmental

conditions associated with its deposition. For instance, biomarkers can help in reconstructing the episodes of photic zone euxinia (PZE) which can occur in stratified marine and lacustrine settings dominated by anoxic conditions and high concentrations of H₂S at the chemocline produced by anaerobic sulfate reducing bacteria (SRB) degrading organic matter anerobically at the sediment water interface. This process persists in very few current day locations, the better known occurrence being remote deep Fjords (e.g. Millero, 1991) and the extant Black Sea (Murray et al., 2007), but has been prevalent in the geological past, especially during global Oceanic Anoxic Events (Grice et al., 2005; Jaraula et al., 2013). Green and brown pigmented *Chlorobiaceae* thrive under PZE conditions and can also be found in shallow microbial mats where euxinic microenvironments are present within the mat (Nicholson et al., 1987; Brocks and Pearson, 2005). These bacteria produce carotenoids and bacteriochlorophylls that lead to biomarkers like isorenieratane (**I**), palaeorenieratane (**II**), chlorobactane (**III**), or a suite of ¹³C-enriched aryl isoprenoids (Summons and Powell, 1986; 1987; Grice et al., 1996; Koopmans et al., 1996). Other biolipids are characteristic of different taxonomic groups (e.g.: 2 α -methylpentakishomohopane characteristic of cyanobacteria (Summons et al., 1999; [Figure 1.9](#)) but others may actually derive from multiple sources (see [Table 1.1](#)).

Biomarkers have also been recognised as highly useful tools to investigate the nature of early-life in the absence of identifiable fossils (Eglinton et al., 1964). Several distinct features from abiogenic organic compounds also make them useful counter-targets in studies attempting to provide convincing evidence for extraterrestrial life (Engel and Macko, 1997).

Recently, much interest has been given to the studies of extant organisms and microbial mats in order to characterise the origin and biosynthetic pathways of novel biomarkers (e.g. perylene, Grice et al., 2009). Finally, industry applications of biomarker studies include petroleum exploration, e.g. oil-oil and oil-source rock correlation and assessment of quality (thermal maturity extent of biodegradation) and economic value of oil reservoirs (e.g. Grosjean et al., 2009).

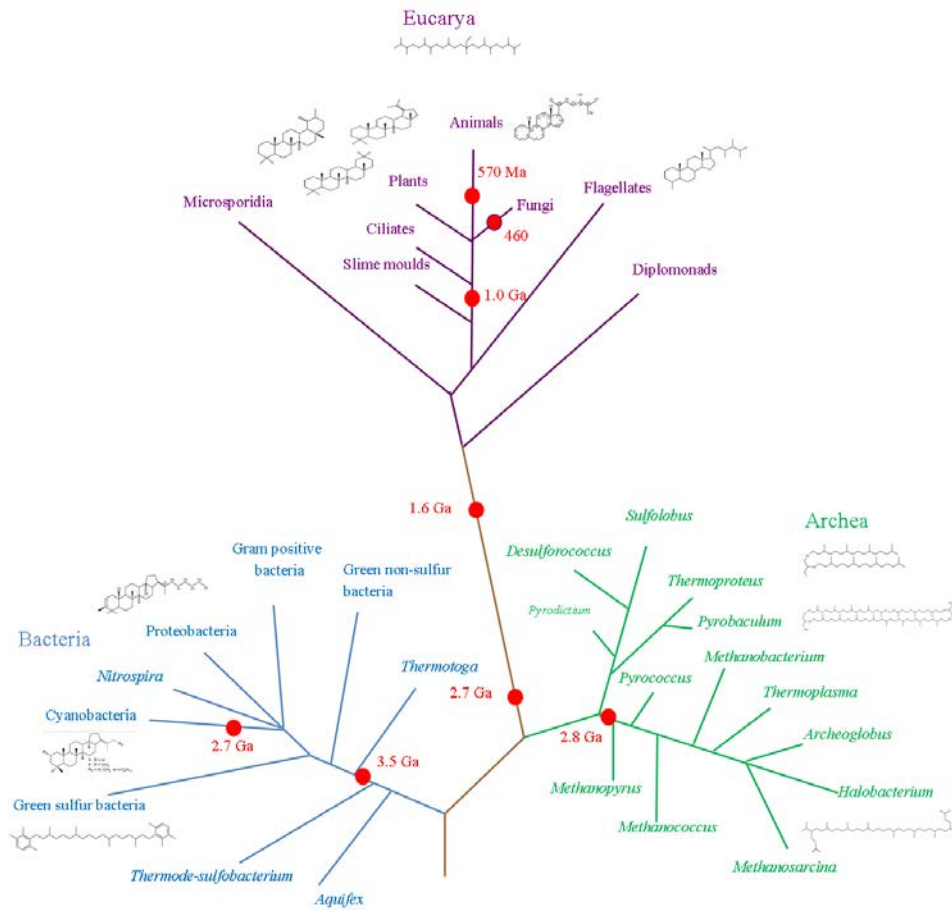


Figure 1.9: The Universal Phylogenetic Tree annotated with examples of diagnostic biomarkers for some taxonomic groups (modified from Brocks and Summons, 2003).

Table 1.1: Comparison of lipids from the three domains of life (modified from Itoh et al., 2001).

Lipids	Archea	Bacteria	Eukarya
Glycerolipids	+	+	+
Hydrocarbon chain	Isoprenoid	Fatty Acid	Fatty Acid
Carbons in compound	C ₁₅ -C ₂₅ /C ₄₀	C ₁₂ -C ₂₄	C ₁₂ -C ₂₄
Phospholipids	+	+	+
Glycolipids	+	+	+
Phosphoglycolipids	+	+	+
Sulfoglycolipids	+	-	+
Phosphosulfoglycolipids	+	-	-
Sulfolipids	-	±	+
Sphingolipids	-	±	+
Hopanoids	-	+	±
Steroids	-	±	+

+ : present in all or most species

- : absent in all species

±: absent in most species

➤ *Diagenesis and preservation of biosignatures*

In marine environments, most biogenic compounds (e.g.: carbohydrates, proteins, nucleic acids) are highly susceptible to biological degradation and are usually rapidly recycled. Organic compounds that survive remineralisation are vulnerable to other diagenetic processes. Diagenesis represents a complex array of biological (i.e. mineralisation) and chemical processes (e.g. condensation, crosslinking reactions, oxidation, reduction, or isomerisation) (Tissot and Welte, 1984). The prevailing physico-chemical conditions (e.g.: salinity, oxygen availability, sulfide concentrations) during and after OM burial strongly influence resultant distributions of diagenetic products (Brocks and Grice, 2011 and references therein). The presence of clay minerals, for instance, enhances the formation of diasteranes (van Kaam-Peters et al., 1998; Nabbefeld et al., 2010).

A major preservation pathway of biosignatures in sediments is the sulfurisation process (Sinninghe Damsté and de Leeuw, 1990 and references therein). Under favourable environmental conditions (e.g. anoxic conditions, minimum bioturbation, low iron(II) concentration and high H₂S concentration) (e.g. Hartgers et al., 1997), reduced sulfur species may react with organic compounds during the first stages of diagenesis. Early sulfurisation of biolipids can lead to polysulfide linking of different organic moieties (intermolecular sulfurisation) or the formation of discrete organic sulfur compounds (OSC). H₂S produced by SRB can react with unsaturated oxygen-sensitive biolipids (e.g. unsaturated isoprenoids) to produce more stable analogues (e.g. isoprenoidal thiols, Hebbing et al., 2006).

The concentration of minerals can also influence the preservation of biolipids. Biolipids have a strong affinity to fine minerals (e.g. clays) that tend to be well cemented and favour the development of euxinic conditions (anoxic and sulfidic), promoting sulfurisation of biolipids. In addition, the adsorption of organic matter onto the surface of mineral particles protects it from remineralisation by heterotrophic bacteria (Brocks and Grice, 2011).

➤ *Aliphatic hydrocarbons in microbial mat settings*

Hydrocarbon composition can reveal significant information regarding the microbial communities of mats. For instance, heptadecane (C_{17:0} *n*-alkane) and heptadecene (C_{17:1} *n*-alkene) reported as dominant hydrocarbons in freshwater calcifying mats (Thiel et al., 1997), hot spring mats (Dobson et al., 1988; Robinson and Eglinton, 1990; Jahnke et al., 2004), hypersaline mats (Grimalt et al., 1992; Fourçans et al., 2004; Rontani and Volkman, 2005; Wieland et al., 2008; Allen et al., 2010) and intertidal microbial mats (Wieland et al., 2003) usually indicate the presence of cyanobacteria (Dobson et al., 1988; Wieland et al., 2003). Although these hydrocarbons have been observed in eukaryotes, (Paoletti et al., 1976; Allard and Templier, 2000) they have shown to be in very high abundance in cyanobacterial isolates such as *Microcoleus chthonoplastes*, *Oscillatoria* spp. and *Spirulina* spp. (Winters et al., 1969; Paoletti et al., 1976). *Microcoleus*

chthonoplastes are also known to produce high abundance of mid-chain monomethyl-branched alkanes (Winters et al., 1969; Des Marais et al., 1992; Grimalt et al., 1992). Cyanobacteria are the only microorganisms that are able to produce mid-chain monomethyl-branched alkanes in the C₁₅–C₂₀ range (Gelpi et al., 1970; Shiea et al., 1990; Des Marais et al., 1992) and these hydrocarbons have also been frequently observed in modern microbial mats (Robinson and Eglinton, 1990; Shiea et al., 1990; Des Marais et al., 1992; Grimalt et al., 1992; Thiel et al., 1997; Jahnke et al., 2004). Particular isomers may be indicative of specific sources. 8-methylhexadecane, for instance, has been reported in hypersaline mats (Grimalt et al., 1992; Fourçans et al., 2004; Rontani and Volkman, 2005; Allen et al., 2010), while the 6-methyl, 7-methyl and 8-methylheptadecanes have been reported in hot springs mats (Dobson et al., 1988; Robinson and Eglinton, 1990; Jahnke et al., 2004), freshwater and marine mats (Shiea et al., 1990; Thiel et al., 1997). Long-chain *n*-alkanes with an odd-over-predominance are characteristic of higher plant inputs (Eglinton and Hamilton, 1967) and have been reported in microbial mats where significant aeolian transport occurs (Allen et al., 2010; Pagès et al., 2014a). Highly branched isoprenoids (HBI) can also be diagnostic markers of specific microbial mat communities. C₂₀ and C₂₅ HBI alkenes, for instance, reported in Shark Bay microbial mats and hypersaline lagoons are diatom markers (Dunlop and Jefferies, 1985; Summons et al., 1993; McKirdy et al., 2010).

Hopanoids and steroid hydrocarbon distributions can also provide information regarding the specific bacterial and eukaryotic sources, respectively. Diploptene, for example, reported in microbial mats from various environments (Boudou et al., 1986; Dobson et al., 1988; Thiel et al., 2001) may derive from cyanobacteria (Gelpi et al., 1970; Dobson et al., 1988), methylotrophs (Summons et al., 1994) or sulfate reducing bacteria (SRB) such as *Desulfovibrio* (Blumenberg et al., 2006). Δ^2 -sterenes, early diagenetic products of sterols, have been observed in modern mats (Rontani and Volkman, 2005; Pagès et al., 2014a) and can derive from diatoms (equal production of C₂₇, C₂₈ and C₂₉), green algae (higher C₂₉), other marine phytoplankton (abundant C₂₈), marine and terrestrial plants (high C₂₉), zooplankton and crustaceans (high C₂₇) (Volkman et al., 1986; 1998; Grice et al., 1998a).

Consequently, hydrocarbon speciation can provide valuable information regarding the microbial composition and organisation of modern microbial systems.

✓ *Common organic geochemical analytical methods*

A pathway for the holistic organic geochemical analysis of modern microbial mats is shown in [Figure 1.10](#).

The free OM was extracted by ultrasonic extraction using a mixture of dichloromethane (DCM) and methanol. To avoid co-elutions, an aliquot of the total lipid extract (TLE, bitumen I) was fractionated by column chromatography in order to obtain aliphatic, aromatic and polar hydrocarbons. The saturate and aromatic fractions, more amenable for Gas Chromatography –Mass Spectrometry (GC-MS) analysis, were analysed by GC-MS and GC-isotope ratio mass spectrometry (irMS) in order to obtain the stable isotopic composition of specific biomarkers.

Raney Nickel was applied to the polar fraction in order to cleave the C-S bonds and release any sulfur-bound biomarkers. The products after Raney Nickel were separated by column chromatography and analysed by GC-MS.

Bound biomarkers in the extracted residue (kerogen) were released by hydrolysis. This technique allows the release of biomarkers covalently bound to the macromolecular matrix of the kerogen (Love et al., 1995). Hydrolysis is conducted at high pressure hydrogen (15 MPa) and requires the use of a sulfided molybdenum catalyst $[(\text{NH}_4)_2\text{MoO}_2\text{S}_2]$. Hydrolysis has been proved to be exceptionally efficient in releasing strongly-bound or highly functionalised biomarkers with optimum preservation of structural arrangement (Love et al., 1995).

Finally, complimentary bulk parameters were investigated by elemental analysis (EA) and bulk stable isotope analysis (see below).

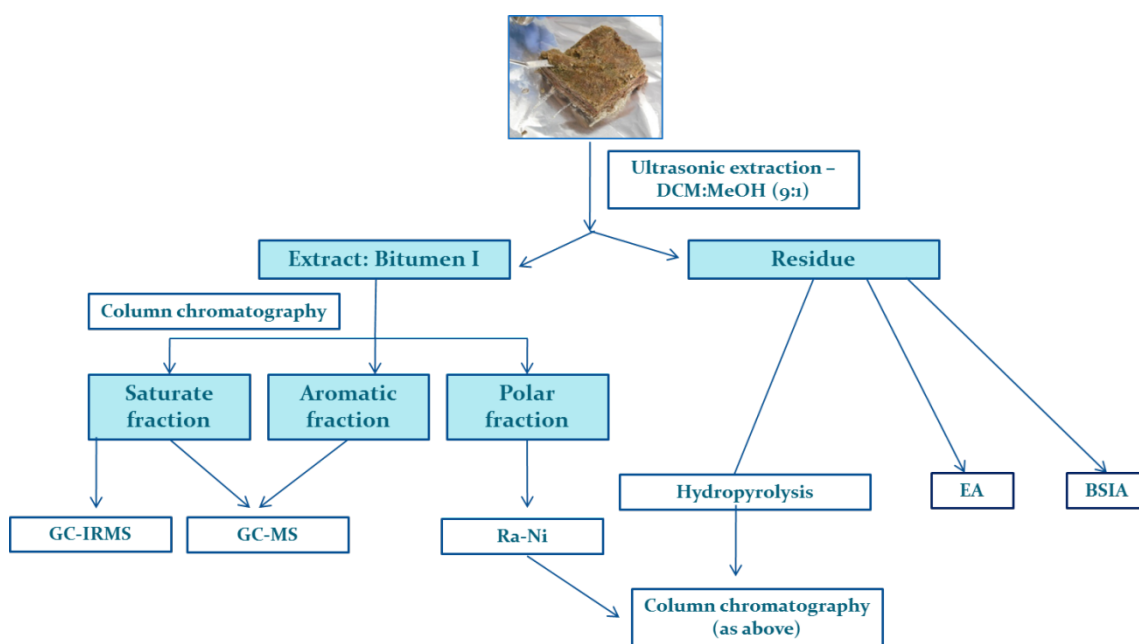


Figure 1.10: Flowchart of analytical steps applied to the modern microbial mats. DCM = Dichloromethane, MeOH: Methanol, GC-irMS = gas chromatography-isotope ratio mass spectrometry; GC-MS = gas chromatography-mass spectrometry; Ra-Ni: Raney-Nickel; BSIA = bulk stable isotope analysis, EA = elemental analysis.

➤ *Phospho-lipid fatty acids (PLFAs) in microbial mat settings*

PLFAs have been used to characterise biomass, community structure, metabolic status and microbial activities (Vestal and White, 1989). PLFAs are recognised to account for most, if not all, microorganisms present in the studied system, including bacteria and eukaryotes (Tunlid and White, 1992; Canuel et al., 1995). All membrane cells contain PLFAs which are rapidly turned over during metabolic activities and metabolised after cell death, meaning that PLFAs are exclusively representative of viable biomass (White et al., 1979; Vestal and White, 1989). As a typical PLFA contains 2 moles of fatty acids for 1 mole of phospholipid, it is possible to determine the phospholipid biomass. Indeed, detritus can significantly contribute to the total fatty acid pool while phospholipids are typically associated with the biomass (Tunlid and White, 1992; Boschker and Middelburg, 2002).

The comparison of the relative abundance of *iso* and *anteiso* compounds, unsaturated and saturated fatty acids can be used to estimate the metabolic status of microbial communities, although the abundances of some PLFAs can vary depending on growth conditions (Guckert et al., 1986; Vestal and White, 1989; Atlas and Bartha, 1998; Navarrete et al., 2000). PLFAs have been used to study microbial communities in sediments and soils, estuarine planktonic communities and microbial mats (Canuel et al., 1995; Cifuentes and Salata, 2001; Villanueva et al., 2004; Schubotz et al., 2009) and biodegraded petroleum samples (Hallmann et al., 2008)

Monoenoic PLFAs are characteristic of most all Gram-negative microorganisms while branched monoenoic unsaturated PLFAs and mid-chain branched saturated PLFAs are common to anaerobic bacteria. Although polyenoic PLFAs have been identified in cyanobacteria, they commonly suggest the presence of microeukaryotes (Ratledge and Wilkinson, 1988). Culture of cyanobacteria have revealed a high abundance of 16:0, 16:1 ω 7 and 18:1 ω 9 (Kenyon et al., 1972; Cohen et al., 1995) and a high abundance of these PLFAs has been reported in modern microbial mats (Jahnke et al., 2004; Bühring et al., 2009; Allen et al., 2010). In the absence of eukaryotes, 18:2 ω 6, 18:3 and 18:4 are also considered as PLFA markers of cyanobacteria and were reported in modern mats (Jahnke et al., 2004; Allen et al., 2010). PLFAs indicative of anaerobic bacteria reported in microbial mats (Zhang et al., 2004; Allen et al., 2010) include *iso*- and *anteiso*-15:0 and 17:0, which are often considered as specific SRB markers (Taylor and Parkes, 1983; 1985) and have been reported in microbial mats settings, however, they have also been found in other groups of bacteria (Vestal and White, 1989). 10-methyl-16:0 and *iso*-17:1 ω 9 are typical markers of SRB (Taylor and Parkes, 1985; Vestal and White, 1989; Londry et al., 2004) and a high abundance of 10-Me-16:0 in comparison with 10-Me-18:0 usually indicates a dominance of the *Desulfobacter*-type SRB (Dowling et al., 1986). 3- and 2-hydroxy fatty acids with 14-18 carbons are indicative of the presence of gram negative bacteria (Wilkinson, 1988).

Finally, long-chain (C₂₀-C₃₀) PLFAs with a predominance of even carbon-numbered fatty acids are usually associated with higher plant inputs (Eglinton and Hamilton, 1967) that can be supplied to the microbial mats by aeolian transport (Allen et al., 2010), especially if co-occurring odd carbon-numbered *n*-alkanes dominate the aliphatic hydrocarbons fraction. However, these long-chain PLFAs have recently been associated with the presence of SRB in ooids from the Bahamas and Shark Bay (Edgcomb et al., 2013a; Summons et al., 2013) and were also identified in hypersaline mats (Pagès et al., 2014a).

A summary of the PLFAs diagnostic of specific microbial groups is presented in Table 1.2.

Table 1.2: Specific PLFA for various organisms (modified from Allen, 2006).

Organisms	PLFA	References
Common to numerous communities	15:0, 16:1 ω 7, 16:1 ω 11, 17:0, 18:1 ω 11, <i>i</i> -19:0, <i>ai</i> -19:0	Vestal and White, 1989
Cyanobacteria	16:0, 16:2 ω 9,12,18:0, 18:2 ω 9,12	Kenyon et al., 1972; Cohen et al., 1995
SRB	<i>i</i> -17:1 ω 9, 10-Me16:0	Taylor and Parkes, 1985; Londry et al., 2004
SOB	Cy-19:0	Kneif, 2003
Iron oxidising bacteria	Cy-17:0	Kneif, 2003
Nitrate oxidising bacteria	11-Me16:0	Lipski et al., 2000
Methanotrophic bacteria	16:1 ω 8, 18:1 ω 10	Bowman et al., 1990
Actinomycetes	10-Me18:0	Vestal and White, 1989
Diatoms	16:1 ω 13, 16:4 ω 6,9,12,15, 20:5 ω 3,6,9,12,15	Vestal and White, 1989; Parrish et al., 2000
Green algae	16:1 ω 3, 18:3 ω 9,12,15	Vestal and White, 1989
Higher plants	18:1 ω 7; 20:5 ω 5,8,11,14,17, 24:0, 26:0, 28:0	Vestal and White, 1989

➤ *Intact Polar Lipids (IPLs)*

Analysis of intact polar membrane lipids (IPLs), like PLFAs, is considered to specifically target viable biomass since the polar head groups rapidly decompose after cell death (White et al., 1979; Harvey et al., 1986; Rütters et al., 2002; Sturt et al., 2004). IPLs present higher taxonomic specificity than PLFAs, do not discriminate against Archea and bear a great potential to qualitatively and quantitatively assess biomass composition in various ecosystems (e.g. Rütters et al.,

2002; Sturt et al., 2004; Zink and Mangelsdorf, 2004). Over the past decade, the analysis of IPL by high-performance liquid chromatography–electrospray ionisation mass spectrometry (HPLC–ESI-MS) has significantly expanded the characterisation of lipid diversity (Rütters et al., 2002; Sturt et al., 2004). This technique simultaneously detects IPLs from all main microbial community organisms that significantly contribute to the bulk biomass (Rossel et al., 2008; Ertefai et al., 2008; Schubotz et al., 2009). Culture-independent methods (i.e. fluorescence *in situ* hybridisation (FISH) and catalysed reporter deposition-FISH (CARD-FISH)), however, are much more selective and provide exclusive information on selected organisms without taking into account the relationships between microbial communities and their environments. IPLs, on the other hand, can provide clues on habitats characteristics as the structural composition of lipid membranes depends on pH (Minnikin and Abdolrahimzadeh, 1974), growth temperature (Oliver and Colwell, 1973; Shimada et al., 2008) and nutrient limitation (Van Mooy et al., 2006).

Whilst the analysis of IPLs is quite recently developed technology, it has already significantly contributed to the characterisation of microbial communities in several environments, including marine sediments (e.g. Rütters et al., 2002; Zink et al., 2003; Lipp et al., 2008), a meromictic lake (Ertefai et al., 2008), marine surface waters (Van Mooy et al., 2006) and microbial mats (Rossel et al., 2008; 2011). In microbial mats, IPLs played a significant role in characterising the influence of environmental factors on anaerobic methanotrophic archaea from seeps (Rossel et al., 2011). A lower abundance of phosphate-based IPLs was detected in microorganisms from calcified microbial mats, suggesting that phosphate was a limiting nutrient in these mats (Rossel et al., 2011).

A wide range of IPL groups are found in microorganisms. Glycerolipids are present in all domains of life and are the most widespread IPLs (Christie, 2003). Sphingolipids are characteristic of eukaryotic organisms and are only rarely found in bacteria (Olsen and Jantzen, 2001). On the other hand, ornithine lipids are exclusively found in bacteria (López-Lara et al., 2003).

➤ *Lipophilic pigments*

Photosynthetic pigments can highlight the distribution patterns of phototrophic organisms in sediments or microbial mats (Watts et al., 1977; Boon et al., 1983; Palmisano et al., 1988; Villanueva et al., 1994). Cyanobacteria have been recognised to produce significant amounts of zeaxanthin (**IV**), *o*-carotene, myxoxanthophyll (**V**), echineone (**VI**) and chlorophyll *a* (**VII**) (Goodwin, 1980). Cyanobacteria-derived photopigments (chl *a*, zeaxanthin, echineone and *p*-carotene) have been reported as dominant photopigments in certain types of hypersaline microbial mats from Shark Bay (Palmisano et al., 1989). In cyanobacteria, chl *d* can replace chl *a* in the photosystems of oxygenic photosynthesis, extending to the red the light spectrum that can be used for carbon fixation (Kühl et al., 2007). Additional chlorophyll, chl *f* was recently found in cyanobacteria and shown to absorb even further to the red (Chen et al., 2010).

The presence or absence of diatoms can also be revealed by pigment analysis. Fucoxanthin (**VIII**) and chlorophyll *c* (chl *c*, **IX**), for instance, are abundant diatoms markers (Jeffrey, 1989). The occurrence of diatoms in Shark Bay mats was revealed by the identification of fucoxanthin, diadinoxanthin (**X**) and diatoxanthin (**XI**) (Palmisano et al., 1989). Comparison of chl's *a* and *c* proportions was used to indicate the relative abundance of diatoms in microbial mats (Palmisano et al., 1989; Villanueva et al., 1994). Spirilloxanthin, rhodopsin, and bacteriochlorophyll *a* (bchl *a*, **XII**) are representative of purple phototrophic bacterial communities (Schmidt, 1979). Bchl *a* is the only pigment from purple phototrophic organisms so far detected in Shark Bay mats (Palmisano et al., 1989). Bacteriochlorophylls *c*, *d* and *e* (bchls *c*, *d*, *e*) are exclusively produced by green phototrophic bacteria and were reported in both multicellular green filamentous bacteria (Pierson and Castenholz, 1971) and GSB (Caple et al., 1978). Study of photopigments degradation in modern microbial mats showed that bchl *a* and *c* have a greater preservation potential because of their production under anoxic conditions, in contrast with chl *a* that is produced under oxic conditions, and consequently, more prone to degradation.

- **Significance of stable isotopes in organic geochemistry**

Biomarkers studies can help reconstruct microbial communities in modern environments, however, a high number of lipids can derive from multiple organisms, limiting the use of biolipids as source specific biomarkers (e.g. Koopmans et al., 1996; Volkman et al., 1998). Yet, stable isotope studies can help characterise specific microbial communities and the nature and pace of environmental and ecological changes in modern and ancient oceans.

Isotopes are “atoms whose nuclei contain the same number of protons but a different number of neutrons” (Hoefs, 2009). Isotopes occupy the same position in the periodic table. About 300 stable isotopes have been discovered whilst over 1,200 unstable ones have been identified so far. Stable isotopes of the major elements of biolipids are displayed in [Table 1.3](#). In this PhD study, stable isotope analysis of carbon and nitrogen were performed.

Table 1.3: Stable isotope abundances (atom %, Faure and Mensing, 2005 and references therein).

Carbon		Hydrogen		Sulfur		Oxygen		Nitrogen	
¹² C	98.899 %	¹ H	99.985 %	³² S	95.02 %	¹⁶ O	99.762 %	¹⁴ N	99.9634 %
¹³ C	1.111 %	D	0.015 %	³³ S	0.75 %	¹⁷ O	0.038 %	¹⁵ N	0.3663 %
				³⁴ S	4.21 %	¹⁸ O	0.200 %		
				³⁶ S	0.02 %				

➤ *Isotopic fractionation*

Discrepancies in chemical and physical properties deriving from differences in atomic mass of an element are described as isotopic effects (Hoefs, 2009). For instance, the replacement of any atom in a molecule by one of its isotopes leads to a very small variation in chemical behavior. Lighter elements (e.g. hydrogen) usually show much more important isotope effects as a result of the greater relative mass difference between the isotopes. Lighter elements will, in general, react more

rapidly than heavier elements thus giving rise to characteristic isotopic fractionations.

Isotopic fractionation is defined as “the partitioning of isotopes between two substances or two phases of the same substance with different isotope ratios” (Hoefs, 2009). Two processes generate isotopic fractionations: isotope exchange reactions and kinetic processes. The isotope exchange is characterised by a change in isotope distribution between different chemical substances, between different phases, or between individual molecules. The intensity of fractionation is temperature dependent and the effects are reversible. Since heavier isotopes tend to form stronger bonds, they are generally enriched in the phase with stronger intramolecular interactions or in molecules with stronger covalent bonds (Urey, 1947).

The evaporation–condensation mechanisms, for instance, are of particular interest because differences in the vapor pressures of isotopic compounds can produce significant isotope fractionations. Kinetic processes, however, are related to unidirectional processes (e.g. evaporation, diffusion) generating irreversible isotopic fractionations. Since heavier isotopes are usually characterised by slower reaction rates, they tend to become more depleted in the products (Bigeleisen and Wolfsberg, 1958).

➤ *Notation, standards and instrumentation*

Isotopic compositions are not measured as absolute isotopic abundances but as ratio (delta δ value) in units of per mil (‰) of the heavier to the lighter isotopes relative to an international reference standard (i.e. for carbon isotopic analysis, isotopic compositions are determined as a ratio of ^{13}C to ^{12}C in an analyte relative to the same ratio measured from the international Vienna Pee Dee Belemnite (‘VPDB’) calibrated to the original marine limestone from the Pee Dee formation in South Carolina (USA)). For δD analyses, Vienna Standard Mean Ocean Water (VSMOW) is used as the international standard while $\delta^{18}\text{O}$ can be reported relative to either of the before-mentioned standards. For $\delta^{14}\text{N}$, atmospheric nitrogen is used as the international standard.

The ratio is calculated as follow:

$$\delta E_{\text{Sample}} = \left(\frac{R_{\text{sample}}}{R_{\text{reference}}} - 1 \right) \text{‰}$$

R stands for the ratio of the heavier to the lighter isotope (e.g. $^{13}\text{C}/^{12}\text{C}$).

Stable isotope carbon isotope the analysis is performed using an irMS. For CSIA analysis, the GC is connected to an isotope ratio mass spectrometer *via* a combustion interface (Matthews and Hayes, 1978). An organic analyte is then converted to CO_2 on which stable isotope ratios are measured. For $\delta^{13}\text{C}$ analysis, the isotope ratio mass spectrometer measures the abundances of the ions m/z 44 ($^{12}\text{CO}_2$), 45 ($^{13}\text{CO}_2$) and 46 ($^{12}\text{C}^{18}\text{O}^{16}\text{O}_2$), thus allowing contribution of oxygen isotopologues to be determined.

➤ *Bulk stable isotope analysis (BSIA)*

Traditional BSIA can provide valuable information regarding the source of organic matter and isotopic fractionation mechanism. For instance, the bulk $\delta^{13}\text{C}$ values of terrestrial plants are about 10 ‰ less enriched in ^{13}C than marine plants (Wickman, 1952; Craig, 1953). The discrepancy between bulk $\delta^{13}\text{C}$ values of different plants has been associated with different photosynthetic pathways. Most terrestrial plants (80–90%) use the C3 (Calvin) photosynthetic pathway resulting in a carbon isotopic fractionation of 18 ‰. In contrast, approximately 10–20 % of carbon uptake by modern land plants is realised through the C4 (Hatch–Slack) photosynthetic pathway resulting in organic carbon on average 6 ‰ more depleted than atmospheric CO_2 . The C4 pathway may signify an adaptation to CO_2 limited photosynthesis, presenting a strong advantage under warm, dry, and saline environmental conditions. Consequently, the discrepancy between isotopic

compositions of C3 and C4 plants are broadly used to characterise paleoenvironments.

BSIA also bears a great potential to investigate the environmental factors influencing carbon isotopic compositions in marine phytoplankton. Different latitudinal carbon isotopic trends of plankton have been observed between the northern and the southern oceans. These results implied that the availability of aqueous CO₂ regulates the carbon isotopic composition of marine plankton, although other internal parameters can also affect this distribution (e.g. cell size, cell wall permeability) (Popp et al., 1998).

BSIA measurements are frequently combined with compound-specific isotope analysis (CSIA). Marine OM often shows $\delta^{13}\text{C}$ values characteristic of microbial communities, plant detritus or primary production (Hoefs, 2009). In such materials, CSIA is performed to differentiate the isotopic compositions deriving from primary sources and secondary inputs. Hence, the use of biomarkers and their associated carbon isotopic values can help assess the proportion of biologically sourced organic materials deriving to the total biomass.

Bulk nitrogen isotope can also provide additional information regarding OM sources. N-autotrophic organisms can use materials presenting a wide range of $\delta^{15}\text{N}$ values, as controlled by key environmental conditions. Yet, most plants show $\delta^{15}\text{N}$ values ranging between -5 and $+2\%$ while plants fixing atmospheric nitrogen present a narrower range of values (between 0 and $+2\%$). Nitrogen isotopic fractionation usually arises when the inorganic nitrogen source is in excess (Fogel and Cifuentes, 1993).

✓ *Methods and instrumentation*

BSIA measures the average isotopic composition of the total sample. Stable isotope ratios are measured in a continuous-flow (CF) system combined with an elemental analyser (EA, for C and N) linked to an irMS. The sample is first converted to the suitable gas target, by-products are then removed by purification

and the isolated gas target is finally analysed in the irMS relative to a reference gas of known isotopic composition. For $^{13}\text{C}/^{12}\text{C}$ and $^{15}\text{N}/^{14}\text{N}$ analysis, the samples are weighed into tin capsules and oxidized in a high temperature combustion furnace ($\sim 1050^\circ\text{C}$). Further clean-up steps include a reduction furnace for the removal of residual oxygen and reduction of NO_x -compounds and use of a nafion- membrane or cold-trap to remove H_2O .

A pre-treatment is often applied to the samples. For instance, selective $\delta^{13}\text{C}$ or $\delta^{18}\text{O}$ analysis of organic carbon (kerogen) requires the removal of carbonates with hydrochloric acid prior to BSIA.

$\delta^{13}\text{C}$ values of carbonates can be measured with a gas-bench connected to an irMS. Carbonates present in the sample can be selectively digested and converted into CO_2 by the addition of phosphoric-acid under a helium atmosphere that does not affect the organic carbon. The generated CO_2 is then diverted into the irMS.

➤ *Compound specific stable isotope analysis (CSIA)*

Carbon and hydrogen are the main components of organic matter and are strongly involved in biochemical, ecological, environmental, hydrologic and atmospheric processes. CSIA allows the measurement of stable isotope ratios in individual compounds providing a highly detailed insight into biogeochemical processes. CSIA have been utilised to investigate biomarkers origins, variations in carbon cycle, paleoclimates and biogeochemical cycling (Summons and Powell, 1986; Freeman et al., 1990; Summons et al., 1994; Nabbefeld et al., 2010).

✓ *Methods and instrumentation*

CSIA is now routinely applied with a GC connected to an irMS through an interface converting the compounds into gases amenable to irMS. Compounds are GC separated based on mass volatility and structural surface area differences. In an

irMS, different isotopes of the same compound are separated based on relative mass differences. For C-CSIA, the organic analytes are converted into CO₂ and H₂O at ~850 – 940 °C in a combustion furnace commonly using CuO as oxidant. H₂O is then removed by a liquid nitrogen-trap or a Nafion-membrane. The CO₂ target gas is subsequently ionised by an ion source and the ions of different isotope masses over a range of mass/charge ratios are then detected by the electron multiplier.

➤ *Significance of $\delta^{13}\text{C}$ analysis*

The $\delta^{13}\text{C}$ of atmospheric CO₂ is relatively constant at -7.7 ‰ although slight seasonal and regional variations have been observed (Keeling et al., 1989). The equilibrium between atmospheric CO₂ and aqueous dissolved inorganic carbon (DIC; Mook et al., 1974) leads to a significant isotopic fractionation in the carbon cycle. The connectivity of atmospheric CO₂, dissolved bicarbonate and carbonate precipitation is of high interest as it partially regulates the pH of oceans. Temperature influences the isotopic fractionation between CO₂ and the marine carbonate system (CO_{2, gas} ↔ CO_{2, aq} ↔ HCO₃⁻ ↔ CO₃²⁻) resulting in ¹³C-enriched marine DIC in surface waters ($\delta^{13}\text{C}$ values up to 2 ‰) (Mook et al., 1974; Zhang et al., 1995). The DIC measured in marine carbonates and deep water usually presents less enriched values of around 0 ‰. The precipitation of carbonate minerals usually involves very minor isotopic fractionation (Zhang et al., 1995); nonetheless, further diagenetic effects can significantly modify $\delta^{13}\text{C}$ values of carbonates (Scholle, 1995).

In shallow marine systems, biomarkers from different organism can present characteristic isotopic signals. Indeed, the $\delta^{13}\text{C}$ values of biomolecules depend on the isotopic fractionation related to their biosynthetic pathways (e.g. Hayes, 1993; Schouten et al., 1998). Consequently, stable isotopic analysis of specific biomarkers can help characterise the sources of OM in sediments and modern microbial systems (e.g. Grice and Brocks, 2011 and references therein). GSB, for instance, fix CO₂ *via* the (reductive) tricarboxylic acid (TCA)-cycle leading to ¹³C-enriched biomass with $\delta^{13}\text{C}$ values on average 15 ‰ heavier than oxygenic phototrophic organisms using the Calvin-Benson cycle (Quandt et al., 1977). Consequently, the

identification of *Chlorobiaceae*-specific carotenoids such as isorenieratane with heavy $\delta^{13}\text{C}$ values indicates the presence of PZE. Biomarkers from purple sulfur bacteria (*Chromatiaceae*) can also present characteristic carbon isotopic values. The carotenoid pigment okenone, precursor of okenane, can be significantly depleted in ^{13}C relatively to phytoplankton biomarkers. Similar to phytoplankton, purple sulfur bacteria utilise the Calvin-Benson cycle, however, these bacteria generally inhabit water bodies below the thermocline of euxinic waters and use ^{13}C -depleted CO_2 deriving from remineralised organic matter.

Diatoms have been recognised to be ^{13}C -rich organisms in comparison to other primary producers as they usually grow in blooms that lead to localised depletions in $\text{CO}_2(\text{aq})$, producing ^{13}C -enriched biomass. Some species are also able to assimilate HCO_3^- (Freeman et al., 1994, Canuel et al., 1997). This leads to ^{13}C -enriched markers of diatoms such as C_{25} and C_{30} highly branched isoprenoidal (HBI) alkene, as reported, for instance, in sediments from the hypersaline Coorong lagoon (McKirdy et al., 2010).

Methane is a source of carbon that presents very characteristic $\delta^{13}\text{C}$ values. In marine sediments, methane is generally produced by anaerobic microbial CO_2 reduction and is extremely depleted in ^{13}C with $\delta^{13}\text{C}$ values as low as -60‰ (Games et al., 1978). Consequently, organisms using isotopically light methane are usually significantly depleted in ^{13}C . The anaerobic oxidation of methane with sulfate is of great interest as this process is a major methane sink in marine systems (Niemann and Elvert, 2008) and favours alkalinity increase, leading to the precipitation of carbonates. Markers of SRB and methanotrophic archaeae involved in this process are highly depleted in ^{13}C (Birgel et al., 2008).

In shallow marine settings, land plant inputs can also significantly contribute to marine OM (Allen et al., 2010). Long-chain *n*-alkanes are characteristic of epicuticular waxes from the leaves of higher plants (Eglinton and Hamilton, 1967). CSIA can be specifically applied to these relatively common analytes to help differentiate vegetation sources. Typically, $\delta^{13}\text{C}$ of biomass

deriving from terrestrial plants using the C3 pathway ranges from -34 to -23 ‰ in contrast to the more ^{13}C -enriched biomass produced by higher plants using the C4 pathway such as grasses, saltmarsh or desert plants. Consequently, CSIA has been used to measure the $\delta^{13}\text{C}$ values of long-chain *n*-alkyl compounds detected in various settings such as soils (Conte et al., 2003), dust particles (Huang et al., 2000) and sediments from marine and terrestrial environments (Ficken et al., 2000; Huang et al., 2000) to help identify their actual source of origin.

Study of biogeochemical cycling

- **Complex biogeochemical cycling in microbial mats**

Since the most important microbial mats processes are light-driven, it seems important to differentiate day and night time microbial processes (Visscher and Stolz, 2005) (Table 1.4). Primary producers are oxygenic phototrophic organisms (cyanobacteria) that fix CO_2 . Fixed organic carbon is subsequently being used by heterotrophic bacteria, in addition to O_2 that is used as a terminal electron acceptor. SRB produce sulfide that is later oxidised by SOB, using O_2 or nitrate as terminal electron acceptors (Stal et al., 1985; Visscher et al., 1992a; van Gemerden, 1993; Visscher et al., 1998).

Table 1.4: Day and night metabolic processes of main functional groups present in microbial mats (modified from Visscher and Stolz, 2005).

Functional groups	Metabolic functions - Daylight conditions	Metabolic functions - Dark conditions
Cyanobacteria	Carbon fixation (photosynthesis) $\text{CO}_2 + \text{H}_2\text{O} \rightarrow \text{CH}_2\text{O} + \text{O}_2$	Fermentation, N_2 fixation, glycogen degradation
Aerobic heterotrophs	Carbon oxidation (respiration) $\text{CH}_2\text{O} + \text{O}_2 \rightarrow \text{CO}_2 + \text{H}_2\text{O}$	Fermentation, denitrification $5\text{CH}_2\text{O} + 2\text{H}_2\text{O} \rightarrow \text{HCO}_3^- + \text{H}^+ + 4\text{CH}_3\text{O}$ $5\text{CH}_2\text{O} + 4\text{NO}_3^- \rightarrow 5\text{HCO}_3^- + \text{H}^+ + 2\text{N}_2 + \text{H}_2\text{O}$
Sulfide oxidisers	Sulfide oxidation $\text{H}_2\text{S} + 2\text{O}_2 \rightarrow \text{SO}_4^{2-} + 2\text{H}^+$	Fermentation, denitrification $5\text{HS}^- + 8\text{NO}_3^- \rightarrow 5\text{SO}_4^{2-} + 4\text{N}_2 + \text{H}_2\text{O} + 3\text{OH}^-$
Phototrophic sulfide oxidisers	Carbon fixation (anoxygenic photosynthesis coupled to sulfide oxidation) $2\text{CO}_2 + \text{H}_2\text{S} + 2\text{H}_2\text{O} \rightarrow 2\text{CH}_2\text{O} + \text{SO}_4^{2-} + 2\text{H}^+$	Fermentation, glycogen degradation, Bchl <i>a</i> synthesis
Anaerobic heterotrophic sulfate-reducers	Carbon oxidation (sulfide respiration) $2\text{CH}_2\text{O} + \text{SO}_4^{2-} \rightarrow 2\text{CHO}_3^- + 2\text{H}_2\text{S}$	Sulfide respiration
Anaerobic heterotrophic methanogens	Carbonate respiration $4\text{H}_2 + \text{CO}_2 \rightarrow \text{CH}_4 + 2\text{H}_2\text{O}$ $2\text{CH}_2\text{O} \rightarrow \text{CH}_4 + \text{CO}_2$	Carbonate respiration

➤ *Carbon and oxygen cycles in microbial mats*

During the day, cyanobacteria and anoxygenic photoautotrophs perform photosynthesis that generates organic matter beneficial for other microbial communities. In microbial mats, the oxygen profile is closely related to light penetration which rapidly decreases with depth (Jørgensen and Des Marais, 1988). Carbon fixation occurs through oxygenic and anoxygenic photosynthesis (Figure 1.11). Dissolved inorganic carbon (DIC) necessary for primary production can derive from O_2 and anaerobic respiration as well as heterotrophic activity (Canfield and Des Marais, 1991). Dissolved organic carbon (DOC) present in the water column or in the mat can also contribute to biomass production. O_2 is exclusively produced by oxygenic photosynthesis that strongly depends on i) the oxidation state of the carbon fixed; ii) the quantity of nitrate that needs to be further reduced to ammonia and iii) the rate of carbon fixation. O_2 usually diffuses towards the water column or the deep part of the mat where it is used to oxidise toxic elements such as sulfide or ammonia. Conversely, under dark conditions, O_2 concentrations rapidly decrease and heterotrophic anaerobic processes dominate. DIC can be used by nonphotosynthetic organisms, however, most of the DIC diffuses outwards of the mat during organic matter oxidation. DOC is usually recycled within the mat but can also diffuse out of the mat.

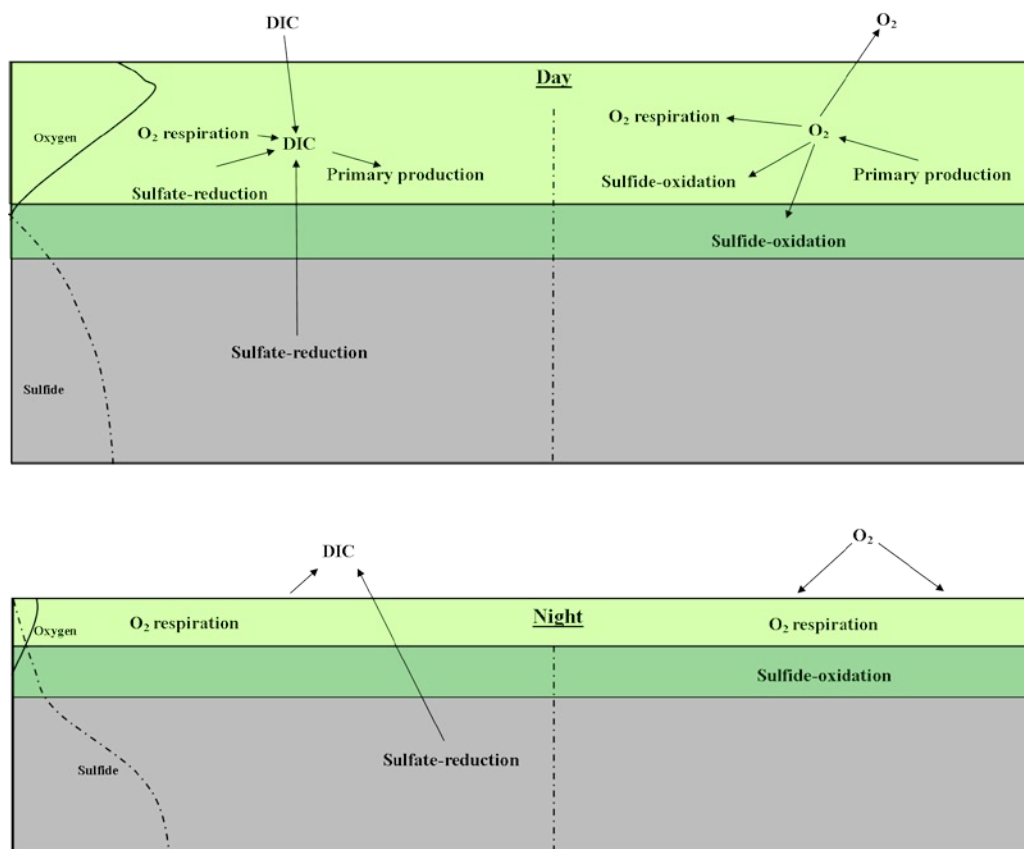


Figure 1.11: Carbon and oxygen cycling in microbial mats during daytime and night time (modified from Canfield and Des Marais, 1993).

➤ *Iron and sulfur cycles in microbial mats*

Oxic conditions in the upper layer of the mats usually lead to the oxidation of sulfide to sulfate by aerobic chemoautotrophic bacteria or chemical reaction with oxygen (Figure 1.12). However, a sharp and highly fluctuating redoxcline is often observed between the oxygen produced in the cyanobacteria layer and the sulfide produced by SRB, resulting in partial exposure of cyanobacteria to varying concentrations of sulfide. At depth, in the more anoxic part of the mat, biological oxidation of sulfide likely occurs through anoxygenic photosynthesis (De Wit and Van Gemerden, 1988). Aerobic sulfate-reduction also occurs in microbial mats (Canfield and Des Marais, 1991). Higher daytime temperatures may favour higher rates of sulfate-reduction (Jørgensen, 1994). Anoxygenic phototrophic bacteria (e.g.: GSB) use sulfide as electron donor to produce sulfate and require light to perform photosynthesis but can survive in low-light environments (Overmann et al., 1992). Chemical and biological oxidations in oxic and anoxic layers are recognised

as important microbial processes regulating sulfide mat concentrations during the daytime. Oxidic conditions can also result in the chemical oxidation of iron(II) into iron(III).

At night, the oxygen accumulated during the daylight is rapidly consumed by microorganisms and anoxic conditions prevail in the mat. In the absence of oxygen, sulfide accumulates due to the activity of SRB and a concomitant absence of sulfide uptake by anoxygenic photosynthesis and biological and chemical reoxidation associated with oxygenic photosynthesis result in the upper sulfide boundary moving towards the higher layers of the mat. In addition, the Fe(III) accumulated during the day can react with HS^- to form FeS and S^0 . Fe(II), periodically released as a result of redoxcline migration, usually leads to the precipitation of FeS. An increase in Fe(II) can occur as a result of the oxidation of FeS by acidophilic sulfur-oxidising bacteria that produce Fe(II) and sulfuric acid (Emerson and Weiss, 2004). However, a high portion of Fe(II) is usually precipitated as FeS (Joye et al., 1996). Fe(II) and FeS can be further converted to Fe(III) by anoxygenic photosynthesis from green phototrophic bacteria (Ehrenreich and Widdel, 1994), bacteria capable of coupling nitrate reduction with Fe(II) oxidation (Hafenbrandl et al., 1996) or bacteria combining Fe(II) oxidation with perchlorate reduction (Chaudhuri et al., 2001).

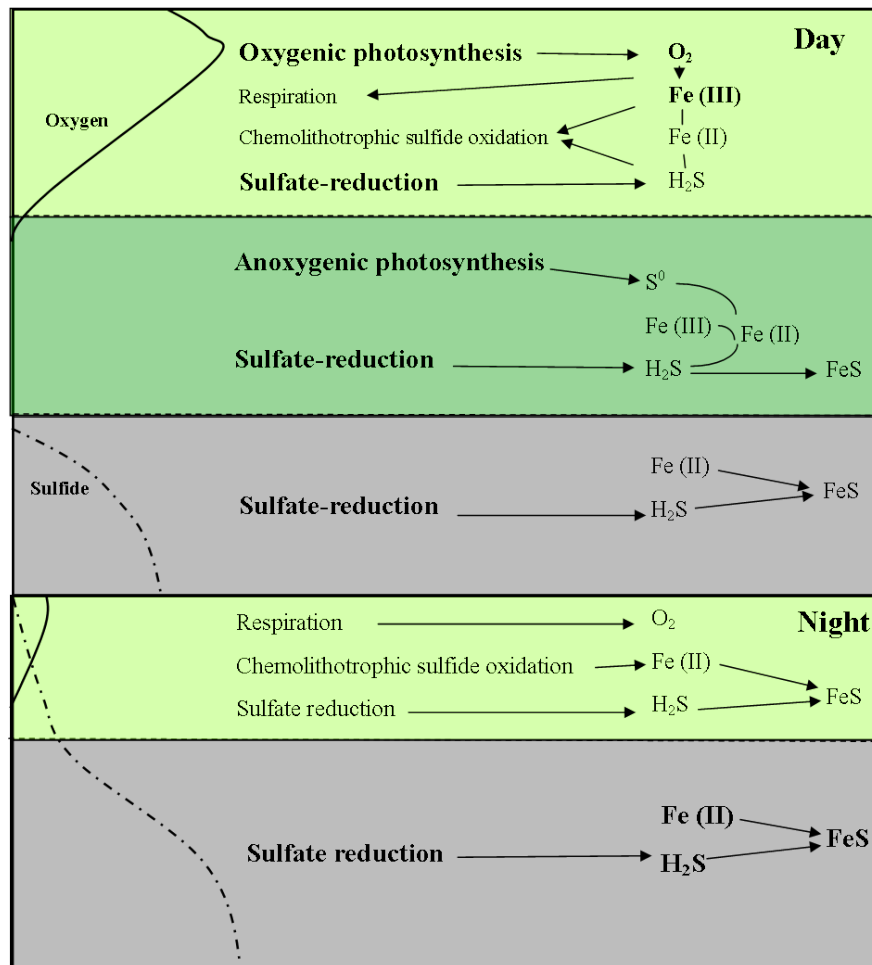


Figure 1.12: Sulfide and iron(II) interactions in microbial mats during daytime and night time (modified from Wieland et al., 2003).

➤ *Nitrogen cycle in microbial mats*

Nitrogen is a crucial nutrient required for biomass growth in microbial mats. The availability of nitrogen in mats is dependent on a balance between sources (dissolved nitrogen from the overlying water, nitrogen fixation and nitrogen from mineralisation) and sinks (efflux, denitrification and burial of nitrogen). Nitrogen cycling includes the coupling of nitrification (obligate aerobic process) and denitrification (anaerobic process) (see Herbert, 1999 for a review) (Figure 1.13).

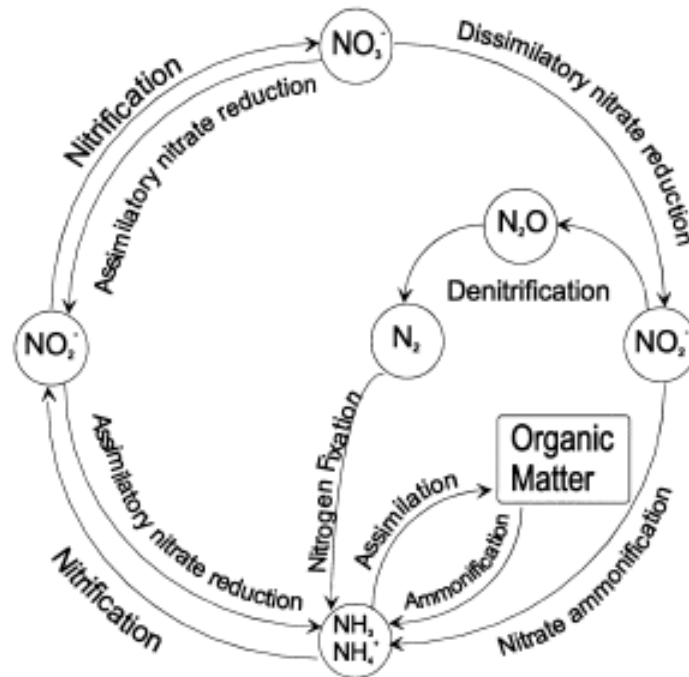


Figure 1.13: Key processes involved in the nitrogen cycle (Herbert, 1999).

Biological nitrogen fixation in which N_2 is converted to NH_4^+ is performed by specific microorganisms (Figure 1.14) and is partly dependent on light energy (Bebout et al., 1987). Photoautotrophic cyanobacteria are usually involved in daylight N_2 fixation whereas heterotrophic and chemoautotrophic bacteria perform N_2 fixation under dark conditions (Bebout et al., 1987). However, nitrogenase activity and oxygenic photosynthesis in cyanobacterial mats could not occur at the same time as nitrogenase is highly sensitive to oxygen (Villbrandt et al., 1991). During the day, the production of oxygen by cyanobacteria inhibits nitrogenase activity. However, heterotrophic bacteria are capable of generating anoxic microzones through the respiration process. NH_4^+ can also be released from nitrogenous OM through ammonification (Lomstein et al., 1998). Nitrite is generated by nitrification, a process which converts NH_4^+ to NO_3^- with NO_2^- as an intermediate component. The nitrification process strongly depends on the presence of O_2 as nitrifying bacteria are obligate aerobes. It is also highly dependent on NH_4^+ concentrations which are lower under daylight conditions because of a higher uptake by photosynthetic bacteria to support aerobic processes (Jørgensen et al., 1979). Consequently, the nitrification production of nitrite is controlled by the

balance between nitrifying bacteria activity, optimum under daylight conditions, and NH_4 concentrations which is likely to increase with anoxic conditions at night and when there is minimum NH_4 uptake by bacteria.

Under dark conditions and the absence of oxygenic photosynthesis, O_2 in the mat is rapidly depleted and nitrifying bacteria compete with other heterotrophic bacteria that have a stronger affinity for oxygen (Jørgensen, 1994). Denitrification is a process fuelled by NO_3^- either produced by nitrification or originating from the overlying water and produces nitrite as an intermediate component. This process decreases the availability of nitrogen in mats as the end-products are gaseous compounds (N_2O and N_2) that diffuse into the atmosphere. This process, strongly inhibited by O_2 , is occurring in the upper layers exclusively under dark conditions, when O_2 is fully depleted in these layers.

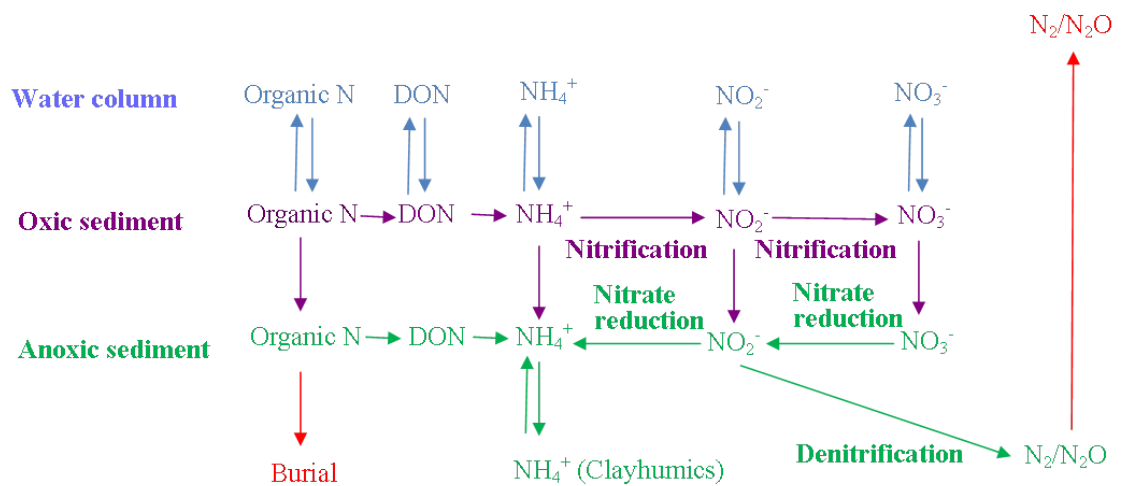


Figure 1.14: Nitrogen cycling in marine sediments (modified from Herbert, 1999).

- **Diffusional Equilibration in Thin-films (DET) and Diffusional Gradient in Thin-films (DGT) samplers**

- *Heterogeneity in microbial mats*

In modern microbial mats, exceptionally high metabolic rates (Jørgensen et al., 1979) lead to steep biogeochemical gradients (e.g. redox potential and pH), which display significant temporal and spatial fluctuations. The rapid changes in oxygen concentration between day and night conditions strongly influence solute distributions and concentrations. Significant heterogeneity in oxygen distributions has been reported due to high rates of oxygen production and consumption within these complex mats (Jørgensen et al., 1983; Glud et al., 1999). Changes in oxygen distributions can strongly influence other biogeochemical cycles and the distributions of various solutes, resulting in micro-scale heterogeneity of biogeochemical zonation varying over time (Paerl and Pinckney, 1996). The production and excretion of EPS also favours small-scale spatial heterogeneity within mats since micro-domains of EPS presenting different physical and chemical properties have been identified at very small scale (Decho, 2000). Consequently, the classical view of microbial mats as strictly organised and static structure has been reassessed (Visscher et al., 1998) and one-dimensional profiles of biogeochemical conditions within the mats are now considered unrepresentative. Consequently, two-dimensional distributions of solutes are required to help understanding the complex biogeochemical processes occurring within dynamic systems. Conventional techniques such as core-slicing or microelectrodes, although they present high temporal resolution, are not adequate to measure two-dimensional distributions of porewater solutes at mm-scale (see Stockdale et al., 2009 for a review). Furthermore, artefacts associated with sample handling and mixing of porewater solutes during sampling have been observed for traditional porewater extraction methods and sediment peepers (de Lange et al., 1992). Major breakthroughs were achieved with the development of planar optodes (Glud et al., 1996; Hulth et al., 2002), DGT (Davison et al., 1997; Teasdale et al., 1999; Robertson et al., 2008) and DET (Shuttleworth et al., 1999; Jézéquel et al., 2007; Robertson et al., 2008) technologies able to measure two-dimensional distributions of porewater solutes at mm resolution. These techniques allowed the identification of heterogeneous features such as sulfidic micro-niches (Devries and Wang, 2003;

Widerlund and Davison, 2007), faunal burrows (Zhu et al., 2006; Robertson et al., 2008; Pagès et al., 2011) and iron hot-spots within sulfidic sediment (Robertson et al., 2009).

Recently, colourimetric DGT and DET techniques have been developed to rapidly obtain two-dimensional, high-resolution distributions of a range of solutes (Teasdale et al., 1999; Jézéquel et al., 2007; Robertson et al., 2008, 2009; Pagès et al., 2011; Bennett et al., 2012; 2014). Any selective chemical reaction that produces a distinct colour change when an analyte is bound or precipitated is potentially suitable for a colourimetric DGT. For instance, the sulfide DGT technique uses an $\text{AgI}_{(s)}$ -impregnated binding gel, which is a white colour but turns black when S^{2-} or HS^- ions displace the iodide to form stable $\text{Ag}_2\text{S}_{(s)}$. The colour change can then be quantified using computer imaging densitometry (CID) which is directly associated with sulfide concentrations by an empirical calibration curve (Robertson, 2008). Since multiple hydrogels can be included within a single sampling probe, these techniques allow the simultaneous measurement of co-distributions of different solutes, overcoming problems of making separate measurements in heterogeneous systems and providing an exceptional insight into biogeochemical interactions (Robertson et al., 2008; 2009; Pagès et al., 2011; 2012).

➤ *Description of DET technique*

The DET technique is based on the use of a polyacrylamide hydrogel (95% water), which accumulates porewater solutes by diffusion until the internal and external concentrations are at equilibrium (Davison et al., 2000). The DET can be deployed in two ways: 1) constrained, with pieces of hydrogel located in small compartments, which does not permit relaxation of the solute concentration gradients or 2) unconstrained, by using a hydrogel sheet that needs to be rapidly sliced or preserved to minimise diffusional relaxation (Davison et al., 1991). A colourimetric DET method utilising a staining reagent to measure high-resolution, two-dimensional distributions of iron(II) on an unconstrained hydrogel was recently developed (Jézéquel et al., 2007; Robertson et al., 2008) and continues to be refined for improved performance (Bennett et al., 2012).

➤ *Description of DGT technique*

The DGT technique requires two key layers; a diffusion layer, that is effectively the same as the polyacrylamide hydrogel used for unconstrained DET, and a binding layer (Davison et al., 1997; Davison et al., 2000), as highlighted in Figure 1.15. The binding layer is most commonly a binding resin encapsulated in a polyacrylamide hydrogel (e.g. Chelex 100, ferrihydrite), but other types of binding layers have also been used (Teasdale et al., 1995). Soluble and labile analyte species diffuse through the layer and are accumulated on the binding layer. The flux across the diffusive layer is described by Fick's First Law of Diffusion, where there is an assumed zero concentration of each measurable species at the interface between the diffusive and binding layers and the concentration gradient is therefore mathematically equivalent with the external solution concentration (C_{DGT} , ng mL⁻¹) of analyte species. The mass accumulated (M , ng) is proportional to C , the deployment time (t , s), the area of the probe exposed to the solution (A , cm²), and the analyte diffusion coefficient (D , cm² s⁻¹) and inversely proportional to the diffusive layer thickness (Δg , cm), which defines the DGT equation that is used to determine the analyte concentration:

$$C_{DGT} = M\Delta g/DA t$$

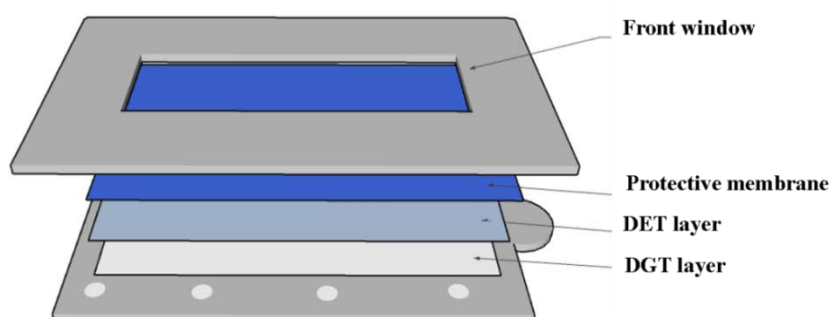


Figure 1.15: Schematic of a DGT/DET sampler.

➤ *DET and DGT deployments in sediment*

Deployment of DET and DGT probes in sediment and microbial mat porewaters necessitates consideration of how the environment responds to the perturbation (Davison et al., 2000). The equilibration or accumulation of analytes by DET and DGT sampling decreases the porewater concentrations in close vicinity of the samplers. The sediment can respond in three ways: 1) unsustained case, 2) sustained case or 3) partially sustained case (Figure 1.16).

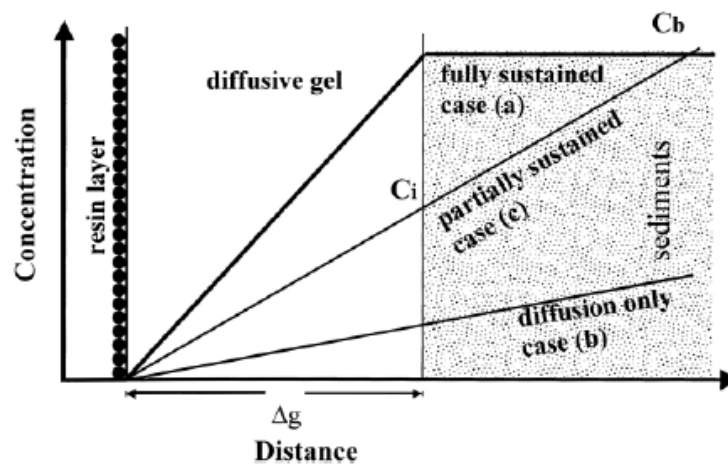


Figure 1.16: Cross-section through a DGT sampler in sediment. Concentration gradients are shown for three cases: a) sustained, b) unsustained and c) partially sustained (Zhang et al., 2002).

(1) Unsustained case

In this case, there is no resupply of analytes to the pore water and the DGT sampler is only supplied by the diffusion of solutes through the porewater that becomes depleted.

(2) Sustained Case

The porewater concentration is sustained at the bulk pore water concentration during the entire probe deployment. This situation usually occurs if solute mixing rates in the sediment are rapid enough (e.g. through bioirrigation), or if the rate of resupply from the solid phase is rapid compared to the rate of removal by the DGT sampler. In this situation, the C_{DGT} can be interpreted as the concentration of labile porewater metals.

(3) Partially Sustained Case

In this situation, a significant resupply of the solute from the solid phase is observed, yet, it is not sufficient to fully sustain porewater concentrations. The mass of analyte accumulated results from a balance between the capacity of the solid phase to resupply the porewater in response to the depletion induced by the DGT sampler.

The main implications for DET are that equilibration will take much longer with poorly sustained or non-sustained sediment, consequently, peaks will be underestimated and the normally sharp peaks will show some broadening. For DGT, the rate of accumulation will decrease as the porewater concentration is depleted and peaks will also be underestimated (Harper et al., 1999).

Aims of the thesis

The main goals of the thesis were to use complimentary molecular, physiological and biogeochemical approaches to characterise microbial communities forming the modern microbial mats in Shark Bay, Western Australia. Diurnal biogeochemical cycles were thoroughly investigated and correlated with microbial communities to get a better understanding of the role that specific communities play in elemental cycling and carbonate precipitation within mats. In addition, the relationships between water depth or salinity on microbial biomarkers and their stable isotope composition were explored. In order to correlate biosignatures in modern and ancient microbial systems, preservation pathways of biosignatures through time (e.g. through sulfurisation) were also investigated into a living stromatolite.

The purpose of the research presented in **Chapter 2** was to visualise small scale lateral variations in biogeochemical conditions and solute concentrations in a layered microbial mat under natural day and night conditions. Two-dimensional co-distributions of sulfide/alkalinity and iron(II)/phosphate were investigated at sub-mm resolution using DGT/DET samplers. In order to further understand the role of specific microbial communities on biogeochemical cycles and solute distributions, the lipid biomarker (hydrocarbons and PLFAs) composition of each mat layer was analysed.

In **Chapter 3**, DGT/DET samplers were used to investigate changes in the distributions of porewater solutes in hypersaline layered microbial mats, over a natural diurnal cycle. Microelectrodes measurements of oxygen and sulfide in the microbial mat helped determine the redox conditions during day and night. Silver foil analyses were also undertaken in order to map sulfate-reducing activity in the mat. Colourimetric DET and DGT techniques were used to investigate the microbial processes regulating the co-distributions of sulfide, iron(II) and phosphate and the alkalinity distributions which are related to carbonate precipitation/dissolution dynamics.

In **Chapter 4**, the main intention was to systematically observe how the lipids and isotopic composition of the microbial mats changed with water depth and salinity. For this purpose, lipid biomarkers (aliphatic hydrocarbons and PLFAs), bulk carbon and nitrogen isotopes and CSIA of aliphatic hydrocarbons and PLFAs were

investigated in four microbial mats along a tidal flat gradient. In addition, smooth mats from different sites (Nilemah, Garden Point and Rocky Point) presenting different salinity levels were also analysed to identify any potential microbial structural or functional relationship with salinity variations.

Chapter 5 described a further investigation of water depth and salinity influences on IPLs and pigment distribution. IPLs and lipophilic pigments were analysed from the same microbial mats analysed in **Chapter 4**. Temporal changes (i.e. dynamics) of lipophilic pigment distributions in Shark Bay microbial mats were considered by comparison of the present results to the corresponding data reported from Hamelin Pool mats by Palmisano et al. (1989).

Chapter 6 investigated the early diagenetic conditions that favoured the preservation of molecular biosignatures in modern microbial mats. For this purpose, free and sulfur-bound biomarkers from the four layers of a laminated smooth mat from Shark Bay were analysed. Complimentary 16s rRNA analysis and two-dimensional porewater analyte measurements were also undertaken to identify specific microbial species and characterise biogeochemical conditions, respectively, present in the microbial mat.

Preservation pathways of biosignatures were further investigated in **Chapter 7**. Kerogen-bound and carbonate-bound biomarkers were investigated in a 2.3 billion years microbial mat in order to get a better insight into the role of carbonates in biomarker preservation. Complimentary thin-sections and Raman spectroscopy analysis were performed to help validating the syngenetic origin of the biomarkers in this ancient sample.

References

- Allard B. and Templier J.** (2000) Comparison of neutral lipid profile of various trilaminar outer cell wall (TLS)-containing microalgae with emphasis on algaenan occurrence. *Phytochemistry* **54**, 369–380.
- Allen M.** (2006). PhD thesis. An astrobiology-focused analysis of microbial mat communities from Hamelin Pool, Shark Bay, Western Australia.
- Allen M. A., Neilan B. A., Burns B. P., Jahnke L. L. and Summons R. E.** (2010) Lipid biomarkers in Hamelin Pool microbial mats and stromatolites. *Org. Geochem.* **41**, 1207–1218.
- Allwood A. C., Walter M. R., Kamber B. S., Marshall C. P. and Burch I. W.** (2006) Stromatolite reef from the Early Archaean era of Australia. *Nature* **441**, 714–718.
- Atlas R. and Bartha R.** (1998) *Microbiology ecology: fundamental and applications*. Addison-Wiley, Reading.
- Awramik S. M.** (1984) Ancient stromatolites and microbial mats. In *Microbial Mats: Stromatolites*. (eds. Y. Cohen, R. W. Castenholz and H. O. Halvorson). Alan Liss, New York, pp. 1–21.
- Bebout B. M., Paerl H. W., Crocker K. M. and Prufert E.** (1987) Diel interactions of oxygenic photosynthesis and N₂ fixation (acetylene reduction) in a marine microbial mat. *Appl. Environ. Microbiol.* **53**, 2353–2362.
- Bennett W. W., Teasdale P. R., Welsh D. T., Panther J. G. and Jolley D. F.** (2012) Optimization of colorimetric DET technique for the in situ, two-dimensional measurement of iron(II) distributions in sediment porewaters. *Talanta* **88**, 490–495.
- Bigeleisen J. and Wolfsberg M.** (1958) Theoretical and experimental aspects of isotope effects in chemical kinetics. *Adv. Chem. Phys.* **1**, 15-76.
- Birgel D., Elvert M., Han X. and Peckmann J.** (2008) ¹³C depleted biphytanic diacids as tracers of past anaerobic oxidation of methane. *Org. Geochem.* **39**, 152–156.
- Blumenberg M., Krüger M., Nauhaus K., Talbot H. M., Oppermann B. I., Seifert R., Pape T. and Michaelis W.** (2006) Biosynthesis of hopanoids by sulfate-reducing bacteria (genus *Desulfovibrio*). *Environ. Microbiol.* **8**, 1220–1227.
- Bolhar, R. and Van Kranendonk M. J.** (2007) A non-marine depositional setting for the northern Fortescue Group, Pilbara Craton, inferred from trace element geochemistry of stromatolitic carbonates. *Precambrian Res.* **3-4**, 229-250.

- Boon J. J., Hines H., Burlingame A. L., Klok J., Rijpastra W. I. C., de Leeuw J. W., Edmonds K. E. and Eglinton G.** (1983) Organic geochemical studies of Solar Lake laminated cyanobacterial mats. In *Advances in Organic Geochemistry*. (eds. M. Bjoroy, C. Albrecht, C. Cornford et al.) John Wiley & Sons, Chichester, pp 207-227.
- Boschker H. and Middelburg J.** (2002) Stable isotopes and biomarkers in microbial ecology. *FEMS Microbiol. Ecol.* **40**, 85–95.
- Boudou J. P., Trichet J., Robinson N. and Brassell S. C.** (1986) Profile of aliphatic hydrocarbons in a recent polynesian microbial mat. *Int. J. Environ. Anal. Chem.* **26**, 137–155.
- Brocks J. J., Logan G. A., Buick, R. and Summons, R. E.** (1999) Archean molecular fossils and the early rise of eukaryotes. *Science* **285**, 1033–1036.
- Brocks J. J. and Summons R. E.** (2003) Sedimentary hydrocarbons, biomarkers for early-life. *Treatise on Geochemistry* (eds. W. H. Schlesinger, H. D. Holland and K. K. Turekian) Elsevier, pp 63-115.
- Brocks J. J. and Pearson A.** (2005) Building the biomarker tree of life. *Rev. Mineral. Geochemistry* **59**, 233–258.
- Brocks J. and Grice K.** (2011) Biomarker (Organic, Compound-Specific Isotopes). In *Encyclopedia of Geobiology* (eds. J. Reitner, V. Thiel). Springer, Dordrecht, pp. 147–166.
- Bühning S. I., Smittenberg R. H., Sachse D., Lipp J. S., Golubic S., Sachs J. P., Hinrichs K.-U. and Summons R. E.** (2009) A hypersaline microbial mat from the Pacific Atoll Kiritimati: insights into composition and carbon fixation using biomarker analyses and a ¹³C-labeling approach. *Geobiology* **7**, 308–323.
- Burne R. V. and Johnson K.** (2012) Sea-level variation and the zonation of microbialites in Hamelin Pool, Shark Bay, Western Australia. *Mar. Freshw. Res.* **63**, 994–1004.
- Canfield D. E. and Des Marais D. J.** (1991) Aerobic sulfate reduction in microbial mats. *Science* **251**, 1471–1473.
- Canfield D. E. and Des Marais D. J.** (1993) Biogeochemical cycles of carbon, sulfur, and free oxygen in a microbial mat. *Geochim. Cosmochim. Acta* **57**, 3971–3984.
- Canuel E. A., Cloern J. E., Ringelberg D. B., Guckert J. B. and Rau G. H.** (1995) Molecular and isotopic tracers used to examine sources of organic matter and its incorporation into the food webs of San Francisco Bay. *Limnol. Oceanogr.* **40**, 67–81.

- Caple M. B., Chow H. and Strouse C. E.** (1978) Photosynthetic pigments of green sulfur bacteria. The esterifying alcohols of bacteriochlorophylls *c* from *Chlorobium limicola*. *J. Biol. Chem.* **253**, 6730–6737.
- Chaudhuri S., Lack J. and Coates J.** (2001) Biogenic magnetite formation through anaerobic biooxidation of Fe(II). *Appl. Environ. Microbiol.* **67**, 2844–2848.
- Chen M., Schliep M., Willows R. D., Cai Z.-L., Neilan B. A. and Scheer H.** (2010) A red-shifted chlorophyll. *Science*. **329**, 1318–1319.
- Christie W.** (2003) *Lipid Analysis, third ed.* The Oily Press, Bridgwater.
- Cifuentes L. A. and Salata G. G.** (2001) Significance of carbon isotope discrimination between bulk carbon and extracted phospholipid fatty acids in selected terrestrial and marine environments. *Org. Geochem.* **32**, 613–621.
- Cohen Z., Margheri M. C. and Tomaselli L.** (1995) Chemotaxonomy of cyanobacteria. *Phytochemistry* **40**, 1155–1158.
- Conte M. H., Weber J. C., Carlson P. J. and Flanagan L. B.** (2003) Molecular and carbon isotopic composition of leaf wax in vegetation and aerosols in a northern prairie ecosystem. *Oecologia* **135**, 67–77.
- Craig H.** (1953) The geochemistry of the stable carbon isotopes. *Geochim. Cosmochim. Acta* **3**, 53–92.
- Davison W., Grime G. W., Morgan J. A. W. and Clarke K.** (1991) Distribution of dissolved iron in sediment pore waters at submillimetre resolution. *Nature* **352**, 323–325.
- Davison W., Fones G. R. and Grime G. W.** (1997) Dissolved metals in surface sediment and a microbial mat at 100- μ m resolution. *Nature* **387**, 885–888.
- Davison W., Fones G. R., Harper M., Teasdale P. R. and Zhang H.** (2000) Dialysis, DET and DGT: in situ diffusional techniques for studying water, sediments and soils. In *In situ monitoring of aquatic systems: chemical analysis and speciation*. (eds. J. Buffle, G. Horvai). John Wiley & Sons, pp. 495–569.
- Decho A. W.** (2000) Microbial biofilms in intertidal systems: an overview. *Cont. Shelf Res.* **20**, 1257–1273.
- De Lange G. J., Cranston R. E., Hydes D. H. and Boust D.** (1992) Extraction of pore water from marine sediments: A review of possible artifacts with pertinent examples from the North Atlantic. *Mar. Geol.* **109**, 53–76.
- De Wit R. and Van Gernerden H.** (1988) Growth of the cyanobacterium *Microcoleus chthonoplastes* on sulfide. *FEMS Microbiol. Ecol.* **53**, 203–209.

- De Wit R., Jonkers H. M., van den Ende F. P. and van Gernerden H.** (1989) In situ fluctuations of oxygen and sulphide in marine microbial sediment ecosystems. *Netherlands J. Sea Res.* **23**, 271–281.
- Des Marais D., Bauld J., Palmisano A., Summons R. and Ward D.** (1992) The biogeochemistry of carbon in modern microbial mats. In *The Proterozoic Biosphere: A multidisciplinary study* (eds. J. W. Schopf, C. Klein). Cambridge University Press, Cambridge, pp. 299–308.
- Des Marais D. J.** (2003) Biogeochemistry of hypersaline microbial mats illustrates the dynamics of modern microbial ecosystems and the early evolution of the biosphere. *Biol. Bull.* **204**, 160–167.
- Devries C. and Wang F.** (2003) In situ two-dimensional high-resolution profiling of sulfide in sediment interstitial waters. *Environ. Sci. Technol.* **37**, 792–797.
- Dobson G., Ward D. M., Robinson N. and Eglinton G.** (1988) Biogeochemistry of hot spring environments: Extractable lipids of a cyanobacterial mat. *Chem. Geol.* **68**, 155–179.
- Dowling N., Widdel F. and White D. C.** (1986) Phospholipid ester-linked fatty acid biomarkers of acetate-oxidizing sulfate reducers and other sulfide-forming bacteria. *J. Gen. Microbiol.* **132**, 1815–1825.
- Dunlop R. W. and Jefferies P. R.** (1985) Hydrocarbons of the hypersaline basins of Shark Bay, Western Australia. *Org. Geochem.* **8**, 313–320.
- Dupraz C., Reid R. P. and Visscher P. T.** (2011) Microbialite, Modern. In *Encyclopedia of Geobiology* (eds. J. Reitner, J. and V. Thiel). Springer, Dordrecht, pp. 617–635.
- Dutkiewicz A., Volk H., George S. C., Ridley J. and Buick R.** (2006) Biomarkers from Huronian oil-bearing fluid inclusions: An uncontaminated record of life before the Great Oxidation Event. *Geology* **34**, 437–440.
- Edgcomb V. P., Bernhard J. M., Beaudoin D., Pruss S. B., Welander P. V, Schubotz F., Mehay S., Gillespie a L. and Summons R. E.** (2013a) Molecular indicators of microbial diversity in oolitic sands of Highborne Cay, Bahamas. *Geobiology* **11**, 234–51.
- Eglinton G., Scott P., Belsky T., Burlingame A. and Calvin M.** (1964) Hydrocarbons of biological origin from a one billion year old sediment. *Science* **145**, 263–264.
- Eglinton G. and Hamilton R. J.** (1967) Leaf Epicuticular waxes. *Science* **156**, 1322–1335.
- Ehrenreich A. and Widdel F.** (1994) Anaerobic oxidation of ferrous iron by purple bacteria, a new type of phototrophic metabolism. *Appl. Envir. Microbiol.* **60**, 4517–4526.

- Emerson D. and Weiss J. V.** (2004) Bacterial iron oxidation in circumneutral freshwater habitats: findings from the field and the laboratory. *Geomicrobiol. J.* **21**, 405–414.
- Engel M. H. and Macko S. A.** (1997) Isotopic evidence for extraterrestrial non-racemic amino acids in the Murchison meteorite. *Nature* **389**, 265–268.
- Ertefai T. F., Fisher M. C., Fredricks H. F., Lipp J. S., Pearson A., Birgel D., Udert K. M., Cavanaugh C. M., Gschwend P. M. and Hinrichs K.-U.** (2008) Vertical distribution of microbial lipids and functional genes in chemically distinct layers of a highly polluted meromictic lake. *Org. Geochem.* **39**, 1572–1588.
- Faure G. and Mensing T.** (2005) *Isotopes, Principles and Applications, Third Edition*. John Wiley & Sons, Inc., Hoboken, New Jersey.
- Ficken K. J., Li B., Swain D. L. and Eglinton G.** (2000) An *n*-alkane proxy for the sedimentary input of submerged/floating freshwater aquatic macrophytes. *Org. Geochem.* **31**, 745–749.
- Flannery D. T. and Walter M. R.** (2011) Archean tufted microbial mats and the Great Oxidation Event: new insights into an ancient problem. *Aust. J. Earth Sci.* **59**, 1–11.
- Fogel M. L. and Cifuentes L. A.** (1993) Isotope fractionation during primary production. In *Organic geochemistry, principles and applications*. (eds. M.H. Engel and S. A. Macko) Springer US. pp. 73–98.
- Fourçans A., de Oteyza T. G., Wieland a, Solé A., Diestra E., van Bleijswijk J., Grimalt J. O., Kühl M., Esteve I., Muyzer G., Caumette P. and Duran R.** (2004) Characterization of functional bacterial groups in a hypersaline microbial mat community (Salins-de-Giraud, Camargue, France). *FEMS Microbiol. Ecol.* **51**, 55–70.
- Freeman K. H., Hayes J. M., Trendel J. M. and Albrecht P.** (1990) Evidence from carbon isotope measurements for diverse origins of sedimentary hydrocarbons. *Nature* **343**, 254–256.
- Freeman K. H., Wakeham S. G. and Hayes J. M.** (1994) Predictive isotopic biogeochemistry: hydrocarbons from anoxic marine basins. *Org. Geochem.* **21**, 629–644.
- Games L. M., Hayes J. M., and Gunsalus R. P.** (1978) Methane-producing bacteria: natural fractionations of the stable carbon isotopes. *Geochim. Cosmochim. Acta* **42**, 1295–1297.
- Gelpi E., Schneider H., Mann J. and Oro J.** (1970) Hydrocarbons of geochemical significance in microscopic algae. *Phytochemistry* **9**, 603–612.

- Glud R. N., Ramsing N., Gundersen J. and Klimant I.** (1996) Planar optodes: a new tool for fine scale measurements of two-dimensional O₂ distribution in benthic communities. *Mar. Ecol. Prog. Ser.* **140**, 217–226.
- Glud R. N., Kühl M., Kohls O. and Ramsing N. B.** (1999) Heterogeneity of oxygen production and consumption in a photosynthetic microbial mat as studied by planar optodes. *J. Phycol.* **279**, 270–279.
- Golubic S. and Hoffman H. J.** (1976) Comparison of holocene and mid-precambrian Entophysalidaceae (Cyanophyta) in stromatolitic algal mats: cell division and degradation. *J. Paleontol.* **50**, 1074–1082.
- Goodwin T. W.** (1980) *The Biochemistry of the Carotenoids, Volume 2, Animals.* Chapman and Hall. New York.
- Grice K., Schaeffer P., Schwark L. and Maxwell J. R.** (1996) Molecular indicators of palaeoenvironmental conditions in an immature Permian shale (Kupferschiefer, Lower Rhine Basin, north-west Germany) from free and S-bound lipids. *Org. Geochem.* **25**, 131–147.
- Grice K., Klein Breteler W. C. M., Schouten S., Grossi V., de Leeuw J. W. and Sinnighe-amsté J. S.** (1998a) Effects of zooplankton herbivory on biomarker proxy records. *Paleoceanography* **13**, 686–693.
- Grice K., Cao C., Love G. D., Bottcher M. E., Twitchett R., Grosjean E., Summons R. E., Turgeon S. E., Dunning W. and Jin Y.** (2005) Photic Zone Euxinia During the Permian-Triassic Superanoxic Event. *Science* **307**, 706–709.
- Grice K., Lu H., Atahan P., Asif M., Hallmann C., Greenwood P., Maslen E., Tulipani S., Williford K. and Dodson J.** (2009) New insights into the origin of perylene in geological samples. *Geochim. Cosmochim. Acta* **73**, 6531–6543.
- Grice K., Brocks J.** (2011) Biomarkers (Molecular fossils). In *Encyclopedia of Geobiology*. (eds. J. Reitner, V. Thiel). Springer, Dordrecht, pp. 147-167.
- Grimalt J. O., de Wit R., Teixidor P. and Albaigés J.** (1992) Lipid biogeochemistry of Phormidium and Microcoleus mats. *Org. Geochem.* **19**, 509–530.
- Grosjean E., Love G. D., Stalvies C., Fike D. A. and Summons R. E.** (2009) Origin of petroleum in the Neoproterozoic–Cambrian South Oman Salt Basin. *Org. Geochem.* **40**, 87–110.
- Grotzinger J. P. and Knoll A. H.** (1999) Stromatolites in Precambrian carbonates: evolutionary mileposts or environmental dipsticks? *Annu. Rev. Earth Planet. Sci.* **27**, 313–358.

- Guckert J. B., Hood M. A. and White D. C.** (1986) Phospholipid ester-linked fatty acid profile changes during nutrient deprivation of *Vibrio cholerae*: increases in the trans/cis ratio and proportions of cyclopropyl fatty acids. *Appl. Environ. Microbiol.* **52**, 794–801.
- Hafenbrandl D., Keller M., Dirmeier R., Rachel R., Robnagel P., Burggraf S., Huber H. and Stetter K.** (1996) *Ferroglobusplacidus* gen. nov., sp. nov. a novel hyperthermophilic archaeum that oxidizes Fe²⁺ at neutral pH under anoxic conditions. *Arch. Mikrobiol.* **166**, 308–314.
- Hallmann C., Schwark L., Grice K.** (2008) Community dynamics of anaerobic bacteria in deep petroleum reservoirs. *Nature Geoscience* **1**, 588–591.
- Harper M. P., Davison W. and Tych W.** (1999) Estimation of porewater concentrations from DGT profiles: a modelling approach. *Aquat. Geochemistry* **5**, 337–355.
- Hartgers W. A., Lopez J. F., Sinninghe Damste J. S., Reiss C., Maxwell J. R. and Grimalt J. O.** (1997) Sulfur-binding in recent environments: II. Speciation of sulfur and iron and implications for the occurrence of organo-sulfur compounds. *Geochim. Cosmochim. Acta* **61**, 4769–4788.
- Harvey H. R., Fallo R. D. and Pattom J. S.** (1986) The effect of organic matter and oxygen on the degradation of bacterial membrane lipids in marine sediments. *Geochim. Cosmochim. Acta* **50**, 795–804.
- Hayes J. M.** (1993) Factors controlling ¹³C contents of sedimentary organic compounds: Principles and evidence. *Mar. Geol.* **113**, 111–125.
- Hebting Y., Schaeffer P., Behrens A., Adam P., Schmitt G., Schneckenburger P., Bernasconi S. M. and Albrecht P.** (2006) Biomarker evidence for a major preservation pathway of sedimentary organic carbon. *Science* **312**, 1627–1631.
- Herbert R. A.** (1999) Nitrogen cycling in coastal marine ecosystems. *FEMS Microbiol. Rev.* **23**, 563–590.
- Hoefs J.** (2009) *Stable isotope geochemistry*. Springer.
- Hoehler T. M., Bebout B. M. and Des Marais D. J.** (2001) The role of microbial mats in the production of reduced gases on the early Earth. *Nature* **412**, 324–327.
- Hoffman P.** (1976) Stromatolite morphogenesis in Shark Bay, Western Australia. In *Stromatolites*. (ed. M. R. Walter) Elsevier, Amsterdam. pp. 261–272.
- Huang Y., Freeman K. H., Wilkin R. T., Arthur M. A. and Jones A. D.** (2000) Black Sea chemocline oscillations during the Holocene: molecular and isotopic studies of marginal sediments. *Org. Geochem.* **31**, 1525–1531.

- Hulth S., Aller R., Engström P. and Selander E.** (2002) A pH plate fluorosensor (optode) for early diagenetic studies of marine sediments. *Limnol. Ocean.* **47**, 212–220.
- Itoh Y., Sugai A., Uda I. and Itoh T.** (2001) The evolution of lipids. *Adv. Sp. Res. Off. J. Comm. Sp. Res.* **28**, 719–724.
- Jahnert R. and Collins L.** (2012) Characteristics, distribution and morphogenesis of subtidal microbial systems in Shark Bay, Australia. *Mar. Geol.* **303-306**, 115–136.
- Jahnert R. and Collins L.** (2013) Controls on microbial activity and tidal flat evolution in Shark Bay, Western Australia. *Sedimentology* **60**, 1071–1099.
- Jahnke L. L., Embaye T., Hope J., Turk K. A., Van Zuilen M., Des Marais D. J., Farmer J. D. and Summons R. E.** (2004) Lipid biomarker and carbon isotopic signatures for stromatolite-forming, microbial mat communities and *Phormidium* cultures from Yellowstone National Park. *Geobiology* **2**, 31–47.
- Jaraula C., Grice K., Twitchett R., Boettcher M., Lemetayer P., Dastidar A. G. and Opazzo L. P.** (2013) Elevated pCO₂ leading to End Triassic Extinction, photic zone euxinia and rising sea levels. *Geology* **41**, 955–958.
- Jeffrey S. W.** (1989) Chlorophyll *c* pigments and their distribution in the chromophyte algae. In *The Chromophyte algae: problems and perspectives*. (eds. J. C. Green, B. S. C. Leadbeater and W. L. Diver) Clarendon Press. pp 13-36.
- Jézéquel D., Brayner R., Metzger E., Viollier E., Prévot F. and Fiévet F.** (2007) Two-dimensional determination of dissolved iron and sulfur species in marine sediment pore-waters by thin-film based imaging. Thau lagoon (France). *Estuar. Coast. Shelf Sci.* **72**, 420–431.
- Jørgensen B. B., Revsbech N. P., Blackburn T. H. and Cohen Y.** (1979) Diurnal cycle of oxygen and sulfide microgradients and microbial photosynthesis in a cyanobacterial mat sediment. *Appl. Envir. Microbiol.* **38**, 46–58.
- Jørgensen B. B., Revsbech N. P. and Cohen Y.** (1983) Photosynthesis and structure of benthic microbial mats: microelectrode and SEM studies of four cyanobacterial communities. *Limnol. Ocean. (United States)* **28:6**, 1075–1093.
- Jørgensen B. B., Cohen Y. and Des Marais D. J.** (1987) Photosynthetic action spectra and adaptation to spectral light distribution in a benthic cyanobacterial mat. *Appl. Environ. Microbiol.* **53**, 879–886.
- Jørgensen B. B. and Des Marais D. J.** (1988) Optical properties of benthic photosynthetic Fiber-optic studies of cyanobacterial mats communities. *Limnol. Oceanogr.* **33**, 99–113.

- Jørgensen B.** (1994) Diffusion processes and boundary layers in microbial mats. *Microb. Mats NATO ASI* **35**, 243–253.
- Joye S. B., Mazzotta M. L. and Hollibaugh J. T.** (1996) Community metabolism in microbial mats: the occurrence of biologically-mediated iron and manganese reduction. *Estuar. Coast. Shelf Sci.* **43**, 747–766.
- Keeling C., Bacastow R., Carter A., Piper S., Whorf T., Heimann M., Mook W. and Roeloffzen H.** (1989) A three-dimensional model of atmospheric CO₂ transport based on observed winds. 1. Analysis of observational data. Aspects of Climate Variability in the Pacific and the Western Americas. *Geophys. Monogr. Ser.* **55**, 165–236.
- Kenyon C. N., Rippka R. and Stanier R. Y.** (1972) Fatty acid composition and physiological properties of some filamentous blue-green algae. *Arch. Mikrobiol.* **83**, 216–236.
- Knoll A.** (2003) *Life on a Young Planet*. Princeton University Press, Princeton, NJ.
- Knoll A. H., Javaux E. J., Hewitt D. and Cohen P.** (2006) Eukaryotic organisms in Proterozoic oceans. *Philos. Trans. R. Soc. Lond. B. Biol. Sci.* **361**, 1023–1038.
- Koopmans M. P., Koster J., van Kaam-peters H. M. E., Kenig F., Schouten S., Hartgers W. A., De Leeuw J. W. and Sinninghe-Damsté J. S.** (1996) Diagenetic and catagenetic products of isorenieratene: Molecular indicators for photic zone anoxia. *Geochim. Cosmochim. Acta* **60**, 4467–4496.
- Kühl M., Chen M. and Larkum A. W. D.** (2007) Cellular Origin, Life in Extreme Habitats and Astrobiology. In *Algae and cyanobacteria in extreme environments, volume 11*. (ed. J. Seckbach). Springer, Dordrecht, pp. 101–123.
- Lipp J. S., Morono Y., Inagaki F. and Hinrichs K.-U.** (2008) Significant contribution of Archaea to extant biomass in marine subsurface sediments. *Nature* **454**, 991–994.
- Logan B. W.** (1961) Cryptozoon and Associate Stromatolites from the recent, Shark Bay, Western Australia. *J. Geol.* **69**, 517–533.
- Logan B. W. and Cebulski D. E.** (1970) Sedimentary Environments of Shark Bay, Western Australia. *Am. Assoc. Pet. Geol. Mem* **13**, 1–37.
- Logan B. W.** (1974) Evolution and diagenesis of Quarternary carbonate sequences, Shark Bay, Western Australia. *Am. Assoc. Pet. Geol. Mem.* **22**, 195–249.
- Lomstein B., Jensen A., Hansen J., Andreasen J., Hansen L., Berntsen J. and Kunzendorf H.** (1998) Budgets of sediment nitrogen and carbon cycling in the shallow water of Knebel Vig, Denmark. *Aquat. Microb. Ecol.* **14**, 69–80.

- Londry K. L., Jahnke L. L. and Des Marais D. J.** (2004) Stable carbon isotope ratios of lipid biomarkers of sulfate-reducing bacteria. *Appl. Environ. Microbiol.* **70**, 745–751.
- López-Lara I. M., Sohlenkamp C. and Geiger O.** (2003) Membrane lipids in plant-associated bacteria: their biosyntheses and possible functions. **16**, 567–579.
- Love D., Snape C., Carr A. D. and Houghton C.** (1995) Release of covalently-bound alkane biomarkers in high yields from kerogen via catalytic hydrolysis. *Org. Geochem.* **23**, 981–986.
- Matthews D. and Hayes J.** (1978) Isotope-ratio-monitoring gas chromatography-mass spectrometry. *Anal. Chem.* **50**, 1465–1473.
- McKirdy D. M., Thorpe C. S., Haynes D. E., Grice K., Krull E. S., Halverson G. P. and Webster L. J.** (2010) The biogeochemical evolution of the Coorong during the mid- to late Holocene: an elemental, isotopic and biomarker perspective. *Org. Geochem.* **41**, 96–110.
- Melendez I., Grice K. and Schwark L.** (2013) Exceptional preservation of Palaeozoic steroids in a diagenetic continuum. *Nat. Sci. Reports* **3**, 1–6.
- Mendelson C. and Schopf J. W.** (1992) Proterozoic and selected Early Cambrian microfossils and microfossil-like objects. In *The Proterozoic Biosphere: A multidisciplinary study* (eds. J. W. Schopf, C. Klein). Cambridge University Press, Cambridge, pp. 865–951.
- Millero F. J.** (1991) The oxidation of H₂S in Framvaren Fjord. *Limnol. Oceanogr.* **36**, 1007–1014.
- Minnikin D. E. and Abdolrahimzadeh H.** (1974) Effect of pH on the proportions of polar Lipids in chemostat cultures of *Bacillus subtilis*. *J. Bacteriol.* **120**, 999–1003.
- Mook W. G., Bommerson J. C. and Staverman W. H.** (1974) Carbon isotope fractionation between dissolved bicarbonate and gaseous carbon dioxide. *Earth Planet. Sci. Lett.* **22**, 169–176.
- Murray J., Stewart K., Kassakian S., Krynytzky M. and Di Julio D.** (2007) Oxic, suboxic, and anoxic conditions in the Black Sea. In *The black sea flood question, changes in coastline, climate and human settlement*. (eds. V. Yanko-Hombach, A. S. Gilbert, N. Panin, P. M. Dolukhanow) Springer, Dordrecht, pp. 1–21.
- Nabbefeld B., Grice K., Schimmelmann A., Summons R. E., Troitzsch U. and Twitchett R. J.** (2010) A comparison of thermal maturity parameters between freely extracted hydrocarbons (Bitumen I) and a second extract (Bitumen II) from within the kerogen matrix of Permian and Triassic sedimentary rocks. *Org. Geochem.* **41**, 78–87.

- Navarrete A.** (1999) PhD thesis. Caracterización bioquímica y ecofisiológica de los tapetes microbianos del delta del Ebro. Universitat de Barcelona, Barcelona, Spain.
- Navarrete A., Peacock A., Macnaughton S. J., Urmeneta J., Mas-Castellà J., White D. C. and Guerrero R.** (2000) Physiological status and community composition of microbial mats of the Ebro Delta, Spain, by signature lipid biomarkers. *Microb. Ecol.* **39**, 92–99.
- Nicholson J., Stolz J. F. and Pierson B.** (1987) Structure of a microbial mat at Great Sippewissett Marsh, Cape Cod, Massachusetts. *FEMS Microbiol. Ecol.* **45**, 343–364.
- Niemann H. and Elvert M.** (2008) Diagnostic lipid biomarker and stable carbon isotope signatures of microbial communities mediating the anaerobic oxidation of methane with sulphate. *Org. Geochem.* **39**, 1668–1677.
- Oliver J. D. and Colwell R. R.** (1973) Extractable lipids of gram-negative marine bacteria: fatty - acid composition. *Int. J. Syst. Bacteriol.* **23**, 442–458.
- Olsen I. and Jantzen E.** (2001) Sphingolipids in bacteria and fungi. *Anaerobe* **7**, 103–112.
- Overmann J., Cypionka H. and Pfennig N.** (1992) An extremely low-light-adapted phototrophic sulfur bacterium from the Black Sea. *Limnol. Oceanogr.* **37**, 150–155.
- Paerl H. W. and Pinckney J. L.** (1996) A mini-review of microbial consortia: Their roles in aquatic production and biogeochemical cycling. *Microb. Ecol.* **31**, 225–247.
- Pagès A., Teasdale P. R., Robertson D., Bennett W. W., Schäfer J. and Welsh D. T.** (2011) Representative measurement of two-dimensional reactive phosphate distributions and co-distributed iron(II) and sulfide in seagrass sediment porewaters. *Chemosphere* **85**, 1256–1261.
- Pagès A., Welsh D. T., Robertson D., Panther J. G., Schäfer J., Tomlinson R. B. and Teasdale P. R.** (2012) Diurnal shifts in co-distributions of sulfide and iron(II) and profiles of phosphate and ammonium in the rhizosphere of *Zostera capricorni*. *Estuar. Coast. Shelf Sci.* **115**, 282–290.
- Pagès A., Grice K., Vacher M., Teasdale P., Welsh D., Bennett W. and Greenwood P.** (2014a) Characterising microbial communities and processes in a modern stromatolite (Shark Bay) using lipid biomarkers and two-dimensional distributions of porewater solutes. *Environ. Microbiol.*, accepted.
- Palmisano A., Cronin S. and Des Marais D. J.** (1988) Analysis of lipophilic pigments from a phototrophic microbial mat community by high performance liquid chromatography. *J. Microbiol. Methods* **8**, 209–217.

- Palmisano A. C., Summons R. E., Cronin S. E. and Des Marais D. J.** (1989) Lipophilic pigments from cyanobacterial (blue-green algal) and diatom mats in Hamelin Pool, Shark Bay, Western Australia. *J. Phycol.* **25**, 655–661.
- Paoletti C., Pushparaj B., Florenzano G., Capella P. and Lercker G.** (1976) Unsaponifiable matter of green and blue-green algal lipids as a factor of biochemical differentiation of their biomasses: I. Total unsaponifiable and hydrocarbon fraction. *Lipids* **11**, 258–265.
- Peters K. E., Walters C. C. and Moldowan J. M.** (2005) *The Biomarker Guide: Biomarkers and isotopes in the environment and human history, Volume 1*. Cambridge University Press.
- Pierson B. K. and Castenholz R. W.** (1971) Bacteriochlorophylls in gliding filamentous prokaryotes from hot springs. *Nature* **233**, 25–27.
- Playford P. E.** (1990) Geology of the Shark Bay area, Western Australia. In *Research in Shark Bay. Report of the France-Australe Bicentenary Expedition Committee. Western Australian Museum, Perth.* (eds. P.F. Berry, , S. D. Bradshaw and B. R. Wilson, B.R.), pp. 13–33.
- Popp B. N., Lawa E. A., Bidigare R. R., Dore J. E., Hanson K. L. and Wakeham S. G.** (1998) Effect of phytoplankton cell geometry on carbon isotopic fractionation. *Geochim. Cosmochim. Acta* **62**, 69–77.
- Price R. M., Skrzypek G., Grierson P. F., Swart P. K. and Fourqurean J. W.** (2012) The use of stable isotopes of oxygen and hydrogen to identify water sources in two hypersaline estuaries with different hydrologic regimes. *Mar. Freshw. Res.* **63**, 952–966.
- Quandt L., Gottschalk G., Ziegler H., and Stichler W.** (1977) Isotopic discrimination by photosynthetic bacteria. *FEMS Microbiol. Lett.* **1**, 125–128.
- Rasmussen B., Fletcher I. R., Brocks J. J. and Kilburn M. R.** (2008) Reassessing the first appearance of eukaryotes and cyanobacteria. *Nature* **455**, 1101–1104.
- Ratledge C. and Wilkinson S.** (1988) *Microbial lipids*. Academic Press.
- Revsbech N. P., Jorgensen B. B., Blackburn T. H. and Cohen Y.** (1983) Microelectrode studies of the photosynthesis and H₂S, and pH profiles of a microbial mat. *Limnol. Oceanogr.* **28**, 1062–1074.
- Riding R.** (2000) Microbial carbonates: the geological record of calcified bacterial-algal mats and biofilms. *Sedimentology* **47**, 179–214.
- Robertson D., Teasdale P. R. and Welsh D. T.** (2008) A novel gel-based technique for the high resolution, two-dimensional determination of iron(II) and sulfide in sediment. *Limnol. Oceanogr. Methods* **6**, 502–512.

- Robertson D., Welsh D. T. and Teasdale P. R.** (2009) Investigating biogenic heterogeneity in coastal sediments with two-dimensional measurements of iron(II) and sulfide. *Environ. Chem.* **6**, 60–69.
- Robinson N. and Eglinton G.** (1990) Lipid chemistry of Icelandic hot spring microbial mats. *Org. Geochem.* **15**, 291–298.
- Rontani J.-F. and Volkman J. K.** (2005) Lipid characterization of coastal hypersaline cyanobacterial mats from the Camargue (France). *Org. Geochem.* **36**, 251–272.
- Rossel P. E., Lipp J., Fredricks H., Arnds J., Boetius A., Elvert M. and Hinrichs K.-U.** (2008) Intact polar lipids of anaerobic methanotrophic Archaea and associated bacteria. *Org. Geochem.* **39**, 992–999.
- Rossel P. E., Elvert M., Ramette A., Boetius A. and Hinrichs K.-U.** (2011) Factors controlling the distribution of anaerobic methanotrophic communities in marine environments: Evidence from intact polar membrane lipids. *Geochim. Cosmochim. Acta* **75**, 164–184.
- Rütters H., Sass H., Cypionka H. and Rullkötter J.** (2002) Phospholipid analysis as a tool to study complex microbial communities in marine sediments. *J. Microbiol. Methods* **48**, 149–160.
- Schmidt K.** (1979) Biosynthesis of carotenoids. In *The Photosynthetic Bacteria*. (eds. R. K. Clayton and W. R. Sistrom) Plenum Press, pp. 729–750.
- Scholle P.** (1995) Carbon and Sulfur Isotope Stratigraphy of the Permian and Adjacent Intervals. In *The Permian of Northern Pangea*. (eds. P. Scholle, T. Peryt, D. Ulmer-Scholle) Springer Berlin Heidelberg, pp. 133–149.
- Schopf J. W.** (1999) *Cradle of Life*. Princeton University Press, Princeton, NJ.
- Schopf J. W., Kudryavtsev A. B., Agresti D. G., Czaja A. D. and Wdowiak T. J.** (2005) Raman imagery: a new approach to assess the geochemical maturity and biogenicity of permineralized precambrian fossils. *Astrobiology* **5**, 333–371.
- Schopf J. W., Kudryavtsev A. B., Czaja A. D. and Tripathi A. B.** (2007) Evidence of Archean life: stromatolites and microfossils. *Precambrian Res.* **158**, 141–155.
- Schouten S., Klein Breteler W. C., Blokker P., Schogt N., Rijpstra W. I. C., Grice K., Baas M. and Sinninghe-Damsté J. S.** (1998) Biosynthetic effects on the stable carbon isotopic compositions of algal lipids: implications for deciphering the carbon isotopic biomarker record. *Geochim. Cosmochim. Acta* **62**, 1397–1406.

- Schubotz F., Wakeham S. G., Lipp J. S., Fredricks H. F. and Hinrichs K.-U.** (2009) Detection of microbial biomass by intact polar membrane lipid analysis in the water column and surface sediments of the Black Sea. *Environ. Microbiol.* **11**, 2720–2734.
- Semikhatov M. A., Gebelein C. D., Could P., Awramik S. M. and Benmore W. C.** (1979) Stromatolite morphogenesis-progress and problems. *Can. J. Earth Sci.* **16**, 992–1015.
- Shiea J., Brassell S. C. and Ward D. M.** (1990) Mid-chain branched mono- and dimethyl alkanes in hot spring cyanobacterial mats: A direct biogenic source for branched alkanes in ancient sediments? *Org. Geochem.* **15**, 223–231.
- Shimada H., Nemoto N., Shida Y., Oshima T. and Yamagishi A.** (2008) Effects of pH and temperature on the composition of polar lipids in *Thermoplasma acidophilum* HO-62. *J. Bacteriol.* **190**, 5404–5411.
- Shuttleworth S. M., Davison W. and Hamilton-Taylor J.** (1999) Two-dimensional and fine structure in the concentrations of iron and manganese in sediment porewaters. *Environ. Sci. Technol.* **33**, 4169–4175.
- Sinninghe Damsté J. S. and de Leeuw J. W.** (1990) Analysis, structure and geochemical significance of organically-bound sulphur in the geosphere: State of the art and future research. *Org. Geochem.* **16**, 1077–1101.
- Smith S. V. and Atkinson M. J.** (1983) Mass balance of carbon and phosphorus Shark Bay, Western Australia. *Limnol. Oceanogr.* **28**, 625–639.
- Stal L., Van Gernerden H. and Krumbein W.** (1985) Structure and development of a benthic marine microbial mat. *FEMS Microbiol. Ecol.* **31**, 111–125.
- Stal L. J.** (2001) Coastal microbial mats: the physiology of a small-scale ecosystem. *South African J. Bot.* **67**, 399–410.
- Stockdale A., Davison W. and Zhang H.** (2009) Micro-scale biogeochemical heterogeneity in sediments: A review of available technology and observed evidence. *Earth-Science Rev.* **92**, 81–97.
- Sturt H. F., Summons R. E., Smith K., Elvert M. and Hinrichs K.-U.** (2004) Intact polar membrane lipids in prokaryotes and sediments deciphered by high-performance liquid chromatography/electrospray ionization multistage mass spectrometry-new biomarkers for biogeochemistry and microbial ecology. *Rapid Commun. Mass Spectrom.* **18**, 617–628.
- Summons R. E. and Powell T. G.** (1986) *Chlorobiaceae* in Paleozoic seas revealed by biological markers, isotopes and geology. *Nature* **319**, 763–765.
- Summons R. E. and Powell T. G.** (1987) Identification of aryl isoprenoids in source rocks and crude oils: Biological markers for the green sulphur bacteria. *Geochim. Cosmochim. Acta* **51**, 557–566.

- Summons R. E., Barrow R., Capon R., Hope J. and Stranger C.** (1993) The Structure of a new C₂₅ isoprenoid alkene biomarker from diatomaceous microbial communities. *Aust. J. Chem.* **46**, 907-915.
- Summons R. E., Jahnke L. L. and Roksandic Z.** (1994) Carbon isotopic fractionation in lipids from methanotrophic bacteria: Relevance for interpretation of the geochemical record of biomarkers. *Geochim. Cosmochim. Acta* **58**, 2853–2863.
- Summons R. E., Jahnke L. L., Hope J. and Logan G. A.** (1999) 2-Methylhopanoids as biomarkers for cyanobacterial oxygenic photosynthesis. *Nature* **400**, 554–557.
- Summons R. E., Bird L. R., Gillespie A L., Pruss S. B., Roberts M. and Sessions A. L.** (2013) Lipid biomarkers in ooids from different locations and ages: evidence for a common bacterial flora. *Geobiology* **11**, 420–436.
- Taylor J. and Parkes R. J.** (1983) The cellular fatty acids of the sulphate-reducing bacteria. *J. Gen. Microbiol.* **129**, 3303–3309.
- Taylor J. and Parkes R. J.** (1985) Identifying different populations of sulphate-reducing bacteria within marine sediment systems, using fatty acid biomarkers. *Microbiology* **131**, 631–642.
- Teasdale P. R., Batley G. E., Apte S. C. and Webster I. T.** (1995) Pore water sampling with sediment peepers. *Trends Anal. Chem.* **14**, 250–256.
- Teasdale P. R., Hayward S. and Davison W.** (1999) In situ, high-resolution measurement of dissolved sulfide using Diffusive Gradients in Thin Films with computer-imaging densitometry. *Anal. Chem.* **71**, 2186–2191.
- Thiel V., Merz-preiß M., Reitner J. and Michaelis W.** (1997) Biomarker studies on microbial carbonates: extractable lipids of a calcifying cyanobacterial mat (Everglades , USA). *Facies* **36**, 163–172.
- Thiel V., Peckmann J., Richnow H. H., Luth U., Reitner J. and Michaelis W.** (2001) Molecular signals for anaerobic methane oxidation in Black Sea seep carbonates and a microbial mat. *Mar. Chem.* **73**, 97–112.
- Tissot B. and Welte D.** (1984) *Petroleum Formation and Occurrence*. Springer, Berlin.
- Tunlid A. and White D. C.** (1992) Biochemical analysis of biomass, community structure, nutritional status, and metabolic activity of microbial communities in soil. In *Soil Biochemistry* (eds. J. M. Bollag and G. Stotzk). Marcel Dekker, pp. 229–262.
- Urey H.** (1947) The thermodynamic properties of isotopic substances. *J. Chem. Soc.*, 562–581.

- Van Gernerden H., Tughan C. S., de Wit R. and Herbert R. A.** (1989) Laminated microbial ecosystems on sheltered beaches in Scapa Flow, Orkney Islands. *FEMS Microbiol. Lett.* **62**, 87–101.
- Van Gernerden H.** (1993) Microbial mats: A joint venture. *Mar. Geol.* **113**, 3–25.
- Van Kaam-Peters H. M. ., Köster J., van der Gaast S. J., Dekker M., de Leeuw J. W. and Sinninghe Damsté J. S.** (1998) The effect of clay minerals on diasterane/sterane ratios. *Geochim. Cosmochim. Acta* **62**, 2923–2929.
- Van Mooy B. A. S., Rocap G., Fredricks H. F., Evans C. T. and Devol A. H.** (2006) Sulfolipids dramatically decrease phosphorus demand by picocyanobacteria in oligotrophic marine environments. *Proc. Natl. Acad. Sci. U. S. A.* **103**, 8607–8612.
- Vestal J. R. and White D. C.** (1989) Lipid analysis microbial ecology. *Bioscience* **39**, 535–541.
- Villanueva J., Grimalt J. O., de Wit R., Keely B. J. and Maxwell J. R.** (1994) Chlorophyll and carotenoid pigments in solar saltern microbial mats. *Geochim. Cosmochim. Acta* **58**, 4703–4715.
- Villanueva L., Navarrete A., Urmeneta J. and White D. C.** (2004) Physiological status and microbial diversity assessment of microbial mats: the signature lipid biomarker approach. *Ophelia* **58**, 165–173.
- Villbrandt M., Krumbein W. and Stal L.** (1991) Diurnal and seasonal variations of nitrogen fixation and photosynthesis in cyanobacterial mats. *Plant Soil* **137**, 13–16.
- Visscher P. T., Prins R. and van Gernerden H.** (1992a) Rates of sulfate reduction and thiosulfate consumption in a marine microbial mat. *FEMS Microbiol. Lett.* **86**, 283–294.
- Visscher P. T., Reid R. P., Bebout B. M., Hoefft S. E. H., Macintyre I. G. and Thompson Jr. J. A.** (1998) Formation of lithified micritic laminae in modern marine stromatolites (Bahamas): the role of sulfur cycling. *Am. Mineral.* **83**, 1482–1493.
- Visscher P. T. and Stolz J. F.** (2005) Microbial mats as bioreactors: populations, processes, and products. *Palaeogeogr. Palaeoclimatol. Palaeoecol.* **219**, 87–100.
- Volkman J. K.** (1986) A review of sterol markers for marine and terrigenous organic matter. *Org. Geochem.* **9**, 83–99.
- Volkman J. K., Barrett S. M., Blackburn S. I., Mansour M. P., Sikes E. L. and Gelin F.** (1998) Microalgal biomarkers: A review of recent research developments. *Org. Geochem.* **29**, 1163–1179.

- Walter M. R.** (1976) *Stromatolites*. Elsevier, Amsterdam.
- Watts C., Maxwell J. and Kjosén H.** (1977) The potential of carotenoids as environmental indicators. I. In *Advances in Organic Geochemistry* (eds. R. Campos, J. Gofii). Enadimsa, Madrid. pp. 391–413.
- White D. C., Davis W. M., Nickels J. S., King J. D. and Bobbie R. J.** (1979) Determination of the sedimentary microbial biomass by extractable lipid phosphate. *Oecologia* **40**, 51–62.
- Wickman F. E.** (1952) Variations in the relative abundance of the carbon isotopes in plants. *Geochim. Cosmochim. Acta* **2**, 243–254.
- Widerlund A. and Davison W.** (2007) Size and density distribution of sulfide-producing microniches in lake sediments. *Environ. Sci. Technol.* **41**, 8044–8049.
- Wieland A., Kühl M., McGowan L., Fourçans A., Duran R., Caumette P., García de Oteyza T., Grimalt J. O., Solé A., Diestra E., Esteve I. and Herbert R. A.** (2003) Microbial mats on the Orkney Islands revisited: microenvironment and microbial community composition. *Microb. Ecol.* **46**, 371–390.
- Wieland A., Pape T., Möbius J., Klock J.-H. and Michaelis W.** (2008) Carbon pools and isotopic trends in a hypersaline cyanobacterial mat. *Geobiology* **6**, 171–186.
- Wilkinson S. G.** (1988) Gram-negative bacteria. In *Microbial Lipids, Volume 1* (eds. C. Ratledge and S. G. Wilkinson). Academic Press, London, pp. 299–489.
- Winters K., Parker P. L. and Van Baalen C.** (1969) Hydrocarbons of blue-green algae: geochemical significance. *Science* **163**, 467–468.
- Zhang C. L., Fouke B. W., Bonheyo G. T., Peacock A. D., White D. C., Huang Y. and Romanek C. S.** (2004) Lipid biomarkers and carbon-isotopes of modern travertine deposits (Yellowstone National Park, USA): Implications for biogeochemical dynamics in hot-spring systems. *Geochim. Cosmochim. Acta* **68**, 3157–3169.
- Zhang H., Davison W., Mortimer R., Krom M., Hayes P. and Davies I.** (2002) Localised remobilization of metals in a marine sediment. *Sci. Total Environ.* **296**, 175–187.
- Zhang J., Quay P. and Wilbur D.** (1995) Carbon isotope fractionation during gas-water exchange and dissolution of CO₂. *Geochim. Cosmochim. Acta* **59**, 107–114.

Zhu Q., Aller R. and Fan Y. (2006) A new ratiometric, planar fluorosensor for measuring high resolution, two-dimensional pCO₂ distributions in marine sediments. *Mar. Chem.* **101**, 40–53.

Zink K.-G., Wilked H., Disko U., Elvert M. and Horsfield B. (2003) Intact phospholipids; microbial “life markers” in marine deep subsurface sediments. *Org. Geochem.* **34**, 755–769.

Zink K.-G. and Mangelsdorf K. (2004) Efficient and rapid method for extraction of intact phospholipids from sediments combined with molecular structure elucidation using LC–ESI–MS–MS analysis. *Anal. Bioanal. Chem.* **380**, 798–812.

Appendix

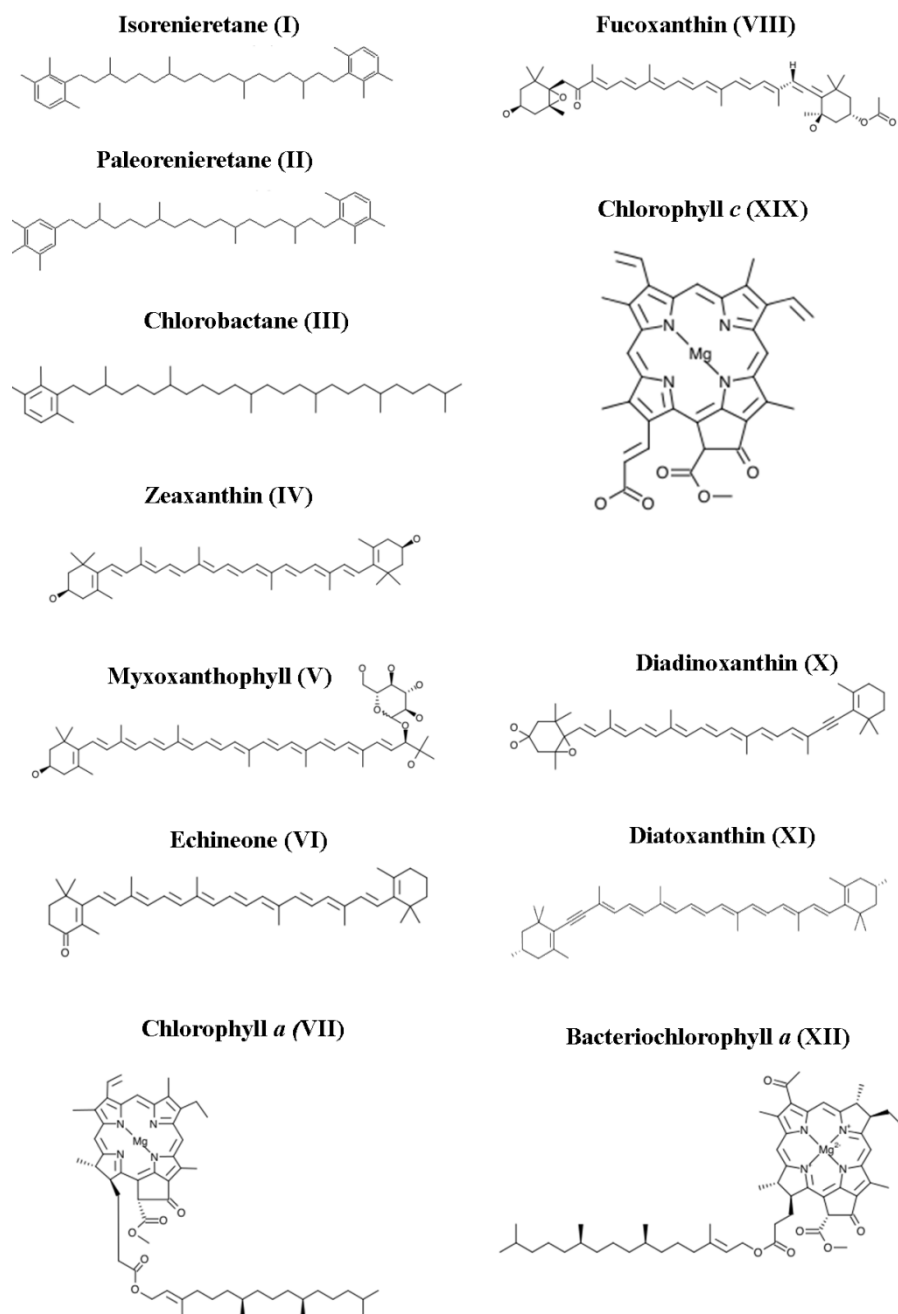


Figure A 1.1: Structures referred to in the text.

Chapter 2

Characterising microbial communities and processes in
a modern stromatolite (Shark Bay) using lipid
biomarkers and two-dimensional distributions of
porewater solutes.

**Anais Pagès, Kliti Grice, Michael Vacher, Peter R. Teasdale, David T. Welsh,
William W. Bennett, Paul Greenwood**

Environmental Microbiology, in press.

(impact factor 5.76)

Chapter 2

Abstract

Introduction

Materials and Methods

- Sampling site
- Sample description
- DET/DGT probes
 - Preparation of DGT and DET gels and assembly of combined DET/DGT probes
 - Deployment of combined DET-DGT probes
 - Analysis of sulfide and alkalinity co-distributions
 - Analysis of iron(II)-phosphate and co-distributions
- Lipid biomarkers
 - Sampling
 - Extraction
 - Column chromatography
 - Phospho-lipid fatty acids (PLFA)
 - Gas-Chromatography Mass-Spectrometry (GC-MS)

Results and Discussion

- Two-dimensional distributions of solute indicative of microbial activity
 - Co-distribution of alkalinity and sulfide
 - Co-distribution of phosphate and iron(II)
- Lipid biomarkers
 - Hydrocarbons
 - Phospho-lipid fatty acids (PLFAs)
- Microbial communities and biogeochemical cycles

Conclusions

Abstract

Modern microbial mats are highly complex and dynamic ecosystems. Diffusive equilibration in thin films (DET) and diffusive gradients in thin films (DGT) samplers were deployed in a modern smooth microbial mat from Shark Bay in order to observe, for the first time, two-dimensional distributions of porewater solutes during day and night time. Two-dimensional sulfide and alkalinity distributions revealed a strong spatial heterogeneity and a minor contribution of sulfide to alkalinity. Phosphate distributions were also very heterogeneous, while iron(II) distributions were quite similar during day and night with a few hotspots of mobilization. Lipid biomarkers from the three successive layers of the mat were also analysed in order to characterise the microbial communities regulating analyte distributions. The major hydrocarbon products detected in all layers included *n*-alkanes and isoprenoids, whilst other important biomarkers included hopanoids. Phospho-lipid fatty-acid (PLFA) profiles revealed a decrease in cyanobacterial markers with depth, whereas sulfate-reducing bacteria (SRB) markers increased in abundance in accordance with rising sulfide concentrations with depth. Despite the general depth trends in community structure and physiochemical conditions within the mat, two-dimensional solute distributions showed considerable small-scale lateral variability, indicating that the distributions and activities of the microbial communities regulating these solute distributions were equally heterogeneous and complex.

Introduction

Smooth microbial mats, commonly organised as stratified communities, are self-sustained ecosystems that exhibit intense recycling of carbon, sulfur, iron and nutrients (Des Marais, 2003). These modern mats have been increasingly studied by microbial ecologists as syntrophic microbial communities (van Gemerden, 1993) and because they are considered to be extant analogues of ancient stromatolites that have been observed in the rock record up to 3.5 Gyr (Walter et al., 1980; Hoffman, 2000; Allwood et al., 2006; Van Kranendonk et al., 2008). Modern microbial mats and strombolitic structures are present in the Shark Bay World Heritage area, located on the western coast of Australia (Logan, 1974).

Lipid analysis of microbial mats has provided significant information on the microbial community composition of mats and the preservation of biosignatures in the fossil record (Jahnke et al., 2004; Allen et al., 2010) and studies of the modern mats from Hamelin Pool and Garden Point (Shark Bay) have revealed a high degree of microbial biodiversity (Burns et al., 2004; Papineau et al., 2005; Allen et al., 2009; 2010). Consequently, lipid analyses of stratified microbial mats can lead to a better understanding of the structural distribution of the microbial communities involved in the major biogeochemical cycles of these systems.

In modern microbial mats, exceptionally high metabolic rates (Jørgensen et al., 1979) lead to steep biogeochemical gradients (e.g. redox potential and pH), although these gradients exhibit significant temporal and spatial fluctuations. Under light conditions, cyanobacterial photosynthesis leads to the production of oxygen, which can inhibit anaerobic processes such as dissimilatory sulfate reduction (Van Gemerden, 1993). In contrast, under dark conditions, oxygen is rapidly depleted and heterotrophic anaerobic processes dominate. These changes strongly influence solute distributions and variations in their concentrations between oxic and anoxic conditions are thus expected. However, considerable heterogeneity in oxygen distributions has been observed (Jørgensen et al., 1983; Glud et al., 1999), due to the high rates of oxygen production and consumption within these complex mats. Concentrations of oxygen have been shown to vary from > 1 atmospheric partial

pressure to complete depletion within only a few minutes (Jørgensen, 1994). Changes in oxygen distributions also significantly impact other biogeochemical cycles and the distributions of various solutes, resulting in micro-scale heterogeneity of biogeochemical zonation, that change over time (Paerl and Pinckney, 1996). This biogeochemical heterogeneity generates different microhabitats where niche microbial populations can live in close vicinity (Paerl et al., 2000) and form mutually beneficial relationships based on the diffusional transfer of nutrients, electron acceptors and donors (Van Gemerden, 1993).

The production and excretion of exo-polymeric substances (EPS) also favours small-scale spatial heterogeneity within mats. Microbes excrete many types of polymeric compounds that act as a cohesive matrix to bind particles and thus stabilize the mat structure (Decho, 2000; Braissant et al., 2009) and micro-domains of EPS presenting different physical and chemical properties have been reported at microscale (Decho, 2000). Consequently, the classical view of microbial mats as being strictly organised and of static structure has been revised (Visscher et al., 1998) suggesting that the typical one-dimensional profiles of physiochemical conditions within the mats may be unrepresentative. Thus, two-dimensional measurements and models are needed to understand the complex biogeochemical processes occurring within mats.

Conventional techniques such as core-slicing or microelectrodes are unable to accurately assess two-dimensional distributions of solutes (see Stockdale et al., 2009 for a review) at appropriate spatial scales. Additionally, artefacts associated with sample handling and mixing of porewater solutes during sampling have been reported for porewater extraction methods and sediment peepers (de Lange et al., 1992). Such artefacts can be minimised by using *in situ* passive sampling techniques, such as DET and DGT. The high resolution, two-dimensional distributions obtained by recently-described colourimetric DET and DGT techniques are powerful tools for the study of biogeochemical cycles in dynamic, heterogeneous environments (Robertson et al., 2008, 2009; Pagès et al., 2011, 2012; Bennett et al., 2012).

DET and DGT techniques are passive samplers developed for monitoring various natural waters, including porewaters (Davison et al., 1991; Davison and Zhang, 1994; Davison et al., 2000). DET is a diffusive equilibrium technique that uses a thin layer of hydrogel and protective membrane that equilibrates with porewater solutes in the sediment (Davison et al., 1991) or within microbial mats (Davison et al., 1997), typically over a deployment time of several hours (Davison et al., 2000). The DGT technique contains a similar thin hydrogel layer and membrane, but also contains a second thin layer, usually another hydrogel containing a binding agent selective for the solute(s) of interest (Davison and Zhang, 1994; Davison et al., 2000). The first hydrogel layer acts as a defined diffusive transport layer, while the analyte species are accumulated in the binding layer, resulting in the formation of a diffusive gradient between the sampled water and the binding gel surface. The DGT equation, derived from Fick's First Law of Diffusion, defines this process and relates the amount of analyte accumulated within the binding layer to the concentration in the waters being measured (Zhang and Davison, 1995; Davison et al., 2000):

$$C = M\Delta g / DtA$$

where, C is the time-averaged concentration of the analyte ($\mu\text{mol}\cdot\text{cm}^{-3} = 1.10^{-3}\mu\text{M}$), M is the mass of analyte accumulated (μmol), Δg the thickness (cm) of the diffusive layer (hydrogel layer and protective membrane), D the diffusive coefficient of the solute, t the time (s) and A the surface area (cm^2).

Recently, colourimetric DGT and DET methods (Teasdale et al., 1999; Jézéquel et al., 2008; Robertson et al., 2008; 2009; Pagès et al., 2011; Bennett et al., 2012; 2014) have been developed in order to rapidly obtain two-dimensional, high-resolution distributions of a range of solutes. Colour changes due to direct colouration of the DGT binding gel or staining of DET gels are quantified by computer imaging densitometry (CID) (Teasdale et al., 1999) using empirical calibration curves (Robertson et al., 2008). Since multiple hydrogels can be included in a single sampling probe, these methods also allow co-distributions of

different solutes to be measured simultaneously at the same location, overcoming problems of making separate measurements in heterogeneous systems and providing unprecedented information on solute and biogeochemical interactions (Robertson et al., 2008; 2009; Pagès et al., 2011; 2012). DGT samplers have previously been deployed in microbial mats in order to study dissolved metals at high resolution and revealed strong heterogeneity in the distributions of Zn, Fe, Mn and As (Davison et al., 1997).

In this study, for the first time in a modern microbial mat from Shark Bay, Western Australia, two-dimensional co-distributions of sulfide/alkalinity and iron(II)/phosphate under natural day and night conditions were measured at sub-mm resolution using colourimetric DET and DGT techniques. In order to further understand the role of specific microbial communities on biogeochemical cycling and solute distributions, we also investigated the distributions of lipid biomarkers (hydrocarbons and PLFAs) present in each layer of the smooth mat.

Materials and Methods

- **Sampling site**

The studied microbial mat was sampled from Nilemah, Shark Bay. Shark Bay is situated in Western Australia, about 800 km north of Perth. Nilemah is located on the southern area of Hamelin Pool which is the easterly embayment of this semi-enclosed zone and covers more than 123,800 ha with a maximum depth of 10 m. Water inflow is constrained by the presence of the Fauré Sill sandbank covered by seagrass beds in the northern part of the bay. In Hamelin Pool, the water is hypersaline (56-70 psu) because of limited rainfall and high evaporation rates (Logan and Cebulski, 1970) and the pH ranges between 7.5 and 8.4 (Jahnert and Collins, 2013). Seven types of microbial mats have been reported in Hamelin Pool (Logan et al., 1974) and mats cover approx. 300 km² of the total 1400 km² area (Jahnert and Collins, 2012). These microbial mats contain a wide variety of species (Allen et al., 2009) and present striking similarities to ancient stromatolites that are regarded as early-life organisms (Logan, 1961). The microbial smooth mats are composed of “millimetric laminae of fine sediment interbedded with laminae of

organic matter” (Jahnert and Collins, 2012). They have been observed in a variety of intertidal environments, fluctuating between 0.13 and 0.45 m Australian height datum (Burne and Johnson 2012). Microbial smooth mats are considered to be pioneering microbial assemblages colonizing recently deposited sediments (Burne and Johnson, 2012).

- **Sample description**

The microbial mat was sampled from Nilemah, Shark Bay, Western Australia. This highly stratified microbial mat consisted of 3 distinct layers visible to the naked eye: a first layer (pale yellow-green, characteristic of cyanobacteria) (1 mm), a second dark green layer (4 mm) and a third black layer likely containing FeS (5 mm). Microbial smooth mats from Nilemah have been previously described as “laminated microbial smooth stromatolites showing internal fabrics composed of flat sub-horizontal millimetric laminae made of fine grained carbonate sediment interbedded with laminae of microbial organic matter that become lithified as micrite laminae” (Jahnert and Collins, 2012). Their macro-fabric is easily identifiable as it shows laminar parallel layers similar to those in ‘classic’ stromatolites (Jahnert and Collins, 2013). Filamentous cyanobacteria contribute to the production of exopolymers that trap sediments and carbonate grains usually deriving from peloids, ooids, foraminifera, shell fragments or seagrass (Jahnert and Collins, 2013). This process has also been previously reported in Bahamian stromatolites (Visscher et al., 1998; Reid et al., 2000).

- **DET/DGT probes**

- *Preparation of DGT and DET gels and assembly of combined DET-DGT probes*

Deionised water (Milli-Q Element) was used to prepare all solutions. All DGT and DET probe components and glassware, including the plates used for gel castings were acid-cleaned in 10% (v/v) HNO₃ (AR grade, Merck) for at least 24 h and rinsed thoroughly with deionised water prior to use. The bisacrylamide cross-linked polyacrylamide diffusive gels (0.4 mm final thickness), used for iron(II),

phosphate and alkalinity DETs, DGT-sulfide binding gels, and staining gels for colorimetric iron(II), phosphate and alkalinity determinations, were prepared, cast and stored as previously described (Robertson et al., 2008).

Custom built sediment DGT/DET probes were constructed and assembled according to Robertson et al. (2008) with a DGT binding gel layer overlain by a diffusive gel layer and a 0.45 μm pore size polysulfone filter (Supor, Pall) of 0.1 mm thickness to protect the diffusive gel from damage during deployment and retrieval. The DET layer was disposed on top of the DGT layer, allowing both layers to record analyte distributions in the exact same position. Two probe combinations were used. The first was a two-layer probe combining an AgI-DGT for colourimetric sulfide and a diffusive layer for colourimetric alkalinity in order to assess two-dimensional co-distributions of sulfide and alkalinity. The second was a two layer probe with a first diffusive gel used as a colorimetric DET for iron(II) and a second diffusive layer used as a colorimetric DET for phosphate.

Prior to all deployments probes were deoxygenated by bubbling with N_2 for at least 3 h and were transported to the field in sealed containers under an N_2 atmosphere, to avoid possible artefacts that could be induced by the introduction of oxygen into the sediment during probe deployment.

➤ *Deployment of combined DET-DGT probes*

All field deployments were for approximately 8 h (exact times were recorded for the sulfide DGT calculation) which is more than the minimum time required for DET equilibration (Pagès et al., 2011) on the 26th and 27th of April 2012. For the night deployment, the probes were deployed after sunset (9 pm) and retrieved the following morning before sunrise (5 am). Blank probes were then deployed in the exact same area in order to easily identify the location for the second probes deployment (daytime deployment) 3 hours later and be able to compare day/night measurements. A second set of probes was then deployed in the

exact same area under daylight conditions between 8 am and 4 pm. Each probe was carefully pushed into the microbial mat.

➤ *Analysis of sulfide and alkalinity co-distributions*

The probes were immediately washed upon retrieval to remove sediment. Then a new stainless steel scalpel was used to rapidly cut out the two gel layers from the probe window. The alkalinity DET was immediately transferred onto a transparent sheet on a flat-bed scanner, stained using a reagent impregnated staining gel and distributions were acquired as previously described (Bennett et al., 2014). The sulfide-DGTs are stable and were stored in the dark and scanned as described by Robertson et al. (2008) 1 h later. In all cases, the scanned images were converted to greyscale (applying a green filter for alkalinity) and the file saved in TIFF format. The greyscale images were then re-sized so that 1 pixel was equal to 0.8 x 0.8 mm and the image was exported to Scion Image (Version 4.0.3.2, ScionCorp) where greyscale intensity values were converted to alkalinity and sulfide concentrations using the appropriate greyscale versus concentration calibration curve (Robertson et al., 2008, Bennett et al., 2014).

➤ *Analysis of iron(II)-phosphate and co-distributions*

Similarly to sulfide/alkalinity probes, the probes were immediately washed upon retrieval to remove all sediment. The gel layers were then cut out from the probe window. The iron(II) DET was immediately transferred onto a transparent sheet on a flat-bed scanner, stained using a ferrozine reagent impregnated staining gel and distributions were acquired as previously described by Robertson et al. (2008) and modified by Bennett et al., (2012). Similarly, the phosphate DET was laid over a molybdate-ascorbic acid impregnated staining gel between two transparency sheets. Distributions were acquired as previously described by Pagès et al., 2011. In both cases, the scanned images were converted to greyscale (applying a green filter for iron(II) and a red filter for phosphate) and the file saved in TIFF format. The greyscale images were then resized so that 1 pixel was equal to 0.8 x 0.8 mm and the image was exported to Scion Image (Version 4.0.3.2, ScionCorp) where greyscale intensity values were converted to iron(II), and

phosphate concentrations using the appropriate greyscale versus concentration calibration curve (Pagès et al., 2011; Bennett et al., 2012).

- **Lipid biomarkers**

- *Sampling*

The microbial mat was sampled in the field using an aluminum push core and immediately frozen (-18°C). The sample was taken in the exact same mat in which the DGT/DET samplers were deployed and during the same deployment period (April 2012). The sample was taken as close as possible to the DGT/DET samplers without perturbing the locations where the samplers were deployed. Prior to extraction, the sample was defrosted and the three different layers were sampled with a spatula, carefully removing the edges of the sample that were in contact with the coring material. Each layer was homogenised in order to obtain enough organic matter for further biolipids extraction. The spatula was carefully washed with dichloromethane (DCM) between each sample preparation.

- *Extraction*

The three different layers were then ultrasonically extracted (5 h) using a mixture of [9:1 DCM: Methanol (MeOH)]. The solvent was filtered to remove particulates from the samples and the excess solvent was removed from the extracts by rotary evaporation. Activated copper turnings were added and the extract was stirred (72 h) to remove elemental sulfur. The syringe used to transfer the extracts was cleaned with hexane a minimum of 20 times between each sample. Procedural blanks were performed throughout the entire process to confirm that the compounds identified were indigenous to the samples. The residue of each layer was stored in the dark at 5°C prior further analyses

- *Column chromatography*

Aliquots (500 µL out of 1 mL) of the extract of each layer were separated using a small column (5.5 cm x 0.5 cm i.d.) filled with activated silica gel (120°C, 8 h). The saturated hydrocarbon fraction was eluted with *n*-hexane (2 mL); the

aromatic hydrocarbon fraction with a mixture of (1:3 DCM: hexane, 2 mL) and the polar fraction with a mixture of (1:1 DCM: MeOH, 2 mL). The saturated fractions were reduced to near dryness by purging with N₂ and the fractions analysed by gas chromatography - mass spectrometry (GC-MS).

➤ *Phospho-Lipid Fatty Acids (PFLAs)*

PLFAs were analysed as fatty acid methyl esters, prepared using a modification of previously reported procedures (Bobbie and White, 1980; Zelles et al., 1995). Lipids were extracted by ultrasonication (15 min) of dry mat material (2 g) in a CHCl₃: CH₃OH: phosphate buffer (K₂HPO₄/ HCl) mixture (0.8:2:1; v/v/v) and isolated with additional CHCl₃ in the presence of water. The total-lipid extract was separated into different polarity fractions by successive elution through silica bonded columns (SPE-Si, Supelco, Poole, UK) with CHCl₃ (2 mL), acetone (2 mL) and CH₃OH (1mL) to sequentially remove neutral fatty acid (FA), free FA and PLFA fractions, respectively. The PLFA fraction was methylated by the addition of 0.2 M KOH-CH₃OH (0.5 mL) and heating up to 75 °C, cooled and neutralised with 0.2 M acetic acid (0.5 mL). Methylated PLFAs were subsequently isolated with an aqueous CHCl₃ mixture. PLFA fractions were analysed with an Agilent 6890/5975b GC-MS. The gas chromatograph was used in pulsed splitless mode, with He as carrier gas at a constant flow of 1.1 mL.min⁻¹ and the oven was programmed from 70 °C (held isothermal for initial 1 min) to 140 °C at 20 °C.min⁻¹, then to 290°C (held 15 min) at 4 °C.min⁻¹. 70 eV full scan (*m/z* 50–550) and selected ion data (*m/z* 55, 74, 87, 270, 284, 298, 312) were simultaneously acquired. Product identifications were based on effective chain length values measured using relative retention times. Relative product abundances were measured by integration of peaks in the total selected ion chromatogram.

➤ *Gas-Chromatography Mass-Spectrometry (GC-MS)*

GC-MS analyses were performed using an Agilent 6890 GC interfaced to an Agilent 5973 mass selective detector (MSD). The saturated hydrocarbon fractions, dissolved in *n*-hexane, were introduced *via* an Agilent 6890 Series Injector into the electronically pressure controlled (EPC) split/splitless injector (320°C) which was

operated in the pulsed splitless mode. The GC was fitted with a 60 m x 0.25 mm i.d. WCOT fused silica capillary column coated with a 0.25 μm film (DB-5MS, JandW Scientific). The oven temperature was programmed from 40 $^{\circ}\text{C}$ to 325 $^{\circ}\text{C}$ (at 3 $^{\circ}\text{C}\cdot\text{min}^{-1}$) with initial and final temperature hold times of 1 and 50 min, respectively. Ultra high purity helium was used as the carrier gas and maintained at a constant flow of 1.1 $\text{mL}\cdot\text{min}^{-1}$. The MSD was operated at 70 $e\text{V}$ and the mass spectra were acquired in full scan mode, 50-600 Daltons at ~ 4 scans per second and with a source temperature of 230 $^{\circ}\text{C}$.

Results and Discussion

- **Two-dimensional distributions of solutes indicative of microbial activity**

- *Co-distribution of alkalinity and sulfide*

Two-dimensional high-resolution (mm) co-distributions of alkalinity and sulfide, measured using combined DET/DGT probes for day and night conditions are presented in [Figure 2.1](#). These measurements provided information on each of the three microbial layers studied for their microbial composition, although only a few rows of pixels may actually correspond to the first and particularly second mat layers, and the surrounding biogeochemical conditions.

Alkalinity in microbial mats is an accurate proxy for carbonate precipitation (Arp et al., 2001; Dupraz et al., 2009). During the day, a background alkalinity ranging between 3 and 4 $\text{meq}\cdot\text{L}^{-1}$ was observed across the three different layers of the mat and remained stable in the underlying sediment ([Figure 2.1](#)). At several points, zones of higher concentration of alkalinity were observed. A small hotspot reaching 7.1 $\text{meq}\cdot\text{L}^{-1}$ was observed at a lateral position between 70 and 75 mm. At a lateral position of 5 mm, a vertical feature of alkalinity (up to 8 $\text{meq}\cdot\text{L}^{-1}$) was observed across the second and third layers and a horizontal feature (up to 7.6 $\text{meq}\cdot\text{L}^{-1}$) was present entirely within the second microbial layer between 6 and 12 mm depth. Several other higher alkalinity features were also present below the deepest microbial layer ([Figure 2.1](#)).

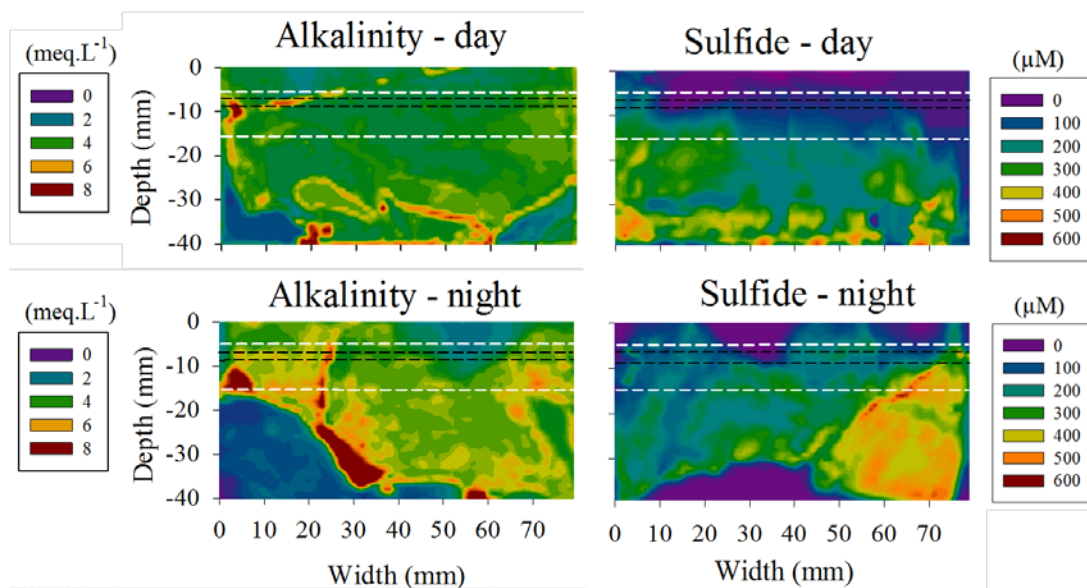


Figure 2.1: Two-dimensional distributions of sulfide and alkalinity from DGT and DET samplers in the mat during day and night. The white lines represent the entire mat. The black dotted lines represent the limits between the first, second and third layers. The region above the top white line represents the water and the area underneath the deeper white line represents the sediment.

The day-time sulfide distribution was more heterogeneous than the alkalinity distribution (Figure 2.1). Low to moderate concentrations of sulfide (0 to 100 μM) were observed across the two top layers at a lateral position between 20 and 80 mm. Concentrations up to 200 μM were measured for the first 20 mm, laterally. Higher sulfide concentrations (up to 370 μM) were present in the deeper part of the third layer implying the presence of strongly anoxic conditions; however, concentrations lower than 150 μM were also visible across this deep layer between 40 and 80 mm. Under anoxic conditions, sulfide accumulates as a result of bacterial sulfate-reduction. Sulfate-reduction is a key respiratory pathway (anaerobic respiration) (Canfield and Des Marais, 1993) using sulfate as the terminal electron acceptor and leading to the production of sulfide. Previous two-dimensional mapping of sulfate-reduction in microbial mats from the Bahamas highlighted both lateral and vertical variability in the activity of SRB, which is concordant with the heterogeneous sulfide distribution observed in this study (Visscher et al., 2000; Dupraz et al., 2004). The zones of lower sulfide concentration suggested a higher availability of oxygen in or near these particular areas. It is possible that a higher abundance of cyanobacteria was present in or close to these specific zones providing more oxygen for chemical or biological oxidation

of sulfur. Indeed, changes in pO_2 conditions within microns have been observed in a marine microbial mat, leading to dynamic microscale variations between O_2 supersaturation and anoxic conditions (Paerl et al., 1989). In addition, a mosaic in which the highest oxygen consumption sites were surrounded by the highest oxygen production areas has been previously observed in the cyanobacteria layer of a microbial mat (Glud et al., 1999), confirming heterogeneity in oxygen production and consumption. It is also possible that a higher proportion of photoautotrophic sulfur oxidising bacteria was present in these areas leading to higher rates of anaerobic sulfide consumption.

At night the distributions of solutes within the biofilm layers and surrounds were quite different to the daytime (Figure 2.1). For instance, the alkalinity distribution within the biofilm was much more heterogeneous during the night. A somewhat consistent background alkalinity (ca. $3.2\text{-}4\text{ meq.L}^{-1}$) was still observed within the microbial mat and extending above and below it. These background alkalinity values were slightly higher on average than those measured under daylight conditions. Several external features intruding into the mat, from above and below, produced some heterogeneity with concentrations outside this range. A zone of lower alkalinity value ($< 2\text{ meq.L}^{-1}$) above the biofilm crossed the top two layers of the biofilm at a lateral position between 50 and 65 mm. At a lateral position of about 25 mm, a vertical feature that resembled a small burrow with higher alkalinity, sometimes reaching 8 meq.L^{-1} , crossed the entire biofilm (see below for further discussion on burrowing organisms within the biofilm). Several other features with concentrations up to 6 and 8 meq.L^{-1} appeared, particularly within the deepest layer of the biofilm. These included a hotspot several mm across at a lateral position of 5 mm. Other large zones of intense alkalinity production similar to this hotspot also appeared below the biofilm, and were all adjacent to a zone below the biofilm with alkalinity $< 2\text{ meq.L}^{-1}$. This alkalinity distribution strongly suggested that the biofilm was both influencing and being influenced by its surrounds with this two-way interaction greatly contributing to lateral and vertical heterogeneity.

Sulfide was observed almost throughout the entire biofilm during the night time deployment and the concentrations were significantly higher than during the day. This increase in sulfide concentration at night is concordant with previous studies on microbial mats (Jørgensen and Revsbech, 1979; Revsbech et al., 1983; Dupraz and Visscher, 2005). Once again, features from the underlying sediment have clearly influenced sulfide concentrations and distributions within the biofilm. In the top two biofilm layers, sulfide concentrations did not exceed 240 μM with one exception, but were much lower ($< 100 \mu\text{M}$) at many points along the biofilm. On the far right of the distribution, a large sulfide hotspot several cm across and with sulfide concentrations from 400-600 μM crossed all layers of the biofilm, producing concentrations above 400 μM in layers 1 and 2. Zones of sulfide depletion (with concentrations approaching 0 μM) were also present between 30-40 mm and 60-70 mm, laterally. This horizontal heterogeneity may be related to changes in the surface topography of the mat which has been shown to strongly affect the properties of the diffusive boundary layer and highly favour lateral heterogeneity in the distribution of porewater analytes (Jørgensen, 1994; de Beer and Kühl, 2001). Sulfide concentrations were higher in the third layer with background concentrations reaching 300 μM and a line of sulfide over 600 μM was present within the large sulfide hotspot. The region of high sulfide concentration below the microbial mat suggested significant anaerobic activity in the underlying sediment. This has been reported previously in sediments underlying hypersaline cyanobacterial mats (Mouné et al., 2003). Several vertical features producing lower sulfide concentrations, where they intersected the biofilm, may have been burrows. Co-distributions of sulfide and iron(II) in a microcosm actually showed very specific distributions when the DGT/DET sampler was deployed adjacent to an amphipod burrow (Roberston et al., 2009).

Burrowing organisms such as nematodes have been reported in various microbial mats (Des Marais, 2003) and especially in Shark Bay modern microbial mats (Allen et al., 2009; 2010). Nematodes can form burrows that strongly affect biogeochemical processes and contribute to significant lateral heterogeneity in solute distributions (Pike et al., 2001). Sulfide concentrations around these suspected burrows (zones of zero sulfide) reached 400 μM within a few mm

suggesting a high rate of sulfate-reduction in the burrow walls. Burrow walls have been reported as organic-rich zones lined with secretions of mucus (Aller et al., 1983; Aller and Aller, 1986; Kristensen, 2000). In addition, macrofauna excrete organic acids such as lactate, succinate, acetate and propionate that can enhance the growth of SRB and lead to higher rates of sulfate-reduction in burrow walls (Hansen et al., 1996).

Alkalinity production represents a balance between the processes producing alkalinity (e.g. cyanobacterial photosynthesis, anoxygenic phototrophy and sulfate-reduction) and those favouring an alkalinity decrease (e.g. aerobic heterotrophy, sulfide oxidation and fermentation) (Visscher and Stolz, 2005; Dupraz et al., 2009). Biomarker distributions highlighted the presence of SRB and reducing conditions in the deepest mat layer suggesting that sulfate-reduction may have been a dominant process in the deep anoxic layer of the mat (see below). Sulfate-reduction can increase HCO_3^- concentration (equation 1) and consequently, directly leads to an alkalinity increase (Abd-el-Malek and Rizk, 1963).



As HCO_3^- can further react with Ca^{2+} ions to precipitate carbonate minerals (Lyons et al., 1984) (equation 2), sulfate-reduction has also been recognised as a major process favouring carbonate precipitation (Visscher et al., 2000; Dupraz and Visscher, 2005; Baumgartner et al., 2006). Indeed, Visscher et al. (2000) showed that sulfate-reduction rates were higher in areas of CaCO_3 precipitation highlighting the role of microbial communities in producing lithified micritic laminae close to the surface of the Bahamian stromatolites.



HS^- produced by sulfate-reduction can also react with H^+ to form H_2S and thus generate an alkalinity increase (Knull and Richards, 1969). However, the

organic matter breakdown also generates a suite of compounds other than sulfide that also influence alkalinity (e.g.: H₂, CO₂, acetate and other weak organic acids and inorganic nutrients such as phosphate or ammonium) (Knull and Richards, 1969).

The microniche of alkalinity across the second and third layer observed at a lateral position in the first 5 mm and a smaller alkalinity hot spot (between 10 and 20 mm) were not concordant with a rise in sulfide concentration. Anoxygenic phototrophy might have been the dominant process in this specific area which would lead to a higher alkalinity value without increasing sulfide concentrations. The presence of these organisms in the microbial mat was confirmed by biomarker results (see below). In addition, the timescales of the DGT and DET techniques also have to be considered. Sulfide concentrations measured with the DGT technique are representative of a time-integrated average of the sulfide concentrations over the entire deployment period (8 h). However, DET is based on equilibrium between the hydrogel and porewater solutes, therefore the alkalinity concentrations mainly represent the concentrations of the last few hours of the deployment period. Consequently, it is also possible that alkalinity hot spots were only present during the last period of the deployment and therefore, did not appear to concord with the time-integrated sulfide concentrations.

Under dark conditions, oxygen in the mat is rapidly depleted and anoxic conditions prevail (Canfield and Des Marais, 1993). As cyanobacteria and anoxygenic phototrophs switch to fermentation and denitrification, sulfate-reduction is usually the main bacterial process favouring alkalinity increase at night (Dupraz et al., 2009). The global increase in alkalinity values and sulfide concentrations under dark conditions was concordant with a predominance of sulfate-reduction in the mat. However, maximum alkalinity values were obtained between 0 and 10 mm in the deepest mat layer and this did not coincide with high sulfide concentrations, suggesting that sulfide did not make a major contribution to total alkalinity. Indeed, the maximum alkalinity value obtained reached 8 meq.L⁻¹, however, the maximum sulfide concentration measured was 0.6 mM.

Consequently, sulfide concentrations were significantly lower than alkalinity concentrations, suggesting that sulfide did not make a major contribution to total alkalinity in this microbial mat during day or night.

➤ *Co-distribution of phosphate and iron(II)*

Two-dimensional distributions of phosphate and iron(II) under daylight and night-time conditions, both measured by colorimetric DET techniques, are presented in Figure 2.2. Phosphate concentrations were highly heterogeneous for the daytime measurement. Background concentrations ranging between 1 and 2 μM were observed in the lateral zone between 20 and 75 mm, with a few small hotspots of over 3 μM also present and a highly localised hotspot of phosphate (up to 3.2 μM) visible at 75 mm in the third layer of the mat. Whereas, in the lateral zone between 0 and 20 mm, background phosphate concentrations ranged between 2.5 and 3.8 μM , with a maximum of 4 μM in the deeper layer.

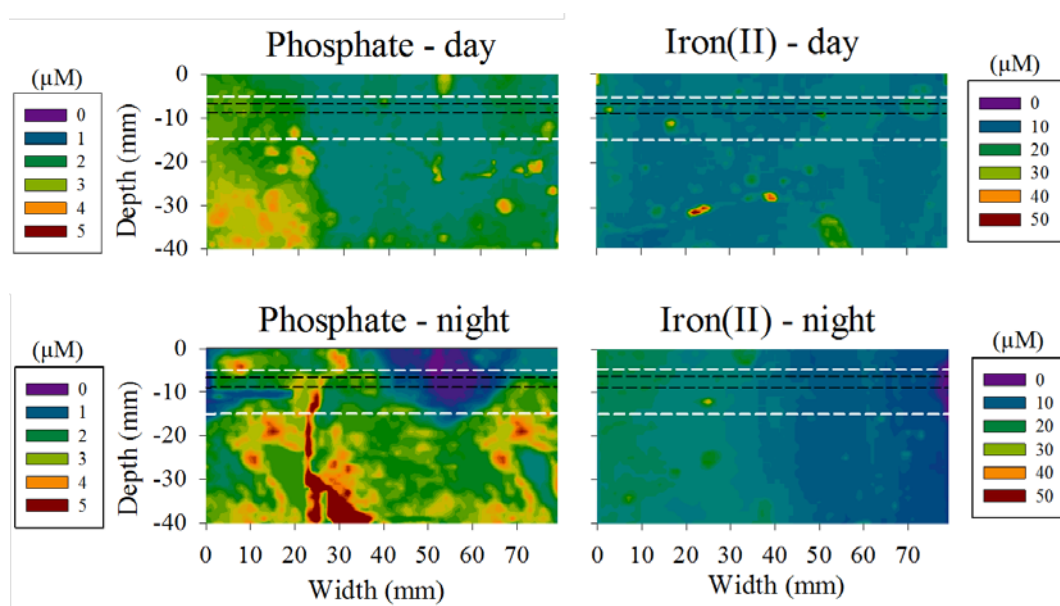


Figure 2.2: Two-dimensional distributions of phosphate and iron(II) from DET samplers in the mat during day and night. The white lines represent the entire mat. The black dotted lines represent the limits between the first, second and third layers. The region above the top white line represents the water and the area underneath the line represents the sediment.

The daytime iron(II) distribution was somewhat more homogeneous, with concentrations around 15 μM in the zone between lateral positions 0 and 40 mm and concentrations around 10 μM from 40 mm onwards, with a single hotspot of up to 25 μM intersecting the uppermost microbial layer in the top left hand corner of the distribution (Figure 2.2). A similar distribution was observed in the underlying sediment. These concentrations were low and it seems likely that the concentration of dissolved iron(II) was regulated by reaction with either oxygen or sulfide to generate Fe(III)OOH and Fe(II)S precipitates, respectively. As the probe was deployed during daytime, photosynthetic activity may have been dominant in the first layer. It appears that oxygen distributions might have been heterogeneous and lower for the first 40 mm. Indeed, higher oxygen concentrations between 40 and 80 mm, possibly related to the presence of burrows, could have transported oxygenated water, leading to the oxidation of iron(II) to iron(III) minerals. In this zone, phosphate would be expected to be trapped by these iron(III) oxyhydroxides (Parfitt et al., 1975), resulting in lower concentrations of both iron(II) and phosphate.

For the night-time measurement, porewater phosphate distributions were extremely heterogeneous and varied between 0 and 5 μM throughout the biofilm layers. Background concentrations ranging between 2 and 3.6 μM were visible at lateral positions between 0 and 40 mm and the last 10 mm. In between, a zone of near zero phosphate concentrations was observed across all three microbial layers. In the third layer, a microniche of phosphate was observed (5 μM) at 25 mm laterally, however, a strong depletion in phosphate was also observed in this layer for the first 20 mm, relatively close to the microniche and this local depletion was only visible in the third layer. The higher concentrations of phosphate at night may be related to the presence of more reducing conditions in the mat leading to an increase in porewater phosphate levels due to the reductive dissolution of iron(III)-phosphate complexes (Parfitt et al., 1975).

The daytime iron(II) distribution was very similar to the night-time distribution; iron(II) concentrations were lower in all three layers of the biofilm and in the underlying sediment between 40 and 80 mm. The biofilm layers 1-3 presented a similar distribution, with background concentrations varying between 12 to 25 μM for the first 40 mm and much lower concentrations (0 to 20 μM) over the next 40 mm. Within the third layer a microniche of iron(II) was present at 25 mm with concentrations reaching 35 μM . Some of the iron(II) microniches seemed to coincide with a line of higher phosphate concentrations, but the phosphate concentrations had very little in common with the iron(II) concentrations. Perhaps precipitation of iron(III) hydr(oxides) was effective at removing phosphate from solution but the phosphate was not being remobilised with subsequent iron(III) reduction.

- **Lipid biomarkers**

- *Hydrocarbons*

In order to characterise microbial communities present in each layer of the mat and those playing a role in regulating solute distributions and concentrations, lipid biomarkers from each layer of the mat were analysed. A wide variety of aliphatic hydrocarbons were observed in the mat layers analysed (Figure 2.3). *n*-alkanes, as highlighted in Figure 2.4, $m/z = 85$ fragmentogram, showed a bimodal distribution: short-chain *n*-alkanes ranging from C_{15} to C_{22} largely deriving from bacteria (Schirmer et al., 2010) and longer chain *n*-alkanes (C_{27} - C_{33}), with a predominance of odd-over-even chain lengths, largely of higher plant origin. Leaf waxes may have been imported to the mat in dust particles, as previously reported by Allen et al. (2010). The relatively high abundance of $\text{C}_{17:0}$ and the presence of $\text{C}_{17:1}$ confirmed the presence of a high proportion of cyanobacteria within the mat (Thiel et al., 1997; Wieland et al., 2003). Phytane, phytene and phytadiene isomers were present in all layers. Anaerobic microbial processes are known to degrade free phytol to form sedimentary phytene, *via* phytadiene intermediates (Grossi et al., 1998), and similar anaerobic processes within the mat are a potential source here. However, anaerobic hydrogenation of phytene does not seem to lead to phytane formation (Rontani et al., 2013). Phytane can also be derived from archaeal ether

lipids (Volkman, 1986) and this isoprenoid was identified in microbial mats where both ether-bound phytane and phytene were proposed to be derived from archaeol (Jahnke et al., 2008). No highly branched isoprenoid (HBI) alkenes characteristic of diatoms (C_{20} and C_{25}) were found in the mat, although diatoms have been previously reported in microbial mats from Shark Bay (Summons et al., 1993; Allen et al., 2010) and other contemporary hypersaline environments (McKirdy et al., 2010).

Hopanoids, markers of certain bacteria, were present in all layers. They ranged from C_{27} to C_{31} , and with common absence of C_{28} . Diploptene was the most abundant hopanoid in all layers, and its relative abundance decreased with depth (Figure 2.3). Diploptene may originate from a wide range of bacteria including cyanobacteria (Rohmer et al., 1984), methylotrophs (Summons et al., 1994) and sulfate reducing bacteria (SRB) such as *Desulfovibrio* (Blumenberg et al., 2006). Steroids (C_{27} - C_{29} sterenes) were also identified in all layers, with a strong predominance of cholestene (C_{27}). Cholest-5-en-3 β -ol, a precursor of C_{27} sterene, however, is recognised as a marker of eukaryotes (Volkman, 1986). The predominance of this sterene in the steroid fraction suggested a predominant eukaryotic input. Higher plants are a common source of 24-ethylcholest-5-en-3 β -ol, a precursor of C_{29} sterene, but this sterol has also been reported to be abundant in marine phytoplankton (e.g. green algae, Prymnesiophycean algae and cyanobacteria) (Volkman, 1986).

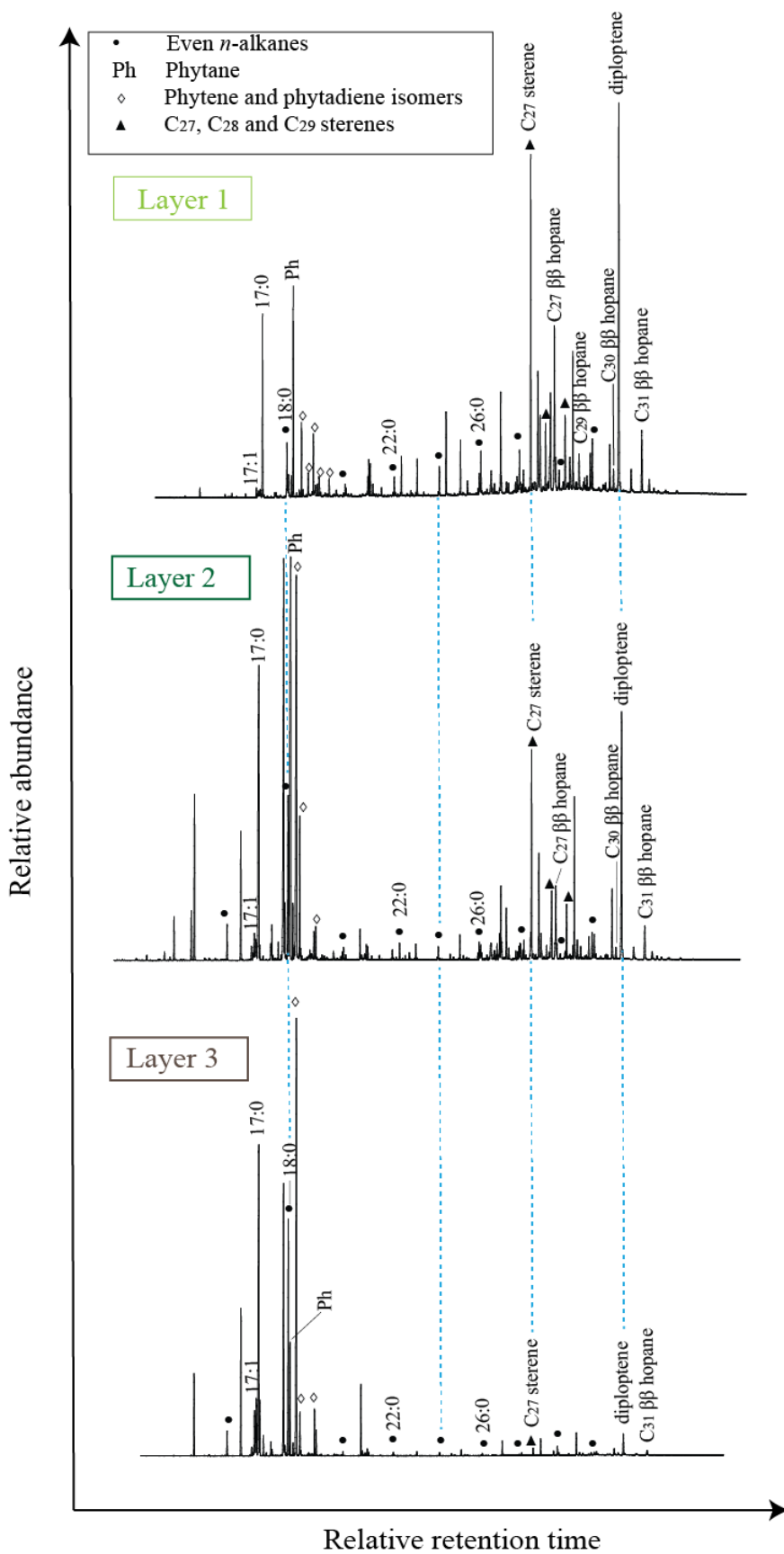


Figure 2.3: Total ion chromatograms from gas chromatography-mass spectrometry (GC-MS) analysis of the aliphatic hydrocarbon fractions from layers 1-3 of the smooth mat.

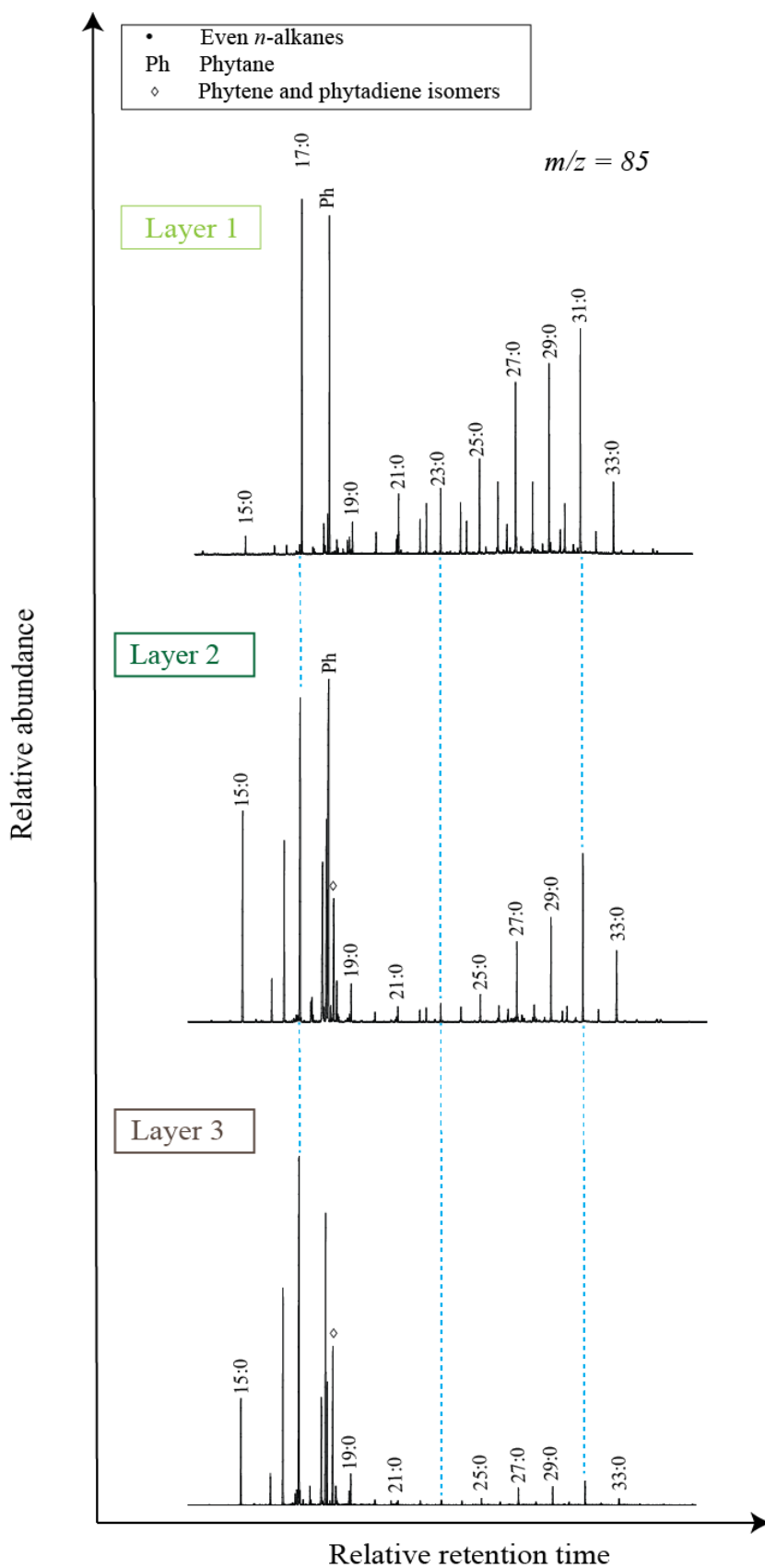


Figure 2.4: M/z 85 fragmentogram from GC-MS analysis of the aliphatic hydrocarbon fractions from layers 1-3 of the smooth mat.

The hydrocarbon distribution of the three layers reflected several changes in microbial community structure with depth (Figure 2.5). These results clearly demonstrated an increase in bacterial input with depth and a concomitant decrease in eukaryotes including land plant contributions. Figure 2.5A highlights the high abundance of hopanoids in the first layer as well as a strong contribution from eukaryotes (marine phytoplankton and higher plants), revealed by the presence of steroids and long-chain *n*-alkanes. In the deeper layers, the proportion of short-chain *n*-alkanes (C₁₆ – C₂₂) significantly increased. From layer 1 to layer 3 the abundances of the short chain *n*-alkanes increased from 12 to 84 %; the long-chain *n*-alkanes (C₂₇ – C₃₃) decreased from 24 to 8 %; and steroids decreased from 22 to 1 %. This confirmed the deposition of eukaryotic input (from the water column) at the surface of the mat as well as the aerosol transportation of leaf waxes (Allen et al., 2010). Hopanoid abundances strongly decreased with depth. Hopanoids are highly abundant in cyanobacteria (Talbot et al., 2008); however, they can also derive from other bacteria (e.g. SRB; Blumenberg et al., 2006). The much higher abundance in hopanoids in the top layer of the mat suggested a dominant cyanobacterial origin. There was a strong increase (10 to 64 %) in the proportion of phytene and phytadiene in the deeper layers (Figure 2.5B), implying the presence of reducing conditions at depth. These results are concordant with the general increase in sulfide concentration with depth, as recorded by DGT samplers (Figure 2.1).

The distribution of hopanes (Figure 2.5C) did not change significantly with depth, however, C₃₁ 17β (H), 21β (H)-homohopane increased by 4 % in the deeper layer (cf. surface layer). This compound has been reported in cyanobacteria (Talbot et al., 2008) but can also derive from *Desulfovibrio* strains (Blumenberg et al., 2006). Fatty acids characteristic of *Desulfovibrio* were identified in the deepest layer of the mat (see below), suggesting SRB were the main source of the C₃₁ homohopane.

The distribution of sterenes was consistent in the first two layers showing a regular predominance of C₂₇ cholest-2-ene, which was the only steroid detected in the deepest layer probably because of a similar high relative abundance (Figure 2.5D).

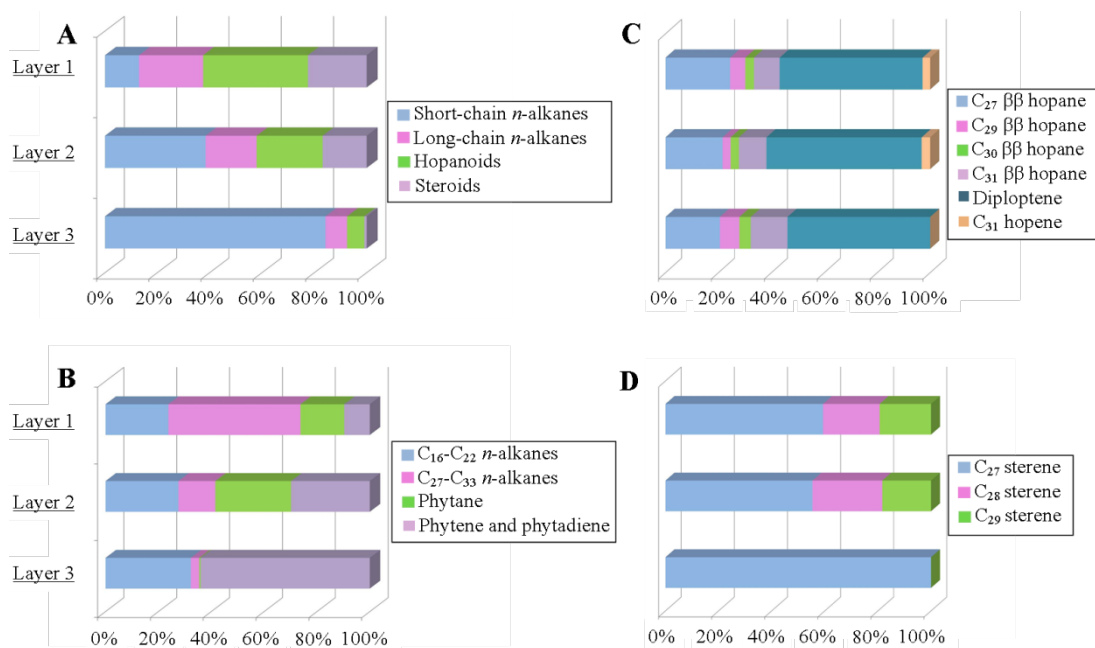


Figure 2.5: Lipid biomarker distribution over depth: (A) aliphatic hydrocarbons (short-chain/C₁₆-C₂₂ *n*-alkanes, long-chain/ C₂₇-C₃₃ *n*-alkanes, hopanoids, steroids); (B) short C₁₆-C₂₂ and long C₂₇-C₃₃ chain *n*-alkanes and highly branched isoprenoids (phytane, phytene and phytadiene isomers); (C) hopanoids (C₂₇ ββ hopane, C₂₉ ββ hopane, C₃₀ ββ hopane, C₃₁ ββ hopane, diploptene, C₃₁ hopene); (D) steroids (C₂₇ sterene, C₂₈ sterene, C₂₉ sterene).

➤ *Phospho-lipid fatty acids (PLFAs)*

The distributions of PLFAs (detected as their methyl esters) in the mat was dominated by straight-chain saturated and monounsaturated acids (Table 2.1). *Iso*- and *anteiso*-PLFAs, usually indicative of gram-positive bacteria (Navarrete et al., 2000) were not major components. Conversely, several PLFAs common to cyanobacterial communities (i.e., 16:0, 16:1 ω 7 and 18:1 ω 9 (Kenyon et al., 1972; Grimalt et al., 1991; Cohen et al., 1995) were detected in high abundance. Allen et al. (2010) similarly reported a dominance of these PLFAs in a smooth mat from Shark Bay. A decrease in the abundance of these biomarkers (cf. total PLFA signal)

with depth is also consistent with a cyanobacterial origin. The presence of highly abundant cyanobacterial markers in the upper layer confirmed that oxygen was being produced in this layer during the day, leading to lower concentrations in sulfide and iron(II) under daylight conditions, as measured by the DGT/DET samplers (Figure 2.1 and Figure 2.2, respectively).

Although the PLFA cyclopropyl-19:0 was detected in very low abundance in the mat, its presence might be indicative of SOB (Fourçans et al., 2004), suggesting the presence of green sulfur bacteria (*Chlorobi*) or colorless sulfur bacteria in the mat. This PLFA has also previously been identified in *Desulfobacter* (Londry et al., 2004), so may also reflect the presence of SRB. *Iso-17:1 ω 9*, a common marker of SRB, was identified in all mat layers suggesting the presence of these bacteria in the upper oxic layer, although the relative abundance of this PLFA significantly increased in the deeper anoxic layers. Although SRB are considered to be obligate anaerobic organisms, they have previously been observed in oxic waters and sediments (Cohen, 1984a; Hastings and Emerson, 1988; Saas et al., 1997), oxygen supersaturated mat layers (Visscher et al., 1992a; Krekeler et al., 1997; 1998; Minz et al., 1999) and sulfate-reduction can take place under fully oxic conditions (Dilling and Cypionka, 1990; Canfield and Des Marais 1991). Some SRB species are even capable of performing limited aerobic respiration (Dilling and Cypionka, 1990) and glycolate, a product of cyanobacterial photorespiration, has been suggested as a potential substrate for aerobic sulfate reduction (Fründ and Cohen, 1992). The vertical distribution of SRB is usually regulated by the presence of oxygen with oxygen-tolerant groups living at the surface of mats whilst strict anaerobes occur at some depth (Risatti et al., 1994). Additional lipid biomarkers indicative of SRB, such as *iso-* and *anteiso-17:0* previously reported in *Desulfovibrio* (Taylor and Parkes, 1985; Londry et al., 2004), were identified in all layers but were relatively more abundant in the deepest layer, which is concordant with the trend of increased sulfide concentrations with depth (Figure 2.1). Methyl octadecanoic acid, characteristic of *Actinomyces*, was not detected although previous studies on similar smooth mats from Shark Bay employing DNA analyses have confirmed the presence of these organisms (Allen et al., 2009).

3- and 2-hydroxy fatty acids (OH-FAs) typical of Gram negative bacteria were also detected and showed similar increases in relative abundance with depth. These fatty acids are constituents of the lipopolysaccharides found in the outer membrane of Gram negative bacteria (Wilkinson, 1988). Other organisms such as Gram-positive *Actinomyces* and certain fungi can also produce OH-FAs (Breman, 1988). However, OH-FAs with 14-18 carbons such as those detected here are usually attributed to Gram negative bacteria (Wilkinson, 1988).

Table 2.1: Distribution of PLFAs in the smooth mat (layers 1-3): PLFA are represented in % abundances of total PLFA.

	Layer 1	Layer 2	Layer 3		Layer 1	Layer 2	Layer 3
<u>Straight chain saturated</u>				<u>Monounsaturated</u>			
<i>n</i> -12:0	1	0.3	0.1	17:1 ω 3	<0.1	<0.1	0.2
<i>n</i> -14:0	8.2	6.5	4.4	<i>iso</i> -18:1	<0.1	<0.1	0.1
<i>n</i> -15:0	1.3	2.0	2.4	18:1 ω 9	2.6	3.0	1.5
<i>n</i> -16:0	48.9	44.1	29.7	18:1 ω 6	0.7	1.5	0.7
<i>n</i> -17:0	1.6	2.0	1.4	19:1 ω 11	0.1	<0.1	0.1
<i>n</i> -18:0	9.0	8.2	5.8	20:1 ω 9	0.2	0.4	0.2
Sum	70.0	63.1	43.8	cyclopropyl-19:0	<0.1	<0.1	0.1
<u>Branched saturated</u>				Sum	10.2	11.5	16.8
<i>iso</i> -14:0	0.4	0.5	0.7	<u>Polyunsaturated</u>			
<i>iso</i> -15:0	2.8	4.5	4.7	18:3 ω 6	<0.1	0.1	<0.1
<i>anteiso</i> -15:0	0.9	1.7	3.1	18:4 ω 3	0.2	0.2	0.3
<i>iso</i> -16:0	1.1	2.6	6.2	19:2 ω 6	0.1	<0.1	0.1
<i>iso</i> -17:0	1.0	1.4	1.3	20:4 ω 6	<0.1	<0.1	0.1
<i>anteiso</i> -17:0	0.5	1.0	2.5	Sum	0.3	0.3	0.5
<i>iso</i> -19:0	0.1	<0.1	0.1	<u>3-Hydroxy</u>			
<i>iso</i> -20:0	0.1	<0.1	0.1	<i>iso</i> -14:0	<0.1	<0.1	0.1
Sum	6.9	11.7	18.7	15:0	2.1	4.3	9.7
<u>Monounsaturated</u>				Sum	2.1	4.3	9.8
16:1 ω 9	0.1	<0.1	0.3	<u>2-Hydroxy</u>			
16:1 ω 7	3.1	2.3	1.2	16:1	<0.1	<0.1	0.1
16:1 ω 5	2.1	1.4	0.8	18:1	0.1	<0.1	<0.1
<i>iso</i> -17:1 ω 9	0.9	2.1	10.8	18:0	<0.1	<0.1	0.1
17:1 ω 8	0.2	0.3	0.3	Sum	0.1	0.1	0.2
17:1 ω 6	0.2	0.5	0.5	<u>Other</u>	10.2	8.8	10.0

- **Microbial communities and biogeochemical cycles**

Biogeochemical cycles strongly depend on microbial community structure, function and dynamics, as well as a range of important external parameters (e.g. diurnal or seasonal cycles). The first layer of the studied mat was characterised by a high abundance of cyanobacteria (Table 2.2) that would have regulated oxygen levels through photosynthetic activity, which would have led to a decrease in sulfide and iron(II) concentrations during the day through chemical oxidation and the activity of photo- and/or chemoautotrophic iron and sulfur oxidisers (see above). The presence of anoxygenic photoautotrophs in the anoxic layers also suggested that sulfide was biologically oxidised during the day in the deeper layers, which is consistent with the observed relatively low to moderate sulfide concentrations (0 to 100 μM) in the second layer of the mat during the day. The bottom layer, however, was dominated by SRB communities (Table 2.2) that played a crucial role in the sulfur cycle and would have contributed to higher sulfide concentrations in the deep anoxic layer. In addition, the rise in sulfide concentration observed at night in the mat may have resulted from a rapid decrease in oxygen concentration in the uppermost layer through microbial respiration and active bacterial sulfate-reduction in this and the deeper mat layers.

Table 2.2: Two-dimensional distributions of phosphate and iron(II) from DET samplers in the mat during day and night. The white lines represent the entire mat. The black dotted lines represent the limits between the first, second and third layers. The region above the top white line represents the water and the area underneath the line represents the sediment.

Layers	Hydrocarbons	Communities	PLFAs	Communities
Layer 1	Long-chain <i>n</i> -alkanes	Higher plant input	<i>n</i> -16:0, 16:1 ω 7	Cyanobacteria
	Sterenes	Eukaryotic input	<i>Iso</i> -17:1 ω 9	Presence of SRB
Layer 2	Relative increase in short-chain <i>n</i> -alkanes	Dominance in bacterial input	Relative increase in <i>i</i> - and <i>ai</i> -17:0 Relative decrease in <i>n</i> -16:0	Increase in SRB abundance Lower abundance of cyanobacteria
Layer 3	Relative increase in C ₃₁ $\beta\beta$ hopane	Possible SRB marker	Cy-19:0	Possible SOB marker
	Increase in phytene and phytadiene isomers	Reducing conditions	Increase in <i>Iso</i> -17:1 ω 9	Dominance of SRB

ANOXIC CONDITIONS

Conclusions

Results from the DET and DGT probes clearly showed that porewater distributions of analysed solutes were highly heterogeneous under both light and dark conditions in the studied smooth mat. These distributions demonstrate that in addition to expected variations over a diurnal cycle, solute distributions can exhibit extensive horizontal fluctuations even within a single layer of the mat (Glud et al., 1999), as well as the more comprehensive shifts that occur associated with changes in light environment and depth. These data also suggest that the distributions and activities of the microbial communities that regulate solute concentrations were also highly heterogeneous.

The visualisation of “hot spots” of high concentrations and micro-zones of low concentrations that would be difficult to detect with conventional methods clearly demonstrated the exceptional spatial resolution and advantages of two-dimensional DGT and DET measurements. In addition, measurements of solute co-distributions provided a strong insight into the biogeochemical cycles operating within the mat. Therefore, two-dimensional distributions of porewater solutes, indicative of key biogeochemical processes and conditions are needed to observe these small scale variations within the different mat layers, in order to assess their role(s) in overall processes.

A very new perspective, into the biogeochemical processes within the smooth microbial mat, was obtained with these two highly complementary methods. Lipid biomarkers can provide significant information regarding the microbial communities present in the microbial mat. Here, they highlighted a predominance of cyanobacteria in the first layer implying significant photosynthetic activity at this outer part of the mat, concordant with the lower concentrations of sulfide and iron(II) recorded in this layer during the day. The increase in SRB abundance with depth was also consistent with the general rise in sulfide concentrations with depth within the mat. Our results emphasized the strong horizontal and vertical heterogeneity of porewater analyte distributions within the microbial mat. These results support the growing body of evidence that microbial

mats are highly complex ecosystems and that in addition to vertical stratifications of physicochemical conditions, there is considerable lateral variations in conditions and solute concentrations, and therefore in the distributions of the microbial communities which regulate and generate these physicochemical variables. This heterogeneity would increase the rates and coupling of biogeochemical cycling by decreasing the diffusional path length and increasing the area of contact between, for instance oxic and anoxic zones, and these shifting spectra of conditions would favour a high degree of functional and taxonomic diversity within the mat microbial community. Further investigation would be required to fully understand the biogeochemical interactions in such a complex ecosystem and two-dimensional distributions of oxygen, for instance, would be a strong asset to better visualise these dynamic biogeochemical processes. This study, however, allowed the visualisation of two-dimensional distributions of key solutes in a modern microbial mat and the detailed observation of biogeochemical interactions.

Acknowledgements

This research was supported by a grant from the Australian Research Council's Discovery Projects scheme (2010-2013, Grice, Greenwood, Snape, and Summons). AP thanks WA-Organic and Isotope Geochemistry Centre, Curtin University and CSIRO for top-up scholarship. Geoff Chidlow is thanked for technical support regarding GC-MS. We would like to acknowledge two anonymous reviewers and Editor Dr Victoria Orphan for constructive and helpful comments.

References

- Abd-el Malek Y. and Rizk S. G.** (1963) Bacterial sulphate reduction and the development of alkalinity . III . Experiments under natural conditions in the Wadi Natriin. *J. Appl. Bacteriol.* **26**, 20–26.
- Allen M. A., Goh F., Burns B. P. and Neilan B. A.** (2009) Bacterial, archaeal and eukaryotic diversity of smooth and pustular microbial mat communities in the hypersaline lagoon of Shark Bay. *Geobiology* **7**, 82–96.
- Allen M. A., Neilan B. A., Burns B. P., Jahnke L. L. and Summons R. E.** (2010) Lipid biomarkers in Hamelin Pool microbial mats and stromatolites. *Org. Geochem.* **41**, 1207–1218.
- Aller J. Y. and Aller R. C.** (1986) Evidence for localized enhancement of biological associated with tube and burrow structures in deep-sea sediments at the HEEBLE site, western North Atlantic. *Deep Sea Res. Part A. Oceanogr. Res. Pap.* **33**, 755–790.
- Aller R. C., Yingst J. Y. and Ullman W. J.** (1983) Comparative biogeochemistry of water in intertidal *Onuphis* (polychaeta) and *Upogebia* (crustacea) burrows: temporal patterns and causes. *J. Mar. Res.* **41**, 571–604.
- Allwood A. C., Walter M. R., Kamber B. S., Marshall C. P. and Burch I. W.** (2006) Stromatolite reef from the Early Archaean era of Australia. *Nature* **441**, 714–718.
- Arp G., Reimer A. and Reitner J.** (2001) Photosynthesis-induced biofilm calcification and calcium concentrations in Phanerozoic oceans. *Science* **292**, 1701–1704.
- Baumgartner L. K., Reid R. P., Dupraz C. P., Decho A. W., Buckley D. H., Spear J. R., Przekop K. M. and Visscher P. T.** (2006) Sulfate reducing bacteria in microbial mats: Changing paradigms, new discoveries. *Sediment. Geol.* **185**, 131–145.
- De Beer D. and K  lh M.** (2001) Interfacial microbial mats and biofilms. In *The Benthic Boundary Layer* (eds. B. P. Boudreau, B. B. J  rgensen). Oxford University Press, New York, pp. 374–394.
- Bennett W. W., Teasdale P. R., Welsh D. T., Panther J. G. and Jolley D. F.** (2012) Optimization of colorimetric DET technique for the in situ, two-dimensional measurement of iron(II) distributions in sediment porewaters. *Talanta* **88**, 490–495.
- Bennett W. W., Serriere A., Panther J. G., Welsh D. T. and Teasdale P. R.** (2014) A rapid, high-resolution, gel-based technique for the in situ measurement of two-dimensional porewater alkalinity distributions. *Chemosphere*, under review.

- Blumenberg M., Krüger M., Nauhaus K., Talbot H. M., Oppermann B. I., Seifert R., Pape T. and Michaelis W.** (2006) Biosynthesis of hopanoids by sulfate-reducing bacteria (genus *Desulfovibrio*). *Environ. Microbiol.* **8**, 1220–1227.
- Bobbie R. J. and White D. C.** (1980) Characterization of benthic microbial community structure by high-resolution gas chromatography of fatty acid methyl esters. *Appl. Environ. Microbiol.* **39**, 1212–1222.
- Braissant O., Decho A. W., Przekop K. M., Gallagher K. L., Glunk C., Dupraz C. P. and Visscher P. T.** (2009) Characteristics and turnover of exopolymeric substances in a hypersaline microbial mat. *FEMS Microbiol. Ecol.* **67**, 293–307.
- Breman, P. J.** (1988) Mycobacterium and other actinomycetes. In *Microbial lipids* (eds. C. Ratledge, S. G. Wilkinson). Academic Press, London, pp. 204–298.
- Burne R. V. and Johnson K.** (2012) Sea-level variation and the zonation of microbialites in Hamelin Pool, Shark Bay, Western Australia. *Mar. Freshw. Res.* **63**, 994–1004.
- Burns B. P., Goh F., Allen M. A. and Neilan B. A.** (2004) Microbial diversity of extant stromatolites in the hypersaline marine environment of Shark Bay, Australia. *Environ. Microbiol.* **6**, 1096–1101.
- Canfield, D. E. and Des Marais, D. J.** (1991) Aerobic sulfate reduction in microbial mats. *Science* **251**, 1471–1473.
- Canfield D. E. and Des Marais D. J.** (1993) Biogeochemical cycles of carbon, sulfur, and free oxygen in a microbial mat. *Geochim. Cosmochim. Acta* **57**, 3971–3984.
- Cohen Y.** (1984) Micro-sulfate reduction measurements at the H₂S-O₂ interface in organic rich sediments. *Eos.* **65**, 905.
- Cohen Z., Margheri M. C. and Tomaselli L.** (1995) Chemotaxonomy of cyanobacteria. *Phytochemistry* **40**, 1155–1158.
- Davison W., Grime G. W., Morgan J. A. W. and Clarke K.** (1991) Distribution of dissolved iron in sediment pore waters at submillimetre resolution. *Nature* **352**, 323–325.
- Davison W. and Zhang H.** (1994) In situ speciation measurements of trace components in natural waters using thin-film gels. *Nature* **367**, 546–548.
- Davison W., Fones G. R. and Grime G. W.** (1997) Dissolved metals in surface sediment and a microbial mat at 100- μ m resolution. *Nature* **387**, 885–888.

- Davison W., Fones G. R., Harper M., Teasdale P. R. and Zhang H.** (2000) Dialysis, DET and DGT: in situ diffusional techniques for studying water, sediments and soils. In *In situ monitoring of aquatic systems: chemical analysis and speciation*. (eds. J. Buffle and G. Horvai). John Wiley & Sons, pp. 495–569.
- Decho, A. W.** (2000) Exopolymer microdomains as a structuring agent for heterogeneity within microbial biofilms. In *Microbial Sediments* (eds. R. Riding, S. M. Awramik). Springer, Berlin, pp. 9–15
- De Lange G. J., Cranston R. E., Hydes D. H. and Boust D.** (1992) Extraction of pore water from marine sediments: A review of possible artifacts with pertinent examples from the North Atlantic. *Mar. Geol.* **109**, 53–76.
- Des Marais D. J.** (2003) Biogeochemistry of hypersaline microbial mats illustrates the dynamics of modern microbial ecosystems and the early evolution of the biosphere. *Biol. Bull.* **204**, 160–167.
- Dilling W. and Cypionka H.** (1990) Aerobic respiration in sulfate-reducing bacteria. *FEMS Microbiol. Lett.* **71**, 123–127.
- Dupraz C. P., Visscher P. T., Baumgartner L. K. and Reid R. P.** (2004) Microbe-mineral interactions: early carbonate precipitation in a hypersaline lake (Eleuthera Island, Bahamas). *Sedimentology* **51**, 745–765.
- Dupraz C. P. and Visscher P. T.** (2005) Microbial lithification in marine stromatolites and hypersaline mats. *Trends Microbiol.* **13**, 429–38.
- Dupraz C. P., Reid R. P., Braissant O., Decho A. W., Norman R. S. and Visscher P. T.** (2009) Processes of carbonate precipitation in modern microbial mats. *Earth-Science Rev.* **96**, 141–162.
- Fourçans A., de Oteyza T. G., Wieland a, Solé A., Diestra E., van Bleijswijk J., Grimalt J. O., Kühl M., Esteve I., Muyzer G., Caumette P. and Duran R.** (2004) Characterization of functional bacterial groups in a hypersaline microbial mat community (Salins-de-Giraud, Camargue, France). *FEMS Microbiol. Ecol.* **51**, 55–70.
- Fründ C. and Cohen Y.** (1992) Diurnal cycles of sulfate reduction under oxic conditions in cyanobacterial mats. *Appl. Environ. Microbiol.* **58**, 70–77.
- Glud R. N., Kühl M., Kohls O. and Ramsing N. B.** (1999) Heterogeneity of oxygen production and consumption in a photosynthetic microbial mat as studied by planar optodes. *J. Phycol.* **279**, 270–279.
- Grimalt J. O., Yruela I., Saiz-Jimenez C., Toja J., De Leeuw J. W. and Albaiges J.** (1991) Sedimentary lipid biogeochemistry of an hypereutrophic alkaline lagoon. *Geochim. Cosmochim. Acta* **55**, 2555–2577.

- Grossi V., Hirschler a, Raphel D., Rontani J.-F., de Leeuw J. W. and Bertrand J.-C.** (1998) Biotransformation pathways of phytol in recent anoxic sediments. *Org. Geochem.* **29**, 845–861.
- Hansen K., King G.M. and Kristensen E.** (1996) Impact of the soft-shell clam *Mya arenaria* on sulfate reduction in an intertidal sediment. *Aquat. Microb. Ecol.* **10**, 181-194.
- Hastings D. and Emerson S.** (1988) Sulfate reduction in the presence of low oxygen levels in the water column of the Cariaco Trench. *Limnol. Oceanogr.* **33**, 391–396.
- Hoffman H. J.** (2000) Archean stromatolites as microbial archives. In *Microbial Sediments* (eds. R. Riding, S. M. Awramik). Springer, Berlin, pp. 315–327.
- Jahnert R. and Collins L.** (2012) Characteristics, distribution and morphogenesis of subtidal microbial systems in Shark Bay, Australia. *Mar. Geol.* **303-306**, 115–136.
- Jahnert R. and Collins L.** (2013) Controls on microbial activity and tidal flat evolution in Shark Bay, Western Australia. *Sedimentology* **60**, 1071–1099.
- Jahnke L. L., Embaye T., Hope J., Turk K. A., Van Zuilen M., Des Marais D. J., Farmer J. D. and Summons R. E.** (2004) Lipid biomarker and carbon isotopic signatures for stromatolite-forming, microbial mat communities and *Phormidium* cultures from Yellowstone National Park. *Geobiology* **2**, 31–47.
- Jahnke L. L., Orphan V. J., Embaye T., Turk K. A., Kubo M. D., Summons R. E. and Des Marais D. J.** (2008) Lipid biomarker and phylogenetic analyses to reveal archaeal biodiversity and distribution in hypersaline microbial mat and underlying sediment. *Geobiology* **6**, 394–410.
- Jézéquel D., Brayner R., Metzger E., Viollier E., Prévot F. and Fiévet F.** (2007) Two-dimensional determination of dissolved iron and sulfur species in marine sediment pore-waters by thin-film based imaging. Thau lagoon (France). *Estuar. Coast. Shelf Sci.* **72**, 420–431.
- Jørgensen B. B. and Revsbech N. P.** (1979) Diurnal cycle of oxygen and sulfide microgradients and microbial photosynthesis in a cyanobacterial mat sediment *Appl. Environ. Microbiol.* **38**, 46–58.
- Jørgensen B. B., Revsbech N. P. and Cohen Y.** (1983) Photosynthesis and structure of benthic microbial mats: microelectrode and SEM studies of four cyanobacterial communities. *Limnol. Ocean.* **28**, 1075-1093.
- Jørgensen B.** (1994) Diffusion processes and boundary layers in microbial mats. *Microb. Mats NATO ASI* **35**, 243–253.

- Kenyon C. N., Rippka R. and Stanier R. Y.** (1972) Fatty acid composition and physiological properties of some filamentous blue-green algae. *Arch. Mikrobiol.* **83**, 216–236.
- Krekeler D., Sigalevich P., Teske a., Cypionka H. and Cohen Y.** (1997) A sulfate-reducing bacterium from the oxic layer of a microbial mat from Solar Lake (Sinai), *Desulfovibrio oxyclinae* sp. nov. *Arch. Microbiol.* **167**, 369–375.
- Krekeler D., Teske A. and Cypionka H.** (1998) Strategies of sulfate-reducing bacteria to escape oxygen stress in a cyanobacterial mat. *FEMS Microbiol. Ecol.* **25**, 89–96.
- Kristensen, E.** (2000) Organic matter diagenesis at the oxic/anoxic interface in coastal marine sediments, with emphasis on the role of burrowing animals. *Hydrobiologia* **426**, 1-24.
- Logan B. W.** (1961) Cryptozoon and associate stromatolites from the recent, Shark Bay, Western Australia. *J. Geol.* **69**, 517–533.
- Logan B. W.** (1974) Evolution and diagenesis of Quarternary carbonate sequences, Shark Bay, Western Australia. *Am. Assoc. Pet. Geol. Mem.* **22**, 195–249.
- Londry K. L., Jahnke L. L. and Des Marais D. J.** (2004) Stable carbon isotope ratios of lipid biomarkers of sulfate-reducing bacteria. *Appl. Environ. Microbiol.* **70**, 745–751.
- Lyons, W. B., Long, D. T., Hines, M. E., Gaudette, H. E. and Armstrong, P. B.** (1984) Calcification of cyanobacterial mats in Solar Lake, Sinai. *Geology* **12**, 623-626.
- McKirby D. M., Thorpe C. S., Haynes D. E., Grice K., Krull E. S., Halverson G. P. and Webster L. J.** (2010) The biogeochemical evolution of the Coorong during the mid- to late Holocene: an elemental, isotopic and biomarker perspective. *Org. Geochem.* **41**, 96–110.
- Minz D., Flax J. L., Green S. J., Muyzer G., Cohen Y., Wagner M., Rittmann B. E. and Stahl D. A.** (1999) Diversity of sulfate-reducing bacteria in oxic and anoxic regions of a microbial mat characterised by comparative analysis of dissimilatory sulfite reductase genes. *Appl. Environ. Microbiol.* **65**, 4666–4671.
- Mouné S., Caumette P., Matheron R. and Willison J. C.** (2003) Molecular sequence analysis of prokaryotic diversity in the anoxic sediments underlying cyanobacterial mats of two hypersaline ponds in Mediterranean salterns. *FEMS Microbiol. Ecol.* **44**, 117–130.

- Navarrete A., Peacock A., Macnaughton S. J., Urmeneta J., Mas-Castellà J., White D. C. and Guerrero R. (2000) Physiological status and community composition of microbial mats of the Ebro Delta, Spain, by signature lipid biomarkers. *Microb. Ecol.* **39**, 92–99.
- Paerl H. W., Bebout B. M. and Prufert L. (1989) Naturally occurring patterns of oxygenic photosynthesis and N₂ fixation in a marine microbial mat: physiological and ecological ramifications. In *Microbial mats: physiological ecology of benthic microbial communities* (eds. Y. Cohen, E. Rosenberg). American Society Microbiology, Washington, pp. 326–341.
- Paerl H. W. and Pinckney J. L. (1996) A mini-review of microbial consortia: Their roles in aquatic production and biogeochemical cycling. *Microb. Ecol.* **31**.
- Paerl H. W., Pinckney J. L. and Steppe T. F. (2000) Cyanobacterial-bacterial mat consortia: examining the functional unit of microbial survival and growth in extreme environments. *Environ. Microbiol.* **2**, 11–26.
- Pagès A., Teasdale P. R., Robertson D., Bennett W. W., Schäfer J. and Welsh D. T. (2011) Representative measurement of two-dimensional reactive phosphate distributions and co-distributed iron(II) and sulfide in seagrass sediment porewaters. *Chemosphere* **85**, 1256–1261.
- Pagès A., Welsh D. T., Robertson D., Panther J. G., Schäfer J., Tomlinson R. B. and Teasdale P. R. (2012) Diurnal shifts in co-distributions of sulfide and iron(II) and profiles of phosphate and ammonium in the rhizosphere of *Zostera capricorni*. *Estuar. Coast. Shelf Sci.* **115**, 282–290.
- Parfitt, R. L., Atkinson, R. J. and Smart R. St. C. (1975) The mechanism of phosphate fixation by iron oxides. *Soil Sci. Soc. Am. J.* **39**, 837–841.
- Pike J., Bernhard J. M., Moreton S. G. and Butler I. B. (2001) Microbioirrigation of marine sediments in dysoxic environments: Implications for early sediment fabric formation and diagenetic processes. *Geology* **29**, 923–926.
- Reid R. P., Visscher P. T., Decho A. W., Stolz J. F. and Bebout B. M. (2000) The role of microbes in accretion, lamination and early lithification of modern marine stromatolites. *Nature* **406**, 989–992.
- Revsbech N. P., Jørgensen B. B., Blackburn T. H. and Cohen Y. (1983) Microelectrode studies of the photosynthesis and H₂S, and pH profiles of a microbial mat. *Limnol. Oceanogr.* **28**, 1062–1074.
- Risatti J. B., Capman W. C. and Stahl D. A. (1994) Community structure of a microbial mat: the phylogenetic dimension. *Proc. Natl. Acad. Sci. U. S. A.* **91**, 10173–10177.

- Robertson D., Teasdale P. R. and Welsh D. T.** (2008) A novel gel-based technique for the high resolution, two-dimensional determination of iron(II) and sulfide in sediment. *Limnol. Oceanogr. Methods* **6**, 502–512.
- Robertson D., Welsh D. T. and Teasdale P. R.** (2009) Investigating biogenic heterogeneity in coastal sediments with two-dimensional measurements of iron(II) and sulfide. *Environ. Chem.* **6**, 60–69.
- Rohmer M., Bouvier-Nave P. and Ourisson G.** (1984) Distribution of hopanoid triterpenes in prokaryotes. *Microbiology* **130**, 1137–1150.
- Rontani J.-F., Bonin P., Vaultier F., Guasco S. and Volkman J. K.** (2013) Anaerobic bacterial degradation of pristenes and phytene in marine sediments does not lead to pristane and phytane during early diagenesis. *Org. Geochem.* **58**, 43–55.
- Saas H., Cypionka H. and Babenzien H.-D.** (1997) Vertical distribution of sulfate-reducing bacteria at the oxic-anoxic interface in sediments of the oligotrophic lake Stechlin. *FEMS Microbiol. Ecol.* **22**, 245–255.
- Schirmer A., Rude M. A., Li X., Popova E. and del Cardayre S. B.** (2010) Microbial biosynthesis of alkanes. *Science* **329**, 559–562.
- Stockdale A., Davison W. and Zhang H.** (2009) Micro-scale biogeochemical heterogeneity in sediments: A review of available technology and observed evidence. *Earth-Science Rev.* **92**, 81–97.
- Summons R. E., Barrow R., Capon R., Hope J. and Stranger C.** (1993) The structure of a new C₂₅ isoprenoid alkene biomarker from diatomaceous microbial communities. *Aust. J. Chem.* **46**, 907–915.
- Summons R. E., Jahnke L. L. and Roksandic Z.** (1994) Carbon isotopic fractionation in lipids from methanotrophic bacteria: Relevance for interpretation of the geochemical record of biomarkers. *Geochim. Cosmochim. Acta* **58**, 2853–2863.
- Talbot H. M., Summons R. E., Jahnke L. L., Cockell C. S., Rohmer M. and Farrimond P.** (2008) Cyanobacterial bacteriohopanepolyol signatures from cultures and natural environmental settings. *Org. Geochem.* **39**, 232–263.
- Taylor J. and Parkes R. J.** (1985) Identifying different populations of sulphate-reducing bacteria within marine sediment systems, using fatty acid biomarkers. *Microbiology* **131**, 631–642.
- Teasdale P. R., Hayward S. and Davison W.** (1999) In situ, high-resolution measurement of dissolved sulfide using diffusive gradients in thin films with computer-imaging densitometry. *Anal. Chem.* **71**, 2186–2191.

- Thiel V., Merz-preiß M., Reitner J. and Michaelis W.** (1997) Biomarker studies on microbial carbonates: extractable lipids of a calcifying cyanobacterial mat (Everglades, USA). *Facies* **36**, 163–172.
- Tolker-Nielsen, T. and Molin, S.** (2000) Spatial organization of microbial biofilm communities. *Microb. Ecol.* **40**: 75–84.
- van Gernerden, H.** (1993) Microbial mats: A joint venture. *Mar. Geol.* **113**: 3–25.
- Van Kranendonk M., Philippot P., Lepot K., Bodorkos S. and Pirajno F.** (2008) Geological setting of Earth's oldest fossils in the ca. 3.5Ga Dresser Formation, Pilbara Craton, Western Australia. *Precambrian Res.* **167**, 93–124.
- Visscher P. T.** (1992a) Rates of sulfate reduction and thiosulfate consumption in a marine microbial mat. *FEMS Microbiol. Lett.* **86**, 283–288.
- Visscher P. T., Reid R. P., Bebout B. M., Hoefft S. E. H., Macintyre I. G. and Thompson Jr. J. A.** (1998) Formation of lithified micritic laminae in modern marine stromatolites (Bahamas): The role of sulfur cycling. *Am. Mineral.* **83**, 1482–1493.
- Visscher P. T., Reid R. P. and Bebout B. M.** (2000) Microscale observations of sulfate reduction: Correlation of microbial activity with lithified micritic laminae in modern marine stromatolites. *Geology* **2**, 919–922.
- Visscher P. T. and Stolz J. F.** (2005) Microbial mats as bioreactors: populations, processes, and products. *Palaeogeogr. Palaeoclimatol. Palaeoecol.* **219**, 87–100.
- Volkman J. K.** (1986) A review of sterol markers for marine and terrigenous organic matter. *Org. Geochem.* **9**, 83–99.
- Walter M. R., Buick R. and Dunlop J. S. R.** (1980) Stromatolites 3,400–3,500 Myr old from the North pole area, Western Australia. *Nature* **284**, 443–445.
- Wieland A., Kühl M., McGowan L., Fourçans A., Duran R., Caumette P., García de Oteyza T., Grimalt J. O., Solé A., Diestra E., Esteve I. and Herbert R. A.** (2003) Microbial mats on the Orkney Islands revisited: microenvironment and microbial community composition. *Microb. Ecol.* **46**, 371–90.
- Wilkinson S. G.** (1988) Gram-negative bacteria. In *Microbial Lipids* (eds. C. Ratledge and S. G. Wilkinson). Academic Press, London, pp. 299–489.
- Zelles L., Bai Q. Y., Rackwitz R., Chadwick D. and Beese F.** (1995) Determination of phospholipid- and lipopolysaccharide-derived fatty acids as an estimate of microbial biomass and community structures in soils. *Biol. Fertil. Soils* **19**, 115–123.

Zhang H. and Davison W. (1995) Performance characteristics of diffusion gradients in thin films for the in situ measurement of trace metals in aqueous solution. *Anal. Chem.* **67**, 3391–3400.

Chapter 3

Diel fluctuations in solute distributions and biogeochemical cycles in a hypersaline microbial mat from Shark Bay, Western Australia.

Anais Pagès, David T. Welsh, Peter R. Teasdale, Kliti Grice, Michael Vacher, William W. Bennett, Pieter T. Visscher

Marine Chemistry, in press

(impact factor 3.00)

Chapter 3

Abstract

Introduction

Materials and Methods

- Site description
- Sample description
- Microelectrode profiles of oxygen, sulfide and pH
- 2D mapping of sulfate-reducing activity using $^{35}\text{SO}_4^{2-}$ -labelled silver foils
- Preparation of DGT and DET gels and assembly of combined DET-DGT probes
- Deployment of combined DET-DGT probes
- Analysis of Fe(II), phosphate and sulfide co-distributions
- Analysis of alkalinity distributions

Results and Discussion

- Microelectrode profiles of oxygen and sulfide
- Small scale two-dimensional heterogeneity in sulfide, iron(II) and phosphate distributions
- Biogeochemical changes over a diel cycle
- Alkalinity measurements and the carbonate cycle

Conclusions

Abstract

Studying modern microbial mats can provide insights into how microbial communities interact with biogeochemical cycles. High-resolution, two-dimensional distributions of porewater analytes were determined in the upper three layers of a modern microbial mat from Nilemah, Shark Bay, Western Australia, using colorimetric diffusive equilibration in thin films (DET) and diffusive gradients in thin films (DGT) techniques. The colorimetric DET and DGT techniques were used to investigate the co-distributions of sulfide, iron(II), phosphate and alkalinity. Two-dimensional distributions of sulfide, iron(II) and phosphate showed a high degree of spatial heterogeneity under both light and dark conditions. However, average concentration profiles showed a clear shift in overall redox conditions between light and dark conditions. During light deployments, iron(II) and sulfide concentrations were generally low throughout the entire microbial mat. In contrast, during dark deployments, when anoxic conditions prevailed, higher concentrations of iron(II) and sulfide were observed and the sulfide boundary migrated towards the upper layer of the mat. Similar to the iron(II) profile, the phosphate profile showed an increase in concentration at night, suggesting that phosphate was released through the dissolution of iron-phosphate complexes under anoxic conditions. However, two-dimensional distributions revealed that hot spots of phosphate and iron(II) did not coincide, suggesting that pore water phosphate was mainly regulated by diel metabolic changes in the mat. Alkalinity profiles also demonstrated an increase in concentration at night, probably related to high rates of sulfate reduction under dark conditions. Complimentary microelectrode measurements of oxygen and sulfide confirmed light-limited microbial communities play a significant role in regulating porewater solute concentrations, especially through photosynthetic activity that supports rapid re-oxidation of sulfide during the day. Sulfide was not detected in the upper layers (ca. 4 mm) of the mat by microelectrode measurements, but was found at those depths by the time-integrated DGT measurements. Complimentary silver foil deployments also showed a 2D distribution of sulfate-reducing activity occurring under oxic conditions in the top layers. DGT, O₂ and sulfide microelectrode profiles and silver

foils confirmed hotspots of sulfide production coinciding with cyanobacterial photosynthesis. Two-dimensional pore water analyte distributions showed significant small-scale heterogeneity, highlighting the complexity of such dynamic ecosystems and the advantage of two-dimensional methods.

Introduction

Stromatolites have been present on Earth for ~3.5 Ga (Walter et al., 1980). These laminated structures were presumably built through mineral precipitation within microbial communities in surface mats (Dupraz et al., 2009) and preserved through diagenetic processes (Walter, 1976). Such microbial communities caused global change of Earth's redox conditions through the production of oxygen and hydrogen (Hoehler et al., 2001). Modern microbial mats develop in a variety of environments, including freshwater lakes, hypersaline ponds, host springs and open marine settings (Dupraz and Visscher, 2005; Van Gernerden and Visscher, 2003). The characteristic laminated structure of microbial mats resembles that of stromatolites and extant mats are studied as modern day analogues of those ancient formations (Dupraz and Visscher, 2005; Logan, 1974). Consequently, modern microbial mats represent natural laboratories to study early-life processes, to provide insight into past environments, and to understand how microbial communities contribute to biogeochemical cycles (Visscher and van Gernerden, 1993).

The typical lamination within mats is due to the vertically changing light regime and the intense interaction between microbial metabolisms and solutes; cyanobacteria are in the upper mm of the mat, with purple-sulfur bacteria just below and strict anaerobic green-sulfur bacteria near the bottom of the photic zone (Des Marais, 1995; van Gernerden, 1993). The deeper mat layers are typically black due to iron sulfide precipitation, but sometimes contain pigmented layers representing past surface communities. The overall metabolic activity of the microbial mat community leads to rapidly fluctuating chemical conditions (e.g., of oxygen and sulfide concentrations, pH and E_h), showing a typical diel pattern (Revsbech and Jørgensen, 1986; Visscher et al., 2002). The diel fluctuations in the photon flux drive changes in specific biogeochemical processes (Jørgensen and Des Marais, 1988). During the light period, cyanobacteria and anoxygenic phototrophs generate organic matter that is required for heterotrophic activity. Conversely, under dark conditions, the oxygen concentration is rapidly depleted and anaerobic heterotrophic processes such as sulfate-reduction prevail, causing the sulfide

concentration to increase. The characteristic diel fluctuations of oxic and anoxic conditions within the mat will also influence iron(II) and nutrient distributions (Joye et al., 1996), as well as the precipitation/dissolution of carbonate minerals (Dupraz and Visscher, 2005). Alkalinity and dissolved inorganic carbon (DIC) are significant parameters influencing lithification within mats and are highly dependent on microbial processes (Dupraz et al., 2009).

Accurate measurements of the distributions of solutes at small spatial scales in such dynamic environments present analytical challenges. Conventional coring methods, with extraction of pore waters, or peepers (Teasdale et al., 1995) do not allow for determination of analyte distributions at relevant spatial scales (see Stockdale et al., 2009 for a review) and artefacts can arise from sample handling (de Lange et al., 1992; Robertson and Liber, 2009) or in pore waters that are highly heterogeneous (Robertson et al., 2008). Accurate two-dimensional distribution of analytes have been obtained in dynamic environments such as sediments, seagrass beds and microbial mats using thin layer diffusive passive samplers (Davison et al., 1997; Pagès et al., 2012, 2011; Robertson et al., 2009) - DGT (diffusive gradients in a thin film) and DET (diffusive equilibration in a thin film) techniques. DET methods utilise a thin hydrogel layer that equilibrates quickly with pore water solutes (Davison et al., 2000). DGT techniques use a selective binding agent that accumulates target solutes and is overlain by a hydrogel and protective membrane, which act as a defined diffusive layer (Davison and Zhang, 1994; Davison et al., 2000). Analyte species diffuse through the diffusive layer and accumulate in the binding gel layer according to the DGT equation, derived from Fick's First Law of Diffusion, and which allows calculation of the solute concentration adjacent to the DGT device (Davison and Zhang, 1994; Davison et al., 2000). These concentrations can be interpreted as pore water solute concentrations with some assumptions (Davison et al., 2000). Recently, colorimetric DGT and DET techniques have been developed in order to rapidly and accurately assess two-dimensional distributions of key porewater solutes at high (sub-mm) spatial resolution (Bennett et al., 2012; Jézéquel et al., 2007; Pagès et al., 2012, 2011; Robertson et al., 2009, 2008; Teasdale et al., 1999). After probe retrieval, DGT

binding gels or stained-DET gels are scanned and analyte concentrations determined by computer imaging densitometry (CID) (Teasdale et al., 1999). The diffusive gel layer of a DGT probe can also serve as a DET for other porewater analytes, allowing co-distributions of solutes to be plotted.

The aim of this study was to investigate changes in the distributions of pore water solutes, over a natural diel cycle, in hypersaline microbial mats from Shark Bay. Microelectrode measurements were performed in the microbial mat in order to determine the oxygen and sulfide concentrations during peak photosynthesis (i.e. daytime) and maximum sulfide accumulation (i.e. the end of the night). Colorimetric DET and DGT techniques were used to investigate the microbial processes regulating the co-distributions of sulfide, iron(II) and phosphate and the alkalinity distributions (related to carbonate precipitation/dissolution dynamics) and $^{35}\text{SO}_4^{2-}$ -labelled silver foils were deployed to map the distribution of sulfate-reducing activity.

Materials and Methods

- **Site and sample descriptions**

Shark Bay is located in Western Australia, 800 km north of Perth. Hamelin Pool is the south-easterly embayment of this “U” shaped, semi-enclosed area. Water influx is restricted by the presence of a sill covered by seagrass in the northern area of the bay, leading to Hamelin Pool being hypersaline (56-70 PSU) because of low rainfall and high evaporation rates (Playford, 1990). These hypersaline conditions limit the presence of metazoans (Edgcomb et al., 2013). Water temperature varies between 17.3 and 30.8°C (Jahnert and Collins, 2013). The Hamelin Coquina, geological units made primarily of bivalve skeletons, is located on the beach ridges of Hamelin Pool (Jahnert and Collins, 2012). The high abundance of shells leads to a saturation of calcium carbonate in the water, which favours the formation of microbialites. Various types of microbial mats have been reported in Hamelin Pool (Logan, 1974; Playford, 1990) that occupy ~300 km² of the total ~1400 km² area (Jahnert and Collins, 2012). The lamination of the

microbial mats resembles that of ancient stromatolites, which possibly represent the earliest life on Earth (Logan, 1961).

The experiments were carried out in a so-called smooth mat (Jahnert and Collins, 2013, 2012; Logan, 1974) from Nilemah (Figure 3.1A, B), which was ca. 10-12 mm thick. Three distinct layers were visible with the naked eye: an uppermost brown layer containing extracellular polymeric substances (EPS) with photopigments, a subsurface green-colored layer characteristic of cyanobacteria, and a third black-colored layer containing iron sulfides (Figure 3.1C, D).



Figure 3.1: Photographs of A, View of Nilemah, Shark Bay. The smooth mats are located close to the waterline. B, a smooth microbial mat. C, a sample of the smooth mat showing the characteristic vertical layering in cross-section. D, a close-up view of the smooth microbial mat.

- **Microelectrode profiles of oxygen, sulfide and pH**

Depth profiles of oxygen, sulfide and pH were determined in triplicate using needle microelectrodes (Myshrall et al., 2010; Visscher et al., 2002, 1998) both *in situ* (daytime only) and *ex situ* under ambient temperature and light intensity (daytime and night-time). *In situ* measurements (18 profiles total) were carried out during low tide in the light when the water level over the mats was less than 7 cm. *Ex situ* measurements (36 depth profiles in total) were carried out during the light and dark in a field laboratory 5 km from the sampling site during two diel cycles. For these *ex situ* measurements, small samples (~5x5 cm) were taken, submerged in 3 cm of water collected from the site, and pre-incubated for 12-24 h under temperature, salinity and light conditions identical to the field site values prior to the first measurement. The sensors, which had a tip diameter between 100 and 150 μm , were deployed in 200-250 μm depth increments using a manual micromanipulator (National Aperture, New Hampshire). Daytime electrode readings were carried out during the peak of photosynthesis between midday and 2 pm during two consecutive light periods. Night time measurements (i.e., covering two complete diel cycles) were made at the end of the dark period between 3:30 and 5:30 am, also during two consecutive dark periods. Each profile was obtained within 20 min. Polarographic oxygen and sulfide electrodes (Unisense, Denmark) were used in combination with a Unisense PA 2000 picoammeter, pH (Diamond General, Ann Arbor, MI) and ion-selective sulfide needles (Microscale Measurements, The Netherlands) were deployed with a high-impedance microscale measurements millivolt meter. The polarographic sulfide electrodes measure H_2S and the ion-selective probes measure S^{2-} . These measurements were combined with pH observations to calculate total free sulfide ($\Sigma(\text{S}^{2-} + \text{HS}^- + \text{H}_2\text{S})$). Light measurements were done using a LiCor LI 250 meter equipped with a SA190A quantum sensor. Salinity and temperature measurements were obtained with an Accumet AP75 temperature/conductivity meter and pH of the overlying water and the sediment at 5-10 mm depth were determined with a handheld Hanna pH-meter.

- **2D mapping of sulfate-reducing activity using $^{35}\text{SO}_4^{2-}$ -labelled silver foils**

Two-dimensional measurements of sulfate-reduction activity were made using $^{35}\text{SO}_4^{2-}$ -coated silver foil and a modification of the method developed by Cohen (Cohen and Helman, 1997; Cohen, 1984). Strips of Ag foil (75 × 75 mm and 0.1 mm thick; Sigma Chemical Co., St. Louis, Missouri) were treated with acetone, rinsed with water, and coated with a solution of $^{35}\text{SO}_4^{2-}$ (1 mCi per foil; Amersham, Chicago, Illinois) prepared in sterilized seawater from the site. The foil was then allowed to air dry for 24 h. A freshly cut sample of mat was placed on the silver foil, and, after an incubation time of 6–8 h in the dark, the sample was removed, and the silver foil was rinsed to remove residual $^{35}\text{SO}_4^{2-}$. The reduced sulfate, which had precipitated as Ag_2^{35}S , was digitally mapped using a BioRad Molecular Imager System GS-525 (Hercules, California) radioactive gel scanner. The silver foil analysis were performed on samples from the same microbial structure, taken a few meters away from the location where the DGT/DET samplers were deployed to avoid disturbing the area. These silver foil measurements were performed at the same time as the DGT/DET deployments.

- **Preparation of DGT and DET gels, and assembly of combined DET-DGT probes**

Deionised water (Milli-Q Element, Millipore) was used to prepare all solutions. All DGT and DET probe components and glassware, including the plates used for gel casting were acid-cleaned in 10% (v/v) HNO_3 (AR grade, Merck) for at least 24 h and rinsed thoroughly with deionised water prior to use. The bisacrylamide cross-linked polyacrylamide diffusive gels (0.4 mm final thickness) used for iron(II), phosphate, alkalinity and nitrite DETs, DGT-sulfide binding gels, and staining gels for colorimetric iron(II), phosphate, alkalinity and nitrite determinations, were prepared, cast and stored as previously described (Bennett et al., 2012; Pagès et al., 2011; Robertson et al., 2008).

Sediment DGT/DET sampling devices were assembled according to Robertson et al. (2008). Two probe combinations were used. The first was a triple-layered probe composed of an AgI-DGT binding hydrogel for determination of sulfide by CID (Teasdale et al., 1999), a diffusive hydrogel used as a colorimetric DET for iron(II) (Robertson et al., 2008; Bennett et al., 2012), and a second diffusive hydrogel for colorimetric measurement of phosphate (Pagès et al., 2011). This combination of gels allowed the measurement of two-dimensional co-distributions of sulfide, iron(II) and phosphate in the exact same sediment. Double-layered probes have been previously used for this type of investigation – to our knowledge this is the first time that triple-layered probes have been used for the investigation of porewater analyte distributions *in situ*. The second probe combination was a double-layered probe with the first diffusive hydrogel used as a colorimetric DET for alkalinity and a second diffusive hydrogel used as a colorimetric DET for nitrite (results not shown).

Ten replicates of each of the two combination probes were prepared and stored in deionised water. Prior to all deployments probes were deoxygenated by sparging the storage solution with N₂ for ca. 3 hours and then transported to the field in sealed containers under an N₂ atmosphere, to avoid possible artefacts that could be induced by the introduction of oxygen into the sediment during probe deployment.

- **Deployment of combined DET-DGT probes**

All field deployments were for approximately 8 hours (exact times recorded), which exceeded the minimum time required for equilibration (Davison et al., 2000; Pagès et al., 2011), on the 26th and 27th of April 2012. Five replicates of each of the two DGT-DET probe types were deployed on each occasion by carefully pushing each probe into the microbial mat. The first set of probes (light incubation) were deployed at the same time in the morning and retrieved in the afternoon (approx. 8 am to 4 pm). After these probes had been processed, the second set of probes (dark incubation) were deployed at the same time in the same

manner, after sunset and retrieved at low tide the following morning before sunrise (approx. 9 pm to 5:30 am). The same site was investigated under daylight and dark conditions. The maximum water depth at high tide reached 70 cm.

- **Analysis of Fe(II), phosphate and sulfide co-distributions**

Probes were briefly washed immediately upon retrieval to remove sediment and a new stainless steel scalpel was used to quickly cut out the gel layers from the probe window. The iron(II), phosphate and alkalinity DETs were immediately transferred onto a transparent sheet on a flat-bed scanner, stained by overlaying them with staining gels equilibrated in ferrozine, molybdate-ascorbic and bromophenol blue reagents, respectively (Bennett et al., 2012; Pagès et al., 2011; Bennett et al., 2014). Gels were stained for 15 min and distributions acquired as previously described. Sulfide-DGTs are stable and were stored in the dark and scanned as described by Robertson et al. (2008) one hour later. In all cases, the scanned images were converted to greyscale, applying a green filter for iron(II) and alkalinity and a red filter for phosphate, and the file saved in TIFF format. The greyscale images were then resized so that 1 pixel was equal to 0.8 x 0.8 mm and the image was exported to Scion Image (Version 4.0.3.2, ScionCorp) where greyscale intensity values were converted to iron(II), phosphate and alkalinity concentrations using the appropriate calibration curve. DGT-labile sulfide (HS^- and S^{2-}) was determined as described by Robertson et al. (2008).

In order to obtain individual depth profiles of iron (II), phosphate, alkalinity and sulfide from each probe, data for each horizontal line of pixels were averaged across the width of the image in order to get a mean value for each depth interval. These mean values were then averaged and standard errors were calculated in order to yield mean concentration profiles.

- **Analysis of alkalinity distributions**

The alkalinity DET was immediately transferred to a transparent sheet on a flat-bed scanner, stained using a reagent impregnated staining gel and distributions were acquired as previously described (Bennett et al., 2014). The scanned images were then converted to greyscale (applying a green filter) and the file saved in TIFF format. The greyscale images were then re-sized so that 1 pixel was equal to 0.8×0.8 mm and the image was exported to Scion Image (Version 4.0.3.2, ScionCorp) where greyscale intensity values were converted to alkalinity concentrations using the appropriate greyscale versus concentration calibration curve (Bennett et al., 2014).

Results and discussion

- **Microelectrode profiles of oxygen and sulfide**

Microelectrodes for O₂, pH and sulfide measurements have been developed in order to measure depth profiles and rates of oxygen production and consumption using the dark-light shift within sediments (Revsbech and Jørgensen, 1983; Revsbech et al., 1983, 1980; Visscher et al., 1998; 1991a). These microelectrodes have been deployed in environments exhibiting high biological activity such as microbial mats in order to investigate oxygen and sulfide dynamics at high spatial and temporal resolution (Dupraz et al., 2004; Jørgensen et al., 1979; Revsbech et al., 1983; Visscher et al., 2002, 1992a, 1991a). As oxygen production is highly dependent on light availability and microbial mat topography fluctuates over small distances (see dashed lines in Fig 7), representative light and dark oxygen and sulfide microelectrodes profiles are shown in [Figure 3.2](#).

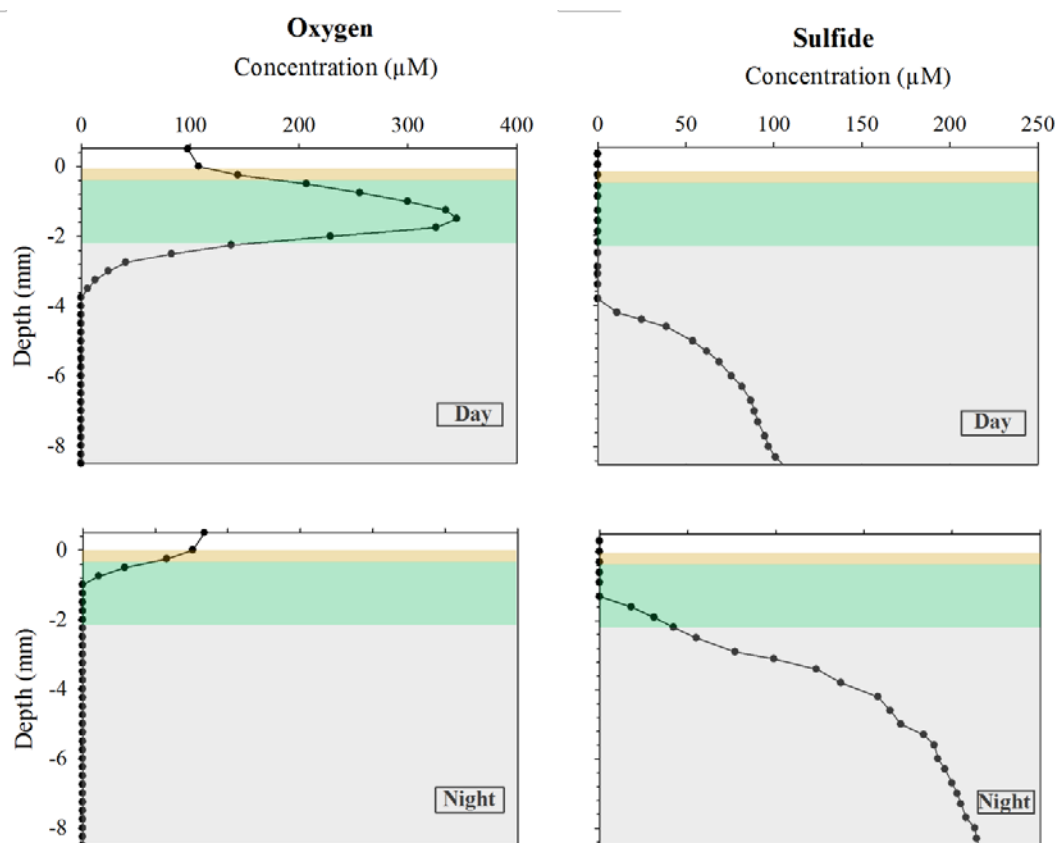


Figure 3.2: Representative oxygen and sulfide profiles measured with microelectrodes in the layered microbial mat during light ($I = 1982 \mu\text{E}\cdot\text{m}^{-2}\cdot\text{s}^{-1}$) and dark deployments ($I = 0 \mu\text{E}\cdot\text{m}^{-2}\cdot\text{s}^{-1}$). The yellow layer represents the first layer of the mat, the green layer represents the second layer characteristic of cyanobacteria and the grey layer represents the deepest part of the mat.

Under light conditions, oxygen concentrations increased rapidly with depth in the subsurface cyanobacterial layer, with a maximum concentration of $345 \mu\text{M}$ recorded at 1.8 mm depth (average and standard error of six measurements was $354 \pm 18 \mu\text{M}$ at a depth of $1.9 \pm 0.2 \text{ mm}$). The salinity averaged $68 \pm 2 \text{ PSU}$, the day time temperature was $29.5 \pm 0.9 \text{ }^\circ\text{C}$, and the night time was temperature $17.2 \pm 1.4 \text{ }^\circ\text{C}$ during the measurements. The differences observed among replicate profiles were therefore most likely due to fluctuations in the light regime ($1603\text{-}2123 \mu\text{E}\cdot\text{m}^{-2}\cdot\text{s}^{-1}$; Revsbech and Jørgensen 1986, 1983; Visscher et al. 2002). Below the O_2 maximum the concentrations rapidly decreased with depth, and oxygen was not detectable below 3.5 mm depth (average and standard error of six profiles 4.0 ± 0.1

mm), confirming permanent anoxic conditions in the third (black-colored) mat layer. During the daytime, sulfide was not detected in the upper 3.8 mm of the mat (average and standard error of six sulfide profiles 4.4 ± 0.1 mm). Concentrations then increased rapidly to $\sim 50 \mu\text{M}$ in all measured profiles, and then slowly increased up to $100\text{-}150 \mu\text{M}$ at 10 mm depth. Oxidic conditions present in the upper 4 mm of the mat during peak photosynthesis likely supported the oxidation of sulfide to sulfate, elemental sulfur, polysulfides and thiosulfate by chemoautotrophic bacteria and anoxygenic photoautotrophs or chemical reaction with oxygen (Visscher et al., 1992b). However, the depth of the oxycline is changing with light availability (Dupraz and Visscher, 2005; Visscher et al., 2002) and so is the depth horizon of chemolithotrophic sulfide oxidation mediated by O_2 . Anoxygenic phototrophic bacteria (e.g., purple sulfur bacteria) use sulfide as electron donor for CO_2 fixation and produce sulfate, with zero-valence sulfur being an intermediate (Visscher and van Gemerden, 1993). These organisms require red light to perform photosynthesis (which is not used by cyanobacteria and penetrates deeper into the sediment) but can survive in low-light environments (Overmann et al., 1992). Sulfide oxidation can also be carried out under anoxic conditions by chemolithotrophs if nitrate is present, but the populations of these denitrifiers in mats is typically an order of magnitude lower than that of aerobic chemolithotrophs (Visscher et al., 1992b). Chemical oxidation can also act as a sulfide sink, however, the affinity of chemolithotrophs for sulfide and their oxidation rate typically outpaces that of chemical oxidation (Visscher et al. 1992b).

At night, in the absence of photosynthetic O_2 production, diffusion from the overlying water is the only O_2 source, and depth profiles show that this was rapidly consumed by microbial respiration within the uppermost mm of the mat (Figure 3.2). Anoxic conditions prevailed below 1 mm depth in all profiles measured leading to a migration of the sulfide profile with concentrations increasing rapidly from $0 \mu\text{M}$ to $200\text{-}250 \mu\text{M}$ in the first 5 mm. Thus, much higher concentrations of sulfide were present at shallower depths during the night. For example, there was $50\text{-}75 \mu\text{M}$ sulfide present at 2 mm depth at night compared to $0 \mu\text{M}$ sulfide during the day. In the absence of O_2 , organic carbon oxidation may take place *via*

fermentation, denitrification and iron(III)- and sulfate-reduction. In the absence of oxygen and light, the sulfide generated by sulfate-reducing bacteria can no longer be chemically or biologically consumed, which results in the migration of the sulfide profile towards the surface and an increase in sulfide concentrations throughout the mat. Similar microelectrodes profiles of oxygen and sulfide have been measured in other microbial mats (e.g., Jørgensen et al., 1979; Revsbech et al., 1983; Visscher et al., 2002, 1991a).

Microelectrodes have many advantages to measure chemical conditions at high temporal and spatial resolution in microbial mats. However, the use of microelectrodes do not readily allow evaluation of sediment heterogeneity (see Stockdale et al., 2009 for a review), as they provide only one-dimensional vertical profiles of solute concentrations and do not take into account horizontal heterogeneity within the system. Additionally, with a few exceptions (e.g., Luther et al., 2001; Visscher et al., 1991a), microelectrodes are not capable of measuring solute co-distributions at exactly the same sampling point. In contrast, the DET and DGT techniques used in this study, although they lack the spatial and especially temporal resolution of microelectrodes, are able to measure the co-distributions of solutes in two dimensions at sub-mm resolution (Pagès et al., 2011; Robertson et al., 2008). Therefore, the combination of microelectrodes and DET/DGT techniques can provide highly complimentary results.

- **Small scale two-dimensional heterogeneity in sulfide, iron(II) and phosphate distributions**

Figure 3.3 shows the five replicate distributions of sulfide measured during day and night deployments. Probes A, B, C and D showed sulfide distributions somewhat similar to those obtained with the micro-electrodes for day-time conditions, although with considerable variation in the sulfide concentration. Of the night-time conditions, only probe I showed sulfide distributions similar to those measured with micro-electrodes, with a large zone from 7 to 30 mm of depth of high sulfide concentration up to 350 μM extending into the microbial mat. There

was considerable variability in the sulfide distributions and concentrations measured by the different probes, even though they were deployed in close proximity. For example, probes F, H and J (night deployments) show relatively homogenous distributions of low to moderate (only at depth below the microbial mat) sulfide concentrations throughout, which was very similar to probe E (day deployment). Probe G had a unique distribution with moderate sulfide concentrations extending through the microbial mat into the overlying waters.

In addition to this inter-probe heterogeneity, strong intra-probe heterogeneity was also visible in sulfide distributions from individual probes from both the day and night deployments. In the day deployment a small “hotspot” of sulfide (up to 200 μM) was visible at ~ 10 mm depth in probe C, while probes A and B showed a generally higher sulfide concentration at depth on the right and left hand sides, respectively. Similarly, in night deployments, probe G recorded a narrow vertical zone of high (300-350 μM) sulfide on the right hand side of the gel at 20-30 mm depth and as discussed above, probe I had an extensive zone of similarly high sulfide concentrations but surrounded by low sulfide concentrations on both sides. These two-dimensional distributions demonstrate the high degree of both vertical and lateral variability in sulfide concentrations that occur within the mat structure, which has significant implications for biogeochemical cycling within the mat (Pagès et al., 2014). Two-dimensional distributions of iron(II), phosphate and alkalinity replicates similarly showed significant heterogeneity and can be found in the Supplementary Information ([Figures A3.1, A3.2 and A3.3](#)).

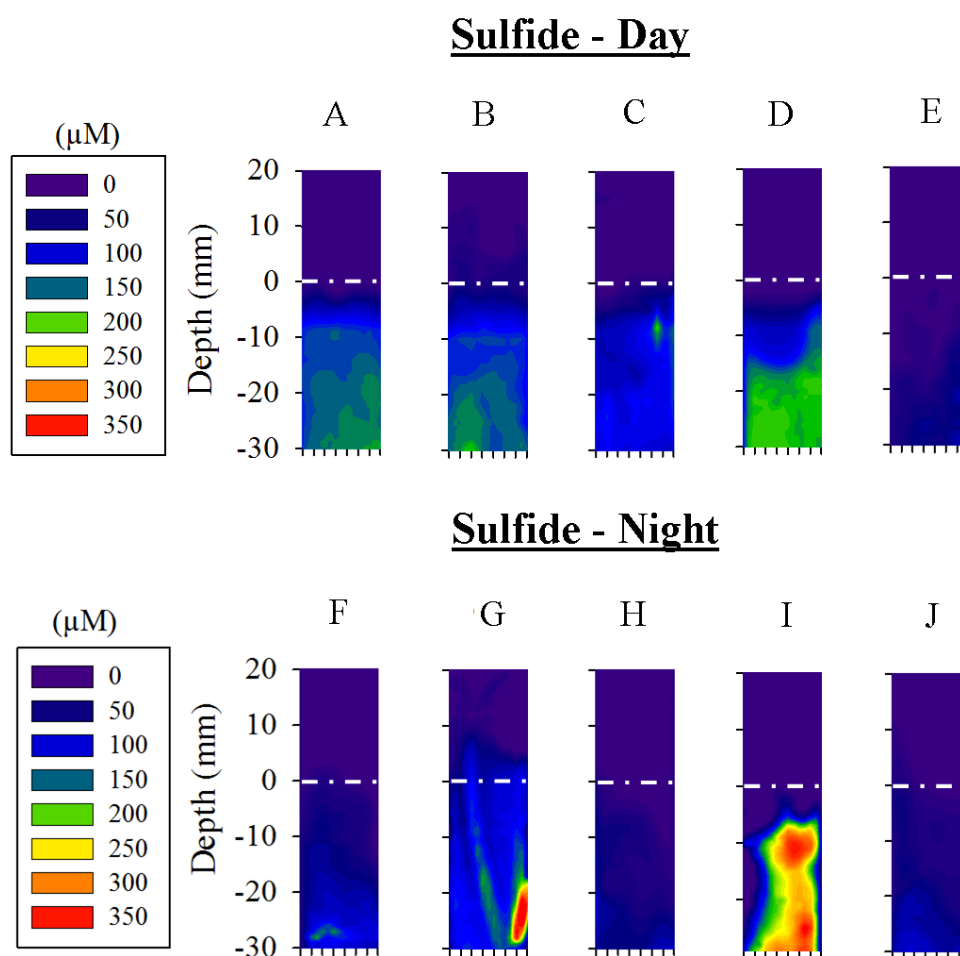


Figure 3.3: Two-dimensional distributions of sulfide measured by five DGT probes in the microbial mat during light and dark deployments. The width of all gels is 14 mm. The white dotted line represents the mat surface.

In addition to providing two-dimensional data, DGT/DET techniques enable the deployment of multiple gel layers within a single probe, allowing the co-distributions of solutes to be obtained for the exact same location of the microbial mat, overlying water and underlying sediment. This allows solute interactions and the combination of microbial metabolisms that generate these distributions to be studied in detail (Pagès et al., 2012, 2011; Robertson et al., 2009, 2008). Figure 3.4 shows an example of day and night co-distributions of sulfide, iron(II) and phosphate obtained from individual triple-layered DGT/DET probes. Probe B (daytime) showed sulfide concentrations that were relatively low for the first 15 mm, but a zone of moderate sulfide concentrations occurred in the deeper part of the mat (up to 200 μM). Iron(II) presented a more patchy distribution with a zone

of relatively high iron(II) (up to 12 μM) throughout the entire mat on the left side of the distribution while the right side exhibited lower background concentrations (~ 2 μM), with the exception of one small hotspot at about 8 mm depth in the mat. There was little overlap between the iron(II) and sulfide distributions with zones of high iron(II) concentrations coinciding with the absence, or low concentrations, of sulfide and vice versa, as would be expected, since sulfide co-precipitates with iron(II) to form insoluble iron monosulfide (Luther and Church, 1988). In contrast, the night deployed probe I showed a large overlap of the iron(II) and sulfide distributions with moderate concentrations of iron(II) coinciding with the large vertical feature of high sulfide concentrations in the right-hand side of the probe (from 5 mm deep). Such a co-occurrence would not normally be expected (see above). These contradictory results could be explained by the different timescales investigated by the DGT and DET samplers. DGT is a kinetic passive sampling measurement where the analyte accumulates on the binding gel over the deployment period. Consequently, the measured concentrations are a time-integrated average of the analyte porewater concentration at the probe-sediment interface over the entire deployment period (Robertson et al., 2008). However, DET is based on equilibrium between the hydrogel and porewater solutes, therefore, the measured concentrations are representative of the last few hours of the deployment period (Pagès et al., 2011; Robertson et al., 2008). Hence, it is possible that sulfide and iron(II) were present in the exact same location of the microbial mats but at different time periods over the deployment. This reinforces the complementary nature of these measurements, which record all sulfide conditions over the deployment period, to microelectrodes, with their superior temporal resolution (Visscher et al. 1992a).

Phosphate distributions differed between the day and night deployments. During the day, the background phosphate was very low with several hot spots of phosphate of various sizes and concentrations of up to 3 μM (Figure 3.4). This suggests that phosphate was removed from solution except in hotspots where it was mobilized. In the night, however, phosphate was mobilized much more extensively within the mat where several hotspots of up to 5 μM observed. The availability of

solid phase iron(III) oxyhydroxides has been proposed to be a factor regulating porewater phosphate concentrations in marine and freshwater sediments (Smolders et al., 1995), as phosphate adsorbs onto the surfaces of iron(III) oxyhydroxides (Jensen et al., 1998). Vivianite ($\text{Fe}_3^{2+}(\text{PO}_4)_2 \cdot 8\text{H}_2\text{O}$), for instance, can be formed from the precipitation of phosphate with iron(II). Consequently, reductive dissolution of these phosphate-iron(III) complexes by iron(III)-reducing bacteria, or chemically by sulfide produced during sulfate-reduction, could result in a concomitant release of phosphate and iron(II) to the porewater. However, as can be clearly seen in the example co-distributions, the zones of high phosphate do not correspond to zones of active iron(III)-reduction (high iron(II) concentrations) or sulfidic zones, where theoretically all biologically available iron(III) oxyhydroxides have been reduced. This suggests that, in this case, iron geochemistry was not a major determinant regulating porewater phosphate concentrations. It is more plausible that the zones of elevated phosphate concentrations represent hotspots of organic matter mineralisation, which would generate phosphate regardless of which microbial respiration process was involved. It should be noted that in general, iron(III)-reduction represents a minor pathway of microbial organic carbon oxidation in hypersaline mats (Wieland et al., 2005).

The absence of an anticipated correlation between the two-dimensional co-distribution of porewater iron(II) and phosphate has been noted previously in seagrass rhizosphere sediments (Pagès et al., 2012, 2011). While Pagès et al. (2011) found a strong correlation between laterally-averaged depth profiles of iron(II) and phosphate, this relationship proved to be largely coincidental due to laterally separated zones of high phosphate and iron(II) occurring at similar depths and there was no significant correlation for the two-dimensional distribution of iron(II) and phosphate (Pagès et al., 2011). Although further studies across a range of aquatic ecosystems are required to confirm these findings, they clearly demonstrate the need for two dimensional techniques when studying complex, heterogenous systems, as conventional porewater extraction and sediment peeper techniques both result in lateral averaging of porewater concentrations due to the large sampling volumes and potential artefacts due to mixing of pore waters with different

compositions that produce undesirable reactions (Pagès et al., 2012, 2011; Robertson et al., 2009, 2008).

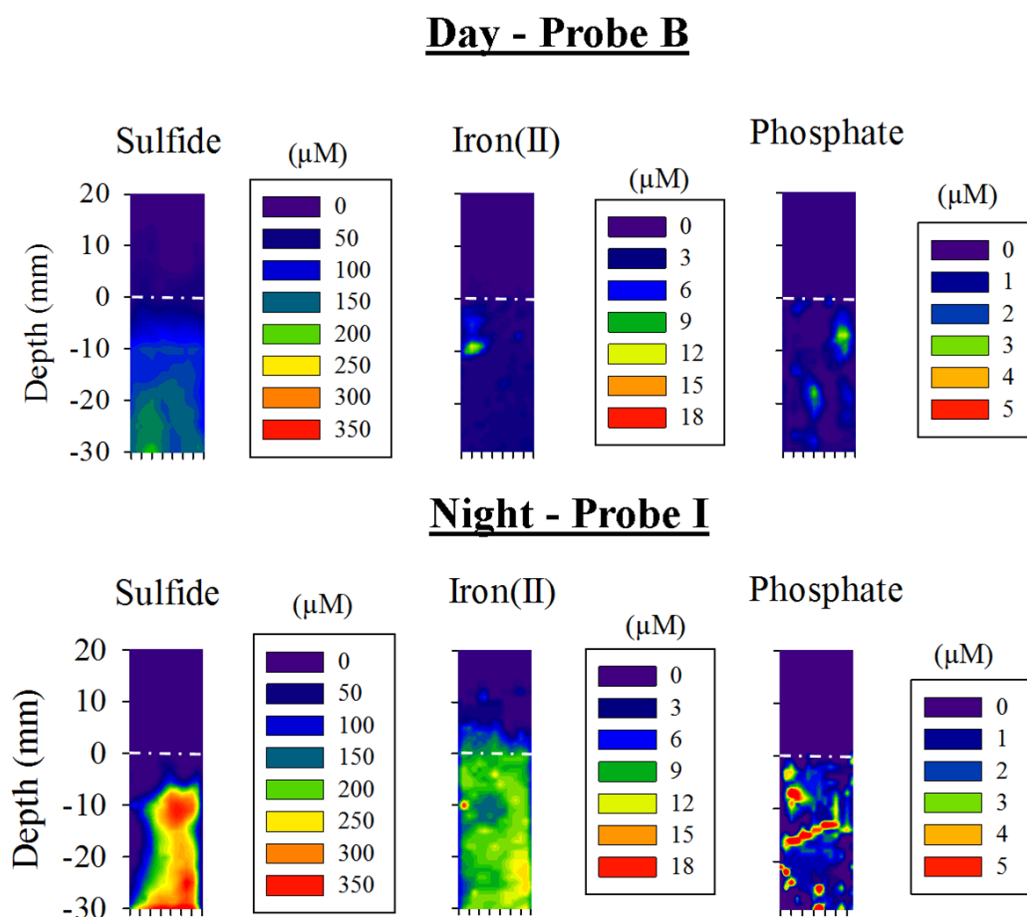


Figure 3.4: Two-dimensional co-distributions of sulfide, iron(II) and phosphate measured in the layered microbial mat by combined DGT/DET probes during light (probe B) and dark (probe I) deployments. The width of all gels is 14 mm. The white dotted line represents the mat surface.

- **Biogeochemical changes over a diel cycle**

Although the high-resolution, two-dimensional measurements clearly demonstrate the high degree of spatial heterogeneity that existed in the distributions of individual solutes within the microbial mat, that same heterogeneity makes it difficult to quantify the more general changes observed between the day and night deployments. Therefore, in order to clearly visualise the global diel changes in porewater conditions, over the biofilm layers, the data from each probe were horizontally averaged across the width of each probe to generate concentration

profiles which were subsequently averaged to provide mean depth profiles with standard errors for each solute for day and night deployments (Figure 3.5).

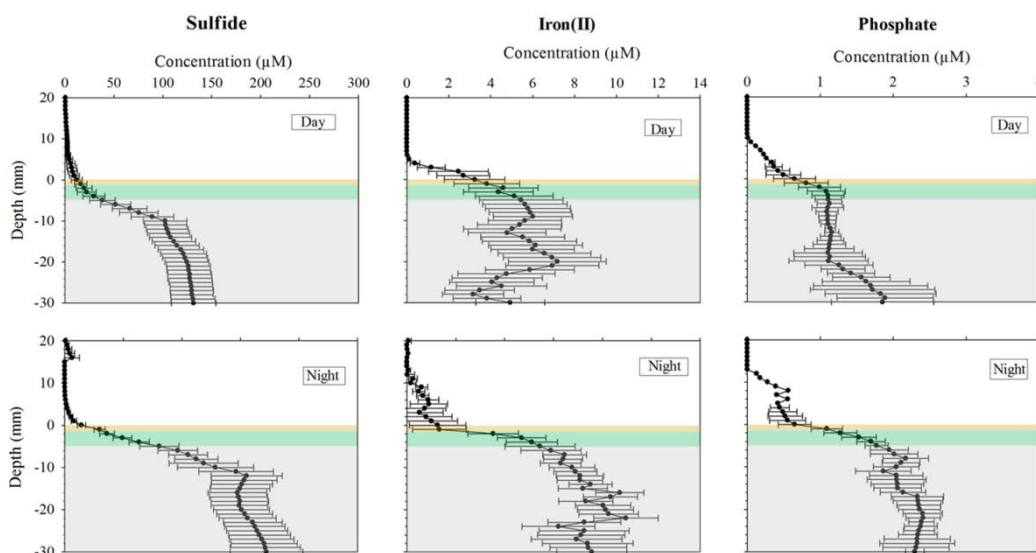


Figure 3.5: Mean depth profiles of sulfide, iron(II) and phosphate concentrations during light and dark deployments. Error bars indicate the standard error of the mean (n=5). The yellow layer represents the first layer of the mat, the green layer represents the second layer characteristic of cyanobacteria and the grey layer represents the deepest part of the mat.

Under light conditions, mean sulfide concentrations increased from 12 μM at the mat surface to 102 μM at 10 mm depth. Sulfide concentrations increased slowly with depth in the permanently anoxic part of the microbial mat to reach a maximum of 132 μM at 30 mm depth (Figure 3.5). Sulfide seemed to diffuse from the bottom layer of the mat to the upper layer, however, the non-linear decrease in sulfide in the upper layers of the mat (0-5 mm) suggested that sulfide distribution was controlled by chemical and biological reactions rather than diffusion only, which is a characteristic feature of mats (Visscher and van Gernerden, 1993; Visscher et al., 1992a, 1991a). Iron(II) concentration at the mat surface was 3 μM and progressively increased to reach 6 μM at 9 mm depth and then, slowly decreased before increasing again to a maximum of 7 μM at 20 mm depth. This distribution is consistent with the presence of anoxic conditions in the deeper part of the mat.

At night, in the absence of photosynthetic oxygen production, the concentration of sulfide and iron(II) showed steep increases within the microbial mat (Figure 3.5): the sulfide concentration increased from 14 μM at the surface to 205 μM at 10 mm depth and reached 239 μM at 30 mm depth, while the iron(II) concentration increased from 1 μM to 7 μM at 7 mm depth. In deeper layers, both sulfide and iron(II) concentrations remained relatively constant, except for a sudden increase in iron(II) concentration at 19 mm depth, but at concentrations almost double those that were recorded during the day deployments (Figure 3.5). The maximum sulfide concentration recorded in the deeper part of the mat increased from 132 μM during the day to 242 μM at night, indicating that the rate of sulfide diffusion to the surface of the mat was much higher at night (van Gemerden, 1993; Visscher et al., 2002, 1991a). The iron(II) profile showed a relatively progressive increase in concentration, similar to the one measured in iron(II) profiles of marine coastal sediments (Thamdrup et al., 1994).

The presence of low concentrations of both sulfide and iron(II) in water above the mat surface during both day and night deployments is somewhat surprising, given that microelectrode profiles (Figure 3.2) showed the presence of oxygen and absence of sulfide in this water. During the day, DGT profile ranged from 12 μM sulfide at the surface of the mat to 102 μM at 10 mm depth. However, the microelectrode profile showed an absence of sulfide for the upper 4 mm and reached approximately 100 μM at 8 mm depth. This may reflect that the heterogeneity in solute distributions observed within the mat also extended into the diffusive boundary layer of water above the mat. A lower concentration scale (0-100 μM) was applied with Sigma Plot to better visualise sulfide distribution at the water-mat interface in probe G (Figure 3.6). For this specific probe, sulfide distribution was clearly present in the water column and the distribution implies one or more plumes of sulfide crossing the water-microbial mat interface. Lower concentrations and anticipated depth profiles were apparent for three other sulfide probes (Figure 3.3A, B and C). As this sulfide diffusion across the mat-water interface was only observed for a few replicates, it might be related to the presence of nematodes that were previously identified in Shark Bay mats (Allen et al., 2009)

and can cause significant bioirrigation in the sediments (Pike et al., 2001). However, visual inspection of mat samples using a dissection microscope did not reveal high numbers of nematodes. A recent molecular diversity study of eukaryotes in Shark Bay mats, which included smooth mats, found a diverse community of protists but did not report high abundances of nematodes or other bioturbators (Edgcomb et al., 2013). As outlined above, a more plausible explanation is that the sulfide originates from the high rates of sulfate reduction present near the surface of the mat (Visscher et al., 2000, 1992a). This sulfide production, in combination with the low rates of sulfide re-oxidation at night, could produce such an efflux of sulfide into the overlying waters.

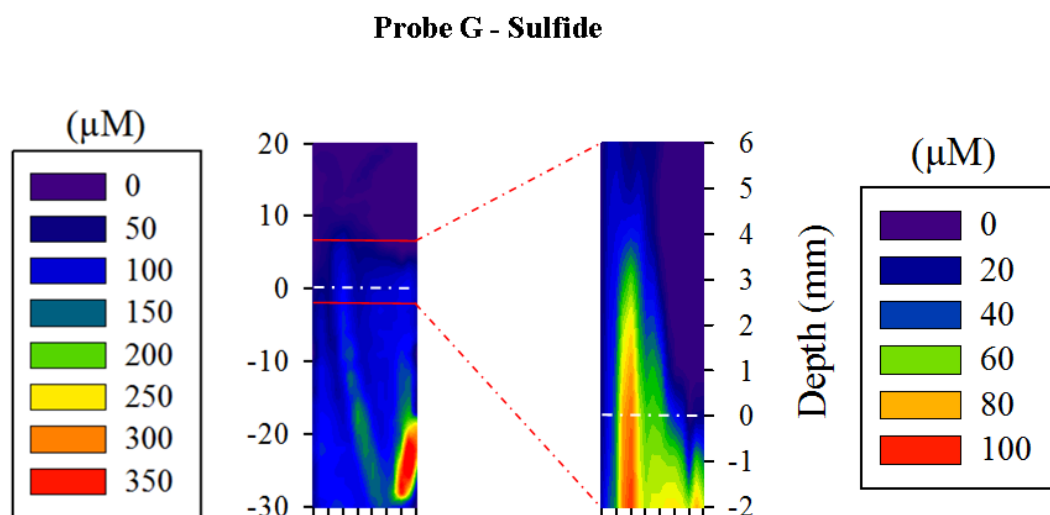


Figure 3.6: Visualisation of sulfide heterogeneity at the mat-water interface in probe G using a smaller concentration scale (0 to 100 µM). The white dotted line represents the mat-water interface.

It has been known for decades that sulfate-reduction is not a strict anaerobic process (Baumgartner et al., 2006; Cypionka et al., 1985). Actual measurements of this anaerobic metabolism in a variety of microbial mats have corroborated that the maximum rates are found where cyanobacterial photosynthesis is also peaking and supersaturated concentrations of oxygen exist during a large part of the light period (Canfield and Des Marais, 1991; Jørgensen, 1994; Visscher et al., 2000; 1992a). However, no microelectrode measurements have reported sulfide in the upper part

of microbial mats. In order to visualise the distribution of sulfate-reducing activities at high resolution (tens to hundreds of micrometers), $^{35}\text{SO}_4^{2-}$ -coated Ag foils were also deployed in the smooth mat. The pixels (Figure 3.7) correlate with areas of sulfate reduction activity; the darker the pixels, the higher the metabolic activity of the sulfate-reducing microbes. The 2D distribution map of sulfate reduction shows the typical pattern of peak activity in the green layer (Figure 3.7, layer 2). Likewise, the deepest (black) mat layer, in which easily degradable organic carbon concentrations are also low (Decho et al., 2005; Visscher and van Gemerden, 1993), displays lower rates (i.e., lower pixel density; Figure 3.7, layer 4). The layer in which purple sulfur bacteria are sometimes found (Figure 3.7, layer 3) revealed a similar or slightly lower rate of sulfide production. These results corroborate previous $^{35}\text{SO}_4^{2-}$ coated Ag foil deployments in a variety of marine and hypersaline mats and microbialites, including open marine stromatolites of the Bahamas, all of which show a peak in sulfate reduction activity close to the peak of O_2 (Dupraz et al., 2004; Visscher et al., 2010, 2002, 2000). In addition, the results from the $^{35}\text{SO}_4^{2-}$ coated Ag foils were strongly concordant with the detection of sulfide in the upper part of the mat from the DGT sampler and confirmed that sulfate-reduction can take place in the upper layers of the mats under daylight conditions.

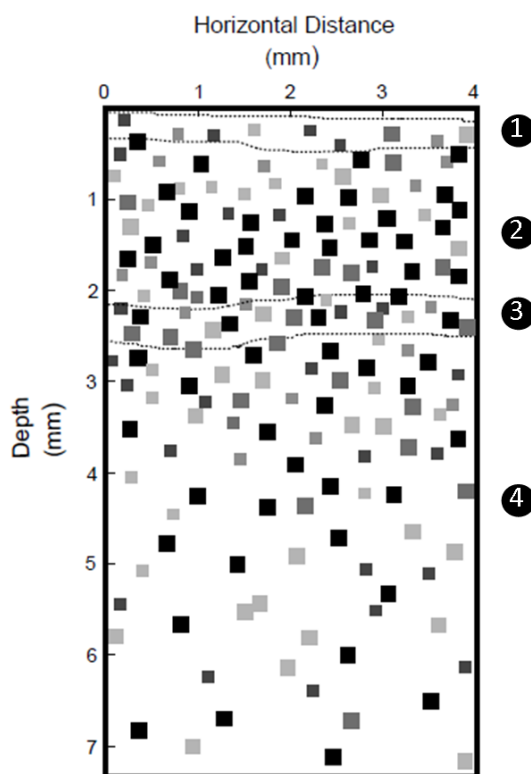


Figure 3.7: 2D distribution of sulfate reducing activity in a smooth mat from Nilemah measured in April 2012; density and size of black and grey pixels indicate locations and relative degree of sulphate reducing activity. Darker pixels represent higher levels of sulfate-reducing activity. The size of the pixel indicates the approximate true size of the sulfate-reducing activity (see text and Visscher et al. 2000). The numbers on the right side (1-4) indicate the layer's number (1 = tan surface layer; 2 = green cyanobacterial layer; 3 = thin layer of purple sulfur bacteria (not always present in smooth mats); 4 = black layer of FeS).

During the day, both DGT and microelectrodes profiles showed a rapid increase of sulfide concentration below 5 mm depth ($50 \mu\text{M}$ for both profiles at 5 mm) followed by a slower increase in the deeper parts of the mat (Figure 3.2 and Figure 3.5). At night, DGT-measured sulfide concentrations increased from $14 \mu\text{M}$ to $205 \mu\text{M}$ at 10 mm depth while the electrode profile showed an absence of sulfide for the first mm and a rapid increase up to $210 \mu\text{M}$ at 8 mm depth. Sulfide concentration increased more rapidly in the electrode profile with sulfide concentration reaching $150 \mu\text{M}$ at 4 mm deep vs. $70 \mu\text{M}$ for the DGT profile. It appeared that both DGT and microelectrode profiles revealed the same trends and similar range of concentrations. However, noticeable differences in the gradient

steepness were present and might be due to the timescale difference between the two measurements. The DGT profiles presented average sulfide concentrations measured by 5 replicates over the entire period of deployment (8 h). In contrast, the microelectrode profile presented the measurement made at one particular instant during the day and the night with a much greater temporal resolution. In addition, due to the 2D nature of the colorimetric DET and DGT, the variability of analyte distribution was taken into account (e.g. hotspots), whereas microelectrodes could only measure this if the individual profile happened to traverse these regions. Although the presence of the DET/DGT samplers in the mat may contribute to an increased heterogeneity by affecting hydrodynamics, the light/dark changes in the sulfide and iron(II) profiles are consistent with the diel changes in microbial metabolism (Dupraz and Visscher, 2005; van Gemerden, 1993) and are largely consistent with the oxygen distributions measured with microelectrodes.

During the day, the upper mat layers were oxic with only a few patches of low concentrations of sulfide and iron(II), possibly associated with micro-zones within the mat (Figure 3.5). This would be expected, since, as confirmed by the microelectrode profiles, there was supersaturation of oxygen during the light period in the subsurface layer of the mat (Figure 3.2). The high concentrations of oxygen support rapid chemical and microbial oxidation of sulfide and iron(II). Microbial sulfide oxidation is a major process in microbial mats, which is carried out by chemolithoautotrophs predominantly under oxic but also under denitrifying conditions (Visscher and van Gemerden, 1993; Visscher et al., 1992a;). Moreover, in anoxic zones where light was present, the use of sulfide and iron(II) as electron donors for anoxygenic photosynthesis (van Gemerden, 1993) would also tend to reduce their concentrations. Thus, the profiles and concentrations of sulfide and iron(II) reflect the dominance of autotrophic, particularly photolithoautotrophic metabolism in the light, which results in the production of oxygen and exploitations of sulfide and iron(II) by photo- and chemolithoautotrophs.

In contrast, at night, photolithoautotrophic metabolisms are absent and the metabolism of chemolithoautotrophs is limited by oxygen diffusion from the overlying water and the availability of nitrate, resulting in a dominance of anaerobic heterotrophic metabolisms (e.g., sulfate reduction) within the mat. The diffusion of O_2 from the water column is kinetically limited and the rapid consumption of oxygen results in anoxic conditions in the bulk of the mat (Fig. 2; Visscher and van Gemerden, 1993; Visscher et al., 1991). This favors iron and sulfate reduction and limited chemical and/or microbial reoxidation of the end products (i.e., iron(II) and sulfide), which would migrate toward the surface of the mat. The interactions that occur between the iron and sulfur cycles could also influence the accumulation of iron(II) and sulfide within the mat. For example, solid phase iron oxyhydroxide generated within the mat by chemical and microbial oxidation during the day would react with sulfide to produce iron(II) and S^0 , the iron(II) produced could precipitate with sulfide as FeS and this could further react with S^0 or polysulfides, produced by reaction of S^0 with sulfide, to form pyrite (FeS_2) (Azzoni et al., 2001; Luther and Church, 1988; Rickard and Morse, 2005; Visscher and van Gemerden, 1993). The net effect of these reactions is to buffer the porewater concentration of sulfide by converting it to solid phase S^0 , FeS and FeS_2 .

Overall, our results are in accordance with what would be expected from previous microelectrode studies which have shown strong diel shifts in redox conditions within microbial mats (Jørgensen et al., 1979; Revsbech et al., 1983; Visscher et al., 2010, 2002, 1992a,b, 1991a,b). However, as clearly shown by the two dimensional distributions of sulfide and iron(II) in [Figure 3.3](#) and [Figure 3.4](#), these shifts are not the result of simple vertical migrations of the oxygen and sulfide profiles but rather changes in the size, intensity and distribution of redox zones.

Diel distributions of phosphate were also obtained with the DET sampler. In Shark Bay water, phosphorus has been shown to be the limiting nutrient while nitrogen requirements are met by nitrogen fixation (Smith and Atkinson, 1983), although changes in phosphorus and nitrogen concentrations overtime are expected. The C:P ratio taken up by primary producers in Shark Bay water and in sediments were respectively 320:1 and 300:1, suggesting that sediments reflect net biological uptake (Smith and Atkinson, 1983). During both day and night deployment, profiles of phosphate (Figure 3.5) showed fluxes from the mat into the water column which suggested that the microbial mat may have been one of the sources of phosphate necessary for the production in the phosphate-limited water column.

During the day deployments, phosphate concentration rapidly increased from 0.5 μM at the mat surface to 1 μM in the upper 4 mm and at greater depth increased much more slowly to a maximum of 1.5 μM at 13 mm. Under light conditions, the phosphate that may be released during organic matter breakdown would likely be taken up by the microbial population. In the oxic layers, phosphate could also have been complexed by solid-phase iron oxyhydroxides.

At night, phosphate concentrations increased rapidly with depth from a surface value of 1 μM to a maximum of 2 μM at 9 mm deep. Deeper in the mat, phosphate decreased at 10 mm depth and increased again to a maximum of 2.5 μM at 16 mm. This steep increase in phosphate suggested a significant release of phosphate after dissolution of iron-phosphorus complexes. The rapid decrease in dissolved oxygen concentration observed during the night with microelectrodes lowers the redox potential leading to liberation of phosphate from the redox-labile iron compounds (Borovec et al., 2010). This would imply that bacteria have access to an extra pool of phosphate during the night, which could favor development of sulfate-reducing microbes. In addition, under anoxic conditions, ferric phosphate could react with sulfide, releasing phosphate ions to the porewater (Ehrlich, 1996). The increase in iron(II) and phosphate at night between 0 and 20 mm depth (Figure 3.5) seemed to coincide with dissolution of iron-phosphate complexes leading to

the release of phosphate and iron in the porewater. However, the 2D distribution clearly showed that phosphate hot spots did not coincide with iron(II) hotspots (zones of effective iron(III) reduction) or sulfidic hot spots (areas where the total iron(III) pool should have been reduced to iron(II) (Figure 3.4, Figures A3.1 and A3.2). This is in agreement with previous observations made in marine and hypersaline mats that iron(III) reduction is generally a minor contributor to overall microbial metabolism (Dupraz and Visscher, 2005; Visscher and Stolz, 2005; Wieland et al., 2005). Furthermore, the correlation between iron(II) and phosphate was estimated for each 2D probe, as well as for the average concentration profiles, and showed that the profiles consistently reported a higher correlation than data from 2D probes (Table A3.1). The iron and phosphate concentrations from averaged data presented r values ranging between 0.23 and 0.88, with a mean r value of 0.65. However, the iron and phosphate concentrations from 2D probes showed r values ranging from 0.12 to 0.68, with a mean value of 0.39. Therefore, the correlation between iron(II) and phosphate concentrations calculated from the 1D profiles is always about 1.5 times higher than the correlation from the 2D concentrations. This confirms that 1D profiles may not reflect biogeochemical processes occurring in microniches. The 2D distributions, however, seemed to confirm that phosphate hot spots resulted from the decomposition of particulate organic matter in the mat by various microbial processes. Consequently, porewater phosphate distribution was most likely driven by diel metabolic changes in the microbial mat rather than being directly solubilised by iron(III)-reduction.

- **Alkalinity measurements and the carbonate cycle**

Alkalinity in microbial mats is a valuable proxy for carbonate precipitation (Arp et al., 2001; Dupraz et al., 2009; Visscher et al., 1998). Calcium carbonate precipitation is a key process for the formation and preservation of lithified microbial mats (Dupraz and Visscher, 2005). Day and night alkalinity profiles measured with the DET method are presented in Figure 3.8. During the day, the alkalinity increased with depth from 3 meq.L⁻¹ at the surface of the mat to 3.5 meq.L⁻¹ in the bottom layer of the FeS-rich layer at 8 mm depth. It progressively

decreased in the deeper part of the mat to reach a minimum of 2 meq.L^{-1} at 28 mm depth. Oxygenic and anoxygenic phototrophy consumed CO_2 , which increases the alkalinity during the day (Visscher and Stolz, 2005). In contrast, aerobic heterotrophic respiration, chemolithoautotrophic sulfide oxidation and fermentation decreased the alkalinity (Visscher and Stolz, 2005). In addition, chemical or microbial oxidation of iron(II) to iron(III) could have resulted in precipitation of iron oxyhydroxide that would further decrease the OH^- concentration and consequently, decrease the alkalinity. In the deeper anoxic layers, HS^- could have reacted with iron(II) to form FeS but this reaction does not consume alkalinity. However, FeS precipitation leads to the production of two fewer alkalinity equivalents than can be expected from sulfate- and iron(III)-reduction (Krumins et al., 2012).

At night, a general increase in alkalinity was observed. The lowest concentration, still detected in the top layer, was significantly higher than during the day (4 meq.L^{-1}). The maximum alkalinity ($> 4 \text{ meq.L}^{-1}$) was observed at 4 mm and 15 mm depth, with slightly lower alkalinity values in between. Under dark conditions, with a rapid depletion of oxygen, sulfate reduction is usually a dominant microbial process in microbial mats (Canfield and Des Marais, 1993; Visscher et al., 1992a). For instance, in a hypersaline microbial mat from Camargue (France), 64-99% of the DIC released at night was found to result from sulfate reduction (Wieland et al., 2005). Incubations of microbial mats showed that the flux of DIC from the mat to the water was \sim ten times higher under dark conditions, corroborating that sulfate reduction is the dominant process at night in microbial mats (Joye et al. 1996). Ample evidence supports that sulfate reduction is as an important process favoring carbonate precipitation in modern mats (Baumgartner et al., 2006; Dupraz and Visscher, 2005; Gallagher et al., 2012; Lyons et al., 1984; Visscher et al., 2000). In Bahamian stromatolite mats, maximum rates of sulfate-reduction were coincided with precipitation of microcrystalline CaCO_3 , showing the role of sulfate-reducing bacteria in shaping stromatolite fabric (Visscher et al. 2000). It should be noted that some weak acids and bases may also contribute to the total alkalinity (Knull and Richards, 1969).

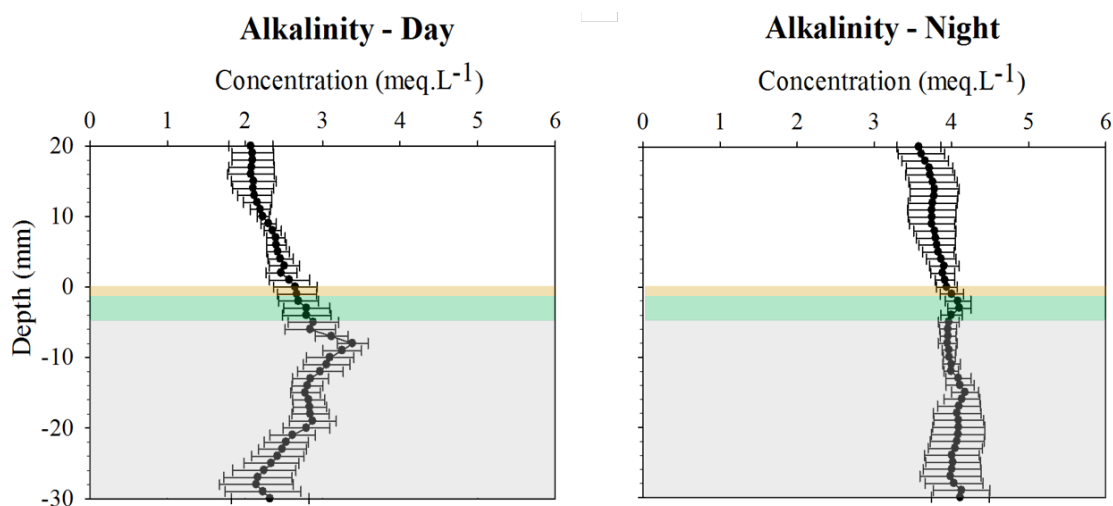


Figure 3.8: Mean depth profiles of alkalinity concentrations during light and dark deployments. Error bars indicate the standard error of the mean ($n=5$). The yellow layer represents the first layer of the mat, the green layer represents the second layer characteristic of cyanobacteria and the grey layer represents the deepest part of the mat.

Microbial metabolic processes are clearly involved in the diel shifts of alkalinity and lithification is the result of a balance between microbial processes favoring alkalinity increase and therefore, carbonate precipitation and alkalinity decrease leading to carbonate dissolution (Visscher and Stolz 2005). In addition to a change in alkalinity, a nucleation site is also needed for CaCO_3 mineral precipitation (Dupraz and Visscher 2005). EPS has also been shown to play this role in microbial mats (Dupraz et al., 2004; Reid et al., 2000).

Conclusions

Microelectrode measurements showed a rapid decrease in oxygen concentration at night and, coupled to this, anoxic conditions in most of the smooth mat. While the two-dimensional distributions of porewater solutes obtained with DET and DGT techniques, agreed generally with the microelectrode results they showed a strong vertical and lateral heterogeneity under both light and dark conditions of sulfide, iron(II) and phosphate. These distributions show that in addition to typical diel fluctuations resulting from photoautotrophy near the surface of the mat, analyte distributions can vary significantly laterally (Glud et al., 1999). The DGT measurements also occasionally showed sulfide in the upper layers of the

microbial mat. This observation was supported by silver foil measurements, which confirmed that sulfate-reducing activity was taking place under oxic conditions in this mat. Daytime averaged profiles of sulfide and iron(II) concentrations showed significant variations and appeared to be highly influenced by light, and thus, the production of O₂. Although the distribution of phosphate is often correlated with the distribution of iron(II), our observations revealed that phosphate distributions were mainly driven by diel metabolic changes in the microbial mat.

Alkalinity distribution seemed to result from various microbial interactions increasing and decreasing the alkalinity. In a microbial mat, which is the quintessential example of a dynamic ecosystem, two-dimensional DGT and DET measurements provide the important advantage of being able to visualise microniches and small-scale variations that would be challenging to detect with conventional methods. In addition, co-distributions of porewater analytes measured by DET/DGT allowed a better insight into the biogeochemical cycles and interactions occurring within the mat. Microelectrodes, however, have an advantage over DGT and DET when short temporal variations are of importance. Consequently, these techniques provide highly complementary measurements, which provide the high spatial and temporal resolution required to study the complex biogeochemical processes occurring in microbial mat systems.

Acknowledgements

This research was supported by a grant from the Australian Research Council's Discovery Projects scheme (2010-2013, Grice, Greenwood, Snape, and Summons). AP thanks WA-Organic and Isotope Geochemistry Centre, Curtin University and CSIRO for a top-up scholarship.

References

- Allen M. A., Goh F., Burns B. P. and Neilan B. A.** (2009) Bacterial, archaeal and eukaryotic diversity of smooth and pustular microbial mat communities in the hypersaline lagoon of Shark Bay. *Geobiology* **7**, 82–96.
- Arp G., Reimer A. and Reitner J.** (2001) Photosynthesis-induced biofilm calcification and calcium concentrations in Phanerozoic oceans. *Science* **292**, 1701–1704.
- Baumgartner L. K., Reid R. P., Dupraz C. P., Decho A. W., Buckley D. H., Spear J. R., Przekop K. M. and Visscher P. T.** (2006) Sulfate reducing bacteria in microbial mats: changing paradigms, new discoveries. *Sediment. Geol.* **185**, 131–145.
- Bennett W. W., Teasdale P. R., Welsh D. T., Panther J. G. and Jolley D. F.** (2012) Optimization of colorimetric DET technique for the in situ, two-dimensional measurement of iron(II) distributions in sediment porewaters. *Talanta* **88**, 490–495.
- Bennett W. W., Serriere A., Panther J. G., Welsh D. T. and Teasdale P. R.** (2014) A rapid, high-resolution, gel-based technique for the in situ measurement of two-dimensional porewater alkalinity distributions. *Chemosphere*, under review.
- Borovec J., Sirová D., Mošnerová P., Rejmánková E. and Vrba J.** (2010) Spatial and temporal changes in phosphorus partitioning within a freshwater cyanobacterial mat community. *Biogeochemistry* **101**, 323–333.
- Braissant O., Decho A. W., Dupraz C. P., Glunk C., Przekop K. M. and Visscher P. T.** (2007) Exopolymeric substances of sulfate-reducing bacteria: Interactions with calcium at alkaline pH and implication for formation of carbonate minerals. *Geobiology* **5**, 401–411.
- Canfield D. E. and Des Marais D. J.** (1991) Aerobic sulfate reduction in microbial mats. *Science* **251**, 1471–1473.
- Canfield D. E. and Des Marais D. J.** (1993) Biogeochemical cycles of carbon, sulfur, and free oxygen in a microbial mat. *Geochim. Cosmochim. Acta* **57**, 3971–3984.
- Cohen Y.** (1984) Comparative N and S cycles: Oxygenic photosynthesis, anoxygenic photosynthesis, and sulfate-reduction in cyanobacterial mats. In *Recent advances in microbial ecology* (M. J. Klug, C. A. Redd.) Washington, D.C., American Society for Microbiology Press. pp. 435–441.

- Cohen Y. and Helman Y.** (1997) Two-dimensional sub-millimetric mapping of sulfate reduction in marine sediments. In *American Society for Microbiology 97th General Meeting, Miami Beach, Florida, Abstracts*. p. 393.
- Cypionka H., Widdel F. and Pfennig N.** (1985) Survival of sulfate-reducing bacteria after oxygen stress, and growth in sulfate-free oxygen-sulfide gradients. *FEMS Microbiol. Lett.* **31**, 39–45.
- Davison W. and Zhang H.** (1994) In situ speciation measurements of trace components in natural waters using thin-film gels. *Nature* **367**, 546–548.
- Davison W., Fones G. R. and Grime G. W.** (1997) Dissolved metals in surface sediment and a microbial mat at 100- μ m resolution. *Nature* **387**, 885–888.
- Davison W., Fones G. R., Harper M., Teasdale P. R. and Zhang H.** (2000) Dialysis, DET and DGT: in situ diffusional techniques for studying water, sediments and soils. In *In-situ monitoring of aquatic systems: chemical analysis and speciation* (eds. J. Buffle, G. Horvai). John Wiley & Sons pp. 495–569.
- Decho A. W., Visscher P. T. and Reid R. P.** (2005) Production and cycling of natural microbial exopolymers (EPS) within a marine stromatolite. *Palaeogeogr. Palaeoclimatol. Palaeoecol.* **219**, 71–86.
- De Lange G. J., Cranston R. E., Hydes D. H. and Boust D.** (1992) Extraction of pore water from marine sediments: A review of possible artifacts with pertinent examples from the North Atlantic. *Mar. Geol.* **109**, 53–76.
- Des Marais D. J.** (1995) The biogeochemistry of hypersaline microbial mats. *Adv. Microb. Ecol.* **14**, 251–274.
- Dupraz C. P., Visscher P. T., Baumgartner L. K. and Reid R. P.** (2004) Microbe-mineral interactions: early carbonate precipitation in a hypersaline lake (Eleuthera Island, Bahamas). *Sedimentology* **51**, 745–765.
- Dupraz C. P. and Visscher P. T.** (2005) Microbial lithification in marine stromatolites and hypersaline mats. *Trends Microbiol.* **13**, 429–438.
- Dupraz C. P., Reid R. P., Braissant O., Decho A. W., Norman R. S. and Visscher P. T.** (2009) Processes of carbonate precipitation in modern microbial mats. *Earth-Science Rev.* **96**, 141–162.
- Edgcomb V. P., Bernhard J. M., Beaudoin D., Pruss S. B., Welander P. V., Schubotz F., Mehay S., Gillespie A. L. and Summons R. E.** (2013a) Molecular indicators of microbial diversity in oolitic sands of Highborne Cay, Bahamas. *Geobiology* **11**, 234–51.

- Edgcomb V., Bernhard J., Summons R. E., Orsi W., Beaudoin D. and Visscher P. T.** (2013b) Active eukaryotes in microbialites from Highborne Cay, Bahamas, and Hamelin Pool (Shark Bay), Australia. *ISME J.*
- Ehrlich H. L.** (1996) How microbes influence mineral growth and dissolution. *Chem. Geol.* **132**, 5–9.
- Gallagher K. L., Kading T. J., Braissant O., Dupraz C. and Visscher P. T.** (2012) Inside the alkalinity engine: the role of electron donors in the organomineralization potential of sulfate-reducing bacteria. *Geobiology* **10**, 518–530.
- Glud R. N., Kühl M., Kohls O. and Ramsing N. B.** (1999) Heterogeneity of oxygen production and consumption in a photosynthetic microbial mat as studied by planar optodes. *J. Phycol.* **279**, 270–279.
- Hoehler T. M., Bebout B. M. and Des Marais D. J.** (2001) The role of microbial mats in the production of reduced gases on the early Earth. *Nature* **412**, 324–327.
- Jahnert R. and Collins L.** (2012) Characteristics, distribution and morphogenesis of subtidal microbial systems in Shark Bay, Australia. *Mar. Geol.* **303-306**, 115–136.
- Jahnert R. and Collins L.** (2013) Controls on microbial activity and tidal flat evolution in Shark Bay, Western Australia. *Sedimentology* **60**, 1071–1099.
- Jensen M. B., Hansen H. C. B., Nielsen N. E. and Magid J.** (1998) Phosphate mobilization and immobilization in two soils incubated under simulated reducing conditions. *Acta Agriculturae Scand. Sect. B, Soil Plant Sci.* **48**, 11–17.
- Jézéquel D., Brayner R., Metzger E., Viollier E., Prévot F. and Fiévet F.** (2007) Two-dimensional determination of dissolved iron and sulfur species in marine sediment pore-waters by thin-film based imaging Thau lagoon (France). *Estuar. Coast. Shelf Sci.* **72**, 420–431.
- Jørgensen B. B., Revsbech N. P., Blackburn T. H. and Cohen Y.** (1979) Diurnal cycle of oxygen and sulfide microgradients and microbial photosynthesis in a cyanobacterial mat sediment. *Appl. Environ. Microbiol.* **38**, 46–58.
- Jørgensen B. B. and Des Marais D. J.** (1988) Optical properties of benthic photosynthetic Fiber-optic studies of cyanobacterial mats communities. *Limnol. Oceanogr.* **33**, 99–113.
- Jørgensen B.** (1994) Diffusion processes and boundary layers in microbial mats. *Microb. Mats NATO ASI* **35**, 243–253.

- Joye S. B., Mazzotta M. L. and Hollibaugh J. T.** (1996) Community metabolism in microbial mats: the occurrence of biologically-mediated iron and manganese reduction. *Estuar. Coast. Shelf Sci.* **43**, 747–766.
- Knoll J. R. and Richards F. A.** (1969) A note on the sources of excess alkalinity in anoxic waters. *Deep-Sea Res.* **16**, 205–212.
- Krumins V., Gehlen M., Arndt S., van Cappellen P. and Regnier P.** (2012) Dissolved inorganic carbon and alkalinity fluxes from coastal marine sediments: model estimates for different shelf environments and sensitivity to global change. *Biogeosciences Discuss.* **9**, 8475–8539.
- Logan B. W.** (1961) Cryptozoon and associate stromatolites from the recent, Shark Bay, Western Australia. *J. Geol.* **69**, 517–533.
- Logan B. W.** (1974) Evolution and diagenesis of Quarternary carbonate sequences, Shark Bay, Western Australia. *Am. Assoc. Pet. Geol. Mem.* **22**, 195–249.
- Luther III G. W. and Church T. M.** (1988) Seasonal cycling of sulfur and iron in porewaters of a Delaware salt marsh. *Mar. Chem.* **23**, 295–309.
- Luther III G. W., Glazer B. T., Hohmann L., Popp J. I., Taillefert M., Rozan T. F., Brendel P. J., Theberge S. M. and Nuzzio D. B.** (2001) Sulfur speciation monitored in situ with solid state gold amalgam voltammetric microelectrodes: polysulfides as a special case in sediments, microbial mats and hydrothermal vent waters. *J. Environ. Monit.* **3**, 61–66.
- Lyons W. B., Long D. T., Hines M. E., Gaudette H. E. and Armstrong P. B.** (1984) Calcification of cyanobacterial mats in Solar Lake, Sinai. *Geology* **12**, 623–626.
- Myshrall K. L., Mobberley J. M., Green S. J., Visscher P. T., Havemann S. A., Reid R. P. and Foster J. S.** (2010) Biogeochemical cycling and microbial diversity in the thrombolitic microbialites of Highborne Cay, Bahamas. *Geobiology* **8**, 337–354.
- Overmann J., Cypionka H. and Pfennig N.** (1992) An extremely low-light-adapted phototrophic sulfur bacterium from the Black Sea. *Limnol. Oceanogr.* **37**, 150–155.
- Pagès A., Teasdale P. R., Robertson D., Bennett W. W., Schäfer J. and Welsh D. T.** (2011) Representative measurement of two-dimensional reactive phosphate distributions and co-distributed iron(II) and sulfide in seagrass sediment porewaters. *Chemosphere* **85**, 1256–1261.

- Pagès A., Welsh D. T., Robertson D., Panther J. G., Schäfer J., Tomlinson R. B. and Teasdale P. R.** (2012) Diurnal shifts in co-distributions of sulfide and iron(II) and profiles of phosphate and ammonium in the rhizosphere of *Zostera capricorni*. *Estuar. Coast. Shelf Sci.* **115**, 282–290.
- Pagès A., Grice K., Vacher M., Welsh D. T., Teasdale P. R., Bennett W. W. and Greenwood P.** (2014). Characterising microbial communities and processes in a modern stromatolite (Shark Bay) using lipid biomarkers and two-dimensional distributions of porewater solutes. *Environ. Microbiol.*, doi:10.1111/1462-2920.12378.
- Pike J., Bernhard J. M., Moreton S. G. and Butler I. B.** (2001) Microbioirrigation of marine sediments in dysoxic environments: Implications for early sediment fabric formation and diagenetic processes. *Geology* **29**, 923–926.
- Playford P. E.** (1990) Geology of the Shark Bay area, Western Australia. In *Research in Shark Bay. Report of the France-Australe Bicentenary Expedition Committee. Western Australian Museum, Perth* (eds. P. F. Berry, S. D. Bradshaw, B. R. Wilson). pp. 13–33.
- Reid R. P., Visscher P. T., Decho A. W., Stolz J. F. and Bebout B. M.** (2000) The role of microbes in accretion, lamination and early lithification of modern marine stromatolites. *Nature* **406**, 989–992.
- Revsbech N. P., Sorensen J., Blackburn T. H. and Lomholt J. P.** (1980) Distribution of oxygen in marine sediments measured with microelectrodes. *Limnol. Ocean.* **25**, 403–411.
- Revsbech N. P. and Jørgensen B. B.** (1983) Photosynthesis of benthic microflora measured with high spatial resolution by the oxygen microprofile method: capabilities and limitations of the method. *Limnol. Oceanogr.*
- Revsbech N. P., Jørgensen B. B., Blackburn T. H. and Cohen Y.** (1983) Microelectrode studies of the photosynthesis and H₂S, and pH profiles of a microbial mat. *Limnol. Oceanogr.* **28**, 1062–1074.
- Revsbech N. P. and Jørgensen B. B.** (1986) Microelectrodes: their use in microbial ecology. *Adv. Microb. Ecol.* **9**, 193–352.
- Rickard D. and Morse J. W.** (2005) Acid volatile sulfide (AVS). *Mar. Chem.* **97**, 141–197.
- Robertson D., Teasdale P. R. and Welsh D. T.** (2008) A novel gel-based technique for the high resolution, two-dimensional determination of iron(II) and sulfide in sediment. *Limnol. Oceanogr. Methods* **6**, 502–512.

- Robertson D., Welsh D. T. and Teasdale P. R.** (2009) Investigating biogenic heterogeneity in coastal sediments with two-dimensional measurements of iron(II) and sulfide. *Environ. Chem.* **6**, 60–69.
- Robertson E. L. and Liber K.** (2009) Effect of sampling method on contaminant measurement in pore-water and surface water at two uranium operations: can method affect conclusions? *Environ. Monit. Assess.* **155**, 539–553.
- Smith S. V. and Atkinson M. J.** (1983) Mass balance of carbon and phosphorus Shark Bay, Western Australia. *Limnol. Oceanogr.* **28**, 625–639.
- Smolders A. J. P., Nijboer R. C. and Roelofs J. G. M.** (1995) Prevention of sulphide accumulation and phosphate mobilization by the addition of iron(II) chloride to a reduced sediment: an enclosure experiment. *Freshw. Biol.* **34**, 559–568.
- Stockdale A., Davison W. and Zhang H.** (2009) Micro-scale biogeochemical heterogeneity in sediments: A review of available technology and observed evidence. *Earth-Science Rev.* **92**, 81–97.
- Teasdale P. R., Batley G. E., Apte S. C. and Webster I. T.** (1995) Pore water sampling with sediment peepers. *Trends analytical Chem.* **14**, 250–256.
- Teasdale P. R., Hayward S. and Davison W.** (1999) In situ, high-resolution measurement of dissolved sulfide using Diffusive Gradients in Thin films with computer-imaging densitometry. *Anal. Chem.* **71**, 2186–2191.
- Thamdrup B., Fossing H. and Jørgensen B. B.** (1994) Manganese, iron, and sulfur cycling in a coastal marine sediment, Aarhus Bay, Denmark. *Geochim. Cosmochim. Acta* **58**, 5115–5129.
- van Gernerden H.** (1993) Microbial mats: A joint venture. *Mar. Geol.* **113**, 3–25.
- Visscher P. T., Beukema J. and van Gernerden H.** (1991a) In-situ characterization of sediments: Measurements of oxygen and sulfide profiles with a novel combined needle electrode. *Limnol. Ocean.* **36**, 1476–1480.
- Visscher P. T., Quist P. and van Gernerden H.** (1991b) Methylated sulfur compounds in microbial mats: in situ concentrations and metabolism by a colorless sulfur bacterium. *Appl. Environ. Microbiol.* **57**, 1758–1763.
- Visscher P. T., Prins R. and van Gernerden H.** (1992a) Rates of sulfate reduction and thiosulfate consumption in a marine microbial mat. *FEMS Microbiol. Lett.* **86**, 283–294.
- Visscher P. T., Ende F., Schaub B. E. M. and Gernerden H.** (1992b) Competition between anoxygenic phototrophic bacteria and colorless sulfur bacteria in a microbial mat. *FEMS Microbiol. Lett.* **101**, 51–58.

- Visscher P. T. and van Gernerden H.** (1993) Sulfur cycling in laminated marine microbial ecosystems. In *Biogeochemistry of Global Change: Radiatively Active Tracegases* (ed. R. S. Oremland). Chapman and Hall, New York. pp. 672–690.
- Visscher P. T., Reid R. P., Bebout B. M., Hoefft S. E. H., Macintyre I. G. and Thompson Jr. J. A.** (1998) Formation of lithified micritic laminae in modern marine stromatolites (Bahamas): The role of sulfur cycling. *Am. Mineral.* **83**, 1482–1493.
- Visscher P. T., Reid R. P. and Bebout B. M.** (2000) Microscale observations of sulfate reduction: correlation of microbial activity with lithified micritic laminae in modern marine stromatolites. *Geology* **2**, 919–922.
- Visscher P. T., Hoefft S. M., Surgeon T. L., Rogers R. B., Bebout B. M., Thompson J. S. and Reid R. P.** (2002) Microelectrode measurements in stromatolites: unraveling the Earth's past? I. In *Environmental Electrochemistry: Analyses of Trace Element Biogeochemistry*. (eds. M. Taillefert, T. Rozan) Oxford University Press, Washington, D.C. pp. 265–282.
- Visscher P. T. and Stolz J. F.** (2005) Microbial mats as bioreactors: populations, processes, and products. *Palaeogeogr. Palaeoclimatol. Palaeoecol.* **219**, 87–100.
- Visscher P. T., Dupraz C., Braissant O., Gallagher K. L., Glunk C., Casillas L. and Reed R. E. S.** (2010) Biogeochemistry of carbon cycling in hypersaline mats: linking the present to the past through biosignatures. In *Microbial Mats: Modern and ancient microorganisms in stratified systems, cellular origin, life in extreme habitats and astrobiology 14* (eds. J. Seckbach and A. Oren). Springer Netherlands, Dordrecht. pp. 443–468.
- Walter M. R.** (1976) *Stromatolites*. Elsevier, Amsterdam.,
- Walter M. R., Buick R. and Dunlop J. S. R.** (1980) Stromatolites 3,400–3,500 Myr old from the North pole area, Western Australia. *Nature* **284**, 443–445.
- Wieland A., Zopfi J., Benthien M. and Kühl M.** (2005) Biogeochemistry of an iron-rich hypersaline microbial mat (Camargue, France). *Microb. Ecol.* **49**, 34–49.

Appendix

Supplementary figures

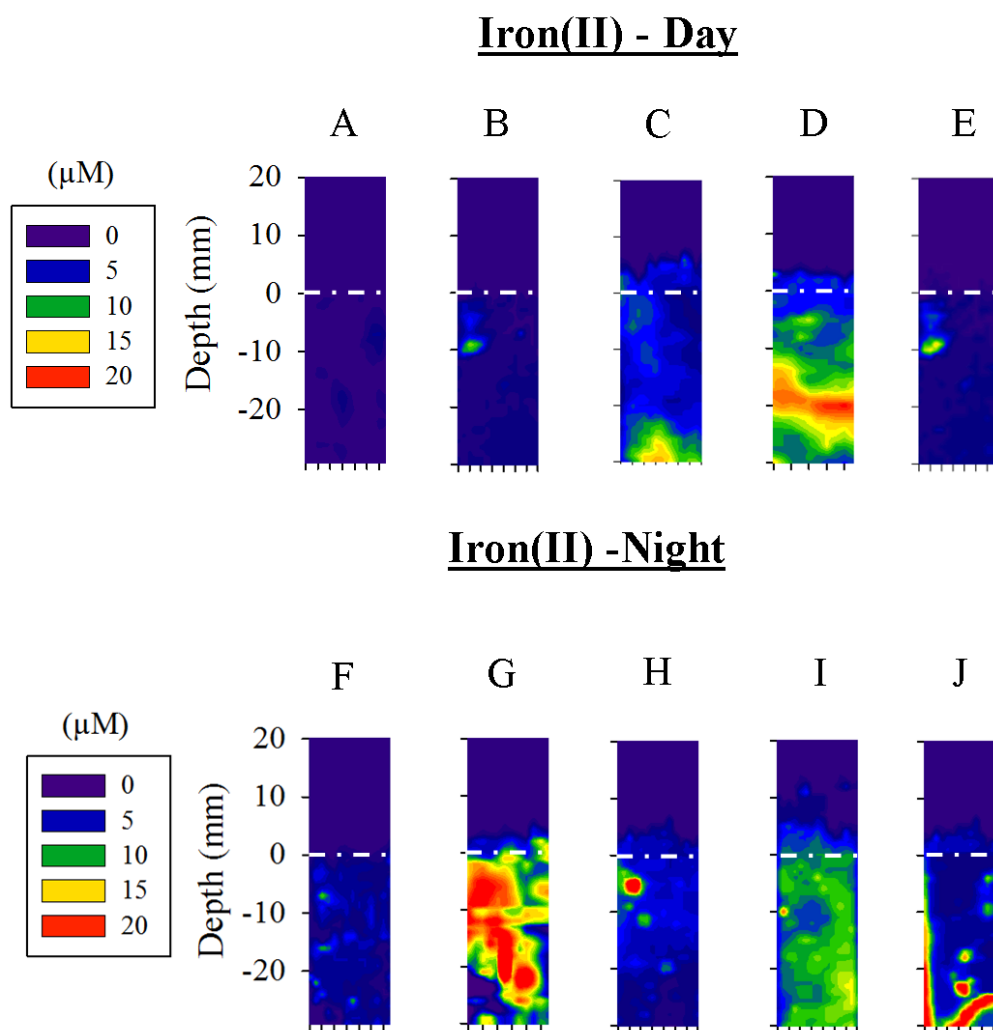


Figure A 3.1: Two-dimensional distributions of iron(II) measured by five DET probes in the layered microbial mat during light and dark deployments. The white dotted line represents the mat surface. The region above the top white line represents the water. The width of all gels was 14 mm.

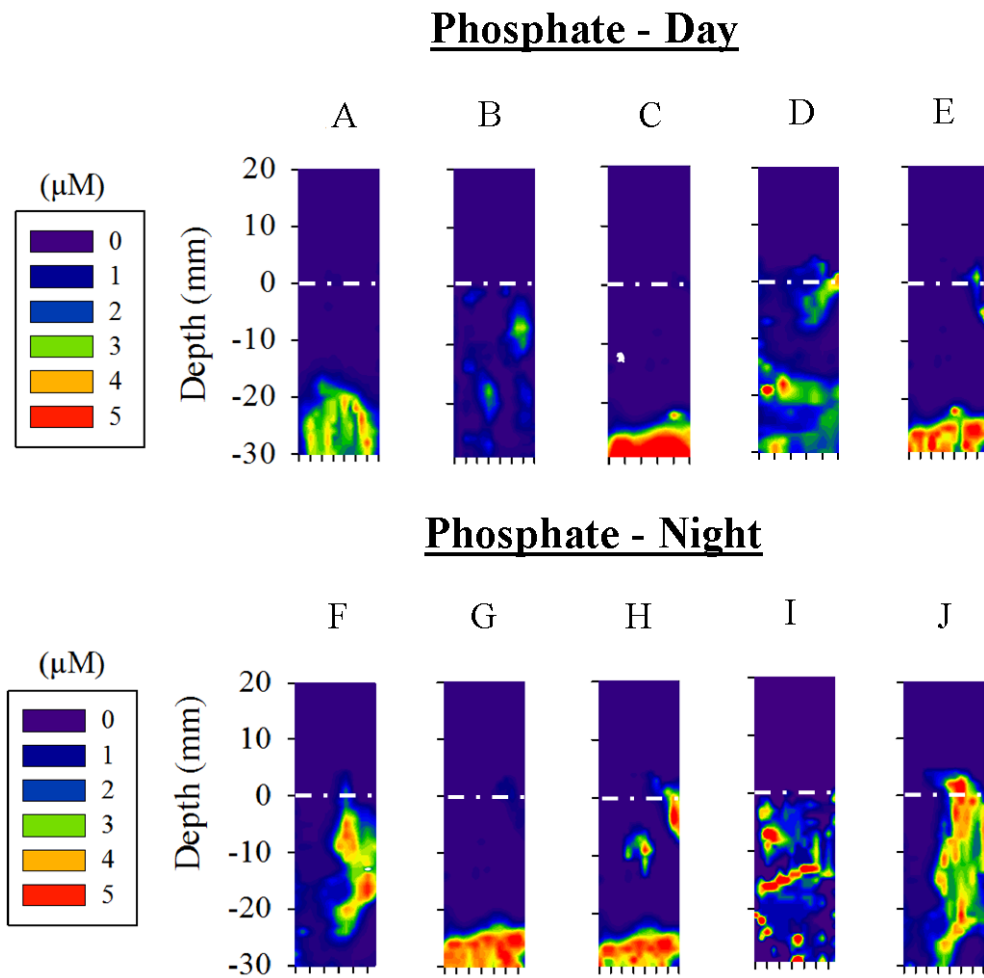


Figure A 3.2: Two-dimensional distributions of phosphate measured by five DET probes in the layered microbial mat during light and dark deployments. The white dotted line represents the mat surface. The region above the top white line represents the water. The width of all gels was 14 mm. No data was available for the small white areas on probes C and F due to physical damage.

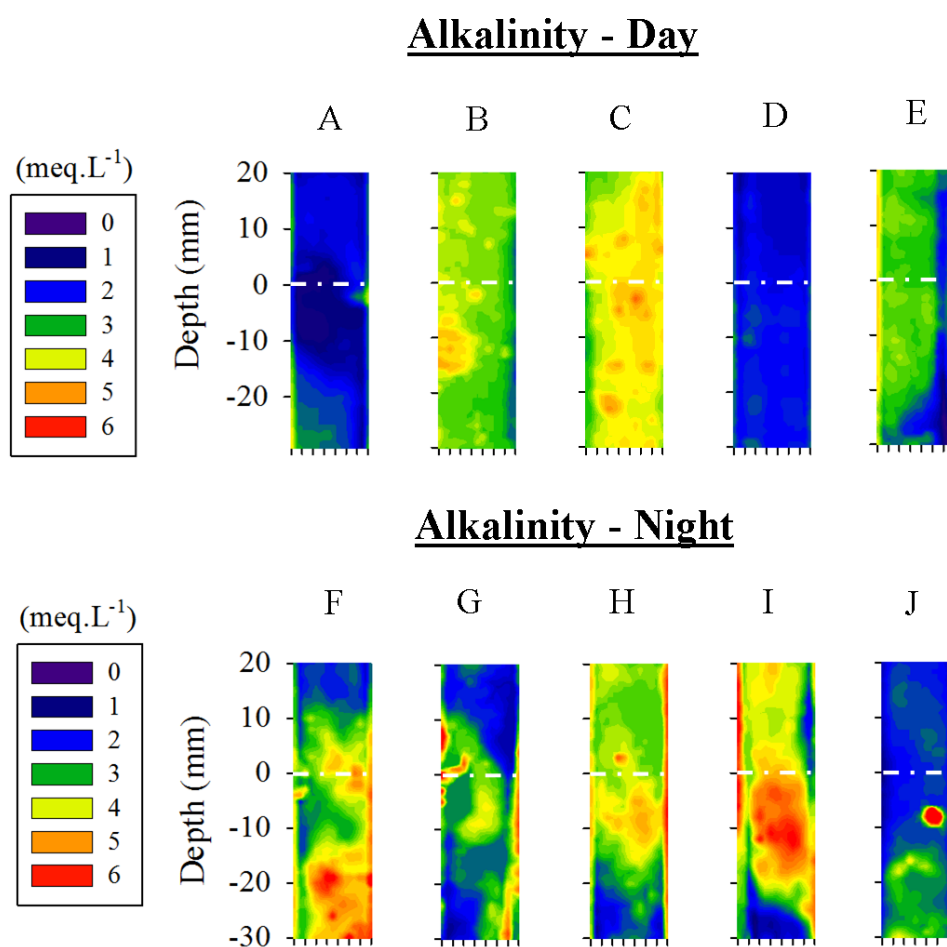


Figure A 3.3: Two-dimensional distributions of alkalinity measured by five DET probes in the layered microbial mat during light and dark deployments. The white dotted line represents the mat surface. The region above the top white line represents the water. The width of all gels was 14 mm.

Supplementary table:**Table A 3.1: Correlation between phosphate and iron(II) concentrations (r values) for 2D images and 1D profiles from each probe.**

r value	2D image	1D profile
Probe A	0.43	0.62
Probe B	0.47	0.86
Probe C	0.12	0.23
Probe D	0.68	0.83
Probe E	0.20	0.31
Probe F	0.43	0.88
Probe G	0.62	0.76
Probe H	0.33	0.64
Probe I	0.18	0.60
Probe J	0.45	0.73
Mean	0.39	0.65

Chapter 4

Organic geochemical studies of modern microbial mats from Shark Bay – Part I. Influence of depth and salinity on lipid biomarkers and their isotopic signatures.

Anais Pagès, Kliti Grice, Tobias Ertefai, Grzegorz Skrzypek, Ricardo Jahnert, Paul Greenwood

Geobiology, under review

(**impact factor 3.04**)

Chapter 4

Abstract

Introduction

Materials and Methods

- Sampling sites along salinity gradient
- Description of microbial mats along depth gradient
- Lipid laboratory preparation
 - Sampling
 - Extraction
 - Column chromatography
- Identification and isotopic characterisation of lipid biomarkers
 - Gas-Chromatography Mass-Spectrometry (GC-MS)
 - GC-Isotope Ratio Mass-Spectrometry (GC-irMS)
- Bulk parameters
 - Sample preparation
 - Measurements
- Water parameters

Results

- Depth gradient
 - Bulk parameters
 - Aliphatic hydrocarbons and their carbon isotopic compositions
 - Phospho-lipid fatty acids (PLFAs) and their carbon isotopic compositions
- Salinity gradient
- Bulk parameters
 - Aliphatic hydrocarbons
 - Phospho-lipid fatty acids (PLFAs)

Discussion

- Nilemah mats of different depth
 - Common features of all microbial mats
 - Changes along the Nilemah littoral gradient
- Salinity gradient

Conclusions

Abstract

The present study investigated the influence of abiotic conditions on microbial mat communities from Shark Bay, a World Heritage area well-known for a diverse range of extant mats presenting structural similarities with ancient stromatolites. The distributions and stable carbon isotopic values of lipid biomarkers [aliphatic hydrocarbons, and polar lipid fatty acids (PLFAs)], and bulk carbon and nitrogen isotope values of biomass were analysed in four different types of mats along a tidal flat gradient to characterise the microbial communities and systematically investigate the relationship of the above parameters with water depth. Cyanobacteria were dominant in all mats, as demonstrated by the presence of diagnostic hydrocarbons (e.g., $n\text{-C}_{17}$ and $n\text{-C}_{17:1}$). Several subtle but important differences in lipid composition across the littoral gradient were however evident. For instance, the shallower mats contained a higher diatom contribution, concordant with previous mat studies from other locations (e.g., Antarctica). Conversely, the organic matter (OM) of the deeper mats showed evidence for a higher seagrass contribution [high C:N, ^{13}C depleted long chain n -alkanes]. The morphological structure of the mats may have influenced CO_2 diffusion leading to more ^{13}C -enriched lipids in the shallow mats. Alternatively, changes in CO_2 fixation pathways, such as increase in the acetyl COA-pathway by sulfate-reducing bacteria, could have also caused the observed shifts in $\delta^{13}\text{C}$ values of the mats. In addition, three smooth mats from different Shark Bay sites were analysed to investigate potential functional relationship of the microbial communities with differing salinity levels. The $\text{C}_{25:1}$ HBI was identified in the high salinity mat only and a lower abundance of PLFAs associated with diatoms was observed in the less saline mats, suggesting a higher abundance of diatoms at the most saline site. Furthermore, it appeared that the most and least saline mats were dominated by autotrophic biomass using different CO_2 fixation pathways.

Introduction

Shark Bay, a World Heritage area located on the Western coast of Australia, is well-known for having a diverse range of extant microbial mats (Logan, 1974) regarded as modern analogues of fossilised stromatolites dating back 3.5 Ga. Some of these specimens have been shown to contain the earliest traces of life (Walter et al., 1980; Hoffmann, 2000; Allwood et al., 2006; van Kranendonk et al., 2008). Geological maps of the Shark Bay microbial deposits including descriptions of their morphologies and internal fabrics have been recently reported (Jahnert and Collins, 2011; 2012; 2013). Diverse types of microbial mats distributed along the littoral gradient with specimens spanning a range of different localised environmental conditions have been described (Jahnert and Collins, 2011; 2012; 2013). These highly dynamic and complex ecosystems support remarkably high metabolic rates leading to steep biogeochemical gradients (e.g. redox potential and pH) (Jørgensen et al., 1979). A strong recycling of OM has been observed at the mm-scale of these ecosystems (Paerl and Pinckney, 1996; Paerl et al., 2000). Since a majority of the mats are located on mudflats, terrestrial or marine sources of carbon (e.g. detritus from seagrass or algae) may also be utilised by the microbial assemblages (Volkman et al., 1980; Meziane et al., 1997; Meziane and Tsuchiya, 2000).

Lipid analysis has often been used to characterise the microbial composition of mats (Navarrete et al., 2000; Jahnke et al., 2004; Bühring et al., 2009; Allen et al., 2010; Pagès et al., 2014a) and previous applications to the modern pustular and smooth mats from Shark Bay have revealed a high degree of microbial diversity (Burns et al., 2004; Papineau et al., 2005; Allen et al., 2009; 2010; Pagès et al., 2014a,b). Stable isotopic ratios of bulk OM (C and N) or from compound-specific isotopic analysis (CSIA) can also complement molecular characterisation and help illuminate the major OM sources of specific organisms (Cook et al., 2004). The integration of lipid biomarker and stable isotope analyses has proven particularly complimentary for studies of the structure and functioning (e.g. carbon utilisation) of modern microbial mats (Bauersachs et al., 2011; Pagès et al., 2014a).

Biological proxies can illuminate the composition and organisation of extant microbial communities. In order to study the nature of environmental change in Shark Bay using biological proxies, it is highly important to understand which factors control the structure of microbial communities. The influence of abiotic conditions (depth and salinity) on microbial communities of Shark Bay mats was specifically addressed. The distributions and stable isotopic values of lipid biomarkers [aliphatic hydrocarbons and PLFAs], and bulk carbon and nitrogen isotope values were analysed in four microbial mats along a tidal flat gradient to systematically observe how the lipids and isotopic composition of the microbial mats changed with water depth. Previously, differences in the relative abundances and isotopic compositions of lipids in microbial mats have been reported along a littoral gradient (Bauersachs et al., 2011) and changes in stable isotope signatures of OM have also been observed with varying salinity (Chmura and Aharon, 1995). Turnover in cyanobacterial communities and diatom species with depth were also observed in a previous study of modern microbial mats from Antarctica (Sabbe et al., 2004). In addition, salinity has been recognised as a major factor regulating biodiversity, microbial abundance and function (Jiang et al., 2007). In various settings (e.g. solar salterns, ponds, intertidal flats), a decrease in the relative abundance of cyanobacteria has been reported with an increase in salinity levels (Pedrós-Alió et al., 2000; Benlloch et al., 2002; Abed et al., 2007). To investigate further the relationships of salinity on microbial community populations, particularly of cyanobacteria and diatoms, and their stable isotope compositions, three microbial laminated smooth mats from different Shark Bay sites (Nilemah, Garden Point and Rocky Point) presenting different salinity levels were also investigated. To date, hydrocarbon studies have been only performed on the pustular and smooth mats from Hamelin Pool (Allen et al., 2010; Pagès et al., 2014a) and no isotopic analysis of these mats has been reported. Here, we present a comprehensive study of biolipids and stable isotopic compositions of six different mat specimens sampled in Hamelin pool, l'Haridon Bight and Henry Freycinet.

Materials and methods

- **Sampling sites along salinity gradient**

Shark Bay is located in Western Australia, about 800 km north of Perth. Microbial mats were sampled along the tidal flat of Nilemah which is located on the southern area of Hamelin Pool (Figure 4.1). Hamelin Pool is the easterly embayment of this semi-enclosed shallow (<10m) area and extends up to 1400 km². Hence, the pools' volume is relatively small (~7km³), favouring high rates of evaporation. Hamelin Pool evaporative loss is compensated by an inflow through shallow Faure Sill. Consequently, 70–200 % of the pools' volume is replaced every year because of combined tidal fluctuation and evaporation losses (Price et al., 2012). Microbial mats cover 300 km² of the area (Jahnert and Collins, 2012). In Nilemah, the water is hypersaline - 56-70 practical salinity units (psu) because of limited rainfall and intense evaporation (Logan and Cebulski, 1970) and the pH ranges between 7.5 and 8.4 (Jahnert and Collins, 2013). To observe changes in stable isotopic and lipid compositions of the mats with depth, the following four specimens were taken: an intertidal pustular mat (0.20-0.80 m of water depth), a subtidal laminated smooth mat (0.80-1.20 m), a subtidal colloform mat (1-1.50 m) and a subtidal microbial pavement (2-6 m). (Nb. the deepest structure in this succession of microbial mats) (Figure 4.1). A detailed schematic model for the distribution of microbial mats at Nilemah is reported by Jahnert and Collins (2013).

Microbial mats from two additional sites were also selected so as to investigate the influence of salinity on the microbial compositions of the smooth mats. These were two subtidal laminated smooth mats from Garden Point and Rocky Point. Garden Point is a re-entrant located on the eastern area of Henry Freycinet embayment, located on the western part of Shark Bay (Figure 4.1). In this area, metahaline calm waters favour the formation of coarse stratified microbial mats. Considerable aeolian sand supply occurs during summer when strong southerly winds are present. The pH ranges between 7.8 and 8.7 in this area (Jahnert and Collins, 2013). Rocky Point, located on the western side of L'Haridon Bight (Figure 4.1), is a tidal flat covering 8 km². The water inflow in this area is

highly restricted, favouring microbial growth. The formation of microbial deposits at Rocky Point occurred before the formation of microbial mats in Garden Point. Rocky Point presents metahaline waters and a pH varying between 7.4 and 8 (Jahnert and Collins, 2013). The salinity of these three sites ranged from 64 psu (hypersaline) at Nilemah, 54 psu (metahaline) at Garden Point and 40 psu (metahaline) at Rocky Point. For ease of discussion, the three mats reflecting increasing salinity will be referred to as S1 to S3. The characteristics of these three sites are summarised in Table 4.1. The smooth mats sampled from these three sites presented a highly similar laminated structure and were found at the same water depth (0.80 to 1.20 m) (Jahnert and Collins, 2013).

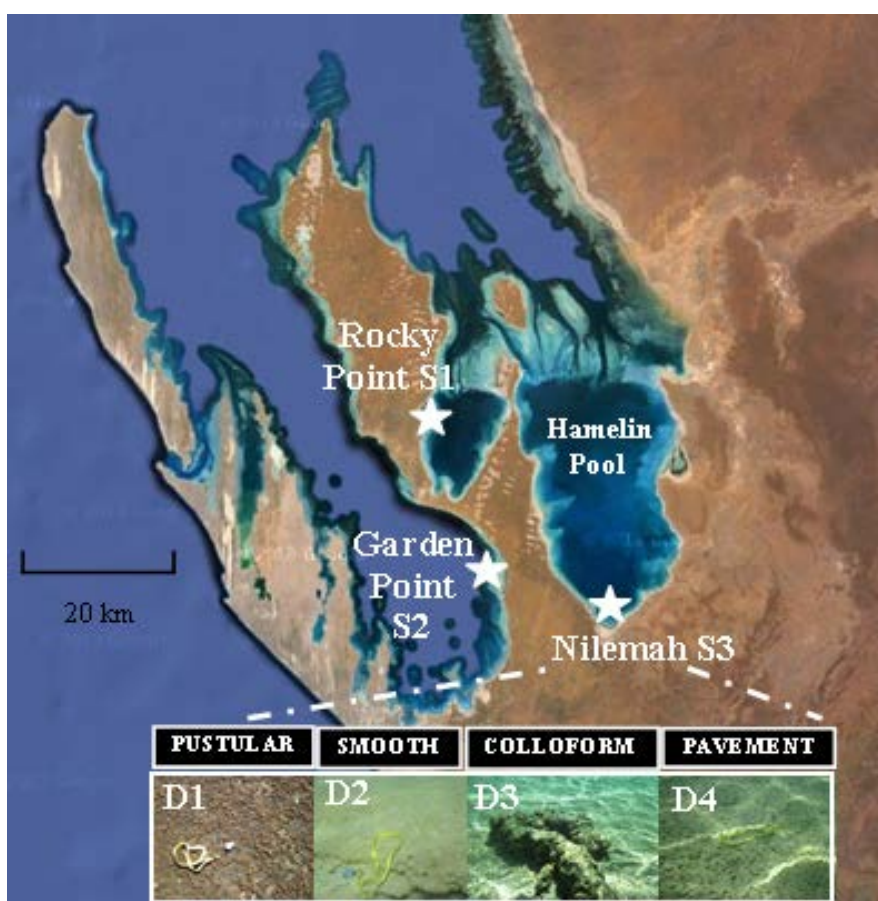


Figure 4.1: Google Earth image of Shark Bay showing the location of investigated tidal flats (Nilemah, Garden Point and Rocky Point) and photographs of the microbial mats investigated along the Nilemah S3 tidal flat gradient. The pustular mat was the shallowest mat (0.20-0.80m, D1), followed by the smooth mat (0.80-1.20m, D2), the colloform mat (1-1.50m, D3) and the microbial pavement that was the deepest structure (2-6m, D4). Rocky Point presented the lowest salinity (40psu, S1), Garden Point an intermediate salinity (54psu, S2) and Nilemah the highest salinity (64psu, S3).

Table 4.1: Main characteristics of the three study sites.

Study site	Characteristics	Salinity
Rocky Point S1	Western area of L'Haridon Bight, between Hamelin Pool and Henry Freycinet. Highly restricted water inflow. pH range: 7.4 - 8	40 psu
Garden Point S2	Eastern area of the Henry Freycinet westerly embayment. Very calm waters. Considerable aeolian sand supply during summer. pH range: 7.8 - 8.7	54 psu
Nilemah S3	Southern area of the Hamelin Pool easterly embayment. High evaporation rates. Water inflow through Faure Sill. pH range: 7.5 - 8.4	64 psu

- **Description of microbial mats along depth gradient**

A detailed description of the microbial mats from Nilemah has been reported elsewhere (Jahnert and Collins, 2012; 2013) and is summarised in [Table 4.2](#). Briefly, the Nilemah intertidal pustular mat, present between 0.20 and 0.80 m of water depth, contained coccoid cyanobacteria and presented an irregular clotted fabric characteristic of thrombolitic deposits covered by a brown mucilage (Golubic and Hoffmann, 1976). The laminated smooth mat from 0.80 and 1.20 m water depth presented flat surfaces and was composed of “sub-horizontal millimetric laminae made of fine-grained carbonate sediments interbedded with laminae of microbial OM that had become lithified as micrite laminae” (Jahnert and Collins, 2012). At the surface of this mat, filamentous cyanobacteria produced exopolymeric substances (EPS) that bind the sediment and favour a relatively flat surface appearance. In Shark Bay, microbial smooth mats are considered to be pioneering microbial assemblages colonizing newly deposited sediments (Burne and Johnson, 2012). The colloform mat (1 to 1.50 m depth) presented a globular shape with coarse laminated wavy structures made of peloids and lithified micrite. Coccoid cyanobacteria were responsible for the production of mucilage binding bioclasts that were further converted to lithified laminae (Jahnert and Collins, 2013). The microbial pavement, carbonate cryptomicrobial deposits containing fragments of bivalves, algae and micro-gastropods, was the deepest microbial deposit in Nilemah and was found between 2 and 6 m of depth (Jahnert and Collins,

2013). For ease of comparison, the shallowest (pustular) to deepest (microbial pavement) Nilemah mats will be referred to as D1 – D4. All microbial mats were sampled in May 2010.

Table 4.2: Main characteristics of the microbial mats sampled along the Nilemah tidal flat.

Mat type	Characteristics	Water depth
Pustular D1	Irregular clotted fabric covered by a brown mucilage.	0.2 - 0.8 m
Smooth D2	Laminae of organic matter interbedded with carbonate laminae.	0.8 - 1.2 m
Colloform D3	Coarse wavy structure made of peloids and lithified micrite.	1.0 - 1.5 m
Microbial pavement D4	Carbonate cryptomicrobial deposit containing shell fragments.	2 - 6 m

- **Lipid laboratory preparation**

- *Sampling*

The microbial mats were sampled in the field using an aluminium push core and immediately frozen (-18°C). Prior to extraction, the samples were defrosted and the top 2 cm of each mat were sampled with a spatula, carefully removing the edges of the samples that were in contact with the coring material. The spatula was carefully washed with dichloromethane (DCM) between each sample preparation. Each microbial mat sample was separated into three different aliquots: a first one for hydrocarbon analysis, a second one for polar lipid fatty acid analysis and the last one for measurement of bulk parameters.

- *Extraction*

For hydrocarbon analysis, dry aliquots (10 g) of the different microbial mats were ultrasonically extracted (5 h) using a 9:1 mixture of DCM: Methanol (MeOH). The solvent was filtered with pre-extracted cotton wool to remove particulates from

the extract and the solvent was reduced to 2 mL by rotary evaporation. Activated copper turnings were added and the extract stirred (72 h) to remove elemental sulfur (Blumer, 1957). The syringe used to transfer the extracts was cleaned with *n*-hexane (a minimum of 20 times) between each sample preparation. Procedural blanks were performed regularly to confirm that the compounds identified were indigenous to the samples.

A second aliquot of each microbial mat was used for PLFA analysis. PLFAs were analysed as fatty acid methyl esters, prepared using a modification of previously reported procedures (Bobbie and White, 1980; Zelles *et al.*, 1995). Lipids were extracted by ultrasonication (15 min) of the dry mat material (2 g) in a chloroform CHCl₃: MeOH: phosphate buffer (K₂HPO₄/ HCl) mixture (0.8:2:1; v/v/v) and isolated with additional CHCl₃ in the presence of double distilled water.

➤ Column chromatography

Aliquots (500 µL) of all hydrocarbon extracts were separated using a small column (5.5 cm x 0.5 cm i.d.) filled with activated silica gel (120°C, 8 h). The aliphatic hydrocarbon fraction was eluted with *n*-hexane (2 mL); the aromatic hydrocarbon fraction with a 1:3 mixture of DCM: *n*-hexane (2 mL) and the polar fraction with a mixture of 1:1 DCM: MeOH (2 mL). The aliphatic fractions were reduced to near dryness under a N₂ purge and then analysed by gas chromatography - mass spectrometry (GC-MS).

For PLFA analysis, the total-lipid extract was separated into neutral lipids, free FA (FA) and PLFA by successive elution through silica bonded columns (SPE-Si, Supelco, Poole, UK) with CHCl₃ (2 mL), acetone (2 mL) and MeOH (1mL). The PLFA fraction was methylated by the addition of 0.2 M potassium hydroxide (KOH) in MeOH (0.5 mL) and heated up to 75 °C for 5 min, then cooled and neutralised with 0.2 M acetic acid (0.5 mL). Methylated PLFAs were subsequently isolated with an aqueous CHCl₃ mixture and this fraction was analysed by GC-MS analysis.

- **Identification and isotopic characterisation of lipid biomarkers**

- *Gas-Chromatography Mass-Spectrometry (GC-MS)*

GC-MS analyses of the hydrocarbon fractions were performed using a Hewlett Packard 6890 GC interfaced to a Hewlett Packard 5973 mass selective detector (MSD). The aliphatic hydrocarbon fractions, dissolved in *n*-hexane, were introduced *via* a Hewlett Packard 6890 Series Injector into the electronically pressure controlled (EPC) split/splitless injector (320°C) which was operated in the pulsed splitless mode. The GC was fitted with a 60 m x 0.25 mm i.d. WCOT fused silica capillary column coated with a 0.25 µm film (DB-5MS, JandW Scientific). The oven temperature was programmed from 40 °C to 325 °C (at 3° C.min⁻¹) with initial and final temperature hold times of 1 and 50 min, respectively. Ultra high purity He was used as the carrier gas and maintained at a constant flow of 1.1 mL.min⁻¹. The MSD was operated at 70 eV and the mass spectra were acquired in full scan mode, 50-600 Daltons at ~ 4 scans per second and a source temperature of 230 °C.

PLFA analysis were performed with an Agilent 6890/5975b GC-MS. The gas chromatograph (GC) was used in pulsed splitless mode, with a 60 m x 0.25 mm i.d. DB5-MS (JandW) column and with He as carrier gas at a constant flow of 1.1 mL.min⁻¹ and the oven was programmed from 70 °C (held isothermally for 1 min) to 140 °C at 20 °C.min⁻¹, then to 290 °C (held 15 min) at 4 °C.min⁻¹. Full scan (50–550 Daltons) and selected ion data (*m/z* 55, 74, 87, 270, 284, 298 and 312) were simultaneously acquired. Product identifications were based on effective chain length values measured using relative retention times and compared with authentic standards. Relative product abundances were measured by integration of peaks in the total selected ion chromatogram.

➤ *GC- Isotope Ratio Mass Spectrometry (GC-iRMS)*

Aliphatic hydrocarbons and PLFAs were further analysed with a Micromass IsoPrime isotope ratio - mass spectrometer (ir-MS) coupled to a Hewlett Packard HP6890 GC fitted with a 60 m x 0.25 mm i.d., 0.25 µm thick DB-1 phase column to measure the $\delta^{13}\text{C}$ value of the most abundant products in the fractions. The samples were injected in pulsed splitless mode. The GC oven was programmed with the same temperature program used for the GC-MS analyses. The $\delta^{13}\text{C}$ values were reported in parts per mil (‰) relative to the international Vienna Pee Dee belemnite (VPDB) standard. Isotopic compositions were determined by integration of the m/z 44, 45 and 46 ion currents of CO_2 peaks from each analyte and reported relative to CO_2 reference gas pulses of known $\delta^{13}\text{C}$. Each sample was analysed at least in duplicate and all reported values had standard deviations <0.5 ‰. To ensure accuracy, in house standard solutions containing *n*-alkanes with a known isotopic composition were analysed after every second hydrocarbon or PLFA fraction.

As the conversion of free fatty acids to their methyl ester analogue involved the addition of one methyl group per fatty acid molecule, the isotope ratio of the original fatty acid was calculated using the measured isotope ratio of the fatty acid methyl ester and MeOH and the fractional carbon contribution of the free fatty acid to the ester (Abrajano *et al.*, 1994).

Isotopic fractionations between average $\delta^{13}\text{C}$ values of PLFAs and biomass ($\epsilon_{\text{PLFA-Biomass}}$) and biomass and CO_2 ($\epsilon_{\text{Biomass-CO}_2}$) were calculated using the following equation:

$$\epsilon_{\text{A-B}} = ((\delta^{13}\text{C}_\text{A} + 1000)/(\delta^{13}\text{C}_\text{B} + 1000) - 1) * 1000$$
 with A and B being two different substances (Zhang *et al.*, 2004).

- **Bulk parameters**

- *Sample preparation*

The samples for stable nitrogen and carbon isotope bulk analyses were manually separated, decalcified with 4% HCl, washed with deionized water, freeze-dried and powdered using a ball-mill (Retsch, model MM400 (Retsch Technology GmbH., Haan, Germany)). Samples aliquots were weighed (between 1 and 10 mg) depending on C and N concentrations, in order to match signals obtained from standards, and placed into tin capsules. Porewater from sediments for $\delta^{13}\text{C}$ of Dissolved Inorganic Carbon (DIC) and Dissolved Organic Carbon (DOC) was extracted using a centrifuge, filtered using a sterile syringe (0.21 mm filters) to sterile vials and stored in a fridge until analysed.

- *Measurements*

The stable carbon and nitrogen isotope compositions of bulk OM were analysed on a continuous flow system using an elemental analyser (Thermo Flash EA 1112) coupled with a Thermo Delta V Plus, an isotope ratio mass spectrometer (IrMS). The δ -values were normalised according to multipoint normalisation (Skrzypek, 2013), based on international standards (NBS19, LSVEC, USGS24 and NBS22 for $\delta^{13}\text{C}_{\text{OM}}$; N1, N2, N3 for $\delta^{15}\text{N}_{\text{OM}}$) provided by International Atomic Energy Agency from Vienna (IAEA), using the approach proposed by Skrzypek et al. (2010).

The stable carbon isotope composition of DIC ($\delta^{13}\text{C}_{\text{DIC}}$) was analysed using a GasBench II coupled with a Delta XL Mass Spectrometer (Thermo-Fisher Scientific). The $\delta^{13}\text{C}_{\text{DIC}}$ of head space gas was analysed after reaction with 100 % H_3PO_4 at 25 °C (24 h). All results were normalised to VPDB scale using three international reference materials from IAEA analysed with each batch of samples: L-SVEC, NBS19 and NBS18 (each replicated twice) following multipoint normalization (Skrzypek, 2013).

The stable carbon isotope composition of DOC ($\delta^{13}\text{C}_{\text{DOC}}$) was analysed using LC IsoLink coupled with a Delta V Thermo Scientific IrMS. The system worked in a continuous flow mode and CO_2 was continuously extracted directly from the liquid sample by passing through a reactor. The oxidation occurred at 100 °C in the presence of peroxodisulfate and H_3PO_4 reagents admixed to the samples. The reagent solutions were prepared using degassed MilliQ water and kept in a 0.5 L glass bottle purged by ultra-high pure He. Normalisation to VPDB scale was based on analyses of a solution of IAEA reference materials IAEA601, IAEA CH6, USGS40, and USGS41 with $\delta^{13}\text{C}$ as given by Skrzypek (2013).

The uncertainties associated with stable isotope analyses (1σ standard deviation) calculated based on long term-monitoring of laboratory reference materials were as follows: 0.10 ‰ for $\delta^{13}\text{C}_{\text{OM}}$ and $\delta^{15}\text{N}_{\text{OM}}$ in bulk OM, 0.10 ‰ for $\delta^{13}\text{C}_{\text{DIC}}$ and 0.30 ‰ for $\delta^{13}\text{C}_{\text{DOC}}$.

- **Water parameters**

Water parameters were measured with a Thermo-Fisher Scientific (TPS) WP-81 conductivity–salinity–pH–temperature instrument. The water depth measurements are relative to the highest sea-level reached under high-tide and low-wind conditions, corresponding to the ‘Winter High-Water Level’ (WHWL) of Logan (1974).

Results

- **Depth gradient**

- *Bulk parameters*

For all four microbial structures, the organic carbon content per dry weight of sediment was always greater than 20 % dry weight (Figure 4.2A, Table 4.3). The nitrogen content increased from 1.4 % (D1) to 2.7 % dry weight (D4) with water depth. The C: N ratio of D1 (10.6) and D2 (10.5) were similar but then showed a progressive increase for D3 (12.5) and D4 (15.4), suggesting a different source of OM in the deeper structures (Figure 4.2, Table 4.3). Similarly, D1 had the highest $\delta^{15}\text{N}_{\text{biomass}}$ (4.4 ‰) and D4 (greatest depth) showed the lowest $\delta^{15}\text{N}_{\text{biomass}}$ (1.4 ‰) (Figure 4.2B, Table 4.3). D2 and D3 had similar $\delta^{15}\text{N}_{\text{biomass}}$ values of 1.8 ‰ and 2.0 ‰, respectively. D1 (-14.4 ‰) and D2 (-14.2‰) had heavier $\delta^{13}\text{C}_{\text{OM}}$ values than D3 (-16.5 ‰) and D4 (-17.3 ‰) (Figure 4.2B, Table 4.3).

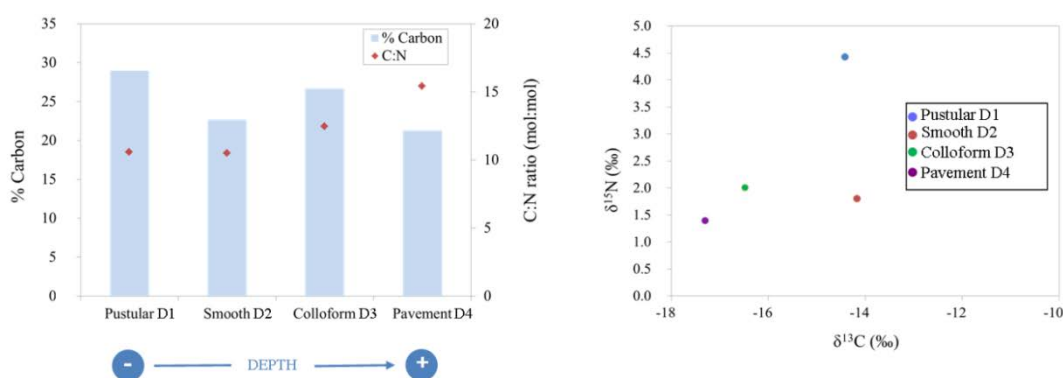


Figure 4.2: A) % carbon and C:N ratios and B) $\delta^{13}\text{C}$ and $\delta^{15}\text{N}$ of the total biomass in the different microbial mats from Nilemah.

Mat	% C	% N	$\delta^{13}\text{C-biomass}$	$\delta^{15}\text{N-biomass}$	C:N	DOC(mg.L ⁻¹)	$\delta^{13}\text{C-DOC}$	DIC(mg.L ⁻¹)	$\delta^{13}\text{C-DIC}$	T(°C)	$\delta^{13}\text{C-CO}_2$	Location
Pustular	29	2.7	-14.4	4.4	10.6	1475	-17.3	14	-4.2	26	-13.0	Intertidal
Smooth	22.7	2.2	-14.2	1.8	10.5	1378	-12.0	13	-1.4	26	-10.2	Subtidal
Colloform	26.7	2.1	-16.5	2.0	12.5	1180	-16.8	13	-3.3	26	-12.2	Subtidal
Pavement	21.3	1.4	-17.3	1.4	15.4	895	-17.5	12	-5.1	26	-13.9	Subtidal

Table 4.3: Carbon and nitrogen contents, molar ratios, $\delta^{13}\text{C}$ and $\delta^{15}\text{N}$ and other environmental parameters of the Nilemah mats. $\delta^{13}\text{C}_{\text{CO}_2}$ (dissolved) was calculated from $\delta^{13}\text{C}_{\text{DIC}}$ according to Mook et al., 1974. $\delta^{13}\text{C}_{\text{HCO}_3}$ ($\sim\delta^{13}\text{C}_{\text{DIC}}$) using the equations of $\delta^{13}\text{C}_{\text{CO}_2} = \varepsilon (\text{CO}_2\text{-HCO}_3) \times (1000 + \delta^{13}\text{C}_{\text{HCO}_3})/1000$ and $\varepsilon (\text{CO}_2\text{-HCO}_3) = 24.12 - 9866/T$, where T is absolute temperature and $\varepsilon (\text{CO}_2\text{-HCO}_3)$ is the fractionation between dissolved CO_2 and HCO_3 .

➤ *Aliphatic hydrocarbons and their carbon isotopic compositions*

Aliphatic hydrocarbons were analysed to investigate molecular features indicative of specific bacterial communities as well as higher plant or other eukaryotic contributions. *N*-alkanes and *n*-alkenes were the most dominant hydrocarbons. *N*-alkanes ranged from C_{15} to C_{36} in all mats, apart from an absence of *n*- C_{15} in D4. The aliphatic fractions of D1, D2 and D3 were all dominated by an *n*- C_{17} alkane and $\text{C}_{17:1}$ alkene (Figure 4.3). *N*- C_{21} alkane was the most abundant aliphatic of D4. The long-chain *n*-alkanes ($\text{C}_{21}\text{-C}_{33}$) of all mats showed a predominance of odd-over-even carbon numbers. The $\delta^{13}\text{C}$ values of the long chain *n*-alkanes ($\text{C}_{24}\text{-C}_{33}$) were more ^{13}C -depleted than short chain *n*-alkanes ($\text{C}_{16}\text{-C}_{18}$). This difference was on average 6.4 ‰ for D1, 4.7 ‰ for D2, and 2.8 ‰ for D4, reflecting a decrease in isotopic difference between long and short chain *n*-alkanes with increasing water depth (Figure 4.4). The $\delta^{13}\text{C}$ values of only three aliphatic hydrocarbons (*n*- C_{15} , 17:1 and *n*- C_{17}) could be measured in D3, as the relative abundance of the other hydrocarbons was too low, limiting its isotopic correlation with the other microbial mats. The $\text{C}_{25:1}$ HBI alkene was detected in D1 and D2, but not the deeper mats. It was very ^{13}C -enriched with $\delta^{13}\text{C}$ values of -16.9 ‰ and -16.5 ‰ in D1 and D2, respectively. Phytane or phytene was present in all mats, whereas pristane was detected only in D4. Hop-22(29)-ene (diploptene) was detected in all microbial mats, however, C_{29} to C_{32} hopanes with a biological isomeric configuration (i.e., 17 β (H), 21 β (H)) were only detected in D2. C_{31} $\beta\beta$ -homohopane was also present in D4. Cholest-2-ene (C_{27}) was exclusively detected in D2. No steroids were detected in the other mats. Overall comparison of the $\delta^{13}\text{C}$

values of the aliphatic hydrocarbons measured in the four mats revealed that D2 consistently presented higher $\delta^{13}\text{C}$ values (Figure 4.4).

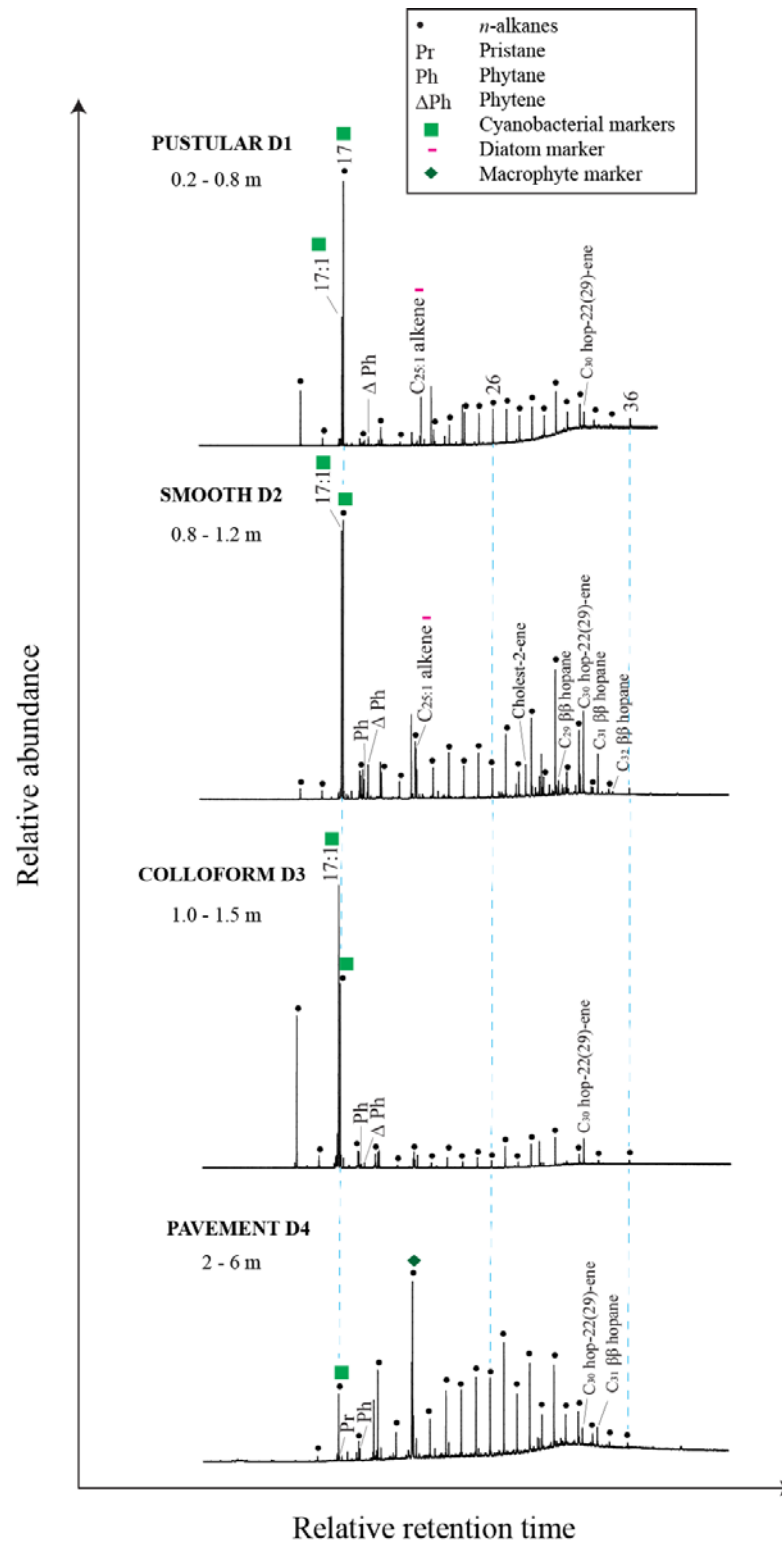


Figure 4.3: Total ion chromatograms from GC-MS analysis of the aliphatic hydrocarbon fractions of the Nilemah mats.

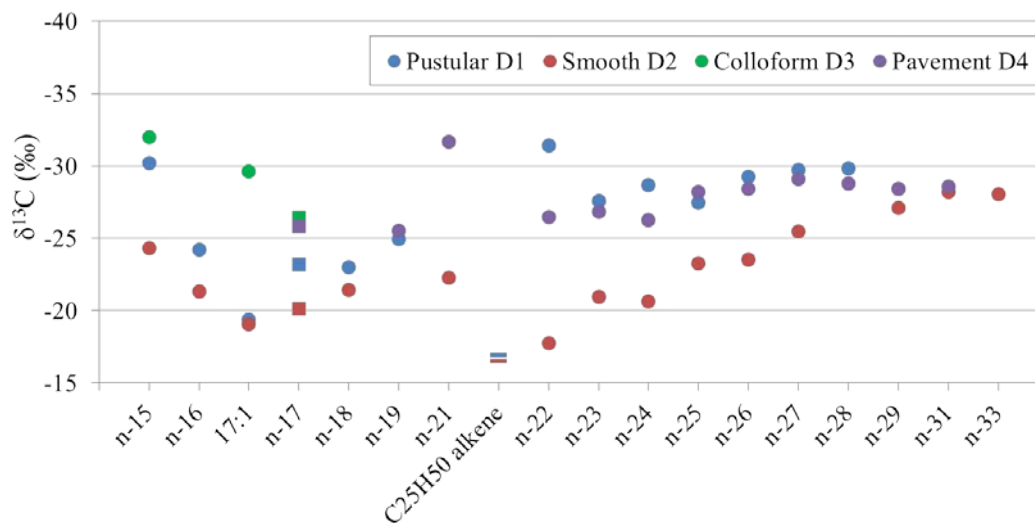


Figure 4.4: The $\delta^{13}\text{C}$ values of hydrocarbons of Nilemah mats at different water depths (D1-D4). The maximum standard deviation of the $\delta^{13}\text{C}$ values is $\pm 0.3\%$. The squares indicate a cyanobacterial marker and the dashes indicate a potential diatom marker.

➤ *Phospho-lipid fatty acids (PLFAs) and their carbon isotopic compositions*

The PLFA composition of all mats was dominated by 16:0, 18:1 ω 9 and 18:0 (Figure 4.5), and also contained 24:0 in relatively high abundance (ranging between 2.0 and 9.5% of the total abundance of the mats) and lesser abundances of 16:4 ω 1, 18:4 ω 3, 20:5 ω 3, *iso*- and *anteiso*-15:0 and 17:0, *iso*-17:1 ω 9, 10-methyl-16:0 and very long-chain fatty acids with a predominance of even-over-odd carbon numbers. Only 10-methyl-16:0 showed a continuous trend with water depth increasing in abundance from 0.1 % in D1 to 1 % in D4. However, the relative abundances of 20:5 ω 3 and 16:4 ω 1 were highest in D1 (2 % and 3 %, respectively) and lowest in D4 (0.6 % and 0.2 %, respectively). 10-methyl-18:0, characteristic of *Actinomycetes*, was not detected in any of the mats analysed here, although these bacteria were previously detected by molecular phylogenetic analysis of Shark Bay mats (Allen *et al.*, 2009). 18:1 ω 7, derived from gram-negative bacteria (Oliver and Colwell, 1973), was also present in low abundance in all mats except D2.

PLFAs from D2 were the most enriched in ^{13}C , with $\delta^{13}\text{C}$ values ranging between -12.1 ‰ to -17.3 ‰ (Figure 4.6). In comparison the $\delta^{13}\text{C}$ values of D4 PLFAs ranged between -21.2 ‰ and -26.1 ‰. The heaviest values were measured for *iso*-15:0 (-12.4 ‰ and -15.1 ‰) and *iso*-17:1 ω 9 (-12.1 ‰ and -14.7 ‰) in D2 and D3. Apart from D1, the PLFA $\delta^{13}\text{C}$ data reflected a progressive depletion in ^{13}C with depth. D2 PLFAs had an average $\delta^{13}\text{C}$ value of -15.8 ‰, D3 an average value of -18.5 ‰ and D4 of -24.2 ‰. D1, however, presented an average $\delta^{13}\text{C}_{\text{PLFA}}$ value of -23.7 ‰. The $\delta^{13}\text{C}$ values of CO_2 and total biomass of D2 to D4 mats also showed more negative values with depth, ranging from -10.2 ‰ and -14.2 ‰ in D2 mat to -13.9 ‰ and -17.3 ‰, respectively, in D4 (Table 4.3, Figure 4.6). The corresponding D1 data, however, again did not follow this trend.

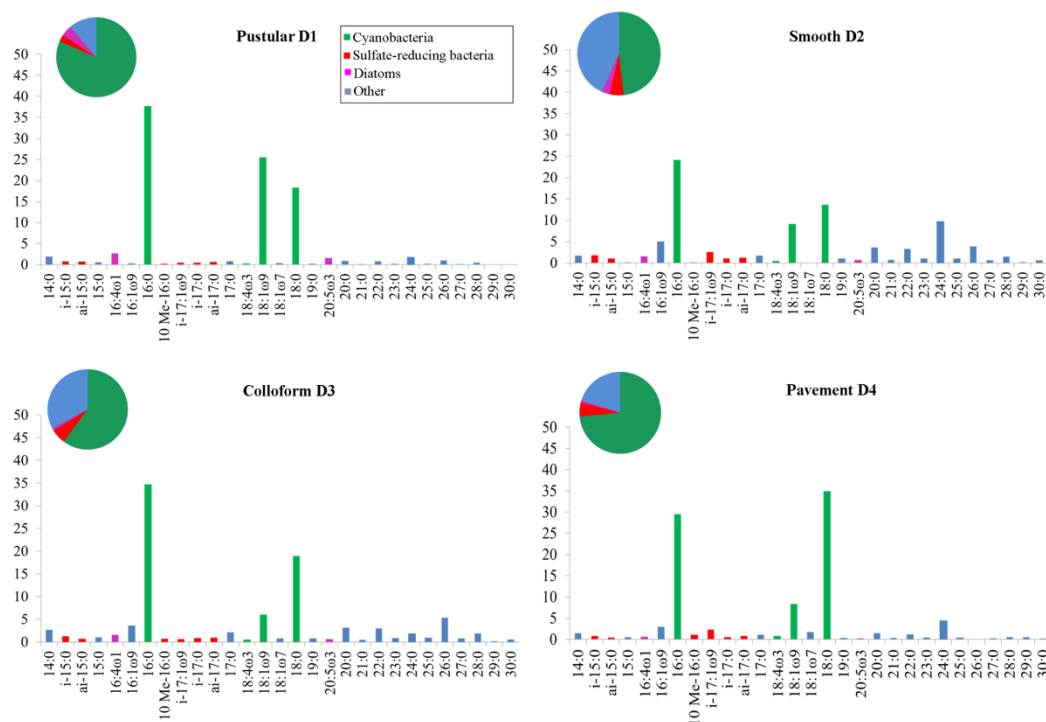


Figure 4.5: Histograms showing relative abundances of PLFA (%) for the different types of the Nilemah mats. Data from GC-MS analysis of PLFA fractions. The pie charts indicate the relative proportion of cyanobacterial PLFAs, sulfate-reducing bacteria (SRB) PLFAs, diatom PLFAs and PLFAs from other sources for each mat.

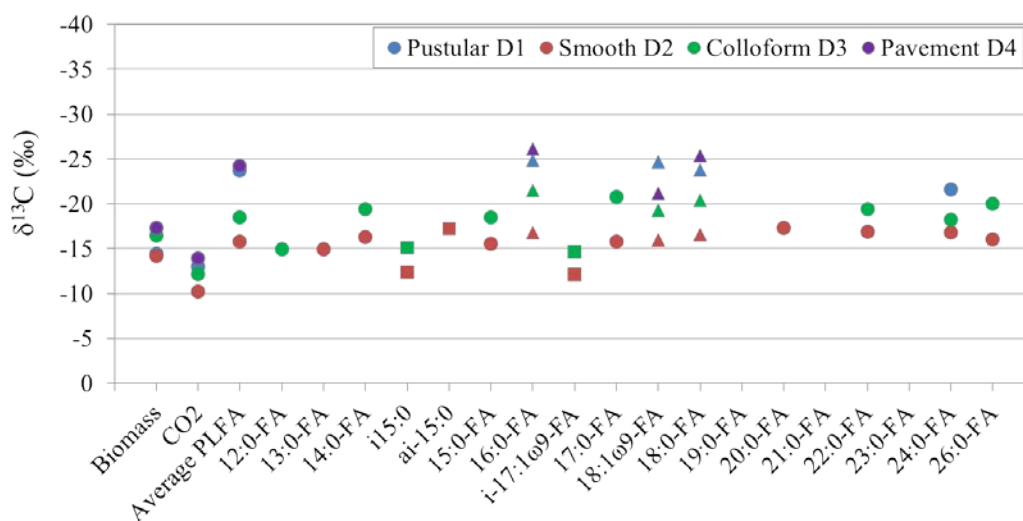


Figure 4.6: $\delta^{13}\text{C}$ of PLFA, biomass and CO_2 (calculated from the DIC according to Mooke *et al.*, 1974) of the Nilemah mats. The maximum standard deviation of the $\delta^{13}\text{C}$ values is $\pm 0.4\%$. The squares indicate cyanobacterial markers and the triangles indicate potential SRB markers.

- **Salinity gradient**

- *Bulk parameters*

The mats from S1 and S3 had organic carbon contents per dry weight of sediment greater than 20 %; however, it was lower than 10 % in the mat from S2 (Figure 4.7A, Table 4.4). The C:N ratios of S3 and S1 were similar (10.5 and 10.9, respectively) and slightly lower than S2 (11.7) (Figure 4.7A, Table 4.4). DIC concentration in S1 was below the detection limit but it showed very similar $\delta^{13}\text{C}_{\text{biomass}}$ and $\delta^{15}\text{N}_{\text{biomass}}$ values to the ones in S3: $\delta^{13}\text{C}_{\text{biomass}}$ values (-14.9 ‰ and -14.2 ‰, respectively) and $\delta^{15}\text{N}_{\text{biomass}}$ values (1.81 ‰ and 1.78 ‰) (Figure 4.7B, Table 4.4). However, S2 had a very different isotopic composition: -9.7 ‰ for $\delta^{13}\text{C}_{\text{OM}}$ and -0.7 ‰ for $\delta^{15}\text{N}_{\text{biomass}}$.

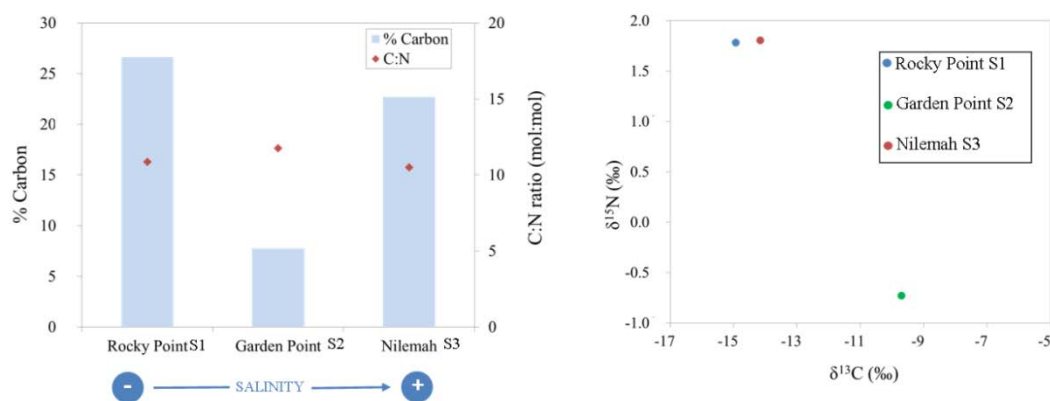


Figure 4.7: A) % carbon and C: N ratios and B) $\delta^{13}\text{C}$ and $\delta^{15}\text{N}$ of the total biomass in S1, S2 and S3.

Location	% C	% N	$\delta^{13}\text{C}$ -biomass	$\delta^{15}\text{N}$ -biomass	C:N	DOC(mg.L ⁻¹)	$\delta^{13}\text{C}$ -DOC	DIC(mg.L ⁻¹)	$\delta^{13}\text{C}$ -DIC	T(°C)	$\delta^{13}\text{C}$ -CO ₂	Salinity
Rocky Point	26.6	2.5	-14.9	1.8	10.9	627	-17.7	n.m.	n.m.	28	n.d.	40
Garden Point	7.8	0.7	-9.7	-0.7	11.7	1093	-13.1	10	-3.9	25	-12.8	58
Nilemah	22.7	2.2	-14.2	1.8	10.5	1378	-12.0	13	-1.4	26	-10.2	64

Table 4.4: Carbon and nitrogen contents, molar ratios, natural abundances of $^{13}\text{C}/^{12}\text{C}$ and $^{15}\text{N}/^{14}\text{N}$ and other environmental parameters for S1, S2 and S3. $\delta^{13}\text{C}_{\text{CO}_2}$ was calculated from $\delta^{13}\text{C}_{\text{DIC}}$ according to Mook et al., 1974. n.m.: not measured. n.d.: not determined.

➤ Aliphatic hydrocarbons

N-alkanes and alkenes were the most dominant hydrocarbons in the microbial smooth mats. *N*-alkanes ranged from C₁₅ to C₃₆ for S3 and from C₁₇ to C₃₆ for S1 and S2. The most dominant hydrocarbon in S3 was the *n*-C₁₇ alkane, however, *n*-C₁₈ alkane and phytane/phytene were the most dominant compounds in S2 (Figure 4.8). S1 presented only *n*-alkanes in low abundance and with no obvious carbon number preference. In S2 and S3, however, a predominance of odd-over-even long-chain *n*-alkanes was observed, suggesting an input from terrestrial plants or seagrass. Whilst S3 showed the presence of a C_{25:1} HBI alkene, this product was not detected in S2 and S1. Hop-22(29)-ene was detected in S3 and S2. S3 presented the highest diversity of $\beta\beta$ -hopanes ranging from C₂₉ to C₃₂. However, S2 also presented C₂₇ and C₃₁ $\beta\beta$ -hopanes. Cholest-2-ene, indicative of eukaryotic input, was detected in S3 and S2. No steranes or sterenes were detected in S1.

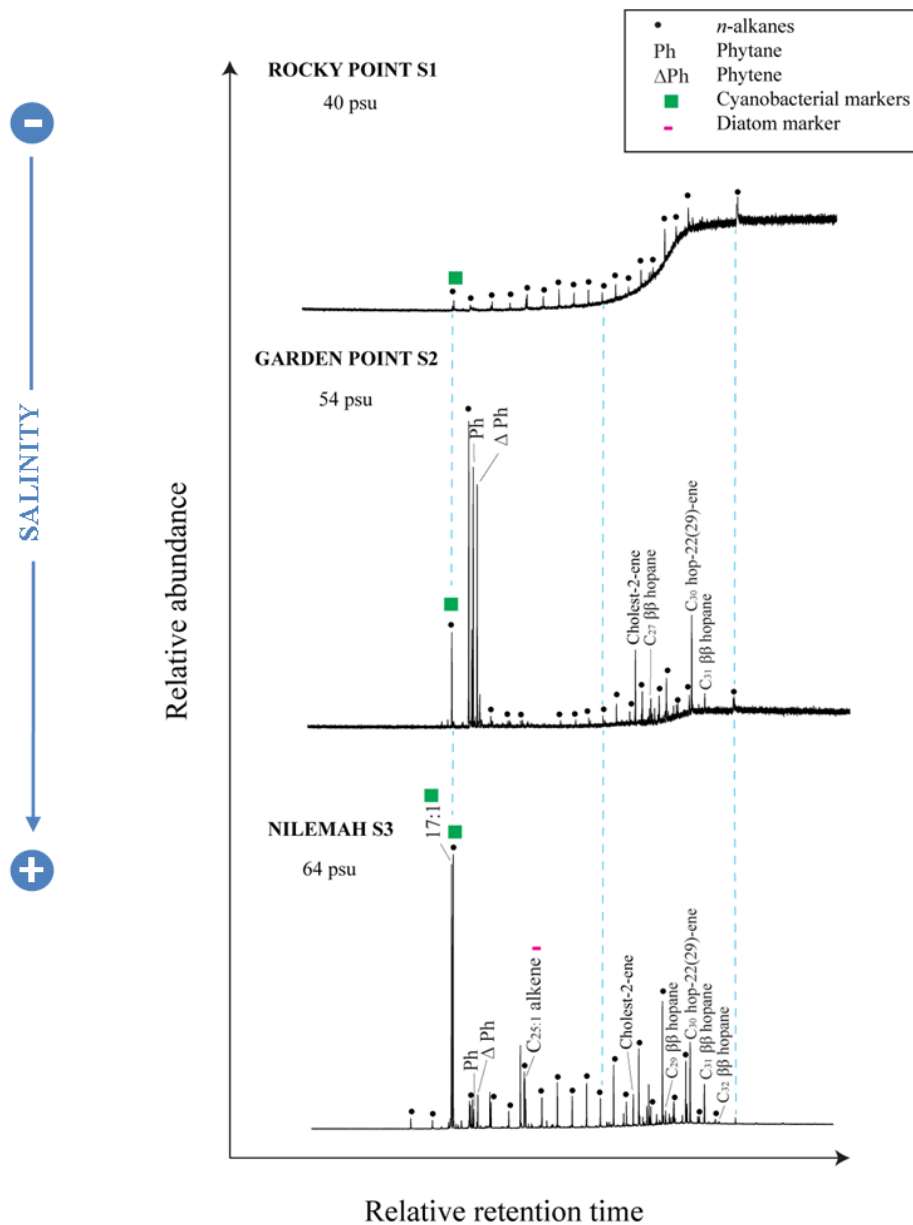


Figure 4.8: Total ion chromatograms from GC-MS analysis of the aliphatic hydrocarbon fractions of S1, S2 and S3.

➤ *Phospho-lipid fatty acids*

The PLFA profiles of all mats presented some similarities with the previously described distribution of S3. 16:0, 18:1 ω 9 and 18:0 were all major PLFAs in S1 (Figure 4.9). These were present but less prominent in S2 in which *iso*-17:1 ω 9 was a major PLFA. *Iso*- and *anteiso*-15:0 and 17:0 as well as *iso*-17:1 ω 9 were present in all mats except for an absence of *iso*-15:0 in the S2. S2, however, showed the highest total abundance of these products largely due to the high abundance of *iso*-17:1 ω 9. PLFA 24:0 was detected in relatively high abundance in S3 (10 %), compared to the other mats where it was present in much lower abundances. The PLFA 18:1 ω 7, deriving from gram-negative bacteria (Oliver and Colwell, 1973), was detected only in S2 and in trace abundance (1 %). The PLFA 16:4 ω 1 was detected in all mats but presented a higher abundance in S3 and the PLFA 20:5 ω 3 was absent in S1. Long-chain PLFAs up to C₃₀ with an even over odd predominance were also observed in all mats although these only extended to C₂₆ in S1 and their abundance was much lower in S2 and S1 than in S3.

CSIA of individual PLFAs revealed that almost all PLFAs from S1 were more depleted in ¹³C than the PLFAs from S2 and S3 (Figure 4.10). For instance, the $\delta^{13}\text{C}$ values of 16:0 and 18:0 were -16.8 ‰ and -16.6 ‰, respectively for S3 and -21.3 ‰ and -23.5 ‰ for S1. In both S3 and S1, the PLFA *iso*-17:1 ω 9 presented the most positive $\delta^{13}\text{C}$ value of all PLFAs (-12.1 ‰ and -16.2 ‰, respectively). The $\delta^{13}\text{C}$ values of the > C₂₂ even carbon-numbered PLFAs of S1 were nearly 10 ‰ lighter than in the two other mats which showed $\delta^{13}\text{C}$ values similar to the lower molecular weight PLFAs, suggesting a different source in S1. A progressive enrichment in ¹³C was observed for the $\delta^{13}\text{C}$ value of average PLFA with increasing salinity. S1 presented a $\delta^{13}\text{C}_{\text{PLFA}}$ value of -21.2 ‰, S2 -17.0 ‰ and S3 -15.8 ‰. The $\delta^{13}\text{C}$ values of CO₂ also showed more positive values with increasing salinity, with $\delta^{13}\text{C}$ values of -12.8 ‰ for S2 and -10.2 ‰ for S3. The $\delta^{13}\text{C}_{\text{CO}_2}$ of S1, on the other hand, could not be measured since the DIC concentration was below the detection limit. The $\delta^{13}\text{C}_{\text{biomass}}$ values, however, did not show more positive values with increasing salinity. S3 and S1 presented similar

$\delta^{13}\text{C}_{\text{biomass}}$ values (-14.2 and -14.9 ‰, respectively) while S2 presented a more positive $\delta^{13}\text{C}_{\text{biomass}}$ value (-9.7 ‰).

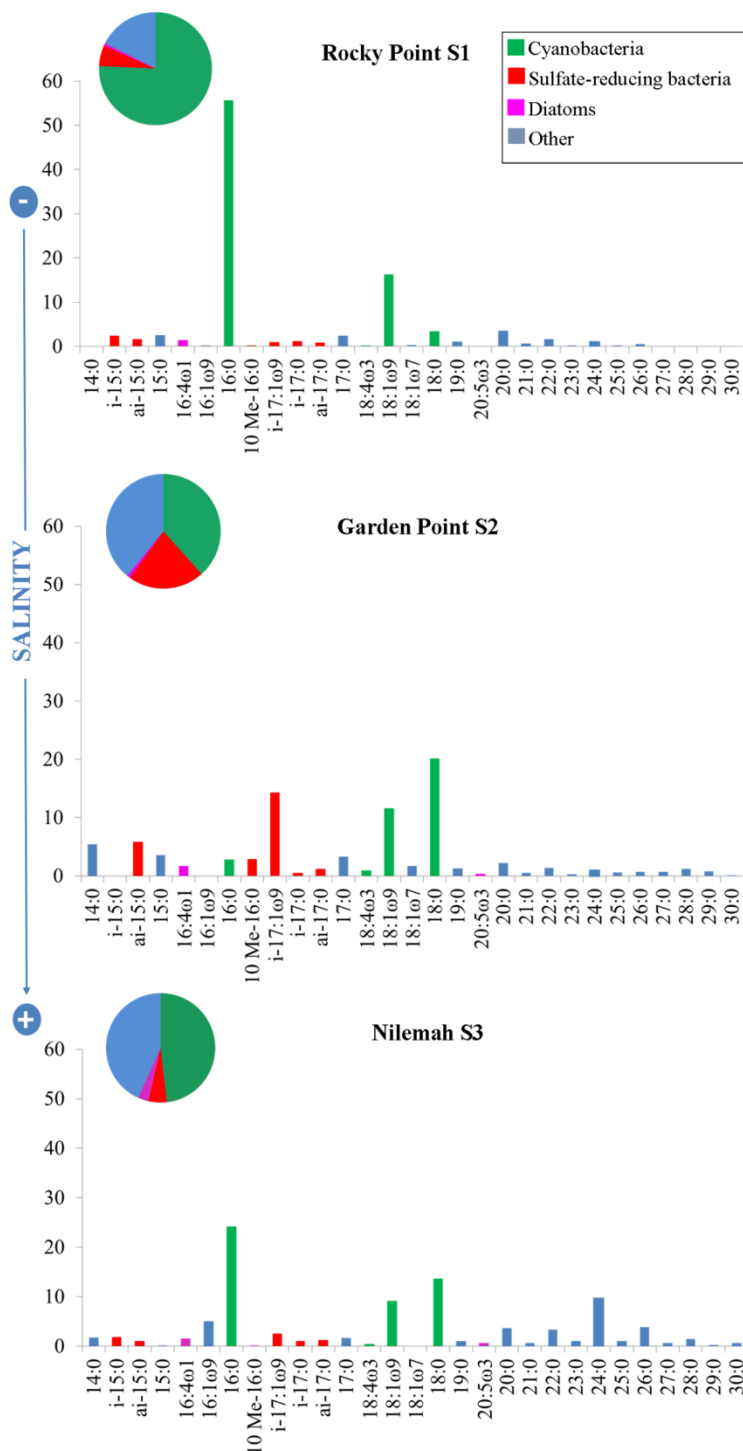


Figure 4.9: Histograms showing relative abundances of PLFA (%) for S1, S2 and S3. Data from GC-MS analysis of PLFA fractions. The pie charts indicate the relative proportion of cyanobacterial PLFAs, SRB PLFAs, diatom PLFAs and PLFAs from other sources for each mat.

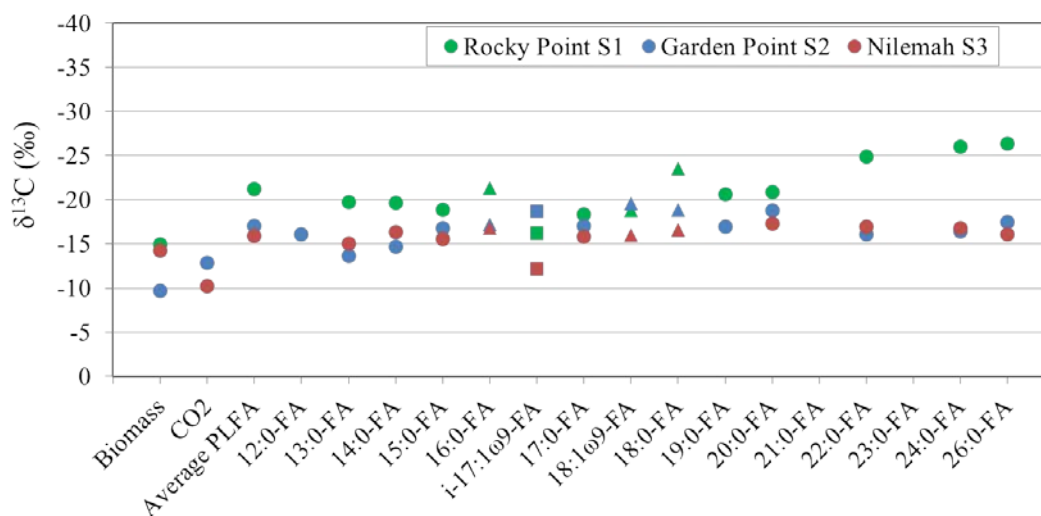


Figure 4.10: $\delta^{13}\text{C}$ of values of PLFA, biomass, CO_2 (calculated from the DIC according to Mook *et al.*, 1974) of S1, S2 and S3. The maximum standard deviation of the $\delta^{13}\text{C}$ values is $\pm 0.3\text{‰}$. The squares indicate cyanobacterial markers and the triangles indicate potential SRB markers.

Discussion

- **Nilemah mats of different depth**

- *Common features of all microbial mats*

The microbial community structure of all mats seemed generally similar, with only slight differences in their biomarker distributions and stable isotopic compositions were noticeable along the littoral gradient. The aliphatic hydrocarbon distributions of all mats were dominated by $n\text{-C}_{17}$ and $n\text{-C}_{17:1}$ (Figure 4.3) which have been previously observed to be the major hydrocarbons of cultured filamentous cyanobacteria (Winters *et al.*, 1969; Paoletti *et al.*, 1976) as well as cyanobacterial mats from hot springs (Robinson and Eglinton, 1990), freshwater (Thiel *et al.*, 1997) and hypersaline environments (Grimalt *et al.*, 1992; Fourçans *et al.*, 2004; Rontani and Volkman, 2005). The same C_{17} aliphatic hydrocarbons have also been reported to be major constituents of pustular and smooth mats from Hamelin Pool associated with the presence of cyanobacteria (Allen *et al.*, 2010). Additionally, the hopane, namely diploptene, detected in all mats is common to many microbial mat environments (Boudou *et al.*, 1986; Dobson *et al.*, 1988; Thiel *et al.*, 2001) and has been associated with both cyanobacterial (Gelpi *et al.*, 1970;

Dobson et al., 1988) and sulfate reducing bacterial (e.g., *Desulfovibrio*) sources (Blumenberg et al., 2006). The dominant 16:0 and 18:0 PLFAs can derive from various sources of bacteria including cyanobacteria and sulfate-reducing bacteria (e.g. Cohen et al., 1995; Londry et al., 2004). Based on additional evidence such as the high relative abundances of 18:1 ω 9- a dominant PLFA of cultured cyanobacteria (Kenyon et al., 1972; Cohen et al., 1995); C_{17:1} hydrocarbons; and stable carbon isotope data concordant with the presence of cyanobacteria and previously reported evidence for a dominance of cyanobacteria in Shark Bay mats (Burns et al., 2004; Allen et al., 2009); it is quite plausible that the 16:0 and 18:0 PLFAs also derived from cyanobacteria. 18:1 ω 9, also highly abundant in the mats, was previously identified as a dominant PLFA in cultured cyanobacteria (Kenyon et al., 1972; Cohen et al., 1995). In addition, PLFA 18:4 ω 3 present in all mats in lower abundance was also related to the presence of cyanobacteria (Kenyon et al., 1972; Vestal and White, 1989; Jahnke et al., 2004). Hence, cyanobacteria were present in all mats although they PLFA markers seemed to be more abundant in the shallowest mat (D1 – 82 % of the total PLFA abundance) (Figure 4.5).

Sulfur-cycling organisms were also common to all microbial mats. The detection of 10-methylhexadecanoic acid in all mats confirmed the presence of sulfate-reducing bacteria (Vestal and White, 1989). This biomarker was slightly more abundant in the deeper mats. *Iso*- and *anteiso*-15:0 and 17:0 as well as *iso*-17:1 ω 9 were also present in all mats (Figure 4.5) and can also derive from sulfate-reducing bacteria. Diagnostic sulfate-reducing bacteria PLFAs such as *iso*-15:0 and *iso*-17:1 ω 9 presented higher $\delta^{13}\text{C}$ values than the other PLFAs (Figure 4.6). This could be related to the carbon source utilised by the sulfate-reducing bacteria. In a previous study, cultures of *Desulfovibrio desulfuricans* grown heterotrophically with lactate, for instance, showed PLFAs enriched in ^{13}C compared to other fatty acids present in these bacteria (i.e. 16:0, 17:0 or 18:0) (Londry et al., 2004). In addition, it is possible that the higher $\delta^{13}\text{C}$ values for *iso*-15:0 and *iso*-17:1 ω 9 resulted from the heterotrophy of the ^{13}C -enriched diatomaceous ooze present in the mats by the sulfate-reducing bacteria.

Additionally, long-chain PLFA with a strong even-over-odd predominance were detected in all mats. These fatty acids, responsible for the commonly detected odd carbon-numbered *n*-alkane bias (i.e., aliphatic fraction; Figure 4.3) have been previously attributed to higher plant inputs (Eglinton and Hamilton, 1967) that can be supplied to the mats by aeolian transport (Allen et al., 2010). All mats showed a predominance of odd carbon-numbered *n*-alkanes (Figure 4.3). However, the isotopic values of the *n*-alkanes were more ^{13}C -depleted (3.4-7.3 ‰ for D2, for instance) than the co-occurring fatty acids (Figure 4.4 and Figure 4.6), suggesting that even long-chain fatty acids and odd *n*-alkanes were from different sources. Distribution of long-chain PLFA and $\delta^{13}\text{C}$ values and trends similar to those observed here have been reported in sediments impacted by vascular plants and bacteria (Gong and Hollander, 1997) as well as in ooids from the Bahamas (Edgcomb et al., 2013a; Summons et al., 2013) and Shark Bay (Summons et al., 2013). These previous studies similarly reported the $\delta^{13}\text{C}$ values of the *n*-alkanes to be depleted relative to the long-chain fatty acids by 4-5‰ and was proposed to reflect a sulfate-reducing *Firmicute* bacteria (Summons et al., 2013), based on the identification of PLFAs with highly similar distributions in spore-forming *Desulfotomaculum* sp. (Rezanka et al., 1990; Rezanka and Sigler, 2009). *Firmicute* bacteria have previously been identified by DNA analyses of microbial mats from Shark Bay (Allen et al., 2009). Hence, it is possible that the predominantly even over odd long-chain fatty acids detected in the different microbial mats were also indicative of the sulfate-reducing bacteria present in these structures.

Pristane was absent in all mats, except for D4 where it was in low abundance whilst phytane or phytene were detected in all mats (Figure 4.3). Absence or low abundance of pristane relative to phytane is usually associated with the presence of reducing conditions ($\text{Pr/Ph} < 1$; Powell and McKirdy, 1973) suggesting that anoxic conditions were present in all investigated microbial structures. This is concordant with a previous study on Nilemah smooth mats that revealed high concentrations of sulfide across the different mat layers (Pagès et al., 2014b).

➤ *Changes along the Nilemah littoral gradient*

Subtle but important differences in the biomarker distributions and isotopic compositions of the mats were noticed along the littoral gradient. A decrease in mat $\delta^{15}\text{N}_{\text{biomass}}$ was observed with water depth (Figure 4.2B). Bauersachs et al. (2011) reported a similar decrease in $\delta^{15}\text{N}$ values of microbial mats along the littoral gradient and associated this with higher contribution of biological N. In addition, high $\delta^{15}\text{N}_{\text{biomass}}$ values such as the one observed in D1 have been previously associated with the presence of diatoms (Davey, 1993). We have identified additional evidence for a decrease in diatom abundance with water depth. First, the $\delta^{13}\text{C}_{\text{biomass}}$ values of the D1 and D2 mats were $>$ D3 and D4 (Figure 4.2B). Diatoms are a source of moderately ^{13}C -depleted carbon and have been attributed to mat $\delta^{13}\text{C}_{\text{biomass}}$ values similar to those observed for D1 and D2 (Fry and Wainright, 1991). Cholest-2-ene was also detected in D2 (Figure 4.3). Δ^2 -sterenes are usually associated with eukaryotes, including for instance green algae and other phytoplankton, terrestrial higher plants or submerged macrophytes (Volkman, 1986; Volkman et al., 1998), however, diatoms and zooplankton are also a major sources for C_{27} sterenes (Volkman, 1986). $\text{C}_{25:1}$ alkene was only detected in D1 and D2 mats and had a relatively heavy $\delta^{13}\text{C}$ value compared to the other hydrocarbon products (Figure 4.4). This alkene has previously been identified in microbial mats (including previous analysis of D1 and D2) and a subtidal sediment from Hamelin Pool (Dunlop and Jefferies, 1985; Allen et al., 2010). In addition, the C_{25} HBI has been previously identified in diatoms (Grossi et al., 2004) and the detection of C_{25} and $\text{C}_{20:0}$ HBIs with relatively heavy $\delta^{13}\text{C}$ values (~ 6.6 ‰ heavier than the TOC) in sediments from the hypersaline Coorong lagoon has been associated with the presence of diatoms (McKirdy et al., 2010). Relatively ^{13}C -enriched $\text{C}_{25:1}$ and $\text{C}_{25:2}$ HBI alkenes from diatomaceous ooze have also previously been detected in Hamelin Pool samples (-12.0 ‰ and -12.8 ‰) (Summons et al., 1993). Diatoms have been recognised to be ^{13}C -rich organisms in comparison to other primary producers as they usually grow in blooms that lead to localised depletions in $\text{CO}_2(\text{aq})$ producing enriched ^{13}C biomass and some species are also able to assimilate HCO_3^- (Freeman et al., 1994, Canuel et al., 1997). This is concordant with a previous identification of eukaryotic organisms in Hamelin Pool microbial

mats (Allen et al., 2010; Edgcomb et al., 2013b). Furthermore, the relative abundance of 20:5 ω 3 and 16:4 ω 1 PLFA that can be associated with the presence of diatoms (Volkman et al., 1989; Dunstan et al., 1993) progressively decreased with depth (Figure 4.5). These results are concordant with a previous study on Antarctic microbial mats in which the presence of diatoms was strongly related to microbial mat depth and the highest diatoms species richness occurred in the shallower mats (Sabbe et al., 2004).

An increase in non-diatom macrophyte input was also evident with water depth. The deeper D3 and D4 mats had C:N ratios of 12.5 and 15.4, respectively, which were higher than the shallower mats (Figure 4.2A). C:N ratios > 12 are indicative of terrestrial OM, whilst values of 6 - 9 are more characteristic of marine OM (Prahl et al., 1980). However, it seems unlikely that the deeper structures would receive more aeolian input than the shallower structures and the $\delta^{13}\text{C}_{\text{biomass}}$ values of these two deeper microbial structures were more positive than typical terrestrial OM values (Kohn, 2010) (Figure 4.2B). Nonetheless, Shark Bay is known for the presence of some of the largest seagrass beds reported (Walker et al., 1988) which can contribute to very high C:N ratios (15-20) (Duarte, 1990). Furthermore, OM from the hypersaline Coorong lagoon with similar C:N ratios and $\delta^{13}\text{C}_{\text{biomass}}$ values (> 20‰) to the deeper D3 mat and D4 mats was suggested to derive from submergent aquatic macrophytes. This suggests a possible contribution from seagrass detritus to the total biomass in the deeper Shark Bay mats. Long-chain *n*-alkanes with an odd over even predominance were detected in all mats (Figure 4.3). The $\delta^{13}\text{C}$ values of the aliphatic fraction of the mats showed that long-chain *n*-alkanes (C₂₄-C₃₃) were on average more depleted than *n*-C₁₇ (-2.8 to -5.8 ‰), consistent with a terrestrial plant or submerged macrophytes origin for the long-chain *n*-alkanes (Figure 4.4), because long-chain *n*-alkanes from plants present ¹³C-depleted values (typically ranging from -31 to -39 ‰ for terrestrial C₃ plants and -19 to -34 ‰ for some species of coastal macrophytes) (Collister et al., 1994; Canuel et al., 1997). A molecular proxy P_{aq} , based on relative abundance of long-chain *n*-alkanes ($P_{\text{aq}} = (\text{C}_{23} + \text{C}_{25})/(\text{C}_{23} + \text{C}_{25} + \text{C}_{27} + \text{C}_{29})$), has been developed to evaluate the input from submerged/floating aquatic macrophytes to the total

biomass relative to the input from emergent and terrestrial plants in lake sediments (Ficken et al., 2000) as well as lagoons and estuaries (Xu et al., 2006; McKirdy et al., 2010). An intermediate value between 0.1 and 0.4 has been assigned to a mixture of inputs from terrestrial plants and submerged macrophytes (Ficken et al., 2000). A value between 0.4 and 1, however, was associated with higher inputs from submerged macrophytes. The P_{aq} ranged between 0.28 and 0.36 for D1 to D3 mats, suggesting a mixed contribution from terrestrial plants and submerged macrophytes (Table 4.5). D4, however, presented a P_{aq} value of 0.41 confirming a higher contribution from seagrass beds to this deepest microbial structure. In addition, the aliphatic fraction of D4 was dominated by the n -C₂₁ alkane. This n -alkane has been reported as a dominant compound in seagrass meadows (Canuel et al., 1997; Jaffé et al., 2001) and it is possible that the predominance of this compound in the deepest structure might be related with the presence of Faure Sill seagrass banks located in the north of Hamelin Pool.

Mat type	P_{aq} value	Source
Pustular D1	0.29	Mixed input: terrestrial and macrophytes
Smooth D2	0.28	
Colloform D3	0.36	
Pavement D4	0.41	Macrophytes

Table 4.5: Value of molecular proxy P_{aq} , based on relative abundance of long-chain n -alkanes and suggested sources for these n -alkanes in the Nilemah mats.

The $\delta^{13}\text{C}$ values of PLFA, biomass and CO_2 also showed differences with water depth (Figure 4.6). Because the stable isotope composition of DIC in surface water is influenced by atmospheric CO_2 dissolution (usually between ~ -7 and -8 ‰), more positive $\delta^{13}\text{C}$ values would be expected in the shallower mats than in the

deeper microbial structures in which isotopic signatures are expected to be influenced by near bottom decomposition processes and recycling of OM (e.g. Grice, 2001). However, both processes depend on water depth and mixing due to tidal and wave action. In addition, morphological structure can also strongly affect the $\delta^{13}\text{C}$ values in microbial mats and an overall enrichment in ^{13}C , as observed for the more cohesive microbial mats, could be due to a greater CO_2 limitation (Des Marais et al., 1992; Jahnke et al., 2004). Of the Nilemah mats, the smooth D2 mat had the most laminated and cohesive structure while the colloform D3 mat and microbial pavement D4 contained fragments of bivalves, microgastropods, foraminifera and algae (Jahnert and Collins, 2012). Thus, the less cohesive structures of the deeper microbial mats, more negative $\delta^{13}\text{C}$ of CO_2 , biomass and lipids would be expected. With the exception of the pustular D1 mat, the $\delta^{13}\text{C}$ PLFA data was concordant with this hypothesis with D2 showing consistently heavier values and a trend towards lighter values in the deeper structures. In addition, the $\delta^{13}\text{C}$ values of CO_2 and biomass also decreased with depth with D2 showing heavier values D4 lighter ones. D1, however, did not follow the same trend, which suggested a specific functionality (van der Meer et al., 2000) or a different pathway for CO_2 fixation. The $\epsilon_{\text{Biomass-CO}_2}$ of D2, D3 and D4 mats showed very similar values, suggesting that the isotopic composition of DIC had a strong influence on the changing isotopic compositions of OM in these mats. D1, however, showed a much lower value, confirming that a different CO_2 fixation pathway was likely used in this mat. With the exception of the pustular D1 mat, the $\epsilon_{\text{PLFA-Biomass}}$ showed a progressive decrease with depth, ranging from -1.6 ‰ for D2 to -6.9 ‰ for D4. Different CO_2 fixation pathways have been shown to result in different isotopic fractionations between PLFA and biomass. For a cyanobacterium, isotopic fractionation between PLFA and biomass associated with the Calvin cycle ranged between -7.6 and -9.9 ‰ (Sakata et al., 1997) while fractionation associated with the reverse tricarboxylic acid (rTCA) cycle can vary from 2.0 to -16.0 ‰ in green sulfur bacteria or sulfate-reducing bacteria, for instance (van der Meer et al., 1998; Zhang et al., 2002; Londry et al., 2004). A smaller range from 0.2 to -1.9 ‰ was observed for a green non-sulfur bacterium using the 3-hydroxypropionic acid (HP)-pathway (van der Meer et al., 2001). The decrease in $\epsilon_{\text{PLFA-Biomass}}$ with depth

suggested a progressive change in dominant communities. This could be related to an increase in sulfur-cycling organisms with depth, as shown by the slightly higher abundance of the 10-methyl-16:0 PLFA in the deeper mats, and therefore, potential changes in CO₂ fixation pathways, such as an increase in the acetyl COA-pathway by sulfate-reducing bacteria or higher rates of heterotrophic remineralisation in the deeper mats. The highest $\epsilon_{\text{PLFA-Biomass}}$, however, was observed for D1 (-9.3 ‰). A previous study of Shark Bay (Hamelin Pool) microbial mats revealed a higher abundance of cyanobacteria in the shallowest pustular mat than in the deeper smooth mat (Allen et al., 2009). In addition, the PLFA data revealed a higher proportion in the pustular mat (Figure 4.5), in comparison with the other mats. Cyanobacteria use the Calvin cycle that results in isotopic fractionation similar to the one observed in the pustular mat (Sakata et al., 1997). Therefore, it is likely that the greater isotopic fractionation observed in this mat, in comparison with the other mats at greater depth, resulted from a higher proportion of cyanobacteria in this structure.

- **Salinity gradient**

As previously discussed (see above), the lipid and PLFA composition of the hypersaline Nilemah smooth mat (S3) showed evidence for a strong marine influence. Both of the less saline smooth mats, particularly the Garden Point mat (S2), had a more significant terrestrial input. The presence of phytane and absence of pristane in both the S3 and S2 was indicative of reducing conditions (Powell and McKirdy, 1973) (Fig. 8). Further, S2 showed a high relative abundance of PLFAs indicative of sulfate-reducing bacteria including *anteiso*-15:0, *iso*- and *anteiso*-17:0 and *iso*-17:1 ω 9 (Taylor and Parkes, 1983; Taylor and Parkes, 1985; Londry et al., 2004) (Figure 4.9) as well as 10-methylhexadecanoic acid (Vestal and White, 1989).

The higher abundances of *n*-C₁₇ and *n*-C_{17:1} in S3 suggested a high abundance of cyanobacteria in the hypersaline mat (Fig. 8). S3 was also the only mat to contain C_{25:1} HBI attributed to a diatom source and it contained higher

concentrations of 20:5 ω 3 and 16:4 ω 1 (Fig. 9) which may also derive from diatoms (Volkman et al., 1989; Dunstan et al., 1993). These data suggested a much lower abundances of diatoms in smooth mats from less saline waters. Salinity has been reported to be a major control of diatoms species distribution in various environments (e.g. Wilson et al., 1994; Underwood et al., 1998; Sabbe et al., 2004). A diatom sequence related to *Navicula cryptotenella* has been previously found in a smooth mat from Hamelin Pool (Allen et al., 2009). These diatoms can thrive in a broad range of salinity (1-102 mS/cm) (Blinn et al., 2004), possibly explaining their higher abundance at the most saline site.

S2 and S3 mats both showed long-chain *n*-alkanes with an odd carbon preference (Figure 4.8), but they showed different P_{aq} values suggesting different sources. S2 had a P_{aq} value of 0.1 typical of terrestrial sources (Ficken et al., 2000). The $\delta^{13}C_{OM}$ of S2 was more positive than the other mats (Figure 4.7B), possibly reflecting a relatively high contribution of the C4 plants inhabiting Shark Bay (e.g. *Atriplex* spp.). S3 had a P_{aq} value of 0.3 characteristic of a mixed input from terrestrial plants and submerged macrophytes (Ficken et al., 2000), suggesting a higher contribution of seagrass compared to S2. The long chain *n*-alkanes in S1 showed no carbon number preference (Figure 4.8), but its long-chain PLFAs showed a predominance of even carbon numbers (Figure 4.9) and these were significantly ^{13}C depleted (about 10‰) compared to the other mats (Figure 4.10). These may reflect higher plant contributions (Eglinton and Hamilton, 1967) whereas the correspondingly heavier PLFAs of S3 and S2 may have originated from sulfate-reducing *Firmicute* organisms (Summons et al., 2013)

It has been suggested that CO_2 is more limited in microbial mats from environments of enhanced salinity (Schidlowski et al., 1984; 1994), which should be reflected by heavier $\delta^{13}C$ values. Indeed, $\delta^{13}C_{PLFA}$ values were lightest in the S1 smooth mat of the least saline water and became heavier in the more saline mats (Figure 4.10). The $\delta^{13}C_{CO_2}$ value of S3 was also heavier than S2 (Nb. Not measured in S1). The $\delta^{13}C_{biomass}$ was also expected to follow the same trend since previous

studies on both microbial mats along a slope gradient (Schidlowski et al., 1994) and sediments from salt marshes (Chmura and Aharon, 1995) showed $\delta^{13}\text{C}_{\text{biomass}}$ values increase with salinity. However, this was not the case in Shark Bay since the $\delta^{13}\text{C}_{\text{biomass}}$ values of S1 and S3 were very similar. The $\epsilon_{\text{Biomass-CO}_2}$ of S3 (-4.0 ‰) was lighter than S2 (3.1 ‰). These values seemed to be influenced by the specific community composition of each mat. For instance, the predominance of sulfur-cycling organisms in S2 (Nb., PLFA biomarkers) potentially contributed to high rates of heterotrophic remineralisation. The $\delta^{13}\text{C}$ values of heterotrophic biomass reflects the substrate carbon and hence also the physiology of the substrates primary source organism (e.g., algae, higher plants) (Pancost and Sinninghe Damsté, 2003). Consequently, the carbon substrate of the higher abundance of heterotrophic biomass in S2 may have influenced the isotopic composition of this mat. Based on biomarker distributions, S1 and S3 appeared to be dominated by autotrophic biomass, however, different $\epsilon_{\text{PLFA-Biomass}}$ were observed for these mats (-6.2 ‰ for S1 and -1.8 ‰ for S3). As the ϵ values of S3 were very similar to the other mats from Nilemah (D3-D4), this mat was likely dominated by autotrophic biomass, strongly influenced by the isotopic composition of the DIC. S1 presented more cyanobacterial PLFAs (76 % of the total PLFA abundance) than S3 (48 %) (Figure 4.9). This is concordant with other studies that have showed an increase in the proportion of cyanobacteria with a decrease in salinity (Pedrós-Alió et al., 2000; Benlloch et al., 2002). Investigation of microbial communities in mats from the Arabian Gulf, for instance, revealed a dramatic decrease in the relative abundance of cyanobacteria (62% to 5%) with increasing salinity (Abed et al., 2007). Hence, it is possible that the least saline mat, S1, was influenced by an autotrophic biomass using the Calvin cycle, leading to a greater isotopic fractionation than in S3.

- **Implications for paleoenvironmental reconstructions**

Modern microbial mats such as the ones found in Shark Bay are potential analogues of Precambrian stromatolites (Walter, 1994). Hence, the correlation of lipids and isotopic compositions in modern mats with corresponding biomarker features of fossil mats may provide a useful insight into ancient ecosystems.

However, as observed herein, environmental and physiological factors can strongly influence the $\delta^{13}\text{C}_{\text{biomass}}$ values. For instance, the $\delta^{13}\text{C}_{\text{biomass}}$ values of the shallowest mat (D1) at 0.20 m depth and the deepest one (D4) at 6 m differed by -2.9 ‰ (Table 4.3). This difference could be due to different morphological structure of the mats or alternatively, changes in CO_2 fixation pathways with depth. Clearly, characteristics of microbial mat facies such as water depth should be taken into account for isotopic interpretations as water depth likely had a very significant impact on the marine carbon cycle of the Proterozoic period (Logan et al., 1995; Rothman et al., 2013). In shallow-water environments, for instance, OM is quite rapidly buried and will therefore be likely to have an isotopic composition reflecting its biological source and paleodepositional conditions. On the other hand, the longer residence time of OM that persists to deeper depths makes it vulnerable to greater alteration (Rothman et al., 2003).

Additionally, the $\delta^{13}\text{C}_{\text{biomass}}$ value of the most saline mat (S3) was higher than the least saline mat (S1), concordant with higher CO_2 limitation with enhanced salinity (Schidlowski et al., 1984; 1994). The mat at intermediate salinity (S2), however, presented the highest $\delta^{13}\text{C}_{\text{biomass}}$ value, reflecting an isotopic influence from other environmental and physiological factors. Jahnke et al. (2004) previously attributed significantly different $\delta^{13}\text{C}_{\text{biomass}}$ values (6.4 ‰) measured for two microbial mats with similar microbial communities and from similar environmental settings (e.g. temperature, pH, $\delta^{13}\text{C}_{\text{DIC}}$) to differences in their macroscopic structure. Since a high number of factors such as environmental conditions and carbon uptake physiologies can influence isotopic signatures, the $\delta^{13}\text{C}$ of recent and fossil sedimentary OM need to be considered cautiously and should be supported as much as possible by additional biological, sedimentological and geochemical evidence.

Conclusions

This study represents the first detailed characterisation of Shark Bay mats, using a combined approach based on biolipids and stable isotopic analysis, and provided a better insight into the complex relationship between microbial mats and their surrounding environment. The molecular and isotopic compositions of Nilemah microbial mats located in different water depths identified a major cyanobacterial community common to all mats. Sulfate-reducing bacteria were also present in all mats (e.g. ^{13}C enriched *iso*-15:0 and *iso*-17:1 ω 9). Subtle differences indicating that water depth does have some influence over microbial communities included i) a possible seagrass input (e.g. high abundance of *n*-C₂₁) to the deepest mat; ii) a contribution from diatoms in the shallowest mats (pustular D1 and smooth D2) based on the C_{25:1} HBI alkene, PLFA and isotopic values; iii) a higher abundance of cyanobacteria in the shallowest mat (based on PLFA data) iv) a decrease in $\delta^{15}\text{N}$ along the littoral gradient possibly due to a higher input of biological fixed N to the total N pool with depth; and v) more negative $\delta^{13}\text{C}$ values of PLFAs, biomass and CO₂ with depth. The main differences between the smooth mats at different salinities were i) a higher abundance of diatoms and macrophytes in the hypersaline Nilemah mat (S3) ii) a higher terrestrial input in the mats in metahaline waters, particularly at Rocky Point (S1) and iii) a higher relative abundance of cyanobacteria in the least saline mat. The $\delta^{13}\text{C}$ values of the biomass, CO₂ and PLFA $\delta^{13}\text{C}$ values did include significant differences between the three mats, but these were most likely related to different biomass (autotrophic *versus* heterotrophic) and CO₂ fixation pathways. Our results highlighted different microbial communities in the different types of mats and showed the contribution of cyanobacteria, diatoms and seagrass to the OM of the mats was controlled to a degree by water depth and salinity.

By holistically considering the biological nature of the Shark Bay mats and the physicochemical nature of their host marine environments, the present study has confirmed that environmental conditions such as water depth and salinity can have a significant influence on the microbial composition of stromatolites. Thus, an

important interplay between abiotic parameters and biotic response of stromatolites has been identified. A similar integrated approach might also be applied to the characterisation of ancient stromatolites. Some of the hydrocarbon lipids sourced from extant stromatolites have been shown to persist in the geological record for long periods of time (e.g. Logan et al., 1995). Correlation of these biomarkers with other geochemical evidence of paleodepositional conditions may help illuminate our understanding of the evolution of stromatolites from the ancient past to their present forms.

Acknowledgements

This research was supported by a grant from the Australian Research Council's Discovery Projects scheme (2010-2013, Grice, Greenwood, Snape, and Summons). AP thanks WA-Organic and Isotope Geochemistry Centre, Curtin University and CSIRO for top-up scholarship. Geoff Chidlow is thanked for technical support regarding GC-MS. G. Skrzypek is supported by a Future Fellowship from the Australian Research Council (FT110100352).

References

- Abed R. M. M., Kohls K. and de Beer D.** (2007). Effect of salinity changes on the bacterial diversity, photosynthesis and oxygen consumption of cyanobacterial mats from an intertidal flat of the Arabian Gulf. *Environ. Microbiol.* **9**, 1384–1392.
- Abrajano Jr T. A., Murphy D. E., Fang J., Comet P. and Brooks J. M.** (1994) $^{13}\text{C}/^{12}\text{C}$ ratios in individual fatty acids of marine mytilids with and without bacterial symbionts. *Org. Geochem.* **21**, 611–617.
- Allen M. A., Goh F., Burns B. P. and Neilan B. A.** (2009) Bacterial, archaeal and eukaryotic diversity of smooth and pustular microbial mat communities in the hypersaline lagoon of Shark Bay. *Geobiology* **7**, 82–96.
- Allen M. A., Neilan B. A., Burns B. P., Jahnke L. L. and Summons R. E.** (2010) Lipid biomarkers in Hamelin Pool microbial mats and stromatolites. *Org. Geochem.* **41**, 1207–1218.

- Allwood A. C., Walter M. R., Kamber B. S., Marshall C. P. and Burch I. W.** (2006) Stromatolite reef from the Early Archaean era of Australia. *Nature* **441**, 714–718.
- Bauersachs T., Compaoré J., Severin I., Hopmans E. C., Schouten S., Stal L. J. and Sinninghe Damsté J. S.** (2011) Diazotrophic microbial community of coastal microbial mats of the southern North Sea. *Geobiology* **9**, 349–359.
- Benloch S., López-López A., Casamayor E. O., Øvreas L., Goddard V., Daae F. L., Smerdon G., Massana R., Joint I., Thingstad F., Pedrós-Allió C. and Rodríguez-Valera F.** (2002). Prokaryotic genetic diversity throughout the salinity gradient of a coastal solar saltern. *Environ. Microbiol.* **4**, 349–360.
- Blinn D., Halse S., Pinder A. and Shiel R.** (2004). Diatom and micro-invertebrate communities and environmental determinants in the western Australian wheatbelt: a response to salinization. *Hydrobiologia* **528**, 229–248.
- Blumenberg M., Krüger M., Nauhaus K., Talbot H. M., Oppermann B. I., Seifert R., Pape T. and Michaelis W.** (2006) Biosynthesis of hopanoids by sulfate-reducing bacteria (genus *Desulfovibrio*). *Environ. Microbiol.* **8**, 1220–1227.
- Blumer M.** (1957) Removal of elemental sulphur from hydrocarbon fractions. *Anal. Chem.* **29**, 1039–1041.
- Bobbie R. J. and White D. C.** (1980) Characterization of benthic microbial community structure by high-resolution gas chromatography of fatty acid methyl esters. *Appl. Environ. Microbiol.* **39**, 1212–1222.
- Boon P. I. and Sorrell B.K.** (1991) Biogeochemistry of billabong sediments. I. The effect of macrophytes. *Fresh. Biol.* **26**, 209–226.
- Boudou J. P., Trichet J., Robinson N. and Brassell S. C.** (1986) Profile of aliphatic hydrocarbons in a recent polynesian microbial mat. *Int. J. Environ. Anal. Chem.* **26**, 137–155.
- Bühring S. I., Smittenberg R. H., Sachse D., Lipp J. S., Golubic S., Sachs J. P., Hinrichs K.-U. and Summons R. E.** (2009) A hypersaline microbial mat from the Pacific Atoll Kiritimati: insights into composition and carbon fixation using biomarker analyses and a ¹³C-labeling approach. *Geobiology* **7**, 308–323.
- Burne R. V. and Johnson K.** (2012) Sea-level variation and the zonation of microbialites in Hamelin Pool, Shark Bay, Western Australia. *Mar. Freshw. Res.* **63**, 994–1004.

- Burns B. P., Goh F., Allen M. A. and Neilan B. A.** (2004) Microbial diversity of extant stromatolites in the hypersaline marine environment of Shark Bay, Australia. *Environ. Microbiol.* **6**, 1096–101.
- Canuel E. A., Freeman K. H. and Wakeham S. G.** (1997) Isotopic compositions of lipid biomarker in estuarine compounds plants and surface sediments. *Limnol. Oceanogr.* **42**, 1570–1583.
- Chmura G. L. and Aharon P.** (1995) Stable carbon isotope signatures of sedimentary carbon in coastal wetlands as indicators of salinity regime. *J. Coast. Res.* **11**, 124–135.
- Cohen Z., Margheri M. C. and Tomaselli L.** (1995) Chemotaxonomy of cyanobacteria. *Phytochemistry* **40**, 1155–1158.
- Collister J. W., Rieley G., Stern B., Eglinton G. and Fry B.** (1994) Compound-specific $\delta^{13}\text{C}$ analyses of leaf lipids from plants with different carbon dioxide metabolism. *Org. Geochem.* **21**, 619–627.
- Cook P. L. M., Reville A., Clementson L. A. and Volkman J. K.** (2004) Carbon and nitrogen cycling on intertidal mudflats of a temperate Australian estuary. III. Sources of organic matter. *Mar. Ecol. Prog. Ser.* **280**, 55–72.
- Davey M. C.** (1993) Carbon and nitrogen dynamics in a maritime Antarctic stream. *Freshw. Biol.* **30**, 319–330.
- Des Marais D. J., Cohen Y., Nguyen H., Cheatham M., Cheatham T., Munoz E.** (1989) Carbon isotopic trends in the hypersaline ponds and microbial mats at Guerrero Negro, Baja California Sur, Mexico: implications for Precambrian stromatolites. In *Microbial mats: physiological ecology of benthic microbial communities* (eds Cohen Y., Rosenberg E.) American Society for Microbiology, Washington, pp. 191–203.
- Des Marais D. J., Bauld J., Palmisano A., Summons R. E., Ward D.** (1992). The biogeochemistry of carbon in modern microbial mats. In *The Proterozoic Biosphere: A Multidisciplinary Study* (eds Schopf J. W., Klein C.) Cambridge University Press, Cambridge, pp. 299–308.
- Dobson G., Ward D. M., Robinson N. and Eglinton G.** (1988) Biogeochemistry of hot spring environments: Extractable lipids of a cyanobacterial mat. *Chem. Geol.* **68**, 155–179.
- Duarte C. M.** (1990) Seagrass nutrient content. *Mar. Ecol. Prog. Ser.* **67**, 201–207.
- Dunlop R. W. and Jefferies P. R.** (1985) Hydrocarbons of the hypersaline basins of Shark Bay, western Australia. *Org. Geochem.* **8**, 313–320.

- Dunstan G. A., Volkman J. K., Barrett S. M., Leroi J. M. and Jeffrey S. W.** (1993) Essential polyunsaturated fatty acids from 14 species of diatom (Bacillariophyceae). *Phytochemistry* **35**, 155–161.
- Edgcomb V. P., Bernhard J. M., Beaudoin D., Pruss S. B., Welander P. V., Schubotz F., Mehay S., Gillespie A. L. and Summons R. E.** (2013a) Molecular indicators of microbial diversity in oolitic sands of Highborne Cay, Bahamas. *Geobiology* **11**, 234–251.
- Edgcomb V. P., Bernhard J. M., Summons R. E., Orsi W., Beaudoin D. and Visscher P. T.** (2013b) Active eukaryotes in microbialites from Highborne Cay, Bahamas, and Hamelin Pool (Shark Bay), Australia. *ISME J.*
- Eglinton G. and Hamilton R. J.** (1967) Leaf Epicuticular waxes. *Science* **156**, 1322–1335.
- Ficken K. J., Li B., Swain D. L. and Eglinton G.** (2000) An *n*-alkane proxy for the sedimentary input of submerged/floating freshwater aquatic macrophytes. *Org. Geochem.* **31**, 745–749.
- Fourçans A., de Oteyza T. G., Wieland A., Solé A., Diestra E., van Bleijswijk J., Grimalt J. O., Kühl M., Esteve I., Muyzer G., Caumette P. and Duran R.** (2004) Characterization of functional bacterial groups in a hypersaline microbial mat community (Salins-de-Giraud, Camargue, France). *FEMS Microbiol. Ecol.* **51**, 55–70.
- Freeman K. H., Wakeham S. G. and Hayes J. M.** (1994) Predictive isotopic biogeochemistry: hydrocarbons from anoxic marine basins. *Org. Geochem.* **21**, 629–644.
- Fry B. and Wainright S. C.** (1991) Diatom sources of ^{13}C -rich carbon in marine food webs. *Mar. Ecol. Prog. Ser.* **76**, 149–157.
- Fry B.** (1996) $^{13}\text{C}/^{12}\text{C}$ fractionation by marine diatoms. *Mar. Ecol. Prog. Ser.* **134**, 283–294.
- Gelpi E., Schneider H., Mann J. and Oro J.** (1970) Hydrocarbons of geochemical significance in microscopic algae. *Phytochemistry* **9**, 603–612.
- Golubic S. and Hoffman H. J.** (1976) Comparison of Holocene and Mid-Precambrian Entophysalidaceae (Cyanophyta) in stromatolitic algal mats: cell division and degradation. *J. Paleontol.* **50**, 1074–1082.
- Gong C. and Hollander D. J.** (1997) Differential contribution of bacteria to sedimentary organic matter in oxic and anoxic environments, Santa Monica Basin, California. *Org. Geochem.* **26**, 545–563.

- Grice K.** (2001) $\delta^{13}\text{C}$ as an indicator of paleoenvironments: A molecular approach. In *Application of stable isotope techniques to study biological processes and functioning ecosystems* (eds. Unkovich M, Pate J, McNeill A and Gibbs J), pp. 247-281
- Grimalt J. O., de Wit R., Teixidor P. and Albaigés J.** (1992) Lipid biogeochemistry of Phormidium and Microcoleus mats. *Org. Geochem.* **19**, 509–530.
- Grossi V., Beker B., Geenevasen J. A. J., Schouten S., Raphel D., Fontaine M.-F. and Sinninghe Damsté J. S.** (2004) C_{25} highly branched isoprenoid (HBI) alkenes from the marine benthic diatom *Pleurosigma strigosum*. *Phytochem.* **65**, 3049-3055.
- Hoffman H. J.** (2000) Archean stromatolites as microbial archives. In *Microbial Sediments*. (eds. R. E. Riding, S.M. Awramik) Springer-Verlag, Berlin, pp. 315–327.
- Jaffé R., Mead R. N., Hernandez M. E., Peralba M. C. and Diguída O. A.** (2001) Origin and transport of sedimentary organic matter in two subtropical estuaries: a comparative, biomarker-based study. *Org. Geochem.* **32**, 507–526.
- Jahnert R. and Collins L.** (2011) Significance of subtidal microbial deposits in Shark Bay, Australia. *Mar. Geol.* **286**, 106–111.
- Jahnert R. and Collins L.** (2012) Characteristics, distribution and morphogenesis of subtidal microbial systems in Shark Bay, Australia. *Mar. Geol.* **303-306**, 115–136.
- Jahnert R. and Collins L.** (2013) Controls on microbial activity and tidal flat evolution in Shark Bay, Western Australia. *Sedimentology* **60**, 1071–1099.
- Jahnke L. L., Embaye T., Hope J., Turk K. A., Van Zuilen M., Des Marais D. J., Farmer J. D. and Summons R. E.** (2004) Lipid biomarker and carbon isotopic signatures for stromatolite-forming, microbial mat communities and *Phormidium* cultures from Yellowstone National Park. *Geobiology* **2**, 31–47.
- Jiang H., Dong H., Yu B., Liu X., Li Y., Ji S. and Zhang C. L.** (2007). Microbial response to salinity change in Lake Chaka, a hypersaline lake on Tibetan plateau. *Environ. Microbiol.* **9**, 2603–2621.
- Jørgensen B. B., Revsbech N. P., Blackburn T. H. and Cohen Y.** (1979) Diurnal cycle of oxygen and sulfide microgradients and microbial photosynthesis in a cyanobacterial mat sediment. *Appl. Envir. Microbiol.* **38**, 46–58.
- Kenyon C. N., Rippka R. and Stanier R. Y.** (1972) Fatty acid composition and physiological properties of some filamentous blue-green algae. *Arch. Mikrobiol.* **83**, 216–236.

- Kohn M. J.** (2010) Carbon isotope compositions of terrestrial C₃ plants as indicators of (paleo)ecology and (paleo)climate. *Proc. Natl. Acad. Sci. U. S. A.* **107**, 19691–19695.
- Logan B. W. and Cebulski D. E.** (1970) Sedimentary environments of Shark Bay, Western Australia. *Am. Assoc. Pet. Geol. Mem* **13**, 1–37.
- Logan B. W.** (1974) Evolution and diagenesis of Quaternary carbonate sequences, Shark Bay, Western Australia. *Am. Assoc. Pet. Geol. Mem.* **22**, 195–249.
- Londry K. L., Jahnke L. L. and Des Marais D. J.** (2004) Stable carbon isotope ratios of lipid biomarkers of sulfate-reducing bacteria. *Appl. Environ. Microbiol.* **70**, 745–751.
- McKirdy D. M., Thorpe C. S., Haynes D. E., Grice K., Krull E. S., Halverson G. P. and Webster L. J.** (2010) The biogeochemical evolution of the Coorong during the mid- to late Holocene: an elemental, isotopic and biomarker perspective. *Org. Geochem.* **41**, 96–110.
- Meziane T., Bodineau L., Retiere C. and Thoumelin G.** (1997) The use of lipid markers to define sources of organic matter in sediment and food web of the intertidal salt-marsh-flat ecosystem of Mont-Saint-Michel Bay, France. *J. Sea Res.* **38**, 47–58.
- Meziane T. and Tsuchiya M.** (2000) Fatty acids as tracers of organic matter in the sediment and food web of a mangrove/intertidal flat ecosystem, Okinawa, Japan. *Mar. Ecol. Prog. Ser.* **200**, 49–57.
- Mook W. G., Bommerson J. C. and Staverman W. H.** (1974) Carbon isotope fractionation between dissolved bicarbonate and gaseous carbon dioxide. *Earth Planet. Sci. Lett.* **22**, 169–176.
- Navarrete A., Peacock A., Macnaughton S. J., Urmeneta J., Mas-Castellà J., White D. C. and Guerrero R.** (2000) Physiological status and community composition of microbial mats of the Ebro Delta, Spain by signature lipid biomarkers. *Microb. Ecol.* **39**, 92–99.
- Oliver J. D. and Colwell R. R.** (1973) Extractable lipids of gram-negative marine bacteria: fatty - acid composition. *Int. J. Syst. Bacteriol.* **23**, 442–458.
- Paerl H. W. and Pinckney J. L.** (1996) A mini-review of microbial consortia: their roles in aquatic production and biogeochemical cycling. *Microb. Ecol.* **31**, 225–247.
- Paerl H. W., Pinckney J. L. and Steppe T. F.** (2000) Cyanobacterial-bacterial mat consortia: examining the functional unit of microbial survival and growth in extreme environments. *Environ. Microbiol.* **2**, 11–26.

- Pagès A., Grice K., Vacher M., Teasdale P., Welsh D., Bennett W. and Greenwood P.** (2014a) Characterising microbial communities and processes in a modern stromatolite (Shark Bay) using lipid biomarkers and two-dimensional distributions of porewater solutes. *Environ. Microbiol.*, accepted.
- Pagès A., Welsh D. T., Teasdale P. R., Grice K., Vacher M., Bennett W. W. and Visscher P. T.** (2014b) Diel fluctuations in solute distributions and biogeochemical cycling in a hypersaline microbial mat from Shark Bay, WA. *Mar. Chem.*, accepted.
- Pancost R. D., Freeman K. H., Wakeham S. G. and Robertson C. Y.** (1997) Controls on carbon isotope fractionation by diatoms in the Peru upwelling region. *Geochim. Cosmochim. Acta* **61**, 4983–4991.
- Pancost R. D. and Sinninghe Damsté J. S.** (2003) Carbon isotopic compositions of prokaryotic lipids as tracers of carbon cycling in diverse settings. *Chem. Geol.* **195**, 29–58.
- Paoletti C., Pushparaj B., Florenzano G., Capella P. and Lercker G.** (1976) Unsaponifiable matter of green and blue-green algal lipids as a factor of biochemical differentiation of their biomasses: I. Total unsaponifiable and hydrocarbon fraction. *Lipids* **11**, 258–265.
- Papineau D., Walker J. J., Mojzsis S. J. and Pace N. R.** (2005) Composition and structure of microbial communities from stromatolites of Hamelin Pool in Shark Bay, Western Australia. *Appl. Environ. Microbiol.* **71**, 4822–4832.
- Pedrós-Alió C., Calderón-Paz J. I., MacLean M. H., Medina G., Marrasé C., Gasol J. M. and Guixa-Boixereu N.** (2000). The microbial food web along salinity gradients. *FEMS Microbiol. Ecol.* **32**, 143–155.
- Popp B. N., Lawa E. A., Bidigare R. R., Dore J. E., Hanson K. L. and Wakeham S. G.** (1998) Effect of phytoplankton cell geometry on carbon isotopic fractionation. *Geochim. Cosmochim. Acta* **62**, 69–77.
- Powell T. G. and McKirdy D. M.** (1973) relationship between ratio of pristane to phytane, crude oil composition and geological environment in Australia. *Nature* **243**, 37–39.
- Prahl F. G., Bennett J. T. and Carpenter R.** (1980) The early diagenesis of aliphatic hydrocarbons and organic matter in sedimentary particulates from Dabob Bay, Washington. *Geochim. Cosmochim. Acta* **44**, 1967–1976.
- Price R. M., Skrzypek G., Grierson P. F., Swart P. K. and Fourqurean J. W.** (2012) The use of stable isotopes of oxygen and hydrogen to identify water sources in two hypersaline estuaries with different hydrologic regimes. *Mar. Freshw. Res.* **63**, 952–966.

- Rezanka T., Sokolov M. and Viden I.** (1990) Unusual and very-long- chain fatty acids in *Desulfotomaculum*, a sulfate-reducing bacterium. *FEMS Microbiol. Lett.* **73**, 231–237.
- Rezanka T. and Sigler K.** (2009) Odd-numbered very-long-chain fatty acids from the microbial, animal and plant kingdoms. *Prog. Lipid Res.* **48**, 206–238.
- Robinson N. and Eglinton G.** (1990) Lipid chemistry of Icelandic hot spring microbial mats. *Org. Geochem.* **15**, 291–298.
- Rontani J.-F. and Volkman J. K.** (2005) Lipid characterization of coastal hypersaline cyanobacterial mats from the Camargue (France). *Org. Geochem.* **36**, 251–272.
- Sabbe K., Hodgson D. A., Verleyen E., Taton A., Wilmotte A., Vanhoutte K. and Vyverman W.** (2004) Salinity, depth and the structure and composition of microbial mats in continental Antarctic lakes. *Freshw. Biol.* **49**, 296–319.
- Sakata S., Hayes J. M., McTaggart A. R., Evans R. A., Leckrone K. J. and Togasaki R. K.** (1997) Carbon isotopic fractionation associated with lipid biosynthesis by a cyanobacterium: relevance for interpretation of biomarker records. *Geochim. Cosmochim. Acta* **61**, 5379–5389.
- Schidlowski M., Matzigkeit U. and Krumbein W. E.** (1984) Superheavy organic carbon from hypersaline microbial mats. *Naturwissenschaften* **71**, 303–308
- Schidlowski M., Gorzawski H. and Dor I.** (1994) Carbon isotope variations in a solar pond microbial mat: Role of environmental gradients as steering variables. *Geochim. Cosmochim. Acta* **58**, 2289–2298.
- Schouten S., Klein Breteler W. C. ., Blokker P., Schogt N., Rijpstra W. I. C., Grice K., Baas M. and Sinninghe Damsté J. S.** (1998) Biosynthetic effects on the stable carbon isotopic compositions of algal lipids: implications for deciphering the carbon isotopic biomarker record. *Geochim. Cosmochim. Acta* **62**, 1397–1406.
- Skrzypek G., Sadler R. and Paul D.** (2010) Error propagation in normalization of stable isotope data: a Monte Carlo analysis. *Rapid Commun. Mass Spectrom.* **24**, 2697–2705.
- Skrzypek G.** (2013) Normalization procedures and reference material selection in stable HCNOS isotope analyses: an overview. *Anal. Bioanal. Chem.* **405**, 2815–2823.
- Smith S. V. and Atkinson M. J.** (1983) Mass balance of carbon and phosphorus Shark Bay, Western Australia. *Limnol. Oceanogr.* **28**, 625–639.

- Summons R., Barrow R., Capon R., Hope J. and Stranger C.** (1993) The Structure of a new C₂₅ isoprenoid alkene biomarker from diatomaceous microbial communities. *Aust. J. Chem.* **46**, 907–915.
- Summons R. E., Bird L. R., Gillespie A. L., Pruss S. B., Roberts M. and Sessions A. L.** (2013) Lipid biomarkers in ooids from different locations and ages: evidence for a common bacterial flora. *Geobiology* **11**, 420–436.
- Taylor J. and Parkes R. J.** (1983) The cellular fatty acids of the sulphate-reducing bacteria. *J. Gen. Microbiol.* **129**, 3303–3309.
- Taylor J. and Parkes R. J.** (1985) Identifying different populations of sulphate-reducing bacteria within marine sediment systems, using fatty acid biomarkers. *Microbiology* **131**, 631–642.
- Thiel V., Peckmann J., Richnow H. H., Luth U., Reitner J. and Michaelis W.** (2001) Molecular signals for anaerobic methane oxidation in Black Sea seep carbonates and a microbial mat. *Mar. Chem.* **73**, 97–112.
- Underwood G. and Smith D.** (1998). Predicting epipelagic diatom exopolymer concentrations in intertidal sediments from sediment chlorophyll *a*. *Microb. Ecol.* **35**, 116–125.
- Van der Meer M. T. J., Schouten S. and Sinninghe Damsté J. S.** (1998) The effect of the reversed tricarboxylic acid cycle on the ¹³C contents of bacterial lipids. *Org. Geochem.* **28**, 527–533.
- Van der Meer M. T. J., Schouten S., de Leeuw J. W. and Ward D. M.** (2000) Autotrophy of green non-sulphur bacteria in hot spring microbial mats: biological explanations for isotopically heavy organic carbon in the geological record. *Environ. Microbiol.* **2**, 428–435.
- Van der Meer, M. T. J., Schouten S., van Dongen B. E., Rijpstra W. I. C., Fuchs G., Sinninghe Damsté J. S., de Leeuw J. W. and Ward D.** (2001) Biosynthetic controls on the ¹³C contents of organic components in the phototrophic bacterium *Chloroflexus aurantiacus*. *J. Biol. Chem.* **14**, 10971–10976.
- Van Kranendonk M., Philippot P., Lepot K., Bodorkos S. and Pirajno F.** (2008) Geological setting of Earth's oldest fossils in the ca. 3.5Ga Dresser Formation, Pilbara Craton, Western Australia. *Precambrian Res.* **167**, 93–124.
- Vestal J. R. and White D. C.** (1989) Lipid analysis microbial ecology. *Bioscience* **39**, 535–541.
- Volkman J. K., Johns R. B., Gillan F. T. and Perry G. J.** (1980) Microbial lipids of an intertidal sediment. I. Fatty acids and hydrocarbons. *Geochim. Cosmochim. Acta* **44**, 1133–1143.

- Volkman J. K.** (1986) A review of sterol markers for marine and terrigenous organic matter. *Org. Geochem.* **9**, 83–99.
- Volkman J. K., Jeffrey S. W., Nichols P. D., Rogers G. I. and Garland C. D.** (1989) Fatty acid and lipid composition of 10 species of microalgae used in mariculture. *J. Exp. Mar. Bio. Ecol.* **128**, 219–240.
- Volkman J. K., Barrett S. M., Blackburn S. I., Mansour M. P., Sikes E. L. and Gelin F.** (1998) Microalgal biomarkers: A review of recent research developments. *Org. Geochem.* **29**, 1163–1179.
- Walker D. I., Kendrick G. A. and McComb A. J.** (1988) The distribution of seagrass species in Shark Bay, Western Australia, with notes on their ecology. *Aquat. Bot.* **30**, 305–317.
- Walter M. R., Buick R. and Dunlop J. S. R.** (1980) Stromatolites 3,400-3,500 Myr old from the North pole area, Western Australia. *Nature* **284**, 443–445.
- Walter M.** (1994). Stromatolites: the main source of information on the evolution of the early benthos. In *Early Life on Earth* (ed. Bengtson S.) Columbia University Press, New York, pp. 270–286.
- Wilson S. E., Cumming B. F., Smol J. P.** (1994). Diatom-salinity relationships in 111 lakes from the Interior Plateau of British Columbia, Canada: the development of diatom-based models for paleosalinity reconstructions. *J. Paleolimnol.* **12**, 197–221.
- Winters K., Parker P. L. and Van Baalen C.** (1969) Hydrocarbons of blue-green algae: geochemical significance. *Science* **163**, 467–468.
- Xu Y., Mead R. N. and Jaffé R.** (2006) A molecular marker-based assessment of sedimentary organic matter sources and distributions in Florida Bay. *Hydrobiologia* **569**, 179–192.
- Zelles L., Bai Q. Y., Rackwitz R., Chadwick D. and Beese F.** (1995) Determination of phospholipid- and lipopolysaccharide-derived fatty acids as an estimate of microbial biomass and community structures in soils. *Biol. Fertil. Soils* **19**, 115–123.
- Zhang H., Davison W., Mortimer R., Krom M., Hayes P. and Davies I.** (2002) Localised remobilization of metals in a marine sediment. *Sci. Total Environ.* **296**, 175–187.

Chapter 5

Organic geochemical studies of modern microbial mats from Shark Bay – Part II. Influence of depth and salinity on lipophilic pigment and intact polar lipid distributions

Anais Pagès, Cédric Hubas, Kliti Grice, Tobias Ertefai, Ricardo Jahnert, Tarik Meziane

***Geobiology*, in preparation**

(impact factor 3.04)

Chapter 5

Abstract

Introduction

Materials and Methods

- Sampling sites
- Description of microbial mats
- Lipid biomarkers
 - Sampling
 - Intact polar lipid extraction
 - Analysis of intact polar lipids by high performance liquid chromatography–mass spectrometry (HPLC-MS)
 - Pigment extraction
 - Analysis of pigments by HPLC

Results

- Depth gradient
 - Intact polar lipids
 - Lipophilic pigments
- Salinity gradient
 - Intact polar lipids
 - Lipophilic pigments

Discussion

- Depth gradient
 - Common features for all mats
 - Changes along the littoral gradient
 - Changes in Hamelin Pool microbial mat communities through time
- Salinity gradient

Conclusions

Abstract

The distributions of intact polar lipids (IPLs) and lipophilic pigments were analysed in the same four microbial mats studied in [Chapter 4](#) to investigate how the distribution and abundance of these compounds changed with water depth. A comparison of lipophilic pigment distributions in the mats between this study and the study by Palmisano et al. (1989) was also undertaken in order to observe community changes in the mats through time. The IPLs and lipophilic pigment composition of Nilemah microbial mats along the littoral gradient highlighted the presence of sulfur-cycling organisms, alphaproteobacteria and cyanobacteria in all mats. Subtle differences between the mat communities were also detected, suggesting that water depth did influence microbial mats communities, as previously suggested in [Chapter 4](#). For instance, the concentration in bacteriochlorophyll *a* decreased with depth, highlighting the decrease in the abundance of purple phototrophic bacteria. In addition, chlorophyll *c*, indicative of diatoms, was only detected in the shallow pustular and smooth mats. To investigate the impact of salinity on microbial structures, two additional smooth mats from lower salinity waters (Garden Point and Rocky Point) were also studied. The highest diversity of IPLs was found in the least saline mat suggesting that microbial mats from more saline environments favour fewer organisms capable of surviving in harsher environments. Cyanobacteria were present in all mats whereas chlorophyll *c* from diatoms was only detected in the mat from Nilemah, further evidence for a higher abundance of diatoms in the most saline site. Compared to the previous study by Palmisano et al. (1989) the presently detected lipophilic pigment distribution reflect significant changes in microbial communities in the Hamelin Pool mats through time. The diatom communities seemed to be exclusively present in the shallower mats (pustular and smooth) whereas back in 1989, diatoms were only detected in the colloform mats. The abundance of purple phototrophic bacteria was also observed to increase over the more than 20 years between the two studies, suggesting significant change in environmental conditions.

Introduction

Fossilised stromatolites from the Pilbara Craton, Western Australia, 3.45 billion years old (Walter et al., 1980; Allwood et al., 2006) provide the oldest trace of biological activity on Earth (Grotzinger and Knoll, 1999). Modern microbial mats from Exuma Sound in the Bahamas and from Shark Bay in Western Australia present strong structural resemblances to ancient stromatolites and are considered modern day analogues of these ancient structures (Logan, 1974; Hoehler et al., 2001). Consequently, modern microbial mats provide a remarkable insight into past environmental conditions and microbial communities. Biological proxies can help understand the mechanisms regulating the composition and organisation of microbial communities and provide a better insight into the complex relationship between environmental conditions and microbial mat distributions in Shark Bay. In [Chapter 4](#), the distributions and stable carbon isotopic values of lipid biomarkers [aliphatic hydrocarbons and phospho-lipid fatty acids (PLFAs)] and bulk carbon and nitrogen isotope values of biomass were analysed in four different mats (pustular, smooth, colloform and pavement) along a tidal flat gradient to investigate their relationship with water depth. Common features of all microbial mats included the presence of cyanobacteria and sulfur-cycling organisms. A higher diatom contribution noted in the shallower mats was concordant with studies of water depth on mats in Antarctica (Sabbe et al., 2004). Conversely, the organic matter (OM) of the deeper mats showed evidence for higher seagrass contribution. Three microbial laminated smooth mats from Shark Bay sites (Rocky Point, Garden Point and Nilemah) of different salinity levels suggested sulfur-cycling organisms were favoured by lower salinities (e.g., Garden Point mat) whereas diatoms were in highest levels in the hypersaline mat (i.e., Nilemah).

IPLs can also provide significant and complimentary taxonomic information as they contain core lipids and signature polar head groups (Rütters et al., 2002; Schubotz et al., 2009). In addition, lipophilic pigments can be related to specific source organisms and are highly valuable for chemotaxonomic information. The earlier study by Palmisano et al. (1989) also considered the lipophilic pigment composition (including chlorophylls and carotenoids) of

different types of Hamelin Pool mats (tufted, pustular, smooth and colloform mats) and identified significant differences in mat communities. The aim of the present study was to further characterise the IPL and lipophilic pigment composition of the same suite of Shark Bay mats, investigate the influence water depth and salinity have on these biomarkers, and integrate this information from the complimentary [Chapter 4](#) data to holistically consider the control these important abiotic environmental parameters have on the microbial community structure of the mats.

Materials and Methods

- **Sampling sites**

Shark Bay is located in Western Australia, about 800 km north of Perth. Three sites were investigated: Nilemah, Garden Point and Rocky Point. A detailed description of these sites was provided in [Chapter 4](#). Briefly, Nilemah is located in the southern area of Hamelin Pool and presents hypersaline waters [56-70 practical salinity units (psu)]. Garden Point is a re-entrant located on the eastern side of Henry Freycinet embayment, on the western part of Shark Bay and presents metahaline waters (54 psu). Rocky Point is located on the western part of L'Haridon Bight and presents waters with the lowest salinity (40 psu). A detailed map highlighting the locations of the sampling sites can be found in [Chapter 4](#).

- **Description of microbial mats**

A more detailed description of the microbial mats of each three locations has been reported in [Chapter 4](#). Briefly, four microbial mats were sampled along the Nilemah tidal flat gradient: an intertidal pustular mat (0.2–0.8 m), presented a surface made of gelatinous mucilage pustules, a subtidal smooth mat (0.8–1.2 m) presented flat surface and flat horizontal mm-scale laminae composed of carbonate minerals interbedded with organic matter, a subtidal colloform mat (1–1.5 m) was a spherical structure that showed small globular forms rich in peloids and ooids and a subtidal microbial pavement (2-6 m), carbonate deposit lithified as bioclastic grainstone. The smooth mats from Garden Point and Rocky Point were found at the

same water depth than the smooth mat from Nilemah (0.2-0.8 m). All microbial mats were sampled in May 2010.

- **Lipid biomarkers**

- *Sampling*

The microbial mats were sampled in the field using an aluminium push core and immediately frozen (-18°C). The samples were freeze-dried in the laboratory and kept at -80°C until further analysis.

- *Intact polar lipid (IPL) extraction*

For IPLs, a modified Bligh and Dyer extraction method with four steps (Sturt et al., 2004) was applied, followed by centrifugation at 800 g for 10 min. The combined supernatants were washed with water and evaporated to dryness.

- *Analysis of intact polar lipids by high performance liquid chromatography–mass spectrometry (HPLC-MS)*

Analyses of IPLs were performed at the University of Bremen according to Sturt et al., (2004) by high performance liquid chromatography/ electrospray ionisation-multiple stage mass spectrometry (HPLC/ESI-MSn). Positive and negative ion mass spectra were separately obtained to provide complementary structural information. A LiChrospher Diol column (125 mm x 2.1 mm, 5 µm; Alltech Associates Inc., Deerfield, IL, USA) was fitted with a 7.5 mm x 4 mm guard column of the same packing material and was used at 30 °C in a column oven using a ThermoFinnigan Surveyor HPLC system. The following linear gradient of eluants was used with a flow rate of 0.2 mL.min⁻¹: 100% A to 35% A: 65% B over 45 min, then back to 100% A for 1 h to re-equilibrate the column for the next run (A = mixture of hexane/2-propanol/formic acid/14.8M NH₃(aq) in the portions of 79:20:0.12:0.04 v/v; and B = 2-propanol/water/formic acid/14.8M NH₃(aq),

88:10:0.12:0.04 v/v). Multiple stage mass spectrometry experiments (MS_n) were performed using a ThermoFinnigan LCQ Deca XP plus ion trap mass spectrometer (ThermoFinnigan, San Jose, CA, USA) with an electrospray ionization interface (ESI). ESI settings derived from tuning with diester- C_{16} -phosphatidylethanol-amine have been described previously (Sturt et al., 2004). A typical mass range of m/z 500–2000 was scanned while sequentially fragmenting the base peaks up to MS_3 stage of acquisition. Compound identification is based on characteristic molecular masses of ionized IPLs shown in the mass spectra, and product ions formed by loss of the neutrally charged headgroups, indicating ether or ester bonds between the hydrophilic headgroup and the core lipid with different numbers of carbon atoms attached (Rütters et al., 2002; Sturt et al., 2004). Relative abundances and total concentrations of IPL classes were obtained by integration of peak areas in mass chromatograms. Therefore, individual molecular ions of each IPL class were extracted from the full scan chromatograms and compared with the peak area of the internal standard. A similar response factor for the internal standard was assumed as for individual IPL classes, resulting in semi-quantitative data. The relative abundance of the acyl/alkyl moieties directly associated with the polar headgroups was determined by comparing the relative intensities of diagnostic ions in the corresponding mass spectra.

➤ *Pigment extraction*

Pigments were extracted from a sub-sample of about 0.5 g of freeze-dried sediment with 2 mL of 95 % cold buffered MeOH (2 % ammonium acetate) for 15 min at -20 °C, in the dark. Samples were sonicated (37 kHz) for 30 s prior to extraction. Extracts were then filtered (0.2 μ m) immediately before HPLC analysis.

➤ *Analysis of pigments by HPLC*

Pigment extracts were analysed using an Agilent 1260 Infinity HPLC composed of a quaternary pump (VL 400bar), a UV-VIS photodiode array detector (DAD 1260 VL, 190 to 950 nm), and a 100 μ L sample injection loop (overfilled

with 250 μL). Chromatographic separation was carried out using a C18 column for reverse phase chromatography (Supelcosil, 25 cm long, 4.6 mm inner diameter). The solvents used were A: 0.5 M ammonium acetate in methanol and water (85:15, v:v), B: acetonitrile and water (90:10, v:v), and C: 100 % ethyl acetate. The solvent gradient followed Brotas and Plante-Cuny method (2003) with a flow rate of 0.6 $\text{mL}\cdot\text{min}^{-1}$. Identification and calibration of the HPLC peaks was performed with chlorophyll *a*, astaxanthin, β -carotene, chlorophyll *c*, fucoxanthin and bacteriochlorophyll *a* standards. Using the Brotas and Plante-Cuny method (2003), thirty different lipophilic pigments could be detected (Table 5.2). Pigments were identified by their absorption spectra and relative retention times. Quantification was performed by repeated injections of standards over a range of dilutions to determine the relationship between peak area and standard concentrations. The relative abundance of each pigment (%) was calculated from their respective concentration ($\mu\text{g}\cdot\text{g}^{-1}$ DW).

Results

- **Depth gradient**

- *Intact polar lipids (IPLs)*

For ease of comparison between the mats, Nilemah mats will be referred to as D1 – D4, D1 being the shallowest mat (pustular mat) and D4 the deepest (microbial pavement). The total IPL concentration was highest in D1 ($362.1 \mu\text{g}\cdot\text{kg}^{-1}$ TOC) and progressively decreased with depth to D3 ($42.5 \mu\text{g}\cdot\text{kg}^{-1}$ TOC) (Figure 5.1). D4 ($222.9 \mu\text{g}\cdot\text{kg}^{-1}$ TOC) had a similar IPL concentration to D2 ($281.6 \mu\text{g}\cdot\text{kg}^{-1}$ TOC). Eight distinct IPL groups were identified across D1- D4 (Figure 5.2 and Table 5.1). Only four of these lipid groups were identified in D2, while the other mats presented six or seven different IPL groups. Ornithine lipids (OL) were highly abundant in all microbial mats ranging from 80 % in D4 and 34 % in D3. Betaine lipids (BL) were another dominant IPL group of D3 where it represented 44 % of the total IPL signal. Lesser amounts of B3 were detected in D1 and D2, respectively, but none was identified in D4. Phosphatidylcholines with DAG (PC-DAG) were present in all mats and most abundant in D2 (26 %).

Phosphatidylethanolamines with DAG (PE-DAG) were exclusive to D3. Common cyanobacterial lipids such as monoglycosyldiacylglycerols (GlyA-DAG) and glycolipid diglycosyldiacylglycerols (DGDG) (Okazaki et al., 2006) were detected in all mats except D2. Phosphatidylglycerols with DAG (PG-DAG), also potential indicators of cyanobacteria, were common to all mats and may represent the only evidence of cyanobacteria in D2. Sulfoquinovosyldiacylglycerols (SQ-DAG), another cyanobacterial marker, was additionally identified in D4.

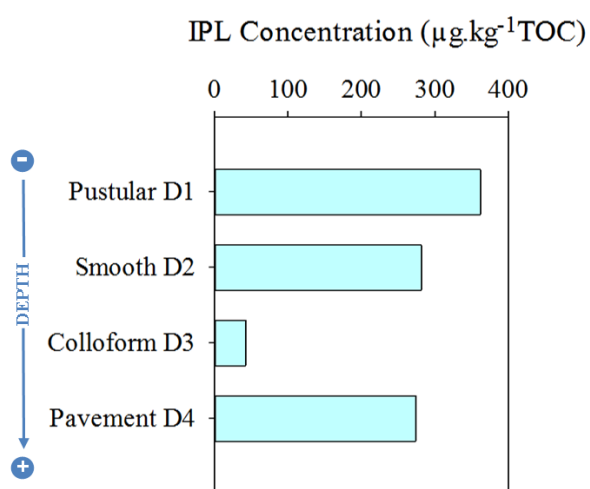


Figure 5.1: Bar chart representing the concentrations in IPL (µg.kg⁻¹of TOC) in the different types of mats from Nilemah, Hamelin Pool.

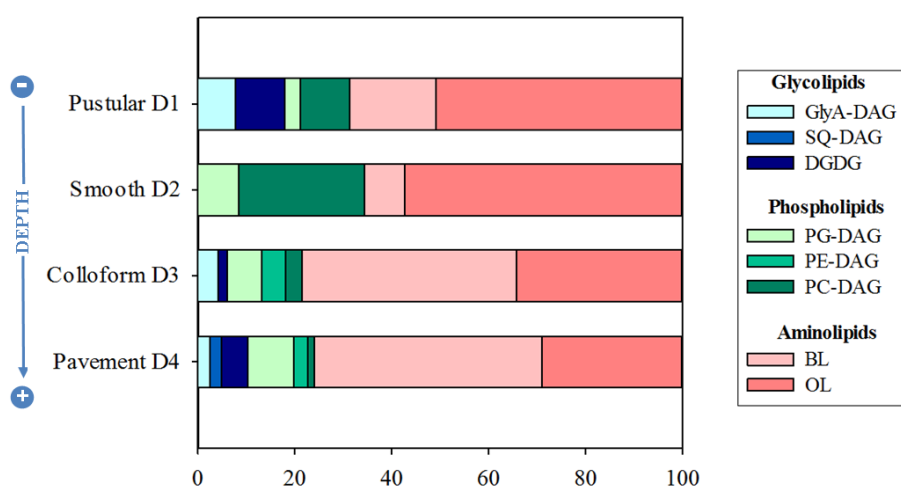


Figure 5.2: Bar chart representing the relative abundance of IPLs groups (%) in the different types of mats from Nilemah, Hamelin Pool. The arrow indicates the increase in depth.

Table 5.1: Overview of IPL detected in the mats.

Type	Class	Structure
Glycolipids	Monoglycosyl diacylglycerol (GlyA-DAG)	
	Sulfoquinovosyldiacylglycerol (SQ-DAG)	
	Digalactosyldiacylglycerol (DGDG)	
Phospholipids	Phosphatidylglycerol diacylglycerol (PG-DAG)	
	Phosphatidylethanolamine diacylglycerol (PE-DAG)	
	Phosphatidylcholine diacylglycerol (PC-DAG)	
Aminolipids	Betaine lipids (BL)	
	Ornithine lipids (OL)	

➤ *Lipophilic pigments*

D1 presented ten different pigments as shown in Figure 5.3 and Table 5.2. The most abundant being bac *a* and a chl *a*/chl *a* epimer/allomer which represented 68 % and 23.8 %, respectively, of the total pigment signal. D2 presented nine of the same pigments – just missing astaxanthin- and was also dominated by the bac *a* (60 %) and the chl *a*/chl *a* epimer/allomer (29.6 %). D3 presented ten different pigments (Figure 5.3) - and was also clearly dominated by the bac *a* (59.3 %) and the chl *a*/chl *a* epimer/allomer (31.3 %). The deepest structure (D4) presented eight different pigments – no chl *c*, β -carotene, bac *a* - and was dominated by the chl *a*/chl *a* epimer/allomer (82.6 %) and neoxanthin (10.7 %) β -carotene was detected in the three shallowest mats but not D4. Echineone was present in all mats but its abundance was slightly higher in D2 (3 %). Zeaxanthin and neoxanthin were also common to all mats, but were notably more abundant in the deeper structures (1.4 % and 10.7 %, respectively, for D4 versus 0.8 % and 1.5 % for D1). Similarly, lutein was exclusive to the deeper D3 and D4. Astaxanthin was detected in all mats except D2. Finally, chl *c* was only present in D1 and D2.

Sheath pigment was also detected in all mats, but could not be quantified since no standards were available. Nevertheless, a semi-quantitative comparison of the peak area for this pigment showed a very high abundance in the shallowest structures (peak area = 358.4 for D1, 51.3 for the D2, 2.2 for the D3 and 33.6 for D4).

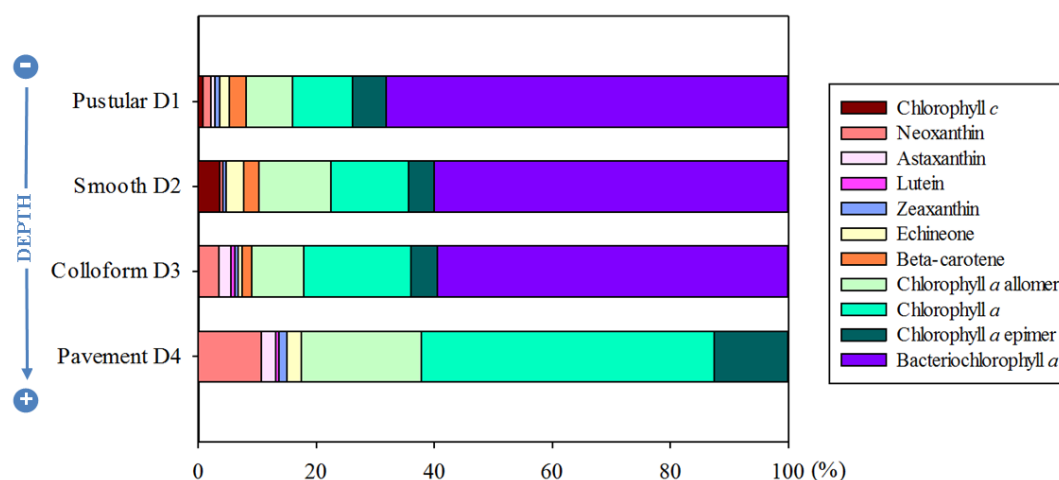


Figure 5.3: Bar chart representing the relative abundance of lipophilic pigments (%) in the different types of mats from Nilemah, Hamelin Pool.

Table 5.2: Summary of pigments that could be identified with the HPLC method used in this study and their taxonomic affinities (compiled from Jeffrey et al., 1997; Leavitt and Hodgson, 2001) and relative abundances of the pigments (%) identified in the different Nilemah mats. N.b. the % of chl *a*, chl *a* epimer and chl *a* allomer were combined.

Pigment	Source organisms or processes	Pustular D1	Smooth D2	Colloform D3	Pavement D4
Chlorophylls/Bacteriochlorophyll					
Chlorophyll <i>a</i> , epimer and allomer	Photosynthetic algae, higher plants	23.8 %	29.6 %	31.3 %	82.6 %
Chlorophyll <i>b</i> , divinyl-chl <i>b</i>	Green algae, higher plants, euglenophytes	-	-	-	-
Chlorophylls <i>c</i>	Diatoms, Dinoflagellates, Chrysophytes, Primmnesiophytes	1.0 %	3.8 %	-	-
Bacteriochlorophyll <i>a</i>	Purple phototrophic bacteria	68.1 %	60.0 %	59.3 %	-
Carotenoids					
β - carotene	Algae and plants	2.9 %	2.6 %	1.9 %	-
α -carotene	Cryptophytes, Prochlorophytes, Rhodophytes	-	-	-	-
Alloxanthin	Cryptophytes	-	-	-	-
Fucoxanthin, fucoxanthin-like	Diatoms, Primmnesiophytes, Chrysophytes, Dinoflagellates	-	-	-	-
Diadinoxanthin	Diatoms, Primmnesiophytes, Chrysophytes, Dinoflagellates	-	-	-	-
Dinoxanthin	Diatoms, Chrysophytes, Dinoflagellates	-	-	-	-
Diatoxanthin	Diatoms, Chrysophytes, Dinoflagellates	-	-	-	-
Mg-DVP	Diatoms, Dinoflagellates, Chrysophytes, Primmnesiophytes	-	-	-	-
Peridinin, peridinin isomer	Dinoflagellates	-	-	-	-
Zeaxanthin	Cyanobacteria, Chlorophytes, Prochlorophytes	0.8 %	0.5 %	0.6 %	1.4 %
Myxoxanthophyll	Colonial cyanobacteria	-	-	-	-
Echineone	Cyanobacteria	1.5 %	3.0 %	0.7 %	2.3 %
Lutein, dihydrolutein	Green algae, higher plants	-	-	0.8 %	0.6 %
Neoxanthin	Green algae, higher plants	1.4 %	0.5 %	3.4 %	10.7 %
Violaxanthin	Green algae, higher plants	-	-	-	-
Astaxanthin	Meiofaunal crustacean	0.5 %	-	2.0 %	2.4 %
Prasinolaxanthin	Algae	-	-	-	-
Lycopene	Anoxygenic phototrophic bacteria or algae (<i>Botryococcus braunii</i>)	-	-	-	-
Chlorophyll degradation products					
Pheophytin <i>a</i>	Chl <i>a</i> derivative	-	-	-	-
Pheophorbide <i>a</i>	Grazing, senescent diatoms	-	-	-	-

- **Salinity gradient**

- *Intact polar lipids (IPLs)*

The smooth mats from the different sites will be referred to as S1 for the lowest salinity (Rocky Point) to S3 with greatest salinity (Nilemah). S2 presented a much higher concentration of IPLs ($2404.1 \mu\text{g.kg}^{-1}$ TOC) than S3 ($281.6 \mu\text{g.kg}^{-1}$ TOC) and S1 ($96.3 \mu\text{g.kg}^{-1}$ TOC) (Figure 5.4). Although the least saline S1 mat presented the lowest concentration in IPL, it also showed the highest diversity of IPL suggesting higher organism diversity (Figure 5.5 and Table 5.1). The lower diversity apparent in the hypersaline may reflect the fewer number of organisms able to survive this harsher environment. OL dominated the IPL composition of all three smooth mats, particularly S2 (62 %). BL was the second most abundant group in S2 (9 %) and S1 (29 %) and also significant in S3 (8 %). PC-DAG, was highly abundant in S3 (26 %), but present in much lower abundance (4 %) in S1 and absent in S2 suggesting a low proportion of alpha and gammaproteobacteria in these higher salinity mats (Sohlenkamp et al., 2003). But PE-DAG, usually associated with alpha, gamma- or deltaproteobacteria (Zhang and Rock, 2008) were only present in the hypersaline S1 (4 %). SQ-DAG and GlyA-DAG were present in both S1 and S2, but absent in S3. PG-DAG, reported in many sources of bacteria including photosynthetic bacteria (Wada and Murata, 2007) were present in S3 and S1 but were absent in S2. PG-DAG was the only cyanobacterial marker in S3. DGDG was not detected in any of the three smooth mats.

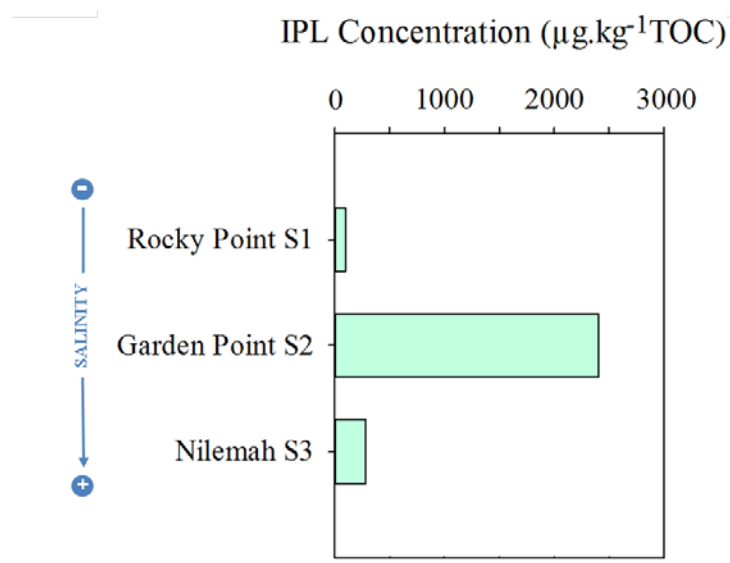


Figure 5.4: Bar chart representing the concentrations in IPL ($\mu\text{g.kg}^{-1}$ of TOC) in the smooth mats from the different Shark Bay sites.

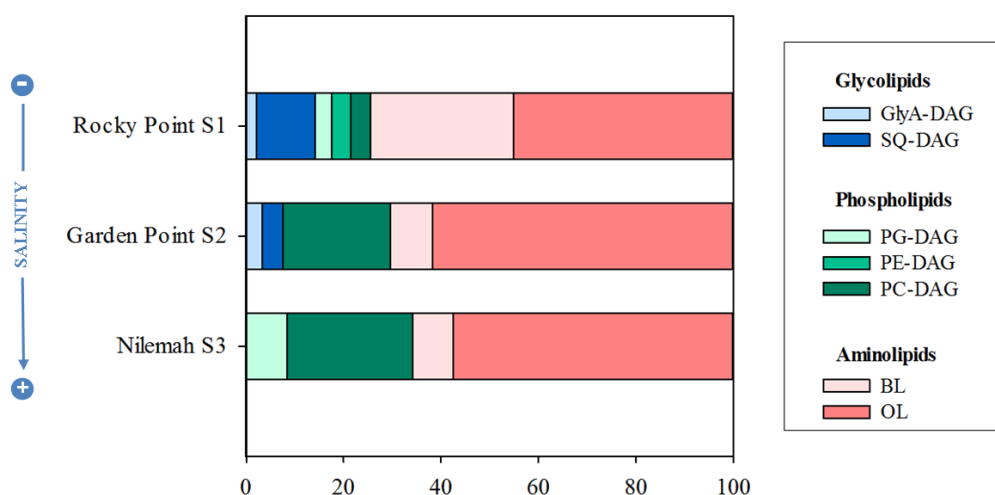


Figure 5.5: Bar chart representing the relative abundance of IPLs groups (%) in the smooth mats from the different Shark Bay sites. The arrow indicates the increase in salinity.

➤ *Lipophilic pigments*

The pigment distributions of S1 and S2 were generally similar to S3, but although some subtle differences were detected. Eight pigments were detected in S1 which was clearly dominated by the bac *a* (70.8 %) and with chl *a*/chl *a* epimer/allomer (8.6 %) the next most abundant pigment (Figure 5.6). S2 presented nine pigments and its distribution was also dominated by the bac *a* (70.8 %) and the chl *a*/chl *a* epimer/allomer (24.8 %). S3 also presented nine pigments including a major bac *a* (60 %) and significant chl *a*/chl *a* epimer/allomer (29.6 %). Neoxanthin showed a slightly higher abundance in the least saline S1 mat, whilst β -carotene, echineone and zeaxanthin showed a slight increase in abundance with rising salinity. Astaxanthin was only detected in S2 and chl *c* was exclusively present in S3.

The sheath pigment (not absolutely quantified) was of higher relative abundance in S2 (peak area = 227.6) than in S3 (51.3), and not detected in S1.

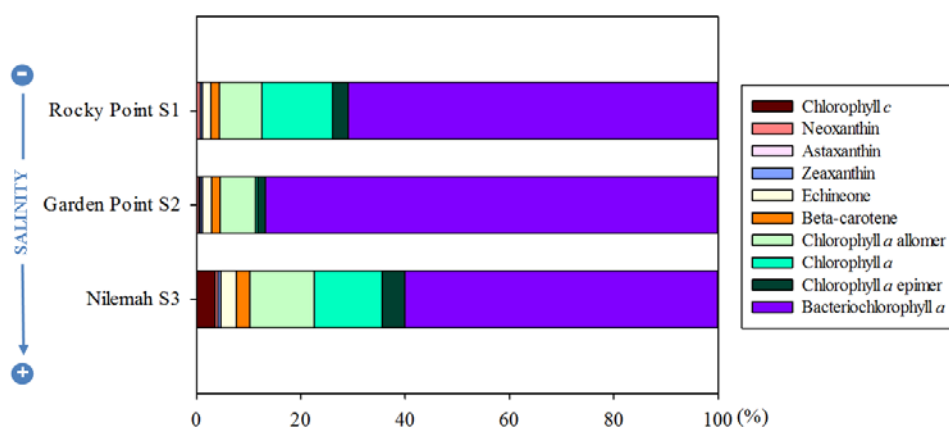


Figure 5.6: Bar chart representing the relative abundance of lipophilic pigments (%) in the smooth mats from the different Shark Bay sites. The arrow indicates the increase in salinity.

Discussion

- **Depth gradient**

- *Common features for all mats*

All Nilemah mats showed the same major microbial communities. The consistent presence of zeaxanthin - highly abundant in most cyanobacteria - and echineone - frequently described as a specific cyanobacterial marker although it is not present in some species including *Phormidium percinium*, *Phormidium ectocarpi* and *Phormidium valderianum* (Hertzberg et al., 1971) - highlighted the ubiquity of cyanobacteria (Figure 5.3). Chl *a*, chl *a* epimer and allomer were additionally detected in high relative abundance in all mats. These are diagnostic pigments of photosynthetic organisms and confirm the relatively high abundance of cyanobacteria in all mats. Chl *a*, β -carotene, zeaxanthin and echineone were previously reported as dominant pigments in microbial mats from solar saltern systems (Boon et al., 1983; Barbe et al., 1990; Grimalt et al., 1992; Villanueva et al., 1994). Myxoxanthophyll, a characteristic marker of colonial and filamentous cyanobacteria (Hertzberg et al., 1971; Leavitt, 1993), however, was not detected in any of the mats. Common cyanobacterial IPL such as GlyA-DAG and DGDG (Okazaki et al., 2006) were present in all mats except D2 (Figure 5.2) and SQ-DAG was detected in D4. PG-DAGs, previously identified in all photosynthetic membranes (Wada and Murata, 1998), were present in all mats and were the only potential IPL markers of cyanobacteria detected in D2. Consequently, it is possible that the lowest diversity in cyanobacterial IPLs reflects a lower diversity of cyanobacterial species in this mat.

OL were detected in all mats (Figure 5.2). These lipids seem exclusive to bacteria with no previous detection in eukarya or archaea (López-Lara et al., 2003). They have been identified in a sulfate-reducing bacteria (SRB) *Desulfovibrio* strain (Makula and Finnerty, 1975) and in sulfur-oxidising bacteria (Shively and Knoche, 1969), so may be generally associated with sulfur-cycling bacteria. Their detection in all Nilemah mats suggested the common occurrence of sulfur-cycling organisms.

BL were also detected in all mats (Figure 5.2). These lipids may indicate a lower plant input (Sato, 1992). Significant aeolian input has been reported in Shark Bay mats (Allen et al., 2010; Jahnert and Collins, 2013), however, their much higher abundance in D3 compared to D2 (i.e, shallower) is not consistent with this source. Further, diatoms were mainly found in the shallower D1 and D2 mats (Chapter 4) which suggests the higher D3 abundance of BLs were not likely due to marine algae. Several BL have been previously associated with phosphate-limited alphaproteobacteria (Geiger et al., 1999; 2010; Edgcomb et al., 2013a). In Shark Bay water, phosphorus is in limited supply whereas nitrogen fixation produces sufficient nitrogen (Smith and Atkinson, 1983). Total phosphorus concentrations as low as $0.007 \text{ mmol.g}^{-1}$ have been reported in Shark Bay sediments. The present study on smooth mats from Nilemah (Chapter 3) reported porewater phosphate concentrations reaching maximum levels of $1.3 \text{ }\mu\text{M}$ during the day and $2.2 \text{ }\mu\text{M}$ at night. These values are relatively low in comparison with the concentrations of porewater phosphate in other hypersaline microbial mats (e.g. maximum value of $11.1 \text{ }\mu\text{M}$ in a microbial mat from Lake Chiprana, Spain; Ludwig et al., 2006), suggesting that phosphate-limited alphaproteobacteria could have been present in the mats.

Neoxanthin was also detected in all mats, suggesting the common presence of green algae in all structures (Mueller et al., 2005; Fernandez-Valiente et al., 2007).

➤ *Changes along the littoral gradient*

Small differences in the community composition of the mat were also observed along the littoral gradient. *Bac a* identified in all mats except D4 was characteristic of purple phototrophic bacteria (Schmidt, 1979). Its concentration was much higher in the shallower structures and gradually decreased with depth ($50.8 \text{ }\mu\text{g.g}^{-1}\text{DW}$ in D1 to $14.3 \text{ }\mu\text{g.g}^{-1}\text{DW}$ in D3) (Figure 5.7) reflecting a decrease in the relative abundance of purple phototrophic bacteria with depth. The D1 concentration of *bac a* ($50.8 \text{ }\mu\text{g.g}^{-1}\text{DW}$) was generally similar to concentrations

measured in microbial mats from other hypersaline settings including Mediterranean microbial mats ($44 \mu\text{g}\cdot\text{g}^{-1}$; Caumette et al., 1994) and solar slattern microbial mats ($77 \mu\text{g}\cdot\text{g}^{-1}$; Villanueva et al., 1994). Higher bac *a* concentrations (up to $600 \mu\text{g}\cdot\text{g}^{-1}$), however, have been reported in South Pacific microbial mats (Mao Che et al., 2001).

Furthermore, chl *c* was only detected in D1 and D2 (Figure 5.3), with respective concentration of 0.4 and $1.6 \mu\text{g}\cdot\text{g}^{-1}\text{DW}$. This pigment can derive from Bacillariophyta (diatoms), Chrysophyta, Prymnesiophyta and Phaeophyta (Goodwin, 1980). It was previously identified in Shark Bay mats and has been associated with the presence of diatoms (Palmisano et al., 1989) which are common to Shark Bay mats (Palmisano et al., 1989; Allen et al., 2010; Jahnert and Collins, 2013; Edgcomb et al., 2013b; Chapter 4). The present study of the biolipid composition of these microbial mats also suggested diatoms were most abundant in the shallower mats (D1 and D2) (Chapter 4). Consequently, the distribution of chl *c* observed herein seems concordant with the greater abundance of diatoms in the shallowest structures. A previous study on Antarctic microbial mats also correlated diatom abundances of microbial mats with water depth and showed the highest species diversity in the shallower mats (Sabbe et al., 2004).

Sheath pigments were detected in all mats, however, was in highest relative abundance in the two shallowest mats (peak area = 358.4 and 51.4 for D1 and D2), although D4 (peak area = 33.6) showed a higher abundance than D3 (peak area = 2.2). Sheath pigments can derive from cyanobacteria and scytonemin (Nageli, 1849). For instance, they have been reported in more than 30 cyanobacteria species (Garcia-Pinchel and Castenholz, 1991), and were present in the top layers of cyanobacterial mats due to production from an adaptive photoprotection strategy against solar irradiance (mainly UV-A, 320-400 nm) (Garcia-Pinchel and Castenholz, 1991). Sheath pigments were also previously reported in Shark Bay microbial mats (Palmisano et al., 1989) that are exposed to surface irradiance that can reach $2000 \mu\text{E}\cdot\text{m}^{-2}\cdot\text{s}^{-1}$ (Bauld, 1984). The different mats were found at different

water depths. Intertidal pustular D1 mats have been reported between 0.20 and 0.80 m of water depth, the subtidal laminated smooth D2 mat between 0.80 and 1.20 m and the colloform D3 mats between 1 and 1.50 m (Jahnert and Collins, 2013). The microbial pavement D4 was found at depths greater than 1.50 m. The higher relative abundance of the sheath pigment in the shallower mats would be consistent with a need for greater photoprotection in shallower structures, more exposed to high irradiance.

Astaxanthin, characteristic of meiofaunal crustaceans (Burford et al., 1994) was detected in all mats, except for D2 (Figure 5.3). The absence of meiofaunal crustaceans in D2, however, was likely more related to the structure of the mats than the water depth. Indeed the morphologies differed, with D2 having a highly laminated cohesive structure while the other mats, particularly the deeper ones, presented an irregular clotted or wavy fabric composed of shell fragments and peloids (Jahnert and Collins, 2013).

Although markers of green sulfur bacteria were identified in very low abundance in a Garden Point mat (Chapter 6), the method used here did not allow the identification of bac *c*, *d*, *e* or isorenieretene, indicative of green phototrophic bacteria, including *Chlorobiaceae* (Caple et al., 1978) and multicellular green filamentous bacteria (Pierson and Castenholz, 1971).

➤ *Changes in Hamelin Pool microbial mat communities through time*

A previous analysis of lipophilic pigments from microbial mats present in Hamelin Pool was conducted in 1989 by Palmisano et al. Pigments from pustular, tufted, smooth and colloform mats were investigated. A comparison of pigment distributions in D1, D2 and D3 between this study and the 1989 study is presented in Table 5.3. The 1989 study revealed a predominance of cyanobacterial lipophilic pigments in the shallow mats (D1 and D2) and a predominance of diatom pigments in the deeper ones (D3). D1 previously showed the presence of canthaxanthin,

marker of cyanobacteria, that was not detected herein (Palmisano et al., 1989). In addition, the pigments chl *c*, neoxanthin, astaxanthin and lutein detected here were not previously reported in this mat. Similar to the 1989 study, the pigment distribution from this study also highlighted a high contribution from cyanobacteria, however, the presence of lutein and neoxanthin suggested a higher input from higher plants or green algae to the mat. In addition, the presence of chl *c* suggested the presence of diatoms that were not previously identified in this mat. The comparison of the pigment distribution in the smooth D2 mats showed that myxoxanthophyll was only detected in the previous study while chl *c*, neoxanthin and echineone were exclusively detected in this study. Similarly to D1, this suggested a higher input from higher plants/green algae and the presence of diatoms in the mat. In addition, the concentration in chl *a* and β -carotene were much higher in the 1989 study (46.9 and 22 $\mu\text{g}\cdot\text{g}^{-1}\text{DW}$ on average, respectively) than in this study (5.6 and 1.1 $\mu\text{g}\cdot\text{g}^{-1}\text{DW}$, respectively) (Figure 5.7). The pigment distributions in the colloform D3 mats presented the highest discrepancy. Specific markers of diatoms such as chl *c*, fucoxanthin, diadinoxanthin and diatoxanthin were detected in colloform D3 mats from the previous study while neoxanthin, astaxanthin, lutein, zeaxanthin and sheath pigment were only found in this study. These results suggested significant changes in the microbial communities of the D3. Bac *a* was present in the D1, D2 and D3, however, no other characteristic pigments for purple phototrophic bacteria such as spirilloxanthin or rhodopsin (Schmidt, 1979) were identified in both studies. Comparison of the concentrations in bac *a* showed that much higher abundance of this pigment was found in this study (Figure 5.7). Maximum bac *a* concentrations previously reported reached 0.2 $\mu\text{g}\cdot\text{g}^{-1}\text{DW}$ versus 50.8 $\mu\text{g}\cdot\text{g}^{-1}\text{DW}$ in this study for D1, 22.0 $\mu\text{g}\cdot\text{g}^{-1}\text{DW}$ versus 25.8 $\mu\text{g}\cdot\text{g}^{-1}\text{DW}$ for D2 and 2.0 $\mu\text{g}\cdot\text{g}^{-1}\text{DW}$ versus 14.3 $\mu\text{g}\cdot\text{g}^{-1}\text{DW}$ for D3. Sheath pigments were previously identified in D1 and D2 but not in D3.

Table 5.3: Comparison of lipophilic pigments identified in the different types of mats from Hamelin Pool from this study and the previous study by Palmisano et al. (1989). X indicates that the pigment was present.

Pigments	Pustular mat		Smooth mat		Colloform mat		Pavement
	Present study	1989 study	Present study	1989 study	Present study	1989 study	Present study
Chlorophyll <i>c</i>	X		X			X	
Fucoxanthin						X	
Neoxanthin	X		X		X		X
Astaxanthin	X				X		X
Myxoxanthophyll				X			
Diadinoxanthin						X	
Diatoxanthin						X	
Lutein	X				X		
Zeaxanthin	X	X	X	X	X		X
Echineone	X	X	X		X		X
β -carotene	X	X	X	X	X	X	
Chlorophyll <i>a</i>	X	X	X	X	X	X	X
UV pigment	X	X	X	X	X		X
Bacteriochlorophyll <i>a</i>	X	X	X	X	X	X	

Pigment concentrations ($\mu\text{g}\cdot\text{g}^{-1}$ DW)

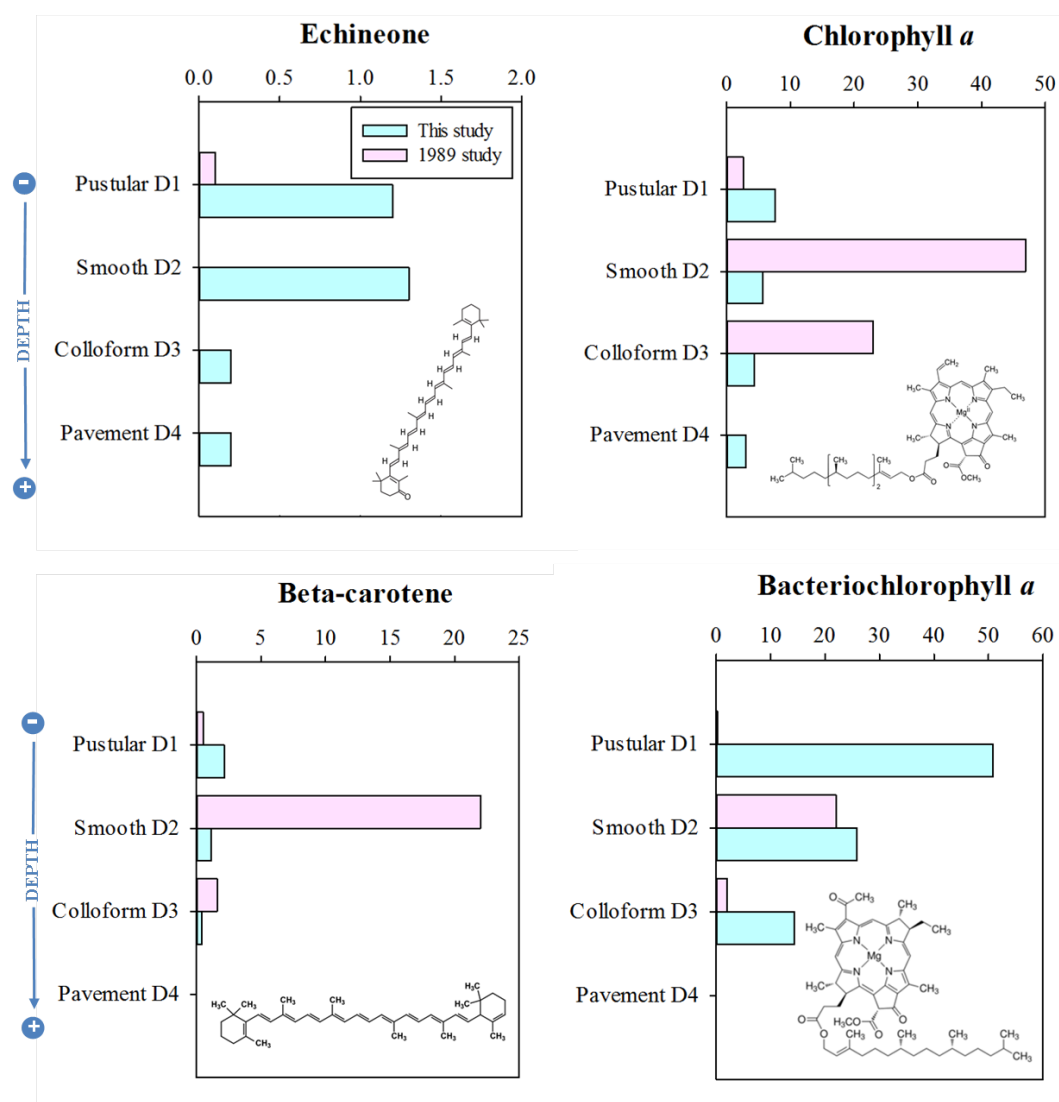


Figure 5.7: Bar chart representing the concentration in echineone, chlorophyll *a*, β -carotene and bacteriochlorophyll *a* in the different types of mats from Hamelin Pool from this study (blue bars) and the previous study by Palmisano et al. (1989) (pink bars).

This comparison of both studies highlighted potential changes in microbial communities of the different types of mats. Based on the presence of chl *c* in D1 and D2, diatoms seem to be now present in microbial mats that were previously referred to as “cyanobacterial mats”, as opposed to D3 that was described as a “diatom mat”. In addition, a higher contribution from higher plants or green algae, based on the presence of lutein and neoxanthin, was detected in this study. Surprisingly, in this study, no diatom marker was detected in D3. These results actually suggested a higher abundance of cyanobacteria to D3 and no significant diatom contribution. The clear increase in bac *a* concentration in D1 and D3 mats suggested an increase in the abundance of purple phototrophic bacteria through time. In addition, the detection of sheath pigment in D3 in this study as opposed to the previous study, possibly suggests a lower relative abundance of carotenoids that were previously playing a role in the photoprotection of the mat (Palmisano et al., 1989) or a higher need for UV-protection. These significant changes in microbial communities through time were highly unexpected. Changes in microbial mat communities have been observed in microbial mats exposed to physical and chemical disturbance (Ferris et al., 1997; Abed et al., 2002). In addition, environmental factors such as temperature or sulfide concentrations can strongly influence microbial mats communities (Skirnisdottir et al., 2000). Nutrient concentrations can also strongly affect microbial community structure, particularly the relative abundance of cyanobacteria and diatoms. Pinckney et al. (1995) showed that addition of N and P in a microbial mat resulted in an increase in the relative abundance of diatoms whereas addition of P only led to an increase in the abundance of cyanobacteria. N addition, however, did not seem to favour one community over the other. In addition, at a large scale, climate variations can also affect microbial communities, as observed in the Arctic microbial ecosystems (Vincent, 2010). Another possible reason for such a high difference in communities’ distributions could be explained by the sampling site location. In this study, microbial mats were sampled in the southern part of Hamelin Pool (Nilemah S3 tidal flat) whereas microbial mats described in the Palmisano et al. (1989) study were mainly sampled in the eastern part of the Bay. However, two sites described in the 1989 study (1 and 4) were located only a few km away from our sampling site, possibly suggesting a high diversity in microbial communities from the same type

of mats within very close vicinity. However, no major difference in the pigment distribution of similar mat types from the different sampled sites was previously reported by Palmisano et al. (1989). Further investigations would be required to fully understand the reasons of these potential changes in microbial mat communities through time, however, this comparison highlighted potential changes in the Hamelin Pool environment through time, affecting the structure of modern mats.

- **Salinity gradient**

Microbial microbial from the different sites showed consistent presence of cyanobacterial markers such as zeaxanthin and echineone (Figure 5.6). In addition, the presence of chl *a* epimer and allomer and chl *a* confirmed a photosynthetic activity in all mats. However, SQ-DAG and GlyA-DAG were present in both S1 and S2, while PG-DAG was the only cyanobacterial marker in S3 (Figure 5.5). This possibly suggested a lower diversity or a different community of cyanobacteria in the most saline mat, however, the previous comparison with other microbial mats from S3 (see above) actually suggested that this specific IPL distribution might only be related to this smooth mat and not directly associated with higher salinity.

OL were present in all mats, however, a higher abundance was detected in S2 (Figure 5.5). The higher abundance of OL in S2 strongly suggested a high abundance of sulfur-cycling organisms (Shively and Knoche, 1969; Makula and Finnerty, 1975). In addition, the concentration in bac *a* was much more abundant in S2 (85.8 $\mu\text{g}\cdot\text{g}^{-1}\text{DW}$) than in S3 and S1 (25.8 $\mu\text{g}\cdot\text{g}^{-1}\text{DW}$ and 13.8 $\mu\text{g}\cdot\text{g}^{-1}\text{DW}$, respectively) (Figure 5.8). This high abundance in bac *a* is concordant with previous analysis on smooth mats from S2 in which 16s *rRNA* analysis on the mats revealed a strong predominance of purple-sulfur bacteria (Chapter 6) and with the high abundance of PLFAs from sulfur-cycling organisms in this mat (Chapter 4).

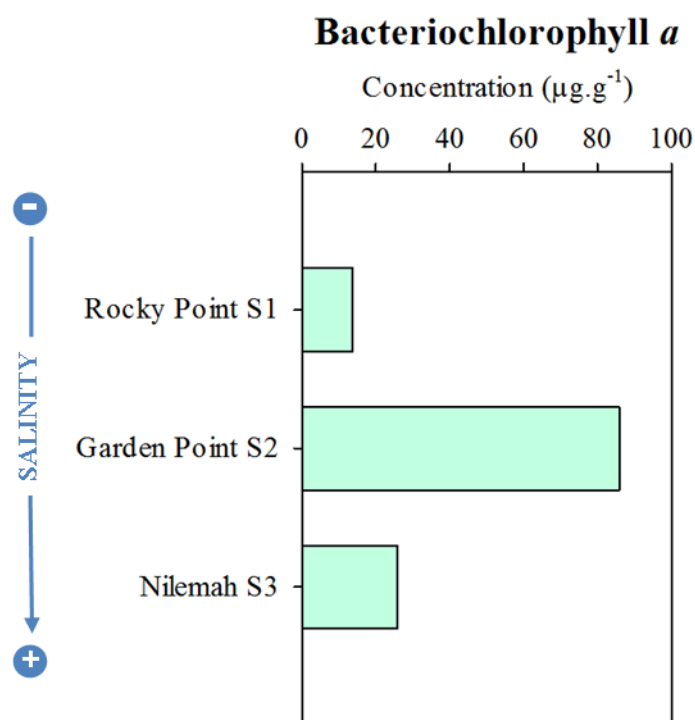


Figure 5.8: Bar chart representing the concentration in bacteriochlorophyll *a* in the smooth mats from the different Shark Bay sites.

BL were relatively abundant in all mats (Figure 5.5). It has been suggested that high abundances in BL in microbial mats could indicate an adaptation to environmental stress, such as hypersalinity (Bühning et al., 2009). However, in this case, the relative concentration in BL gradually increased with decreasing salinity. Lower and higher plants are a possible source of BL (Dembitsky, 1996). However, a study of hydrocarbon composition of the three smooth mats revealed an absence of odd over even carbon-numbered *n*-alkanes, typical higher plant biomarkers (Eglinton and Hamilton, 1967) in S1 (Chapter 4). As BL were relatively more abundant in S1 (29 %) and no typical plants biomarkers were detected in this mat, it is likely that BL actually derived from phosphate-limited alphaproteobacteria that might have been more abundant in the least saline sites, possibly due to a higher availability in phosphate in more saline sites.

Another difference observed the salinity gradient was related to the abundance of chl *c* (Figure 5.6). S3 was the only mat showing the presence of this pigment, suggesting the presence of diatoms in the most saline mat only. These results are concordant with previous analysis of hydrocarbons and phospho-lipid fatty acids on all three mats that revealed a higher abundance of diatoms in the most saline setting (S3) (Chapter 4).

Finally, no sheath pigment was detected in the least saline structure (S1). Based on the relative abundance and diversity of carotenoids in this mat, it is unlikely that carotenoids were playing a significant role in photoprotection for this mat. Consequently, it is possible that S1 only contained cyanobacterial species less capable of sheath pigment production or that this less saline mat presented a lower need for photoprotection.

Conclusions

This study of IPL and pigment composition of microbial mats can complement more traditional biolipid and isotopic analysis (e.g., Chapter 4). The present application of these analyses to Shark Bay mats has extended our understanding of the controls of water depth and salinity on compositional structure of microbial mat communities. By comparison to previous studies – in this instance, a similar study over two decades earlier, microbial dynamics over long timeframes (e.g., capturing notable changes in climate) can be additionally monitored.

The IPL and lipophilic pigments composition of Nilemah mats along the littoral gradient highlighted the presence of sulfur-cycling organisms, possibly phosphate-limited alphaproteobacteria and cyanobacteria in all mats, although D2 presented a much lower diversity of cyanobacterial derived IPLs - suggesting a lower diversity of cyanobacterial species unrelated to water depth. Subtle differences observed between the four mats suggested that water depth can influence microbial mats communities. The concentration in bac *a*, for instance,

decreased with depth, highlighting a decrease in purple phototrophic bacteria with depth. Chl *c* was only detected in D1 and D2, indicating a higher abundance of diatoms in the shallower mats. D2 also corresponds to S3 of the salinity study. Contrary to the occurrence of chl *c* in S3, it was not detected in S1 or S2 reflecting the association with diatoms and the most saline site – both depth and salinity controls on diatoms were consistent with those reported in [Chapter 4](#). The highest diversity of IPL was found in the least saline mat (S1) suggesting that hypersalinity reduces microbial diversity by being selective to organisms capable of surviving the harsher salinity environments. Cyanobacteria were present in all mats, although a lower diversity of cyanobacterial IPLs was detected in the most saline mat S3. A decrease in BL, possibly deriving from phosphate-limited alphaproteobacteria, was observed with an increase in salinity, suggesting greater phosphate limitation with decreased salinity, although porewater phosphate measurements in S1 and S2 would be required to confirm this. A much higher abundance of purple phototrophic bacteria in S2 mat seemed unrelated to salinity, but might be influenced by the very calm waters of Garden Point which support the development of thick microbial mat layers (Jahnert and Collins, 2013). The present distributions of lipophilic pigments showed several differences to those reported by Palmisano et al. (1989). Presently, diatoms seem isolated to the shallower mats and cyanobacteria are abundant in D3, whereas some 20 years ago diatoms were highly abundant in D3 and absent from the shallower mats. Furthermore, purple phototrophic bacteria seemed to have intensified over this time frame. Physical, chemical or biogeochemical factors can influence microbial dynamics (Pinckney et al., 1995; Ferris et al., 1997; Skirnisdottir et al., 2000; Abed et al., 2002; Vincent, 2010) and a more dedicated study would be required to fully understand the cause of the changes in microbial structure identified here to have occurred in recent times. In addition, long-term monitoring of different Shark Bay sites would also be recommended as an extension to the present study and to observe how changes in salinity levels at specific sites affects mats communities.

Acknowledgements

This research was supported by a grant from the Australian Research Council's Discovery Projects scheme (2010-2013, Grice, Greenwood, Snape and Summons). AP thanks WA-Organic and Isotope Geochemistry Centre, Curtin University and CSIRO for top-up scholarship. Dr Julius Lipp is thanked for his help with IPL analysis. Prof. Kai-Uwe Hinrichs is thanked for providing access to the Hinrichs laboratory (University of Bremen).

References

- Abed R. M. M., Safi N. M. D., Köster J., de Beer D., El-Nahhal Y., Rullkötter J., Beer D. De and Garcia-pichel F.** (2002) Microbial diversity of a heavily polluted microbial mat and its community changes following degradation of petroleum compounds. *Appl. Environ. Microbiol.* **68**, 1674–1683.
- Allen M. A., Neilan B. A., Burns B. P., Jahnke L. L. and Summons R. E.** (2010) Lipid biomarkers in Hamelin Pool microbial mats and stromatolites. *Org. Geochem.* **41**, 1207–1218.
- Allwood A. C., Walter M. R., Kamber B. S., Marshall C. P. and Burch I. W.** (2006) Stromatolite reef from the Early Archaean era of Australia. *Nature* **441**, 714–718.
- Bauld J.** (1984) Microbial mats in marginal marine environments: Shark Bay, Western Australia. In *Microbial mats: Stromatolites*. (eds. Y. Cohen, R.W. Castenholz, H.O. Halvorson). Alan R. Liss, New York, pp 39-58.
- Boon J. J., Hines H., Burlingame A. L., Klok J., Rijpastra W. I. C., de Leeuw J. W., Edmonds K. E. and Eglinton G.** (1983) Organic geochemical studies of Solar Lake laminated cyanobacterial mats. In *Advances in Organic Geochemistry*. (eds. M. Bjoroy, C. Albrecht, C. Cornford et al.). John Willey & Sons, Chichester, pp 207-227.
- Bühring S. I., Smittenberg R. H., Sachse D., Lipp J. S., Golubic S., Sachs J. P., Hinrichs K.-U. and Summons R. E.** (2009) A hypersaline microbial mat from the Pacific Atoll Kiritimati: insights into composition and carbon fixation using biomarker analyses and a ¹³C-labeling approach. *Geobiology* **7**, 308–323.
- Burford M. A., Long B. G. and Rothlisberg P. C.** (1994) Sedimentary pigments and organic carbon in relation to microalgal and benthic faunal abundance in the Gulf of Carpentaria. *Mar. Ecol. Prog. Ser.* **103**, 111–117.

- Brotas V. and Plante-Cuny M.-R.** (2003) The use of HPLC pigment analysis to study microphytobenthos communities. *Acta Oecologica* **24**, S109–S115
- Caple M. B., Chow H. and Strouse C. E.** (1978) Photosynthetic pigments of green sulfur bacteria. The esterifying alcohols of bacteriochlorophylls *c* from *Chlorobium limicola*. *J. Biol. Chem.* **253**, 6730–6737.
- Caumette P., Matheron T., Raymond N. and Relexans J.-C.** (1994) Microbial mats in the hypersaline ponds of Mediterranean salterns (Salins-de-Giraud, France). *FEMS Microbiol. Ecol.* **13**, 273–286.
- Dembitsky V. M.** (1996) Betaine ether-linked glycerolipids: chemistry and biology. *Prog. Lipid Res.* **35**, 1–51.
- Edgcomb V. P., Bernhard J. M., Beaudoin D., Pruss S. B., Welander P. V., Schubotz F., Mehay S., Gillespie A. L. and Summons R. E.** (2013a) Molecular indicators of microbial diversity in oolitic sands of Highborne Cay, Bahamas. *Geobiology* **11**, 234–251.
- Eglinton G. and Hamilton R. J.** (1967) Leaf Epicuticular waxes. *Science* **156**, 1322–1335.
- Ferris M. J., Nold S. C., Revsbech N. P. and Ward D. M.** (1997) Population structure and physiological changes within a hot spring microbial mat community following disturbance. *Appl. Envir. Microbiol.* **63**, 1367–1374.
- Fourçans A., de Oteyza T. G., Wieland a, Solé A., Diestra E., van Bleijswijk J., Grimalt J. O., Kühl M., Esteve I., Muyzer G., Caumette P. and Duran R.** (2004) Characterization of functional bacterial groups in a hypersaline microbial mat community (Salins-de-Giraud, Camargue, France). *FEMS Microbiol. Ecol.* **51**, 55–70.
- Garcia-Pinchel F. and Castenholz R. W.** (1991) Characterization and biological implications of scytonemin, a cyanobacterial sheath pigment. *J. Phycol.* **27**, 395–409.
- Geiger O., Rohrs V., Weissenmayer B., Finan T. M. and Thomas-Oates J. E.** (1999) The regulator gene *phoB* mediates phosphate stress-controlled synthesis of the membrane lipid diacylglyceryl-N,N,N-trimethylhomoserine in *Rhizobium* (*Sinorhizobium*) *meliloti*. *Mol. Microbiol.* **32**, 63–73.
- Geiger O., González-Silva N., López-Lara I. M. and Sohlenkamp C.** (2010) Amino acid-containing membrane lipids in bacteria. *Prog. Lipid Res.* **49**, 46–60.
- Golubic S. and Hoffman H. J.** (1976) Comparison of Holocene and Mid-Precambrian Entophysalidaceae (Cyanophyta) in stromatolitic algal mats: cell division and degradation. *J. Paleontol.* **50**, 1074–1082.

- Goodwin T. W.** (1980) *The Biochemistry of the Carotenoids. Volume 2. Animals.* Chapman and Hall. New York.
- Grimalt J. O., de Wit R., Teixidor P. and Albaigés J.** (1992) Lipid biogeochemistry of Phormidium and Microcoleus mats. *Org. Geochem.* **19**, 509–530.
- Grotzinger J. P. and Knoll A. H.** (1999) Stromatolites in Precambrian carbonates: evolutionary mileposts or environmental dipsticks? *Annu. Rev. Earth Planet. Sci.* **27**, 313–358.
- Hertzberg S., Liaaen-Jensen S. and Siegelman H. W.** (1971) The carotenoids of blue-green algae. *Phytochemistry* **10**, 3121–3127.
- Hoehler T. M., Bebout B. M. and Des Marais D. J.** (2001) The role of microbial mats in the production of reduced gases on the early Earth. *Nature* **412**, 324–327.
- Jahnert R. and Collins L.** (2011) Significance of subtidal microbial deposits in Shark Bay, Australia. *Mar. Geol.* **286**, 106–111.
- Jahnert R. and Collins L.** (2012) Characteristics, distribution and morphogenesis of subtidal microbial systems in Shark Bay, Australia. *Mar. Geol.* **303-306**, 115–136.
- Jahnert R. and Collins L.** (2013) Controls on microbial activity and tidal flat evolution in Shark Bay, Western Australia. *Sedimentology* **60**, 1071–1099.
- Jeffrey S. W., Mantoura R. F. C. and Wright S. W.** (1997) *Phytoplankton pigments in oceanography.* UNESCO Publishing.
- Leavitt P. R.** (1993) A review of factors that regulate carotenoid and chlorophyll deposition and fossil pigment abundance. *J. Paleolimnol.* **9**, 109–127.
- Leavitt P. R. and Hodgson D. A.** (2001) Sedimentary pigments. In *Tracking environmental change using lake sediments. Volume 3: Terrestrial, algal, and siliceous indicators.* (eds. J. P. Smol, H. J. B. Birks, W. M. Last). Kluwer Academic Publishers, pp 295-325
- Logan B. W. and Cebulski D. E.** (1970) Sedimentary environments of Shark Bay, Western Australia. *Am. Assoc. Pet. Geol. Mem* **13**, 1–37.
- Logan B. W.** (1974) Evolution and diagenesis of Quarternary carbonate sequences, Shark Bay, Western Australia. *Am. Assoc. Pet. Geol. Mem.* **22**, 195–249.
- López-Lara I. M., Sohlenkamp C. and Geiger O.** (2003) Membrane lipids in plant-associated bacteria: their biosyntheses and possible functions. *Mol. Plant Microbe Inter.* **16**, 567-579.

- Ludwig R., Pringault O., de Wit R., de Beer D. and Jonkers H. M.** (2006) Limitation of oxygenic photosynthesis and oxygen consumption by phosphate and organic nitrogen in a hypersaline microbial mat: a microsensor study. *FEMS Microbiol. Ecol.* **57**, 9–17.
- Makula R. A. and Finnerty W. R.** (1975) Isolation and characterization of an ornithine-containing lipid from *Desulfovibrio gigas*. *J. Bacteriol.* **123**, 523–529.
- Mao Che L., Andréfouët S., Bothorel V., Guezennec M., Rougeaux H., Guezennec J., Deslandes E., Trichet J., Matheron R., Campion T. Le, Payri C. and Caumette P.** (2001) Physical, chemical, and microbiological characteristics of microbial mats (KOPARA) in the South Pacific atolls of French Polynesia. *Can. J. Microbiol.* **47**, 994–1012.
- Mueller D. R., Vincent W. F., Bonilla S. and Laurion I.** (2005) Extremotrophs, extremophiles and broadband pigmentation strategies in a high arctic ice shelf ecosystem. *FEMS Microbiol. Ecol.* **53**, 73–87.
- Nageli C.** (1849) *Gattungen einzelliger Algen*. Zurich.
- Okazaki K., Sato N., Tsuji N., Tsuzuki M. and Nishida I.** (2006) The significance of C₁₆ fatty acids in the sn-2 positions of glycerolipids in the photosynthetic growth of *Synechocystis* sp. PCC6803. *Plant Physiol.* **141**, 546–556.
- Palmisano A. C., Summons R. E., Cronin S. E. and Des Marais D. J.** (1989) Lipophilic pigments from cyanobacterial (blue-green algal) and diatom mats in Hamelin Pool, Shark Bay, Western Australia. *J. Phycol.* **25**, 655–661.
- Pierson B. K. and Castenholz R. W.** (1971) Bacteriochlorophylls in gliding filamentous prokaryotes from hot Springs. *Nature* **233**, 25–27.
- Pinckney J. L., Paerl H. W. and Fitzpatrick M.** (1995) Impacts of seasonality and nutrients on microbial mat community structure and function. *Mar. Ecol. Prog. Ser.* **123**, 207–216.
- Rütters H., Sass H., Cypionka H. and Rullkötter J.** (2002) Phospholipid analysis as a tool to study complex microbial communities in marine sediments. *J. Microbiol. Methods* **48**, 149–160.
- Sabbe K., Hodgson D. A., Verleyen E., Taton A., Wilmotte A., Vanhoutte K. and Vyverman W.** (2004) Salinity, depth and the structure and composition of microbial mats in continental Antarctic lakes. *Freshw. Biol.* **49**, 296–319.
- Sato, N.** (1992) Betaine lipids. *Bot. Mag. Tokyo* **105**, 185–197.

- Schubotz F., Wakeham S. G., Lipp J. S., Fredricks H. F. and Hinrichs K.-U.** (2009) Detection of microbial biomass by intact polar membrane lipid analysis in the water column and surface sediments of the Black Sea. *Environ. Microbiol.* **11**, 2720–34.
- Shively J. M. and Knoche H. W.** (1969) Isolation of an ornithine-containing lipid from *Thiobacillus thiooxidans*. *J. Bacteriol.* **98**, 829–830.
- Skirnisdottir S., Hreggvidsson G. O., Hjörleifsdottir S., Marteinson V. T., Solveig K., Holst O. and Kristjansson J. K.** (2000) Influence of sulfide and temperature on species composition and community structure of hot spring microbial mats. *Appl. Environ. Microbiol.* **66**, 2835–2841.
- Smith S. V. and Atkinson M. J.** (1983) Mass balance of carbon and phosphorus Shark Bay, Western Australia. *Limnol. Oceanogr.* **28**, 625–639.
- Sohlenkamp C., Lopez-Lara I. M. and Geiger O.** (2003) Biosynthesis of phosphatidylcholine in bacteria. *Prog. Lipid Res.* **42**, 115–162.
- Sturt H. F., Summons R. E., Smith K., Elvert M. and Hinrichs K.-U.** (2004) Intact polar membrane lipids in prokaryotes and sediments deciphered by high-performance liquid chromatography/electrospray ionization multistage mass spectrometry new biomarkers for biogeochemistry and microbial ecology. *Rapid Commun. Mass Spectrom.* **18**, 617–628.
- Villanueva J., Grimalt J. O., de Wit R., Keely B. J. and Maxwell J. R.** (1994) Chlorophyll and carotenoid pigments in solar saltern microbial mats. *Geochim. Cosmochim. Acta* **58**, 4703–4715.
- Vincent W. F.** (2010) Microbial ecosystem responses to rapid climate change in the Arctic. *ISME J.* **4**, 1087–1090.
- Wada H. and Murata N.** (1998) Membrane lipids in cyanobacteria. In *Lipids in Photosynthesis: Structure, Function and Genetics* (eds P. A. Siegenthaler, N. Murata). Kluwer Academic Publishers, Dordrecht, pp. 65–81.
- Wada H. and Murata N.** (2007) The essential role of phosphatidylglycerol in photosynthesis. *Photosynth. Res.* **92**, 205–215.
- Walter M. R., Buick R. and Dunlop J. S. R.** (1980) Stromatolites 3,400–3,500 Myr old from the North pole area, Western Australia. *Nature* **284**, 443–445.
- Zhang Y.-M. and Rock C. O.** (2008) Membrane lipid homeostasis in bacteria. *Nat. Rev. Microbiol.* **6**, 222–233.

Chapter 6

Keeping the smell down: Microbial environment and community diversity in a modern stromatolite from Shark Bay, Western Australia.

Anais Pagès, Kliti Grice, Ricardo J. Jahnert, Michael Vacher, Peter R. Teasdale, David T. Welsh, Lindsay B. Collins, Martin J. Van Kranendonk, James S. Cleverley, Paul F. Greenwood

Geobiology, under review

(**impact factor 3.04**)

Chapter 6

Introduction

Methods

- Sampling site
- Sample description
- Biogeochemical methods: DGT and DET samplers
- Molecular phylogenetic methods
- Organic geochemical methods
 - Sampling
 - Extraction
 - Column chromatography
 - Phospho-lipid fatty acids (PLFAs)
 - Cleavage of C-S bonds by Raney nickel
 - Gas-Chromatography Mass-Spectrometry (GC-MS)
 - GC - multiple reaction monitoring – MS (GC-MRM-MS)
 - GC-Isotope ratio Mass Spectrometry (GC-iRMS)
 - Measurement of $\delta^{13}\text{C}$ of bulk carbonate

Results and Discussion

- Porewater chemistry: co-distributions of iron(II) and sulfide
- Microbial diversity of the smooth mat
- Lipid Biomarkers
 - Aliphatic hydrocarbons
 - Compound-specific carbon isotopic signature of hydrocarbons
 - Phospho-lipid fatty acids
- Significance of sulfur in the modern stromatolite

Conclusions

Abstract

This study represents a comprehensive analysis of the microbial communities and environmental conditions of a living, well-laminated, smooth microbial mat from Shark Bay, Western Australia. Innovative measurement of the two-dimensional distribution of porewater sulfide and iron(II) associated with the living Shark Bay stromatolite revealed highly sulfidic and anoxic conditions in the deeper layers of the mat, optimum for the preservation of organic sulfur compounds (OSCs). Microbial characterisation by 16S *r*RNA gene sequences, biolipids [hydrocarbons and phospho-lipid fatty acids (PLFAs)] and compound-specific isotopic analysis revealed a high abundance of sulfur-cycling organisms [purple sulfur bacteria and sulfate reducing bacteria (SRB)] and a lower proportion of cyanobacteria. Aliphatic and aromatic sulfur-bound biomarkers were detected from the surficial to the deepest layers of the mat, suggesting that sulfurisation occurred at a very early stage of diagenesis and contributed to the preservation of biolipids. Sulfur-bound carotenoids deriving from purple and green sulfur bacteria (e.g. isorenieratane) were observed, confirming strongly anoxic and sulfidic (euxinic) conditions in the mat. As modern microbial mats from Shark Bay strongly resemble ancient stromatolites, the distribution of the microbial communities and processes of diagenetic preservation of Shark Bay mats can also provide a better insight into the true nature of macroscopic bio-signatures and early microbial assemblages.

Introduction

Stromatolites, laminated sedimentary structures of biological origin, extend in the geological record to 3.5 Gyr and are recognised as the earliest visible traces of life on Earth (Walter et al., 1980; Hoffman, 2000; Allwood et al., 2006; Van Kranendonk et al., 2008). However, Archean fossil microbes are not often preserved and little is known about the biogeochemical processes (Semikhatov et al., 1979; Grotzinger and Knoll, 1999) and preservation pathways of these ancient microbial macrostructures. Modern lithifying microbial mats can show close structural similarities to Archean stromatolites (Grotzinger and Knoll, 1999; Riding, 2000). Consequently, studies of modern microbial mats and their preservation pathways are critically important for discerning early microbial assemblages, complex and dynamic elemental cycles, and the true nature of macroscopic bio-signatures. In modern laminated microbial mats, microbial communities orient themselves vertically along microscale physico-chemical gradients such as light, O₂, pH, E_h and nutrients in order to optimise metabolic processes (van Gernerden, 1993). This generates a vertical distribution of main functional groups that interact to change the oxidation states of elements such as C, N, S (Canfield and Des Marais, 1991). Sulfur is a key element in modern microbial mats, however, at high concentration, sulfide is highly toxic to all microorganisms, including those that produce it (sulfate-reducing bacteria) and those that rely on it (anoxygenic phototrophic bacteria and chemolithotrophic bacteria) (De Wit and van Gernerden, 1988). Iron can play a crucial role as a buffer against sulfide accumulation, via interactions such as the precipitation of sulfide by dissolved iron(II) to form FeS.

Modern microbial mats, including laminated lithifying smooth mats have been reported in the World Heritage listed Shark Bay, Western Australia (Jahnert and Collins, 2012, 2013). Microbial mats from Hamelin Pool have been extensively studied and various microbial communities described in both smooth and pustular mats (Burns et al., 2004; Allen et al., 2009). The microstructure of microbial mats from L'Haridon Bight and Henry Freycinet embayment were recently described (Jahnert and Collins, 2013), however, a high number of microbial mats from Shark Bay have not yet been analysed in detail. For instance, no biolipids or phylogenetic studies have been performed on the microbial mats from Garden Point, a remote area of Shark Bay where metahaline calm

waters favour the formation of coarse stratified microbial mats (Jahnert and Collins, 2013). In this study, the composition of the microbial communities and the micro-environmental conditions of a laminated microbial mat from Garden Point were investigated. This study involved *r*RNA gene sequences, biolipids (hydrocarbons and PLFAs) and compound-specific isotopic analysis that were used to characterise the microbial community. Porewater analytes (sulfide and iron(II)) distributions were investigated in two-dimensions using DET (diffusional equilibration in thin-films) and DGT (diffusional gradient in thin-films) to characterise the microbial niches. Evidence for OSCs was given particular attention as the role of sulfur in the preservation of biolipids in this modern stromatolite was also investigated.

Methods

- **Sampling site**

Shark Bay is located in Western Australia, 800 km north of Perth. This area is famous for its various types of microbial mats. While several studies have focused on tidal flats and microbial mats within Hamelin Pool (Logan et al., 1974; Allen et al., 2009; 2010), much less attention has been given to microbial mats from Henry Freycinet embayment, located in the western part of Shark Bay. The samples in this study were obtained from Garden Point, a re-entrant located on the eastern area of the embayment (see Jahnert and Collins, 2013 for detailed maps). Microbial community organisation in microbial mats strongly depends on physical and chemical parameters such as salinity, alkalinity, light intensity, depth, waves and wind intensity (Logan et al., 1974). Aeolian transport and deposition of sand has been recognised to be highly significant (Jahnert and Collins, 2013). In this zone, the oldest carbonate shell was dated at 2150 ± 25 years and the oldest microbial mats at 1040 ± 25 years. The presence of a carbonate coating on microbial deposits was associated with contemporary microbial activity (Jahnert and Collins, 2013).

- **Sample description**

The sampled smooth mat contained small carbonate grains inter-bedded within organised laminae of microbes (Jahnert and Collins, 2013). These structures are classical stromatolites, based on the Kalkowsky definition (1908). The microbial mat was highly stratified and consisted of 4 distinct layers characteristic of laminated microbial mats (Figure 6.1). The decrease in light intensity with depth resulted in a green layer near the surface, characteristic of cyanobacteria, overlaying a purple-pink layer of purple sulfur bacteria, a third layer of green sulfur bacteria and a fourth black layer (Nicholson et al., 1987; Overmann and van Gernerden, 2000). The samples of microbial mat were taken in April 2011.



Figure 6.1: Sampled microbial smooth mat presenting 4 distinct layers: the first a pale yellow-green layer, a second purple layer, a third dark green-brown layer and a fourth black layer.

- **Biogeochemical methods: DGT and DET samplers**

Two-dimensional distributions of sulfide and iron(II) were obtained using colorimetric DGT and DET methods (Robertson et al., 2008), respectively. DGT and DET techniques are passive samplers that are deployed *in-situ* (Davison et al., 2000) and, combined with colorimetric measurements, provide high-resolution, two-dimensional measurements of porewater solutes; the interpretation of these measurements are discussed in detail elsewhere (Robertson et al., 2009; Pagès et al., 2011). The DET technique uses a thin polyacrylamide hydrogel layer that equilibrates with pore water solutes when placed in the sediment. DGT methods are based on the accumulation of target pore water species within a binding gel containing an analyte specific binding

agent (Zhang and Davison, 1995; Davison et al., 2000) which is overlain by a polyacrylamide hydrogel and a membrane (diffusive layer). Analyte species diffuse through the diffusive layer and are accumulated in the binding gel layer. The flux of the target analyte through the diffusive gel layer is described by Fick's First Law of Diffusion and the mass of analyte accumulated by the binding gel allows calculation of the mean analyte concentration in porewater using the DGT equation when the deployment time, the surface area of the gel exposed to the solution, the diffusion coefficient of the analyte and the diffusive gel layer thickness are known (Zhang and Davison, 1995; Davison et al., 2000). The DGT/DET sampler was deployed for 8 daytime hours, from 8 am to 4pm.

- **Molecular phylogenetic methods**

16S *rRNA* analysis was performed by Taxon Biosciences. Genomic DNA was extracted from six samples using a bead beating method (Taxon Soil and Sediment DNA Extraction Protocol version 4.3). A total of about 1.4 g (4 x 0.35 g) of the entire mat was extracted, yielding a range of 0.3 – 2.7 µg/g of genomic DNA as determined by fluorescence DNA Quantitation. To profile the microbial community, a section of the highly conserved 16S *rRNA* gene that included variable regions 5 and 6 was targeted. The 16S *rRNA* based PCR techniques have been highly useful to study the genetic diversity of modern stromatolites from different locations where bacteria and archaea have been detected (Burns et al., 2004; Papineau et al., 2005, Baumgartner et al., 2009; Goh et al., 2009; Allen et al., 2009). The conserved regions separate bacteria and archaea from eukaryotes while the variable regions distinguish species.

Primers TX9 and 1391R were used to PCR amplify a 600-bp region of the 16S *rRNA* gene from the genomic DNA in three rounds. First, the minimum number of PCR cycles needed to get sufficient amplification was determined by small volume PCR cycle titration. Optimizing for the lowest number of cycles reduces PCR-dependent biases and errors from misincorporation of nucleotides. Second, a large volume (200 µL) PCR reaction (PCR#1) was performed with the optimal cycle number, followed by 0.9% agarose gel purification of the 600-bp amplicon and recovery with a QIAquick gel

extraction kit. Lastly, 28 ng of the gel purified amplicon was amplified in a 400 μ L, 7 cycle reaction (PCR#2) with modified TX9 and 1391R primers containing a unique, sample-specific nucleotide sequence (“barcodes”) and the 454 GS FLX Titanium sequencing adaptor sequences. The addition of the barcode to amplicons allows for multiplexing samples and faster more cost effective sequencing.

The PCR#2 product was then purified on a 8% polyacrylamide gel electrophoresis-Tris-borate-EDTA (PAGE-TBE) gel and isolated by a series of steps: excision of the roughly 700-bp amplicon (600-bp + barcode + adaptors), fragmentation of the excised gel, diffusion of the DNA from the gel, and finally recovery of DNA with QIAquick PCR Purification kit. Barcoded PAGE-purified amplicons were merged into one sequencing library (33 ng each) and processed following the GS FLX Titanium emPCR and Sequencing methods (October 2009, rev. January 2010 version). Two sequencing runs were performed for a total of 3,340,600 sequences that passed the GS FLX signal processing filters with an average read length of 466-bp. The data was processed further using Taxon’s internal quality and trimming filters, resulting in a total of 1,275,231 sequences covering variable region 5 and 6. Sequencing data was analysed by correlation and clustering, using sequences observed 100 or more times across all samples. The data was first normalized to sequences per 100,000 and then log transformed before analysis in PC-ORD. Cluster analysis was performed using Ward’s method (Ward, 1963) for both the sequences and the samples. Clustering results were translated back to the normalized sequence table and 675 of the 1210 sequences annotated to division level using NCBI BLAST.

The top 500 most abundant sequences were used for the phylogenetic analysis and the construction of the taxonomic tree. Sequence alignment and taxon-based analysis of diversity within the sample were performed with the QIIME platform (Caporaso et al., 2010). The circular tree (Figure 6.4) represents the various microbial communities and their distribution within the sample.

- **Organic Geochemical Methods**

- *Sampling*

The microbial mat was sampled in the field using an aluminium push core and immediately frozen (-18°C). Prior to extraction, the sample was defrosted and the four layers separated with a metal spatula, carefully removing the edges of the sample that were in contact with the core. The spatula was thoroughly washed with dichloromethane (DCM) between each sampling.

- *Extraction*

Aliquots of the four layers were separately ultrasonicated for 5 h using a 9:1 mixture of dichloromethane (DCM): methanol (MeOH). The solvent was then filtered to remove particles and the solvent volume reduced by rotary evaporation. Activated copper turnings were added to the extract and stirred (72 h) to remove elemental sulfur. The syringe used to transfer the extracts was flushed 20 times with pure solvent to avoid possible contamination. Procedural blanks were performed regularly to confirm the authenticity of analyses. The residues from the extractions of the four layers were stored in the dark at 5°C prior to further analyses.

- *Column chromatography*

Each extract sample was separated by passage through a large column (20 cm x 0.9 cm i.d.) filled with activated silica gel (120°C, 8h) using mobile phases with increasing polarity. A smaller column (5.5 cm x 0.5 cm i.d.) was used for fractionation of the Raney-nickel treated (i.e., desulfurised) extract. The saturated hydrocarbon fraction was eluted with *n*-hexane (35 mL for large column, 2 mL for small column); the aromatic hydrocarbon fraction with a 1:3 mixture of DCM:hexane (40 mL for large column, 2 mL for small column) and the polar fraction with a 1:1 mixture of DCM:MeOH (40 mL for large column, 2 mL for small column). The saturated and aromatic hydrocarbon fractions were reduced to near dryness by purging with N₂ and the fractions analysed by gas chromatography-mass spectrometry (GC-MS) and GC-multiple reaction monitoring (MRM)-MS.

➤ *Phospho-lipid fatty acids (PLFAs)*

A second aliquot of the samples was used to extract PLFAs. PLFAs were prepared using a modification of previously reported procedures (Bobbie and White, 1980; Zelles et al., 1995). Lipids were extracted by ultrasonication (15 min) in a CHCl_3 : CH_3OH :phosphate buffer ($\text{K}_2\text{HPO}_4/\text{HCl}$) mixture (0.8:2:1; v/v/v) and isolated with additional CHCl_3 in the presence of water. The total-lipid extract was separated into polarity based fractions by successive elution through silica bonded columns (SPE-Si, Supelco, Poole, UK) with CHCl_3 (2 mL), acetone (2 mL) and CH_3OH (1 mL) to sequentially remove neutral fatty acid (FA), free FA and PLFA fractions, respectively. The PLFA fraction was methylated by addition of 0.2 M $\text{KOH-CH}_3\text{OH}$ (0.5 mL) and heating to 75°C, cooled and neutralised with 0.2 M acetic acid (0.5 mL). Methylated PLFAs were subsequently isolated with an aqueous CHCl_3 mixture and analysed with the same GC-MS equipment used to analyse the free and sulfur-bound fractions.

➤ *Cleavage of C-S bonds by Raney nickel*

Aliquots of the polar fractions (ca. 20 mg) were desulfurised with Raney nickel, as follows. Each fraction was dissolved in a 1:1 mixture of ethanol (EtOH):toluene (2 mL) together with a suspension of Raney nickel (0.25 g in 0.5 mL EtOH) and refluxed under a N_2 stream (3 h). The desulfurisation products were obtained by subsequent extraction with DCM (5 mL, 3 times). The organic phase was passed through a large column (20 cm x 0.9 cm i.d.) of anhydrous MgSO_4 to ensure H_2O removal. The solvent was removed by using a rotary evaporation. The extract was then separated on a small activated silica gel column and the saturate and aromatic fractions analysed by GC-MS. This method has previously been utilised to efficiently release sulfur-bound biomarkers from various types of samples (Adam et al., 1993; Schaeffer et al., 1995a; Wakeham et al., 1995; Grice et al., 1998b; Adam et al., 2000; Hebbing et al., 2006).

➤ *Gas-Chromatography Mass-Spectrometry (GC-MS)*

GC-MS analyses were performed using a Hewlett Packard 6890 gas chromatograph (GC) interfaced to a Hewlett Packard 5973 mass selective detector (MSD). The aromatic and saturated hydrocarbon fractions, dissolved in *n*-hexane, were

introduced *via* a Hewlett Packard 6890 Series Injector to the electronically pressure controlled (EPC) split/splitless injector (320 °C) which was operated in the pulsed splitless mode. The GC was fitted with a 60 m x 0.25 mm i.d. WCOT fused silica capillary column coated with a 0.25 µm film (DB-5MS, J and W Scientific). The oven temperature was programmed from 40°C to 325°C (at 3°C.min⁻¹) with initial and final temperature hold times of 1 and 50 min, respectively. Ultra high purity helium was used as the carrier gas and maintained at a constant flow of 1.1 mL.min⁻¹. Full scan (50-600 Daltons) mass spectra were acquired at ~ 4 scans per second with ionisation energy of 70 eV, and a source temperature of 230°C. Carotenoid standards were used to identify sulfur-bound carotenoids present in the aromatic fractions.

➤ *GC-multiple reaction monitoring-MS (GC-MRM-MS)*

MRM GC-MS affords high signal to noise ratio and elevated selectivity for targeted lipid classes. Sulfur-bound saturated hydrocarbons were analysed in MRM mode on a Micromass Autospec Ultima mass spectrometer interfaced to an Agilent 6890N gas chromatograph with an autosampler. The GC was fitted with a DB-5MS fused silica capillary column (60 m; 0.25 mm i.d.; 0.25 µm film thickness; J andW Scientific). He at a constant flow of 2 mL min⁻¹ was the carrier gas. The GC temperature program was: 60°C (2 min) to 150°C at 10°C min⁻¹, thus to 315°C (held 24 min) at 3°C min⁻¹. The source was operated in electron impact, 70 eV mode at 250°C, with 8 kV accelerating voltage, using predetermined precursor–product reactions (see Table 1). Data were acquired and processed using MassLynx 4.0 (Micromass Ltd.).

➤ *GC- Isotope-Ratio Mass-Spectrometry (GC-iRMS)*

A Micromass IsoPrime isotope ratio - mass spectrometer (ir-MS) coupled to a Hewlett Packard HP6890 gas chromatograph fitted with a 60 m x 0.25 mm i.d., 0.25 µm thick DB-1 phase column was used to measure the δ¹³C values of the hydrocarbons and PLFAs. The samples were injected in pulsed splitless mode (30 seconds hold time at 15 psi above the head pressure of the column and 35 seconds for purge). The GC oven was programmed with the same temperature program as for the GC-MS analyses. The δ¹³C compositions are reported in parts per mil (‰) relative to the international Vienna Peedee

Belemnite (VPDB) standard. Stable carbon isotope ratios for individual PLFAs were calculated from FAME data by correcting for the one methyl carbon that was added during derivatisation. Reported values are the average of at least two analyses.

➤ *Measurement of $\delta^{13}\text{C}$ of bulk carbonate*

Samples were analysed for $\delta^{13}\text{C}$ using a GasBench II coupled with Delta XL Mass Spectrometer (Thermo-Fisher Scientific) following procedure outlined in Paul et al., 2007. All $\delta^{13}\text{C}$ (‰, VPDB) were determined by three point normalization with international standards provided by IAEA (i.e., L-SVEC, NBS19 and NBS18). The external error for $\delta^{13}\text{C}$ analyses was <0.10‰.

Results and discussion

- **Porewater chemistry: co-distributions of iron(II) and sulfide**

Porewater sulfide and iron(II) distributions are presented in [Figure 6.2](#). Sulfide concentrations which varied between 0 and 500 μM in the microbial mat were lowest in the top layer (0 to 250 μM) and increased with depth, confirming intensification of anoxic conditions with depth. Sulfide distribution, however, was highly heterogeneous. The concentrations were higher for the first 40 mm of sample width and progressively decreased afterwards, reaching 0 μM on the far right area. At 10 and 15 mm wide, small hotspots of sulfide (concentrations reaching 488 μM) were visible. Other large zones of high sulfide production also appeared below the microbial mat as well as an area of zero sulfide (60 mm wide) suggesting the presence of fauna in the sediment. This sulfide distribution implied that the microbial mat was influencing and being influenced by its surrounds; this two-way interaction contributing to significant heterogeneity in analyte distributions. The sulfide concentrations measured during daylight conditions are probably lower than they would be at night when, in the absence of sulfide consumption by anoxygenic photosynthesis, and biological and chemical reoxidation coupled to oxygen production by oxygenic photosynthesis, whereas, at night in the absence of photosynthesis sulfide would tend to accumulate within the mat (Pagès et al., 2014a).

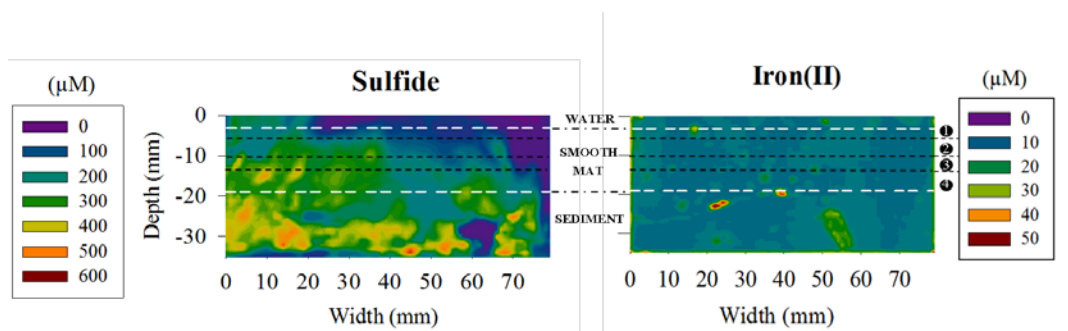


Figure 6.2: Two-dimensional distributions of sulfide (DGT) and iron(II) (DET) samplers in the microbial mat under daylight conditions. The white lines represent the entire mat. The region above the top white line represents the water and the area underneath the line represents the sediment. The black dotted lines represent the four different layers of the mat.

The porewater iron(II) distribution was a lot more homogeneous, with maximum concentrations reaching 14 μM in the mat and 50 μM in the underlying sediment. Background concentrations ranged between 8 and 14 μM . Similar to sulfide, iron(II) concentration was lower in the far right area of the mat, corroborating the possible presence of a burrow and penetration of oxygen to depth. Indeed, in oxic areas, the presence of oxygen would have led to the direct chemical oxidation of sulfide and iron(II) by dissolved oxygen and/or biological oxidation via the metabolism of chemoautotrophic iron and sulfur oxidising bacteria, resulting in lower concentrations in sulfide and iron(II) (Stal, 2001). With the exception of this specific area, layers 3 and 4 presented more anoxic conditions, as shown by the increase in sulfide concentration. Under anoxic conditions, anaerobic respirations including iron and sulfate reduction are favoured and in the absence of significant chemical or biological reoxidation, iron(II) and sulfide accumulated in the deeper layers of the mat. However, there are strong interactions between the iron and sulfur cycles, which would also influence the distribution of iron(II) and sulfide within the mat. For example, iron(III) present in oxic zones of the mat can be reduced to iron(II) by sulfide and this could further react with sulfide to produce insoluble iron monosulfide (Rickard and Morse, 2005). Consequently, since iron(II) and sulfide co-precipitate to form FeS and they should not coexist in the same sediment zone (Viaroli et al., 2004; Rickard and Morse 2005). However, a consistent background iron(II) concentration (8-14 μM) was visible in the deeper part of the mat where sulfide concentrations were also high. This discrepancy may be explained by the different

timescales of measurement of the DGT and DET samplers (Robertson et al., 2008; Pagès et al., 2011; 2012).

DGT accumulates analytes during the over the whole deployment period and therefore the measured concentrations represent a time-integrated average of the actual porewater concentrations over the sampling period (Robertson et al., 2008). In contrast, DET measurements depend on the dynamic diffusive equilibrium between the porewater and sampling gel and therefore measured porewater concentrations are mostly representative of conditions over the last few hours of the deployment (Robertson et al., 2008; Pagès et al., 2011). Therefore, the overlap observed in sulfide and iron(II) distributions measured by combined DGT/DET samplers may be due to iron(II) and sulfide being present at the same location in the sediment, but at different periods during the probe deployment. Thus, the sulfide distribution may reflect the more reduced conditions in the morning when the samplers were deployed whereas, the iron(II) distribution may reflect the more oxidised conditions following an entire day of oxygen production by photosynthesis (Pagès et al., 2012). In addition, porewater iron(II) concentrations are still very low in comparison with other hypersaline microbial mats (56 mM) (Wieland et al., 2005) and coastal sediments (100 μ M) (Thamdrup et al., 1994). Relatively low concentration of iron(II) and high concentration of sulfide suggest highly dynamic sulfur cycling, as previously observed in Bahamian stromatolites and associated with the formation of lithified micritic layers and consequently, could significantly promote lithification in this mat (Visscher et al., 1998). In addition, these chemical conditions can favour the preservation of biolipids through the formation of OSCs. Indeed, anoxic conditions and high concentrations of sulfide are prerequisites for the formation of these compounds. Additionally, since formation of FeS is thought to occur more rapidly than OSCs (Hartgers et al., 1997) the generally low concentrations of porewater iron(II) in this mat may favour the formation of OSCs.

- **Microbial diversity of the smooth mat**

The microbial community of the smooth mat was comprised of ~ 94% of bacteria and ~ 5% of archaea (Figure 6.3), on the basis of 16s *r*RNA analysis. Three groups of archaea were identified: Crenarchaeota, Traumarchaeota and Euryarchaeota, the latter phylum included Halobacteria, an archeal class characteristic of hypersaline environments (Oren, 2002), as well as the methanogens Thermoplasmata, Thermococci and Methanomicrobia (Figure 6.4). This latter class exclusively contains methylotrophic methanogens that have been previously identified in hypersaline Guerrero Negro microbial mats (Orphan et al., 2008). It has been proposed that sulfate-rich environments would provide little support of methanogenesis (Burns et al., 2004); however, the identification of methanogens in the sample is concordant with other studies of Shark Bay microbial mats (Burns et al., 2004; Papineau et al., 2005; Allen et al., 2009). Their presence might be explained by an accumulation of glycine betaine as a compatible solute for osmotic balance by halotolerant cyanobacteria and other bacteria in the mat. This osmolyte and its breakdown products such as trimethylamine can provide non-competitive substrates for methanogens, allowing them to co-exist with SRB in sulfate-rich environments (see Welsh, 2000 for a review). This co-existence in the sample is of particular interest as methane has been reported to be anaerobically oxidised by SRB acting syntrophically with methanotrophic archaea (Boetius et al., 2000).

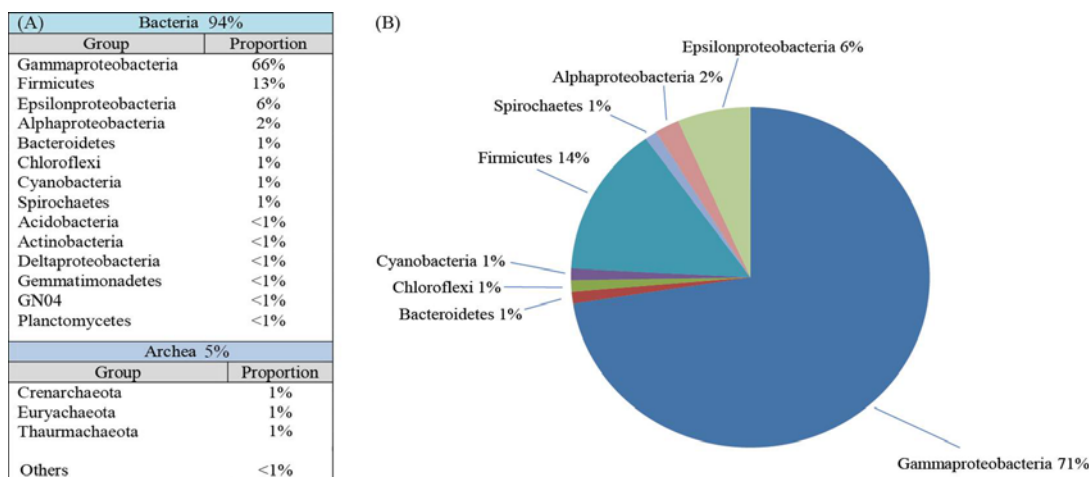


Figure 6.3: A. Phylogenetic affiliations and proportion of groups of bacteria and archaea present in the smooth mat. B. Relative proportion of the 10 most abundant bacterial groups.

The bacterial community exhibited a very high biodiversity (Figure 6.4). The dominant bacterial classes were Proteobacteria (Gammaproteobacteria, Epsilonproteobacteria and Alphaproteobacteria) and Firmicutes. Allen et al. (2009) similarly reported a dominance of Gammaproteobacteria and Firmicutes in a smooth mat from Hamelin Pool. Alphaproteobacteria are also common to these microbial mats (Burns et al., 2004; Papineau et al., 2005; Goh et al., 2009). Cyanobacteria were present in the mat in relatively low abundance. Potential sulfate-reducers can be found among the Deltaproteobacteria group and the dominant Firmicutes group. As previously reported by Allen et al. (2009), a low proportion of cyanobacteria and a contrastingly high abundance of potential sulfate-reducers observed in these mats may favour calcium carbonate precipitation and lithification (Visscher et al., 1998; Dupraz and Visscher, 2005). In addition, the deep purple zone observed in the mat (layer 2, Figure 6.1) and the high abundance of Gammaproteobacteria suggest that, in comparison with previously studied microbial mats from Shark Bay (Allen et al., 2009; Burns et al., 2004), this microbial mat presented a unique distribution of microorganisms and a highly dynamic sulfur cycle in which purple sulfur bacteria must have played a significant role. Purple sulfur bacteria are capable of assimilating CO_2 by means of H_2S photo-oxidation. Through this reaction, two weak acids are transformed to neutral components which results in an alkalinity increase favouring carbonate precipitation (Warthmann et al., 2011). Studies of the microbial mats from Lagoa Vermelha showed that carbonates were nucleating and

growing in the purple sulfur bacteria layer of the mat, confirming the important role of purple sulfur bacteria can play in carbonate precipitation and mat lithification (Van Lith et al., 2003; Vasconcelos et al., 2006).

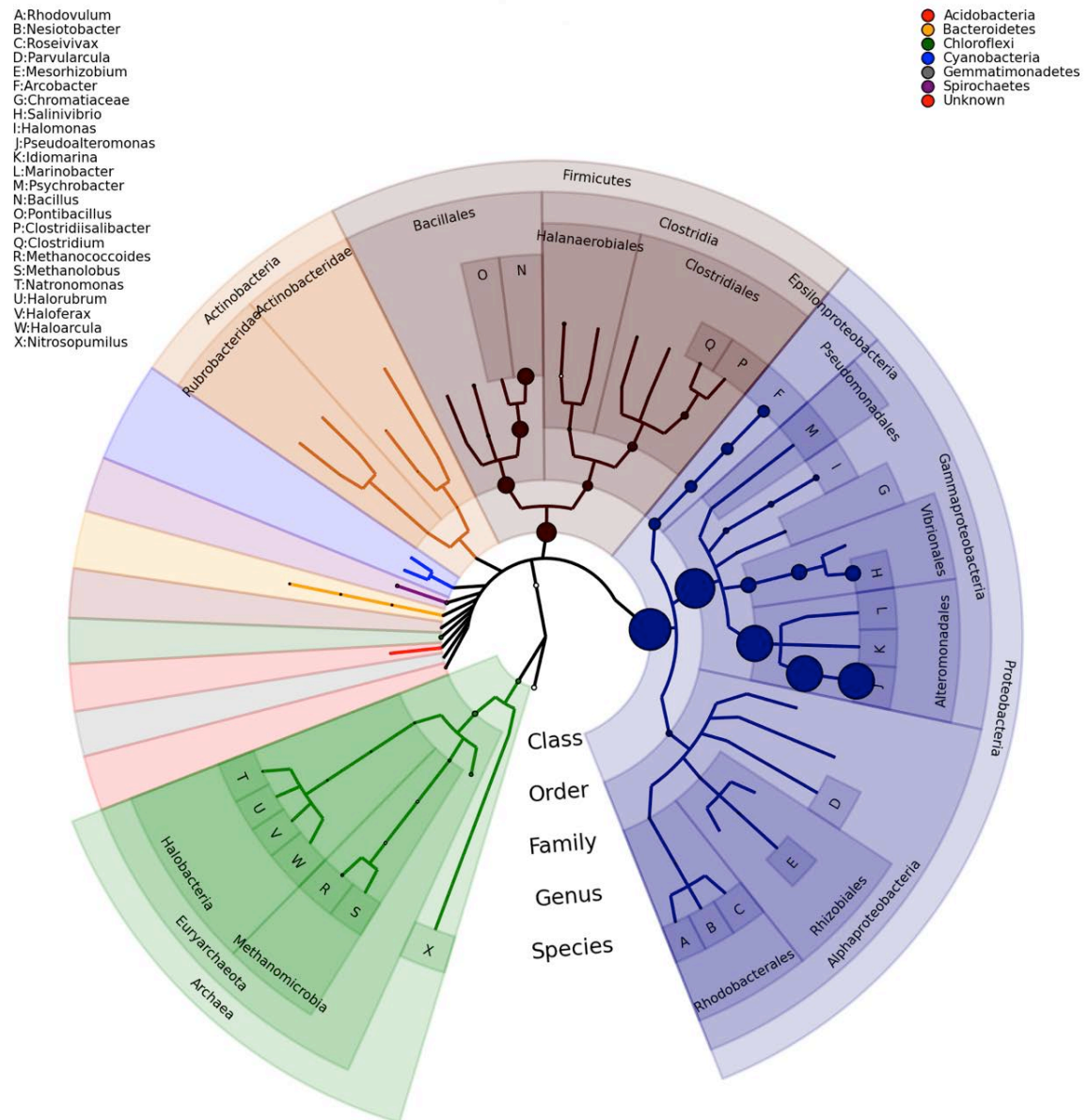


Figure 6.4: Phylogenetic tree of the Garden Point microbial mat 16s ribosomal RNA gene sequences. The size of the nodes is directly proportional to the number of sequences observed for the given taxonomic units it represents.

- **Lipid biomarkers**

Hydrocarbons and PLFAs were analysed in the four different layers of the mat. The free extracts of the four layers showed different distributions of aliphatic hydrocarbons. This is consistent with the light and oxygen gradients influencing the distribution of microbial communities in the mat. The surficial layer is usually dominated by cyanobacterial photosynthesis under daytime conditions leading to oxic conditions whereas the deepest layer is under permanently anoxic conditions implying the presence of anaerobic microbes, as detected in the hydrocarbons and PLFA fractions (Stal, 2001). However, anthropogenic contamination can be an issue when studying biolipids from modern systems. Consequently, to avoid any possible anthropogenic impact on the biolipids composition of the microbial mat (e.g.: oil spill), most of the analyses discussed therein relate to the indigeneous organic matter of the deeper layers (3 and 4).

➤ *Aliphatic hydrocarbons*

Aliphatic hydrocarbons were analysed to investigate the major bacterial, higher plant or eukaryotic contributions to the mat. *N*-alkanes ranged from C₁₅ to C₃₄ with a predominance of short-chain *n*-alkanes (<C₂₀). C₁₇ *n*-alkane was the most abundant *n*-alkane and C_{18:1} alkene was also highly abundant, as shown for the deepest layer (Figure 6.5). Although *n*-C₁₇ alkane can be found in eukaryotic algae (Paoletti et al., 1976), it was also the most dominant hydrocarbon in cultures of filamentous cyanobacteria (Winters et al., 1969; Paoletti et al., 1976). *n*-C₁₇ alkane has been interpreted as a marker of cyanobacteria in microbial mats from Shark Bay (Allen et al., 2010) and cyanobacterial mats from hot springs (Robinson and Eglinton, 1990), freshwater (Thiel et al., 1997) or hypersaline environments (Grimalt et al., 1992; Fourçans et al., 2004; Rontani and Volkman, 2005). Phytane and phytene were highly abundant in the mat but no pristane was detected. A pr/ph ratio < 1 implies reducing conditions (Powell and McKirdy, 1973). The total absence of pristane may reflect the significant contribution of anaerobic bacteria (e.g. SRB) to the total biomass. The presence of reducing conditions in this deep layer is consistent with the high concentrations of sulfide measured in the mat (see above). The long-chain *n*-alkanes showed a predominance of odd-over-even carbon-numbered *n*-alkanes (C₂₁-C₃₃ carbon preference index = 2.6), as highlighted by the *m/z* = 85 mass

chromatogram (Figure 6.6), characteristic of epicuticular leaf waxes (Eglinton and Hamilton, 1967), suggesting an input from higher plants supplied by aeolian transport, as previously observed in microbial mats from the Hamelin Pool (Allen et al., 2010). However, waxy *n*-alkanes with odd carbon-number predominance have also been reported in coastal seagrass beds (Attaway et al., 1970; Botello and Mandelli, 1978).

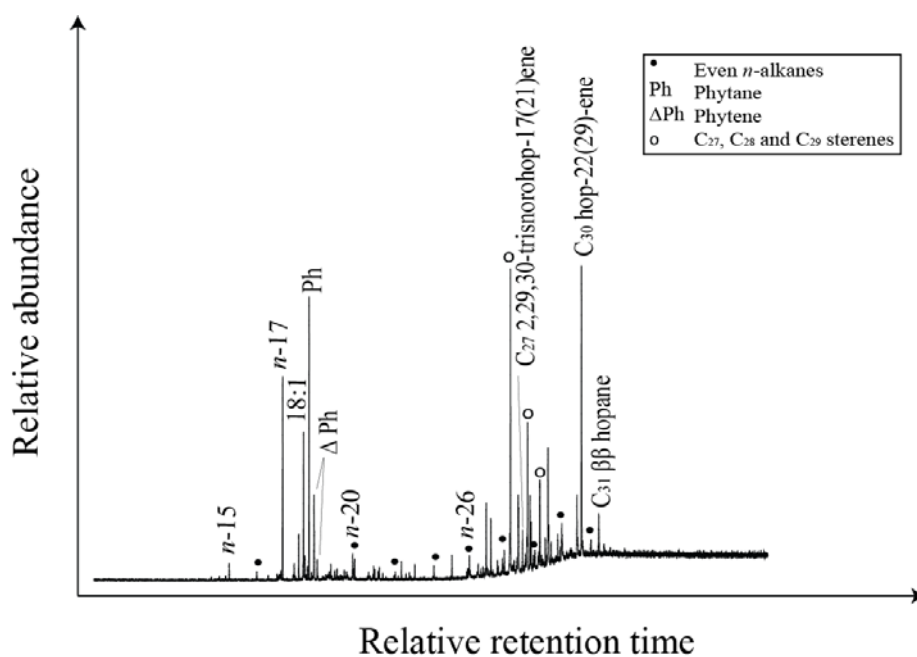


Figure 6.5: Total ion chromatograms from gas chromatography-mass spectrometry (GC-MS) analysis of the aliphatic hydrocarbon fraction of the fourth layer of the microbial mat.

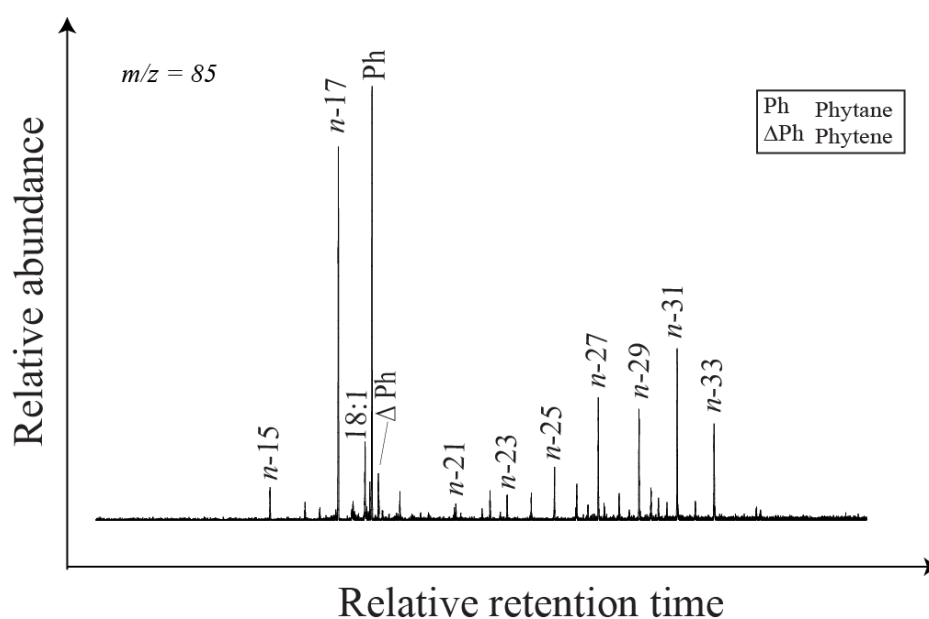


Figure 6.6: Mass fragmentogram ($m/z = 85$) of the aliphatic hydrocarbon fraction of the fourth layer of the microbial mat.

Hopanoids were also detected in the mat: 22,29,30-trisnorhop-17(21)-ene, hop-22(29)-ene (i.e. diploptene) and $17\beta,21\beta$ -homohopane. Diploptene was previously identified in microbial mats from various environments (Boudou et al., 1986; Dobson et al., 1988; Thiel et al., 2001) and has been recognised as a potential marker for cyanobacteria (Gelpi et al., 1970; Dobson et al., 1988), methylotrophs (Summons et al., 1994) or sulfate reducing bacteria (SRB) such as *Desulfovibrio* (Blumenberg et al., 2006). C_{31} $17\beta,21\beta$ -homohopane derives from aminobacteriohopanetetrol possibly deriving from cyanobacteria (Talbot et al., 2008), sulfate reducing bacteria (Blumenberg et al., 2006) or other bacteria (Talbot et al., 2008).

The main hydrocarbons identified in the $m/z = 215$ mass chromatogram selective for unsaturated steroids were the $5\alpha(H),14\alpha(-H),17\alpha(H)$ 20R isomers of cholest-2-ene (C_{27}), 24-methylcholest-2-ene (C_{28}) and 24-ethylcholest-2-ene (C_{29}). Δ^2 -sterenes are usually associated with eukaryotes, including diatoms, green algae and other phytoplankton, zooplankton, terrestrial higher plants and submerged macrophytes (Volkman, 1986; Volkman et al., 1998). In addition to diatoms that produce C_{27} , C_{28} and C_{29} sterenes, zooplankton is the dominant source of C_{27} sterene while C_{28} is mainly

produced by phytoplankton and C₂₉ usually derives from aquatic or terrestrial plants and green algae (Volkman, 1986).

➤ *Compound-specific carbon isotopic signatures of hydrocarbons*

The $\delta^{13}\text{C}$ values of the long chain *n*-alkanes (C₂₄-C₃₃) in the range -28 to -30‰ were notably more depleted than the short chain *n*-alkanes (C₁₆-C₂₀), by 8.8‰ on average, strongly suggesting separate sources (Figure 6.7). Diatoms and dinoflagellates can produce long-chain *n*-alkanes (Volkman et al., 1998), however, the clear predominance of odd-carbon numbered *n*-alkanes is more characteristic of higher plants. Terrestrial C₃ plants produce long-chain *n*-alkanes typically with $\delta^{13}\text{C}$ values ranging from -31 to -39‰ and some species of coastal macrophytes are a source of *n*-alkanes with $\delta^{13}\text{C}$ values between -19 and -34‰ (Collister et al., 1994; Canuel et al., 1997). C₂₇, C₂₈ and C₂₉ sterenes presented more enriched $\delta^{13}\text{C}$ values (-16.4, -13.3 and -15.2‰ respectively) suggesting a distinct source for these sterenes. Diatoms have been recognised to produce approximately equal amounts of C₂₇, C₂₈ and C₂₉ sterenes although some centric species produce more C₂₈ sterene (Volkman, 1986). Diatoms are known to be ¹³C-rich organisms in comparison to other primary producers as some species are capable of assimilating HCO₃⁻ and they usually grow in blooms that cause localised depletions in CO₂(aq) leading to enriched ¹³C biomass (Freeman et al., 1994, Canuel et al., 1997). Consequently, the enrichment in ¹³C for the cholest-2-ene (C₂₇), 24-methylcholest-2-ene (C₂₈) and 24-ethylcholest-2-ene (C₂₉) in comparison with $\delta^{13}\text{C}$ values of *n*-alkanes suggested that these biomarkers may derive from diatoms indigenous to the mat. However, no C₂₀ or C₂₅ HBI alkenes were found in the mat, although these biomarkers have been recognised as characteristic markers of diatoms from samples of sediments, diatomaceous ooze and microbial mats from Hamelin Pool (Dunlop and Jefferies, 1985; Summons et al., 1993; Allen et al., 2010). 22,29,30-trisnorhop-17(21)-ene and diploptene also presented enriched $\delta^{13}\text{C}$ values (-17.6 and -17.6‰, respectively). However, C₃₁ 17 β , 21 β -homohopane presented a much more depleted $\delta^{13}\text{C}$ value (-30.6‰) suggesting a different source for the C₂₇/C₃₀ hopenes and the C₃₁ hopane.

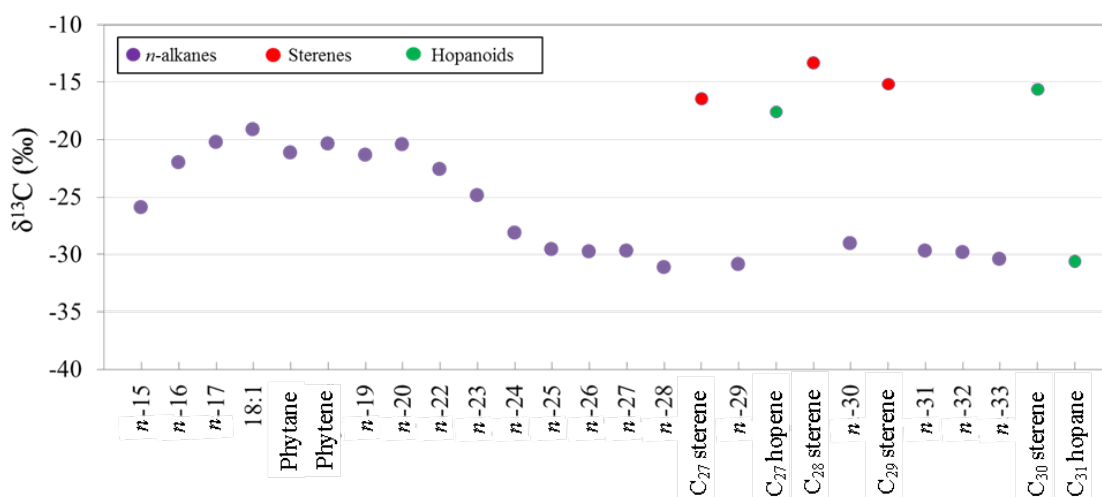


Figure 6.7: $\delta^{13}\text{C}$ of values of hydrocarbons from the saturate fraction of the fourth layer of the microbial mat analysed by gas chromatography – isotope ratio – mass spectrometry (GC-irMS) analysis. The maximum standard deviation of the $\delta^{13}\text{C}$ values is $\pm 0.3\%$.

➤ *Phospho-lipid fatty acids (PLFAs)*

To determine that all 4 layers of the microbial mat presented extant biomass, PLFAs were extracted from each layer. PLFAs are cell membrane components that are rapidly metabolised after cell death (Vestal and White, 1989). Consequently, the presence of PLFAs indicates viable biomass (Vestal and White, 1989). Results from the GC-MS analysis of the PLFA fraction of layer 4 (deep anoxic layer) are presented in Figure 6.8. 16:0, 18:1 ω 9 and 18:0 PLFAs were the most abundant PLFAs in the sample. 16:0 and 18:1 ω 9 are the most abundant PLFAs in cultured cyanobacteria (Kenyon et al., 1972; Cohen et al., 1995) and have also previously been reported in other microbial mats from Shark Bay (Allen et al., 2010). 18:4 ω 3 PLFA, another marker of cyanobacteria, was detected in lower abundance (Kenyon et al., 1972; Vestal and White, 1989; Jahnke et al., 2004). *Iso*- and *anteiso*-15:0 and 17:0 as well as *iso*-17:1 ω 9 were also detected. These PLFAs have been reported in SRB (Taylor and Parkes, 1983; 1985) but also other bacterial groups (Vestal and White, 1989). 10-methylhexadecanoic acid, a more specific marker for SRB, confirmed their presence in the mat (Vestal and White, 1989). 10-methyloctadecanoic acid, characteristic of *Actinomycetes*, was not detected although 16s *r*RNA analysis revealed their presence in the mat (see above).

Cyclopropyl-19:0 was detected in relatively low abundance whereas it has been reported to be highly abundant in other microbial mats from Shark Bay (Allen et al., 2010). This PLFA has been reported in *Desulfobacter* genus (Londry et al., 2004) and purple sulfur bacteria (Grimalt et al., 1991), but it is also relatively abundant in numerous Alpha and Gammaproteobacteria.

Other less abundant products included cyclopropyl-17:0 which is possibly indicative of iron-oxidising bacteria (Knief et al., 2003) and 2-hydroxy fatty acids with 14-18 carbons, which are indicative of the presence of Gram negative bacteria (Wilkinson, 1988).

Finally, very long-chain fatty acids with a predominance of even over odd carbon-numbers were observed in the mat. Even carbon-numbered fatty acids are usually attributed to a vascular plant origin (Eglinton and Hamilton, 1967) which may have been supplied to the mat by aeolian transport (Allen et al., 2010). The hydrocarbon fraction showed a predominance of odd carbon-numbered alkanes (Figure 6.5). However, the $\delta^{13}\text{C}$ values of long-chain fatty acids were more ^{13}C -enriched than the co-occurring odd carbon numbered *n*-alkanes (-7.7‰ discrepancy on average between PLFAs in the C₂₀-C₂₄ range and co-occurring *n*-alkanes) (Figure 6.7 and Figure 6.8), suggesting that even long-chain fatty acids and odd *n*-alkanes were from different sources. Similar distribution of PLFA with comparable $\delta^{13}\text{C}$ values were found in ooids from Shark Bay (Summons et al., 2013). The ooids also showed *n*-alkanes with $\delta^{13}\text{C}$ values more depleted than the co-occurring long-chain fatty acids by 4-5‰ and it were speculated these data might relate to sulfate-reducing Firmicute bacteria (Summons et al., 2013). Firmicute bacteria represent a major bacterial group in the microbial mat (see above). Hence, Firmicute bacteria inhabiting Shark Bay mats may also contribute to the formation of ooids, which occur in Shark Bay.

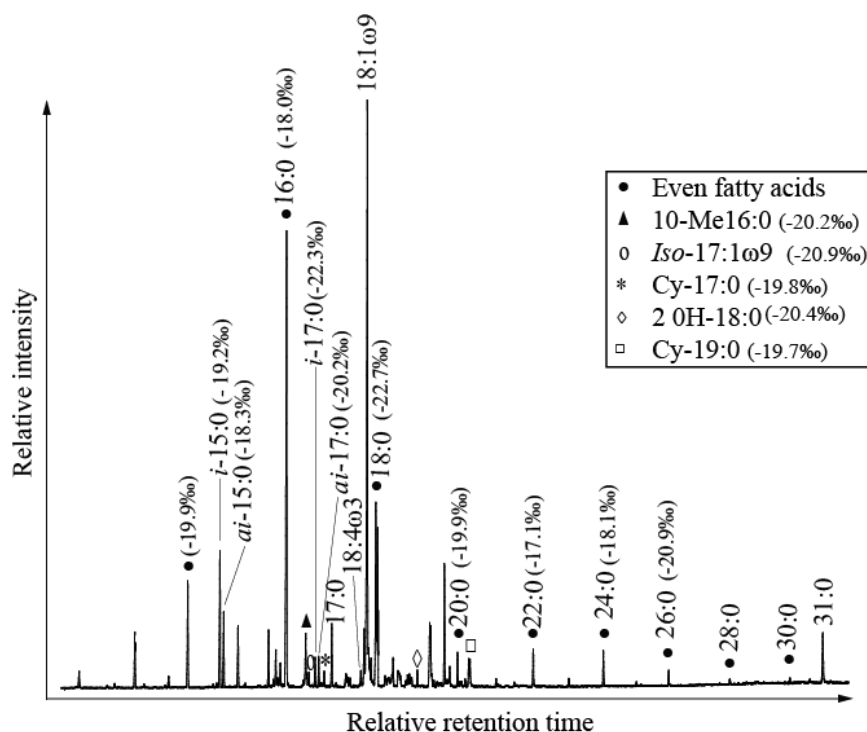


Figure 6.8: Total Ion Chromatogram and $\delta^{13}\text{C}$ values obtained from GC-MS and GC-irMS analysis of the phospho-lipid fatty acid fraction of the fourth layer of the mat. The maximum standard deviation of the $\delta^{13}\text{C}$ values was ± 0.3 ‰.

- **Significance of sulfur in the modern stromatolite**

Sulfur is a crucial element in modern microbial mats. Sulfurisation during primary diagenesis, producing OSCs with intramolecular or intermolecular linkages, is a key process for the preservation of biolipids in the rock record (Sinninghe Damsté and de Leeuw, 1990). SRB organisms are renowned to play a vital role in the sulfur cycle and in the formation of OSCs. These bacteria have existed on Earth for ca. 3.5 billion years (Shen et al., 2001) and their activity has played a significant role in preservation of organic matter in the rock record, for instance in carbonate laminae of ca. 2.72 Ga Tumbiana stromatolites where sulfur-rich globules representing microbial cells encapsulated in minerals have been identified (Lepot et al., 2008). In contemporary sediments, SRB provide H_2S as the reducing agent for abiotic reduction of biolipids (Hebting et al., 2006). To investigate the role of sulfur in the preservation of biolipids

from the presently studied modern stromatolite, C-S bound biomarkers were analysed and compared with biomarkers from the free fractions.

The sulfur-bound aliphatic hydrocarbons from layer 4 (Figure 6.9) showed a different distribution than the free hydrocarbons (Figure 6.5). The C₁₈ and C₂₁ *n*-alkanes were particularly abundant. The unusually high abundance of the *n*-C₃₇ alkane might be attributed to haptophyte-derived alkadienes (Grice et al., 1998b). A similarly prominent *n*-C₃₇ has been reported in the sulfurised fraction of sediments which showed evidence of prymnesiophytes input (Schaeffer et al., 1995b) and the presence of haptophytes has previously been reported in other hypersaline and coastal marine microbial mats (Lopez et al., 2005). Phytane, present in the free aliphatic fraction was also identified in the sulfur-bound fraction. A high abundance of phytane and phytene was recently identified in the raney-nickel released sulfur-bound fraction of estuarine sediments associated with high concentration of monosulfidic black ooze (Lockhart, personal communication). The C₃₁ 17 β ,21 β -homohopane, detected in the free fraction, was also present in the sulfur-bound fraction in relatively low abundance.

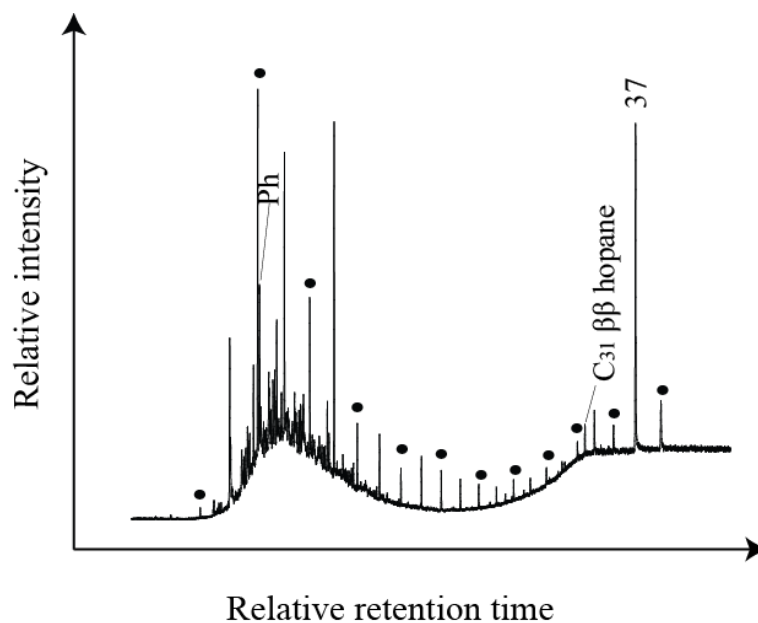


Figure 6.9: Total Ion Chromatogram of the sulfur-bound aliphatic hydrocarbons from the fourth layer of the smooth mat measured by GC-MS. The black dots indicate even carbon-numbered *n*-alkanes.

The $m/z = 191$ chromatogram of the third layer of the mat (Figure 6.10) clearly showed it was the most abundant hopanoid product. Of all the layers, this third layer presented the highest abundance of hopanes (ranging from C_{27} to C_{31}) and a very high abundance of C_{31} $17\beta,21\beta$ -homohopane. High relative of $\beta\beta$ hopanes and these have been previously reported in the sulfur-bound fractions of other sediments such as evaporitic sequences and lignites (Schaeffer et al., 1995b; Sandinson et al., 2002). Other hopanes detected in trace amount included C_{29} $\alpha\beta$ and $\beta\alpha$ hopanes and C_{30} $\alpha\beta$ hopanes. These $\alpha\beta$ isomers are the most thermally mature and are usually dominant in crude oils, however, they have also been reported in recent lacustrine sediments (Innes et al., 1997) and Holocene peat deposits (Pancost et al., 2000). In addition, a clear predominance of $\alpha\beta$ -hopanoids over $\beta\beta$ -hopanoids was reported in a living microbial mat, suggesting that the “geological” isomers can be produced within a living system (Thiel et al., 2003). C_{31} $17\beta,21\beta$ -homohopane usually indicates the presence of cyanobacteria (Talbot et al., 2008) but we also detected in high abundance in the sulfur-bound compounds of mono-sulfidic black ooze sediments (Lockhart, personal communication). These results tend to suggest that a possible source from SRB (Blumenberg et al., 2006) is not negligible for this hopane and could explain its relatively high abundance in an anoxic layer of the mat.

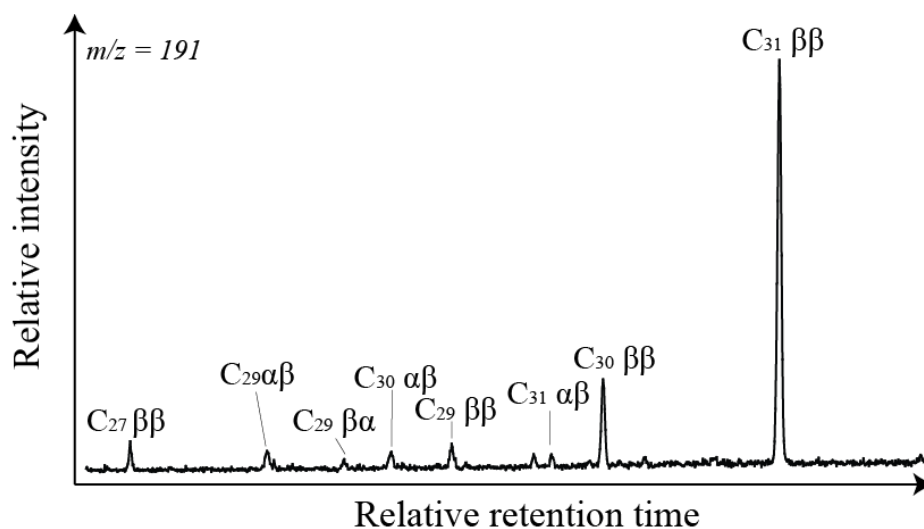


Figure 6.10: Mass fragmentogram ($m/z = 191$) of the sulfur-bound aliphatic hydrocarbons from layer 3.

Sulfur-bound steroids were also identified in the deepest layer of the mat (layer 4). MRM GC-MS analysis of the aliphatic fractions and comparison with laboratory standards confirmed the detection of 20R 5 α -cholestane and 5 α -24-ethylcholestane (Figure 6.11). Sulfur-bound C₂₇ - C₂₉ steranes with a predominance of 5 α over 5 β configuration have been previously reported in early diagenetic sulfurised sediments (Filley et al., 1996; Kok et al., 2000). Trace quantities of sulfur-bound carotenoids were also detected in the three top layers of the mat. These products included β -renierapurpurane in layer 1, renieratane in layers 1 and 2 and isorenieratane in layer 3. They are quite unique and not typical of petroleum contamination. The natural product precursors for β -renierapurpurane and renieratane derive from purple-sulfur bacteria (*Chromatiacea*) (Behrens et al., 2000). Isorenieratane may originate from isorenieratene present in brown-pigmented *Chlorobi* (Summons and Powell, 1986) or actinomycetes (Kohl et al., 1983). As this aryl isoprenoid was exclusively detected in the third layer of the mat, characteristic of green sulfur bacteria (Nicholson et al., 1987; Overmann and van Gemerden, 2000), it is likely that this compound derived from *Chlorobi*. The presence of isorenieratane, a marker of euxinia (Summons and Powell, 1986), in layer 3 suggests strongly sulfidic and anoxic conditions in this layer. The presence of fully reduced carotenoids implies that carotenoids could have been hydrogenated *in-situ* or during the desulfurisation process (Mozingo et al., 1944). The presence of sulfur-bound carotenoids with possible *in-situ* transformation of unstable oxygen-sensitive carotenoids into more stable configurations typical of fossil biomarkers confirms the crucial role that sulfur-cycling organisms play in the preservation of organic matter in modern stromatolites.

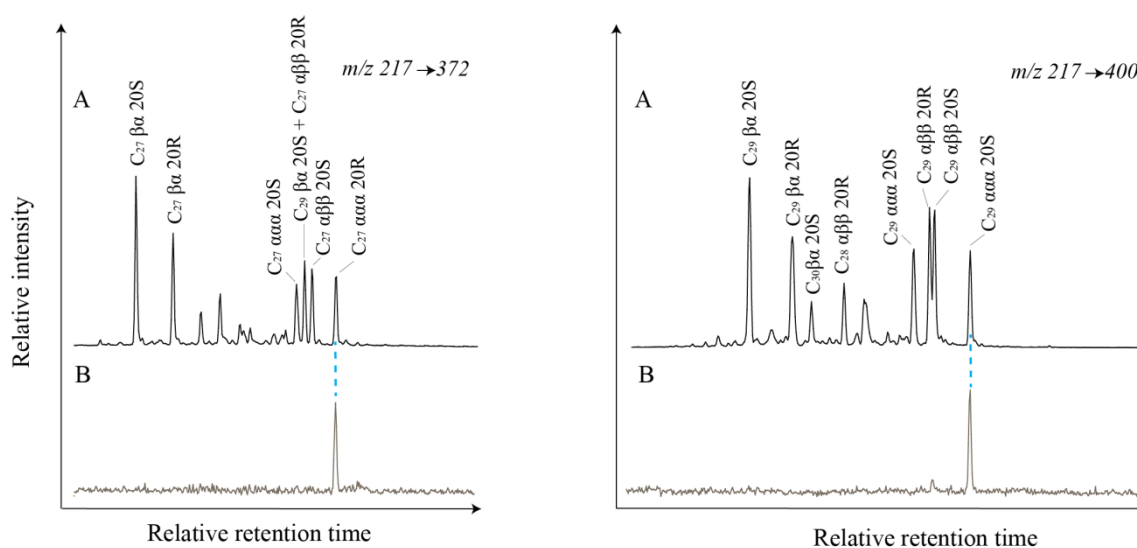


Figure 6.11: Partial GC-MRM chromatograms (m/z 217 \rightarrow 372; 217 \rightarrow 400). A: Steroid standard. B: sulfur-bound aliphatic fraction of layer 4.

Conclusions

The study of the micro-environmental conditions revealed high sulfide concentrations, implying the presence of anoxic conditions deeper in the mat (i.e. up to 10 mm). The composition of the microbial communities revealed a high biodiversity, slightly different from previously studied microbial mats from Shark Bay (Burns et al., 2004; Papineau et al., 2005; Allen et al., 2010). The high abundance of Gammaproteobacteria and Firmicute suggested a predominance of sulfur-cycling organisms which likely contributed to dynamic sulfur cycle and carbonate precipitation in the mat. Biolipids also showed evidence of sulfur-cycling organisms as well as cyanobacteria and maybe diatoms, as shown by the highly ^{13}C -enriched sterenes. Unusual long-chain fatty acids with isotopic signatures significantly different from co-occurring long-chain *n*-alkanes indicated that Firmicute bacteria inhabiting Shark Bay mats may also contribute to the formation of ooids in Shark Bay, as previously suggested by Summons et al. (2013). In addition, OSCs were identified in the four different layers of the mat analysed. Reaction between reduced inorganic sulfur species and labile, oxygen sensitive biolipids contributes to the preservation of organic matter in modern stromatolites. This selective preservation process, occurring at a very early stage of diagenesis, is likely a crucial step in the protection of these biomarkers over geological

time. Preservation of microbial mats can be further enhanced by carbonate precipitation, subsequently leading to the formation of lithified structures commonly referred to as microbialites (Reid et al., 2000; Dupraz and Visscher, 2005; Dupraz et al., 2009). Highest sulfate-reduction rates in lithifying hypersaline mats have been recognised to be concomitant with areas of maximum carbonate precipitation (Visscher et al., 2000), confirming that sulfur cycling organisms play a significant role in lithification of modern stromatolites. In addition, the $\delta^{13}\text{C}$ of the bulk carbonate of layer 4 was measured and its depleted value (-9.7‰) corroborated a biologically-induced carbonate precipitation. A conceptual model summarising the various preservation processes observed in modern mats and relating these to biomarkers preservation is shown in Figure 6.12. This study provided a comprehensive analysis of microbial communities, characterisation of the surrounding environmental conditions and highlighted the significance of sulfur cycling for preservation pathways of biolipids in a modern stromatolite.

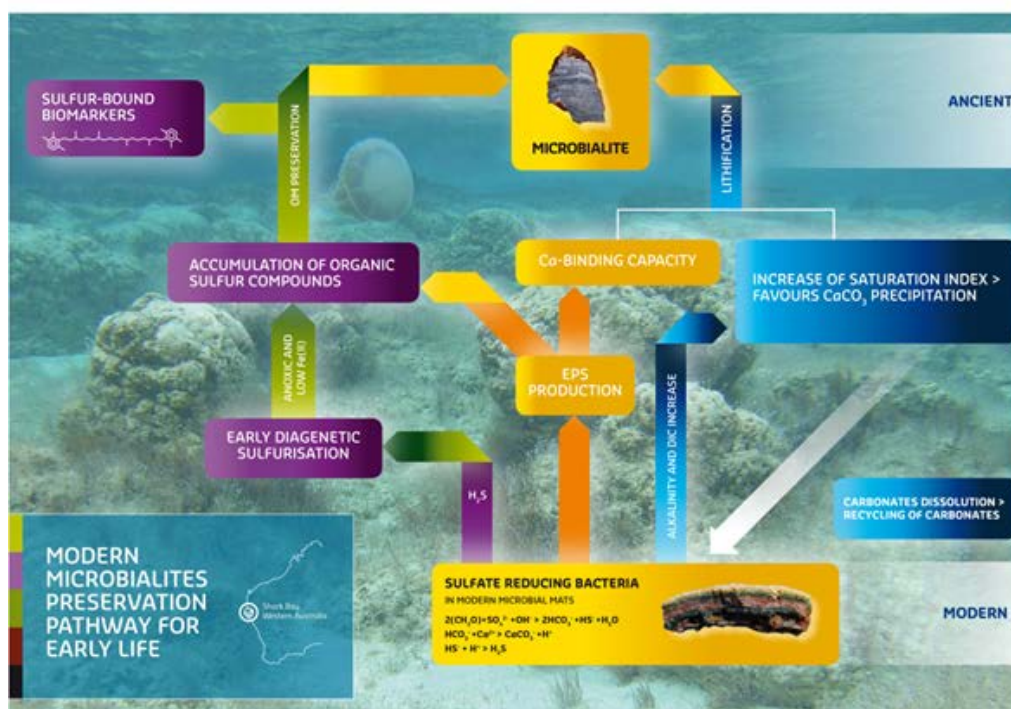


Figure 6.12: The role of sulfate-reducing bacteria in biosignature preservation. Sulfate-reducing bacteria produce H_2S that favour early diagenetic sulfurisation and preservation of organic matter under specific environmental conditions (anoxic, high sulfide and low Fe^{2+} concentrations). They also produce EPS (exo-polymeric substances) that tend to accumulate organic sulfur compounds favouring organic matter preservation and binds Ca^{2+} promoting lithification of the microbialite. Finally, bacterial sulfate-reduction raises the alkalinity favouring carbonate precipitation. Microbial mat lithification occurs if the precipitation of carbonates exceeds their dissolution by aerobic heterotrophs, sulfide oxidisers and fermenters.

Acknowledgements:

This research was supported by a grant from the Australian Research Council's Discovery Projects scheme (2010-2013, Grice, Greenwood, Snape and Summons). AP thanks WA-Organic and Isotope Geochemistry Centre, Curtin University and CSIRO for top-up scholarship. Geoff Chidlow is thanked for GC-MS technical support. Roger E. Summons and Carolyn L. K. Colonero are thanked for MRM GC-MS technical support and data interpretation. Taxon Biosciences is thanked for contribution with 16s *rRNA* analysis.

References

- Adam P., Schmid J. C., Mycke B., Strazielle C., Connan J., Huc A., Riva A. and Albrecht P. A.** (1993) Structural investigation of nonpolar sulfur cross-linked macromolecules in petroleum. *Geochim. Cosmochim. Acta* **57**, 3395–3419.
- Adam P., Schneckenburger P., Schaeffer P. and Albrecht P. A.** (2000) Clues to early diagenetic sulfurization processes from mild chemical cleavage of labile sulfur-rich geomacromolecules. *Geochim. Cosmochim. Acta* **64**, 3485–3503.
- Allen M. A., Goh F., Burns B. P. and Neilan B. A.** (2009) Bacterial, archaeal and eukaryotic diversity of smooth and pustular microbial mat communities in the hypersaline lagoon of Shark Bay. *Geobiology* **7**, 82–96.
- Allen M. A., Neilan B. A., Burns B. P., Jahnke L. L. and Summons R. E.** (2010) Lipid biomarkers in Hamelin Pool microbial mats and stromatolites. *Org. Geochem.* **41**, 1207–1218.
- Allwood A. C., Walter M. R., Kamber B. S., Marshall C. P. and Burch I. W.** (2006) Stromatolite reef from the Early Archaean era of Australia. *Nature* **441**, 714–718.
- Attaway D. H., Parker P. L. and Mears J. A.** (1970) Normal alkanes of five coastal spermatophytes. *Contrib. Mar. Sci.* **15**, 13–19.
- Baumgartner L. K., Spear J. R., Buckley D. H., Pace N. R., Reid R. P., Dupraz C. P. and Visscher P. T.** (2009) Microbial diversity in modern marine stromatolites, Highborne Cay, Bahamas. *Environ. Microbiol.* **11**, 2710–2719.
- Behrens A., Schaeffer P., Bernasconi S. and Albrecht P. A.** (2000) Mono- and bicyclic squalene derivatives as potential proxies for anaerobic photosynthesis in lacustrine sulfur-rich sediments. *Geochim. Cosmochim. Acta* **64**, 3327–3336.

- Blumenberg M., Krüger M., Nauhaus K., Talbot H. M., Oppermann B. I., Seifert R., Pape T. and Michaelis W.** (2006) Biosynthesis of hopanoids by sulfate-reducing bacteria (genus *Desulfovibrio*). *Environ. Microbiol.* **8**, 1220–7.
- Bobbie R. J. and White D. C.** (1980) Characterization of benthic microbial community structure by high-resolution gas chromatography of fatty acid methyl esters. *Appl. Environ. Microbiol.* **39**, 1212–1222.
- Boetius A., Ravensschlag K., Schubert C. J., Rickert D., Widdel F., Gieseke A., Amann R., Jørgensen B. B., Witte U. and Pfannkuche O.** (2000) A marine microbial consortium apparently mediating anaerobic oxidation of methane. *Nature* **407**, 623–626.
- Botello A. V. and Mandelli E. F.** (1978) Distribution of n-paraffins in seagrasses, benthic algae, oysters and recent sediments from Terminos Lagoon, Campeche, Mexico. *Bull. Environ. Contam. Toxicol.* **78**, 162–170.
- Boudou J. P., Trichet J., Robinson N. and Brassell S. C.** (1986) Profile of aliphatic hydrocarbons in a recent polynesian microbial mat. *Int. J. Environ. Anal. Chem.* **26**, 137–155.
- Burns B. P., Goh F., Allen M. A. and Neilan B. A.** (2004) Microbial diversity of extant stromatolites in the hypersaline marine environment of Shark Bay, Australia. *Environ. Microbiol.* **6**, 1096–1101.
- Canfield D. E. and Des Marais D. J.** (1991) Aerobic sulfate reduction in microbial mats. *Science*. **251**, 1471–1473.
- Canuel E. A., Freeman K. H. and Wakeham S. G.** (1997) Isotopic compositions of lipid biomarker in estuarine compounds plants and surface sediments. *Limnol. Oceanogr.* **42**, 1570–1583.
- Caporaso J. G., Kuczynski J., Stombaugh J., Bittinger K., Bushman F. D., Costello E. K., Fierer N. et al.** (2010) QIIME allows analysis of high-throughput community sequencing data. *Nat. Methods* **7**, 335–336.
- Cohen Z., Margheri M. C. and Tomaselli L.** (1995) Chemotaxonomy of cyanobacteria. *Phytochemistry* **40**, 1155–1158.
- Collister J. W., Rieley G., Stern B., Eglinton G. and Fry B.** (1994) Compound-specific $\delta^{13}\text{C}$ analyses of leaf lipids from plants with different carbon dioxide metabolism. *Org. Geochem.* **21**, 619–627.
- Davison W., Fones G. R., Harper M., Teasdale P. R. and Zhang H.** (2000) Dialysis, DET and DGT: in situ diffusional techniques for studying water, sediments and soils. In *In situ monitoring of aquatic systems: chemical analysis and speciation*. (eds. J. Buffle and G. Horvai). John Wiley & Sons, pp. 495–569.

- De Wit R. and Van Gernerden H.** (1988) Growth of the cyanobacterium *Microcoleus chthonoplastes* on sulfide. *FEMS Microbiol. Ecol.* **53**, 203–209.
- Dobson G., Ward D. M., Robinson N. and Eglinton G.** (1988) Biogeochemistry of hot spring environments: extractable lipids of a cyanobacterial mat. *Chem. Geol.* **68**, 155–179.
- Dunlop R. W. and Jefferies P. R.** (1985) Hydrocarbons of the hypersaline basins of Shark Bay, Western Australia. *Org. Geochem.* **8**, 313–320.
- Dupraz C. P. and Visscher P. T.** (2005) Microbial lithification in marine stromatolites and hypersaline mats. *Trends Microbiol.* **13**, 429–438.
- Dupraz C. P., Reid R. P., Braissant O., Decho A. W., Norman R. S. and Visscher P. T.** (2009) Processes of carbonate precipitation in modern microbial mats. *Earth-Science Rev.* **96**, 141–162.
- Edgcomb V. P., Bernhard J. M., Beaudoin D., Pruss S. B., Welander P. V, Schubotz F., Mehay S., Gillespie A. L. and Summons R. E.** (2013a) Molecular indicators of microbial diversity in oolitic sands of Highborne Cay, Bahamas. *Geobiology* **11**, 234–251.
- Eglinton G. and Hamilton R. J.** (1967) Leaf Epicuticular waxes. *Science* **156**, 1322–1335.
- Filley T. R., Freeman K. H. and Hatcher P. G.** (1996) Carbon isotope relationships between sulfide-bound steroids and proposed functionalized lipid precursors in sediments from the Santa Barbara Basin, California. *Org. Geochem.* **25**, 367–377.
- Fourçans A., de Oteyza T. G., Wieland a, Solé A., Diestra E., van Bleijswijk J., Grimalt J. O., Köhl M., Esteve I., Muyzer G., Caumette P. and Duran R.** (2004) Characterization of functional bacterial groups in a hypersaline microbial mat community (Salins-de-Giraud, Camargue, France). *FEMS Microbiol. Ecol.* **51**, 55–70.
- Freeman K. H., Wakeham S. G. and Hayes J. M.** (1994) Predictive isotopic biogeochemistry: hydrocarbons from anoxic marine basins. *Org. Geochem.* **21**, 629–644.
- Gelpi E., Schneider H., Mann J. and Oro J.** (1970) Hydrocarbons of geochemical significance in microscopic algae. *Phytochemistry* **9**, 603–612.
- Goh F., Allen M. A., Leuko S., Kawaguchi T., Decho A. W., Burns B. P. and Neilan B. A.** (2009) Determining the specific microbial populations and their spatial distribution within the stromatolite ecosystem of Shark Bay. *ISME J.* **3**, 383–396.

- Grice K., Schouten S., Nissenbaum A., Charrach J. and Sinninghe Damsté J. S.** (1998b) A remarkable paradox: sulfurised freshwater algal (*Botryococcus braunii*) lipids in an ancient hypersaline euxinic ecosystem. *Org. Geochem.* **28**, 195–216.
- Grimalt J. O., de Wit R., Teixidor P. and Albaigés J.** (1992) Lipid biogeochemistry of *Phormidium* and *Microcoleus* mats. *Org. Geochem.* **19**, 509–530.
- Grotzinger J. P. and Knoll A. H.** (1999) Stromatolites in Precambrian carbonates: evolutionary mileposts or environmental dipsticks? *Annu. Rev. Earth Planet. Sci.* **27**, 313–358.
- Hartgers W. A., Lopez J. F., Sinninghe Damsté J. S., Reiss C., Maxwell J. R. and Grimalt J. O.** (1997) Sulfur-binding in recent environments: II. Speciation of sulfur and iron and implications for the occurrence of organo-sulfur compounds. *Geochim. Cosmochim. Acta* **61**, 4769–4788.
- Hebting Y., Schaeffer P., Behrens A., Adam P., Schmitt G., Schneckenburger P., Bernasconi S. M. and Albrecht P. A.** (2006) Biomarker evidence for a major preservation pathway of sedimentary organic carbon. *Science* **312**, 1627–1631.
- Hoffman H. J.** (2000) Archean stromatolites as microbial archives. In *Microbial Sediments*. (eds. R.E. Riding, S. M. Awramik). Springer, Berlin, pp. 315–327.
- Innes H. E., Bishop A. N., Head I.M. and Farrimond P.** (1997) Preservation and diagenesis of hopanoids in recent lacustrine sediments of Priest Pot, England. *Org. Geochem.* **26**, 565–576.
- Jahnert R. and Collins L.** (2012) Characteristics, distribution and morphogenesis of subtidal microbial systems in Shark Bay, Australia. *Mar. Geol.* **303-306**, 115–136.
- Jahnert R. and Collins L.** (2013) Controls on microbial activity and tidal flat evolution in Shark Bay, Western Australia. *Sedimentology* **60**, 1071–1099.
- Jahnke L. L., Embaye T., Hope J., Turk K. A., Van Zuilen M., Des Marais D. J., Farmer J. D. and Summons R. E.** (2004) Lipid biomarker and carbon isotopic signatures for stromatolite-forming, microbial mat communities and *Phormidium* cultures from Yellowstone National Park. *Geobiology* **2**, 31–47.
- Kalkowsky, V. H. E.** (1908): Oolith und stromatolith im nord- deutschen Buntsandstein. *Z. Deut. Geol. Ges.* **60**, 231-242.
- Kenyon C. N., Rippka R. and Stanier R. Y.** (1972) Fatty acid composition and physiological properties of some filamentous blue-green algae. *Arch. Mikrobiol.* **83**, 216–236.
- Knief C., Altendorf K. and Lipski A.** (2003) Linking autotrophic activity in environmental samples with specific bacterial taxa by detection of ¹³C-labelled fatty acids. *Environ. Microbiol.* **5**, 1155–1167.

- Kohl W., Achenbach H. and Reichenbacht H.** (1983) The pigments of *Brevibacterium unens*: aromatic carotenoids. *Phytochemistry* **22**, 207–210.
- Kok M. D., Rijpstra W. I. C., Robertson L., Volkman J. K. and Sinnighe Damsté J. S.** (2000) Early steroid sulfurisation in surface sediments of a permanently stratified lake. *Geochim. Cosmochim. Acta* **64**, 1425–1436.
- Lepot K., Benzerara K., Brown G. E. and Philippot P.** (2008) Microbially influenced formation of 2, 724 million years old stromatolites. *Nat. Geosci.* **1**, 118–121.
- Logan B. W.** (1974) Evolution and diagenesis of Quarternary carbonate sequences, Shark Bay, Western Australia. *Am. Assoc. Pet. Geol. Mem.* **22**, 195–249.
- Londry K. L., Jahnke L. L. and Des Marais D. J.** (2004) Stable carbon isotope ratios of lipid biomarkers of sulfate-reducing bacteria. *Appl. Environ. Microbiol.* **70**, 745–751.
- Lopez J. F., de Oteyza T. G., Teixidor P. and Grimalt J. O.** (2005) Long chain alkenones in hypersaline and marine coastal microbial mats. *Org. Geochem.* **36**, 861–872.
- Mozingo R., Spencer C. and Folers C.** (1944) Hydrogenation by raney nickel catalyst without gaseous hydrogen. *J. Am. Chem. Soc.* **66**, 1859–1860.
- Nicholson J., Stolz J. F. and Pierson B.** (1987) Structure of a microbial mat at Great Sippewissett Marsh, Cape Cod, Massachusetts. *FEMS Microbiol. Ecol.* **45**, 343–364.
- Oren A.** (2002) Molecular ecology of extremely halophilic Archaea and Bacteria. *FEMS Microbiol. Ecol.* **39**, 1–7.
- Orphan V. J., Jahnke L. L., Embaye T., Turk K. a, Pernthaler a, Summons R. E. and Des Marais D. J.** (2008) Characterization and spatial distribution of methanogens and methanogenic biosignatures in hypersaline microbial mats of Baja California. *Geobiology* **6**, 376–393.
- Overmann J. and van Gemerden H.** (2000) Microbial interactions involving sulfur bacteria: implications for the ecology and evolution of bacterial communities. *FEMS Microbiol. Rev.* **24**, 591–599.
- Pagès A., Teasdale P. R., Robertson D., Bennett W. W., Schäfer J. and Welsh D. T.** (2011) Representative measurement of two-dimensional reactive phosphate distributions and co-distributed iron(II) and sulfide in seagrass sediment porewaters. *Chemosphere* **85**, 1256–1261.
- Pagès A., Welsh D. T., Robertson D., Panther J. G., Schäfer J., Tomlinson R. B. and Teasdale P. R.** (2012) Diurnal shifts in co-distributions of sulfide and iron(II) and profiles of phosphate and ammonium in the rhizosphere of *Zostera capricorni*. *Estuar. Coast. Shelf Sci.* **115**, 282–290.

- Pagès A., Grice K., Vacher M., Teasdale P., Welsh D., Bennett W. and Greenwood P.** (2014a) Characterising microbial communities and processes in a modern stromatolite (Shark Bay) using lipid biomarkers and two-dimensional distributions of porewater solutes. *Environ. Microbiol.*, accepted.
- Pancost R. D., van Geel B., Baas M. and Sinninghe Damsté J. S.** (2000) $\delta^{13}\text{C}$ values and radiocarbon dates of microbial biomarkers as tracers for carbon recycling in peat deposits. *Geology* **28**, 663–666.
- Paoletti C., Pushparaj B., Florenzano G., Capella P. and Lercker G.** (1976) Unsaponifiable matter of green and blue-green algal lipids as a factor of biochemical differentiation of their biomasses: I. Total unsaponifiable and hydrocarbon fraction. *Lipids* **11**, 258–265.
- Papineau D., Walker J. J., Mojzsis S. J. and Pace N. R.** (2005) Composition and structure of microbial communities from stromatolites of Hamelin Pool in Shark Bay, Western Australia. *Appl. Environ. Microbiol.* **71**, 4822–4832.
- Paul D., Skrzypek G. and Forizs I.** (2007) Normalization of measured stable isotope composition to isotope reference scale – a review. *Rapid Commun. Mass Spectrom.* **21**, 3006–3014.
- Powell T. G. and McKirdy D. M.** (1973) Relationship between ratio of pristane to phytane, crude oil composition and geological environment in Australia. *Nature* **243**, 37–39.
- Reid R. P., Visscher P. T., Decho A. W., Stolz J. F. and Bebout B. M.** (2000) The role of microbes in accretion, lamination and early lithification of modern marine stromatolites. *Nature* **406**, 989–992.
- Riding R.** (2000) Microbial carbonates: the geological record of calcified bacterial- algal mats and biofilms. *Sedimentology* **47**, 179–214.
- Robinson N. and Eglinton G.** (1990) Lipid chemistry of Icelandic hot spring microbial mats. *Org. Geochem.* **15**, 291–298.
- Rontani J.-F. and Volkman J. K.** (2005) Lipid characterization of coastal hypersaline cyanobacterial mats from the Camargue (France). *Org. Geochem.* **36**, 251–272.
- Schaeffer P., Reiss C. and Albrecht P. A.** (1995) Geochemical study of macromolecular organic matter from sulfur-rich sediments of evaporitic origin (Messinian of Sicily) by chemical degradations. *Org. Geochem.* **23**, 567–581.
- Semikhatov M. A., Gebelein C. D., Could P., Awramik S. M. and Benmore W. C.** (1979) Stromatolite morphogenesis-progress and problems. *Can. J. Earth Sci.* **16**, 992–1015.

- Shen Y., Buick R. and Canfield D. E.** (2001) Isotopic evidence for microbial sulphate reduction in the early Archaean era. *Nature* **410**, 77–81.
- Stal L. J.** (2001) Coastal microbial mats: the physiology of a small-scale ecosystem. *South African J. Bot.* **67**, 399–410.
- Summons R. E. and Powell T. G.** (1986) *Chlorobiaceae* in Paleozoic seas revealed by biological markers, isotopes and geology. *Nature* **319**, 763–765.
- Summons R. E., Barrow R., Capon R., Hope J. and Stranger C.** (1993) The structure of a new C₂₅ isoprenoid alkene biomarker from diatomaceous microbial communities. *Aust. J. Chem.* **46**, 907.
- Summons R. E., Jahnke L. L. and Roksandic Z.** (1994) Carbon isotopic fractionation in lipids from methanotrophic bacteria: Relevance for interpretation of the geochemical record of biomarkers. *Geochim. Cosmochim. Acta* **58**, 2853–2863.
- Summons R. E., Bird L. R., Gillespie A L., Pruss S. B., Roberts M. and Sessions A. L.** (2013) Lipid biomarkers in ooids from different locations and ages: evidence for a common bacterial flora. *Geobiology* **11**, 420–436.
- Talbot H. M., Summons R. E., Jahnke L. L., Cockell C. S., Rohmer M. and Farrimond P.** (2008) Cyanobacterial bacteriohopanepolyol signatures from cultures and natural environmental settings. *Org. Geochem.* **39**, 232–263.
- Taylor J. and Parkes R. J.** (1983) The cellular fatty acids of the sulphate-reducing bacteria. *J. Gen. Microbiol.* **129**, 3303–3309.
- Taylor J. and Parkes R. J.** (1985) Identifying different populations of sulphate-reducing bacteria within marine sediment systems, using fatty acid biomarkers. *Microbiology* **131**, 631–642.
- Thamdrup B., Fossing H. and Jørgensen B. B.** (1994) Manganese, iron, and sulfur cycling in a coastal marine sediment, Aarhus Bay, Denmark. *Geochim. Cosmochim. Acta* **58**, 5115–5129.
- Thiel V., Peckmann J., Richnow H. H., Luth U., Reitner J. and Michaelis W.** (2001) Molecular signals for anaerobic methane oxidation in Black Sea seep carbonates and a microbial mat. *Mar. Chem.* **73**, 97–112.
- Thiel V., Blumenberg M., Pape T., Seifert R. and Michaelis W.** (2003) Unexpected occurrence of hopanoids at gas seeps in the Black Sea. *Org. Geochem.* **34**, 81–87.
- Van Gernerden H.** (1993) Microbial mats: A joint venture. *Mar. Geol.* **113**, 3–25.
- Van Kranendonk M., Philippot P., Lepot K., Bodorkos S. and Pirajno F.** (2008) Geological setting of Earth's oldest fossils in the ca. 3.5Ga Dresser Formation, Pilbara Craton, Western Australia. *Precambrian Res.* **167**, 93–124.

- Van Lith Y., Warthmann R., Vasconcelos C. and McKenzie J. A.** (2003) Sulphate-reducing bacteria induce low-temperature Ca-dolomite and high Mg-calcite formation. *Geobiology* **1**, 71–79.
- Vasconcelos C., Warthmann R., McKenzie J. A., Visscher P. T., Bittermann A. G. and van Lith Y.** (2006) Lithifying microbial mats in Lagoa Vermelha, Brazil: Modern Precambrian relics? *Sediment. Geol.* **185**, 175–183.
- Vestal J. R. and White D. C.** (1989) Lipid Analysis Microbial Ecology. *Bioscience* **39**, 535–541.
- Viaroli P., Bartoli M., Giordani G., Magni P. and Welsh D. T.** (2004) Biogeochemical indicators as tools for assessing sediment quality/vulnerability in transitional aquatic ecosystems. *Aquat. Conserv. Mar. Freshw. Ecosyst.* **14**, S19–S29.
- Visscher P. T., Reid R. P., Bebout B. M., Hoefft S. E. H., Macintyre I. G. and Thompson Jr. J. A.** (1998) Formation of lithified micritic laminae in modern marine stromatolites (Bahamas): the role of sulfur cycling. *Am. Mineral.* **83**, 1482–1493.
- Visscher P. T., Reid R. P. and Bebout B. M.** (2000) Microscale observations of sulfate reduction: Correlation of microbial activity with lithified micritic laminae in modern marine stromatolites. *Geology* **2**, 919–922.
- Volkman J. K.** (1986) A review of sterol markers for marine and terrigenous organic matter. *Org. Geochem.* **9**, 83–99.
- Volkman J. K., Barrett S. M., Blackburn S. I., Mansour M. P., Sikes E. L. and Gelin F.** (1998) Microalgal biomarkers: a review of recent research developments. *Org. Geochem.* **29**, 1163–1179.
- Wakeham S. G., Sinninghe Damsté J. S., Kohnen M. E. L. and de Leeuw J. W.** (1995) Organic sulfur compounds formed during early diagenesis in Black Sea sediments. *Geochim. Cosmochim. Acta* **59**, 521–533.
- Walter M. R., Buick R. and Dunlop J. S. R.** (1980) Stromatolites 3,400–3,500 Myr old from the North pole area, Western Australia. *Nature* **284**, 443–445.
- Ward, J. H. J.** (1963) Hierarchical grouping to optimize an objective function. *J. Am. Stat. Assoc.* **58**, 236–244.
- Warthmann R., Vasconcelos C., Bittermann A. and McKenzie J.** (2011) The role of purple sulphur bacteria in carbonate precipitation of modern and possibly early precambrian stromatolites. In *Advances in stromatolites biology. Lecture notes in Earth Sciences* (eds. J. Reitner, M. H. Trauth, K. Stüwe, D. Yuen), pp. 141–149.
- Welsh D. T.** (2000) Ecological significance of compatible solute accumulation by microorganisms: from single cells to global climate. *FEMS Microbiol. Rev.* **24**, 263–290.

- Wieland A., Zopfi J., Benthien M. and Kühl M.** (2005) Biogeochemistry of an iron-rich hypersaline microbial mat (Camargue, France). *Microb. Ecol.* **49**, 34–49.
- Wilkinson S. G.** (1988) Gram-negative bacteria. In *Microbial Lipids* (eds. C. Ratledge, S. G. Wilkinson). Academic Press, London, pp. 299–489.
- Winters K., Parker P. L. and Van Baalen C.** (1969) Hydrocarbons of blue-green algae: geochemical significance. *Science* **163**, 467–468.
- Zelles L., Bai Q. Y., Rackwitz R., Chadwick D. and Beese F.** (1995) Determination of phospholipid- and lipopolysaccharide-derived fatty acids as an estimate of microbial biomass and community structures in soils. *Biol. Fertil. Soils* **19**, 115–123.
- Zhang H. and Davison W.** (1995) Performance characteristics of diffusion gradients in thin films for the in situ measurement of trace metals in aqueous solution. *Anal. Chem.* **67**, 3391–3400.

Chapter 7

Investigation of biomarker distributions in a Paleoproterozoic microbial mat from the Turee Creek group, Pilbara, Western Australia

Anais Pagès, Kliti Grice, Lorenz Schwark, Robert Lockhart, David Flannery, Martin van
Kranendonk

In preparation

Chapter 7

Introduction

Geology and Methods

- Geological context
- Sample description
- Organic geochemical analysis
 - Sampling
 - Extraction
 - Column chromatography
 - Hydropyrolysis (HyPy)
 - Carbonate dissolution
 - Gas-Chromatography Mass-Spectrometry (GC-MS)
 - Procedure followed for the analysis of the samples

Results

- Free saturated and alcohol hydrocarbons
- Saturated hydrocarbons after HyPy on kerogen
- Carbonate-bound saturated and alcohol hydrocarbons
- Saturated hydrocarbons after HyPy on carbonate-free kerogen

Discussion

- Diagenetic features of carbonates
- Raman spectroscopy analysis of the microbial mat
- Comparison with two additional samples from the Turee Creek group
- HyPy technique evaluation

Conclusions

Abstract

Hydropyrolysis (HyPy) technique was applied to a Paleoproterozoic (2.3 billion years old) fossilised microbial mat from a thick dolostone unit of the Turee Creek Group, in the Pilbara region of Western Australia. HyPy is known as a reliable method to release kerogen-bound biomarkers that can be unequivocally associated with the stratigraphic interval of the sample. No steranes or hopanes were identified from the freely extractable saturated fraction. After applying HyPy to the kerogen, C₂₇, C₂₈ and C₂₉ steranes and diasteranes in both 20*S* and 20*R* configurations were observed, but with a slight predominance of 20*S* isomers. After dissolving the carbonates present in the kerogen, carbonate-bound steranes and sterols were identified. No steranes were detected after application of HyPy on the carbonate-free kerogen, implying that the previously obtained steranes came from the carbonate-bound steranes and sterols. A thin-section investigation of carbonates in the sample revealed that no post-diagenetic re-precipitation of carbonate occurred; suggesting that carbonate mineral precipitation was generally contemporaneous with formation and diagenetic recrystallisation of the microbial mat. Raman spectroscopy revealed a spectrum similar to other low-metamorphic grade, old carbonate rocks and matched the lowest temperature spectrum for the kerogen formation. A comparison of biomarkers with two additional samples of sedimentary rocks from the Turee Creek Group (clotted microbial mat and stromatolite) confirmed that steroids were only present in the laminated smooth mat. Additional work will be performed to confirm the indigenous signature of steroids in this sample.

Introduction

Although microfossils have demonstrated the first evidence of eukaryotes on Earth up to 1.78–1.68 Gyr ago (Knoll et al., 2006), hydrocarbon biomarkers can also provide insight into the diversity and evolution of life and possibly indicate an earlier appearance of eukaryotes. In Proterozoic samples, biomarkers have been studied to provide informative results regarding the origin of organic matter from the host stratigraphic interval (Summons et al., 1988; Summons and Walter, 1990). However, Proterozoic and Archean samples are commonly highly mature and do not contain high quantity of extractable biomarkers, making these samples prone to contamination from non-indigenous hydrocarbons. Nevertheless, the presence of oil in Archean fluid inclusions (Dutkiewicz et al., 1998) and significant hydrocarbon stability over a range of metamorphic/hydrothermal conditions (Mango, 1991) have been reported, suggesting that biomarkers can be preserved in ancient low-grade rocks. In addition, specific sampling techniques and rigorous laboratory procedures have been developed in order to minimise and identify any possible contamination (Peters and Moldowan, 1993). HyPy is one of the techniques that has been developed in order to release indigenous biomarkers from ancient samples. This method allows the release of kerogen-bound biomarkers with a minimum structural rearrangement (Love et al., 1995). The products released after HyPy are recognised to be unambiguously associated with the specific stratigraphic interval of the sample (Love et al., 1995, 2009). Consequently, this analytical technique appears to be a powerful tool to reveal hydrocarbons in Proterozoic samples. In this study, HyPy was applied to an exceptionally well preserved Proterozoic fossilised microbial mat from the ca. 2.3 billion-year-old Turee Creek Group in the Ashburton region of Western Australia. A variety of analytical techniques were used to investigate the distribution of kerogen-bound and carbonate-bound biomarkers. Complimentary thin-sections and Raman spectroscopy analysis were also performed to characterise the diagenetic features of carbonates and the temperature of metamorphism associated with the geological setting of the sample.

Geology and methods

- **Geological context**

The studied microbial mat was collected from the Paleoproterozoic (ca. 2.4-2.3 Gyr) Turee Creek Group of Western Australia (Trendall, 1979). The microbial mat grew under very shallow water conditions during carbonate precipitation and was partly recrystallized during early diagenesis. The mat was partly silicified when the unit was periodically exposed to subaerial conditions, as evidenced by the fact that silicified stromatolite beds are cut by carbonate dewatering veins in nearby tepee structures. The rocks were deformed during the Paleoproterozoic Ophthalmian and Capricorn orogenies about 2.2 and 1.8 billion years ago (Rasmussen et al., 2005; Muller et al., 2005). The rocks then remained intact until the Phanerozoic evolution of Australia, first through glacial peneplanation at 250 Ma, when the rocks were brought to near-surface levels, and then by deep tropical weathering when Fe was redistributed through the rocks along fractures (e.g., Pillans, 2005).

- **Sample description**

The sample collected for organic geochemical analysis came from a 600 m thick unit of predominantly stromatolitic dolostone from the upper part of the Turee Creek Group. The sample was a millimetre-laminated microbial mat comprising alternating dark brown-weathering, siliceous layers, and blue-grey dolomite layers (Figure 7.1). Lamination was generally smooth, but defines low amplitude (5-10 cm), large wavelength (2-3 m) domes, and oncolites and imbricate flat-pebble conglomerates were locally developed indicative of a microbial origin. The sampled mat lied between layers with small to large stromatolites that varied in shape from columnar, to domical, to club-shaped, some of which were up to 2m high.

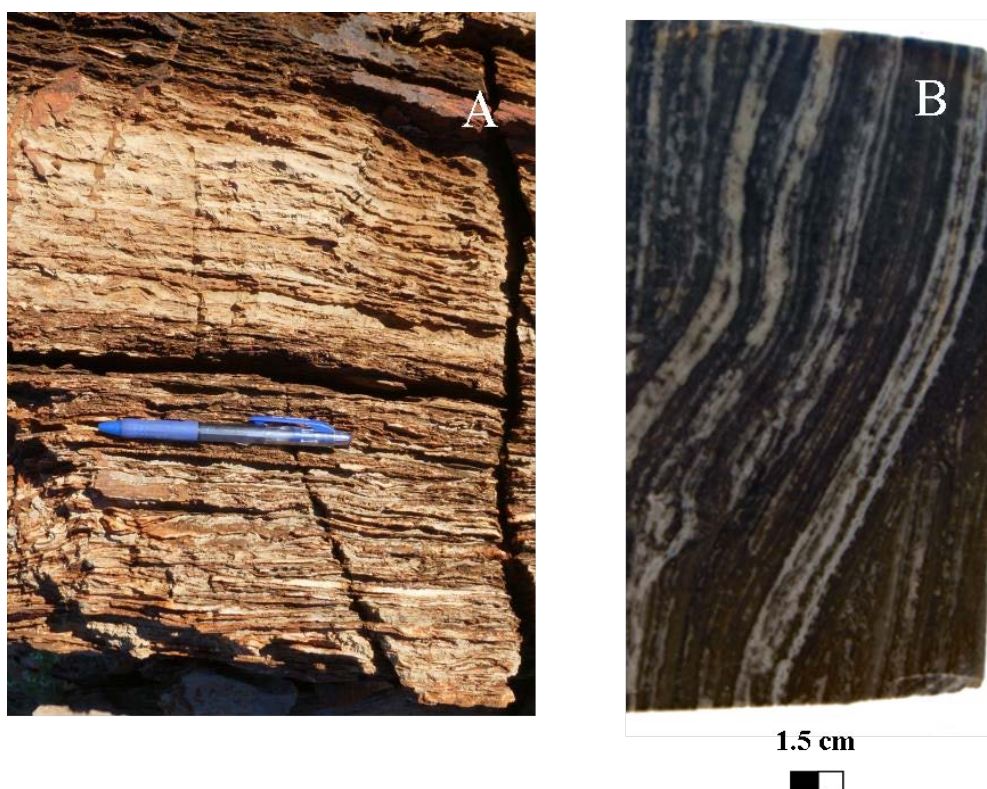


Figure 7.1: (A) Photograph of the outcrop microbial mat and (B) photograph of a fresh surface of the mat.

Organic geochemical analysis

➤ *Sampling*

The microbial mat was sampled in the field and immediately stored in aluminium foil. Three different aliquots of the microbial mat were analysed in order to confirm the validity of the results. Prior to grinding, the samples were pre-washed five times with dichloromethane (DCM) and left in an ultrasonic bath for 30 minutes each time. Each rinse was analysed chromatographically until no more hydrocarbons were detected. Using a rock saw, the edges were removed. The samples were then grinded. Annealed sand was ground three times before and after each sample to avoid any contamination. Samples of the annealed sand were kept for further analysis.

➤ *Extraction*

A powdered aliquot of each microbial mat aliquot was Soxhlet extracted using a 9: 1 (v/v) mixture of [DCM: methanol (MeOH)]. Activated copper turnings were added to remove elemental sulfur. Each aliquot was extracted for 3 days. Excess solvent was removed from the extract by rotary evaporation. Soxhlet extractions of the annealed sand used to clean the grinder, as well as all solvents used in the experimental work, were also undertaken. To avoid contamination, no gloves were used when processing the samples, which were very carefully handled to avoid any direct contact. The syringe used to transfer the bitumens was cleaned for a minimum of 20 times between each sample. Procedural blanks were performed throughout the entire experiments and confirm that the compounds identified belonged to the sample.

➤ *Column chromatography*

The extracts were separated by a small column (5.5 cm x 0.5 cm i.d.) filled with activated silica gel (120 °C, 8 h). The saturated hydrocarbon fractions were eluted with *n*-hexane (2 mL); the aromatic hydrocarbon fractions with a mixture of DCM in *n*-hexane (2 mL, 30 %); the fatty acid fractions with DCM (2 mL), the alcohol fractions with a mixture of ethyl acetate in DCM (2 mL, 20%) and the polar fractions with a mixture of equal parts of DCM and MeOH (2 mL). The saturated and aromatic hydrocarbon fractions as well as the fatty acids and alcohols fractions were reduced to near dryness with a N₂ purge and the fractions analysed by gas chromatography - mass spectrometry (GC-MS). The saturated hydrocarbons and alcohol fractions are presented in this study.

➤ *HydroPyrolysis (HyPy)*

Complimentary biomarkers were obtained after applying catalytic HyPy to the residual kerogen. This technique allows the release of biomarkers covalently bound to the macromolecular matrix of the kerogen (Love et al., 1995). HyPy is conducted at high pressure hydrogen (15 MPa) and requires the use of a sulfided molybdenum catalyst [(NH₄)₂MoO₂S₂]. HyPy has been proved to be exceptionally efficient in releasing

strongly-bound or highly functionalised biomarkers with optimum preservation of structural arrangement (Love et al., 1995).

HyPy was applied to the residual kerogen prior and after carbonates removal using the method described in detail previously (Love et al., 1995). The sample was pyrolysed with resistive heating from 50 °C to 250 °C at 250 °C.min⁻¹, then from 250 °C to 500 °C at 8 °C.min⁻¹. The system was maintained under a constant hydrogen pressure of 15 MPa. The sweep gas flow of 5 L.min⁻¹ allowed the products to be rapidly removed from the reactor before collection in a trap filled with silica and cooled with dry ice (Meredith et al., 2004).

➤ *Carbonate dissolution*

Carbonates from the microbial mat were dissolved using the method described by Pearson et al., 2005. 37 %v/v HCl and distilled water were pre-cleaned using DCM. Three aliquots were weighed (30-32g) and each aliquot was slowly transferred to a 200 mL beaker containing 30 mL of 25 % v/v HCl. Additional 5 mL aliquot of 37 %v/v HCl was slowly added to maintain the reaction (final volume: 70 mL). After total dissolution of carbonates, 30 mL MeOH was added to the mixture. After shaking, the miscible solution was transferred to 200 mL round bottom flasks (1). The beaker was washed 3 times using 10 mL aliquots of methanol which were then added to the flask. 75 mL of DCM was added to the flask and the solution was vigorously shaken. Two layers were formed in the flask (the upper one contained water and MeOH while the lower one contained DCM and MeOH). The upper layer was transferred to another round bottom flask (2) and left aside until complete decantation. Another 75 ml aliquot of DCM was added and the flask vigorously shaken to complete the extraction of MeOH. 75 mL of water was then added to the flask (1), in order to remove excess methanol from the DCM/MeOH layer. The lower layers from flasks (1) and (2) were combined and shaken with additional water in order to remove any trace of MeOH. DCM was carefully pipetted out to another round bottom flask and was evaporated by rotary evaporator.

➤ *Analysis of samples by Gas Chromatography – Mass Spectrometry*

GC-MS analyses were performed with a Hewlett Packard 6890 gas chromatograph (GC) interfaced to a Hewlett Packard 5973 mass selective detector. The aromatic and saturated hydrocarbon fractions, dissolved in *n*-hexane, and the fatty acids and alcohols fractions, dissolved in DCM, were introduced *via* the Hewlett Packard 6890 Series Injector into the electronically pressure controlled (EPC) split/splitless injector (320 °C), which was operated in the pulsed splitless mode. The GC was fitted with a 60 m x 0.25 mm i.d. WCOT fused silica capillary column coated with a 0.25 µm film (DB-5MS, J&W Scientific). The oven temperature was programmed from 40 °C to 325 °C (at 3 °C.min⁻¹) with the initial and final hold times of 1 and 50 min, respectively. Ultra high purity helium was used as the carrier gas and maintained at a constant flow of 1.1 mL.min⁻¹. The MSD was operated at 70 eV and the mass spectra were acquired in full scan mode, 50-600 Daltons at ~ 4 scans per second and a source temperature of 230 °C.

➤ *Procedure followed for the analysis of the samples*

After Soxhlet extraction, an aliquot of the extracted sample (kerogen) was used for HyPy analysis and the hydropyrolysate extract was further analysed by GC-MS. Another aliquot of the kerogen was used to investigate carbonate-bound biomarkers. HCl treatment was applied to the kerogen and the carbonate-bound biomarkers were further extracted and analysed by GC-MS. The carbonate-free kerogen was then used for HyPy and the hydropyrolysate extract was further analysed by GC-MS and compared to the previously obtained HyPy results. This procedure is summarised in [Figure 7.2](#). The entire procedure was repeated on three aliquots of the sample.

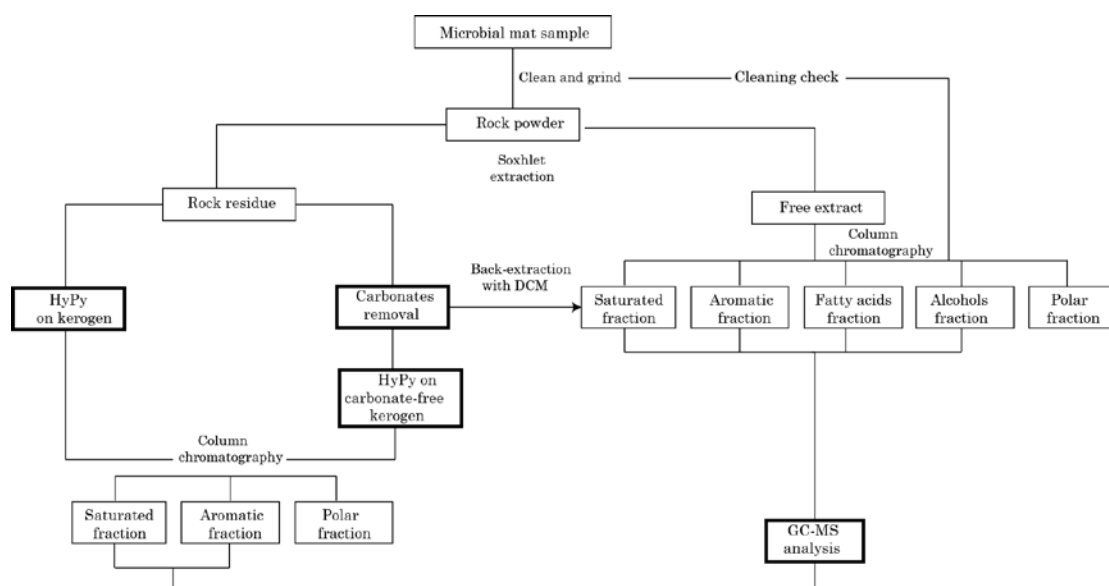


Figure 7.2: Flow chart of the experimental procedure.

Two additional samples from the Turee Creek group were also analysed (a stromatolite and a clotted microbial mat). The free and carbonate-bound biomarkers were analysed in these samples in order to compare the carbonate-bound biomarker signatures in the different samples.

Results

- **Free saturated and alcohol hydrocarbons**

The free saturated fraction of the sample was dominated by *n*-alkanes, ranging from C₁₇ to C₃₃ (Figure 7.3). Pristane and phytane were also present. However, no steranes were detected in this fraction.

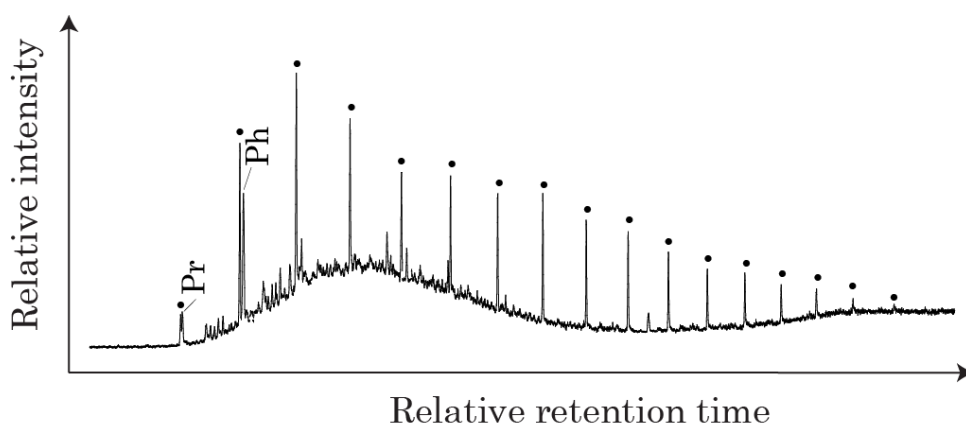


Figure 7.3: Total Ion Chromatogram (TIC) of the freely extractable saturated hydrocarbons measured by Gas Chromatography-Mass Spectrometry (GC-MS).

The free alcohol fraction revealed the presence of sterols: 24-ethylcholest-5-en-3 β -ol (sitosterol) and 24-ethyl-5 α -cholestan-3 β -ol (sitostanol) and steroid ketones (Figure 7.4 and Table 7.1). Sitosterol is one of the most abundant sterols in higher plants, although C₂₉ sterols have also been reported in unicellular algae (Volkman et al., 1986 for a review). Sitostanol is most likely derived from the microbial reduction of the corresponding Δ^5 sterol (sitosterol) which is being controlled by the redox potential (Nishimura and Koyama, 1977; Nishimura, 1978).

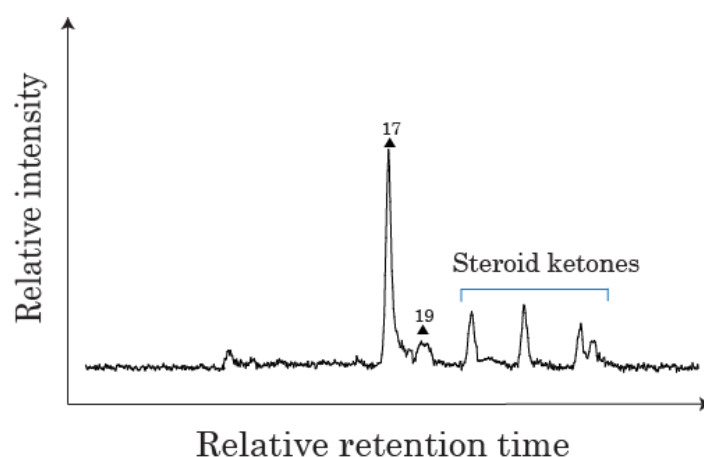


Figure 7.4: TIC of the freely extractable alcohol hydrocarbons measured by GC-MS.

- **Saturated hydrocarbons after HyPy on kerogen**

HyPy was applied to the kerogen of the sample in order to reveal indigenous biomarkers. After applying HyPy to the kerogen, a wide range of steroids were revealed (Figure 7.5 and Table 7.1). Steranes between C₂₇ and C₂₉ were observed. C₂₇ and C₂₈ βα and αβ diasteranes and C₂₉ βα diasteranes were present in the 20*R* and 20*S* configurations but the thermally mature 20*S* configuration appeared to be the most dominant one. Diasteranes usually derive from the conversion of sterols to diasterenes occurring in presence of acidic sites on clays (illite or montmorillonite) (Sieskind et al., 1979). Acidic and oxic conditions can also favour the formation of diasterenes (Moldowan et al., 1986) which can be further reduced predominantly to 13β,17α(H) based diasteranes and in lower proportion, to 13α,17β(H) based diasteranes. C₂₇ steranes (ααα and αββ configurations) were also present in both 20*R* and 20*S* configurations. Traces of C₂₈ and C₂₉ steranes were also observed from the *m/z* = 217 chromatogram. This steroid hydrocarbon distribution revealed after HyPy on kerogen presented a thermally mature sample.

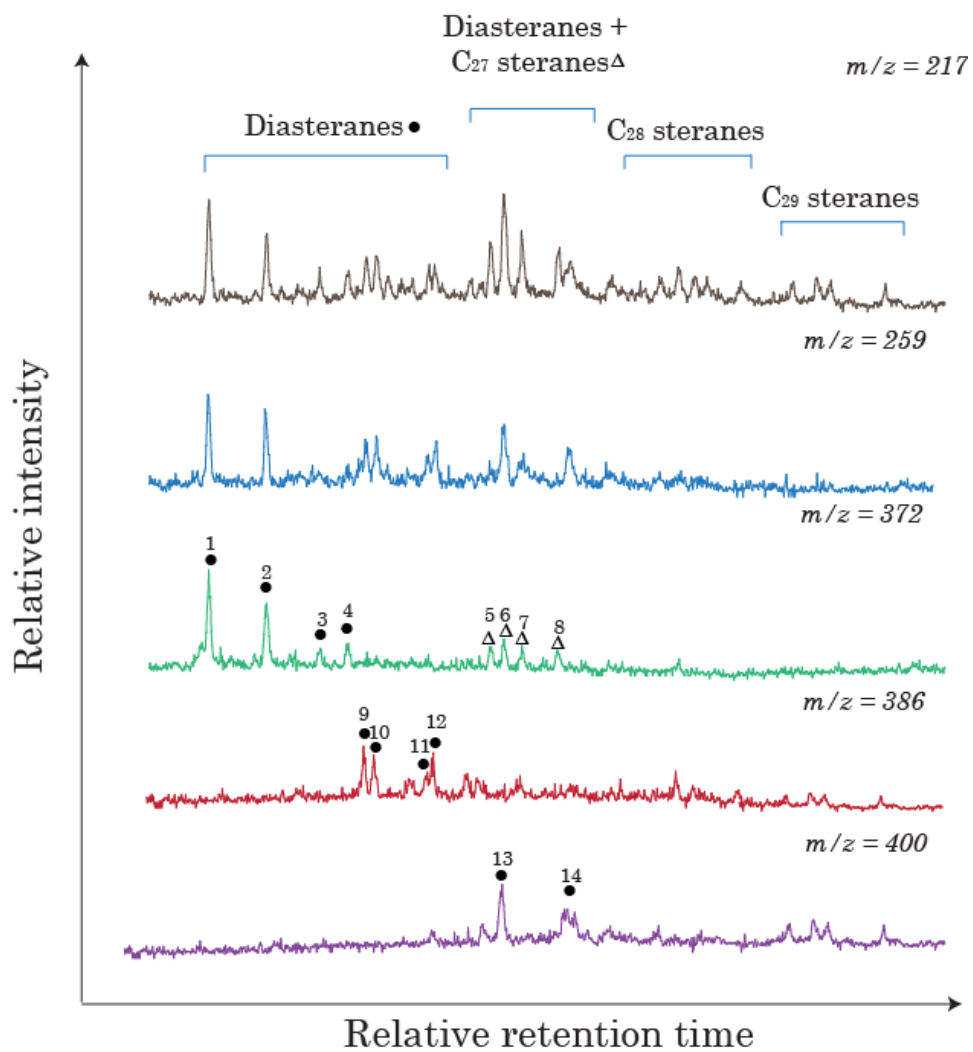


Figure 7.5: Mass fragmentograms of the saturated hydrocarbons, measured by GC-MS, after applying HyPy on the kerogen.

Table 7.1: Identification of steranes and sterols in the sample.

Peak	Compound name
STERANES	
1•	C ₂₇ 13 β ,17 α (H) diacholestane 20 <i>S</i>
2•	C ₂₇ 13 β ,17 α (H) diacholestane 20 <i>R</i>
3•	C ₂₇ 13 α ,17 β (H) diacholestane 20 <i>S</i>
4•	C ₂₇ 13 α ,17 β (H) diacholestane 20 <i>R</i>
5 Δ	C ₂₇ 5 α ,14 α ,17 α (H) cholestane 20 <i>S</i>
6 Δ	C ₂₇ 5 α ,14 β ,17 β (H) cholestane 20 <i>R</i>
7 Δ	C ₂₇ 5 α ,14 β ,17 β (H) cholestane 20 <i>S</i>
8 Δ	C ₂₇ 5 α ,14 α ,17 α (H) cholestane 20 <i>R</i>
9•	C ₂₈ 13 β ,17 α (H) 24-methyldiacholestane 20 <i>S</i>
10•	C ₂₈ 13 β ,17 α (H) 24-methyldiacholestane 20 <i>R</i>
11•	C ₂₈ 13 α ,17 β (H) 24-methyldiacholestane 20 <i>S</i>
12•	C ₂₈ 13 α ,17 β (H) 24-methyldiacholestane 20 <i>S</i>
13•	C ₂₉ 13 β ,17 α (H) 24-ethyldiacholestane 20 <i>S</i>
14•	C ₂₉ 13 β ,17 α (H) 24-ethyldiacholestane 20 <i>R</i>
STEROLS	
15▲	Cholest-5-en-3 β -ol
16▲	24-ethylcholesta-5,22-dien-3 β -ol
17▲	24-ethylcholest-5-en-3 β -ol
18▲	24-ethylcholesta-5,24 (28)-dien-3 β -ol
19▲	24-ethyl-5 α -cholestan-3 β -ol
20▲	24-methyl-9,19 cyclolanost-25-en-3 β -ol

- **Carbonate-bound saturated and alcohol hydrocarbons**

Carbonates from the kerogen were dissolved in order to analyse carbonate-bound biomarkers. Similarly to the steroid fraction after HyPy on kerogen, diasteranes ($\beta\alpha$ configuration) were dominant in the sample (Figure 7.6). However, based on the $m/z = 372$ and $m/z = 386$ chromatograms, no C_{27} $13\alpha,17\beta$ (H) diacholestanes and no C_{28} diasteranes were detected in the fraction. As in the HyPy fraction, C_{27} steranes were present in relatively low abundance.

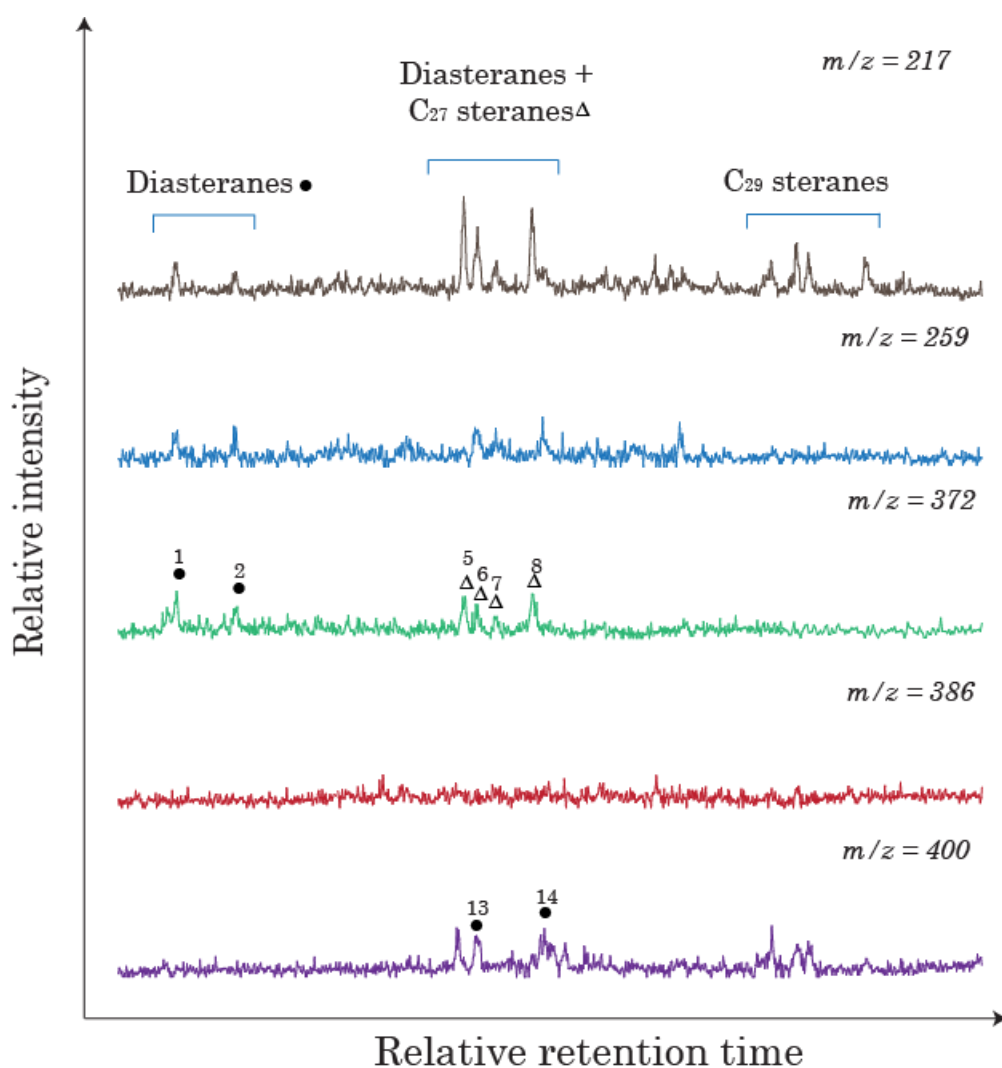


Figure 7.6: Mass fragmentograms of the carbonate-bound saturated hydrocarbons measured by GC-MS.

Carbonate-bound sterols were also analysed and revealed a strong predominance of C₂₉ sterols (Figure 7.7). Cholesterol was a minor component of the fraction while stigmasterol (24-ethylcholesta-5,22-dien-3 β -ol), sitosterol and 24-ethylcholesta-5,24(28)-dien-3 β -ol were more abundant. The 24-methyl-9,19 cyclolanost-25-en-3 β -ol (cyclolaudenol) was also present in the fraction. Although this steroid is commonly recognised as a plant biomarker (Goodwin, 1985), it has also been reported in colourless sulfur-oxidising bacteria (McCaffrey et al., 1989).

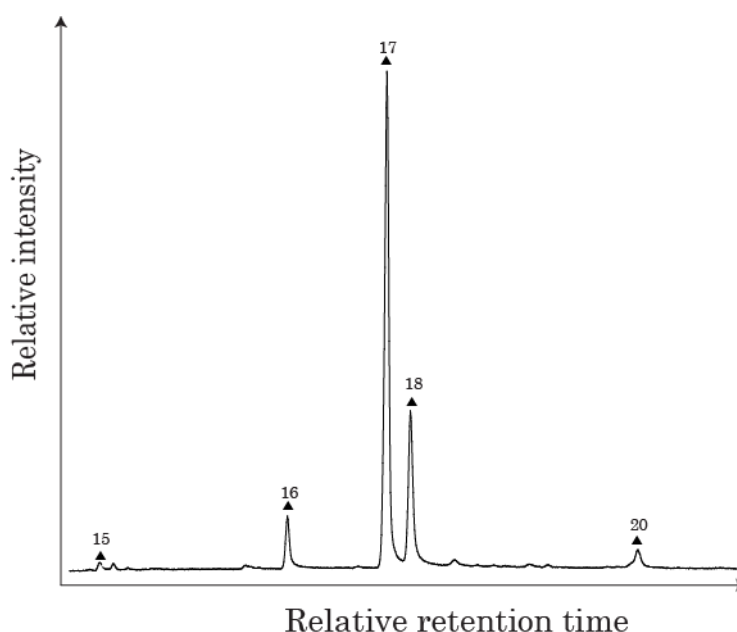


Figure 7.7: Total Ion Chromatogram of the carbonate-bound alcohol hydrocarbons measured by GC-MS.

- **Saturated hydrocarbons after HyPy on carbonate-free kerogen**

HyPy was then applied to the carbonate-free kerogen. In contrast with the saturated fraction obtained after HyPy on the kerogen, no steranes were detected (Figure 7.8). Only *n*-alkanes ranging from C₁₆ to C₃₄ were present. The total absence of steranes in this fraction implied that the steranes observed after HyPy on the kerogen originated from carbonate-bound steranes and carbonate-bound sterols that were further converted to steranes during the HyPy process.

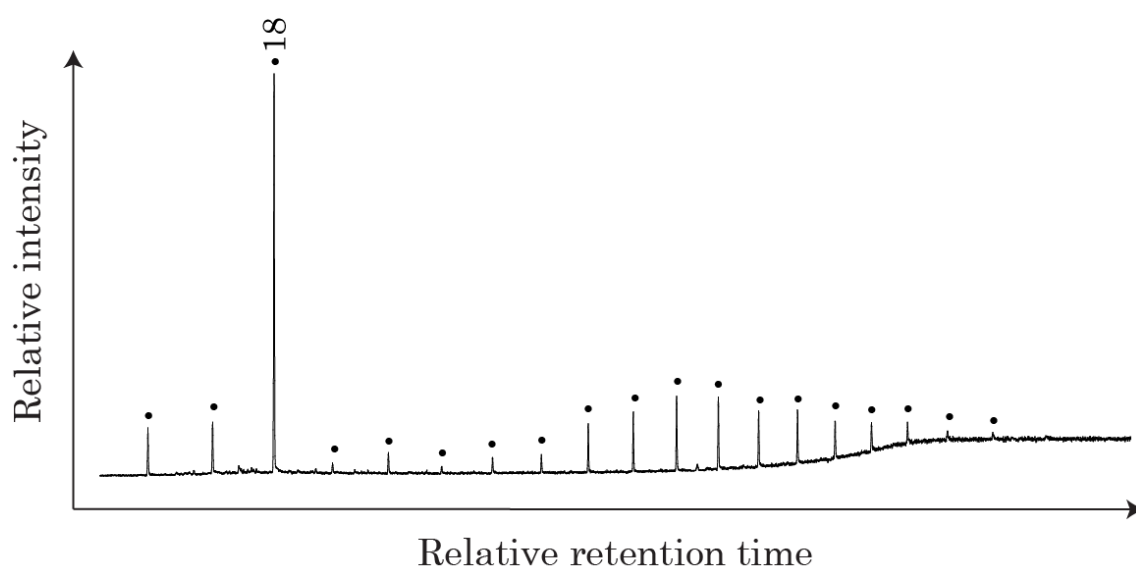


Figure 7.8: Total Ion Chromatogram of the saturated hydrocarbons, measured by GC-MS, after HyPy on carbonate-free kerogen.

Discussion

In order to obtain the hydrocarbon fraction indigenous to the sample and not affected by post-contamination, HyPy was applied to the kerogen. Kerogen-bound hydrocarbons released by HyPy are recognised to undertake minimal structural rearrangement and can be unequivocally associated with specific stratigraphic intervals (Love et al., 1995). Carbonates were dissolved from another aliquot of the kerogen in order to ensure the analysis of carbonate-bound biomarkers. After dissolution of carbonates and subsequent extraction of carbonate-bound biomarkers, steranes were identified as well as sterols. However, after applying HyPy on the carbonate-free kerogen, no steranes were identified, confirming the presence of steroid biomarkers exclusively entrapped in the carbonates. The simple steroid pattern observed in the carbonate-bound fraction could reflect a primitive steroid evolution after the Great Oxidation Event. Consequently, these results could be highly significant regarding the evolution of life and the rise of eukaryotes. Indeed, the oldest fossil evidence for eukaryotes has been found at 1.78–1.68 Gyr ago (Knoll et al., 2006). Since these biomarkers were found in the carbonate fraction only, detailed analysis of thin-sections were performed to try to characterise the diagenetic features of carbonate.

- **Diagenetic features of carbonate**

Analysis of thin sections reveal that the microbial mat was principally composed of fine-grained, thinly-bedded dolomite, with well-developed palisade structure (Figure 7.9A) and local neomorphic recrystallisation to rhombic (sparry) carbonate (Figure 7.9B). The observed palisade structure was similar to herringbone cements observed in many well-preserved carbonates. Such texture has been nicely preserved in outcrops from the area. The cements were early diagenetic and indicated a low degree of recrystallization since deposition at 2.3 Gyr. In places, the recrystallised dolomite became coarser grained, forming two distinct phases of carbonate. Two carbonates phases were detected, both showing early diagenetic features and interlayered at a 1-3mm scale. A first, fine-grained dolomite was dark and well laminated, defining bedding. This was cut by a second phase that was coarser-grained and discordant to bedding (Figure 7.9C). In some samples, the coarse-grained dolomite was associated with macroquartz (Figure 7.9D). From the rhombic shape of the carbonate crystals in the quartz, it clearly appeared that the carbonate and the quartz formed at the same time. No later cracks that could have introduced traces of modern eukaryotes were visible in the sample.

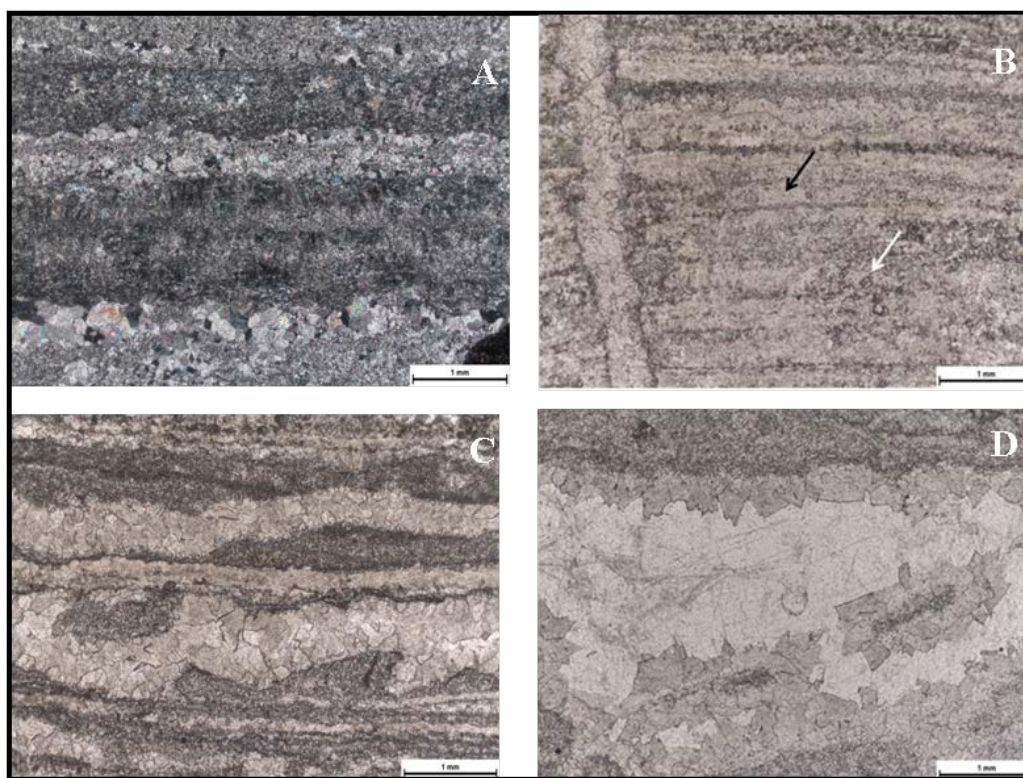


Figure 7.9: Thin-sections showing the first phase (A) Cross-polarised light thin section view of finely laminated microbial mat with weakly radiating palisade structure in fine-grained bedded dolomite (B) Plane light thin section view of finely bedded fine-grained carbonate (black arrow) with neomorphic recrystallization of carbonate into rhombs (white arrow) (C) Plane polarised light thin section view of laminated microbial mat comprising two distinct phases: a fine-grained dark phase that defines bedding and a second, discordant phase of coarser, sparry dolomite (D) Closeup of second phase, coarse sparry carbonate cored by clear silica (macroquartz).

- **Raman spectroscopy analysis of the microbial mat**

Raman spectrographic analysis of finely-bedded carbonate revealed kerogen distributed throughout the sample. The kerogen spectrum was characterised by a well-developed G-band and broad, low amplitude D-band (Figure 7.10). Comparison with other samples indicated a high Raman Index of Preservation (RIP) (Schopf et al., 2010) a spectrum similar to other low-metamorphic grade, old carbonate rocks, consistent with the degree of metamorphism of the sample. This signature was clearly distinct from that obtained for modern organisms. In addition, Raman spectroscopy can also be used as a geothermometer of the maximum temperature conditions reached during regional metamorphism (Beysac et al., 2002). The Raman spectroscopy spectrum of the microbial mat was compared with a variety of spectra over a range of temperature for

analysed kerogen (Figure 7.10). The signature obtained for the Turee Creek microbial mat matched the lowest metamorphism temperature on the scale ($T = 140\text{ }^{\circ}\text{C}$) implying that the temperature was either equal or lower to this value. This low metamorphism temperature may have contributed to an exceptional preservation of carbonates and the biomarkers entrapped within them, particularly functionalised biomarkers, and confirmed an indigenous origin of the kerogen.

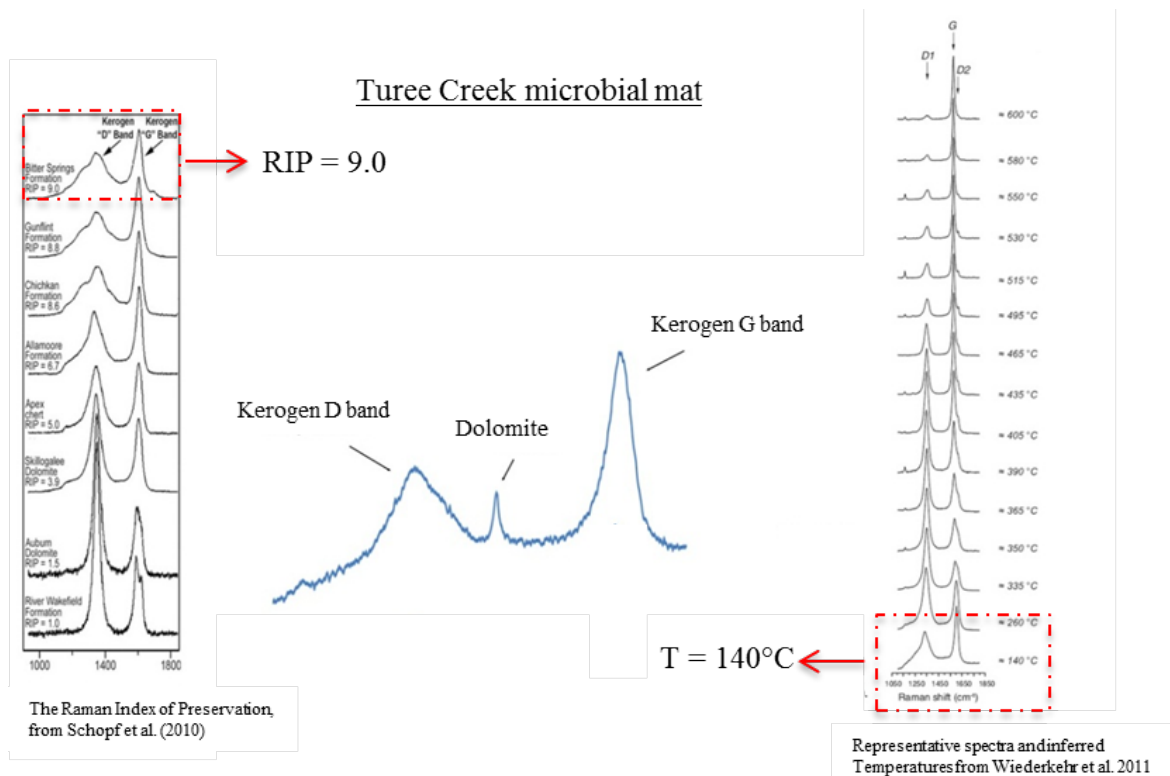


Figure 7.10: Raman spectrographic analysis of kerogen from the sampled Turee Creek microbial mat compared with another low-grade sample from the Neoproterozoic Maddina Formation (Fortescue Group) and the spectra libraries from Schopf et al. (2010) and Wiederkehr et al. (2011) that indicate very low temperature of metamorphism ($\leq 140^{\circ}\text{C}$) and high degree of preservation, similar to that of the Paleoproterozoic Gunflint Formation.

- **Comparison with two additional samples from the Turee Creek group**

Two additional samples from the Turee Creek group were also analysed in order to compare the biomarker signature: a stromatolite and a clotted microbial mat (Figure 7.11). Free and carbonate-bound biomarkers were analysed in both samples. No steroids (steranes or sterols) were detected in the two fractions of both samples. In the free and carbonate-bound aliphatic fractions, only *n*-alkanes were detected in very low relative abundance. The carbonate-bound saturated fraction of the stromatolite, for instance, exclusively showed *n*-alkanes ranging from C₂₁ to C₃₅ (Figure 7.12).

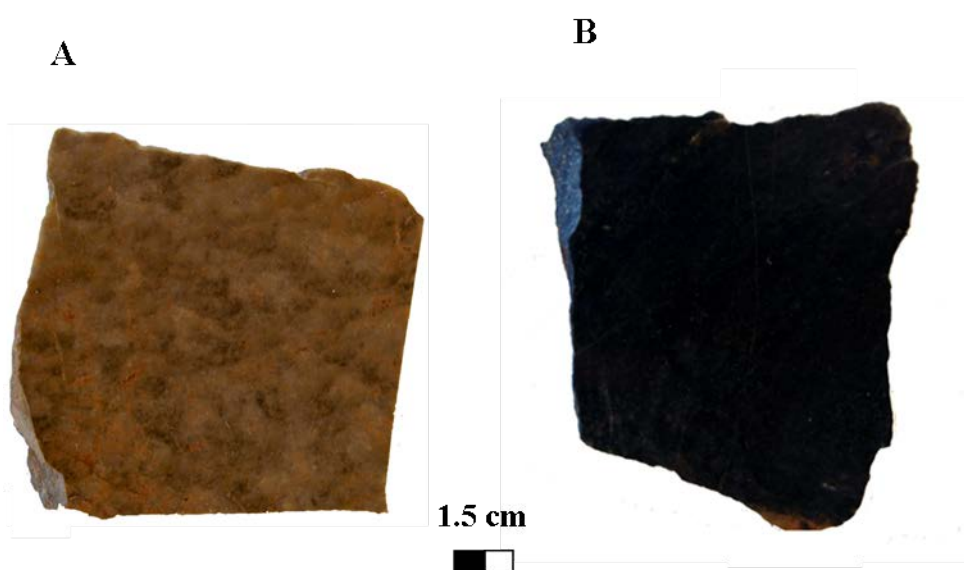


Figure 7.11: Photographs of the additional studied samples from the Turee Creek group: A) a microbialite presented a “clotted” texture and B) a stromatolite.

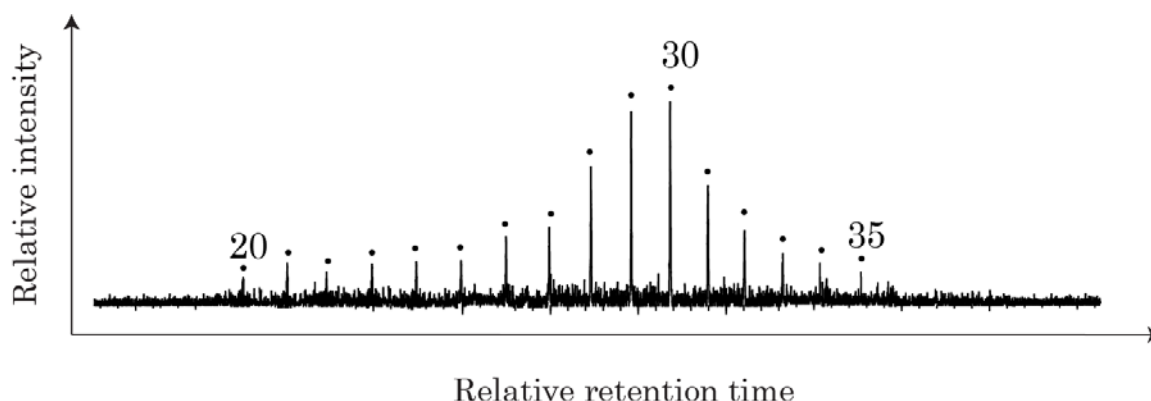


Figure 7.12: Total Ion Chromatogram of the carbonate-bound saturated hydrocarbons of the stromatolite, measured by GC-MS.

- **HyPy technique evaluation**

It clearly appeared that the steranes identified in the HyPy fraction (HyPy on kerogen) originated from the steranes and sterols present in the carbonates. A partial hydrogenation of sterols during HyPy has been previously demonstrated (Love et al., 2005; Sephton et al., 2005), however, no sterenes were detected in the HyPy fraction, implying a complete hydrogenation of the sterols. In addition, the presence of diasteranes in the HyPy fraction could have derived from carbonate-bound diasteranes. However, no C_{27} ($\alpha\beta$) diasteranes and C_{28} ($\beta\alpha$ and $\alpha\beta$) diasteranes were present in the carbonate-bound fraction implying that these diasteranes were HyPy products of the sterols present in the carbonate. Diasterenes are usually more abundant than diasteranes in the steroid products after HyPy because of the hindered unsaturation in the tetracyclic nucleus (Love et al., 2005). However, HyPy experiments on cholesterol previously highlighted the direct formation of diasteranes from sterols (Sephton et al., 2005). Our results also confirmed a structural rearrangement occurring during HyPy. In addition, the presence of 20*S* isomers of these diasteranes implied that sterols were being converted to the thermally mature isomer of diasteranes. Previous studies of HyPy on microbial cultures or sterols standards showed that only steranes with a 20*R* configuration were being produced. However, the formation of diasterenes with a 20*S* configuration has been previously reported after HyPy on microbial cultures (Love et al., 2005). Their presence was associated with the migration of the double bond that generated hydrogen shuttling and exchange (via

dehydrogenation and subsequent non-stereospecific hydrogenation) at carbon sites throughout the tetracyclic steroid backbone (de Leeuw et al., 1989). This mechanism could explain the formation of 20*S* diasteranes from sterols in our sample.

Conclusions

HyPy technique was applied to a Paleoproterozoic microbial mat in order to identify kerogen-bound hydrocarbons associated with this stratigraphic interval. The detection of steroids within the carbonate matrix of this 2.3 Gyr microbial mat could be highly significant as the oldest fossil evidence for eukaryotes was found 1.78–1.68 Gyr ago (Knoll et al., 2006). Additional work will be required to confirm that the biomarkers in this study are demonstrably indigenous and syngenetic and indicate the first evidence of the apparition of the domain Eucarya in the rock record. However, the analysis of thin-sections and results from Raman spectroscopy seem to indicate an exceptional preservation of carbonates and a low temperature of metamorphism for this sample. Melendez et al. (2013) recently reported an exceptional preservation of steroids (from sterols to triaromatic steroids) in a Devonian carbonate concretion from the Gogo formation, suggesting that enclosed carbonaceous systems can strongly contribute to the preservation of biosignatures through time. In addition, the comparison with additional samples from the same geological group showing a different biomarker signature emphasised the unique biomarker signature in this laminated microbial mat. Although further work will be required in this study, the possible exceptional preservation of biosignatures within the carbonate matrix of the microbial mat suggests an outstanding preservation pathway for biomolecules through time. In addition, the discovery and careful analysis of biomarkers in Archean and Paleoproterozoic environments will potentially offer new insights into the early evolution of life.

Acknowledgements:

This research was supported by a grant from the Australian Research Council's Discovery Projects scheme (2010-2013, Grice, Greenwood, Snape and Summons). AP thanks WA-Organic and Isotope Geochemistry Centre, Curtin University and CSIRO for top-up scholarship. Geoff Chidlow is thanked for GC-MS technical support.

References

- Beyssac O., Goffé B., Chopin C. and Rouzaud J. N.** (2002) Raman spectra of carbonaceous material in metasediments: a new geothermometer. *J. Metamorph. Geol.* **20**, 859–871.
- Dutkiewicz A., Rasmussen B. and Buick R.** (1998) Oil preserved in fluid inclusions in Archaean sandstones. *Nature* **395**, 885–888.
- Knoll A. H., Javaux E. J., Hewitt D. and Cohen P.** (2006) Eukaryotic organisms in Proterozoic oceans. *Philos. Trans. R. Soc. Lond. B. Biol. Sci.* **361**, 1023–1038.
- De Leeuw J. W., Cox H. C., van Graas G., van de Meer F. W., Peakman T. M., Baas J. M. A. and van de Graaf B.** (1989) Limited double bond isomerisation and selective hydrogenation of sterenes during early diagenesis. *Geochim. Cosmochim. Acta* **53**, 903–909.
- Goodwin, T. W.** 1985. Biosynthesis of plant sterols, In: *Sterol and Bile Acids*. (eds. H. Danielsson, J. Sjövall). Elsevier, Amsterdam, pp. 175-198.
- Love G. D., Snape C., Carr A. D. and Houghton C.** (1995) Release of covalently-bound alkane biomarkers in high yields from kerogen via catalytic hydrolysis. *Org. Geochem.* **23**, 981–986.
- Love G. D., McAulay A., Snape C. and Bishop A. N.** (1997) Effect of process variables in catalytic hydrolysis on the release of covalently bound aliphatic hydrocarbons from sedimentary organic matter. *Energy & Fuels* **11**, 522–531.
- Love G. D., Bowden S. A., Jahnke L. L., Snape C., Campbell C. N., Day J. G. and Summons R. E.** (2005) A catalytic hydrolysis method for the rapid screening of microbial cultures for lipid biomarkers. *Org. Geochem.* **36**, 63–82.
- Love G. D., Grosjean E., Stalvies C., Fike D. a, Grotzinger J. P., Bradley A. S., Kelly A. E., Bhatia M., Meredith W., Snape C., Bowring S. A., Condon D. J. and Summons R. E.** (2009) Fossil steroids record the appearance of Demospongiae during the Cryogenian period. *Nature* **457**, 718–721.

- Mango F. D.** (1991) The stability of hydrocarbons under the time–temperature conditions of petroleum genesis. *Nature* **352**, 146–148.
- McCaffrey M. A., Farrington J. W. and Repeta D. J.** (1989) Geochemical implications of the lipid composition of *Thioploca* spp. from the Peru upwelling region—15°S. *Org. Geochem.* **14**, 61–68.
- Melendez I., Grice K. and Schwark L.** (2013) Exceptional preservation of Palaeozoic steroids in a diagenetic continuum. *Nat. Sci. Reports* **3**, 1–6.
- Meredith W., Russell C. A., Cooper M., E. Snape C., Love G. D., Fabbri D. and Vane C. H.** (2004) Trapping hydropyrolysates on silica and their subsequent thermal desorption to facilitate rapid fingerprinting by GC–MS. *Org. Geochem.* **35**, 73–89.
- Moldowan J. M., SundaraRaman P. and Schoell M.** (1986) Sensitivity of biomarker properties to depositional environment and/or source input in the Lower Toarcian of SW-Germany. *Org. Geochem.* **10**, 915–926.
- Muller, S. G., Krapez, B., Barley, M. E., and Fletcher, I. R.** (2005) Giant iron-ore deposits of the Hamersley province related to the breakup of Paleoproterozoic Australia: New insights from in situ SHRIMP dating of baddeleyite from mafic intrusions. *Geology* **33**, 577–580.
- Nishimura M. and Koyama T.** (1977) The occurrence of stanols in various living organisms and the behavior of sterols in contemporary sediments. *Geochim. Cosmochim. Acta* **41**, 379–385.
- Nishimura M.** (1978) Geochemical characteristics of the high reduction zone of stanols in Suwa sediments and the environmental factors controlling the conversion of stanols into stanols. *Geochim. Cosmochim. Acta* **42**, 349–357.
- Pearson M. J., Hendry J. P., Taylor C. W. and Russell M. A.** (2005) Fatty acids in sparry calcite fracture fills and microsparite cement of septarian diagenetic concretions. *Geochim. Cosmochim. Acta* **69**, 1773–1786.
- Peters K. E. and Moldowan J. M.** (1993) *The Biomarker Guide*. Prentice Hall, Engelwood Cliffs, NJ.
- Pillans, B.** (2005) Geochronology of Australian Regolith. *CRC LEME*, 1–12.
- Rasmussen, B., Fletcher, I.R., Sheppard, S.** (2005) Isotopic dating of the migration of a low-grade metamorphic front during orogenesis. *Geology* **33**, 773–776.
- Schopf J. W., Kudryavtsev A. B. and Sergeev V. N.** (2010) Confocal laser scanning microscopy and raman imagery of the late Neoproterozoic chichkan microbiota of south Kazakhstan. *J. Paleontol.*, **84**, 402–416.

- Sephton M. A., Meredith W., Sun C.-G. and Snape C.** (2005) Hydrolysis of steroids: a preparative step for compound-specific carbon isotope ratio analysis. *Rapid Commun. Mass Spectrom.* **19**, 3339–3342.
- Sieskind O., Joly G. and Albrecht P. A.** (1979) Simulation of the geochemical transformations of sterols: superacid effect of clay minerals. *Geobiology* **43**, 1675–1679.
- Summons R. E., Powell T. G. and Boreham C. J.** (1988) Petroleum geology and geochemistry of the Middle Proterozoic McArthur Basin, Northern Australia: III. Composition of extractable hydrocarbons. *Geochim. Cosmochim. Acta* **52**, 1747–1763.
- Summons R. E. and Walter M. R.** (1990) Molecular fossils and microfossils of prokaryotes and protists from proterozoic sediments. *Am. J. Sci.* **290**, 212–244.
- Trendall, A. F.** (1979) A revision of the Mount Bruce Supergroup: Geological Survey of Western Australia, Annual Report 1978, pp. 63–71.
- Volkman J. K.** (1986) A review of sterol markers for marine and terrigenous organic matter. *Org. Geochem.* **9**, 83–99.
- Wiederkehr M., Bousquet R., Ziemann M., Berger A. and Schmid S.** (2011) 3-D assessment of peak-metamorphic conditions by Raman spectroscopy of carbonaceous material: an example from the margin of the Lepontine dome (Swiss Central Alps). *Int. J. Earth Sci.* **100**, 1029–1063.

Chapter 8

Conclusions and Outlook



This PhD project provided a comprehensive study of modern microbial mats and allowed a better characterisation of microbial communities, biosignatures and isotopic trends in these unique microbial structures. Integration of the comprehensive biomarker, stable isotope and elemental data provided an in-depth insight into the complexity of biogeochemical cycles and microbial organisation in these modern stromatolites. In addition, the influence of environmental conditions on microbial communities' distribution is crucial while trying to characterise different types of microbial mats or mats from different locations. Changes of salinity in marine settings, for instance, can significantly impact local ecosystems and affect primary production. As a consequence, the influence of water depth and salinity on microbial compositions was investigated. In addition, these modern systems also provide an exceptional opportunity to investigate preservation pathways of biosignatures through time and allow a better understanding of ancient stromatolites that represent the earliest traces of life and extend in the rock record up to 3.5 Gyr (Walter et al., 1980; Hoffman, 2000; Allwood et al., 2006; Van Kranendonk et al., 2008). In this project, preservation pathway of biosignatures in modern stromatolites was explored and the role of sulfur-cycling organisms in preservation of biomolecules was highlighted.

Biogeochemical cycles in modern microbial mats

Microbial mats exhibit exceptionally high metabolic rates (Jørgensen et al., 1979) that lead to steep biogeochemical gradients (e.g. redox potential and pH), presenting significant temporal and spatial fluctuations. These modern systems present strong variations in solute distributions and concentrations between oxic and anoxic conditions. However, micro-scale heterogeneity of biogeochemical zonation and oxygen concentrations has been reported (Jørgensen et al., 1983; Paerl and Pinckney, 1996; Glud et al., 1999). Despite previous studies on biogeochemical cycles in modern microbial mats, including investigations of diurnal variations in oxygen and sulfide (e.g. Jørgensen and Revsbech, 1979; Visscher et al., 1992a,b; 1993; Dupraz et al., 2004; 2009), little was known about diurnal variations in the distribution of porewater solutes, biogeochemical interactions and the role of microbial communities in regulating porewater solute distributions. The present study ([Chapter 2](#)) used biomarker analysis (hydrocarbons and PLFAs) to characterise microbial communities present in the different layers of a

laminated smooth mat. Novel DGT and DET samplers were also deployed in the same mat in order to visualise the two-dimensional co-distributions of porewater alkalinity/sulfide and iron(II)/phosphate. A direct correlation between microbial communities and analyte distributions was established. A predominance of cyanobacteria was detected in the first layer suggesting significant photosynthetic activity at this outer part of the mat, concordant with lower concentrations of sulfide and iron(II) recorded during the day. The increase in sulfate reducing bacteria abundance with depth was also concordant with the general increase in sulfide concentrations with depth within the mat. However, results from DET and DGT samplers also showed that porewater solute distributions were highly heterogeneous under both light and dark conditions indicating that solute distributions can present extensive horizontal fluctuations even within a single layer of the mat (Glud et al., 1999), as well as the more comprehensive shifts associated with changes in light environment and depth. In order to observe general trends in diurnal biogeochemical cycles in modern mats, small replicates of DET and DGT samplers were also deployed (Chapter 3). Complimentary microelectrode measurements of oxygen and sulfide were also obtained. Microelectrode measurements highlighted a strong decrease in oxygen concentration at night and a predominance of anoxic conditions in the smooth mat. Two-dimensional distributions of porewater solutes obtained with the DET and DGT techniques showed, here again, a strong vertical and lateral heterogeneity under both light and dark conditions. Silver foil deployments in the mat revealed a significant sulfate-reducing activity in the upper layers of the mat, concordant with high concentrations of sulfide measured in the cyanobacterial layer with the DGT technique. In order to visualise general trends in solute variations between oxic and anoxic conditions, diurnal averaged profiles of analytes were plotted. Sulfide and iron(II) concentrations presented significant variations and appeared to be highly influenced by light and oxygen gradients. Although phosphate distribution is often associated with iron(II) distribution, our results revealed that phosphate distribution was mainly driven by diurnal metabolic changes in the microbial mat. Alkalinity distribution and carbonate precipitation seem to be the result of a complex balance between microbial processes increasing and decreasing the alkalinity gradient. These results clearly showed that porewater analytes can be regulated by both chemical reactions (e.g: iron(II) and sulfide oxidation, dissolution of phosphorus-iron complexes) and microbial processes.

Influence of abiotic conditions on microbial mats communities

Environmental conditions can strongly influence microbial communities' distribution and organisation. For instance, differences in the relative abundances and isotopic compositions of lipids in microbial mats have been reported along a littoral gradient (Bauersachs et al., 2011) and changes in stable isotope signatures of OM have also been observed with varying salinity (Chmura and Aharon, 1995). The influence of abiotic conditions (depth and salinity) on lipid biomarkers and stable isotopic values of Shark Bay mats was investigated in [Chapter 4](#). Bacterial communities common to all mats (e.g. cyanobacteria, sulfur-cycling organisms) were detected in relatively high abundance. However, subtle differences were observed between the mats along the tidal flat gradient. A possible higher seagrass input (e.g. high abundance of $n\text{-C}_{21}$) in the deepest mat and a likely contribution from diatoms in the shallowest mats (pustular and smooth) based on the $\text{C}_{25:1}$ HBI alkene, PLFAs and isotopic values. The three smooth mats from the different sites presenting varying salinity levels also showed small discrepancies. A lower abundance of diatoms was detected in Garden Point and Rocky Point than in Nilemah, based on hydrocarbons and PLFA distributions, suggesting that diatoms were more present at the most saline site. Macrophytic input also appeared to be higher at Nilemah. The significant differences between the $\delta^{13}\text{C}$ values of the three mats, however, were most likely related to different biomass (autotrophic *versus* heterotrophic) and CO_2 fixation pathways than variations in salinity.

Changes in lipophilic pigments and IPL distributions with depth and salinity were investigated in [Chapter 5](#). A comparison of lipophilic pigment distributions in the mats between this study and the study by Palmisano et al. (1989) was also undertaken in order to observe community changes in the mats through time. The IPLs and lipophilic pigment composition of Nilemah microbial mats along the littoral gradient highlighted the presence of sulfur-cycling organisms, possibly phosphate-limited Alphaproteobacteria and cyanobacteria in all mats. Subtle differences between the mat communities were detected. The concentration of bacteriochlorophyll *a*, for instance, decreased with water depth, highlighting a decrease in purple phototrophic bacteria with depth. In addition, chlorophyll *c*, indicative of diatoms, was only detected in the shallow pustular and smooth mats. These results are concordant with the higher abundance of diatoms in the

shallower mats observed in [Chapter 4](#). The comparison between the Nilemah, Garden Point and Rocky Point mats showed that the highest diversity of IPL was found in the least saline mat. Cyanobacteria were present in all mats, although a lower diversity of cyanobacterial IPL was detected in the most saline Nilemah mat. A decrease in betaine lipids, possibly deriving from phosphate-limited Alphaproteobacteria, was observed with an increase in salinity, suggesting a higher limitation in phosphate in less saline sites. Chlorophyll *c* from diatoms was only detected in the mat from Nilemah, confirming that diatoms were more abundant in the most saline site, as previously observed in [Chapter 4](#). The much higher abundance in purple phototrophic bacteria in the Garden Point mat did not seem to be related to salinity but might actually be associated with the presence of very calm waters in this area, favouring the formation of a thick layer of purple-sulfur bacteria. The comparison of lipophilic pigments distribution in the Hamelin Pool with the previous study by Palmisano et al. (1989) revealed significant changes in microbial communities in the mats through time. The diatoms communities seemed to be exclusively present in the shallower mats and the colloform mats presented a high abundance of cyanobacteria whereas diatoms were highly abundant in the colloform mats and absent from the shallower mats in the 1989 study. In addition, an increase in the abundance of purple phototrophic bacteria through time was observed, suggesting potential changes in environmental conditions through time.

These results clearly highlighted different microbial communities in the different types of mats and showed a close relationship between the presence of diatoms, macrophytes and depth/salinity gradient, as previously suggested in other microbial mats (Sabbe et al., 2004).

Rapid turnover in microbial communities

The comparison of lipophilic pigment distribution in Hamelin pool mats between this study (Chapter 5) and the 1989 study (Palmisano et al.) suggested significant changes in mat communities over time. In addition, the comparison of biomarker distribution from the studies presenting in the different chapters of this thesis also suggested changes in microbial communities over shorter time periods (11-12 months). Indeed, because of strict restrictions related to permits and sample collections in Shark Bay, three different main field missions were needed to collect the entire set of samples studied in this PhD (May 2010 – Chapters 3 and 4, April 2011 – Chapter 6 and April 2012 – Chapters 2 and 3). Subtle differences in the biomarker distributions from Nilemah (Chapters 2 and 4) and Garden Point (Chapters 6 and 4) mats were observed. For instance, no C₂₅ HBI was detected in the smooth mat from Nilemah in Chapter 2, as opposed to Chapter 4, possibly suggesting a lower abundance of diatoms in this mat in 2012 than in 2010. On the other hand, Chapter 6 revealed a possible presence of diatoms in the Garden Point smooth mat, based on more positive $\delta^{13}\text{C}$ values of sterenes, in comparison with other hydrocarbons. In addition, the relative abundance of *iso*-17:1 ω 9 was lower in the Garden Point mat studied in Chapter 6 than in the one analysed in Chapter 4. However, the high abundance of Gammaproteobacteria and the thick purple layer observed in the mat studied in Chapter 6 were concordant with a high abundance of sulfur-cycling organisms in this microbial structure, as suggested in Chapters 4 and 5 by the high abundance of PLFAs from sulfur-cycling organisms and the high concentration in bacteriochlorophyll *a*, respectively. An association of short generation times, large surface to volume ratio and fast evolutionary potential allows microorganisms to rapidly adapt to changes in environmental conditions (Schmidt et al., 2007). Studies of microbial communities in soils revealed a biomass turnover on scales of days to months, leading to significant changes in microbial communities over a year (Schmidt et al., 2007). The comparison of biomarker distribution from microbial mats sampled at different periods in this study confirmed that microbial mats are highly dynamic systems and that rapid turnover in mat communities can take place over very short time-periods.

Preservation pathway of biosignatures in microbialites

Preservation pathway of biosignatures in stromatolites through time is not yet well understood. In [Chapter 6](#), a multidisciplinary approach including 16s *rRNA* technique, DGT and DET samplers, biomarkers and stable isotope analysis was used to characterise microbial communities in a smooth mat from Garden Point and investigate the role of sulfur-cycling organisms on the preservation of biolipids. The high abundance of Gammaproteobacteria and Firmicute suggested a predominance of sulfur-cycling organisms in this mat which likely contributed to a dynamic sulfur cycle and carbonate precipitation. Biolipids also showed evidence for sulfur-cycling organisms as well as cyanobacteria and maybe diatoms, as shown by the highly ^{13}C -enriched sterenes. Unusual long-chain fatty acids with isotopic signatures significantly different from co-occurring long-chain *n*-alkanes indicated that Firmicute bacteria inhabiting Shark Bay mats may also contribute to the formation of ooids in Shark Bay, as previously suggested by Summons et al. (2013). In addition, sulfur-bound biomarkers (aliphatic and aromatic) were identified in the mat. Reaction between reduced inorganic sulfur species and labile, oxygen sensitive biolipids contributes to the preservation of OM in modern stromatolites. This selective preservation process, occurring at a very early stage of diagenesis, is likely a crucial step in the protection of microbial mats biosignatures over geological time.

Preservation of biomarkers in an ancient microbial mat was also investigated in [Chapter 7](#). Hydrolysis was applied to a Paleoproterozoic laminated microbial mat in order to release indigenous biosignatures. This technique allowed the detection of steroid biomarkers entrapped in the carbonate fraction. The analysis of thin-sections seemed to confirm that no re-precipitation of carbonates occurred after 1.8 Gyr at the earliest (and more likely 2.3 Gyr). In addition, the Raman spectroscopy supported exceptional preservation of kerogen and a low temperature of metamorphism. Although further work will be required to confirm the syngenetic origin of these biomarkers, the entrapment of biosignatures in carbonate also appeared as another selective preservation process that will potentially provide a new insight into early microbial life.

Future perspectives

This study allowed a better insight into microbial mats organisation and structures and highlighted the complexity of porewater solutes distributions in these systems. In particular, the investigation of spatial heterogeneity was investigated *via* the use of DGT and DET samplers. Such dynamic ecosystems, however, also present highly temporal variations and further investigation of seasonal influence on microbial communities and biogeochemical cycles, for instance, would also be of high interest. In addition, a direct comparison with microbial mats from other settings (e.g. Bahamas, Guerrero Negro, Solar Saltern, Mediterranean lakes) would also provide a better understanding of microbial systems at a global scale. From a biomarker perspective, this study investigated a high diversity of lipid biomarkers including aliphatic and aromatic hydrocarbons, PLFAs, IPLs and lipophilic pigments. In addition, for the first time, bulk and compound-specific stable isotope measurements were performed on Shark Bay mats and provided further insight into the metabolic processes characterising these microbial mats. Although 16s *r*RNA analysis were performed in this study and other previous studies (Papineau et al., 2005; Burns et al., 2004; Allen et al., 2009), additional analysis would be required to fully characterise mat communities. The use of fluorescent *in situ* hybridisation (FISH) technique (Amann et al., 1995), for instance, would allow the quantification of species *in situ* with a high spatial resolution. This could help visualising the exact location of target species (e.g. Archea, SRB) in the mat and would provide a better understanding of community structure and role of key organisms in carbonate precipitation (Baumgartner et al., 2006). In addition, although some highly interesting studies have been performed on EPS from Bahamian microbial mats (e.g. Kawaguchi and Decho, 2002; Decho et al., 2005; Braissant et al., 2009), additional work on micro-scale characterisation of EPS from Shark Bay mats would be highly beneficial and would provide additional valuable data on mat lithification and preservation of biosignatures through time.

Additional biomarker work on ancient microbial mats and stromatolites will also be required to confirm or not the presence of steroids 2.3 billion years old. Biomarkers analysis from ancient samples of different geological units, for instance, will help providing a global characterisation of ancient biosignatures and will provide new insight into early life evolution.

Bibliography

“Every reasonable effort has been made to acknowledge the owners of copyright material. I would be pleased to hear from any copyright owner who has been omitted or incorrectly acknowledged”

A

- Abd-el Malek Y. and Rizk S. G.** (1963) Bacterial sulphate reduction and the development of alkalinity . III . Experiments under natural conditions in the Wadi Natriin. *J. Appl. Bacteriol.* **26**, 20-26.
- Abed R. M. M., Safi N. M. D., Köster J., de Beer D., El-Nahhal Y., Rullkötter J., Beer D. De and Garcia-pichel F.** (2002) Microbial diversity of a heavily polluted microbial mat and its community changes following degradation of petroleum compounds. *Appl. Environ. Microbiol.* **68**, 1674-1683.
- Abed R. M. M., Kohls K. and de Beer D.** (2007). Effect of salinity changes on the bacterial diversity, photosynthesis and oxygen consumption of cyanobacterial mats from an intertidal flat of the Arabian Gulf. *Environ. Microbiol.* **9**, 1384–1392.
- Abrajano Jr T. A., Murphy D. E., Fang J., Comet P. and Brooks J. M.** (1994) $^{13}\text{C}/^{12}\text{C}$ ratios in individual fatty acids of marine mytilids with and without bacterial symbionts. *Org. Geochem.* **21**, 611-617.
- Adam P., Schmid J. C., Mycke B., Strazielle C., Connan J., Huc A., Riva A. and Albrecht P. A.** (1993) Structural investigation of nonpolar sulfur cross-linked macromolecules in petroleum. *Geochim. Cosmochim. Acta* **57**, 3395-3419.
- Adam P., Schneckenburger P., Schaeffer P. and Albrecht P. A.** (2000) Clues to early diagenetic sulfurization processes from mild chemical cleavage of labile sulfur-rich geomacromolecules. *Geochim. Cosmochim. Acta* **64**, 3485-3503.
- Allard B. and Templier J.** (2000) Comparison of neutral lipid profile of various trilaminar outer cell wall (TLS)-containing microalgae with emphasis on algaenan occurrence. *Phytochemistry* **54**, 369-380.
- Allen M. A.** (2006). PhD thesis. An Astrobiology-Focused Analysis of Microbial Mat Communities from Hamelin Pool, Shark Bay, Western Australia.
- Allen M. A., Goh F., Burns B. P. and Neilan B. A.** (2009) Bacterial, archaeal and eukaryotic diversity of smooth and pustular microbial mat communities in the hypersaline lagoon of Shark Bay. *Geobiology* **7**, 82-96.

Bibliography

- Allen M. A., Neilan B. A., Burns B. P., Jahnke L. L. and Summons R. E.** (2010) Lipid biomarkers in Hamelin Pool microbial mats and stromatolites. *Org. Geochem.* **41**, 1207-1218.
- Aller J. Y. and Aller R. C.** (1986) Evidence for localized enhancement of biological associated with tube and burrow structures in deep-sea sediments at the HEEBLE site, western North Atlantic. *Deep Sea Res. Part A. Oceanogr. Res. Pap.* **33**, 755-790.
- Aller R. C., Yingst J. Y. and Ullman W. J.** (1983) Comparative biogeochemistry of water in intertidal Onuphis (polychaeta) and Upogebia (crustacea) burrows: temporal patterns and causes. *J. Mar. Res.* **41**, 571-604.
- Allwood A. C., Walter M. R., Kamber B. S., Marshall C. P. and Burch I. W.** (2006) Stromatolite reef from the Early Archaean era of Australia. *Nature* **441**, 714-718.
- Amann R. I., Ludwig W., Schleifer K.** (1995) Phylogenetic identification and in situ detection of individual microbial cells without cultivation. *Microbiol. Rev.* **59**, 143-169.
- Arp G., Reimer A. and Reitner J.** (2001) Photosynthesis-induced biofilm calcification and calcium concentrations in Phanerozoic oceans. *Science* **292**, 1701-1704.
- Atlas R. and Bartha R.** (1998) *Microbiology ecology: fundamental and applications*. Addison-Wiley, Reading.
- Attaway D. H., Parker P. L. and Mears J. A.** (1970) Normal alkanes of five coastal spermatophytes. *Contrib. Mar. Sci.* **15**, 13-19.
- Awramik S. M.** (1984) Ancient stromatolites and microbial mats. In *Microbial Mats: Stromatolites*. (eds. Y. Cohen, R. W. Castenholz and H. O. Halvorson). Alan Liss, New York, pp. 1-21.

B

- Bauersachs T., Compaoré J., Severin I., Hopmans E. C., Schouten S., Stal L. J. and Sinninghe Damsté J. S.** (2011) Diazotrophic microbial community of coastal microbial mats of the southern North Sea. *Geobiology* **9**, 349-359.
- Bauld J.** (1984) Microbial mats in marginal marine environments: Shark Bay, Western Australia. In *Microbial mats: Stromatolites*. (eds. Y. Cohen, R.W. Castenholz, H.O. Halvorson). Alan R. Liss, New York, pp 39-58.
- Baumgartner L. K., Reid R. P., Dupraz C. P., Decho A. W., Buckley D. H., Spear J. R., Przekop K. M. and Visscher P. T.** (2006) Sulfate reducing bacteria in microbial mats: Changing paradigms, new discoveries. *Sediment. Geol.* **185**, 131-145.

Bibliography

- Baumgartner L. K., Spear J. R., Buckley D. H., Pace N. R., Reid R. P., Dupraz C. P. and Visscher P. T.** (2009) Microbial diversity in modern marine stromatolites, Highborne Cay, Bahamas. *Environ. Microbiol.* **11**, 2710-2719.
- Bebout B. M., Paerl H. W., Crocker K. M. and Prufert E.** (1987) Diel interactions of oxygenic photosynthesis and N₂ fixation (acetylene reduction) in a marine microbial mat. *Appl. Environ. Microbiol.* **53**, 2353-2362.
- Behrens A., Schaeffer P., Bernasconi S. and Albrecht P. A.** (2000) Mono- and bicyclic squalene derivatives as potential proxies for anaerobic photosynthesis in lacustrine sulfur-rich sediments. *Geochim. Cosmochim. Acta* **64**, 3327-3336.
- Benlloch S., López-López A., Casamayor E. O., Øvreas L., Goddard V., Daae F. L., Smerdon G., Massana R., Joint I., Thingstad F., Pedrós-Allió C. and Rodríguez-Valera F.** (2002). Prokaryotic genetic diversity throughout the salinity gradient of a coastal solar saltern. *Environ. Microbiol.* **4**, 349–360.
- Bennett W. W., Teasdale P. R., Welsh D. T., Panther J. G. and Jolley D. F.** (2012) Optimization of colorimetric DET technique for the in situ, two-dimensional measurement of iron(II) distributions in sediment porewaters. *Talanta* **88**, 490-495.
- Bennett W. W., Serriere A., Panther J. G., Welsh D. T. and Teasdale P. R.** (2014) A rapid, high-resolution, gel-based technique for the in situ measurement of two-dimensional porewater alkalinity distributions. *Chemosphere*, under review.
- Beyssac O., Goffé B., Chopin C. and Rouzaud J. N.** (2002) Raman spectra of carbonaceous material in metasediments: a new geothermometer. *J. Metamorph. Geol.* **20**, 859-871.
- Bigeleisen J. and Wolfsberg M.** (1958) Theoretical and experimental aspects of isotope effects in chemical kinetics. *Adv. Chem. Phys.* **1**, 15-76.
- Birgel D., Elvert M., Han X. and Peckmann J.** (2008) C13 depleted biphytanic diacids as tracers of past anaerobic oxidation of methane. *Org. Geochem.* **39**, 152-156.
- Blinn D., Halse S., Pinder A. and Shiel R.** (2004). Diatom and micro-invertebrate communities and environmental determinants in the western Australian wheatbelt: a response to salinization. *Hydrobiologia* **528**, 229–248.
- Blumenberg M., Krüger M., Nauhaus K., Talbot H. M., Oppermann B. I., Seifert R., Pape T. and Michaelis W.** (2006) Biosynthesis of hopanoids by sulfate-reducing bacteria (genus *Desulfovibrio*). *Environ. Microbiol.* **8**, 1220-1227.
- Blumer M.** (1957) Removal of elemental sulphur from hydrocarbon fractions. *Anal. Chem.* **29**, 1039-1041.

Bibliography

- Bobbie R. J. and White D. C.** (1980) Characterization of benthic microbial community structure by high-resolution gas chromatography of fatty acid methyl esters. *Appl. Environ. Microbiol.* **39**, 1212-1222.
- Boetius A., Ravenschlag K., Schubert C. J., Rickert D., Widdel F., Gieseke a, Amann R., Jørgensen B. B., Witte U. and Pfannkuche O.** (2000) A marine microbial consortium apparently mediating anaerobic oxidation of methane. *Nature* **407**, 623-626.
- Bolhar, R. and Van Kranendonk M. J.** (2007) A non-marine depositional setting for the northern Fortescue Group, Pilbara Craton, inferred from trace element geochemistry of stromatolitic carbonates. *Precambrian Res.* **3-4**, 229-250.
- Boon J. J., Hines H., Burlingame A. L., Klok J., Rijpastra W. I. C., de Leeuw J. W., Edmonds K. E. and Eglinton G.** (1983) Organic geochemical studies of Solar Lake laminated cyanobacterial mats. In *Advances in Organic Geochemistry*. (eds. M. Bjoroy, C. Albrecht, C. Cornford et al.) John Wiley & Sons, Chichester, pp 207-227.
- Boon P. I. and Sorrell B.K.** (1991) Biogeochemistry of billabong sediments. I. The effect of macrophytes. *Fresh. Biol.* **26**, 209-226.
- Borovec J., Sirová D., Mošnerová P., Rejmánková E. and Vrba J.** (2010) Spatial and temporal changes in phosphorus partitioning within a freshwater cyanobacterial mat community. *Biogeochemistry* **101**, 323-333.
- Boschker H. and Middelburg J.** (2002) Stable isotopes and biomarkers in microbial ecology. *FEMS Microbiol. Ecol.* **40**, 85-95.
- Botello A. V. and Mandelli E. F.** (1978) Distribution of n-paraffins in seagrasses, benthic algae, oysters and recent sediments from Terminos Lagoon, Campeche, Mexico. *Bull. Environ. Contam. Toxicol.* **78**, 162-170.
- Boudou J. P., Trichet J., Robinson N. and Brassell S. C.** (1986) Profile of aliphatic hydrocarbons in a recent polynesian microbial mat. *Int. J. Environ. Anal. Chem.* **26**, 137-155.
- Braissant O., Decho A. W., Dupraz C. P., Glunk C., Przekop K. M. and Visscher P. T.** (2007) Exopolymeric substances of sulfate-reducing bacteria: Interactions with calcium at alkaline pH and implication for formation of carbonate minerals. *Geobiology* **5**, 401-411.
- Braissant O., Decho A. W., Przekop K. M., Gallagher K. L., Glunk C., Dupraz C. P. and Visscher P. T.** (2009) Characteristics and turnover of exopolymeric substances in a hypersaline microbial mat. *FEMS Microbiol. Ecol.* **67**, 293-307.
- Breman, P. J.** (1988) Mycobacterium and other actinomycetes. In *Microbial lipids* (eds. C. Ratledge, S. G. Wilkinson). Academic Press, London, pp. 204-298.

Bibliography

- Brocks J. and Grice K.** (2011) Biomarker (Organic, Compound-Specific Isotopes). In *Encyclopedia of Geobiology* (eds. J. Reitner, J. and V. Thiel). Springer, Dordrecht Netherlands, pp. 147-166.
- Brocks J. J. and Pearson A.** (2005) Building the Biomarker Tree of Life. *Rev. Mineral. Geochemistry* **59**, 233-258.
- Brocks J. J. and Summons R. E.** (2003) Sedimentary hydrocarbons, biomarkers for early-life. In *Treatise on Geochemistry* (eds. W. H. Schlesinger, H. D. Holland and K. K. Turekian) Elsevier, pp 63-115.
- Brocks J. J., Logan G. A., Buick, R. and Summons, R. E.** (1999) Archean molecular fossils and the early rise of eukaryotes. *Science* **285**, 1033-1036.
- Brotas V. and Plante-Cuny M.-R.** (2003) The use of HPLC pigment analysis to study microphytobenthos communities. *Acta Oecologica* **24**, S109-S115
- Bühning S. I., Smittenberg R. H., Sachse D., Lipp J. S., Golubic S., Sachs J. P., Hinrichs K.-U. and Summons R. E.** (2009) A hypersaline microbial mat from the Pacific Atoll Kiritimati: insights into composition and carbon fixation using biomarker analyses and a ¹³C-labeling approach. *Geobiology* **7**, 308-323.
- Burford M. A., Long B. G. and Rothlisberg P. C.** (1994) Sedimentary pigments and organic carbon in relation to microalgal and benthic faunal abundance in the Gulf of Carpentaria. *Mar. Ecol. Prog. Ser.* **103**, 111-117.
- Burne R. V. and Johnson K.** (2012) Sea-level variation and the zonation of microbialites in Hamelin Pool, Shark Bay, Western Australia. *Mar. Freshw. Res.* **63**, 994-1004.
- Burns B. P., Goh F., Allen M. A. and Neilan B. A.** (2004) Microbial diversity of extant stromatolites in the hypersaline marine environment of Shark Bay, Australia. *Environ. Microbiol.* **6**, 1096-1101.

C

- Canfield D. E. and Des Marais D. J.** (1991) Aerobic sulfate reduction in microbial mats. *Science* **251**, 1471-1473.
- Canfield D. E. and Des Marais D. J.** (1993) Biogeochemical cycles of carbon , sulfur , and free oxygen in a microbial mat. *Geochim. Cosmochim. Acta* **57**, 3971-3984.
- Canuel E. A., Cloern J. E., Ringelberg D. B., Guckert J. B. and Rau G. H.** (1995) Molecular and isotopic tracers used to examine sources of organic matter and its incorporation into the food webs of San Francisco Bay. *Limnol. Oceanogr.* **40**, 67-81.

Bibliography

- Canuel E. A., Freeman K. H. and Wakeham S. G.** (1997) Isotopic compositions of lipid biomarker in estuarine compounds plants and surface sediments. *Limnol. Oceanogr.* **42**, 1570-1583.
- Caple M. B., Chow H. and Strouse C. E.** (1978) Photosynthetic pigments of green sulfur bacteria. The esterifying alcohols of bacteriochlorophylls *c* from *Chlorobium limicola*. *J. Biol. Chem.* **253**, 6730-6737.
- Caporaso J. G., Kuczynski J., Stombaugh J., Bittinger K., Bushman F. D., Costello E. K., Fierer N. et al.** (2010) QIIME allows analysis of high-throughput community sequencing data. *Nat. Methods* **7**, 335-336.
- Caumette P., Matheron T., Raymond N. and Relexans J.-C.** (1994) Microbial mats in the hypersaline ponds of Mediterranean salterns (Salins-de-Giraud, France). *FEMS Microbiol. Ecol.* **13**, 273-286.
- Chaudhuri S., Lack J. and Coates J.** (2001) Biogenic magnetite formation through anaerobic biooxidation of Fe(II). *Appl. Environ. Microbiol.* **67**, 2844-2848.
- Chen M., Schliep M., Willows R. D., Cai Z.-L., Neilan B. A. and Scheer H.** (2010) A red-shifted chlorophyll. *Science* **329**, 1318-1319.
- Chmura G. L. and Aharon P.** (1995) Stable carbon isotope signatures of sedimentary carbon in coastal wetlands as indicators of salinity regime. *J. Coast. Res.* **11**, 124-135.
- Christie W.** (2003) *Lipid Analysis, third ed.* The Oily Press, Bridgwater.
- Cifuentes L. A. and Salata G. G.** (2001) Significance of carbon isotope discrimination between bulk carbon and extracted phospholipid fatty acids in selected terrestrial and marine environments. *Org. Geochem.* **32**, 613-621.
- Cohen Y.** (1984a) Micro-sulfate reduction measurements at the H₂S-O₂ interface in organic rich sediments. *Eos* **65**, 905.
- Cohen Y.** (1984b) Comparative N and S cycles: Oxygenic photosynthesis, anoxygenic photosynthesis, and sulfate-reduction in cyanobacterial mats. In *Recent advances in microbial ecology* (M. J. Klug, C. A. Redd.) Washington, D.C., American Society for Microbiology Press. pp. 435-441.
- Cohen Y. and Helman Y.** (1997) Two-dimensional sub-millimetric mapping of sulfate reduction in marine sediments. In American Society for Microbiology 97th General Meeting, Miami Beach, Florida, Abstracts. p. 393.
- Cohen Z., Margheri M. C. and Tomaselli L.** (1995) Chemotaxonomy of cyanobacteria. *Phytochemistry* **40**, 1155-1158.

Bibliography

- Collister J. W., Rieley G., Stern B., Eglinton G. and Fry B.** (1994) Compound-specific $\delta^{13}\text{C}$ analyses of leaf lipids from plants with different carbon dioxide metabolism. *Org. Geochem.* **21**, 619-627.
- Conte M. H., Weber J. C., Carlson P. J. and Flanagan L. B.** (2003) Molecular and carbon isotopic composition of leaf wax in vegetation and aerosols in a northern prairie ecosystem. *Oecologia* **135**, 67-77.
- Cook P. L. M., Reville A., Clementson L. A. and Volkman J. K.** (2004) Carbon and nitrogen cycling on intertidal mudflats of a temperate Australian estuary. III . Sources of organic matter. *Mar. Ecol. Prog. Ser.* **280**, 55-72.
- Craig H.** (1953) The geochemistry of the stable carbon isotopes. *Geochim. Cosmochim. Acta* **3**, 53-92.
- Cypionka H., Widdel F. and Pfennig N.** (1985) Survival of sulfate-reducing bacteria after oxygen stress, and growth in sulfate-free oxygen-sulfide gradients. *FEMS Microbiol. Lett.* **31**, 39-45.
- D**
- Davey M. C.** (1993) Carbon and nitrogen dynamics in a maritime Antarctic stream. *Freshw. Biol.* **30**, 319-330.
- Davison W., Grime G. W., Morgan J. A. W. and Clarke K.** (1991) Distribution of dissolved iron in sediment pore waters at submillimetre resolution. *Nature* **352**, 323-325.
- Davison W. and Zhang H.** (1994) In situ speciation measurements of trace components in natural waters using thin-film gels. *Nature* **367**, 546-548.
- Davison W., Fones G. R. and Grime G. W.** (1997) Dissolved metals in surface sediment and a microbial mat at 100- μm resolution. *Nature* **387**, 885-888.
- Davison W., Fones G. R., Harper M., Teasdale P. R. and Zhang H.** (2000) Dialysis, DET and DGT: in situ diffusional techniques for studying water, sediments and soils. In *In situ monitoring of aquatic systems: chemical analysis and speciation*. (eds. J. Buffle and G. Horvai). John Wiley & Sons, pp. 495-569.
- De Beer D. and K  hl M.** (2001) Interfacial microbial mats and biofilms. In *The Benthic Boundary Layer* (eds. B. P. Boudreau, B. B. J  rgensen). Oxford University Press, New York, pp. 374-394.

Bibliography

- De Lange G. J., Cranston R. E., Hydes D. H. and Boust D.** (1992) Extraction of pore water from marine sediments: A review of possible artifacts with pertinent examples from the North Atlantic. *Mar. Geol.* **109**, 53-76.
- De Leeuw J. W., Cox H. C., van Graas G., van de Meer F. W., Peakman T. M., Baas J. M. A. and van de Graaf B.** (1989) Limited double bond isomerisation and selective hydrogenation of sterenes during early diagenesis. *Geochim. Cosmochim. Acta* **53**, 903-909.
- De Wit R. and Van Gernerden H.** (1988) Growth of the cyanobacterium *Microcoleus chthonoplastes* on sulfide. *FEMS Microbiol. Ecol.* **53**, 203-209.
- De Wit R., Jonkers H. M., van den Ende F. P. and van Gernerden H.** (1989) In situ fluctuations of oxygen and sulphide in marine microbial sediment ecosystems. *Netherlands J. Sea Res.* **23**, 271-281.
- Decho A. W.** (2000) Microbial biofilms in intertidal systems: an overview. *Cont. Shelf Res.* **20**, 1257-1273.
- Decho A. W., Visscher P. T. and Reid R. P.** (2005) Production and cycling of natural microbial exopolymers (EPS) within a marine stromatolite. *Palaeogeogr. Palaeoclimatol. Palaeoecol.* **219**, 71-86.
- Decho, A. W.** (2000) Exopolymer microdomains as a structuring agent for heterogeneity within microbial biofilms. In *Microbial Sediments* (eds. R. Riding, S. M. Awramik). Springer, Berlin, pp. 9-15
- Dembitsky V. M.** (1996) Betaine ether-linked glycerolipids: chemistry and biology. *Prog. Lipid Res.* **35**, 1-51.
- Des Marais D. J., Bauld J., Palmisano A., Summons R. and Ward D.** (1992) The biogeochemistry of carbon in modern microbial mats. In *The Proterozoic Biosphere: A multidisciplinary study* (eds. J. W. Schopf, C. Klein). Cambridge University Press, Cambridge, pp. 299-308.
- Des Marais D. J.** (1995) The biogeochemistry of hypersaline microbial mats. *Adv. Microb. Ecol.* **14**, 251-274.
- Des Marais D. J.** (2003) Biogeochemistry of hypersaline microbial mats illustrates the dynamics of modern microbial ecosystems and the early evolution of the biosphere. *Biol. Bull.* **204**, 160-167.
- Devries C. and Wang F.** (2003) In situ two-dimensional high-resolution profiling of sulfide in sediment interstitial waters. *Environ. Sci. Technol.* **37**, 792-797.
- Dilling W. and Cypionka H.** (1990) Aerobic respiration in sulfate-reducing bacteria. *FEMS Microbiol. Lett.* **71**, 123-127.

Bibliography

- Dobson G., Ward D. M., Robinson N. and Eglinton G.** (1988) Biogeochemistry of hot spring environments: Extractable lipids of a cyanobacterial mat. *Chem. Geol.* **68**, 155-179.
- Dowling N., Widdel F. and White D. C.** (1986) Phospholipid ester-linked fatty acid biomarkers of acetate-oxidizing sulfate reducers and other sulfide-forming bacteria. *J. Gen. Microbiol.* **132**, 1815-1825.
- Dunlop R. W. and Jefferies P. R.** (1985) Hydrocarbons of the hypersaline basins of Shark Bay, Western Australia. *Org. Geochem.* **8**, 313-320.
- Duarte C. M.** (1990) Seagrass nutrient content. *Mar. Ecol. Prog. Ser.* **67**, 201–207.
- Dupraz C., Visscher P. T., Baumgartner L. K. and Reid R. P.** (2004) Microbe-mineral interactions: early carbonate precipitation in a hypersaline lake (Eleuthera Island, Bahamas). *Sedimentology* **51**, 745-765.
- Dupraz C. P. and Visscher P. T.** (2005) Microbial lithification in marine stromatolites and hypersaline mats. *Trends Microbiol.* **13**, 429-438.
- Dupraz C. P., Reid R. P., Braissant O., Decho A. W., Norman R. S. and Visscher P. T.** (2009) Processes of carbonate precipitation in modern microbial mats. *Earth-Science Rev.* **96**, 141-162.
- Dupraz C., Reid R. P. and Visscher P. T.** (2011) Microbialite, Modern. In *Encyclopedia of Geobiology* (eds. J. Reitner, J. and V. Thiel). Springer, Dordrecht Netherlands, pp. 617-635.
- Dutkiewicz A., Rasmussen B. and Buick R.** (1998) Oil preserved in fluid inclusions in Archaean sandstones. *Nature* **395**, 885-888.
- Dutkiewicz A., Volk H., George S. C., Ridley J. and Buick R.** (2006) Biomarkers from Huronian oil-bearing fluid inclusions: An uncontaminated record of life before the Great Oxidation Event. *Geology* **34**, 437-440.

E

- Edgcomb V. P., Bernhard J. M., Beaudoin D., Pruss S. B., Welander P. V, Schubotz F., Mehay S., Gillespie A. L. and Summons R. E.** (2013a) Molecular indicators of microbial diversity in oolitic sands of Highborne Cay, Bahamas. *Geobiology* **11**, 234-51.
- Edgcomb V., Bernhard J., Summons R. E., Orsi W., Beaudoin D. and Visscher P. T.** (2013b) Active eukaryotes in microbialites from Highborne Cay, Bahamas, and Hamelin Pool (Shark Bay), Australia. *ISME J.*

Bibliography

- Eglinton G. and Hamilton R. J.** (1967) Leaf Epicuticular waxes. *Science* **156**, 1322-1335.
- Eglinton G., Scott P., Belsky T., Burlingame A. and Calvin M.** (1964) Hydrocarbons of biological origin from a one billion year old sediment. *Science* **145**, 263-264.
- Ehrenreich A. and Widdel F.** (1994) Anaerobic oxidation of ferrous iron by purple bacteria, a new type of phototrophic metabolism. *Appl. Envir. Microbiol.* **60**, 4517-4526.
- Ehrlich H. L.** (1996) How microbes influence mineral growth and dissolution. *Chem. Geol.* **132**, 5-9.
- Emerson D. and Weiss J. V.** (2004) Bacterial iron oxidation in circumneutral freshwater habitats: findings from the field and the laboratory. *Geomicrobiol. J.* **21**, 405-414.
- Engel M. H. and Macko S. A.** (1997) Isotopic evidence for extraterrestrial non-racemic amino acids in the Murchison meteorite. *Nature* **389**, 265-268.
- Ertefai T. F., Fisher M. C., Fredricks H. F., Lipp J. S., Pearson A., Birgel D., Udert K. M., Cavanaugh C. M., Gschwend P. M. and Hinrichs K.-U.** (2008) Vertical distribution of microbial lipids and functional genes in chemically distinct layers of a highly polluted meromictic lake. *Org. Geochem.* **39**, 1572-1588.

F

- Faure G. and Mensing T.** (2005) *Isotopes, Principles and Applications, Third Edition*. John Wiley & Sons, Inc., Hoboken, New Jersey.
- Ferris M. J., Nold S. C., Revsbech N. P. and Ward D. M.** (1997) Population structure and physiological changes within a hot spring microbial mat community following disturbance. *Appl. Envir. Microbiol.* **63**, 1367-1374.
- Ficken K. J., Li B., Swain D. L. and Eglinton G.** (2000) An *n*-alkane proxy for the sedimentary input of submerged/floating freshwater aquatic macrophytes. *Org. Geochem.* **31**, 745-749.
- Filley T. R., Freeman K. H. and Hatcher P. G.** (1996) Carbon isotope relationships between sulfide-bound steroids and proposed functionalized lipid precursors in sediments from the Santa Barbara Basin, California. *Org. Geochem.* **25**, 367-377.
- Flannery D. T. and Walter M. R.** (2011) Archean tufted microbial mats and the Great Oxidation Event: new insights into an ancient problem. *Aust. J. Earth Sci.* **59**, 1-11.
- Fogel M. L. and Cifuentes L. A.** (1993) Isotope fractionation during primary production. In *Organic geochemistry, principles and applications*. (eds. M.H. Engel and S. A. Macko). Springer US, pp. 73-98.

Bibliography

- Fourçans A., de Oteyza T. G., Wieland a, Solé A., Diestra E., van Bleijswijk J., Grimalt J. O., Kühl M., Esteve I., Muyzer G., Caumette P. and Duran R.** (2004) Characterization of functional bacterial groups in a hypersaline microbial mat community (Salins-de-Giraud, Camargue, France). *FEMS Microbiol. Ecol.* **51**, 55-70.
- Freeman K. H., Hayes J. M., Trendel J. M. and Albrecht P. A.** (1990) Evidence from carbon isotope measurements for diverse origins of sedimentary hydrocarbons. *Nature* **343**, 254–256.
- Freeman K. H., Wakeham S. G. and Hayes J. M.** (1994) Predictive isotopic biogeochemistry: hydrocarbons from anoxic marine basins. *Org. Geochem.* **21**, 629-644.
- Fründ C. and Cohen Y.** (1992) Diurnal cycles of sulfate reduction under oxic conditions in cyanobacterial mats. *Appl. Environ. Microbiol.* **58**, 70-77.
- Fry B.** (1996) $^{13}\text{C}/^{12}\text{C}$ fractionation by marine diatoms. *Mar. Ecol. Prog. Ser.* **134**, 283-294.
- Fry B. and Wainright S. C.** (1991) Diatom sources of ^{13}C -rich carbon in marine food webs. *Mar. Ecol. Prog. Ser.* **76**, 149-157.
- 9
- Gallagher K. L., Kading T. J., Braissant O., Dupraz C. and Visscher P. T.** (2012) Inside the alkalinity engine: the role of electron donors in the organomineralization potential of sulfate-reducing bacteria. *Geobiology* **10**, 518-530.
- Games L. M., Hayes J. M. and Gunsalus R. P.** (1978) Methane-producing bacteria: natural fractionations of the stable carbon isotopes. *Geochim. Cosmochim. Acta* **42**, 1295-1297.
- Garcia-Pinchel F. and Castenholz R. W.** (1991) Characterization and biological implications of scytonemin, a cyanobacterial sheath pigment. *J. Phycol.* **27**, 395-409.
- Geiger O., González-Silva N., López-Lara I. M. and Sohlenkamp C.** (2010) Amino acid-containing membrane lipids in bacteria. *Prog. Lipid Res.* **49**, 46-60.
- Geiger O., Rohrs V., Weissenmayer B., Finan T. M. and Thomas-Oates J. E.** (1999) The regulator gene *phoB* mediates phosphate stress-controlled synthesis of the membrane lipid diacylglycerol-N,N,N-trimethylhomoserine in *Rhizobium* (*Sinorhizobium*) *meliloti*. *Mol. Microbiol.* **32**, 63-73.
- Gelpi E., Schneider H., Mann J. and Oro J.** (1970) Hydrocarbons of geochemical significance in microscopic algae. *Phytochemistry* **9**, 603-612.

Bibliography

- Glud R. N., Ramsing N., Gundersen J. and Klimant I.** (1996) Planar optodes: a new tool for fine scale measurements of two- dimensional O₂ distribution in benthic communities. *Mar. Ecol. Prog. Ser.* **140**, 217-226.
- Glud R. N., Kühl M., Kohls O. and Ramsing N. B.** (1999) Heterogeneity of oxygen production and consumption in a photosynthetic microbial mat as studied by planar optodes. *J. Phycol.* **279**, 270-279.
- Goh F., Allen M. A., Leuko S., Kawaguchi T., Decho A. W., Burns B. P. and Neilan B. A.** (2009) Determining the specific microbial populations and their spatial distribution within the stromatolite ecosystem of Shark Bay. *ISME J.* **3**, 383-396.
- Golubic S. and Hoffman H. J.** (1976) Comparison of Holocene and Mid-Precambrian Entophysalidaceae (Cyanophyta) in stromatolitic algal mats: cell division and degradation. *J. Paleontol.* **50**, 1074-1082.
- Gong C. and Hollander D. J.** (1997) Differential contribution of bacteria to sedimentary organic matter in oxic and anoxic environments, Santa Monica Basin, California. *Org. Geochem.* **26**, 545-563.
- Goodwin T. W.** (1980) *The Biochemistry of the Carotenoids, Volume 2, Animals.* Chapman and Hall. New York.
- Goodwin, T.W.** (1985) Biosynthesis of plant sterols, In: *Sterol and Bile Acids.* (eds. H. Danielsson, J. Sjövall). Elsevier, Amsterdam, pp. 175-198.
- Grice K., Schaeffer P., Schwark L. and Maxwell J. R.** (1996) Molecular indicators of palaeoenvironmental conditions in an immature Permian shale (Kupferschiefer, Lower Rhine Basin, north-west Germany) from free and S-bound lipids. *Org. Geochem.* **25**, 131-147.
- Grice K., Klein Breteler W. C. M., Schouten S., Grossi V., de Leeuw J. W. and Sinninghe Damsté J. S.** (1998a) Effects of zooplankton herbivory on biomarker proxy records. *Paleoceanography* **13**, 686-693.
- Grice K., Schouten S., Nissenbaum A., Charrach J. and Sinninghe Damsté J. S.** (1998b) A remarkable paradox: Sulfurised freshwater algal (*Botryococcus braunii*) lipids in an ancient hypersaline euxinic ecosystem. *Org. Geochem.* **28**, 195-216.
- Grice K.** (2001) $\delta^{13}\text{C}$ as an indicator of paleoenvironments: A molecular approach. In *Application of stable isotope techniques to study biological processes and functioning ecosystems* (eds. Unkovich M, Pate J, McNeill A and Gibbs J), pp. 247-281
- Grice K., Cao C., Love G. D., Bottcher M. E., Twitchett R., Grosjean E., Summons R. E., Turgeon S. E., Dunning W. and Jin Y.** (2005) Photic Zone Euxinia During the Permian-Triassic Superanoxic Event. *Science* **307**, 706-709.

Bibliography

- Grice K., Lu H., Atahan P., Asif M., Hallmann C., Greenwood P., Maslen E., Tulipani S., Williford K. and Dodson J.** (2009) New insights into the origin of perylene in geological samples. *Geochim. Cosmochim. Acta* **73**, 6531-6543.
- Grimalt J. O., Yruela I., Saiz-Jimenez C., Toja J., De Leeuw J. W. and Albaiges J.** (1991) Sedimentary lipid biogeochemistry of an hypereutrophic alkaline lagoon. *Geochim. Cosmochim. Acta* **55**, 2555-2577.
- Grimalt J. O., de Wit R., Teixidor P. and Albaigés J.** (1992) Lipid biogeochemistry of Phormidium and Microcoleus mats. *Org. Geochem.* **19**, 509-530.
- Grosjean E., Love G. D., Stalvies C., Fike D. A. and Summons R. E.** (2009) Origin of petroleum in the Neoproterozoic-Cambrian South Oman Salt Basin. *Org. Geochem.* **40**, 87-110.
- Grossi V., Hirschler a, Raphel D., Rontani J.-F., de Leeuw J. W. and Bertrand J.-C.** (1998) Biotransformation pathways of phytol in recent anoxic sediments. *Org. Geochem.* **29**, 845-861.
- Grossi V., Beker B., Geenevasen J. A. J., Schouten S., Raphel D., Fontaine M.-F. and Sinninghe Damsté J. S.** (2004) C₂₅ highly branched isoprenoid (HBI) alkenes from the marine benthic diatom *Pleurosigma strigosum*. *Phytochem.* **65**, 3049-3055.
- Grotzinger J. P. and Knoll A. H.** (1999) Stromatolites in Precambrian carbonates: evolutionary mileposts or environmental dipsticks? *Annu. Rev. Earth Planet. Sci.* **27**, 313-358.
- Guckert J. B., Hood M. A. and White D. C.** (1986) Phospholipid ester-linked fatty acid profile changes during nutrient deprivation of *Vibrio cholerae*: increases in the trans/cis ratio and proportions of cyclopropyl fatty acids. *Appl. Environ. Microbiol.* **52**, 794-801.
- H
- Hafenbrandl D., Keller M., Dirmeier R., Rachel R., Robnagel P., Burggraf S., Huber H. and Stetter K.** (1996) *Ferroglobusplacidus* gen. nov., sp. nov. a novel hyperthermophilic archaeum that oxidizes Fe²⁺ at neutral pH under anoxic conditions. *Arch. Mikrobiol.* **166**, 308-314.
- Hansen K., King G.M. and Kristensen E.** (1996) Impact of the soft-shell clam *Mya arenaria* on sulfate reduction in an intertidal sediment. *Aquat. Microb. Ecol.* **10**, 181-194.
- Harper M. P., Davison W. and Tych W.** (1999) Estimation of porewater concentrations from DGT profiles: a modelling approach. *Aquat. Geochemistry* **5**, 337-355.

Bibliography

- Hartgers W. A., Lopez J. F., Sinninghe Damste J. S., Reiss C., Maxwell J. R. and Grimalt J. O.** (1997) Sulfur-binding in recent environments: II . Speciation of sulfur and iron and implications for the occurrence of organo-sulfur compounds. *Geochim. Cosmochim. Acta* **61**, 4769-4788.
- Harvey H. R., Fallo R. D. and Pattom J. S.** (1986) The effect of organic matter and oxygen on the degradation of bacterial membrane lipids in marine sediments. *Geochim. Cosmochim. Acta* **50**, 795-804.
- Hastings D. and Emerson S.** (1988) Sulfate reduction in the presence of low oxygen levels in the water column of the Cariaco Trench. *Limnol. Oceanogr.* **33**, 391-396.
- Hayes J.** (1993) Factors controlling ^{13}C contents of sedimentary organic compounds: Principles and evidence. *Mar. Geol.* **113**, 111-125.
- Hebting Y., Schaeffer P., Behrens A., Adam P., Schmitt G., Schneckenburger P., Bernasconi S. M. and Albrecht P. A.** (2006) Biomarker evidence for a major preservation pathway of sedimentary organic carbon. *Science* **312**, 1627-1631.
- Herbert R. A.** (1999) Nitrogen cycling in coastal marine ecosystems. *FEMS Microbiol. Rev.* **23**, 563-590.
- Hertzberg S., Liaaen-Jensen S. and Siegelman H. W.** (1971) The carotenoids of blue-green algae. *Phytochemistry* **10**, 3121-3127.
- Hoefs J.** (2009) *Stable isotope geochemistry*. Springer.
- Hoehler T. M., Bebout B. M. and Des Marais D. J.** (2001) The role of microbial mats in the production of reduced gases on the early Earth. *Nature* **412**, 324-327.
- Hoffman H. J.** (2000) Archean stromatolites as microbial archives. In *Microbial Sediments* (eds. R. Riding, S. M. Awramik). Springer, Berlin, pp. 315-327.
- Hoffman P.** (1976) Stromatolite morphogenesis in Shark Bay, Western Australia. In *Stromatolites*. (ed. M. R. Walter) Elsevier, Amsterdam. pp. 261-272.
- Huang Y., Freeman K. H., Wilkin R. T., Arthur M. A and Jones A. D.** (2000) Black Sea chemocline oscillations during the Holocene: molecular and isotopic studies of marginal sediments. *Org. Geochem.* **31**, 1525-1531.
- Hulth S., Aller R., Engström P. and Selander E.** (2002) A pH plate fluorosensor (optode) for early diagenetic studies of marine sediments. *Limnol. Ocean.* **47**, 212-220.

Bibliography

I

Innes H. E., Bishop A. N., Head I.M. and Farrimond P. (1997) Preservation and diagenesis of hopanoids in Recent lacustrine sediments of Priest Pot, England. *Org. Geochem.* **26**, 565-576.

Itoh Y., Sugai A., Uda I. and Itoh T. (2001) The evolution of lipids. *Adv. Sp. Res. Off. J. Comm. Sp. Res.* **28**, 719-724.

J

Jaffé R., Mead R. N., Hernandez M. E., Peralba M. C. and Diguida O. A. (2001) Origin and transport of sedimentary organic matter in two subtropical estuaries: a comparative, biomarker-based study. *Org. Geochem.* **32**, 507-526.

Jahnert R. and Collins L. (2011) Significance of subtidal microbial deposits in Shark Bay, Australia. *Mar. Geol.* **286**, 106-111.

Jahnert R. and Collins L. (2012) Characteristics, distribution and morphogenesis of subtidal microbial systems in Shark Bay, Australia. *Mar. Geol.* **303-306**, 115-136.

Jahnert R. and Collins L. (2013) Controls on microbial activity and tidal flat evolution in Shark Bay, Western Australia. *Sedimentology* **60**, 1071-1099.

Jahnke L. L., Embaye T., Hope J., Turk K. A., Van Zuilen M., Des Marais D. J., Farmer J. D. and Summons R. E. (2004) Lipid biomarker and carbon isotopic signatures for stromatolite-forming, microbial mat communities and Phormidium cultures from Yellowstone National Park. *Geobiology* **2**, 31-47.

Jahnke L. L., Orphan V. J., Embaye T., Turk K. A., Kubo M. D., Summons R. E. and Des Marais D. J. (2008) Lipid biomarker and phylogenetic analyses to reveal archaeal biodiversity and distribution in hypersaline microbial mat and underlying sediment. *Geobiology* **6**, 394-410.

Jaraula C., Grice K., Twitchett R., Boettcher M., Lemetayer P., Dastidar A. G. and Opazzo L. P. (2013) Elevated pCO₂ leading to End Triassic Extinction, photic zone euxinia and rising sea levels. *Geology* **41**, 955-958.

Jeffrey S. W. (1989) Chlorophyll *c* pigments and their distribution in the chromophyte algae. In *The Chromophyte algae: problems and perspectives*. (eds. J. C. Green, B. S. C. Leadbeater and W. L. Diver) Clarendon Press. pp 13-36.

Bibliography

- Jeffrey S. W., Mantoura R. F. C. and Wright S. W.** (1997) *Phytoplankton pigments in oceanography*. UNESCO Publishing.
- Jensen M. B., Hansen H. C. B., Nielsen N. E. and Magid J.** (1998) Phosphate mobilization and immobilization in two soils incubated under simulated reducing conditions. *Acta Agriculturae Scand. Sect. B, Soil Plant Sci.* **48**, 11-17.
- Jézéquel D., Brayner R., Metzger E., Viollier E., Prévot F. and Fiévet F.** (2007) Two-dimensional determination of dissolved iron and sulfur species in marine sediment porewaters by thin-film based imaging. Thau lagoon (France). *Estuar. Coast. Shelf Sci.* **72**, 420-431.
- Jiang H., Dong H., Yu B., Liu X., Li Y., Ji S. and Zhang C. L.** (2007). Microbial response to salinity change in Lake Chaka, a hypersaline lake on Tibetan plateau. *Environ. Microbiol.* **9**, 2603–2621.
- Jørgensen B. B. and Revsbech N. P.** (1979) Diurnal cycle of oxygen and sulfide microgradients and microbial photosynthesis in a cyanobacterial mat sediment. *Appl. Environ. Microbiol.* **38**, 46-58.
- Jørgensen B. B., Revsbech N. P. and Cohen Y.** (1983) Photosynthesis and structure of benthic microbial mats: microelectrode and SEM studies of four cyanobacterial communities. *Limnol. Ocean.* **28**, 1075-1093.
- Jørgensen B. B., Cohen Y. and Des Marais D. J.** (1987) Photosynthetic action spectra and adaptation to spectral light distribution in a benthic cyanobacterial mat. *Appl. Environ. Microbiol.* **53**, 879-886.
- Jørgensen B. B. and Des Marais D. J.** (1988) Optical properties of benthic photosynthetic Fiber-optic studies of cyanobacterial mats communities. *Limnol. Oceanogr.* **33**, 99-113.
- Jørgensen B. B.** (1994) Diffusion processes and boundary layers in microbial mats. *Microb. Mats NATO ASI* **35**, 243-253.
- Joye S. B., Mazzotta M. L. and Hollibaugh J. T.** (1996) Community metabolism in microbial mats: the occurrence of biologically-mediated iron and manganese reduction. *Estuar. Coast. Shelf Sci.* **43**, 747-766.

K

- Kalkowsky, V. H. E.** (1908): Oolith und stromatolith im nord- deutschen Buntsandstein. *Z. Deut. Geol. Ges.* **60**, 231-242.

Bibliography

- Keeling C., Bacastow R., Carter A., Piper S., Whorf T., Heimann M., Mook W. and Roeloffzen H.** (1989) A three-dimensional model of atmospheric CO₂ transport based on observed winds: 1. Analysis of observational data. Aspects of Climate Variability in the Pacific and the Western Americas. *Geophys. Monogr. Ser.* **55**, 165-236.
- Kenyon C. N., Rippka R. and Stanier R. Y.** (1972) Fatty acid composition and physiological properties of some filamentous blue-green algae. *Arch. Mikrobiol.* **83**, 216-236.
- Knief C., Altendorf K. and Lipski A.** (2003) Linking autotrophic activity in environmental samples with specific bacterial taxa by detection of ¹³C-labelled fatty acids. *Environ. Microbiol.* **5**, 1155-1167.
- Knoll A.** (2003) *Life on a Young Planet*. Princeton University Press, Princeton, NJ.
- Knoll A. H., Javaux E. J., Hewitt D. and Cohen P.** (2006) Eukaryotic organisms in Proterozoic oceans. *Philos. Trans. R. Soc. Lond. B. Biol. Sci.* **361**, 1023-1038.
- Knoll J. R. and Richards F. A.** (1969) A note on the sources of excess alkalinity in anoxic waters. *Deep-Sea Res.* **16**, 205-212.
- Kohl W., Achenbach H. and Reichenbacht H.** (1983) The pigments of *Brevibacterium unens*: aromatic carotenoids. *Phytochemistry* **22**, 207-210.
- Kohn M. J.** (2010) Carbon isotope compositions of terrestrial C3 plants as indicators of (paleo)ecology and (paleo)climate. *Proc. Natl. Acad. Sci. U. S. A.* **107**, 19691-19695.
- Kok M. D., Rijpstra W. I. C., Robertson L., Volkman J. K. and Sinninghe Damsté J. S.** (2000) Early steroid sulfurisation in surface sediments of a permanently stratified lake. *Geochim. Cosmochim. Acta* **64**, 1425-1436.
- Koopmans M. P., Koster J., van Kaam-peters H. M. E., Kenig F., Schouten S., Hartgers W. A., De Leeuw J. W. and Sinninghe-Damsté J. S.** (1996) Diagenetic and catagenetic products of isorenieratene: Molecular indicators for photic zone anoxia. *Geochim. Cosmochim. Acta* **60**, 4467-4496.
- Krekeler D., Sigalevich P., Teske a., Cypionka H. and Cohen Y.** (1997) A sulfate-reducing bacterium from the oxic layer of a microbial mat from Solar Lake (Sinai), *Desulfovibrio oxycliniae* sp. nov. *Arch. Mikrobiol.* **167**, 369-375.
- Krekeler D., Teske A. and Cypionka H.** (1998) Strategies of sulfate-reducing bacteria to escape oxygen stress in a cyanobacterial mat. *FEMS Microbiol. Ecol.* **25**, 89-96.
- Kristensen, E.** (2000) Organic matter diagenesis at the oxic/anoxic interface in coastal marine sediments, with emphasis on the role of burrowing animals. *Hydrobiologia* **426**, 1-24.

Bibliography

- Krumins V., Gehlen M., Arndt S., van Cappellen P. and Regnier P.** (2012) Dissolved inorganic carbon and alkalinity fluxes from coastal marine sediments: model estimates for different shelf environments and sensitivity to global change. *Biogeosciences Discuss.* **9**, 8475-8539.
- Kühl M., Chen M. and Larkum A. W. D.** (2007) Cellular origin, Life in extreme habitats and Astrobiology. In *Algae and cyanobacteria in extreme environments, volume 11.* (ed. J. Seckbach). Springer, Dordrecht. pp. 101-123.
- L
- Leavitt P. R.** (1993) A review of factors that regulate carotenoid and chlorophyll deposition and fossil pigment abundance. *J. Paleolimnol.* **9**, 109-127.
- Leavitt P. R. and Hodgson D. A.** (2001) Sedimentary pigments. In *Tracking environmental change using lake sediments. Volume 3: Terrestrial, algal, and siliceous indicators.* (eds. J. P. Smol, H. J. B. Birks, W. M. Last). Kluwer Academic Publishers, pp 295-325.
- Lepot K., Benzerara K., Brown G. E. and Philippot P.** (2008) Microbially influenced formation of 2, 724 million years old stromatolites. *Nat. Geosci.* **1**, 118–121.
- Lipp J. S., Morono Y., Inagaki F. and Hinrichs K.-U.** (2008) Significant contribution of Archaea to extant biomass in marine subsurface sediments. *Nature* **454**, 991-994.
- Logan B. W.** (1961) Cryptozoon and Associate Stromatolites from the Recent , Shark Bay , Western Australia. *J. Geol.* **69**, 517-533.
- Logan B. W. and Cebulski D. E.** (1970) Sedimentary Environments of Shark Bay, Western Australia. *Am. Assoc. Pet. Geol. Mem.* **13**, 1-37.
- Logan B. W.** (1974) Evolution and diagenesis of Quarternary carbonate sequences, Shark Bay, Western Australia. *Am. Assoc. Pet. Geol. Mem.* **22**, 195-249.
- Lomstein B., Jensen A., Hansen J., Andreasen J., Hansen L., Berntsen J. and Kunzendorf H.** (1998) Budgets of sediment nitrogen and carbon cycling in the shallow water of Knebel Vig, Denmark. *Aquat. Microb. Ecol.* **14**, 69-80.
- Londry K. L., Jahnke L. L. and Des Marais D. J.** (2004) Stable carbon isotope ratios of lipid biomarkers of sulfate-reducing bacteria. *Appl. Environ. Microbiol.* **70**, 745-751.
- Lopez J. F., de Oteyza T. G., Teixidor P. and Grimalt J. O.** (2005) Long chain alkenones in hypersaline and marine coastal microbial mats. *Org. Geochem.* **36**, 861-872.

Bibliography

- López-Lara I. M., Sohlenkamp C. and Geiger O.** (2003) Membrane lipids in plant-associated bacteria: their biosyntheses and possible functions. *Mol. Plant Microbe Inter.* **16**, 567-579.
- Love G. D., Snape C., Carr A. D. and Houghton C.** (1995) Release of covalently-bound alkane biomarkers in high yields from kerogen via catalytic hydrolysis. *Org. Geochem.* **23**, 981-986.
- Love G. D., McAulay A., Snape C. and Bishop A. N.** (1997) Effect of process variables in catalytic hydrolysis on the release of covalently bound aliphatic hydrocarbons from sedimentary organic matter. *Energy & Fuels* **11**, 522-531.
- Love G. D., Bowden S. A., Jahnke L. L., Snape C., Campbell C. N., Day J. G. and Summons R. E.** (2005) A catalytic hydrolysis method for the rapid screening of microbial cultures for lipid biomarkers. *Org. Geochem.* **36**, 63-82.
- Love G. D., Grosjean E., Stalvies C., Fike D. a, Grotzinger J. P., Bradley A. S., Kelly A. E., Bhatia M., Meredith W., Snape C., Bowring S. A., Condon D. J. and Summons R. E.** (2009) Fossil steroids record the appearance of Demospongiae during the Cryogenian period. *Nature* **457**, 718-721.
- Ludwig R., Pringault O., de Wit R., de Beer D. and Jonkers H. M.** (2006) Limitation of oxygenic photosynthesis and oxygen consumption by phosphate and organic nitrogen in a hypersaline microbial mat: a microsensor study. *FEMS Microbiol. Ecol.* **57**, 9-17.
- Luther III G. W. and Church T. M.** (1988) Seasonal cycling of sulfur and iron in porewaters of a Delaware salt marsh. *Mar. Chem.* **23**, 295-309.
- Luther, III G. W., Glazer B. T., Hohmann L., Popp J. I., Taillefert M., Rozan T. F., Brendel P. J., Theberge S. M. and Nuzzio D. B.** (2001) Sulfur speciation monitored in situ with solid state gold amalgam voltammetric microelectrodes: polysulfides as a special case in sediments, microbial mats and hydrothermal vent waters. *J. Environ. Monit.* **3**, 61-66.
- Lyons W. B., Long D. T., Hines M. E., Gaudette H. E. and Armstrong P. B.** (1984) Calcification of cyanobacterial mats in Solar Lake, Sinai. *Geology* **12**, 623-626.



- Makula R. A. and Finnerty W. R.** (1975) Isolation and characterization of an ornithine-containing lipid from *Desulfovibrio gigas*. *J. Bacteriol.* **123**, 523-529.
- Mango F. D.** (1991) The stability of hydrocarbons under the time-temperature conditions of petroleum genesis. *Nature* **352**, 146-148.

Bibliography

- Mao Che L., Andréfouët S., Bothorel V., Guezennec M., Rougeaux H., Guezennec J., Deslandes E., Trichet J., Matheron R., Champion T. Le, Payri C. and Caumette P.** (2001) Physical, chemical, and microbiological characteristics of microbial mats (KOPARA) in the South Pacific atolls of French Polynesia. *Can. J. Microbiol.* **47**, 994-1012.
- Matthews D. and Hayes J.** (1978) Isotope-ratio-monitoring gas chromatography-mass spectrometry. *Anal. Chem.* **50**, 1465-1473.
- McCaffrey M. A., Farrington J. W. and Repeta D. J.** (1989) Geochemical implications of the lipid composition of *Thioploca* spp. from the Peru upwelling region-15°S. *Org. Geochem.* **14**, 61-68.
- McKirdy D. M., Thorpe C. S., Haynes D. E., Grice K., Krull E. S., Halverson G. P. and Webster L. J.** (2010) The biogeochemical evolution of the Coorong during the mid- to late Holocene: An elemental, isotopic and biomarker perspective. *Org. Geochem.* **41**, 96-110.
- Melendez I., Grice K. and Schwark L.** (2013) Exceptional preservation of Palaeozoic steroids in a diagenetic continuum. *Nat. Sci. Reports* **3**, 1-6.
- Mendelson C. and Schopf J. W.** (1992) Proterozoic and selected Early Cambrian microfossils and microfossil-like objects. In *The Proterozoic Biosphere: A multidisciplinary study* (eds. J. W. Schopf, C. Klein). Cambridge University Press, Cambridge, pp. 865-951.
- Meredith W., Russell C. A., Cooper M., E. Snape C., Love G. D., Fabbri D. and Vane C. H.** (2004) Trapping hydropyrolysates on silica and their subsequent thermal desorption to facilitate rapid fingerprinting by GC-MS. *Org. Geochem.* **35**, 73-89.
- Meziane T. and Tsuchiya M.** (2000) Fatty acids as tracers of organic matter in the sediment and food web of a mangrove/intertidal flat ecosystem, Okinawa, Japan. *Mar. Ecol. Prog. Ser.* **200**, 49-57.
- Meziane T., Bodineau L., Retiere C. and Thoumelin G.** (1997) The use of lipid markers to define sources of organic matter in sediment and food web of the intertidal salt-marsh-flat ecosystem of Mont-Saint-Michel Bay, France. *J. Sea Res.* **38**, 47-58.
- Millero F. J.** (1991) The oxidation of H₂S in Framvaren Fjord. *Limnol. Oceanogr.* **36**, 1007-1014.
- Minnikin D. E. and Abdolrahimzadeh H.** (1974) Effect of pH on the proportions of polar Lipids in chemostat cultures of *Bacillus subtilis*. *J. Bacteriol.* **120**, 999-1003.

Bibliography

- Minz D., Flax J. L., Green S. J., Muyzer G., Cohen Y., Wagner M., Rittmann B. E. and Stahl D. A.** (1999) Diversity of sulfate-reducing bacteria in oxic and anoxic regions of a microbial mat characterised by comparative analysis of dissimilatory sulfite reductase genes. *Appl. Environ. Microbiol.* **65**, 4666-4671.
- Moldowan J. M., SundaraRaman P. and Schoell M.** (1986) Sensitivity of biomarker properties to depositional environment and/or source input in the Lower Toarcian of SW-Germany. *Org. Geochem.* **10**, 915-926.
- Mook W. G., Bommerson J. C. and Staverman W. H.** (1974) Carbon isotope fractionation between dissolved bicarbonate and gaseous carbon dioxide. *Earth Planet. Sci. Lett.* **22**, 169-176.
- Mouné S., Caumette P., Matheron R. and Willison J. C.** (2003) Molecular sequence analysis of prokaryotic diversity in the anoxic sediments underlying cyanobacterial mats of two hypersaline ponds in Mediterranean salterns. *FEMS Microbiol. Ecol.* **44**, 117-130.
- Mozingo R., Spencer C. and Folers C.** (1944) Hydrogenation by raney nickel catalyst without gaseous hydrogen. *J. Am. Chem. Soc.* **66**, 1859-1860.
- Mueller D. R., Vincent W. F., Bonilla S. and Laurion I.** (2005) Extremotrophs, extremophiles and broadband pigmentation strategies in a high arctic ice shelf ecosystem. *FEMS Microbiol. Ecol.* **53**, 73-87.
- Muller, S. G., Krapez, B., Barley, M. E., and Fletcher, I. R.** (2005) Giant iron-ore deposits of the Hamersley province related to the breakup of Paleoproterozoic Australia: New insights from in situ SHRIMP dating of baddeleyite from mafic intrusions. *Geology* **33**, 577-580.
- Murray J., Stewart K., Kassakian S., Krynytzky M. and Di Julio D.** (2007) Oxic, suboxic, and anoxic conditions in the Black Sea. In *The black sea flood question, changes in coastline, climate and human settlement.* (eds. V. Yanko-Hombach, A. S. Gilbert, N. Panin, P. M. Dolukhanow) Springer, Dordrecht, pp. 1-21.

N

- Nabbefeld B., Grice K., Schimmelmann A., Summons R. E., Troitzsch U. and Twitchett R. J.** (2010) A comparison of thermal maturity parameters between freely extracted hydrocarbons (Bitumen I) and a second extract (Bitumen II) from within the kerogen matrix of Permian and Triassic sedimentary rocks. *Org. Geochem.* **41**, 78-87.
- Nageli C.** (1849) *Gattungen einzelliger Algen.* Zurich.

Bibliography

- Navarrete A.** (1999) PhD thesis. Caracterización bioquímica y ecofisiológica de los tapetes microbianos del delta del Ebro. Universitat de Barcelona, Barcelona, Spain.
- Navarrete A., Peacock A., Macnaughton S. J., Urmeneta J., Mas-Castellà J., White D. C. and Guerrero R.** (2000) Physiological status and community composition of microbial mats of the Ebro Delta, Spain, by signature lipid biomarkers. *Microb. Ecol.* **39**, 92-99.
- Nicholson J., Stolz J. F. and Pierson B.** (1987) Structure of a microbial mat at Great Sippewissett Marsh, Cape Cod, Massachusetts. *FEMS Microbiol. Ecol.* **45**, 343-364.
- Niemann H. and Elvert M.** (2008) Diagnostic lipid biomarker and stable carbon isotope signatures of microbial communities mediating the anaerobic oxidation of methane with sulphate. *Org. Geochem.* **39**, 1668-1677.
- Nishimura M. and Koyama T.** (1977) The occurrence of stanols in various living organisms and the behavior of sterols in contemporary sediments. *Geochim. Cosmochim. Acta* **41**, 379-385.
- Nishimura M.** (1978) Geochemical characteristics of the high reduction zone of stanols in Suwa sediments and the environmental factors controlling the conversion of stanols into stanols. *Geochim. Cosmochim. Acta* **42**, 349-357.
- 
- Okazaki K., Sato N., Tsuji N., Tsuzuki M. and Nishida I.** (2006) The significance of C₁₆ fatty acids in the sn-2 positions of glycerolipids in the photosynthetic growth of *Synechocystis* sp. PCC6803. *Plant Physiol.* **141**, 546-556.
- Oliver J. D. and Colwell R. R.** (1973) Extractable lipids of gram-Negative marine bacteria?: fatty - acid composition. *Int. J. Syst. Bacteriol.* **23**, 442-458.
- Olsen I. and Jantzen E.** (2001) Sphingolipids in bacteria and fungi. *Anaerobe* **7**, 103-112.
- Oren A.** (2002) Molecular ecology of extremely halophilic Archaea and Bacteria. *FEMS Microbiol. Ecol.* **39**, 1-7.
- Orphan V. J., Jahnke L. L., Embaye T., Turk K. A., Pernthaler A., Summons R. E. and Des Marais D. J.** (2008) Characterization and spatial distribution of methanogens and methanogenic biosignatures in hypersaline microbial mats of Baja California. *Geobiology* **6**, 376-393.
- Overmann J., Cypionka H. and Pfennig N.** (1992) An extremely low-light-adapted phototrophic sulfur bacterium from the Black Sea. *Limnol. Oceanogr.* **37**, 150-155.

Bibliography

Overmann J. and van Gernerden H. (2000) Microbial interactions involving sulfur bacteria: implications for the ecology and evolution of bacterial communities. *FEMS Microbiol. Rev.* **24**, 591-599.

P

Paerl H. W., Bebout B. M. and Prufert L. (1989) Naturally occurring patterns of oxygenic photosynthesis and N₂ fixation in a marine microbial mat: physiological and ecological ramifications. In *Microbial mats: physiological ecology of benthic microbial communities* (eds. Y. Cohen, E. Rosenberg). American Society Microbiology, Washington, pp. 326-341.

Paerl H. W. and Pinckney J. L. (1996) A mini-review of microbial consortia: Their roles in aquatic production and biogeochemical cycling. *Microb. Ecol.* **31**, 225-247.

Paerl H. W., Pinckney J. L. and Steppe T. F. (2000) Cyanobacterial-bacterial mat consortia: examining the functional unit of microbial survival and growth in extreme environments. *Environ. Microbiol.* **2**, 11-26.

Pagès A., Teasdale P. R., Robertson D., Bennett W. W., Schäfer J. and Welsh D. T. (2011) Representative measurement of two-dimensional reactive phosphate distributions and co-distributed iron(II) and sulfide in seagrass sediment porewaters. *Chemosphere* **85**, 1256-1261.

Pagès A., Welsh D. T., Robertson D., Panther J. G., Schäfer J., Tomlinson R. B. and Teasdale P. R. (2012) Diurnal shifts in co-distributions of sulfide and iron(II) and profiles of phosphate and ammonium in the rhizosphere of *Zostera capricorni*. *Estuar. Coast. Shelf Sci.* **115**, 282-290.

Pagès A., Grice K., Vacher M., Teasdale P., Welsh D., Bennett W. and Greenwood P. (2014a) Characterising microbial communities and processes in a modern stromatolite (Shark Bay) using lipid biomarkers and two-dimensional distributions of porewater solutes. *Environ. Microbiol.*, accepted.

Pagès A., Welsh D. T., Teasdale P. R., Grice K., Vacher M., Bennett W. W. and Visscher P. T. (2014b) Diel fluctuations in solute distributions and biogeochemical cycling in a hypersaline microbial mat from Shark Bay, WA. *Mar. Chem.*, accepted

Palmisano A., Cronin S. and Des Marais D. J. (1988) Analysis of lipophilic pigments from a phototrophic microbial mat community by high performance liquid chromatography. *J. Microbiol. Methods* **8**, 209-217.

Palmisano A. C., Summons R. E., Cronin S. E. and Des Marais D. J. (1989) Lipophilic pigments from cyanobacterial (blue-green algal) and diatom mats in Hamelin Pool, Shark Bay, Western Australia. *J. Phycol.* **25**, 655-661.

Bibliography

- Pancost R. D., Freeman K. H., Wakeham S. G. and Robertson C. Y.** (1997) Controls on carbon isotope fractionation by diatoms in the Peru upwelling region. *Geochim. Cosmochim. Acta* **61**, 4983-4991.
- Pancost R. D., van Geel B., Baas M. and Sinninghe Damsté J. S.** (2000) $\delta^{13}\text{C}$ values and radiocarbon dates of microbial biomarkers as tracers for carbon recycling in peat deposits. *Geology* **28**, 663-666.
- Pancost R. D. and Sinninghe Damsté J. S.** (2003) Carbon isotopic compositions of prokaryotic lipids as tracers of carbon cycling in diverse settings. *Chem. Geol.* **195**, 29-58.
- Paoletti C., Pushparaj B., Florenzano G., Capella P. and Lercker G.** (1976) Unsaponifiable matter of green and blue-green algal lipids as a factor of biochemical differentiation of their biomasses: I. Total unsaponifiable and hydrocarbon fraction. *Lipids* **11**, 258-265.
- Papineau D., Walker J. J., Mojzsis S. J. and Pace N. R.** (2005) Composition and structure of microbial communities from stromatolites of Hamelin Pool in Shark Bay, Western Australia. *Appl. Environ. Microbiol.* **71**, 4822-4832.
- Parfitt, R. L., Atkinson, R. J. and Smart R. St. C.** (1975) The mechanism of phosphate fixation by iron oxides. *Soil Sci. Soc. Am. J.* **39**, 837-841.
- Paul D., Skrzypek G. and Forizs I.** (2007) Normalization of measured stable isotope composition to isotope reference scale - a review. *Rapid Commun. Mass Spectrom.* **21**, 3006-3014.
- Pearson M. J., Hendry J. P., Taylor C. W. and Russell M. A.** (2005) Fatty acids in sparry calcite fracture fills and microsparite cement of septarian diagenetic concretions. *Geochim. Cosmochim. Acta* **69**, 1773-1786.
- Pedrós-Alió C., Calderón-Paz J. I., MacLean M. H., Medina G., Marrasé C., Gasol J. M. and Guixa-Boixereu N.** (2000). The microbial food web along salinity gradients. *FEMS Microbiol. Ecol.* **32**, 143-155.
- Peters K. E. and Moldowan J. M.** (1993) *The Biomarker Guide*. Prentice Hall, Engelwood Cliffs, NJ.
- Peters K. E., Walters C. C. and Moldowan J. M.** (2005) *The Biomarker Guide: Biomarkers and isotopes in the environment and human history, Volume 1*. Cambridge University Press.
- Pierson B. K. and Castenholz R. W.** (1971) Bacteriochlorophylls in gliding filamentous prokaryotes from hot springs. *Nature* **233**, 25-27.

Bibliography

- Pike J., Bernhard J. M., Moreton S. G. and Butler I. B.** (2001) Microbioirrigation of marine sediments in dysoxic environments: Implications for early sediment fabric formation and diagenetic processes. *Geology* **29**, 923-926.
- Pillans, B.** (2005) Geochronology of Australian Regolith. *CRC LEME*, 1-12.
- Pinckney J. L., Paerl H. W. and Fitzpatrick M.** (1995) Impacts of seasonality and nutrients on microbial mat community structure and function mat community structure and function. *Mar. Ecol. Prog. Ser.* **123**, 207-216.
- Playford P. E.** (1990) Geology of the Shark Bay area, Western Australia. In *Research in Shark Bay. Report of the France-Australe Bicentenary Expedition Committee. Western Australian Museum, Perth.* (eds. P.F. Berry, , S. D. Bradshaw and B. R. Wilson, B.R.), pp. 13-33.
- Popp B. N., Lawa E. A., Bidigare R. R., Dore J. E., Hanson K. L. and Wakeham S. G.** (1998) Effect of phytoplankton cell geometry on carbon isotopic fractionation. *Geochim. Cosmochim. Acta* **62**, 69-77.
- Powell T. G. and McKirdy D. M.** (1973) Relationship between ratio of pristane to phytane, crude oil composition and geological environment in Australia. *Nature* **243**, 37-39.
- Prahl F. G., Bennett J. T. and Carpenter R.** (1980) The early diagenesis of aliphatic hydrocarbons and organic matter in sedimentary particulates from Dabob Bay, Washington. *Geochim. Cosmochim. Acta* **44**, 1967-1976.
- Price R. M., Skrzypek G., Grierson P. F., Swart P. K. and Fourqurean J. W.** (2012) The use of stable isotopes of oxygen and hydrogen to identify water sources in two hypersaline estuaries with different hydrologic regimes. *Mar. Freshw. Res.* **63**, 952-966.

Q

- Quandt L., Gottschalk G., Ziegler H., and Stichler W.** (1977) Isotopic discrimination by photosynthetic bacteria. *FEMS Microbiol. Lett.* **1**, 125-128.

R

- Rasmussen, B., Fletcher, I.R., Sheppard, S.** (2005) Isotopic dating of the migration of a low-grade metamorphic front during orogenesis. *Geology* **33**, 773-776.
- Rasmussen B., Fletcher I. R., Brocks J. J. and Kilburn M. R.** (2008) Reassessing the first appearance of eukaryotes and cyanobacteria. *Nature* **455**, 1101-1104.

Bibliography

- Ratledge C. and Wilkinson S.** (1988) *Microbial lipids*. Academic Press.
- Reid R. P., Visscher P. T., Decho A. W., Stolz J. F. and Bebout B. M.** (2000) The role of microbes in accretion, lamination and early lithification of modern marine stromatolites. *Nature* **406**, 989-992.
- Revsbech N. P., Sorensen J., Blackburn T. H. and Lomholt J. P.** (1980) Distribution of oxygen in marine sediments measured with microelectrodes. *Limnol. Ocean.* **25**, 403-411.
- Revsbech N. P. and Jørgensen B. B.** (1983) Photosynthesis of benthic microflora measured with high spatial resolution by the oxygen microprofile method: capabilities and limitations of the method. *Limnol. Oceanogr.* **28**, 749-756.
- Revsbech N. P. and Jørgensen B. B.** (1986) Microelectrodes: their use in microbial ecology. *Adv. Microb. Ecol.* **9**, 193-352.
- Rezanka T., Sokolov M. and Viden I.** (1990) Unusual and very-long-chain fatty acids in *Desulfotomaculum*, a sulfate-reducing bacterium. *FEMS Microbiol. Lett.* **73**, 231-237.
- Rezanka T. and Sigler K.** (2009) Odd-numbered very-long-chain fatty acids from the microbial, animal and plant kingdoms. *Prog. Lipid Res.* **48**, 206-238.
- Rickard D. and Morse J. W.** (2005) Acid volatile sulfide (AVS). *Mar. Chem.* **97**, 141-197.
- Riding R.** (2000) Microbial carbonates: the geological record of calcified bacterial- algal mats and biofilms. *Sedimentology* **47**, 179-214.
- Risatti J. B., Capman W. C. and Stahl D. A.** (1994) Community structure of a microbial mat: the phylogenetic dimension. *Proc. Natl. Acad. Sci. U. S. A.* **91**, 10173-10177.
- Robertson D., Teasdale P. R. and Welsh D. T.** (2008) A novel gel-based technique for the high resolution, two-dimensional determination of iron(II) and sulfide in sediment. *Limnol. Oceanogr. Methods* **6**, 502-512.
- Robertson D., Welsh D. T. and Teasdale P. R.** (2009) Investigating biogenic heterogeneity in coastal sediments with two-dimensional measurements of iron(II) and sulfide. *Environ. Chem.* **6**, 60-69.
- Robertson E. L. and Liber K.** (2009) Effect of sampling method on contaminant measurement in pore-water and surface water at two uranium operations: can method affect conclusions? *Environ. Monit. Assess.* **155**, 539-553.
- Robinson N. and Eglinton G.** (1990) Lipid chemistry of Icelandic hot spring microbial mats. *Org. Geochem.* **15**, 291-298.

Bibliography

- Rohmer M., Bouvier-Nave P. and Ourisson G.** (1984) Distribution of hopanoid triterpenes in prokaryotes. *Microbiology* **130**, 1137-1150.
- Rontani J.-F. and Volkman J. K.** (2005) Lipid characterization of coastal hypersaline cyanobacterial mats from the Camargue (France). *Org. Geochem.* **36**, 251-272.
- Rontani J.-F., Bonin P., Vaultier F., Guasco S. and Volkman J. K.** (2013) Anaerobic bacterial degradation of pristenes and phytanes in marine sediments does not lead to pristane and phytane during early diagenesis. *Org. Geochem.* **58**, 43-55.
- Rossel P., Lipp J., Fredricks H., Arnds J., Boetius A., Elvert M. and Hinrichs K.-U.** (2008) Intact polar lipids of anaerobic methanotrophic Archaea and associated bacteria. *Org. Geochem.* **39**, 992-999.
- Rossel P. E., Elvert M., Ramette A., Boetius A. and Hinrichs K.-U.** (2011) Factors controlling the distribution of anaerobic methanotrophic communities in marine environments: Evidence from intact polar membrane lipids. *Geochim. Cosmochim. Acta* **75**, 164-184.
- Rütters H., Sass H., Cypionka H. and Rullkötter J.** (2002) Phospholipid analysis as a tool to study complex microbial communities in marine sediments. *J. Microbiol. Methods* **48**, 149-160.

S

- Saas H., Cypionka H. and Babenzien H.-D.** (1997) Vertical distribution of sulfate-reducing bacteria at the oxic-anoxic interface in sediments of the oligotrophic lake Stechlin. *FEMS Microbiol. Ecol.* **22**, 245-255.
- Sabbe K., Hodgson D. A., Verleyen E., Taton A., Wilmotte A., Vanhoutte K. and Vyverman W.** (2004) Salinity, depth and the structure and composition of microbial mats in continental Antarctic lakes. *Freshw. Biol.* **49**, 296-319.
- Sakata S., Hayes J. M., McTaggart A. R., Evans R. A., Leckrone K. J. and Togasaki R. K.** (1997) Carbon isotopic fractionation associated with lipid biosynthesis by a cyanobacterium: relevance for interpretation of biomarker records. *Geochim. Cosmochim. Acta* **61**, 5379-5389.
- Sato, N.** (1992) Betaine lipids. *Bot. Mag. Tokyo* **105**, 185-197.
- Schaeffer P., Reiss C. and Albrecht P. A.** (1995) Geochemical study of macromolecular organic matter from sulfur-rich sediments of evaporitic origin (Messinian of Sicily) by chemical degradations. *Org. Geochem.* **23**, 567-581.

Bibliography

- Schidlowski M., Matzigkeit U. and Krumbein W. E.** (1984) Superheavy organic carbon from hypersaline microbial mats. *Naturwissenschaften* **71**,303-308
- Schidlowski M., Gorzawski H. and Dor I.** (1994) Carbon isotope variations in a solar pond microbial mat: Role of environmental gradients as steering variables. *Geochim. Cosmochim. Acta* **58**, 2289–2298.
- Schirmer A., Rude M. A., Li X., Popova E. and del Cardayre S. B.** (2010) Microbial biosynthesis of alkanes. *Science* **329**, 559-562.
- Schmidt K.** (1979) Biosynthesis of carotenoids. In *The Photosynthetic Bacteria*. (eds. R. K. Clayton and W. R. Sistrom) Plenum Press, pp. 729-750.
- Schmidt S. K., Costello E. K., Nemergut D. R., Cleveland C. C., Reed S. C., Weintraub M. N., Meyer A. F. and Martin A. M.** (2007) Biogeochemical consequences of rapid microbial turnover and seasonal succession in soil. *Ecology* **88**, 1379-1385.
- Scholle P.** (1995) Carbon and Sulfur Isotope Stratigraphy of the Permian and Adjacent Intervals. In *The Permian of Northern Pangea*. (eds. P. Scholle, T. Peryt, D. Ulmer-Scholle) Springer Berlin Heidelberg, pp. 133-149.
- Schopf J. W.** (1999) *Cradle of Life*. Princeton University Press, Princeton, NJ.
- Schopf J. W., Kudryavtsev A. B., Agresti D. G., Czaja A. D. and Wdowiak T. J.** (2005) Raman imagery: a new approach to assess the geochemical maturity and biogenicity of permineralized precambrian fossils. *Astrobiology* **5**, 333-371.
- Schopf J. W., Kudryavtsev A. B., Czaja A. D. and Tripathi A. B.** (2007) Evidence of Archean life: Stromatolites and microfossils. *Precambrian Res.* **158**, 141-155.
- Schopf J. W., Kudryavtsev A. B. and Sergeev V. N.** (2010) Confocal laser scanning microscopy and raman imagery of the late Neoproterozoic chichkan microbiota of south Kazakhstan. *J. Paleontol.*, **84**, 402-416.
- Schouten S., Klein Breteler W. C. ., Blokker P., Schogt N., Rijpstra W. I. C., Grice K., Baas M. and Sinninghe Damsté J. S.** (1998) Biosynthetic effects on the stable carbon isotopic compositions of algal lipids: implications for deciphering the carbon isotopic biomarker record. *Geochim. Cosmochim. Acta* **62**, 1397-1406.
- Schubotz F., Wakeham S. G., Lipp J. S., Fredricks H. F. and Hinrichs K.-U.** (2009) Detection of microbial biomass by intact polar membrane lipid analysis in the water column and surface sediments of the Black Sea. *Environ. Microbiol.* **11**, 2720-2734.
- Semikhatov M. A., Gebelein C. D., Could P., Awramik S. M. and Benmore W. C.** (1979) Stromatolite morphogenesis-progress and problems. *Can. J. Earth Sci.* **16**, 992-1015.

Bibliography

- Sephton M. A., Meredith W., Sun C.-G. and Snape C.** (2005) Hydropyrolysis of steroids: a preparative step for compound-specific carbon isotope ratio analysis. *Rapid Commun. Mass Spectrom.* **19**, 3339-3342.
- Shen Y., Buick R. and Canfield D. E.** (2001) Isotopic evidence for microbial sulphate reduction in the early Archaean era. *Nature* **410**, 77-81.
- Shiea J., Brassell S. C. and Ward D. M.** (1990) Mid-chain branched mono- and dimethyl alkanes in hot spring cyanobacterial mats: A direct biogenic source for branched alkanes in ancient sediments? *Org. Geochem.* **15**, 223-231.
- Shimada H., Nemoto N., Shida Y., Oshima T. and Yamagishi A.** (2008) Effects of pH and temperature on the composition of polar lipids in *Thermoplasma acidophilum* HO-62. *J. Bacteriol.* **190**, 5404-5411.
- Shively J. M. and Knoche H. W.** (1969) Isolation of an ornithine-containing lipid from *Thiobacillus thiooxidans*. *J. Bacteriol.* **98**, 829-830.
- Shuttleworth S. M., Davison W. and Hamilton-Taylor J.** (1999) Two-dimensional and fine structure in the concentrations of iron and manganese in sediment porewaters. *Environ. Sci. Technol.* **33**, 4169-4175.
- Sieskind O., Joly G. and Albrecht P. A.** (1979) Simulation of the geochemical transformations of sterols: superacid effect of clay minerals. *Geobiology* **43**, 1675-1679.
- Sinninghe Damsté J. S. and de Leeuw J. W.** (1990) Analysis, structure and geochemical significance of organically-bound sulphur in the geosphere: State of the art and future research. *Org. Geochem.* **16**, 1077-1101.
- Skirnisdottir S., Hreggvidsson G. O., Hjörleifsdottir S., Marteinson V. T., Solveig K., Holst O. and Kristjansson J. K.** (2000) Influence of sulfide and temperature on species composition and community structure of hot spring microbial mats. *Appl. Environ. Microbiol.* **66**, 2835-2841.
- Skrzypek G., Sadler R. and Paul D.** (2010) Error propagation in normalization of stable isotope data: a Monte Carlo analysis. *Rapid Commun. Mass Spectrom.* **24**, 2697-2705.
- Skrzypek G.** (2013) Normalization procedures and reference material selection in stable HCNOS isotope analyses: an overview. *Anal. Bioanal. Chem.* **405**, 2815-2823.
- Skyring G. W. and Bauld J.** (1990) Microbial mats in Australian coastal environments. In *Advances in Microbial Ecology 11* (ed. K. C. Marshall). Plenum, New York. pp. 461-498.
- Smith S. V. and Atkinson M. J.** (1983) Mass balance of carbon and phosphorus Shark Bay, Western Australia. *Limnol. Oceanogr.* **28**, 625-639.

Bibliography

- Smolders A. J. P., Nijboer R. C. and Roelofs J. G. M.** (1995) Prevention of sulphide accumulation and phosphate mobilization by the addition of iron(II) chloride to a reduced sediment: an enclosure experiment. *Freshw. Biol.* **34**, 559-568.
- Sohlenkamp C., Lopez-Lara I. M. and Geiger O.** (2003) Biosynthesis of phosphatidylcholine in bacteria. *Prog. Lipid Res.* **42**, 115-162.
- Stal L. J., Van Gernerden H. and Krumbein W.** (1985) Structure and development of a benthic marine microbial mat. *FEMS Microbiol. Ecol.* **31**, 111-125.
- Stal L. J.** (2001) Coastal microbial mats: the physiology of a small-scale ecosystem. *South African J. Bot.* **67**, 399-410.
- Stockdale A., Davison W. and Zhang H.** (2009) Micro-scale biogeochemical heterogeneity in sediments: A review of available technology and observed evidence. *Earth-Science Rev.* **92**, 81-97.
- Sturt H. F., Summons R. E., Smith K., Elvert M. and Hinrichs K.-U.** (2004) Intact polar membrane lipids in prokaryotes and sediments deciphered by high-performance liquid chromatography/electrospray ionization multistage mass spectrometry-new biomarkers for biogeochemistry and microbial ecology. *Rapid Commun. Mass Spectrom.* **18**, 617-628.
- Summons R. E. and Powell T. G.** (1986) *Chlorobiaceae* in Paleozoic seas revealed by biological markers, isotopes and geology. *Nature* **319**, 763-765.
- Summons R. E. and Powell T. G.** (1987) Identification of aryl isoprenoids in source rocks and crude oils: Biological markers for the green sulphur bacteria. *Geochim. Cosmochim. Acta* **51**, 557-566.
- Summons R. E., Powell T. G. and Boreham C. J.** (1988) Petroleum geology and geochemistry of the Middle Proterozoic McArthur Basin, Northern Australia: III. Composition of extractable hydrocarbons. *Geochim. Cosmochim. Acta* **52**, 1747-1763.
- Summons R. E. and Walter M. R.** (1990) Molecular fossils and microfossils of prokaryotes and protists from proterozoic sediments. *Am. J. Sci.* **290**, 212-244.
- Summons R. E., Barrow R., Capon R., Hope J. and Stranger C.** (1993) The structure of a new C₂₅ isoprenoid alkene biomarker from diatomaceous microbial communities. *Aust. J. Chem.* **46**, 907-915.
- Summons R. E., Jahnke L. L. and Roksandic Z.** (1994) Carbon isotopic fractionation in lipids from methanotrophic bacteria: Relevance for interpretation of the geochemical record of biomarkers. *Geochim. Cosmochim. Acta* **58**, 2853-2863.
- Summons R. E., Jahnke L. L., Hope J. and Logan G. A.** (1999) 2-Methylhopanoids as biomarkers for cyanobacterial oxygenic photosynthesis. *Nature* **400**, 554-557.

Bibliography

Summons R. E., Bird L. R., Gillespie A. L., Pruss S. B., Roberts M. and Sessions A. L. (2013) Lipid biomarkers in ooids from different locations and ages: evidence for a common bacterial flora. *Geobiology* **11**, 420-436.

T

Talbot H. M., Summons R. E., Jahnke L. L., Cockell C. S., Rohmer M. and Farrimond P. (2008) Cyanobacterial bacteriohopanepolyol signatures from cultures and natural environmental settings. *Org. Geochem.* **39**, 232-263.

Taylor J. and Parkes R. J. (1983) The cellular fatty acids of the sulphate-reducing bacteria. *J. Gen. Microbiol.* **129**, 3303-3309.

Taylor J. and Parkes R. J. (1985) Identifying different populations of sulphate-reducing bacteria within marine sediment systems, using fatty acid biomarkers. *Microbiology* **131**, 631-642.

Teasdale P. R., Batley G. E., Apte S. C. and Webster I. T. (1995) Pore water sampling with sediment peepers. *Trends Anal. Chem.* **14**, 250-256.

Teasdale P. R., Hayward S. and Davison W. (1999) In situ, high-resolution measurement of dissolved sulfide using diffusive gradients in thin films with computer-imaging densitometry. *Anal. Chem.* **71**, 2186-2191.

Thamdrup B., Fossing H. and Jørgensen B. B. (1994) Manganese, iron, and sulfur cycling in a coastal marine sediment, Aarhus Bay, Denmark. *Geochim. Cosmochim. Acta* **58**, 5115-5129.

Thiel V., Merz-preiß M., Reitner J. and Michaelis W. (1997) Biomarker studies on microbial carbonates: extractable lipids of a calcifying cyanobacterial mat (Everglades, USA). *Facies* **36**, 163-172.

Thiel V., Peckmann J., Richnow H. H., Luth U., Reitner J. and Michaelis W. (2001) Molecular signals for anaerobic methane oxidation in Black Sea seep carbonates and a microbial mat. *Mar. Chem.* **73**, 97-112.

Thiel V., Blumenberg M., Pape T., Seifert R. and Michaelis W. (2003) Unexpected occurrence of hopanoids at gas seeps in the Black Sea. *Org. Geochem.* **34**, 81-87.

Tissot B. and Welte D. (1984) *Petroleum Formation and Occurrence*. Springer, Berlin.

Tolker-Nielsen, T. and Molin, S. (2000) Spatial Organization of Microbial Biofilm Communities. *Microb. Ecol.* **40**, 75-84.

Bibliography

Trendall, A. F. (1979) A revision of the Mount Bruce Supergroup: Geological Survey of Western Australia, Annual Report 1978, pp. 63-71.

Tunlid A. and White D. C. (1992) Biochemical analysis of biomass, community structure, nutritional status, and metabolic activity of microbial communities in soil. In *Soil Biochemistry* (eds. J. M. Bollag and G. Stotzk). Marcel Dekker, pp. 229-262.

U

Underwood G. and Smith D. (1998). Predicting epipelagic diatom exopolymer concentrations in intertidal sediments from sediment chlorophyll *a*. *Microb. Ecol.* **35**, 116–125.

Urey H. (1947) The thermodynamic properties of isotopic substances. **J. Chem. Soc.**, 562-581.

V

Van der Meer M. T. J., Schouten S. and Sinninghe Damsté J. S. (1998) The effect of the reversed tricarboxylic acid cycle on the ^{13}C contents of bacterial lipids. *Org. Geochem.* **28**, 527-533.

Van der Meer M. T. J., Schouten S., de Leeuw J. W. and Ward D. M. (2000) Autotrophy of green non-sulphur bacteria in hot spring microbial mats: biological explanations for isotopically heavy organic carbon in the geological record. *Environ. Microbiol.* **2**, 428-435.

Van der Meer, MTJ Schouten S., van Dongen B. E., Rijpstra W. I. C., Fuchs G., Sinninghe Damsté J. S., de Leeuw J. W. and Ward D. (2001) Biosynthetic controls on the ^{13}C contents of organic components in the phototrophic bacterium *Chloroflexus aurantiacus*. *J. Biol. Chem.* **14**, 10971-10976.

Van Gernerden H., Tughan C. S., de Wit R. and Herbert R. A. (1989) Laminated microbial ecosystems on sheltered beaches in Scapa Flow, Orkney Islands. *FEMS Microbiol. Lett.* **62**, 87-101.

Van Gernerden H. (1993) Microbial mats: A joint venture. *Mar. Geol.* **113**, 3-25.

Van Kaam-Peters H. M., Köster J., van der Gaast S. J., Dekker M., de Leeuw J. W. and Sinninghe Damsté J. S. (1998) The effect of clay minerals on diasterane/sterane ratios. *Geochim. Cosmochim. Acta* **62**, 2923-2929.

Bibliography

- Van Kranendonk M., Philippot P., Lepot K., Bodorkos S. and Pirajno F.** (2008) Geological setting of Earth's oldest fossils in the ca. 3.5Ga Dresser Formation, Pilbara Craton, Western Australia. *Precambrian Res.* **167**, 93-124.
- Van Lith Y., Warthmann R., Vasconcelos C. and Mckenzie J. A.** (2003) Sulphate-reducing bacteria induce low-temperature Ca-dolomite and high Mg-calcite formation. *Geobiology* **1**, 71-79.
- Van Mooy B. A. S., Rocap G., Fredricks H. F., Evans C. T. and Devol A. H.** (2006) Sulfolipids dramatically decrease phosphorus demand by picocyanobacteria in oligotrophic marine environments. *Proc. Natl. Acad. Sci. U. S. A.* **103**, 8607-8612.
- Vasconcelos C., Warthmann R., McKenzie J. A., Visscher P. T., Bittermann A. G. and van Lith Y.** (2006) Lithifying microbial mats in Lagoa Vermelha, Brazil: Modern Precambrian relics? *Sediment. Geol.* **185**, 175-183.
- Vestal J. R. and White D. C.** (1989) Lipid Analysis Microbial Ecology. *Bioscience* **39**, 535-541.
- Viaroli P., Bartoli M., Giordani G., Magni P. and Welsh D. T.** (2004) Biogeochemical indicators as tools for assessing sediment quality/vulnerability in transitional aquatic ecosystems. *Aquat. Conserv. Mar. Freshw. Ecosyst.* **14**, S19-S29.
- Villanueva J., Grimalt J. O., de Wit R., Keely B. J. and Maxwell J. R.** (1994) Chlorophyll and carotenoid pigments in solar saltern microbial mats. *Geochim. Cosmochim. Acta* **58**, 4703-4715.
- Villanueva L., Navarrete A., Urmeneta J. and White D. C.** (2004) Physiological status and microbial diversity assessment of microbial mats: The signature lipid biomarker approach. *Ophelia* **58**, 165-173.
- Villbrandt M., Krumbein W. and Stal L.** (1991) Diurnal and seasonal variations of nitrogen fixation and photosynthesis in cyanobacterial mats. *Plant Soil* **137**, 13-16.
- Vincent W. F.** (2010) Microbial ecosystem responses to rapid climate change in the Arctic. *ISME J.* **4**, 1087-1090.
- Visscher P. T., Beukema J. and van Germerden H.** (1991a) In-situ characterization of sediments: Measurements of oxygen and sulfide profiles with a novel combined needle electrode. *Limnol. Ocean.* **36**, 1476-1480.
- Visscher P. T., Quist P. and van Gernerden H.** (1991b) Methylated sulfur compounds in microbial mats: In situ concentrations and metabolism by a colorless sulfur bacterium. *Appl. Environ. Microbiol.* **57**, 1758-1763.
- Visscher P. T.** (1992a) Rates of sulfate reduction and thiosulfate consumption in a marine microbial mat. *FEMS Microbiol. Lett.* **86**, 283-288.

Bibliography

- Visscher P. T., Ende F., Schaub B. E. M. and van Gernerden H.** (1992b) Competition between anoxygenic phototrophic bacteria and colorless sulfur bacteria in a microbial mat. *FEMS Microbiol. Lett.* **101**, 51-58.
- Visscher P. T. and van Gernerden H.** (1993) Sulfur cycling in laminated marine microbial ecosystems. In *Biogeochemistry of global change: Radiatively active trace gases* (ed. R. S. Oremland). Chapman and Hall, New York. pp. 672-690.
- Visscher P. T., Reid R. P., Bebout B. M., Hoefft S. E. H., Macintyre I. G. and Thompson Jr. J. A.** (1998) Formation of lithified micritic laminae in modern marine stromatolites (Bahamas): The role of sulfur cycling. *Am. Mineral.* **83**, 1482-1493.
- Visscher P. T., Reid R. P. and Bebout B. M.** (2000) Microscale observations of sulfate reduction: Correlation of microbial activity with lithified micritic laminae in modern marine stromatolites. *Geology* **2**, 919-922.
- Visscher P. T., Hoefft S. M., Surgeon T. L., Rogers, R. B., Ebout B. M., Thompson J. S. and Reid R. P.** (2002) Microelectrode measurements in stromatolites: unraveling the Earth's past I. In *Environmental Electrochemistry: Analyses of trace element biogeochemistry*. (eds. M. Taillefert, T. Rozan) Oxford University Press, Washington, D.C. pp. 265-282.
- Visscher P. T. and Stolz J. F.** (2005) Microbial mats as bioreactors: populations, processes, and products. *Palaeogeogr. Palaeoclimatol. Palaeoecol.* **219**, 87-100.
- Visscher P. T., Dupraz C., Braissant O., Gallagher K. L., Glunk C., Casillas L. and Reed R. E. S.** (2010) Biogeochemistry of carbon cycling in hypersaline mats: linking the present to the past through biosignatures. In *Microbial mats: modern and ancient microorganisms in stratified systems, cellular origin, life in extreme habitats and astrobiology 14* (eds. J. Seckbach and A. Oren). Springer, Dordrecht. pp. 443-468.
- Volkman J. K., Johns R. B., Gillan F. T. and Perry G. J.** (1980) Microbial lipids of an intertidal sediment-I . Fatty acids and hydrocarbons. *Geochim. Cosmochim. Acta* **44**, 1133-1143.
- Volkman J. K.** (1986) A review of sterol markers for marine and terrigenous organic matter. *Org. Geochem.* **9**, 83-99.
- Volkman J. K., Jeffrey S. W., Nichols P. D., Rogers G. I. and Garland C. D.** (1989) Fatty acid and lipid composition of 10 species of microalgae used in mariculture. *J. Exp. Mar. Bio. Ecol.* **128**, 219-240.
- Volkman J. K., Barrett S. M., Blackburn S. I., Mansour M. P., Sikes E. L. and Gelin F.** (1998) Microalgal biomarkers: A review of recent research developments. *Org. Geochem.* **29**, 1163-1179.

Bibliography

W

- Wada H. and Murata N.** (1998) Membrane lipids in cyanobacteria. In *Lipids in Photosynthesis: structure, function and genetics* (eds P. A. Siegenthaler, N. Murata). Kluwer Academic Publishers, Dordrecht, pp. 65-81.
- Wada H. and Murata N.** (2007) The essential role of phosphatidylglycerol in photosynthesis. *Photosynth. Res.* **92**, 205-215.
- Wakeham S. G., Sinninghe Damsté J. S., Kohnen M. E. L. and de Leeuw J. W.** (1995) Organic sulfur compounds formed during early diagenesis in Black Sea sediments. *Geochim. Cosmochim. Acta* **59**, 521-533.
- Walker D. I., Kendrick G. A. and McComb A. J.** (1988) The distribution of seagrass species in Shark Bay, Western Australia, with notes on their ecology. *Aquat. Bot.* **30**, 305-317.
- Walter M. R.** (1976) *Stromatolites*. Elsevier, Amsterdam.
- Walter M. R., Buick R. and Dunlop J. S. R.** (1980) Stromatolites 3,400-3,500 Myr old from the North pole area, Western Australia. *Nature* **284**, 443-445.
- Walter M.** (1994). Stromatolites: the main source of information on the evolution of the early benthos. In *Early Life on Earth* (ed. Bengtson S.) Columbia University Press, New York, pp. 270-286.
- Ward, J. H. J.** (1963) Hierarchical grouping to optimize an objective function. *J. Am. Stat. Assoc.* **58**, 236-244.
- Warthmann R., Vasconcelos C., Bittermann A. and McKenzie J.** (2011) The role of purple sulphur bacteria in carbonate precipitation of modern and possibly early precambrian stromatolites. In *Advances in stromatolites biology. Lecture notes in Earth Sciences* (eds J. Reitner, M. H. Trauth, K. Stüwe, D. Yuen), pp. 141-149.
- Watts C., Maxwell J. and Kjosén H.** (1977) The potential of carotenoids as environmental indicators. I. In *Advances in Organic Geochemistry* (eds R. Campos, J. Gofii), Enadimsa, Madrid. pp. 391-413.
- Welsh D. T.** (2000) Ecological significance of compatible solute accumulation by microorganisms: from single cells to global climate. *FEMS Microbiol. Rev.* **24**, 263-290.
- White D. C., Davis W. M., Nickels J. S., King J. D. and Bobbie R. J.** (1979) Determination of the sedimentary microbial biomass by extractable lipid phosphate. *Oecologia* **40**, 51-62.

Bibliography

- Wickman F. E.** (1952) Variations in the relative abundance of the carbon isotopes in plants. *Geochim. Cosmochim. Acta* **2**, 243-254.
- Widerlund A. and Davison W.** (2007) Size and density distribution of sulfide-producing microniches in lake sediments. *Environ. Sci. Technol.* **41**, 8044-8049.
- Wieland A., Kühl M., McGowan L., Fourçans A., Duran R., Caumette P., García de Oteyza T., Grimalt J. O., Solé A., Diestra E., Esteve I. and Herbert R. A.** (2003) Microbial mats on the Orkney Islands revisited: microenvironment and microbial community composition. *Microb. Ecol.* **46**, 371-90.
- Wieland A., Zopf J., Benthien M. and Kühl M.** (2005) Biogeochemistry of an iron-rich hypersaline microbial mat (Camargue, France). *Microb. Ecol.* **49**, 34-49.
- Wieland A., Pape T., Möbius J., Klock J.-H. and Michaelis W.** (2008) Carbon pools and isotopic trends in a hypersaline cyanobacterial mat. *Geobiology* **6**, 171-186.
- Wiederkehr M., Bousquet R., Ziemann M., Berger A. and Schmid S.** (2011) 3-D assessment of peak-metamorphic conditions by Raman spectroscopy of carbonaceous material: an example from the margin of the Lepontine dome (Swiss Central Alps). *Int. J. Earth Sci.* **100**, 1029-1063.
- Wilkinson S. G.** (1988) Gram-negative bacteria. In *Microbial Lipids* (eds. C. Ratledge, S. G. Wilkinson). Academic Press, London, pp. 299-489.
- Wilson S. E., Cumming B. F., Smol J. P.** (1994). Diatom-salinity relationships in 111 lakes from the Interior Plateau of British Columbia, Canada: the development of diatom-based models for paleosalinity reconstructions. *J. Paleolimnol.* **12**, 197-221.
- Winters K., Parker P. L. and Van Baalen C.** (1969) Hydrocarbons of blue-green Algae: geochemical significance. *Science* **163**, 467-468.

X

- Xu Y., Mead R. N. and Jaffé R.** (2006) A molecular marker-based assessment of sedimentary organic matter sources and distributions in Florida Bay. *Hydrobiologia* **569**, 179-192.

Y-Z

- Zelles L., Bai Q. Y., Rackwitz R., Chadwick D. and Beese F.** (1995) Determination of phospholipid- and lipopolysaccharide-derived fatty acids as an estimate of microbial biomass and community structures in soils. *Biol. Fertil. Soils* **19**, 115-123.

Bibliography

- Zhang C. L., Fouke B. W., Bonheyo G. T., Peacock A. D., White D. C., Huang Y. and Romanek C. S.** (2004) Lipid biomarkers and carbon-isotopes of modern travertine deposits (Yellowstone National Park, USA): Implications for biogeochemical dynamics in hot-spring systems. *Geochim. Cosmochim. Acta* **68**, 3157-3169.
- Zhang H. and Davison W.** (1995) Performance characteristics of diffusion gradients in thin films for the in situ measurement of trace metals in aqueous solution. *Anal. Chem.* **67**, 3391-3400.
- Zhang H., Davison W., Mortimer R., Krom M., Hayes P. and Davies I.** (2002) Localised remobilization of metals in a marine sediment. *Sci. Total Environ.* **296**, 175-187.
- Zhang J., Quay P. and Wilbur D.** (1995) Carbon isotope fractionation during gas-water exchange and dissolution of CO₂. *Geochim. Cosmochim. Acta* **59**, 107-114.
- Zhang Y.-M. and Rock C. O.** (2008) Membrane lipid homeostasis in bacteria. *Nat. Rev. Microbiol.* **6**, 222-233.
- Zhu Q., Aller R. and Fan Y.** (2006) A new ratiometric, planar fluorosensor for measuring high resolution, two-dimensional pCO₂ distributions in marine sediments. *Mar. Chem.* **101**, 40-53.
- Zink K.-G. and Mangelsdorf K.** (2004) Efficient and rapid method for extraction of intact phospholipids from sediments combined with molecular structure elucidation using LC-ESI-MS-MS analysis. *Anal. Bioanal. Chem.* **380**, 798-812.
- Zink K.-G., Wilked H., Disko U., Elvert M. and Horsfield B.** (2003) Intact phospholipids; microbial "life markers" in marine deep subsurface sediments. *Org. Geochem.* **34**, 755-769.

Appendix

Following pages contain documents stating:

The rights, granted by Wiley to the first author of the publication that forms [Chapter 2](#) of this thesis, to reproduce the contribution in any printed volume (book or thesis).

The rights, granted by Elsevier to the first author of the publication that forms [Chapter 3](#) of this thesis, to reproduce the contribution in any printed volume (book or thesis).



Author Services

Copyright FAQs

- [1. Why is it important to sign a Copyright Transfer Agreement or Exclusive Licence?](#)
- [2. My work is funded by the National Institutes of Health \(NIH\)](#)
- [3. My work is funded by the Research Councils UK \(RCUK\)](#)
- [4. My work is funded by the Wellcome Trust \(WT\)](#)
- [5. What is OnlineOpen?](#)
- [6. What are the permitted uses for OnlineOpen articles?](#)
- [7. I am a UK government employee](#)
- [8. I am a US federal government employee](#)
- [9. I am another government employee](#)
- [10. My employer holds the copyright](#)
- [11. Special conditions relating to military personnel](#)
- [12. What rights do I retain if I sign a Copyright Transfer Agreement \(CTA\)?](#)
- [13. What sections must I sign?](#)
- [14. Must all authors sign the Agreement?](#)
- [15. Can I send a faxed or emailed copy of the Agreement?](#)
- [16. Do all contributions require a signed Agreement?](#)
- [17. What are the 'Contributor representations'?](#)
- [18. Do abstracts require an Agreement?](#)
- [19. What about translations?](#)
- [20. What do I do if some material has been published before?](#)
- [21. I want to reproduce some figures/tables from an already published contribution](#)
- [22. I want to reproduce some material from a website](#)
- [23. Do I need permission to quote someone else's work?](#)
- [24. What is the situation regarding copyright in interviews?](#)
- [25. What is the situation regarding plagiarism?](#)
- [26. What is the situation regarding retractions?](#)
- [27. What is the situation regarding dual publication?](#)
- [28. Can you provide advice regarding libel and slander?](#)

1: FAQs for Authors

1. Why is it important to sign a Copyright Transfer Agreement or Exclusive Licence?

It is a legal requirement for Wiley to receive either a signed Copyright Transfer Agreement (CTA) or an Exclusive Licence Agreement (ELA) before publication of your contribution can proceed. Wiley has adopted the CTA for all Wiley-owned journals. For society-owned journals, the societies for whom we publish decide which versions of the forms they require.

This policy also has the following advantages:

- it facilitates international protection against infringement, libel or plagiarism;
- it enables the most efficient processing of publishing licensing and permissions in order that the contribution can be made available to the fullest extent both directly and through intermediaries, and in both print and electronic form;
- it enables Wiley to maintain the integrity of a contribution once refereed and accepted for publication, by facilitating centralized management of all media forms including linking, reference validation and distribution.

Sample copyright forms are provided via the following links:

- [eCTA-A_sample.pdf](#)
- [eCTA-B_sample.pdf](#)
- [eCTA-PS_sample.pdf](#)
- [eELA-A_sample.pdf](#)
- [eELA-B_sample.pdf](#)
- [eELA-PS_sample.pdf](#)



Sign in

E-mail Address

Password

Sign in

Please sign in using your Wiley Online Library (formerly Wiley InterScience) password.

[Forgotten password?](#)
[Register](#)
[Help](#)

Guidelines by Journal

If you are interested in submitting a manuscript, view the author guidelines for each journal by selecting the journal title below (the guidelines will appear in a new browser window):

Top ↑

2. My work is funded by the National Institutes of Health (NIH)

Further to the NIH mandate, Wiley will post the accepted version of contributions authored by NIH grant-holders to PubMed Central upon acceptance. This accepted version will be made publicly available 12 months after publication. For further information, see <http://authorservices.wiley.com/bauthor/onlineopen.asp>.

Top ↑

3. My work is funded by the Research Councils UK (RCUK)

You must comply with the terms of the RCUK's mandate which came into effect on 1 April 2013 and ensure your article is published Open Access (see <http://authorservices.wiley.com/bauthor/onlineopen.asp>). If you elect to pay to make your article OnlineOpen, you will be asked to sign the Creative Commons Attribution (CC-BY) licence, which permits use, distribution and reproduction in any medium, provided the original work is properly cited. This will be reflected in the copyright statement that accompanies the published version of the article. See <http://www.wileyopenaccess.com/details/content/12f25db4c87/Copyright—License.html> for more information relating to the Creative Commons licences used for Wiley Open Access articles'

Top ↑

4. My work is funded by the Wellcome Trust (WT)

You must comply with the terms of the Wellcome Trust's mandate which came into effect on 1 April 2013 and ensure your article is published Open Access (see <http://authorservices.wiley.com/bauthor/onlineopen.asp>). If you elect to pay to make your article OnlineOpen, you will be asked to sign the Creative Commons Attribution (CC-BY) licence, which permits use, distribution and reproduction in any medium, provided the original work is properly cited. This will be reflected in the copyright statement that accompanies the published version of the article. See <http://www.wileyopenaccess.com/details/content/12f25db4c87/Copyright—License.html> for more information relating to the Creative Commons licences used for Wiley Open Access articles.

Top ↑

5. What is OnlineOpen?

OnlineOpen is a service offered by Wiley that enables authors the opportunity to ensure that their final published contribution is made available for anyone to access online. This option is an important part of Wiley's response to the calls for open access and our commitment to viable high-quality publishing on behalf of societies.

For further details, please see <http://authorservices.wiley.com/bauthor/onlineopen.asp>.

Top ↑

6. What are the permitted uses for OnlineOpen articles?

Authors who elect to make their article OnlineOpen are invited to sign one of three Creative Commons Licences: the Creative Commons Attribution Licence (CC-BY), the Creative Commons Attribution Non-Commercial Licence (CC-BY-NC) and the Creative Commons Attribution Non-Commercial No Derivatives Licence (CC-BY-NC-ND). Further information about these licences, and the permitted uses, can be found at: <http://www.wileyopenaccess.com/details/content/12f25db4c87/Copyright—License.html>

Sample copies of these licences can be found at:

- [eOAA-CC-BY sample.pdf](#)
- [eOAA-CC-BY-NC sample.pdf](#)
- [eOAA-CC-BY-NC-ND sample.pdf](#)

Top ↑

7. I am a UK government employee

The rights in a contribution prepared by an employee of a UK government department, agency or other Crown body as part of his/her official duties, or which is an official government publication, belong to the Crown. Authors must ensure they comply with departmental regulations and submit the appropriate authorization to publish.

Top ↑

8. I am a US federal government employee

A contribution prepared by a US federal government employee as part of the employee's official duties, or which is an official US government publication, is called a 'US Government work', and is in the public domain in the United States. If the contribution was not prepared as part of the employee's duties or is not an official US government publication, it is not a US Government work. In the case of a contribution prepared under US government contract or grant, the US government may reproduce, without charge, all or portions of the contribution and may authorize others to do so, for official US government purposes only, if the US government contract or grant so requires.

Top ↑

9. I am another government employee

If you are employed by the Department of Veterans Affairs in Australia, the World Bank, the International Monetary Fund, the European Atomic Energy Community, the Jet Propulsion Laboratory at California Institute of Technology, or are a Canadian Government civil servant, please download a copy of the relevant license agreement below:

- [WileyJetPropulsionELA.pdf](#)
- [WileyIMFELA.pdf](#)
- [WileyDeptVeteransAffairsELA.pdf](#)
- [WileyCanadianCivilServantsELA.pdf](#)
- [EU-EURATOMPUBLICATIONLICENSE.pdf](#)
- [WileyWorldBankELA.pdf](#)

Top ↑

10. My employer holds the copyright

Where work is carried out by an author in their capacity as an employee of a company, copyright will be owned by the company. An authorized signatory of the company must therefore sign the Agreement.

If you are an employee of Amgen, please download a copy of the company addendum from the link below and return your signed license agreement along with the addendum:

- [WileyAmgenaddendum.pdf](#)

Top ↑

11. Special conditions relating to military personnel

Work carried out by government employees or military personnel may require a statement to the effect that the opinions expressed do not necessarily reflect those of the military or government agency for which they work. Please ensure that you check with the appropriate authorities and include the necessary statement within the body of your contribution. (See also section 7 '[I am a UK government employee](#)' or section 8 '[I am a US federal government employee](#)'.)

Top ↑

12. What rights do I retain if I sign a Copyright Transfer Agreement (CTA)?

The Contributor or, if applicable, the Contributor's Employer, retains all proprietary rights other than copyright, such as patent rights, in any process, procedure or article of manufacture described in the contribution.

Contributors may re-use unmodified abstracts for any non-commercial purpose. For online use of the abstract, Wiley encourages but does not require linking back to the final published contribution.

Contributors may use the articles in teaching duties and in other works such as theses.

Contributors may re-use figures, tables, data sets, artwork, and selected text up to 250 words from their contributions without seeking permission, provided the following conditions are met:

- Full and accurate credit must be given to the contribution.
- Modifications to the figures, tables and data must be noted. Otherwise, no changes may be made.
- The reuse may not be made for direct commercial purposes, or for

- financial consideration to the Contributor.
- Re-use rights shall not be interpreted to permit dual publication in violation of journal ethical practices.

Additional re-use rights are set forth in the actual copyright Agreement.

[Top](#) 

13. What sections must I sign?

You must sign in the space indicated depending on whether you own the copyright in your work, the copyright is owned by your employer or whether you are a government employee. It is essential to check that the CTA or ELA (the Agreement) has been completed, signed and dated correctly before your contribution can be published.

[Top](#) 

14. Must all authors sign the Agreement?

Ideally, all authors should sign the Agreement, with additional signatures attached separately if necessary. However, if it is not possible to obtain a physical signature from all authors, you must have their agreement in writing to enable you to enter into the Agreement on their behalf.

[Top](#) 

15. Can I send a faxed or emailed copy of the Agreement?

Wiley will accept faxes, as well as scanned copies of the signed original forms via e-mail.

[Top](#) 

16. Do all contributions require a signed Agreement?

Yes, signed forms are required for all contribution types (apart from letters and correspondence).

[Top](#) 

17. What are the 'Contributor representations'?

In signing the forms you confirm that:

- The contribution is your own work
- All individuals identified as contributors have actually contributed to the article
- All individuals who contributed are listed
- You have informed your fellow contributors of the terms of the Agreement and obtained their permission in writing to enter into it on their behalf
- The contribution is submitted only to the specified journal and has not been published before
- You have obtained written permission from the copyright owners to reproduce any material owned by third parties, and that you have included appropriate acknowledgement within the text of your contribution
- That the contribution contains no libelous or unlawful statements, does not infringe upon the rights or the privacy of others, and does not contain any material or instructions that might cause harm or injury

[Top](#) 

18. Do abstracts require an Agreement?

Meetings abstracts. We do not require a signed Agreement to publish abstracts of material submitted for poster sessions and presentations at conferences or meetings. The right to publish such material is presumed.

Abstracts specifically created for abstract publications. If you have written an abstract of a previously published article for publication in another journal (e.g. a reviews-type journal), we do require you to sign an Agreement.

Reproduction of existing abstracts. If you wish to include verbatim abstracts from previously published articles, you do not need written permission from the publisher of those articles, although the source should be cited. Abstracts are covered by copyright and are not in the public domain but there is an exception in UK law which permits the copying and publication of scientific and technical abstracts accompanying published periodical articles.

Top 

19. What about translations?

Let's say, for example, that you have published an article in Spanish by Palabra Publications. You have translated the article yourself (or by employing a translator) and want to submit the English translation to a Wiley journal, say *Journal of Indelible Research*.

In order to make the translation, you must first approach Palabra for permission to translate the article for republication. The translation itself would then be held under separate copyright – by you or the translator. You would then be able to sign the *Journal of Indelible Research* Copyright Transfer Agreement for the translation, rather than the original article.

The translation must include a full bibliographic reference to the original publication and you must have obtained permission from the original copyright holder to make the translation.

Top 

20. What do I do if some material has been published before?

The corresponding author is responsible for obtaining written permission to reproduce the material "in print and other media" from the publisher of the original source, and for supplying Wiley with that permission. A RightsLink facility for requesting permission from Wiley journals is available on each journal's website. The corresponding author is also responsible for completing and returning to the editorial office or the publisher the journal-specific copyright transfer form, and any financial disclosure forms that might be required for a particular journal. These forms are found via the Wiley Author Licensing Service or on each journal's website. Forms may also be available from the journal's editorial office.

Following is more information to help you obtain necessary written permissions.

Author retains copyright: If you, the author, have retained the copyright, it is still likely that the first journal will have required an exclusive licence to publish, which means that you are not in a position to authorize another journal to republish. As a general rule it is essential to obtain written permission from the original publisher or society to reproduce the relevant material if this is not made clear in the Agreement or licence you signed for that publisher or society. It will always be necessary to seek permission to re-publish unless the licence you have signed is clearly for non-exclusive rights only.

Copyright rests with the original publisher: Where the previous publisher owns the copyright, the copyright line on the re-published contribution should refer to the previous publisher. In these cases the copyright line that will appear on the published contribution will be e.g., © 2013 Oxford University Press.

Copyright is owned by a third party: If content has been previously published, and a third party is the copyright holder or exclusive licensee of rights in that material, you must seek and obtain permission for re-use, and credit the material in accordance with the permission grant. This applies whether you have written the material yourself or whether it has been written by a third party. Permission is generally not required for brief and insubstantial extracts of text or references to other works, provided that these are properly attributed. In all cases, you should be aware that duplicate publication can constitute an infringement and/or an ethical violation if it is not made clear that the material has been published before.

Top 

21. I want to reproduce some figures/tables from an already published contribution

You must ensure that you have received permission from the copyright holder or exclusive licensee to reproduce in the contribution all material not owned by you, and that you have provided full acknowledgement of the source. In most cases, the original publisher's Rights Department or the journal editorial office will advise you of the exact form of words required. This usually includes a full bibliographic reference to the original publication, and an acknowledgement that the material is reproduced with permission from the rights owner.

Wiley is a signatory to an agreement signed by the majority of scientific, technical and medical (STM) publishers whereby participating publishers do not make reciprocal charges for the reproduction of copyright material. (For further information, please see the Permission Guidelines at : <http://www.stm-assoc.org>.) These guidelines extend to re-use of a small

number of figures and tables from journal articles without seeking permission and a number of large STM publishers have signed up to this.

Top ↑

22. I want to reproduce some material from a website

Just because material is freely available on the web, it does not necessarily mean that the information can be reproduced without permission. We recommend the following actions:

1. You should seek permission from the original source.
2. If the website doesn't provide an original source and/or the source is unknown to you then you should seek permission from the website to reuse the material. You can use the following link to identify the contact details for the name in which the website has been registered <http://www.whois.org>.

If the website has posted material without seeking permission from the copyright holder and/or the source is unknown, then you are taking a risk in including the material in your work. As a last resort, the Authors' Licensing and Collecting Society (ALCS) can be contacted to trace the copyright holder: <http://www.alcs.co.uk>.

Top ↑

23. Do I need permission to quote someone else's work?

Fair use or fair dealing (depending on the country whose laws apply) allow use of a copyrighted work for the purposes of criticism or review. This extends to quotations that form part of book reviews and other critical material. Permission to quote is not required in such instances, provided the extracts are not substantial and are genuinely required for the purposes of review or criticism. For works of shorter length, such as songs, permission to re-use shorter extracts may be required. All sources must be credited – title and author at minimum – in order for fair dealing to apply.

Top ↑

24. What is the situation regarding copyright in interviews?

If the record of an informal conversation you held with a particular interviewee appears in a contribution there is no issue regarding copyright. However, copyright may rest with the interviewee in cases of formal interviews where you record the subject's conversation on a tape recorder or verbatim. It is therefore necessary for the interviewee to sign the Agreement.

In some cases, copyright in interviews is shared jointly between interviewer and interviewee where the conversation being recorded represents a mutual exchange between the two. In such cases both parties should sign the Agreement.

Top ↑

25. What is the situation regarding plagiarism?

The Contributor's representations contained in the Agreement are designed to protect against plagiarism. Wiley policy is based on the 'Guidelines on Good Publication Practice' published by the Committee on Publication Ethics (COPE) and can be found at <http://authorservices.wiley.com/bauthor/publicationethics.asp>.

COPE defines plagiarism as follows:

'Plagiarism ranges from the unreferenced use of others' published and unpublished ideas, including research grant applications, to submission under 'new' authorship of a complete paper, sometimes in a different language. . . It applies to print and electronic versions.'

Dealing with misconduct

It is the duty of journal editors to investigate suspected cases of misconduct. They need to decide whether it is necessary to retract a published contribution and in some cases, whether it is necessary to alert the employers of the accused author(s). Some evidence is required, but if the employers have a process for investigating accusations, it is not necessary for the editor to assemble a complete case as this may entail wider consultation which would bring the author into disrepute before the facts of the matter have been decided.

Editors may decide not to involve employers in cases of less serious misconduct, such as dual publication, deception over authorship or failure to declare a conflict of interest. In all cases, authors must be given the opportunity to respond to accusations of misconduct before any action is taken. (See http://authorservices.wiley.com/bauthor/faq_main.asp).

Available sanctions

The following sanctions are set out in the COPE guidelines, but journal editors should consider the application of any sanction very seriously due to the potential impact on an author's reputation or career. The COPE guidelines have no legal force and it is generally prudent to avoid 'naming and shaming' authors and simply to confirm a retraction, when necessary, in neutral and concise terms.

- A letter of explanation (and education) to the authors, where there appears to be a genuine misunderstanding of principles.
- A letter of reprimand and warning as to future conduct.
- A formal letter to the relevant head of institution or funding body.
- Publication of a notice of dual publication or plagiarism.
- An editorial giving full details of the misconduct.
- Refusal to accept future submissions from the individual, unit or institution responsible for the misconduct, for a stated period.
- Formal withdrawal or retraction of the paper from the scientific literature, informing other editors and the indexing authorities (see section 26, '[What is the situation regarding retractions?](#)').

Reporting the case to the General Medical Council, or other such authority or organization which can investigate and act with due process.

Top ↑

26. What is the situation regarding retractions?

It is Wiley policy strongly to discourage withdrawal of an article in line with the STM guidelines on retractions: 'Preservation of the Objective Record of Science – an STM Guideline' (<http://www.stm-assoc.org>).

The practice of removal, deletion or obscuring of an article or portion thereof should be limited to circumstances such as:

- An inappropriate violation of the privacy of a research subject
- Errors to which a member of the general public might be exposed that, if followed or adopted, would pose a significant risk to health
- Clearly defamatory comment made about others in the relevant field or about their work

Even in these circumstances, bibliographic information about the removed contribution should be retained for the scientific record, and an explanation given, however, brief, about the circumstances of its removal.

For most cases of infringement, Wiley recommends linking a retraction statement to the article in question, while retaining the article as first published in order to maintain the scientific record.

- The retraction will appear on a numbered page in a prominent section of the journal.
- The retraction will be listed in the contents page, and the title of the original contribution will be included in its heading.
- The text of the retraction should explain why the contribution is being retracted.
- The statement of retraction and the original article must be clearly linked in the electronic database so that the retraction will always be apparent to anyone who comes across the original article.

Top ↑

27. What is the situation regarding dual publication?

Dual publication of an article is generally not permitted. In signing the Agreement you are being asked to represent that the contribution has not been submitted elsewhere for publication. There are narrow exceptions to the dual publication rule for some materials, such as standards. In any such case, prior approval from the journal to which you are submitting is likely to be required.

Top ↑

28. Can you provide advice regarding libel and slander?

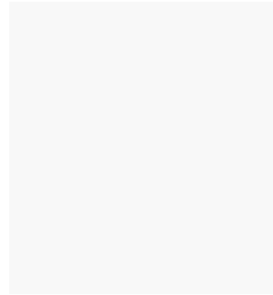
Libel and slander are both forms of defamation and so in defining them it is necessary to look at what is meant by defamation. Broadly, **defamation** arises where a statement is made which is false and which impugns another person's reputation, or adversely affects his or her standing in the community.

Libel can be defined as a statement in print, or some other permanent form, concerning any person, which exposes that person to hatred, or ridicule, or which might injure that person in their profession, trade or calling. In the UK, the printer, publisher and author may all be held liable for libelous statements in printed published form. Ignorance is not an acceptable defence

Appendix

The difference between libel and slander relates to how the defamatory statement is made. In **libel**, the defamatory statement is expressed in a permanent and visual form including written words and printed images. In **slander**, the defamatory statement is in a transient form, conveyed for example by spoken words or gestures.

There is a range of defences to an action for libel. In the UK, the two main defences (apart from 'privilege') are 'justification' and 'fair comment'. In a defence of justification it must be established that the works in question are true in substance and in fact. In a defence of fair comment, which only protects statements of opinion, the defence is that the words in question are a comment – based on actual facts – on a matter of public interest and are not malicious. Laws in other countries differ, but truth is always a defense. If in any doubt, please refer to Wiley for guidance.



© 2014 John Wiley & Sons, Ltd, Company number 00641132, Registered in England and Wales, registered office: The Atrium, Southern Gate, Chichester, West Sussex PO19 8SQ, UK [CarbonFree](#) partner of [Carbonfund.org](#)



[Advanced search](#)

[Follow us](#)

[Help & Contact](#)

[Journals & books](#)

[Online tools](#)

[Authors, editors & reviewers](#)

[About Elsevier](#)

[Store](#)

For Authors

[Home](#)

[Rights & responsibilities](#)

[Funding body agreements](#)

[Open access](#)

[Author services](#)

[Journal performance](#)

[Early career researchers](#)

[Book authors](#)

[Authors' Update](#)

Rights & responsibilities

At Elsevier, we request transfers of copyright, or in some cases exclusive rights, from our journal authors in order to ensure that we have the rights necessary for the proper administration of electronic rights and online dissemination of journal articles. Authors and their employers retain (or are granted/transferred back) significant scholarly rights in their work. We take seriously our responsibility as the steward of the online record to ensure the integrity of scholarly works and the sustainability of journal business models, and we actively monitor and pursue unauthorized and unsubscribed uses and re-distribution (for subscription models).

In addition to [authors' scholarly rights](#), authors have certain responsibilities for their work, particularly in connection with [publishing ethics issues](#).

Rights

As a journal author, you have rights for a large range of uses of your article, including use by your employing institute or company. These rights can be exercised without the need to obtain specific permission.

How authors can use their own journal articles

Authors publishing in Elsevier journals have wide rights to use their works for teaching and scholarly purposes without needing to seek permission.

Table of Authors' Rights

	Preprint version (with a few exceptions- see below *)	Accepted Author Manuscript	Published Journal Articles
Use for classroom teaching by author or author's institution and presentation at a meeting or conference and distributing copies to attendees	Yes	Yes with full acknowledgement of final article	Yes with full acknowledgement of final article
Use for internal training by author's company	Yes	Yes with full acknowledgement of final article	Yes with full acknowledgement of final article
Distribution to colleagues for their research use	Yes	Yes	Yes
Use in a subsequent compilation of the author's works	Yes	Yes with full acknowledgement of final article	Yes with full acknowledgement of final article
Inclusion in a thesis or dissertation	Yes	Yes with full acknowledgement of final article	Yes with full acknowledgement of final article
Reuse of portions or extracts from the article in other works	Yes	Yes with full acknowledgement of final article	Yes with full acknowledgement of final article
Preparation of derivative works (other than for commercial purposes)	Yes	Yes with full acknowledgement of final article	Yes with full acknowledgement of final article
Preprint servers	Yes	Yes with the specific written permission of Elsevier	No
Voluntary posting on open web sites operated by author or author's institution for scholarly purposes	Yes (author may later add an appropriate bibliographic citation, indicating subsequent publication by Elsevier and journal title)	Yes, with appropriate bibliographic citation and a link to the article once published	Only with the specific written permission of Elsevier
Mandated deposit or deposit in or posting to subject-oriented or centralized repositories	Yes under specific agreement between Elsevier and the repository	Yes under specific agreement between Elsevier and the repository**	Yes under specific agreement between Elsevier and the repository
Use or posting for commercial gain or to substitute for services provided directly by journal	Only with the specific written permission of Elsevier	Only with the specific written permission of Elsevier	Only with the specific written permission of Elsevier

**Voluntary posting of Accepted Author Manuscripts in the arXiv subject repository is permitted.

Examples of use or posting for commercial gain:

- Posting by companies of employee-authored works for use by customers of those companies (e.g. pharmaceutical companies and physician prescribers)
- Commercial exploitation such as directly associating advertising with posting or charging fees for document delivery or access

*Which journals have different preprint policies?

If an electronic preprint of an article is placed on a public server prior to its submission to an Elsevier journal, this is not generally viewed by Elsevier as 'prior publication' and will not disqualify the article from further consideration by Elsevier, nor will Elsevier require the removal of that preprint version.

However Cell Press and The Lancet have different preprint policies and will not consider for publication articles that have already been posted publicly. This is a rule agreed upon by The International Committee of Medical Journal Editors. Information on [Cell Press policy on preprints](#) is available, as is [The Lancet preprint policy](#). There are a number of other journals published by Elsevier (principally journals published on behalf of third party owners) that also have their own preprint policies which will be set out in the Guide for Authors for the relevant journal.

Does Elsevier request a transfer of copyright?

Elsevier requests a transfer of copyright for articles published under subscription-based business models but we generally use different licensing approaches for other publishing models where we offer authors a variety of Creative Commons licenses for some of our author-pays journals and are piloting a range of options. [Learn more](#) about Creative Commons licenses.

For subscription-based publishing, we ask for a transfer of copyright for a number of reasons, mainly because:

1. By having the ability to exercise all rights under copyright, Elsevier is able to quickly launch new products and services, and to make agreements with other platforms and services to enrich published content and to make it more accessible and usable. Authors may be based in a number of different countries, which will have their own copyright regimes. Copyright assignments give more legal certainty, particularly in relation to future rights in new technologies.
2. Elsevier uses copyright to protect the integrity of the journal articles in cases of plagiarism, copyright infringement and other third party infringements. The journal subscription business model depends on a substantial body of subscribing customers providing financial support to a particular journal, and "free-riding" infringements diminish this model.
3. An assignment of rights under copyright means that we can more easily show that we own the rights and do not have to seek the participation of the author or obtain power of attorney from the author in order to bring an enforcement action.

Remember, even though we ask for a transfer of copyright, our journal authors retain (or are granted back) significant scholarly rights, as outlined above.

For a more detailed discussion, see the [STM Position Paper](#) on the benefits of copyright assignments.

Does Elsevier claim rights in an author's supporting data?

Elsevier supports the general principle that raw research data should be made freely available to all researchers and encourages the public posting of the raw data outputs of research. (Note that this is distinct from charts, tables, etc. which may be included within an article and in which rights would be transferred or licensed to Elsevier as part of the article, in the same way as text, illustrations or photographs). Elsevier therefore does not claim rights in the raw datasets that may be submitted with an article and the author can make these datasets freely available from other (web) locations.

If supported by the author and journal editor, and when a dataset is hosted in a repository that ensures data integrity and supports long-term preservation and inward linking, Elsevier can further support the discoverability of that dataset by connecting it with the published journal article on ScienceDirect through linking from an article or entity or through article interoperability. [Click here](#) to review examples of how this could work in practice.

For more information on industry positions on this issue supported by Elsevier, view the:

[Joint Statement from STM and DataCite](#) on the Linkability and Citability of Research Data, June 2012

[Brussels Declaration on STM Publishing](#), November 2007

[STM/ALPSP Statement](#), June 2006

Can I post my published journal article on open websites?

A published journal article is the definitive final record of published research that appears in the journal and embodies all value-adding publisher activities, including copy editing, formatting and, if relevant, pagination, along with the stewardship of the scholarly record.

You can use your branded and formatted published article for all of the personal and institutional purposes described above. However, in order to safeguard the correct scientific record, Elsevier does not permit the posting of published journal articles (either the pdf provided by Elsevier or HTML files) on any open websites.

As part of its contribution to the stewardship of the scientific literature, Elsevier works with third parties (e.g. national libraries) to preserve its journal articles for posterity and in perpetuity, and invests to drive their usage. Elsevier strictly enforces an absolute

guideline on the location of its published journal articles: each branded and formatted published journal article will reside only on a completely controlled site because this is the only way that we as the publisher can guarantee that each published journal article is permanent, authentic and unaltered as part of the 'minutes of science'.

Since Elsevier adds significant value to the final published journal article, we need to take these steps to ensure that this value is maintained, both for Elsevier and for our authors. However, we view preprints and accepted author manuscripts as less formal versions of the article and we therefore take a more liberal approach towards these, as described in more detail on our [Article Posting Policies](#) information page.

FAQ

Where can I find more information on Elsevier's posting and copyright policies?

Please visit our [Article Posting Policies](#) information page.

You can also download your practical guide to Elsevier's copyright policy [here](#).

Am I allowed to post my published journal article to websites to fulfil drug regulation authority approval of therapeutic agents?

The posting of the published article to websites to fulfil drug regulation authority approval of therapeutic agents is not permitted. However, Elsevier permits the inclusion of an article title and abstract to fulfil drug regulation authority requirements, provided this is accompanied by a link to the published journal article on Elsevier's website. There are also reprint and license arrangements available to facilitate medical requirements.

Does Elsevier assist its authors to comply with the manuscript archiving requirements of funding bodies?

Elsevier has established agreements and developed policies to allow authors who publish in Elsevier journals to comply with the manuscript archiving requirements of a variety of funding bodies, including the US-based National Institutes of Health. For more information on existing arrangements, or if you are an institution or funding body and would like to discuss putting in place a new agreement with Elsevier, please see the [Funding Body Agreements](#) information page.

When Elsevier changes its author usage policies, are those changes also retroactive?

Yes, when Elsevier changes its policies to enable greater academic use of journal materials (such as the changes several years ago in our web-posting policies) or to clarify the rights retained by journal authors, Elsevier is prepared to extend those author rights retroactively with respect to articles published in journal issues produced prior to the policy change.

How do I obtain a journal publishing agreement?

You will receive a form automatically by post or e-mail once your article is received by Elsevier's Editorial-Production Department. View a [generic example of the agreement](#). Some journals will use another variation of this form.

Can you provide me with a PDF file of my article?

Many Elsevier journals are now offering authors e-offprints – free electronic versions of their published articles. E-offprints are watermarked PDF versions, and are usually delivered within 24 hours, much quicker than print copies. These PDFs may not be posted to public websites. For more information, please see our author [Offprints](#) page or contact authorsupport@elsevier.com

What is Elsevier's position on author rights in the case of a contractor of the US government?

Where work is produced by a contractor under contract to a US government department, Elsevier agrees that the government department will retain the same standard rights to reuse the work as Elsevier would typically grant if the work had been produced by an employee of that department.

Who should I contact if I have a query about my journal publishing agreement?

Please note that the rights listed above apply to journal authors only. For information regarding book author rights and for any questions relating to the author rights outlined here, please contact Elsevier's Global Rights department.

Elsevier Global Rights Department
Phone (+44) 1865 843830
Fax (+44) 1865 853333
Email: oxfordcopyrights@elsevier.com

Responsibilities

The publication of an article in a peer-reviewed journal is an essential building block in the development of a coherent and respected network of knowledge. It is a direct reflection of the quality of work of the author and the institutions that support them. Peer-reviewed articles support and embody the scientific method. It is therefore important to agree upon standards of expected ethical behavior.

Reporting standards

Authors of reports of original research should present an accurate account of the work performed as well as an objective discussion of its significance. Underlying data should be represented accurately in the paper. A paper should contain sufficient detail and references to permit others to replicate the work. Fraudulent or knowingly inaccurate statements constitute unethical behavior and are unacceptable.

Review and professional publication articles should also be accurate and objective, and editorial 'opinion' works should be identified as such.

Data access and retention

Authors may be asked to provide the raw data in connection with a paper for editorial review, and should be prepared to provide public access to such data (consistent with the ALPSP-STM Statement on Data and Databases), if practicable, and should in any event be prepared to retain such data for a reasonable time after publication.

Originality and plagiarism

The authors should ensure that they have written entirely original works, and if the authors have used the work and/or words of others, that this has been appropriately cited or quoted.

Plagiarism takes many forms, from 'passing off' another's paper as the author's own paper, to copying or paraphrasing substantial parts of another's paper (without attribution), to claiming results from research conducted by others. Plagiarism in all its forms constitutes unethical publishing behavior and is unacceptable.

Multiple, redundant or concurrent publication

An author should not in general publish manuscripts describing essentially the same research in more than one journal or primary publication. Submitting the same manuscript to more than one journal concurrently constitutes unethical publishing behavior and is unacceptable.

In general, an author should not submit for consideration in another journal a previously published paper. Publication of some kinds of articles (e.g. clinical guidelines, translations) in more than one journal is sometimes justifiable, provided certain conditions are met. The authors and editors of the journals concerned must agree to the secondary publication, which must reflect the same data and interpretation of the primary document. The primary reference must be cited in the secondary publication. Further detail on acceptable forms of secondary publication can be found at www.icmje.org.

Acknowledgement of sources

Proper acknowledgment of the work of others must always be given. Authors should cite publications that have been influential in determining the nature of the reported work. Information obtained privately, as in conversation, correspondence, or discussion with third parties, must not be used or reported without explicit, written permission from the source. Information obtained in the course of confidential services, such as refereeing manuscripts or grant applications, must not be used without the explicit written permission of the author of the work involved in those services.

Hazards and human or animal subjects

If the work involves chemicals, procedures or equipment that have any unusual hazards inherent in their use, the author must clearly identify these in the manuscript. If the work involves the use of animal or human subjects, the author should ensure that the manuscript contains a statement that all procedures were performed in compliance with relevant laws and institutional guidelines and that the appropriate institutional committee(s) has approved them. Authors should include a statement in the manuscript that informed consent was obtained for experimentation with human subjects. The privacy rights of human subjects must always be observed.

Use of patient images or case details

Studies on patients or volunteers require ethics committee approval and informed consent, which should be documented in the paper.

Appropriate consents, permissions and releases must be obtained where an author wishes to include case details or other personal information or images of patients and any other individuals in an Elsevier publication. Written consents must be retained by the author and copies of the consents or evidence that such consents have been obtained must be provided to Elsevier on request.

Particular care should be taken with obtaining consent where children are concerned (in particular where a child has special needs or learning disabilities), where an individual's head or face appears, or where reference is made to an individual's name or other personal details.

For more information, please review the [Elsevier Policy on the Use of Images or Personal Information of Patients or other Individuals](#).

Disclosure and conflicts of interest

A conflict of interest may exist when an author or the author's institution has a financial or other relationship with other people or organizations that may inappropriately influence the author's work. A conflict can be actual or potential, and full disclosure to the journal is the safest course. All submissions must include disclosure of all relationships that could be viewed as presenting a potential conflict of interest. The journal may use such information as a basis for editorial decisions and may publish such disclosures if they are believed to be important to readers in judging the manuscript. A decision may be made by the journal not to publish on the basis of the declared conflict. At the end of the text, under a subheading 'Disclosure Statement', all authors must disclose any actual or potential conflict of interest including any financial, personal or other relationships with other people or organizations within three (3) years of beginning the work submitted that could inappropriately influence (bias) their work.

Examples of potential conflicts of interest which should be disclosed include employment, consultancies, stock ownership, honoraria, paid expert testimony, patent applications/registrations, and grants or other funding. Potential conflicts of interest should be disclosed at the earliest stage possible.

All sources of financial support for the project should be disclosed. This declaration (with the heading 'Role of the funding source') should be made in a separate section of the text and placed before the References. Authors must describe the role of the study sponsor(s), if any, in study design; in the collection, analysis, and interpretation of data; in the writing of the report; and in the decision to submit the paper for publication. (In addition some funding organizations have particular policies to enable their grant recipients to publish open access in Elsevier journals - for more detail on this, please visit our [Funding Body Agreements](#) page.

Fundamental errors in published works

When an author discovers a significant error or inaccuracy in his/her own published work, it is the author's obligation to promptly notify the journal editor or publisher and cooperate with the editor to retract or correct the paper. If the editor or the publisher learns from a third party that a published work contains a significant error, it is the obligation of the author to promptly retract or correct the paper or provide evidence to the editor of the correctness of the original paper.

Authorship of the paper

Authorship should be limited to those who have made a significant contribution to the conception, design, execution, or interpretation of the reported study. All those who have made significant contributions should be listed as co-authors. Where there are others who have participated in certain substantive aspects of the research project, they should be acknowledged or listed as contributors.

The corresponding author should ensure that all appropriate co-authors and no inappropriate co-authors are included on the paper, and that all co-authors have seen and approved the final version of the paper and have agreed to its submission for publication.

Changes to authorship

This policy concerns the addition, deletion, or rearrangement of author names in the authorship of accepted manuscripts. Note that The Lancet, Cell, and journals published by Elsevier on behalf of learned societies may have different policies.

Before the accepted manuscript is published in an online issue:

Requests to add or remove an author, or to rearrange the author names, must be sent to the Journal Manager by the corresponding author of the accepted manuscript, and must include:

1. The reason the name should be added or removed, or the author names rearranged
2. Written confirmation (e-mail, fax, letter) from all authors that they agree with the addition, removal or rearrangement. In the case of addition or removal of authors, this includes confirmation from the author being added or removed

Requests that are not sent by the corresponding author will be forwarded by the Journal Manager to the corresponding author, who must follow the procedure described above.

Note that:

- Journal Managers will inform the Journal Editors of any such requests
- Publication of the accepted manuscript in an online issue is suspended until authorship has been agreed

After the accepted manuscript has been published in an online issue:

Any requests to add, delete or rearrange author names in an article published in an online issue will follow the same policies as noted above and may result in a corrigendum.

For more information on publishing ethics issues, please consult our [Publishing Ethics Resource Kit](#).

Permissions

Elsevier's Global Rights Department meets the rights and permissions needs of our customers and authors

Our [Author and User Rights](#) guidelines describe additional uses that can be made of Elsevier-owned material by authors, subscribers, and other customers (including content that is free at the point of use or accessed under license).

As an author, you may wish to use references you have found in other publications. Conversely, you may be seeking information on using an Elsevier-published work as a reference.

If you are an author who wishes to obtain permission to include material from other sources in your work being published by Elsevier, please visit:

[Permission seeking guidelines for Elsevier authors](#)

If you wish to obtain permission to re-use material from Elsevier books, journals, databases, or other products, please visit:

[Obtaining permission to re-use Elsevier material](#)

If you are an Elsevier author and are contacted by a requester who wishes to re-use all or part of your article or chapter, please also refer them to our [Obtaining Permission to Re-Use Elsevier Material](#) page.

Contact us

Questions about obtaining permission? Contact the Permissions Helpdesk at permissionshelpdesk@elsevier.com or (+1) 800-523-4069 ext 3808.



[Industries](#) [Advertising](#) [Careers](#) [Feedback](#) [Site Map](#) [Elsevier Websites](#) [A Reed Elsevier Company](#)

Copyright © Elsevier B.V. All rights reserved. [Privacy Policy](#) [Terms & Conditions](#)

Cookies are set by this site. To decline them or learn more, visit our [Cookies page](#).

Appendix
